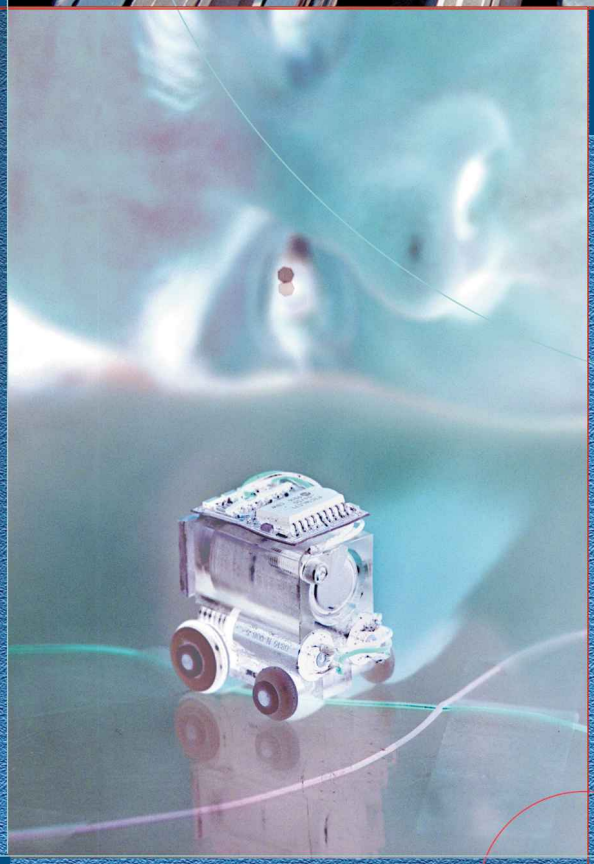

1998

LABORATORY DIRECTED RESEARCH AND DEVELOPMENT

Sandia National Laboratories

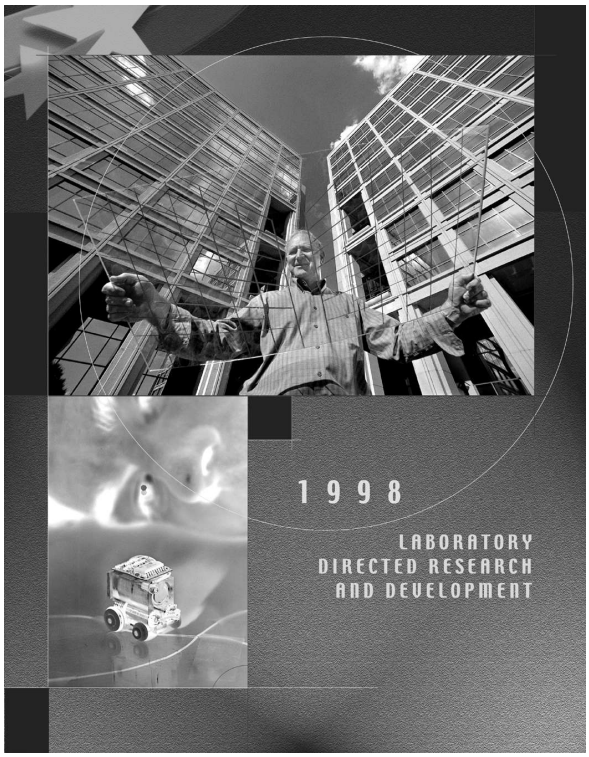

Cover (Above)

Since the 1940s, Sandia has provided engineering and science expertise to protect the nation against foreign military threats. Now, national security is facing a new range of threats, from foreign states to rogue groups within the nation. At the same time, the United States is becoming increasingly dependent on a complex infrastructure, international in scope and vulnerable to this new range of threats. Sandia has capabilities that can improve the surety (confidence that a system will perform in acceptable ways during normal, abnormal, and malevolent circumstances) of infrastructures critical to the security of the United States. Infrastructure surety is the new national security challenge.

Sandian Rudy Matalucci leads a group that applies surety principles to make buildings safer.

(Below)

Miniature robotic vehicles for sensor deployment make possible multiple vehicle mapping of radioactive, chemical, biological, and other characteristics. These integrated technologies provide intelligent miniature systems for DOE and DoD applications.

Sandian Tom Weber examines a self-contained 0.5-cubic-inch robotic vehicle.

Abstract

This report summarizes progress from the Laboratory Directed Research and Development (LDRD) program during fiscal year 1998. In addition to a programmatic and financial overview, the report includes progress reports from 230 individual R&D projects in 12 categories.

This work was supported by the United States Department of Energy under Contract DE-AC04-94-AL85000.

Sandia is a multiprogram laboratory operated by Sandia Corporation, a Lockheed Martin Company, for the United States Department of Energy.

SAND 99-0358

LDRD Annual Report Staff:
Laboratory Directed Research & Development (LDRD) Program Manager: Chuck Meyers, Sandia National Laboratories
Deputy Program Manager: Cynthia Harvey, Sandia National Laboratories
Information Administrator: Donna Chavez, Sandia National Laboratories
Editor, Writer, Page Layout: Carol Whiddon, Technically Write
Researchers: Donna Drayer, Joy Bemesderfer & Carol Whiddon, Technically Write
Designer: Douglas Prout, Technically Write

TECHnically WRITE

1998
LABORATORY DIRECTED RESEARCH AND DEVELOPMENT

THIS PAGE
INTENTIONALLY BLANK

xi "...exceptional service in the national interest."

1 Laboratory Directed Research and Development Program Review

Materials Science & Technology

9 Photonic Bandgap Structures as a Gateway to Nanophotonics

10 Catalytic Membrane Sensors

10 Wide-Bandgap Compound Semiconductors to Enable Novel Semiconductor Devices

12 Ultra-Hard Multilayer Coatings

14 Scanning Probe–Based Processes for Nanometer-Scale Device Fabrication

15 Molecular-Scale Lubricants for Micromachine Applications

16 Surface-Micromachined Flexural Plate-Wave Device Integrated on Silicon

17 Smart Interface Bonding Alloys (SIBA): Tailoring Thin-Film Mechanical Properties

18 Molecular-to-Continuum Fracture Analysis of Thermoset Polymer/Solid Interfaces

19 Monolithic Structures for Nanoseparation

20 Recognizing Atoms in Atomically Engineered Nanostructures: An Interdisciplinary Approach

21 Fundamental Aspects of Micromachine Reliability

22 Atomic-Level Studies of Surfactant-Directed Materials Growth

24 Enabling Science and Technology for Cold-Spray Direct Fabrication

25 Freeforming of Ceramics and Composites from Colloidal Slurries

26 Intelligent Polymers for Nanodevice Performance Control

26 Quantum Dot Arrays

27 Laser-Assisted Arc Welding for Aluminum Alloys

28 Reactivity of Metal-Oxide Surfaces

29 Exploiting LENS Technology Through Novel Materials

Computer Sciences

33 Gradient-Driven Diffusion of Multi-Atom Molecules Through Macromolecules and Membranes

34 Parallel Quantum Chemistry for Material Aging and Synthesis

34 Modeling Complex Turbulent Chemically Reacting Flows on Massively Parallel Supercomputers

35 Automated Geometric Model Builder Using Range Image Sensor Data

36 A Massively Parallel Sparse Eigensolver for Structural Dynamics Finite Element

36 Density-Functional Theory for Classical Fluids at Complex Interfaces

38 Fast and Easy Parallel I/O for Efficient Scientific Computing

38 Novel Load-Balancing for Scalable, Parallel Electromagnetic and Plasma Physics Simulation Software

40 Parallel Computational Chemistry Using Constraints

40 Massively Parallel *Ab Initio* Validation for ASCI Materials Aging

41 Integrated Quantum/Classical Modeling of Hydrogenic Materials

42 Computational Methods for Coupling Microstructural and Micromechanical Materials Response Simulations

43 From Atom-Picoseconds to Centimeter-Years in Simulation and Experiment

44 An Investigation of Wavelet Bases for Multiscale, Grid–Based Simulation

45 The Next Generation of Teraflop Density-Functional Electronic Structure Codes

46 Methodology for Characterizing Modeling and Discretization Uncertainties in Computational Simulation

47 Emergent Behavior of Large Swarms of Intelligent Agents

48 Global Optimization for Engineering Science Problems

49 Dynamic Simulation of Mechanical Systems with Intermittent Contacts

50 Parallel Combinatorial Optimization for Scheduling Problems

50 Programming Paradigms for Massively Parallel Computers

51 Multilevel Techniques for Unstructured Grid Problems on Massively Parallel Computers

52 Scalable Tools for Massively Parallel Distributed Computing

52 Massively Parallel Methods for Simulating the Phase Field Model

53 Visual Explanation and Insight

Electronics & Photonics

57 Advanced Concepts for High-Power VCSELs and VCSEL Arrays

58 Wafer Fusion for Integration of Semiconductor Materials and Devices

58 Highly Parallel, Low-Power, Photonic Interconnects for Inter-Board Signal Distribution

59 Virtual Reactor for the Semiconductor Manufacturing Plant of the Future

60 Selective Oxidation Technology and Its Applications Toward Electronic and Optoelectronic Devices

61 Agile Prototyping of Microelectromechanical Systems (MEMS)

62 Midwave-Infrared (2–6 µm) Emitter–Based Chemical Sensor Systems

62 A Novel Nondestructive Silicon-on-Insulator Nonvolatile Memory

64 Integration of Optoelectronics and MEMS by Free-Space Microoptics

65 Advanced Laser Structures for Short-Pulsed Power in Active Optical Sensor Systems

66 Metal Micro-Heat-Pipe Substrates for High-Power-Density Electronics

66 Vacuum Encapsulation of MEMS Structures

67 Massively Parallel Sensor Arrays for Volatile Organic Detection

68 Integration of Microsensor Technology into a Miniature Robotic Vehicle

68 Precision-Formed Micromagnets

70 Agile Dry Etching of Compound Semiconductors for Science–Based Manufacturing Using *In Situ* Process Control

70 Time-Resolved Ion-Beam–Induced Charge-Collection (TRIBICC) Imaging

71 Compliant Substrates for Epitaxial Integration of Dissimilar Materials

72 Double Quantum-Well Long-Wavelength Opto-electronic Devices

73 Role of Defects in III-Nitride–Based Electronics

74 Composite-Resonator Surface-Emitting Lasers

74 Ultra–Low-Power Sensors for Microtelemetry Systems

75 The Development of Integrated Chemical Microsensors in GaAs

76 Monolithic Integration of VCSELs and Detectors for Microsystems

77 AlGaN Materials Engineering for Integrated Multifunction Systems

78 Post-Processed Integrated Microsystems

Phenomenological Modeling & Engineering Simulation

81 Enhanced Vapor-Phase Diffusion in Porous Media

82 Stress Evaluation and Model Validation Using Laser Ultrasonics

83 Using Higher-Order Gradients to Modeling Localization Phenomena

84 Altered Simulation Properties for Tetrahedral Finite Elements for Use in Engineering Simulation

84 Development, Implementation, and Experimental Validation of the Lattice Boltzmann Method for Modeling Three-Dimensional Complex Flows

86 Capturing Recrystallization of Metals with a Multiscale Material Model

88 Nondeterministic Modeling in Engineering Science

88 Lagrangian Modeling of Radiative Transport

89 High-Resolution Modeling of Multiscale Transient Phenomena in Turbulent Boundary Layers

90 Dispersive Measurements of Velocity in Heterogeneous Materials

90 A Physically–Based Computational Method for Predicting Generalized Fracture

91 Micromechanical Failure Analyses for Finite-Element Polymer Modeling

92 Development of *In Situ* Diagnostics for Simultaneous Measurement of Transient Gas Species and Soot in Large Fires

93 A Phenomenological Model for Multi-component Transport with Electrochemical Reactions in Concentrated Solutions

94 Methodology Optimal Selection of Test and Simulation Levels for Problems Involving Computational Simulation

Manufacturing Science & Technology

97 Ultra-Precise Assembly of Microelectro-mechanical Systems (MEMS)

98 Laser-Spray Fabrication for Net-Shape Rapid Product Realization

99 Solution Synthesis and Processing of PZT Materials for Neutron-Generator Applications

100 Finite-Element Meshing Approached as a Global Minimization Process

100 Investigation of the Impact of Cleaning on Adhesive Bond and the Process Implications

102 Application of Parallel Mechanism Technology to Manufacturing

102 Standard Cells for Microelectromechanical Systems (MEMS)

103 Scripting for Video Inspection

104 Laser Wire Deposition for Fully Dense Shapes

105 High-Throughput Dry Processes for Large-Area Devices

106 Assuring High Reliability and Production Readiness in Low-Volume Manufacturing

106 Advanced Machining Processes for Microfabrication

107 Fusion of Product and Process Data Using Real-Time Streaming Visualization

108 Advanced Production Planning Models

Life-Cycle Systems Engineering

111 Enabling Human Skills with Cooperative Automation

112 Automatic Generation of Multimedia Documentation for Assembly Operations

113 Distributed Life-Cycle Models in Enterprise Simulations to Answer System Questions

114 Immersive CAD

114 Automatic Planning of Life-Cycle Assembly Processes

116 Analysis of Very Large Assemblies

116 Cloud To CAD

117 Feature Reduction of Geometric Solid Models for Analysis Tools

118 Ergonomics in Life-Cycle Assembly Processes

119 System Surety Life-Cycle Engineering

Information Systems

123 Content–Based Search of Geometric Databases

123 Mission Surety for Large-Scale Real-Time Information Systems

124 Integrated Service Provisioning in an “IPv6 over ATM” Research Network

125 Virtual Desktop Engineering with Integrated Multimedia Data

126 Scaled ATM End-to-End Encryption

126 Ten-to-One-Hundred-Gigabit/Second Network Enabling R&D

128 Network Surety Modeling for Wireless ATM Networks

129 Algorithm–Based Fault Tolerance on Heterogeneous Massively Parallel Computers

130 High-Performance Commodity Interconnects for Clustered Scientific and Engineering Computing

130 Low-Power, Reduced-Computation, Public-Key Protocols

131 AVATAR—Navigating and Mining in Massive Data

Precision Sensing & Analysis

135 Sampling and Sensing Systems for High-Priority Analytes

136 Electrokinetic Immunoaffinity Chemical Sensors

136 Information-Efficient Spectral Imaging System (ISIS)

137 Imaging of Moving Targets Using Simultaneous Synthetic Aperture Radar (SAR) and Moving Target Indicator (MTI) Radar

138 Automated Vegetation Height Measurement for Automatic Terrain Mapping

138 Sparse Geophysical Networks for Monitoring Deep Targets

139 Miniature Bioaerosol Concentrator

140 Recognizing Partially Obscured Targets by Combining Multiple Data Sources Using Evidential Reasoning

141 Computational Engineering of Sensor Materials and Integration with a Novel Biological Weapon Detection System

142 Biological Weapon Detector Using Bioaffinity Array Impedance Analysis with Chemical Amplification Through Redox Recycling

142 ATR / Exploitation Utilizing Ultra–High-Resolution, Complex SAR Imaging

Environmental Sciences

147 Designed Molecular Recognition Materials for Chiral Sensors, Separations, and Catalytic Materials

148 Rapid Screening of Complex Chemical Samples Via Capillary Array Analysis

148 Designed Synthesis of Controlled Degradative Materials

149 Adaptive 3-D Sensing

150 Mechanistic Models for Radionuclide Desorption from Soils

150 Development of Innovative Combustion Processes for a Direct-Injection Diesel Engine

152 Hydrogen Production for Fuel Cells by Selective Dehydrogenation of Alkanes in Catalytic Membrane Reactors

153 Hybrid Vehicle Engine Development

154 Aqueous Organic Sensor

154 Designed Ionophores for Liquid-Membrane Separation and Extraction of Metal Ions

156 An Electromagnetic Imaging System for Environmental Site Reconnaissance

Risk & Reliability

159 Integrated Approach to Develop Microelectro-mechanical (MEMS) Reliability Tools

160 Reliability Degradation Due to Stockpile Aging

160 Precursors to Failure of Oxides and Metal Lines in CMOS Technology

162 An Extensible Object-Oriented Framework for Risk and Reliability Analysis

162 Simulation/Optimization Tools for System Variability Analysis

164 A Massively Parallel Microsimulation Model of Infrastructure Interdependency

165 Reliability Predictions for Advanced Electronics in Smoke Environments

166 Physical Models for Predicting the Effect of Atmospheric Corrosion on Microelectronic Reliability

167 Backside Localization of Open and Shorted IC (Integrated Circuits) Interconnections

168 Security of Bulk Power Systems

National Grand Challenges

171 Science on the Microdomain

171 Cooperative, Distributed Sensing and Action Using Microminiature, Intelligent Agents

172 Autonomous MicroChem Laboratory (µChemLab)

Initiatives

177 Computational Methods for Predicting the Response of Critical As-Built Infrastructure to Dynamic Loads (Architectural Surety)

178 Background Radiation Anisotropy Measurement Sensor (BRAMS)

178 Exploitation of Satellite Communications Systems and Networks for Intelligence Applications

179 Microcode Evaluation

179 Real-Time Image Analysis Using Field-Programmable Gate Arrays

180 Advanced 3-D Sensing and Visualization System for Unattended Monitoring

180 System-of-Labs Direct Fabrication Technology

182 Poco Switch Tubes

182 Chemiresistors Based on Metal-Loaded Polymers for Solvent Spill Detection

183 Advanced Neutron-Tube Design and Producibility

183 Surface Hardening by Nanoparticle Precipitation and Atomic Clustering in Ni(Al,O)

184 Dynamical Properties of Polymers: Computational Modeling

184 Calculation and Interpretation of the Energies that Underlie Transition-Metal Surface Structure

185 Interfacial Reactions in Ceramic Systems

186 Direct Fabrication of Multifunctional Nanocomposites Via Supramolecular Self-Assembly

187 Biophotonic Materials for Optical Encryption and Noncomputing

188 Broadening Mechanism in 2-D Excitonic and Electron Gases

188 Low-Stress Amorphous Diamond: A New Material for Sensors

189 Nanoengineered Cu-Al Defects in Al: A Prototype System for Corrosion

190 Novel Energy-Conversion Devices of Icosahedral Borides

191 Ion-Mobility Spectroscopy of Biological Materials

191 Direct Fabrication of Planar Solid-Oxide Fuel Cells

192 Visualization Tools for MEMS Designs in a Virtual 3-D World

192 Micromachining with Ultra-Short Pulsewidth Lasers

193 Molecular Characterization of Energetic Material Initiation

194 Engineering Complex Distributed Systems

196 Global Approaches to Infrastructural Analysis (GAIA)

196 Chemical Feedstocks for the Future: Oxidative Dehydrogenation

198 Laser Communication Nanosatellites

199 Accelerator Technologies for Emerging Threats

200 Collection and Data Synthesis of Atmospheric Explosion Ground Truth for Global Monitoring Systems

201 Advanced Radiation Sources: Rayleigh-Taylor Mitigation Via Perturbation Reduction

201 Microfluidic Engineering

202 InGaAsN: A Novel Material for High-Efficiency Solar Cells and Advanced Photonic Devices

203 Technologies for Countering C/B Terrorism

204 Technologies for System-Level Innovations in Ballistic Missile Defense

205 Aerosol Stand-Off Detection Test-Bed

206 Design and Optimization of High-Power Electromagnetic Source Systems and Engagement Scenarios for Achieving Functional Upset or Damage in Specific Target Electronic Systems

207 Real-Time Design of Improved Powder Pressing Dies Using Finite-Element Method Modeling

208 Development of Fiber-Laser–Based LIF for Detection of SO_2

209 Penetration and Defeat of Hardened Underground Facilities Using a Microhole Drilling Robot

210 IFSAR Tree Phenomenology and Coherence Normalization

210 Electric Launcher for Defense Applications

211 Power-Grid Reliability and Restructuring Policy Changes

212 SAM Telemetry for Measurements While Drilling

212 Advanced Geosphere Transport Simulation

214 Design-for-Manufacturability Applied to Photovoltaic Modules

214 Low-Work-Function Thermionic Emission Materials

216 LIGA Micromachining

216 Applied Microfluidics Science

218 Computational Simulations of Self-Assembling Macro-Systems by Direct Fabrication of Microscopic Structured Materials

218 Self-Stabilizing Optical Solitons and High-Intensity Laser Plasma Channels for Diffraction-Free Propagation and Robust Power Compression

220 Optical Communication System for Remote Monitoring and Adaptive Control of Distributed Ground Sensors Exhibiting Collective Intelligence

222 Low-Cost Cadmium Zinc Telluride Radiation Detectors Based on Electron-Transport-Only Designs

222 Novel Materials for Hydrogen Storage

223 Inversion of Passive Electromagnetic Fields to Locate Weapons of Mass Destruction

224 Z-Pinch–Driven Isentropic Compression

225 Covert, Distributed Biosensors for UXO/CW Based on Amplified Immunoassays Conducted in Porous Inorganic Media

226 Semiconductor Filament Lasers

226 Development of Membrane Devices Using AlN and SiC Films

227 Spectral Information Content in Ion-Mobility Spectra for Explosives, Interferants, and Other Negative-Ionizing Chemicals

228 Picosecond Particle Velocity Measurements

228 Particle-Level Modeling of Flows of Concentrated Suspensions

229 Efficient Processing of Materials Microstructures with Intelligent Feature Extraction for Quantitative Stereology

230 Magnetic Field Profile Measurements in Wire-Array Z-Pinches by Faraday Rotation

230 Nondestructive Evaluation of Wind Turbine Blades

231 Very Small Arrays: Designing Self-Assembled Systems of Light-Antennae and Reaction Centers for Artificial Photosynthesis

232 Enzyme-Mediated Electrochemical Redox Polymer Biosensor for V- and G-Type Chemical Weapons

232 Novel Biosensor Fabrication Techniques

233 Enhancing Multilevel Linear Equation Solvers Using Domain Decomposition Strategies

233 Design for 100-Year-Life Prototype

234 *In Situ* and *Ex Situ* Investigations of Lateral Composition

235 Approximate Methods for Computing Eigensolutions Using Automated Multilevel Substructuring

235 Living Tissue Engineering

237 Appendix A: Author's Index

243 Appendix B: Project Number/Title Index

251 Appendix C: Awards/Recognition List

253 Appendix D: Project Performance Measures

265 Appendix E: DOE Critical Technologies

281 Appendix F: Major National Programs

295 Appendix G: Dual-Benefit Areas and Single-Use Categories

"...exceptional service in the national interest."

Science and technology are at the heart of United States industrial competitiveness, national security, energy resources, environmental quality, and leadership in fundamental and applied science.

At Sandia, the Laboratory Directed Research and Development Program provides the knowledge that drives our future. We initiate research and development that spawn the knowledge that revolutionized technology. Areas of emphasis center on our core technical competencies and the major strategic thrusts of Sandia's Institutional Plan. Leading-edge experiments that validate our work are constructed and operated on schedule, within budget, and in a safe and environmentally responsible manner.

Our work continues to produce many scientific and technological breakthroughs that lead to new technologies, markets, and businesses for the nation.

To all those who have contributed so generously of their time and talent, thanks and congratulations for a job well done.

THIS PAGE
INTENTIONALLY BLANK

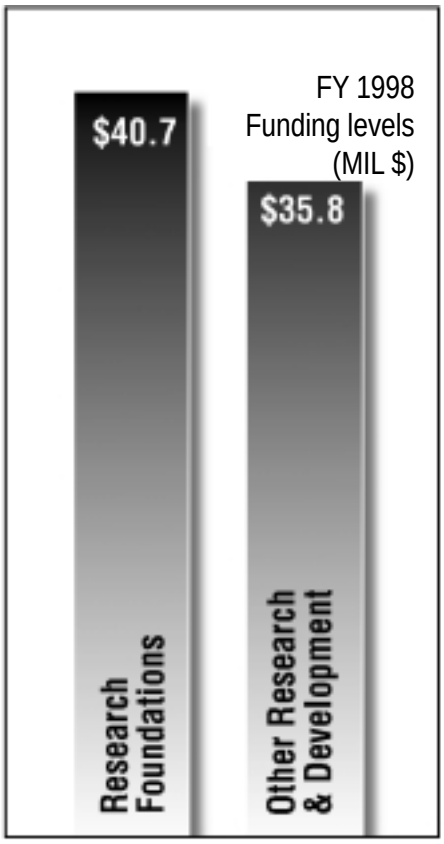

Laboratory Directed Research and Development Program Overview

C. E. Meyers

"Almost every laboratory has found that the most important innovation often comes from the scientists' independent ideas or actions."
The Packard Panel, May 1983, Federal Laboratory Review Panel: Report of the White House Science Council Office of Science and Technology Policy

Strategy

Sandia's value as a national resource is our world-class science, technology, and engineering. These capabilities must remain on the cutting edge because the safety, security, and reliability of U.S. nuclear weapons depend directly on them. Under the guidance of Sandia's Laboratory Director and with the DOE's concurrence, the Laboratory Directed Research and Development (LDRD) Program provides the flexibility to invest in long-term, high-risk, and potentially high-payoff research activities that stretch Sandia's science and technology capabilities.

LDRD supports DOE's missions through Sandia's four primary strategic objectives: nuclear weapons, nonproliferation and materials control, energy and critical infrastructure, and emerging national security threats. To meet these objectives, LDRD promotes creative and innovative research and development by funding initiatives that are inspired by technology needs, often high risk, and that attract exceptional research talent across disciplines.

Authorized by federal law and implemented under DOE Order 413.2, LDRD is Sandia's sole source of discretionary research funds. LDRD is funded by an assessment on all costed work at Sandia. Atomic energy defense activities are supported directly by 67 percent of LDRD projects, although atomic-energy defense activities provide only 48 percent of LDRD annual funding. More than 90 percent of LDRD projects provide benefits in basic and applied research to national security needs.

In FY 1998, LDRD provided $76.5 million to fund 230 projects (selected from 866 submitted). The Sandia LDRD Program was divided into four principal elements: Core Science and Technology Competencies, Systems and Technology Solutions, National Grand Challenges, and Initiatives. Principal elements were further subdivided into areas as follows: **Core Science and Technology Competencies** (Materials Science and Technology, Computer Sciences, Electronics and Photonics, and Phenomenological Modeling and Engineering Simulation), **Systems and Technology Solutions** (Manufacturing Science and Technology, Life-Cycle Systems Engineering,

FY 1998 Selected Statistics

Full-time staff	278
Smallest project	$ 9K
Average project	$ 322K
Average project (FTE)	1.21
Largest project	$ 4.1M
1ST-year projects	116
2ND-year projects	82
3RD-year projects	32

FY 1998 Performance

Refereed publications	407
Other publications	223
Patent disclosures	79
Patent applications	48
Patents	7
Copyrights	12

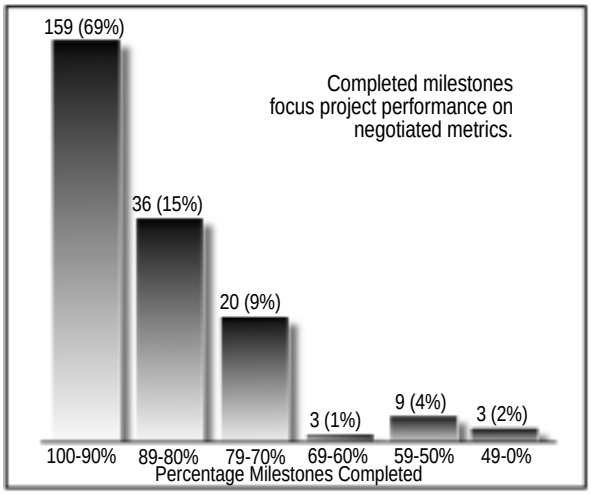

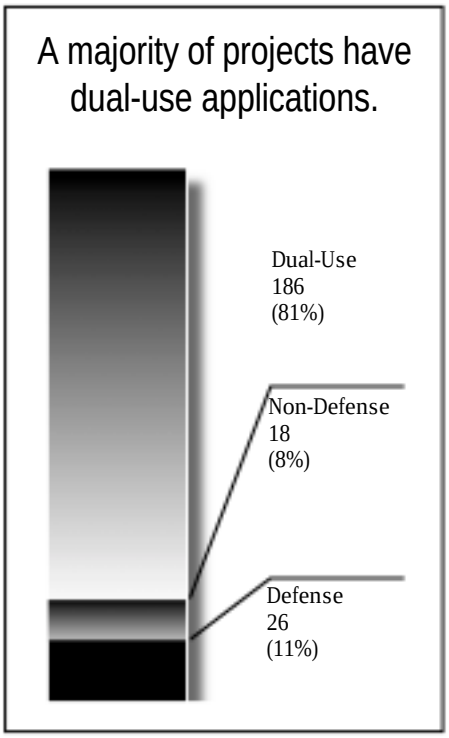

Information Systems, Precision Sensing and Analysis, Environmental Sciences, and Risk and Reliability), **National Grand Challenges**, and **Initiatives**. Investment areas are profiled at the beginning of each section. Each area funded projects that strengthened Sandia's core science and technology base and focused on future DOE and national needs. The projects permitted Sandia staff to explore innovative scientific and technological opportunities that hold high potential for payoff in future applications.

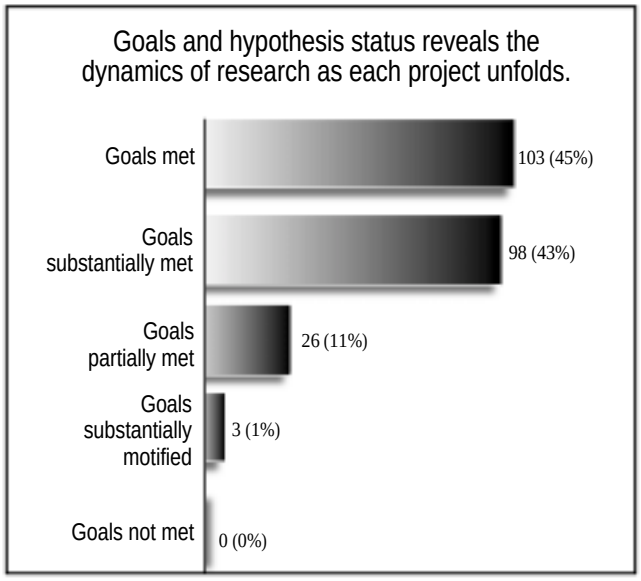

Additional Reading

A comprehensive discussion of DOE and Sandia's LDRD Program management and funding sources may be found in the "Annual Report to Congress on the DOE Laboratory Directed Research and Development Program, FY 1998 LDRD," dated February 1999, and the "Sandia National Laboratories FY 1999–2004 Institutional Plan," dated December 1998.

Achievements

Outcomes are the best measure of achievement for LDRD-funded work. The ultimate measure of success is customer satisfaction with the product.

The achievements described here result from LDRD projects completed during FY 1998 and/or projects that had a major impact on one or more of the Laboratories or DOE's mission areas during the year.

Nuclear Weapons Core Stockpile Stewardship Programs

The United States faces two critical issues that are the focus of Sandia's efforts in nuclear weapons stockpile stewardship. We must maintain confidence in a continuously aging stockpile, and we must reduce and manage the vulnerability of a smaller stockpile to common mode failures. Moreover, we must resolve both issues without underground nuclear testing.

Ceramic Process Selected as Baseline for Neutron-Generator Production

In FY 1996, an LDRD project was initiated to synthesize complex oxide ceramic materials by a new, more controlled process. The focus was on the preparation of a niobium-doped lead zirconate titanate (PZT) because of its wide application in neutron-generator power supplies. The LDRD project ended successfully last September, and subsequent improvements funded by Defense Programs have recently led to selection of this process as a baseline for production of PZT for neutron generators. Additional development work to scale the Sandia process up to the volume required to meet future production needs is under way, with the delivery of the first War Reserve (WR)-qualified material scheduled for late FY 2002.

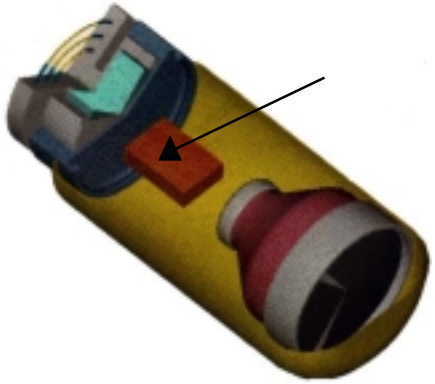

Schematic of an explosively driven neutron generator showing the PZT power supply.

100-Year-Life-Cycle Performance and Modeling

The nuclear weapons stockpile stewardship program requires that the systems and processes that undertake the examination, possible remanufacture, and periodic testing of systems and components continually meet stringent cost and performance standards. As the stockpile moves beyond its initial design life, it is becoming increasingly important that new technology be developed to evaluate performance of the overall weapons complex. Sandia, in collabora-

ration with MIT and other institutions, is working on an LDRD project to develop extended life-cycle enterprise simulation techniques. These techniques are using broad approaches that look at analyzing and understanding the full system capability and performance.

Nuclear Weapons System Components Science and Technology

Chem-Lab-on-a-Chip

Ultimately, the safety and reliability of every nuclear weapon in the stockpile directly reflect the level of perfection with which we discharge our component engineering responsibilities.

Sandia is directing its integrated capabilities in component science toward pioneering developments in advanced miniaturization technologies. A differentiating capability is our expertise in the small, highly integrated, low-power, high-functionality devices known as *integrated microsystems*. Created through integrated circuit fabrication technology, these devices combine diverse functions, potentially ranging from processing electronics and microelectromechanical systems to fabricating sensors and communication devices on a single substrate or in very small multichip modules. We are employing miniature machining, photolithographic semiconductor processes, and silicon micromachining to fabricate research prototypes of these advanced components.

Sandia's explosives-detection portal.

A very complex example of an intelligent, integrated microsystem is the "chem-lab-on-a-chip," which requires the integration of microelectromechanical system actuation devices for pumping microfluids and sensing chemicals, integrated complementary metal-oxide semiconductor electronics for interrogating and interpreting sensors, and communications using either radio frequency or photonic devices based on compound semiconductor technology.

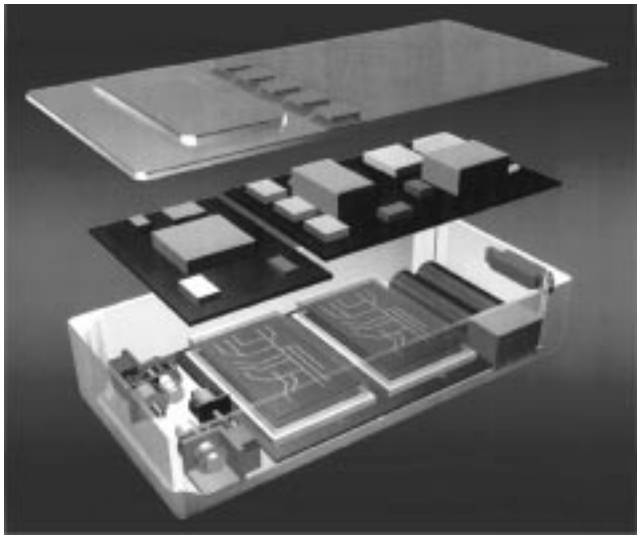

An artist's conception of Sandia's "chem-lab-on-a-chip" shows the push-button controls (top), the encasements for computation and power management (middle), and the analysis system and batteries (bottom).

Energy and Critical Infrastructure

Explosives-Detection Portal

Sandia's explosives-detection portal may help prevent airliner hijackings and bombings. The portal can identify persons who have recently worked with or have been exposed to any of a wide variety of explosives. The portal passes a puff of air over a person, then collects and analyzes the air sample. The detector determines both the type and quantity of even small quantities of explosives and displays this information on a computer screen. The same technology can be adapted to detect narcotics and chemical agents or can be used for environmental monitoring.

Materials and Process Science

Simulation and Experiment for Materials Aging and Synthesis

Stockpile stewardship requires that potential problems in critical materials be identified well before any significant deterioration that might lead to eventual failure occurs. The physical examination of components provides only a limited database and tends to be reactive rather than proactive. Understanding the fundamental science underlying the aging phenomenon is therefore a critical aspect of stewardship. To complete such simulations requires the increasing use of advanced capabilities such as that available in massively parallel architectures. Massively parallel computer simulations offer the promise to predict the aging of materials at levels of detail from atomistic to bulk levels and to enable optimal synthesis of new materials.

Sandia LDRD researchers continue to develop parallel computing codes that efficiently and accurately predict the chain of states of atoms, identify cavities in polymer samples, and render planar shear calculations in metal crystals. These new techniques, when coupled to computational quantum chemistry methods, enhance the ability to treat chemical degradation processes occurring in polymers

and in energetic materials, such as adhesion and corrosion. These results provide scientifically grounded approaches for calibrating the workhorse simulation methods in the weapons program.

New Class of Room-Temperature Gamma-Ray Detectors

Cadmium zinc telluride crystals are being used in a new class of room-temperature gamma-ray detectors. Sandia produced the first detailed characterizations of the properties and performance of these crystals, leading to an explanation of their behavior. Previous radiation detectors could be used only after being cooled to liquid-nitrogen temperatures. The new detectors are smaller and can be left unattended for much longer periods.

Sandia's understanding of cadmium zinc telluride crystals could impact the way nuclear materials are monitored and could accelerate an emerging $1 billion-per-year medical imaging business. *Discover* magazine recognized the Sandia team leader as Innovator of the Year in the Sight category.

Biological Microcavity Laser for Blood Sample Analysis in Minutes

Sandia and the National Institutes of Health patented a hand-held device that analyzes blood samples in minutes rather than in the current time of hours to weeks. The biological microcavity laser can immediately detect sickle-cell anemia and other blood anemias, and may be able to detect tiny changes in cell structure, such as those caused by the AIDS virus. The laser can distinguish between cancerous and noncancerous cells and should allow observers to monitor cancer cell growth and death. The device, based on Sandia's vertical-cavity surface-emitting laser (VCSEL), generates laser light using individual blood cells from a drop of blood in the VCSEL microcavity. The blood cell becomes a light guide that reflects many times through a sample, so deviations in the image created by the blood particle are magnified, greatly increasing the chances of errorless identification. The device eliminates the traditional need to kill or stain blood cells for better visibility. The biological microcavity laser may influence health care by combining the low cost and small size of semiconductors with the high speed and sensitivity of laser microtechnology.

Engineering Sciences

Refrozen-Food Detector

Frozen food that thaws in transit can now be identified by an inexpensive detector placed in the package. Sandia's patented detector changes color when the frozen-food temperature rises above freezing.

Wear-Resistant Diamond Coating

Sandia has developed a simple and inexpensive way to relieve internal stresses of noncrystalline diamond films, a significant advance to produce wear-resistant coating. Crystalline diamond coatings require high temperatures to deposit properly, and they have very rough surfaces. Stress-free coatings are deposited at room temperature and are extremely smooth, which will improve protection and extend lifetimes of tools, auto parts, and plastics (such as those used in biomedical devices). Sandia has applied for a patent.

Microelectronics and Photonics Sciences

Microelectromechanical Systems

Microsystems have the potential to miniaturize weapon functions such as navigation, trajectory sensing, safing, and fusing while increasing reliability and robustness. A Sandia microelectromechanical–based 24-bit countermeshing gear discriminator has been built in the Microelectronics Development Laboratory. We coupled prototype discriminators with custom processing and optical devices from the Compound Semiconductor Research Laboratory to demonstrate optical shuttering and beam steering.

Sandia's technology for integration of microelectromechanical systems and microelectronics has been licensed for commercial production. This technology transfer is important to establishing a commercial source for future integrated microelectromechanical systems applications in navigation, trajectory sensing, and fusing.

Heat-Pipe Substrate to Cool Microelectronic Devices

Sandia developed a high-performance metal heat-pipe substrate (approximately 2 inches square) for microelectronic cooling applications. The design uses embedded microheat pipes to cool components such as microprocessors by transferring large amounts of heat without active fans or pumps. We developed new micromachining processes for manufacturing the device, using photolithographic processes to create patterns on the substrate and electroplating processes to fill the patterns with metal. The devices underwent thermal testing at Sandia to characterize their performance. Sandia is partnering with a microprocessor manufacturer and is considering other applications for the new technology, such as cooling the components of computers, cellular phones, and radar systems.

Semiconductor Filament Lasers

LDRD researchers are creating a new type of high beam-quality semiconductor laser that has the potential to produce over a thousand times more power than that available in conventional semiconductor lasers. Miniature, short-pulse, high-energy lasers are key to direct optical ignition of fuels and explosives, active optical sensors for weapons systems in limited visibility environments, and micromachining micron-size features over large areas. This work significantly advances the understanding of the properties of lasing materials in terms of power, efficiency, reliability and other properties, and so breaks

new ground in defining technologies that will be usable in environments where there is limited available prime power and where a strong laser link may be of high value. This work greatly expands the range of possible applications of semiconductor lasers, particularly in the core national security mission.

Computational and Information Sciences

Asteroid Strike Model Using the Teraflops Supercomputer

Using virtual reality techniques, decades of experience in shock physics, advanced computer programs, and the world's fastest computer, we recently modeled the impact of a 1.4-kilometer asteroid striking the Atlantic Ocean twenty-five miles south of Brooklyn, NY. Sandia's teraflops supercomputer, which performs more than one trillion mathematical operations per second, calculated a three-dimensional (3-D) moving picture of the collision.

The work supports Sandia's DOE mission to develop computer codes that can one day model the extremely complex physics processes that occur during the nuclear weapon blast. In the absence of actual nuclear testing, the DOE and the weapons laboratories are developing increasingly powerful supercomputers and computer codes to simulate the complex 3-D physics involved in nuclear weapon performance and to accurately predict the degradation of nuclear weapon components as they age in the stockpile.

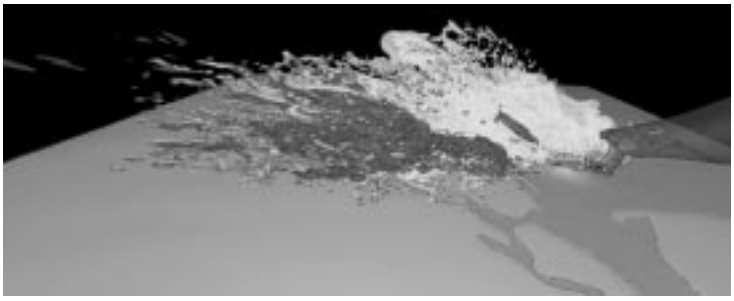

David Crawford sits in front of a computer image generated by Sandia's teraflops supercomputer, which can perform more than one trillion operations per second. This scenario simulates an asteroid 1.4 kilometers in diameter hitting the Atlantic Ocean 25 miles from Brooklyn, NY. The supercomputer is critical in supporting Sandia's stockpile stewardship mission.

THIS PAGE
INTENTIONALLY BLANK

MATERIALS SCIENCE & TECHNOLOGY

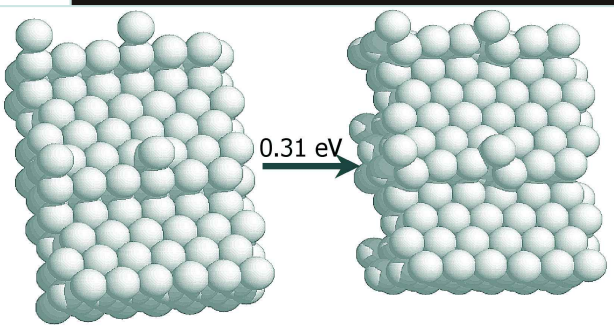

Creating new materials and processes that enhance national security and benefit industry is the objective of the Materials Science and Technology investment area. Projects create materials and products that behave predictably during the fabrication, production, and aging processes. Predictable behavior helps designers choose materials and processes according to the kinds of stress that products must endure. Products range from mechanical, electronic, optic, chemical, and magnetic to "smart" devices that operate on atomic and subatomic levels.

There are three categories of Materials Science and Technology projects: (1) understanding the mechanisms of materials aging to ensure the safety and reliability of the nuclear weapons stockpile, (2) novel materials-processing methods to manufacture high-performance hardware rapidly, affordably, and in low volume with no defects, and (3) nanotechnology projects applying engineering at the atomic scale to develop integrated microsystems.

One such project is working to convert surface impurities from a nuisance to a nanofabrication tool. Common adsorbed atoms acting as "surfactants" can be used to manipulate and direct thin-film growth. The aim is to develop a "surfactant toolkit," a scientifically-based understanding of how foreign atoms modify growth of thin films. This will enable us to produce at will either flat or three-dimensionally nanostructured films on a wide variety of substrates.

This project combines Sandia's special facilities, including the "atom-tracker" scanning-tunneling microscope (AT-STM), low-energy electron microscopy (LEEM), and massively parallel computation (MPC). The project started with model systems, where there is experience in the absence of surfactants, studying surfactant-modified diffusion on and near metal and semiconductor surfaces, and integrating our real-time experimental and advanced computational modeling

A broad rule of physics is that "function is determined by structure." Microscopic measurements from this study indicated the range of potential interactions of surface contaminants, and computational techniques were developed to analyze metal-on-metal atomic-level growth. These conclusions will establish a model for thinking more generally about surfactant-assisted transport near defects.

THIS PAGE
INTENTIONALLY BLANK

3502.040

Photonic Bandgap Structures as a Gateway to Nanophotonics

S. Y. Lin, J. R. Wendt, S. R. Kurtz, G. A. Vawter, E. D. Jones, I. J. Fritz, J. F. Klem, B. E. Hammons, P. L. Gourley, S. K. Lyo

The goal of this project is to explore the fundamental physics of a new class of photonic materials—photonic bandgap (PBG) structures—and to exploit its unique properties for the design and implementation of photonic devices on a nanometer-length scale for the control and confinement of light. The low-loss, highly reflective, and quantum interference nature of a PBG material makes it one of the most promising candidates for realizing an extremely high-Q resonant cavity, > 100,000, for optoelectronic applications and for the exploration of novel photonic physics, such as photonic localization, tunneling, and modification of spontaneous emission rate. Moreover, the PBG concept affords us a new opportunity to design and tailor photonic properties in very much the same way we manipulate, or bandgap-engineer, electronic properties through modern epitaxy.

(1) *Three-dimensional (3-D) silicon (Si) photonic crystal.* Sandia created the first-ever Si 3-D photonic crystal yielding a photonic stop band at infrared (IR) wavelengths. We constructed the crystal in a layer-by-layer fashion from Si using microelectromechanical systems (MEMS) technology. At a thickness equal to only one wavelength of light, 3-D crystal rejects 98% of incident light. Such performance is ten times more effective than the 1-D distributed-feedback mirrors (distributed Bragg reflectors [DBRs]) widely used in vertical-cavity surface-emitting laser (VCSEL) technology. Indeed, a 3-D crystal is equivalent to a 3-D DBR that controls and manipulates light in all three dimensions. Our experimental realization of a Si–based 3-D photonic crystal opens a door for Si photonic crystal devices that is suitable for large-scale integration. Due to its large photonic bandgap, a 3-D photonic crystal can be used as a bandpass filter integratable, for example, to a Si waveguide or a photodetector. By creating a single-mode 3-D defect cavity, a narrowband bandpass filter with an adjustable bandwidth is readily available. Furthermore, with an attenuation constant of 12 dB per unit cell, the 3-D structure is capable of producing a high-quality resonant cavity with a quality factor (Q) exceeding 10,000 and confining light to a fraction of a wavelength. Finally, a 3-D photonic crystal may be utilized to modify and/or suppress the intrinsic thermal emission of a hot object. It will find important applications in the field of IR emissivity engineering and thermal signature recognition.

(2) *Three-dimensional (3-D) single-mode resonant cavity.* We successfully fabricated a 3-D PBG-resonant cavity that is single-mode. This is the smallest 3-D Si Ir (iridium) cavity ever achieved. Combining such a small defect volume with high-Q cavity would enable the realization of truly novel photonic devices such as thresholdless semiconductors and single-mode LEDs. A rather exciting application of this type of cavity is in the development of efficient LEDs from the indirect bandgap Si material. We formed the defect by removing a section of the rods at the fourth layer of the 3-D structure. The defect volume is about 0.2 wavelength cubic, and cavity modal volume is estimated to be one wavelength cubic. A transmission spectrum taken from the cavity sample shows that, indeed, at a proper polarization (transverse electric), we can observe a string resonant transmission within the bandgap.

(3) *Experimental demonstration of guiding and bending of electromagnetic (EM) waves in a photonic crystal.* The efficient guiding and interconnection of light on a chip is important for telecommunication and optical computing applications. Conventional dielectric waveguides can support guided modes along straight lines with high efficiency, yet are restricted by radiation loss to a moderate bending radius. A recent theoretical investigation suggests that photonic crystals hold the key for overcoming this problem.

A linear defect in a photonic crystal can give rise to a band of defect states within the gap and act as a waveguide. Light in the photonic crystal is confined to and guided along the 1-D channel because the gap forbids light from escaping into the bulk crystal. A waveguide bend can then steer light around a sharp 90-degree corner. A simple scattering theory predicts the existence of reflection nodes where 100% transmission efficiency can be achieved through the bend. We demonstrated waveguiding of EM waves by a PBG line defect and, more importantly, observed near-perfect transmission of EM waves around a sharp corner in a photonic crystal. Bending radii were made smaller than one wavelength. We observed an overall high transmission, > 85%, over the entire bandgap regime. More importantly, at two distinct frequencies, we observed 100% transmission. Light at such frequencies travels freely inside the photonic crystal. Such a lossless bending of light would have important application in the field of optical interconnect.

Publications

Refereed

Lin, S. Y., J. G. Fleming, D. L. Hetherington, B. K. Smith, R. Biswas, K. M. Ho, M. M. Sigalas, W. Zubrzycki, S. R. Kurtz, and J. Bur. 1998. "A Three-Dimensional Photonic Crystal Operating at Infrared Wavelengths." *Nature* **394** (16 July): 251.

Lin, S. Y., J. R. Wendt, G. A. Vawter, J. G. Fleming, D. L. Hetherington, B. K. Smith, W. Zubrzycki, K. C. Chow, S. R. Kurtz, P. R. Villeneuve, J. D. Joannopoulos, R. Biswas, K. M. Ho, and M. M. Sigalas. 1998. "Applications of Photonic Crystals in Optoelectronics." *Proc. SPIE* **3419** (9 July): 268.

3502.030

Catalytic Membrane Sensors

T. J. Boyle, R. C. Hughes, C. J. Brinker, A. G. Sault, T. J. Gardner

The goal of this project is to develop a catalytic membrane–based sensor (CMS) with enhanced sensitivity and specificity by modifying a Sandia-developed palladium/nickel (Pd/Ni)–based hydrogen sensor. We accomplished this through overlayers of size-selective gas-separation membranes and an ion-exchangeable titanate catalyst. This report describes in full detail the synthesis and processing of the various overlayers and their effect on the sensor. We designed and synthesized the basic component. Because of the low temperature required to maintain the sensor, we could not determine a suitable catalyst. We began testing new sensors to obtain higher operating temperatures.

We demonstrated the feasibility of synthesizing a CMS component. This involved the development of a process for coating the sensor, synthesis and characterization of the ion-exchanged catalyst precursor (and alternatives), and a process for deposition of the final layer.

Testing the completed CMS device was not feasible for two reasons: (1) the sensor platform could not withstand the high temperatures required to utilize the catalyst efficiently, and (2) the operating temperature of the catalyst could not be lowered sufficiently to maintain a usable sensor platform. We were investigating alternative platforms at the end of the project.

We produced several new concepts and ideas that will prove to be very beneficial for other areas of research. (1) The most promising concept was the use of sol-gel coatings as a protective coating against the poisoning of the sensor surface. We investigated several sol-gel coatings as poison-control agents, and each appeared to prevent poisoning of the surface from H_2S. (2) The coated wafers also displayed an affinity for determining the quantity of O_2 in the presence of H_2 and could potentially be used as an explosive atmosphere sensor. (3) We investigated the use of zirconium (Zr)–based ion-exchanged catalyst in place of the standard titanium-rhodium (Ti-Rh) catalyst; however, due to the low Rh-loading after ion-exchange, we did not pursue these precursors for further development. (4) We also synthesized novel $RhTi_6$ and $ThZr_6$ double alkoxides that omit the ion-exchange step. Unfortunately, the utility of these catalysts as thin films is still ambiguous since the small amount of catalyst led to a small amount of converted material.

We filed a patent application on the basic CMS component and the poison protection ability of the A2** coating.

Publications

Refereed

Boyle, T. J., T. J. Gardner, R. C. Hughes, C. J. Brinker, and A. G. Sault. 1998. "Catalytic Membrane Sensors: A Thin-Film–Modified H_2 Resistive Sensor for Multimolecular Detection." *Comts. on Inorg. Chem.*, accepted.

Gardner, T. J., L. I. McLaughlin, L. R. Evans, and A. K. Datye. 1998. "Preparation and Evaluation of Novel Hydrous Metal Oxide (HMO)-Supported Noble Metal Catalysts." *Studies in Surf. Sci. and Catalysis* **118**: 245.

Hughes, R. C., S. V. Patel, M. W. Jenkins, T. J. Boyle, T. J. Gardner, and C. J. Brinker. 1998. "Thin-Film Porous Membranes Based on Sol-Gel Chemistry for Catalytic Sensors." *Tech. Digest of the 7th Internat. Mtg. on Chem. Sensors* (Beijing, China, 27–30 July): 41.

3502.050

Wide-Bandgap Compound Semiconductors to Enable Novel Semiconductor Devices

M. H. Crawford, A. F. Wright, W. W. Chow, S. R. Lee, E. D. Jones, J. Han

This project is an interdisciplinary investigation into the growth and physical properties of wide-bandgap compound semiconductors for the purpose of enabling both optoelectronic and microelectronic device development. The AlGaInN (aluminum gallium indium nitride) material system is widely considered to be essential to the development of a wide array of ultraviolet (UV) and blue optical devices as well as high-temperature microelectronics. A critical limiting factor in the demonstration of advanced III–N–based devices is the lack of an in-depth understanding of the physics and chemistry that govern the unique properties of these materials. Sandia's work focuses on the investigation of the physical properties of the AlGaInN material system. Analytical investigations include calculations to determine bandstructure and the development of a model for optical gain and lasing, which will include an exact treatment of coulomb effects. We will perform density-functional calculations to evaluate defect levels associated with extended defects (e.g., edge dislocations) in GaN. We will perform steady-state and time-resolved luminescence to evaluate the dominant recombination mechanisms in these materials. We will also perform magnetoluminescence experiments to determine energy dispersion and effective masses, and compare these results directly with bandstructure calculations. A final aspect of our project is an evaluation of how various processing techniques that

are relevant for device fabrication, such as post-growth annealing, reactive ion etching, and implantation, affect the optical and electronic properties of the III–N materials.

We made significant advances in theoretical modeling of Group-III–N materials. We developed a microscopic laser theory for treating bandstructure and many-body coulomb effects in Group-III nitride quantum-well (QW) lasers. We have since furthered this effort by studying the contributions of these many-body effects to the shape and carrier-density dependence of the gain spectrum. We gained predictions for laser behavior of various InGaN QW structures and under different experimental conditions. We used the theory successfully to analyze experimental results. Also, we used these calculations to predict the gain characteristics of GaN/AlGaN QW structures. Our efforts also included a theoretical study of extended defects in Group-III–N materials. We performed density-functional calculations to determine whether there are defect levels associated with the most common type of dislocation (edge-type) in aluminum nitride (AlN) and gallium nitride (GaN). We found that these extended defects do indeed introduce defect levels into the gap. Our results also indicate that the exact defect levels depend on the atomic structure at the core of the dislocation, which, in turn, depends on the background doping level and on the growth conditions. We predict that edge dislocations can become charged in the presence of a background concentration of *n*-type dopants and expect approximately 1.3 electrons per defect site along the dislocation line in moderately doped GaN. In the area of experimental studies, we performed magnetoluminescence experiments to determine the exciton binding energy and reduced mass in GaN thin films. These experiments were performed at the National High Magnetic Field Facility at Los Alamos and employed fields up to 60 Tesla. While we expected to see a shift in the photoluminescence (PL) resonance as a function of applied field, no such shift was seen. As yet, we do not understand our results and have not determined the exciton binding energy and reduced mass in our materials. We expanded time-resolved PL experiments to include GaN/AlGaN QW structures, which are ideal for UV light-emitting diodes (LEDs). We grew various samples with different well widths and with or without silicon (Si) doping in the active region. Our studies showed that for all samples, the measured PL decay time decreased strongly with increasing sample temperature (from 10°–300°K), suggesting that nonradiative recombination is dominating in these samples. Also, we found increased decay times (> 1 ns) at 10°K for wider QWs (> 2 nm), which we believe is due to electron-hole spatial separation resulting from internal piezoelectric fields.

Publications

Refereed

Chow, W. W., H. Amano, J. Han, and T. Takeuchi. 1998. "Theoretical Limit to the Laser Threshold Current Density in an InGaN Quantum-Well Laser." *Appl. Phys. Lett.*, submitted.

Chow, W. W., K. C. Zeng, R. Mair, J. Y. Lin, and H. X. Jiang. 1998. "Carrier-Population Dynamics in Group-III Nitride Quantum-Well Laser Structures." *1998 OSA Tech. Digest Series 6* (Conference on Lasers and Electrooptics, San Francisco, CA, 3–8 May): 282–283.

Chow, W. W., M. H. Crawford, A. Girndt, and S. W. Koch. 1998. "Threshold Conditions for an Ultraviolet Wavelength GaN Quantum-Well Laser." *IEEE J. Selected Topics in Quantum Electron.* **4**: 314–319.

Kim, H. S., J. Y. Lin, H. X. Jiang, W. W. Chow, A. Botchkarev, and H. Morkoc. 1998. "Piezoelectric Effects on the Optical Properties of GaN/AlGaN Multiple Quantum Wells." *Appl. Phys. Lett.*, submitted.

Wright, A. F. 1998. "Theoretical Investigation of an Edge Dislocation in AlN." Paper presented to the 1998 March Meeting of the American Physical Society, Los Angeles, CA, 16–20 March.

Wright, A. F. 1998. "Theoretical Investigation of Edge Dislocations in AlN." Paper presented to the Four Corners American Physical Society Meeting, Albuquerque, NM, 3–4 April.

Wright, A. F. 1998. "Theoretical Investigation of Edge Dislocations in GaN." Paper presented to the 40th Electronic Materials Conference, Charlottesville, VA, 24–26 June.

Wright, A. F., and J. Furthmiller. 1998. "Theoretical Investigation of Edge Dislocations in AlN." *Appl. Phys. Lett.* **72**: 3467.

Zeng, K. C., R. Mair, J. Y. Lin, H. X. Jiang, W. W. Chow, A. Botchkarev, and H. Morkoc. 1998. "Plasma Heating in Highly Excited GaN/AlGaN Multiple Quantum Wells." *Appl. Phys. Lett.*, accepted.

3502.080

Ultra-Hard Multilayer Coatings

T. A. Friedmann, J. A. Knapp, D. M. Follstaedt, M. T. Dugger, N. A. Missert, D. L. Medlin, P. N. Provencio, K. F. McCarty, D. C. Chrzan

Sandia is exploring the production of ceramic multilayer structures that are potentially harder than any natural or artificial material. Diamond and cubic boron nitride (cBN) are the two hardest substances known to man. Numerous proven technologies rely on the superior mechanical properties of these materials. The question arises: Is it possible to manufacture a material that is harder than diamond? In theory, the answer is yes. Experiments indicate that properly grown multilayer coatings of two materials are harder than either of the materials making up the individual layers. The increase in hardness is due mainly to the resistance of dislocation flow across the interfaces between phases of different elasticity. This experimental fact leads to the possibility that a new class of ultra-hard materials—harder than diamond—can be made by growing the appropriate multilayer film. We will establish the state-of-the-art in ultra-hard multilayers by synergistically merging Sandia's capabilities. This work is a combination of growth, analysis, and theoretical modeling capabilities at Sandia that could possibly lead to a revolutionary jump in both materials understanding and performance—a material harder than diamond.

We developed a new multilayer a-tC (amorphous tetrahedral carbon) material that is thick, stress-free, adherent, low friction, and with hardness and stiffness near that of diamond. We deposited the new a-tC material by pulsed-laser deposition (PLD) at room temperature and fully stress-relieved it by a short thermal anneal at 600°C. We built up a thick multilayer by repeated deposition and annealing steps. We measured 88 GPa hardness, 1100 GPa Young's modulus, and 0.1 friction coefficient (under high load). Significantly, these results were all well within the range reported for crystalline diamond. However, this material has important advantages over thin-film diamond; namely, a-tC is smooth, processed at lower temperature, and can be grown on a much broader range of substrates. This breakthrough will enable a host of applications that we are actively pursuing in microelectromechanical systems (MEMs), sensors, LIGA (an acronym for the German words for lithography, electroforming, and molding), etc. In addition, we dramatically improved our cBN films grown by ion-assisted PLD (or IAPLD). We combined x-ray reflectivity, Fourier transform infrared (FTIR), and transmission electron microscopy (TEM) characterization to optimize the IAPLD process to obtain films that have the bulk density of cBN, a columnar cBN grain structure with greatly reduced hBN inclusions, and smooth surfaces. Thus, we are now ready to deposit by PLD multilayers of (arguably) the two hardest substances known to man—stress-relieved a-tC and cBN, due to breakthroughs directly resulting from this project. Additional highlights include development of an electron cyclotron resonance (ECR) ion-assisted sputtering process for B4C that is compatible with our improved cBN deposition process developed earlier. We are using this process to synthesize cBN/B4C multilayers. Also, we vastly improved our finite-element modeling (FEM) techniques to extract yield, elastic stresses, and hardness from nanoindentation curves. Finally, we made progress in modeling dislocation sources and the role they play in pileups as a step toward modeling dislocations in multilayers.

Publications

Refereed

Cardinale, G. F., D. G. Howitt, K. F. McCarty, D. L. Medlin, P. B. Mirkarimi, and N. R. Moody. 1996. "Analysis of Residual Stress in Cubic Boron Nitride Thin Films Using Micromachined Cantilever Beams." *Diamond and Relat. Mater.* **5** (November): 1295–1302.

Cardinale, G. F., D. L. Medlin, P. B. Mirkarimi, K. F. McCarty, and D. G. Howitt. 1997. "Orientation-Dependence of Elastic Strain Energy in Hexagonal and Cubic Boron Nitride Layers in Energetically Deposited BN Films." *J. Vac. Sci. Technol. A-Rapid Commun.* **15** (15 January): 196–200.

Dinardo, N. J., T. W. Mercer, L. J. Martinez-Miranda, M. P. Siegal, T. A. Friedmann, and J. P. Sullivan. 1998. "Analysis and Modification of Amorphous and Partially Crystalline Thin Films." *Proc. Mat. Res. Soc.* **498** (Invited) (May) (Boston, MA, 1–5 December): 67.

Follstaedt, D. M., J. A. Knapp, S. M. Meyers, M. T. Dugger, T. A. Friedmann, J. P. Sullivan, T. Christenson, O. R. Monteiro, J. W. Ager, and I. G. Brown. 1997. "Energetic Particle Synthesis of Metastable Layers for Superior Mechanical Properties." Paper presented to the Fall Meeting of the Materials Research Society (Invited), Boston, MA, 1–5 December.

Friedmann, T. A., J. P. Sullivan, D. R. Tallant, N. A. Missert, J. A. Knapp, D. M Follstaedt, and D. L. Medlin. 1998. "Pulsed-Laser Deposition of Amorphous-Tetrahedral Carbon Film." Paper presented to the Gordon Research Conference on Laser Interactions with Materials, Andover, NH, 7–13 June.

Friedmann, T. A., J. P. Sullivan, J. A. Knapp, D. R. Tallant, D. M. Follstaedt, D. L. Medlin, and P. B. Mirkarimi. 1997. "Thick Stress-Free Amorphous-Tetrahedral Carbon Films with Hardness Near that of Diamond." *Appl. Phys. Lett.* **71** (29 December): 3820–3822.

Friedmann, T. A., J. P. Sullivan, N. A. Missert, D. R. Tallant, J. A. Knapp, D. M. Follstaedt, A. J. Magerkurth, and D. L. Medlin. 1998. "Residual Stress and Hardness in Amorphous Carbon Films Grown by Pulsed-Laser Ablation." Paper presented to the 1998 Fall Meeting of the Materials Research Society (Invited), Boston, MA, 30 November–4 December.

Friedmann, T. A., J. P. Sullivan, N. A. Missert, D. R. Tallant, J. A. Knapp, D. M. Follstaedt, M. P. Siegal, D. L. Medlin, and K. F. McCarty. 1997. "Growth

Properties and Annealing of Amorphous Carbon Films." Paper presented to the Fall Meeting of the Materials Research Society (Invited), Boston, MA, 1–5 December.

Friedmann, T. A., K. F. McCarty, J. C. Barbour, M. P. Siegal, and D. C. Dibble. 1996. "Thermal Stability of Amorphous Carbon Films Grown by Pulsed-Laser Deposition." *Appl. Phys. Lett.* **68** (18 March): 1643–1645.

Friedmann, T. A., N. A. Missert, K. F. McCarty, D. L. Medlin, P. B. Mirkarimi, and P. N. Provencio. 1998. "Ion-Assisted Pulsed-Laser Deposition of Cubic Boron Nitride." Paper presented to the International Conference on Metallurgical Thin Films and Coatings (Invited), San Diego, CA, 27 April–1 May.

Knapp, J. A., D. M. Follstaedt, and T. A. Friedmann. 1998. "Finite-Element Modeling of Nanoindentation for Evaluating Mechanical Properties of Thin Layers." Paper presented to the Spring Meeting of the Materials Research Society, San Francisco, CA, 3–7 April.

Knapp, J. A., D. M. Follstaedt, S. M. Myers, J. C. Barbour, and T. A. Friedmann. 1998. "Finite-Element Modeling of Nanoindentation." *J. Appl. Phys.*, accepted.

Knapp, J. A., D. M. Follstaedt, S. M. Myers, J. C. Barbour, T. A. Friedmann, J. W. Ager, O. R. Monteiro, and I. G. Brown. 1998. "Finite-Element Modeling of Nanoindentation for Evaluating Mechanical Properties of MEMS Materials." *Surf. & Coatings Technol.* **104** (May): 268–275.

Knapp, J. A., D. M. Follstaedt, T. A. Friedmann, A. J. Magerkurth, S. W. Clark, O. R. Monteiro, J. W. Ager, I. G. Brown, B. N. Lucas, and W. C. Oliver. 1997. "Finite-Element Modeling of Nanoindentation for Evaluating Mechanical Properties of Thin Diamond-Like Carbon Layers." Paper presented to the Fall Meeting of the Materials Research Society, Boston, MA, 1–5 December.

Knapp, J. A., D. M. Follstaedt, T. A. Friedmann, A. J. Magerkurth, S. W. Clark, O. R. Monteiro (LBNL), J. W. Ager, III (LBNL), I. G. Brown (LBNL), B. N. Lucas, and W. C. Oliver (Nano Instruments, Inc.). 1998. "Finite-Element Modeling of Nanoindentation for Evaluating Mechanical Properties of Diamond-Like Carbon Films." *Appl. Phys. Lett.*, submitted.

Martinez-Miranda, L. J., J. P. Sullivan, T. A. Friedmann, M. P. Siegal, and N. J. Dinardo. 1997. "Structural Characterization of the Thermal Evolution of Tetrahedrally Coordinated Amorphous Carbon Films." *Proc. Mat. Res. Soc.* **498** (May) (Boston, MA, 1–5 December): 55.

McCarty, K. F., and D. L. Medlin. 1997. "How Plastic Deformation Can Produce Texture in Graphitic Films of Boron Nitride, Carbon Nitride, and Carbon." *Diamond and Relat. Mater.* **6** (May): 1219–1225.

McCarty, K. F., D. L. Medlin, P. B. Mirkarimi, and G. F. Cardinale. 1996. "How Nucleation and Growth Mechanisms Control Microstructural Evolution in Cubic Boron Nitride Films." Paper presented to the Materials Research Society Meeting, Boston, MA, 2–6 December.

McCarty, K. F., P. B. Mirkarimi, D. L. Medlin, T. A. Friedmann, and J. C. Barbour. 1996. "On the Low-Temperature Threshold for Cubic Boron Nitride Formation in Energetic Film Deposition." *Diamond and Relat. Mater.* **5** (December): 1519–1526.

Medlin, D. L., P. B. Mirkarimi, G. F. Cardinale, and K. F. McCarty. 1996. "Microstructural Development in Cubic Boron Nitride Thin Films." Paper presented to the 43rd National Symposium of the American Vacuum Society (Invited), Philadelphia, PA, 14–18 October.

Medlin, D. L., P. B. Mirkarimi, G. F. Cardinale, and K. F. McCarty. 1997. "Microstructure and Texture Development in Cubic Boron Nitride Thin Films." Paper presented to the TMS 1997 Meeting, Orlando, FL, 9–13 February.

Medlin, D. L., P. B. Mirkarimi, T. A. Friedmann, G. F. Cardinale, and K. F. McCarty. 1998. "Origins of Crystallographic Texture in Cubic Boron Nitride Thin Films." Paper presented to the Fall Meeting of the Materials Research Society, Boston, MA, 27 November–1 December.

Mirkarimi, P. B., D. L. Medlin, K. F. McCarty, D. C. Dibble, W. M. Clift, J. A. Knapp, and J. C. Barbour. 1997. "The Synthesis, Characterization, and Mechanical Properties of Thick, Ultrahard Cubic Boron Nitride Films Deposited by Ion-Assisted Sputtering." *J. Appl. Phys.* **82** (15 August): 1617–1625.

Mirkarimi, P. B., K. F. McCarty, and D. L. Medlin. 1997. "Review of Advances in Cubic Boron Nitride Synthesis." *Mater. Sci. Engin. Reports* **21** (15 December): 47–100.

Mirkarimi, P. B., K. F. McCarty, D. L. Medlin, N. R. Moody, and D. C. Dibble. 1996. "Synthesis and Mechanical Characterization of Very Hard Cubic BN–Based Films Deposited by Ion-Assisted Sputtering." Paper presented to the Materials Research Society Meeting, Boston, MA, 2–6 December.

Mirkarimi, P. B., K. F. McCarty, G. F. Cardinale, D. L. Medlin, D. K. Ottesen, and H. A. Johnsen. 1998. "Substrate Effects in Cubic Boron Nitride Film Formation." *J. Vac. Sci. and Technol. A* **14** (January–February): 251–255.

Missert, N. A., T. A. Friedmann, J. P. Sullivan, and R. G. Copeland. 1997. "Characterization of Electron-Emission from Planar Amorphous-Carbon Thin-Films Using *In Situ* Scanning Electron Microscopy." *Appl. Phys. Lett.* **70** (14 April): 1995–1997.

Missert, N. A., T. A. Friedmann, J. P. Sullivan, and R. G. Copeland. 1997. "Evolution of the Electron Emission Characteristics from Amorphous Carbon Thin Films Upon Annealing." Paper presented to the Fall Meeting of the Materials Research Society, Boston, MA, 1–5 December.

Missert, N. A., T. A. Friedmann, P. P. Newcomer, P. B. Mirkarimi, K. F. McCarty, and D. L. Medlin. 1996. "X-Ray Reflectivity Studies of the Density and Thickness of BN Thin Films." Paper presented to the Materials Research Society Meeting, Boston, MA, 2–6 December.

Siegal, M. P., J. C. Barbour, P. N. Provencio, D. R. Tallant, and T. A. Friedman. 1998. "Amorphous-Tetrahedral Diamond-Like Carbon Layered Structures Resulting from Film Growth Energetics." *Appl. Phys. Lett.* **73** (10 August): 759–761.

Sullivan, J. P., T. A. Friedmann, and A. G. Baca. 1997. "Stress Relaxation and Thermal Evolution of Film Properties in Amorphous Carbon." *J. Elect. Mater.* **26** (September): 1021–1029.

Sullivan, J. P., T. A. Friedmann, N. A. Missert, P. A. Schultz, M. P. Siegal, and E. B. Stechel. 1998. "The Electronic Transport Mechanism in Amorphous Tetrahedrally-Coordinated Carbon Films Deduced from Combined Transport and Stress Relaxation Measurements." *Proc. 1st Internat. Specialist Mtg. on Amorphous Carbon '97* **1** (February) (Cambridge, UK, 31 July–1 August): 320.

Sullivan, J. P., T. A. Friedmann, R. G. Dunn, E. B. Stechel, P. A. Schultz, and N. A. Missert. 1997. "The Electronic Transport Mechanism in Amorphous Tetrahedrally Coordinated Carbon Films." *Proc. Mat. Res. Soc.* **498** (May) (Boston, MA, 1–5 December): 97.

Tallant, D. R., T. A. Friedmann, N. A. Missert, M. P. Siegal, and J. P. Sullivan. 1997. "Raman Spectroscopy of Amorphous Carbon." *Proc. Mat. Res. Soc.* **498** (May) (Boston, MA, 1–5 December): 37.

3502.090

Scanning Probe–Based Processes for Nanometer-Scale Device Fabrication

T. M. Mayer, B. S. Swartzentruber, S. A. Casalnuovo, A. J. Ricco

Development of nanometer-scale technologies requires a novel physics base that includes fabrication processes, characterization techniques, and materials properties allowing reliable performance of devices at this very small length scale. This project will expand Sandia's expertise in scanning probe–based fabrication and characterization of nanostructures. Our objective is to achieve an order-of-magnitude decrease in feature size compared to conventional fabrication technology. This order-of-magnitude jump in our ability to make small structures opens new areas of fundamental physics research on the properties of mesoscopic structures and enables new types of electronic and sensing devices with enhanced functionality, speed, and reliability. We are exploring approaches to nanostructure fabrication and characterization using scanning probe–based scanning-tunneling microscopy (STM) and atomic force microscopy (AFM). We also are developing numerical simulations of localized electric-field and emission current to explore mechanisms and characterize limits to processing techniques. We will emphasize novel fabrication processes and characterization of physical, chemical, and electronic effects in nanostructures. We will integrate critical nanoscale components with conventional test structures to allow full electrical accessibility. We will investigate molecular layer resists based on simple adsorbed atoms and molecules that can be patterned by electron-induced desorption or reaction. We also are developing direct-write fabrication processes for nanoscale fabrication using electric fields and the low-energy electron flux from an STM to directly induce deposition processes leading to nanostructure formation. We will perform electrical measurements of nanometer-scale structures to investigate the effect of material structure on these small length scales on electronic properties. We will evaluate novel, high-sensitivity, chemical-sensor prototypes based on alteration of electrical properties of nanowires by adsorption or absorption of gases.

We investigated contrasting surface modification of Au(111) (gold) surfaces in the presence of high electric fields, characteristic of the fields that exist under a scanning probe tip. We observed dramatic surface distortions when a 200 nm tip, biased at -100 V, is brought toward the Au surface, then retracted. Other experiments maintain a constant high-field and field-emission current. STM images, taken after each procedure, show that high electric field causes step retraction, vacancy island formation, and disappearance of small islands beneath the tip. Very high fields result in unstable bump formation beneath the tip. We adapted our nanofabrication simulation code to explore effects of electric fields, mechanical forces, and emission current-induced heating on surface modification processes in scanning probes. We showed that for a tungsten (W) tip interacting with a Au surface, surface diffusion of Au atoms in a lateral electric-field gradient is responsible for formation of nanometer-scale bumps on the Au surface, in agreement with experiments at high field. This work suggests another practical method for controlled fabrication of nanoscale structures.

Publications

Refereed

Cabibil, H., J. E. Houston, T. M. Mayer, and G. E. Franklin. 1998. "Electric Field Effects on the Nanometer-Level Surface Modification of Au(111) Surfaces." *Proc. Mater. Res. Soc.* (San Francisco, CA, 15 April).

Mayer, T. M., J. E. Houston, G. E. Franklin, and T. A. Michalske. 1997. "Electric Field and Emission Current-Induced Surface Modification of Au in the Interfacial Force Microscope." Paper presented to the American Vacuum Society, San Jose, CA, 23 October.

Other

Mayer, T. M. 1998. "Making Things Small, Really Small, with the STM." Presentation to Northern Arizona University, Flagstaff, AZ, 23 September.

3502.110

Molecular-Scale Lubricants for Micromachine Applications

A. R. Burns, T. A. Michalske, T. M. Mayer, J. J. Sniegowski, P. J. McWhorter, M. J. Stevens, S. L. Miller, M. T. Dugger, J. E. Houston

The goal of this work is to develop the physics and chemistry base for designing and understanding molecular-scale lubricants for the reduction of friction- and adhesion-induced failure in silicon (Si) micromachines or microelectromechanical systems (MEMS). Sandia acquired this new knowledge by tailoring the molecular properties of lubricants, applying local probes that can directly monitor the response of lubricants in contact conditions, and evaluating the performance of model lubricants in MEMS devices.

Model lubricants under investigation are the silane coupling agents that form monolayer films on native oxide Si surfaces, which is the substrate in MEMS. These molecules bind via strong surface bonds and produce a layer of hydrocarbon or fluorocarbon chains normal to the substrate. Tailoring the lubricants entails modifying the chain length, the chain chemical reactivity (H [hydrogen] or F [fluorine]), and the density of chain structures. Thus understanding the surface chemistry of silane-silicon oxide coupling is critical. With proximal probes such as atomic force microscopy (AFM), interfacial force microscopy (IFM), and scanning near-field optical microscopy (SNOM), we examined the frictional and adhesive properties of the silane films with very high spatial resolution (< 100 nm) and sensitivity. We treated MEMS structures with silanes under identical conditions and examined them for friction and adhesion under operating conditions. Proper assessment of the lubricants requires quantitative analysis of MEMS performance at high speeds and long operating times. Our proximal probe measurements and MEMS performance analyses form a very important link for molecular dynamics (MD) simulations that, in turn, should be able to predict MEMS performance under all conditions.

We examined friction at the molecular level with a novel scanning probe microscope that observes simultaneously the onset of energy dissipation and attractive forces. We monitored friction by measuring the damped vibrational amplitude of an oscillating probe tip, analogous to shear-force feedback commonly used in SNOMs. We used a mechanically stable interfacial force sensor to measure normal forces at the tip independently and decoupled it from the lateral forces, thus allowing us to observe friction from the early stages of the purely attractive regime to the latter stage of repulsive compression. Measurements on model lubricant silane monolayers indicated that friction dramatically increases with the strength of attractive interactions between the tip and the monolayers. These interactions resulted in significant energy losses due to the tensile deformation of the lubricant chains, collective chain motion, and dissipative bond breaking.

Cross-polymerization in silane self-assembled monolayers (SAMs) was thought to be an essential ingredient of their stability. We used MD simulations to show that cross-polymerization cannot occur due to steric effects. Thus, to form dense, fully covered monolayers, cross-polymerization must be avoided. The structure of the headgroup plays a limiting role in possible monolayer structures. To satisfy the steric constraints, the aliphatic tails must form a herringbone structure.

Silane treatment of MEMS devices continues to produce mixed results, although the overall yield and performance of operating structures improve with silane treatment. Fluorinated silanes are more effective than protonated silanes. The trend is reversed in scanning probe studies here and elsewhere. The fundamental reasons for the latter are not understood and require further investigation.

Publications

Refereed

Burns, A. R., J. E. Houston, R. W. Carpick, and T. A. Michalske. 1998. "Acid-Base Interactions at the Molecular Level: Scanning Probe Studies." *J. Adhesion Sci. Technol.*, submitted.

Burns, A. R., J. E. Houston, R. W. Carpick, and T. A. Michalske. 1998. "Friction and Molecular Deformation in the Attractive Regime." *Phys. Rev. Lett.*, submitted.

Burns, A. R., J. E. Houston, R. W. Carpick, and T. A. Michalske. 1998. "Molecular-Level Friction as Revealed with Novel Scanning Probe." *Langmuir*, submitted.

Kiely, J. D., and J. E. Houston. 1998. "Contact Hysteresis and Friction of Alkanethiol SAMs on Au." *Langmuir*, submitted.

Stevens, M. 1998. "Thoughts on the Structure of Alkylsilane Monolayers." *Langmuir*, submitted.

3502.120

Surface-Micromachined Flexural Plate-Wave Device Integrated on Silicon

B. A. Tuttle, J. H. Smith, D. B. Dimos, W. K. Schubert, J. A. Ruffner

Small, reliable chemical sensors are needed for a wide range of applications, such as weapons state-of-health monitoring, nonproliferation activities, and manufacturing emission monitoring. Advantages of a flexural plate-wave (FPW) architecture for these sensors include improved sensitivity, reduction in operating frequency to be compatible with standard digital microelectronics, and sensing in liquid media. Fabrication of these miniaturized, high-reliability devices requires successful execution and integration of three technologies: acoustic sensor design, silicon (Si) surface micromachining, and high-quality piezoelectric thin-film deposition. Sandia determined the effects of deposition parameters in obtaining reasonable piezoelectric output from aluminum nitride (AlN) films and developed a novel procedure for integrating lead zirconate titanate (PZT) thin films with silicon nitride (SiN)-membraned devices.

We fabricated both surface acoustic-wave (SAW) and FPW PZT piezoelectric thin-film devices. We fabricated PZT SAW devices on both $LaAlO_3$ and Si substrates. These second-generation PZT SAW designs eliminated the conducting ground-plane electrode, which had resulted in low-impedance devices due to the high dielectric constant for the PZT films. The $LaAlO_3$ substrates act as an electrically insulating template for growth of highly oriented PZT films. On the Si substrates, we used zirconia (ZrO_2) as the electrically insulating template layer. The PZT/$LaAlO_3$ SAW devices operated at frequencies ranging from 50 to 175 MHz, depending on the transducer wavelength. Some of the PZT/ZrO_2/Si SAW devices did show acoustic responses that were sensitive to absorbed mass on the surface of the device. However, the resonant frequencies of the devices were much higher than expected for the transducer wavelengths and layer thickness involved, and indeed did not scale with the transducer period. All of the Si–based devices had their strongest response at around 125 MHz, regardless of the transducer-defined wavelength (which varied from 120 to 28 microns). This suggests that bulk modes were excited at frequencies dependent more on layer thickness than on transducer wavelength.

We developed device designs and obtained appropriate masks to fabricate bulk-micromachined FPW devices using PZT films with conducting bottom electrodes. These devices use interdigitated transducers (IDTs) with one of the combs of fingers connected to the ground plane. Since the PZT film thickness is much less than the finger spacing in the IDTs, the electric field between the drive fingers and the ground plane is dominant, and the other set of fingers plays little role in driving the piezoelectric film. Acoustic wavelengths for the bulk-micromachined FPWs ranged from 246 to 320 microns.

Process integration efforts were highlighted by the development of several new techniques that were essential to the fabrication of PZT thin-film//SiN microelectromechanical system (MEMS) devices. A critical development was the efficient, uniform adherence of titanium//platinum (Ti//Pt) electrode technology to SiN membranes through the use of a thin, 60 nm, SiO_2 sputter-deposited layer. Two other important findings that allowed PZT//SiN devices to be fabricated were mask design/patterning to avoid PZT//SiN contact anywhere on the wafer and elimination of the use of hexamethyldisilizane (HMDS) adhesive due to its detrimental effect on the underlying Pt metallurgy. We used a new technology, termed *high-aspect-ratio silicon etch* (HARSE) processing, to define sharp membrane structures in Si for the fabrication of compound clamped–clamped cantilever beam devices. We improved project enhancement of piezoelectric response by a factor of 1000 compared to simple cantilever beam structures. Finally, we developed a metal-etch procedure for chromium/gold (Cr/Au) electrodes on the PZT devices because of yield problems with lift-off patterning of IDTs with the needed dimensions (lines and spaces of around 10 microns). No deleterious effects of the etch process were detectable on the low-frequency piezoelectric properties of the PZT films, so we used this procedure for subsequent SAW lots and the bulk-micromachined FPW lot.

We fabricated AlN films that were highly oriented in terms of both crystallographic and c+/c- domain configurations. We obtained piezoelectric coefficients of 5.4 pM/V from these highly oriented films, in reasonable agreement with single-crystal values. We developed a fundamental understanding of the effect of nanoscale template layers on AlN domain orientation. A thin, approximately 5 nm-thick, ruthenium-dioxide (RuO_2)

layer will alter domain configurations compared to Ru layers. Control of this layer formation results in piezoelectric constants close to single-crystal values. If formation of the nanoscale interface layers is not controlled, essentially no macroscopic piezoelectric response is obtained.

Publications

Refereed

Clem, P. G., B. A. Tuttle, J. A. Voigt, T. J. Garino, and M. Rodriguez. 1998. "Design of CSD Routes for $BaTiO_3$, PZN/PT, and PZT Thin-Film Devices." Paper presented to the 10th International Symposium on Integrated Ferroelectrics, Monterey, CA, 2 March.

Martin, S. J., M. A. Butler, J. J. Spates, M. A. Mitchell, and W. K. Schubert. 1998. "Flexural Plate-Wave Resonator Excited with Lorentz Forces." *J. Appl. Phys.* **83** (5 May): 4589–4601.

Martin, S. J., M. A. Butler, J. J. Spates, M. A. Mitchell, and W. K. Schubert. 1998. "Magnetically-Excited Flexural Plate-Wave Resonator." *IEEE Trans. on Ultrasonics, Ferroelect., and Freq. Control Symp.* **45** (Los Angeles, CA, 15 June): 1381–1387.

Ruffner, J. A., D. Dimos, P. G. Clem, and B. A. Tuttle. 1997. "Effect of Deposition Parameters on Piezoelectric Response of Reactively Sputtered AlN." Paper presented to the ASM/ACerS Meeting, Albuquerque, NM, 3 November.

Tuttle, B. A., T. J. Garino, P. G. Clem, J. A. Ruffner, and W. K. Schubert. 1998. "Materials Analysis of $Pb(Zr,Ti)O_3$ Thin-Film//Si-Micromachined Structures." Paper presented to the Materials Research Society Meeting, Boston, MA, 2 December.

3502.140

Smart Interface Bonding Alloys (SIBA): Tailoring Thin-Film Mechanical Properties

R. Q. Hwang, S. J. Plimpton, N. D. Shinn, N. R. Moody, J. E. Houston, J. C. Hamilton

Sandia will explore the use of the newly discovered, strain-stabilized, 2-D interfacial alloys as smart interface bonding alloys (SIBAs). We will use these materials as templates for the heteroepitaxial growth of metallic thin films. SIBAs are formed by two metallic components that mix at an interface to relieve strain and prevent dislocations from forming in subsequent thin-film growth. The composition of the SIBA is determined locally by the amount of strain, and therefore can react "smartly" to areas of the highest strain to relieve dislocations. In this way, we can use SIBA to tailor the dislocation structure of thin films.

This project will include growth, characterization, and modeling of films grown using SIBA templates. Characterization will include atomic imaging of the dislocations structure, measurement of the mechanical properties of the film using interfacial force microscopy (IFM) and the nanoindenter, and measurement of the electronic structure of the SIBA with synchrotron photoemission. We will also examine resistance of films to sulfidation and oxidation. We will use the Paragon parallel processing computer to calculate the structure of the SIBA and thin films to develop the ability to predict and tailor SIBA and thin-film behavior.

This work will lead to the development of a new class of thin-film materials with properties tailored by varying the composition of the SIBA, serving as a buffer layer to relieve the strain between the substrate and the thin film. Such films will have improved mechanical and corrosion resistance, allowing application as protective barriers for weapons applications. They will also exhibit enhanced electrical conductivity and reduced electromigration, making them particularly suitable for application as interconnects and other electronic needs.

Our accomplishments include the following:

- Measured IFM indentation curves for Au(111) (gold) and investigated the role of surface steps. This result has proven valuable not only for our SIBA project, but also in developing modeling techniques that can be applied to other work.
- Developed and debugged indentation modeling code on the Paragon computer. The ability to use this code to model indentation led to new insights into the atomistic processes governing the onset of plastic deformation.
- Developed an algorithm for automated identification of dislocations in complex structures.
- Modeled indentation on Au(111) and Au(100). The modeling of these two surfaces showed the importance of the crystal structure in defining mechanical properties. In particular, the overall governing nature of (111) slip planes dominates the behavior of both surfaces in response to indentation.
- Measured the effect of surface defects on the local elastic and plastic properties of Au(111). In addition, we also developed new IFM sensors that exhibit greater reliability and performance.
- Measured dislocation structure of silver (Ag) film grown on SIBA material.
- Measured stability of SIBA interface.

Publications

Refereed

Kelchner, C. L., S. J. Plimpton, and J. C. Hamilton. 1998. "Dislocation Structure During Indentation of Passivated Au(111)." *Phys. Rev. B*, accepted.

Kiely, J. D., R. Q. Hwang, and J. E. Houston. 1998. "The Effect of Surface Steps on the Plastic Threshold in Nanoindentation." *Phys. Rev. Lett.*, accepted.

3502.190

Molecular-to-Continuum Fracture Analysis of Thermoset Polymer/Solid Interfaces

M. S. Kent, M. J. Stevens, E. D. Reedy, Jr.

Sandia is investigating submicron debonding processes at polymer/solid interfaces with a combination of continuum stress analysis, molecular dynamics (MD) simulations, and new experimental approaches. Our objective is a validated, molecular-to-continuum fracture theory. On the continuum level, we made considerable headway in an interfacial fracture mechanics approach for preexisting macroscopic cracks between linear elastic materials. Little is known, however, about modeling cracks on a micron or submicron level, how microcracks develop into macroscopic cracks, or about length-scale limitations on the use of a continuum analysis. Furthermore, the effect of interphase structure and molecular properties on fracture mechanics parameters, needed for a fundamental understanding of failure criteria, is unknown. On the molecular scale, much is known about polymer dynamics, the origin of viscoelastic behavior and relaxation phenomena, and the behavior of polymers near surfaces. Yet it is not clear how stress concentrations develop on a molecular scale in an imperfect thermoset polymer, or how nanoscale inhomogeneities grow into microcracks under stress. An understanding of the link between the molecular and continuum levels is required before the goal of a truly comprehensive model of fracture can be approached.

This past year we performed MD simulations using two-bead chains that qualitatively reproduce experimental stress-strain curves in epoxies. We determined distributions of bond lengths as the system was strained. We determined the structure of epoxy near silicon (Si) surface by neutron reflection (NR) as a function of stoichiometry, coating method, cure temperature, and after thermal cycling. We performed NR measurements with samples subjected to three-point bend loading. We developed two experimental methods for continuously varying interface strength based on self-assembled monolayers (SAMs). We discovered that adhesive-to-cohesive transition occurs over a very narrow range of SAM coverage. We also developed a novel, sandwiched aluminum/silicon/epoxy/aluminum, double-cantilevered beam sample to measure the toughness of a Si/epoxy interface under a mode I-like loading.

The development of MD coarse-grained model epoxy systems encountered several (expected) complications. We determined that even short (five-bead) chains exhibited elastomeric response unless we included a bond-bending potential to stiffen the chain. Networks made of stiff chains had stress-strain curves of the epoxy form. However, simulations of larger systems showed that the stiff chains tend to become aligned, and voids form in the liquid. To prevent this behavior, we went to two-bead chains that do not require the bond-bending and do not form the liquid-crystal phases. With two-bead chains, we were able to qualitatively reproduce the experimental (and continuum mechanics [CM]) stress-strain curves. We calculated stress-strain curves as a function of temperature and confirmed that the trends are the same as CM predictions.

We characterized the network structure in a variety of ways. We coded a cluster analysis of the connectivity and used it to calculate the cluster size and distribution within the network. For all our networks, we achieved about 95% of possible crosslinks. The largest cluster contains about 90% of the crosslinks with the remaining strands consisting of small clusters (single chains or a few chains crosslinked). We are also calculating the minimal path in the network from a bonded site on the top substrate to a bonded site on the bottom substrate. We calculated the bond length distributions as the system was strained. Somewhat surprisingly, they show that the bonds are not stretched significantly, even though the system is significantly strained. We devoted further work to determining the local stress field in the MD.

We determined the near-surface structure of an epoxy film on Si as a function of stoichiometry, coating method, and cure temperature. In all cases, we found a layer of elevated density near the interface (less than 50^3). This effect is most likely due to packing of oligamers next to the hard, smooth surface. In further work, we thermal-cycled samples from 40°C to 65°C for 7 months and detected no variation. This is consistent with continuum stress analysis, which indicates that stress acts only on the edges of these samples in this mode of loading. Therefore, a different way of applying a stress must be implemented. To that end, we fabricated reflectivity samples that could be loaded in three-point bend geometry. They consisted of a thin film of epoxy between two polished Si blocks. We successfully performed NR experiments, and preliminary data suggest a variation in the interface structure after cycling.

We devoted much work to measuring fracture energy as a function of interface strength. We had to overcome two difficulties: (1) a method was needed for varying the interface strength in a controlled way, and (2) well-defined fracture tests were needed that could be performed with Si substrates.

We developed two methods for varying interface strength, each based on SAMs: (1) vary time of exposure to coating solution, and (2) use photolithography to vary the ratio of surface area that is exposed/unexposed to the SAM solution.

We studied adhesive/cohesive fracture transition as a function of interface strength using SAMs and a rod/torsion test (nearly pure mode II, ill-defined stress state). We discovered that adhesive-to-cohesive transition occurs over a very narrow range of SAM coverage.

We adapted napkin/ring torsion test to Si substrates (nearly pure mode II, well-defined stress state). We began a study of fracture as a function of interface strength with SAMs using this fracture test.

We developed a novel, sandwiched aluminum/silicon/epoxy/aluminum, double-cantilevered beam sample to measure the toughness of a Si/epoxy interface under a mode I-like loading. We performed detailed finite-element analyses to determine the calibration connecting loading and specimen geometry to energy release rate and mode mixity. We obtained fracture energies for no SAM coverage and for full coverage.

Publications

Refereed

Reedy, E. D. 1998. "Connection Between Interface Corner and Interfacial Fracture Analyses of an Adhesively Bonded Butt Joint." *Internat. J. Solids & Structures, Proc. 22nd Ann. Mtg. Adhesion Soc.* (Panama City Beach, FL, 24 February 1999), accepted.

Other

Kent, M. S., W. F. McNamara, J. Majewski, and G. S. Smith. 1997. "Stress-Induced Degradation of Interface Structure in Epoxy Films on Silicon Substrates: An *In Situ* Study by Neutron Reflection." Paper presented to the Materials Research Society Meeting, Boston, MA, 1–5 December.

Kent, M. S., W. F. McNamara, L. Domeier, and A. P. Y. Wong. 1998. "Characterization of Epoxy Structure Near a Silicon Surface Using Neutron Reflection." *Proc. 21st Ann. Mtg. Adhesion Soc.* (Savannah, GA, 22–25 February): 153.

Kent, M. S., W. F. McNamara, L. Domeier, J. Majewski, G. S. Smith, and S. Satija. 1998. "Structure of an Epoxy Near a Smooth SiO_2 Surface." Paper presented to the Annual Meeting of the American Physical Society, Los Angeles, CA, March.

Stevens, M. J. 1998. "Adhesive Failure in Thermosetting Polymers." Paper presented to the Materials Research Society Meeting, Boston, MA, 30 November–4 December.

3502.210

Monolithic Structures for Nanoseparation

T. J. Shepodd, M. E. Warren, D. S. Anex, A. Martino

Miniaturization in detection and separation technologies requires easily built, rugged devices based on materials that have well-understood interactions with analytes at the molecular level. The goals of this project are to design such materials for state-of-the-art separation science, understand their structure/function relationships, and fabricate them into useful devices. We are utilizing Sandia's expertise in the synthesis of microporous and nanoporous materials to develop continuous, high-surface-area polymers as monolithic nanoporous supports for ultra-efficient separations. We are evaluating these materials using capillary electrochromatography (CEC) as a test-bed. We will quantify the interaction of functionalized surfaces of these supports with analytes, propelled by the electroosmotic flow (EOF), in terms of separation efficiency and selectivity. Our goal is to engineer an open and interconnected network where every nanopore functions as a CEC column. We will integrate these new solid supports, which are cast as fluids and cured to monolithic polymer structures, into micromachined grooves as pre-prototype devices for ultra-efficient separations.

Our work thus far has greatly increased our understanding of analyte/support interactions as influenced by engineered materials. The monoliths have been spectacularly successful in other micromachine-type devices. We made two patent disclosures.

We designed and synthesized monolithic polymer supports that function as CEC columns. We demonstrated that these columns support EOF and showed baseline separation of analytes in simple chromatography experiments. We developed efficient synthetic routes to organic and inorganic monolithic supports. We discovered a way to use inverse emulsion polymerization to simultaneously create the chromatography medium, the species to support EOF, and the bonds connecting the support to the substrate (capillaries in these studies). Thus, we avoid time-consuming and logistically difficult surface modification chemistry. They can be designed to support positive and negative EOF, and the EOF direction can be switched. We synthesized a second generation of supports for immediate testing. The second-generation supports are based on phase-separation polymerization and demonstrated modest separation efficiencies. We also demonstrated that we can modify the micro- and macrostructure of the monoliths, as predicted, by varying synthetic parameters. We incorporated the phase-separation–generated monoliths into devices powered by EOF. These devices have been spectacularly successful, and we released patent disclosures covering the devices and their compositions.

3502.170

Recognizing Atoms in Atomically Engineered Nanostructures: An Interdisciplinary Approach

K. M. Horn, J. S. Nelson, G. C. Osbourn, R. M. Biefeld, M. P. Sears, D. R. Jennison, A. M. Bouchard

Scanning-tunneling microscopy (STM) is a powerful tool for both characterizing and manipulating the atomic topographies of surfaces. However, STM has typically been unable to provide unambiguous chemical recognition of atomic sites in many technologically relevant, but chemically heterogeneous, systems. Sandia will develop the theoretical and experimental underpinnings necessary to enable unambiguous, computer–based identification of atomic sites in multivariate STM imagery, focusing on heterogeneous III–V semiconductor materials and atomically engineered nanostructures. The project will have several subtasks: (1) We will seek to develop the first database of multivariate STM spectral features. (2) We will study the effects of different tip states on the STM spectral features and attempt to establish procedures for computationally removing or minimizing variable tip effects. (3) We will use pattern recognition of STM spectral imagery, based on the results of tasks 1 and 2, to map out the atomic-scale chemical structure of selected cleaved (110) III–V surfaces. We will specifically attempt to understand the alloy ordering and interfacial structure of III–V structures of current programmatic interest for infrared (IR) device applications.

Comparison of topographic and conductance–based STM images showed that surface irregularities in a topographic image do not necessarily indicate the presence of unique electronic structures. Conversely, STM features that appear topographically similar can, in fact, exhibit distinctly different electronic behavior. The use of multispectral image analysis techniques in the reduction of multibias STM conductance data provides a quantitative means of examining atomic surfaces while still maintaining the rich information content inherent in an imaging technique. The use of a computed grouping algorithm greatly streamlines the data-reduction process and provides a rigorous, reproducible means of discriminating features based on their conductance spectra.

The ideal situation is to analyze data acquired from a single STM tip. Multibias conductance images measured with different tips and analyzed with this multivariate classification technique have consistently produced classed images that discriminate between different chemical species and even different bonding states of the same species. However, the exact shape of the conductance spectra defining a specific surface feature differs between tips. This is predominantly due to the variability in both the atom configuration and composition (silicon [Si] and tungsten [W] atoms) on the tip side of the tunneling junction. Thus, at present our classed images discriminate only between surface electronic features, but do not identify them absolutely. We believe that the ability to absolutely identify atoms based on their conductance spectra can be achieved through strict control or characterization of the STM tip, so that reproducible conductance spectra are measured from surface to surface. This may require utilizing field-ion microscopy (FIM) of the tip before multibias measurements. However, it may also be possible to devise post-measurement transformations of the measured conductance spectra that will factor out variations in tip structure. This latter approach holds some promise since such data transformation techniques are already used in other multivariate classification analyses, e.g., chemical sensing, where similar problems with variability of sensor response and uneven signal attenuation are compensated for by sensor recalibration and renormalization of sensor response.

Using a single STM tip, we showed that classed images of simple features in Si(001)-2x1 surfaces correlate well with obvious features suggested by the corresponding topographic images. The periodicity of the 2x1 dimer row structure, A- and B-step edges, kinks in step edges, 2+1 vacancies, and *c*-defects were all resolved in conductance–based images of this atomic surface. The classed, conductance–based images also revealed surface electronic structures not suggested by the topographic images. Classed images of the B-step in the Si(001)-2x1 surface indicate the presence of two electronically distinct rows at the base of the B-step; these features correlate well with the position of rebonded atoms proposed in models of the single B-step. Furthermore, the termination of the dimer trough of the upper terrace at the B-step exhibited unique conductance characteristics while the termination of the dimer row does not. This may reflect the presence of exposed, undimerized dangling bonds at the step edge. This interdisciplinary approach to the data analysis of multivariate STM data adds significant value to the interpretation of the images of atomic surfaces.

We were unable to exploit the power of our approach to study cleaved III–V heterostructures as originally intended.

Publications

Refereed

Horn, K. M., B. S. Swartzentruber, G. C. Osbourn, A. M. Bouchard, and J. W. Bartholomew. 1998. “Electronic Structure Classifications Using Scanning-Tunneling Microscopy Conductance Imaging.” *J. Appl. Phys.* **84** (1 September): 2487–2496.

3502.220

Fundamental Aspects of Micromachine Reliability

M. P. De Boer, J. A. Knapp, T. M. Mayer, J. J. Sniegowski, J. M. Redmond

A fundamental basis for designing micromechanical devices with high-yield, reliable performance and long life is lacking. Mechanical design tools for macroscale machines relate reliability to inertial forces. However, the performance of micron-scale structures of high-aspect ratio is dominated by surface forces. The technical goal of this project is to use experimental reliability results obtained directly from micromachined test structures to develop and verify mechanics models containing interaction terms appropriate to the micron-scale (e.g., capillarity, van der Waals forces, electrostatics, etc.). Issues to be addressed include auto-adhesion (stiction), friction, and wear. Beginning with auto-adhesion, Sandia will design and build microbridge structures with varying geometry and surface properties (roughness, chemical coatings, etc.). We will monitor deformations by interferometry in an environmental chamber. We will develop finite-element models incorporating new surface elements, and verify and refine them by comparing them against experimental results. Next, we will investigate friction and wear using smart micromachined structures that enable self-diagnosis by electrical monitoring of capacitance and Q-factor changes. We will also explore optical detection techniques. We will verify and refine dynamical response models incorporating internal friction terms, as well as damping, using experimental results. We will then extract friction due to energy loss at rubbing surfaces.

This project will develop a new tool set based on an experimental and theoretical foundation. We will use the tool set to calculate and characterize reliability of micromachines for integrated microsystem applications.

We accomplished the following:

• Compared the integrity of various coatings subject to high and low relative humidity (RH). We found adhesion to be exponentially dependent on RH. This trend was explained by comparing to models of capillary condensation. We showed that for a smooth interface, the adhesion should be independent of RH. This agrees well with crack healing data for glass, which fractures in an atomically smooth fashion, but disagrees with our data. However, due to roughness of our material, the surfaces come into contact only at asperity tips. We showed that a single asperity model for adhesion versus RH agrees well with our experimental results.

• Applied analytical techniques (e.g., Fourier-transform infrared [FTIR], ellipsometry) to determine water absorption. Small amounts of water seem to adsorb even on nominally hydrophobic molecular coatings.

• Developed a method to measure adhesion hysteresis. We measured adhesion hysteresis as a function of exposure to RH. At RH > 90%, our hydrophobic molecular coating begins to break down, as evidenced by increasing adhesion.

• Fabricated a device to measure capacitance of adhered beams. We achieved the expected measurement results.

• Invented surface terms that account for interactions between forces, e.g., van der Waals and electrostatic.

• Designed and fabricated a new test chip with simulated friction test structures, and corrected designs from the first test chip.

• Formulated a comprehensive dynamic model incorporating beam vibrations and frictional effects.

• Tested friction test structures statically and showed that they work. We determined the friction coefficient of uncoated beams.

• Tested friction test structures dynamically and demonstrated hysteretic losses.

Publications

Refereed

De Boer, M. P., J. M. Redmond, and T. A. Michalske. 1998. “A Hinged-Pad Test Structure for Sliding Friction Measurement in Micromachining.” *Proc. SPIE, Mater. and Device Characterization in Micromachining* **3512** (Santa Clara, CA, 1 September): 241–250.

De Boer, M. P., P. J. Clews, B. K. Smith, and T. A. Michalske. 1998. “Adhesion of Polysilicon Beams in Controlled Humidity Ambients.” *Proc. Mater. Res. Soc. Symp.* **518** (December) (San Francisco, CA, April).

3502.240

Atomic-Level Studies of Surfactant-Directed Materials Growth

P. J. Feibelman, B. S. Swartzentruber, G. L. Kellogg, J. A. Floro, N. C. Bartelt, J. C. Hamilton

Sandia will convert surface impurities from a nuisance to a systematically applicable nanofabrication tool. Combining Sandia's special facilities, including the atom-tracker scanning-tunneling microscope (AT-STM), low-energy electron microscopy (LEEM), and massively parallel computation (MPC), we will learn how common adsorbed atoms (surfactants) can be used to manipulate and direct thin-film growth. Thus, we will develop a surfactant toolkit that enables us to produce either atomically flat or 3-D nanostructured surfaces. We will start with model systems, where we have experience in the absence of surfactants, studying surfactant-modified diffusion on and near metal and semiconductor surfaces, and integrating our real-time experimental and advanced computational modeling capabilities. We will use the AT-STM to study hydrogen (H)-assisted silicon (Si) adatom diffusion on Si(001), LEEM to investigate both H-assisted step fluctuations on the same surface, and oxygen (O)-assisted island growth on Pt(111) (platinum). Via novel surface stress measurements, we will study germanium (Ge) segregation versus adsorbate overlayer coverage in Si-Ge alloys. We will closely couple theoretical efforts to our experiments; MPC will be indispensable in developing reliable, atomic-scale, mechanistic models.

High-resolution STM measurements of localized strain relief near Ge and Si islands on Si(001) showed debuckling of substrate dimers extending over 3+ lattice sites, indicative of the lateral range of the varying potential interaction. This has implications for growth of Ge and Si, as diffusing atoms interact with preexisting structures. We showed that morphological phase transitions, accelerated coarsening, and self-organization among SiGe-strained islands on Si result from elastic repulsions between neighboring islands. Our first-principles calculations of Pt transport show facile transport down A-type island edges on Pt(111), and thus that O-induced layer-by-layer epitaxy of Pt(111) cannot result from reduced downward transport barriers, as claimed in the literature. We vindicated the theory with the discovery of sample contamination by background carbon-monoxide (CO) in the experiments. Via LEEM we determined the mechanism and energetics of Si(001) etching by oxygen. We quantified observations of O-induced stress relief on Si(001) by measuring terrace widths and the velocity of step retraction. New field-ion microscopy (FIM) measurements generalized the conclusion that H promotes hopping and inhibits exchange diffusion. After LEEM modifications, we made initial observations of nucleation, growth, and coarsening of a metal-on-metal system: Pt islands on Pt(111). We developed a computational technique to analyze such observations by solving the diffusion equation subject to boundary conditions determined by the observed configuration of surface steps. Finally, to see how lattice mismatch affects the structure of growing heteroepitaxial films, we used a combination of 2-D elasticity models and first-principles calculation, accounting for the misfit dislocation structure observed in silver (Ag) monolayers on Pt(111).

Publications

Refereed

Carpinelli, J. M., and B. S. Swartzentruber. 1998. "Detailed Energetic Interactions of Adsorbed Si Dimers on Si(001)." *Surf. Sci.* **411**: L828.

Carpinelli, J. M., and B. S. Swartzentruber. 1998. "Direct Measurement of Field Effects on Surface Diffusion." *Phys. Rev. B*, accepted.

Feibelman, P. J. 1998. "Interlayer Self-Diffusion on Stepped Pt(111)." *Phys. Rev. Lett.* **81** (6 July): 168–171.

Feibelman, P. J. 1998. "Interpretation of O Binding-Site Preferences on Close-Packed Group VIII Metal Surfaces." *Phys. Rev. B*, accepted.

Feibelman, P. J. 1997. "Nature of Adatom Bonds to Transition-Metal Surfaces." Paper presented to the National American Vacuum Society Symposium, San Jose, CA, 23 October.

Feibelman, P. J., J. Hafner, and G. Kresse. 1998. "Vibrations of O on Stepped Pt(111)." *Phys. Rev. B* **58** (15 July): 2179–2184.

Floro, J. A. 1998. "Accelerating Island Coarsening During SiGe MBE Measured by Real-Time Spectroscopic Light Scattering." Paper presented to the Spring 1998 MRS Meeting, San Francisco, CA, April.

Floro, J. A., E. Chason, L. B. Freund, R. D. Twesten, and R. Q. Hwang. 1998. "The Kinetics of Coherent Island Formation in $Si1_{-x}Ge_x$/Si (001)." *Phys. Rev. B*, submitted.

Floro, J. A., E. Chason, M. Sinclair, L. B. Freund, and G. A. Lucadamo. 1998. "Dynamic Self-Organization of Strained Islands During SiGe Epitaxial Growth." *Appl. Phys. Lett.* **73**: 951–953.

Floro, J. A., G. A. Lucadamo, E. Chason, L. B. Freund, M. Sinclair, R. D. Twesten, and R. Q. Hwang. 1998. "SiGe Island Shape Transitions Induced by Elastic Repulsion." *Phys. Rev. Lett.* **80**: 4717–4720.

Hamilton, J. C. 1997. "Frenkel-Kontorova Molecular Dynamics Model for Strained Heteroepitaxial Film Growth." Paper presented to the APS International Conference on Computational Physics, Santa Cruz, CA, 25–28 August.

Hamilton, J. C. 1997. "Frenkel-Kontorova Molecular Dynamics Model for Strained Heteroepitaxial Film Growth." Paper presented to the Gordon Conference on Thin-Film and Crystal Growth Mechanisms, Plymouth, NH, 6–11 July.

Hannon, J. B., N. C. Bartelt, B. S. Swartzentruber, and G. L. Kellogg. 1998. "LEEM Measurements of Step Energies at the (001) Surface of Heavily Boron-Doped Silicon." *Surf. Rev. and Lett.*, accepted.

Hannon, J. B., N. C. Bartelt, B. S. Swartzentruber, J. C. Hamilton, and G. L. Kellogg. 1997. "Step Faceting at the (001) Surface of Boron-Doped Silicon." *Phys. Rev. Lett.* **79**: 4226–4229.

Kellogg, G. L. 1997. "Direct Observations of the Effect of Chemisorbed Hydrogen on Single-Atom Surface Diffusion." Paper presented to the 18th IUVSTA Workshop on Diffusion and Growth in Ultrathin Layers (Invited), New Castle, Australia, 4–22 November.

Kellogg, G. L. 1997. "Direct Observations of the Effect of Hydrogen on Single-Atom Surface Diffusion." Paper presented to the 1997 Symposium of the Pacific Northwest Section of the American Vacuum Society (Invited), Troutdale, OR, 18–19 September.

Kellogg, G. L. 1997. "Field Ion Microscope Studies of the Effect of Hydrogen on Single-Atom Surface Diffusion." Paper presented to the 44th International Field Emission Symposium, Tsukuba, Japan, 7–11 July.

Kellogg, G. L. 1997. "Hydrogen Inhibition of Exchange Diffusion on Pt(100)." Paper presented to the 44th National Symposium of the American Vacuum Society, San Jose, CA, 20–24 October.

Kellogg, G. L. 1997. "Hydrogen Inhibition of Exchange Diffusion on Pt(100)." *Phys. Rev. Lett.* **79**: 4417–4420.

Kellogg, G. L. 1998. "Mechanisms and Energetics of Cluster Nucleation and Diffusion on Surfaces." Paper presented to the 9th International Symposium on Small Particles and Inorganic Clusters (Invited), Lausanne, Switzerland, 1–5 September.

Pohl, K., M. C. Bartelt, J. de la Figuera, N. C. Bartelt, and R. Q. Hwang. 1998. "Identifying the Forces Responsible for Self-Assembled Nanostructures." *Nature*, accepted.

Schmid, A. K., R. Q. Hwang, and N. C. Bartelt. 1998. "Predicting the Future of a Complicated Surface Structure: Grain Coarsening of P(2x2)O/Ru(0001)." *Phys. Rev. Lett.* **80**: 2153–2156.

Swartzentruber, B. S. 1997. "Atomic-Scale Dynamics of Atoms and Dimers on the Si(001) Surface." *Surf. Sci.* **386**: 195.

Swartzentruber, B. S. 1998. "Fundamentals of Surface Step and Island Formation Mechanisms." *J. Crystal Growth* **188**: 1.

Other

Bartelt, N. C. 1998. "Driving Forces for Self-Assembly on Surfaces: Phonons in Vacancy Island Lattices in Ag Films on Ru(0001)." Paper presented to the American Association of Crystal Growth West Meeting, Fallen Leaf, CA, 10 June.

Bartelt, N. C. 1997. "The Different Roles of Near and Far from Equilibrium Theories of the Evolution of Surface Morphology." Paper presented to the Materials Research Society Meeting, Boston, MA, 5 December.

Feibelman, P. J. 1998. "The Forces that Control How Metal Surfaces Evolve." Paper presented to the Colloquium, Arizona State University, Tempe, AZ, 26 February.

Feibelman, P. J. 1997. "The Forces that Control How Metal Surfaces Evolve." Paper presented to the Colloquium, University of Texas–El Paso, El Paso, TX, 15 April.

Feibelman, P. J. 1998. "Vibrations of O on Stepped Pt(111)." Paper presented to the March American Physical Society Meeting, Los Angeles, CA, 17 March.

Floro, J. A. 1997. "Epitaxy with an Attitude: Real-Time Studies of Coherent Islanding Kinetics During SiGe/Si Molecular Beam Epitaxy." Seminar, Johns Hopkins University, Baltimore, MD, 17 September.

Floro, J. A. 1997. "Epitaxy with an Attitude: Real-Time Studies of Coherent Islanding Kinetics During SiGe/Si Molecular Beam Epitaxy." Seminar, University of Texas, El Paso, TX, 1 October.

Floro, J. A. 1997. "Evolution of Self-Organized Si_xGe1_{-x} Island Arrays." Paper presented to the Fall MRS Meeting (Invited), Boston, MA, 1–5 December.

Floro, J. A. 1998. "SiGe Island Formation Kinetics Real-Time Studies of Coarsening Shape Transitions and Self-Assembly." Paper presented to the 16th Annual Conference on Crystal Growth and Epitaxy, Fallen Leaf Lake, CA, 10 June.

Hamilton, J. C. 1997. "Dislocations, Diffusion, and Heteroepitaxial Film Growth." Paper presented to Physics Colloquium at University of Texas–El Paso (Invited), El Paso, TX, 26 November.

Hamilton, J. C. 1998. "Dislocations During Thin-Film Growth and Indentation." Seminar, LANL, Los Alamos, NM, June.

Hamilton, J. C. 1997. "Early Stages of Heteroepitaxial Film Growth on Metals." Paper presented to the 15th Conference on Crystal Growth and Epitaxy (Invited), Fallen Leaf Lake, CA, 1–4 June.

Hamilton, J. C. 1997. "Initial Growth of Heteroepitaxial Films on Close-Packed Metal Substrates." Paper presented to the Fall MRS Symposium (Invited), Boston, MA, 1–5 December.

Swartzentruber, B. S. 1997. "Direct Measurements of Atomic-Scale Surface Kinetics on Si(001)." Paper presented to the Annual Meeting of the American Vacuum Society, San Jose, CA, 20–24 October.

3502.230

Enabling Science and Technology for Cold-Spray Direct Fabrication

M. F. Smith, D. L. Gilmore, J. E. Brockmann, R. C. Dykhuizen, R. A. Neiser, Jr.

Cold-spray processing (CSP) is a new technology that can rapidly deposit (mm/second) metals, polymers, and composites at temperatures < 200° Celsius by accelerating powder particles up to 600–1000 m/s in a supersonic gas jet. Sandia envisions a radical new direct fabrication technology in which a highly focused CSP particle beam with a robotic positioning system can spray-fabricate single- or multimaterial components directly from a computer model. Build rates should be higher than present layer-wise direct fabrication techniques and, since CSP particles are never melted, superior surface finishes, microstructures, and properties might be achieved (finer grain size, no brittle phases, minimal oxidation, less residual stress, etc.). CSP might also deposit functionally graded or layered materials at low temperatures, eliminating joining operations, simplifying design/fabrication, reducing part counts, and decreasing stress cracking (e.g., aluminum can be CSP-deposited directly onto smooth, unprepared glass with excellent adhesion.) CSP may even be a green alternative to technologies such as electroplating, soldering, and painting. A primary technical barrier is focusing the particle stream. Theory indicates major technical challenges, but a noncontact focusing technique known as an aerodynamic lens (AL) *might work. The AL was originally developed with submicron particles at subatmospheric pressures. Sandia previously established a new cold-spray capability and successfully focused a beam of 15+ micron particles down to ~ 1 mm at atmospheric pressure with subsonic gas velocities. Later, we will test higher-pressure AL designs and spray-fabricate proof-of-concept shapes commensurate with the level of focusing achieved. We will also characterize the resulting material properties.*

Tasks included successfully designing/testing multistage aerodynamic focusing; enhancing understanding through substantial experimental/modeling progress; and preliminary characterization of cold-sprayed materials. Based on computational modeling, we built a three-lens stepped focusing system and aerodynamically focused 15+ micron aluminum particles in a subsonic helium jet down to a beam ~ 1 mm in diameter under ambient atmospheric conditions (substantial improvement over ~ 5 mm beam achieved previously). We are currently building a final design for focusing under actual cold-spray conditions. Modeling/variable sensitivity experiments confirmed our analysis of key variable effects; for example, changing from nitrogen to helium can double particle velocity; doubling nitrogen temperature can increase particle velocity by one-third, but a 30% reduction in gun inlet nitrogen pressure reduces particle velocities by only ~ 3%. Our results show that inlet gas temperature is more important than indicated by the Russian inventors of cold spray. Currently, we are modeling and experimentally studying the impact of copper particles cold-sprayed onto steel. Also, we successfully cold-spray–deposited copper, aluminum, stainless steel, a nickel–based alloy, and a nanophase tungsten carbide/cobalt wear coating. Microstructures have similarities to thermally sprayed materials but with highly angular features and no apparent evidence of melting or increase in grain size. Some deposits exhibit compressive residual stress. Copper deposited in an ambient air environment has no measurable increase in oxygen content over the feed powder.

Publications

Refereed

Dykhuizen, R. C., and M. F. Smith. 1998. "Gas Dynamic Principles of Cold Spray." *J. Thermal Spray Technol.* **7** (June): 205–212.

Smith, M. F., R. A. Neiser, D. L. Gilmore, and R. C. Dykhuizen. 1998. "Cold-Spray Deposition Material Consolidation Without Melting or Solidification." Paper presented to the Gordon Conference on High-Temperature Materials, Processing, and Diagnostics (Invited), Plymouth, NH, 19–24 July.

3502.260

Freeforming of Ceramics and Composites from Colloidal Slurries

J. Cesarano, III, M. T. Ensz, M. L. Griffith, M. R. Baer, D. J. Schmitt

Sandia will develop a model–based direct freeform fabrication technique for ceramic, metal, or graded composite components. These components are fabricated by computer-controlled dispensing of colloidal suspensions through an orifice. Any conceivable 2-D pattern may be written layer-by-layer into a 3-D shape. Our goal is to develop model–based processing rules that will aid in the development of slurries with the appropriate rheology, density, and drying kinetics to ensure process success for a variety of ceramics and composites. Software and equipment development is also essential for precise control of layer thickness and feature resolution.

Development of this technique into a manufacturing process requires computer simulations of the relevant physical phenomena; materials expertise for tailoring colloidal slurry properties and processing dissimilar materials; software and equipment expertise for computer-aided design (CAD) model conversion; and robotics expertise for process optimization and incorporation of knowledge–based processing capabilities with closed-loop, sensor–based control.

This work will directly impact the production of neutron tubes and ceramic fixtures for switch tubes.

We made significant progress toward scientific understanding of slurry behavior, fabrication techniques for reliable parts with good properties, fabrication of novel structures for ceramic/metal joins, development of new material systems, software, modeling of flow, and sensing.

For aluminum oxide, in particular, we studied the aging process of slurries, resulting in substantial time-savings for slurry preparation. Slurries can now be processed in two days instead of three weeks, and slurries may be frozen and stored until needed. This, along with the development of controlled drying on wet plaster substrates, yields reliable parts with good tolerance. The density, microstructure, and mechanical properties are comparable to aluminum oxide that is traditionally isopressed and machined. Therefore, we selected an aluminum oxide Defense Programs (DP) neutron-tube component and are attempting to fabricate it with our technology. Another unanticipated accomplishment was the development of corrugated ceramic preforms that, when infiltrated with metal, can form strong interlocking joins with a graded macrostructure. We fabricated crack-free alumina/aluminum structures.

We also developed slurries for the fabrication of lead zirconate titanate (PZT), ZnO, Kaolin, and alumina/Mo composites. We are just beginning multimaterial fabrication.

Developments for software, modeling, and sensing. We developed software that can slice a CAD file into layers and create machine commands for slurry deposition that fills in the layers. We now have the ability to build simple parts directly from a CAD file. We also developed a 3-D model of fluid flow through a nozzle and onto a moving substrate, the first of its kind. In addition, we are developing a structured lighting sensor for real-time dimensional measurement of parts.

Publications

Refereed

Cesarano, J., and R. Segalman. 1998. “Robocasting Provides Moldless Fabrication from Slurry Deposition.” *Ceramic Industry* **148** (April): 94–102.

Cesarano, J., B. King, and H. Denham. 1998. “Recent Developments in Robocasting of Ceramics and Multimaterial Deposition.” *Proc. Solid Freeform Fabrication Symp.* (Austin, TX, 7 August).

Denham, H., J. Cesarano, and B. King. 1998. “Mechanical Behavior of Robocast Alumina.” *Proc. Solid Freeform Fabrication Symp.* (Austin, TX, 7 August).

King, B., S. Morissette, H. Denham, J. Cesarano, and D. Dimos. 1998. “Influence of Rheology on Deposition Behavior of Ceramic Pastes in Direct Fabrication Systems.” *Proc. Solid Freeform Fabrication Symp.* (Austin, TX, 7 August).

Other

Cesarano, J. 1997. “Slurry Processing of Technical Ceramics with Robocasting.” Presentation for AlliedSignal Corporation in preparation for a joint proposal to DARPA, Morristown, NJ, September.

Cesarano, J., B. King, and T. Baer. 1998. “Direct Fabrication of Ceramics and Composites from Slurries: Robocasting Technology.” Paper presented to the Pacific Rim International Conference on Advanced Materials and Processing, Honolulu, HI, July.

3502.250

Intelligent Polymers for Nanodevice Performance Control

G. M. Jamison, M. J. Carr, J. A. Shelnutt, R. S. Saunders, D. R. Wheeler, D. A. Loy

The purpose of this project is to develop organic materials systems that can be predictably manipulated to alter the fundamental optical, electrical, and rheological properties of the materials. Technical insights led to a larger emphasis on manipulating the electrical properties of organic materials than reflected on the original project plan. We will continue to pursue manipulation of both polymer electrical and rheological properties through light, heat, or redox–based stimuli.

Molecular modeling of a family of metal porphyrin-terminated polyenes confirmed molecular orbital overlap between polyene linkers and porphyrin termini in model systems; we predicted photophysical properties to reflect these favorable interactions. Sandia began synthetic efforts on simple polyene systems.

Chemical amplification continues to be an attractive strategy for affecting macroscopic changes in polymer rheological properties and to leverage with existing in-house expertise, e.g., photoresist materials. We are broadening our approach in chemical amplification to include catalyst systems that will be potentially more effective than previously investigated systems. Application of this approach to acid- and base-sensitive polymer systems continues and has allowed us to address technical issues of interest to national security and weapons customers.

This year the project extended computational methods to include semiempirical molecular orbital modeling studies of metal porphines as candidate redox ligands for electrical manipulation of polyacetylenic linkers. These theoretical results allow photophysical property prediction of porphyrin-terminated polyenes. We prepared simple diene- and triene-bridged systems for validation of the modeling predictions.

Our experimental work includes the preparation of organic monomers for potential light-induced conversion of electrically insulating organic polymers to conducting materials and novel hybrid materials bearing conducting organic nanodomains in phase-separated block polymers. Investigations of structural polymers that can be degraded by light-induced liberation of chemical species advanced. Also, we prepared reductively sensitive polyurethanes for potential hydrogen-detection applications (verification of better efficiency). Finally, we applied new metathesis catalysts to the development of novel hybrid polymers. The oligomerization behavior of phosphaalkyne monomers with metal alkylidenes is a fundamental advance in the chemistry of phosphaalkynes and suggests that polyconjugated materials may be accessible by this route.

Publications

Refereed

Jamison, G. M., D. R. Wheeler, R. S. Saunders, and D. A. Loy. 1998. "Double Phosphaalkyne Insertion to a Tungsten Alkylidene: Formation of a Novel Diphosphametallabicyclo-butane." *J. Amer. Chem. Soc.*, submitted.

3502.270

Quantum Dot Arrays

J. E. Martin, R. A. Anderson, D. R. Jennison, P. N. Provencio, J. P. Wilcoxon

The goals of Sandia's research are to investigate methods of synthesizing quantum dot arrays (QDAs)—superlattices of nanoclusters—and to characterize and understand the properties of these novel materials. It is well known that nanoclusters have many unusual properties, including anomalous optical properties, size-dependent bandgaps, high catalytic activity, low melting temperature, anomalous magnetic properties, etc. However, the formation of cluster–based materials requires that these nanoclusters be isolated in a matrix to prevent the spontaneous sintering of clusters to form a bulk material. We can accomplish this by forming these clusters into periodic arrays where clusters are separated by an isolating matrix. These periodic arrays may exhibit coherent effects, or may simply be efficiently close-packed materials.

We developed robust synthetic procedures to synthesize very narrow-size distribution metal nanoclusters (platinum [Pt], gold [Au], palladium [Pd], ruthenium [Rh]) by systematically exploring and optimizing the reactants and procedures. We developed extraction methods to purify the as-synthesized nanoclusters so they spontaneously form 2-D and 3-D superlattices without the need for size fractionation. The 3-D QDAs form in several crystalline habits. We developed software to obtain very detailed structural information from tunneling electron microscope (TEM) images of 2-D QDAs and used this to study the ability of systematically chosen thiol capping agents to control the lattice cell size and interparticle gaps—important in controlling tunneling currents through these materials. We formed a stable microemulsion of Pt nanoclusters in octane—useful in incorporating nanoclusters into periodic mesoporous silica. We made conductivity measurements on thin films of QDAs and found that the sintering temperature of Pt nanoclusters is only ~ 200°C, far below the melting temperature of bulk Pt, 1772°C, which led to further investigations to use these materials as hermetic seals. We showed the direct writing of wires at low temperatures to be possible, as was the selected laser annealing of nanocluster thin films to

form conducting Pt and Au wires. Optical studies show that the optical absorption properties of QDAs are quite different from dilute solutions of nanoclusters, which we believe is because of local field corrections due to nearby dipole radiators. Nonlinear optical studies on Au QDAs demonstrate a very large third nonlinear optical coefficient, measured in four-wave degenerate mixing experiments. A university collaboration showed that 2-D QDAs on graphite can be manipulated with a scanning-tunneling microscope.

Publications

Refereed

Durston, P. J., J. Schmidt, R. E. Palmer, and J. P. Wilcoxon. 1997. "STM Imaging of Ordered Coated Cluster Layers on Graphite." *Appl. Phys. Lett.* **71** (October): 2940–2942.

Durston, P. J., R. E. Palmer, and J. P. Wilcoxon. 1998. "Manipulation of Passivated Gold Clusters on Graphite with the Scanning Tunneling Microscope." *Appl. Phys. Lett.* **72** (January): 176–178.

Newcomer, P. P., J. P. Wilcoxon, J. E. Martin, and J. G. Odinek. 1997. "Studies of Pt and Au Nanocluster Superlattices." Paper presented to the 1997 Fall Meeting of the Materials Research Society, Boston, MA, 1 December.

Wilcoxon, J. P. 1997. "An Overview of Nanocluster Research at Sandia National Laboratories." Paper presented to the Department of Physics Colloquium, University of New Mexico, Albuquerque, NM, 9 October.

Wilcoxon, J. P., J. E. Martin, and P. P. Newcomer. 1997. "Chromatographic Characterization of Metal and Semiconductor Nanoclusters." Paper presented to the 1997 Fall Meeting of the Materials Research Society, Boston, MA, 1 December.

3502.280

Laser-Assisted Arc Welding for Aluminum Alloys

P. W. Fuerschbach

There exists a strong need in the defense programs and automotive, aerospace, and transportation industries for a rapid, robust, high-quality process for welding aluminum alloys, especially for relatively thin-gauge product. While laser beam welding is widely applied in these industries, it has not proved valuable for aluminum because of problems with reflectivity and weld joint variability. Sandia intends to develop a new welding process by combining a fiber-optic–delivered materials-processing laser with a small arc-welding heat source. The new laser-assisted arc-welding (LAAW) process will couple the process advantages of the two heat sources and will also enable process capabilities never before envisioned in arc welding. The project is a System of Laboratories (SOL) collaboration among Oak Ridge National Laboratory, Idaho National Electrical Engineering Laboratory, Sandia National Laboratories, and Y12. Team members will combine their welding expertise to develop the scientific understanding and engineering methods required for the novel process. We anticipate that the team established through this SOL interaction will allow the U.S. to successfully compete with international entities in developing (and hence owning) advanced joining technologies.

Our efforts this year in LAAW furthered our fundamental and practical understanding of hybrid laser/arc-welding technology. Important modifications to the Sandia-developed LAAW end-effector continued this year as new experimental data indicated weaknesses in the prototype. We produced a full set of dimensioned drawings of the end-effector components and the combined assembly. We found variations in the orifice gas flow to produce combined process welds that appeared similar to deep-penetration laser welds. We obtained high-fusion-zone depth-to-width ratios with 150 W of laser and 400 W of arc power. These results indicate that by carefully controlling the LAAW process parameters, we can independently select a wide range of weld-pool geometries with this process. We also modified the end effector to be compatible with continuous-wave (CW) CO_2 laser beam welding. Metallography of early welds with this CO_2 laser indicated that the arc does not penetrate as deeply into the laser keyhole as was observed for Nd:YAG laser welding. Presently, it appears that the arc plasma is absorbing the laser beam and preventing the laser beam from penetrating into the weld pool.

Based on the success of the SOL collaboration, the laboratory and industrial participants submitted a joint proposal to the DOE Office of Industrial Technology to further develop this technology for steel-welding applications. DOE has approved the joint project.

Publications

Other

Fuerschbach, P. W., and F. M. Hooper. 1998. "Laser-Assisted Non-Consumable Arc-Welding Process Development." Paper presented to the 79th Annual AWS Convention, Detroit, MI, 27 April.

3502.310

Reactivity of Metal-Oxide Surfaces

A. G. Sault, R. Q. Hwang, J. A. Ruffner, D. R. Jennison, B. S. Swartzentruber

Sandia will use a combination of experimental and theoretical techniques to explore atomic-scale defect chemistry on technologically important surfaces, with the goal of determining the salient factors that control defect chemistry. The formation, mobility, reactivity, and dissolution of atomic-scale surface defects play important roles in materials areas such as catalysis, corrosion, thin-film growth, semiconductor processing, sensors, and magnetic devices. Important defects include single adatoms, surface steps and kinks, dislocations, and vacancies. It is generally believed that a small number of localized surface defects may be particularly reactive and thereby dominate the surface chemistry of many materials. While past studies of this important problem have been limited by an absence of appropriate experimental probes for imaging atomic-scale defects, the recent advent of specialized scanning probe microscopies largely overcomes this problem and now allows more detailed studies of defect chemistry than previously possible. The unique atom-tracking scanning-tunneling microscope (AT-STM) recently developed at Sandia is a particularly powerful new technique that allows measurement of atomic-scale kinetic processes on a time scale that is more than three orders of magnitude faster than previous techniques. Similarly, a lack of sufficient computing power has severely limited previous theoretical studies of defect properties. The recent development of massively parallel (MP) computational techniques at Sandia, which now allow calculations on systems containing hundreds of atoms per unit cell, will enable studies of surface defects with a level of detail and sophistication far greater than previously possible. By studying well-defined, well-ordered surfaces, we can greatly simplify the study of defect chemistry and obtain detailed fundamental information on defect formation and reactivity. Coupling experimental results with theoretical studies will allow the development of models that explain, predict, and ultimately help to control surface defect reactivity.

We designed and built a new STM for investigation of adsorbate kinetics on metal substrates. This microscope has the capability to perform atom-tracking studies and will be used to study local reactivity at well-characterized defect sites.

We performed STM investigations of the modification of dislocation networks present on strained metal films upon controlled exposure to molecular oxygen. Our study shows that oxygen reacts with a two-monolayer copper (Cu)-strained film, at first only at threading dislocations, and then through the modification of the film mesoscopic structure and removal of atoms from the film. The process responsible for these changes, which is consistent with our STM observations, is the local extraction of the Cu atoms from the film due to oxygen atoms.

We deposited magnesium vanadate and bismuth molybdate films on Si(100) substrates and investigated the effects of deposition variables such as temperature and oxygen pressure on film composition and structure. Initial results are leading us to improved methods for deposition that will allow us to accurately reproduce mixed metal-oxide stoichiometries and orientations of desired crystalline phases.

We studied the perfect interfaces between Al_2O_3 ultra-thin films and Al(111), Mo(110), and Ru(001), discovering that the driving factor in interface geometry is the strong chemisorption of oxygen. In preparation for studying adsorbate interactions with surface dislocations, we computed atomic adsorbates H, O, and S on 1ML Cu/Ru(001), and compared the results to ordinary Cu and to Cu strained at the Ru lattice constant. These calculations are helping us to understand the roles of strain versus chemical effects in binding.

Publications

Refereed

Carpinelli, J. M., and B. S. Swartzentruber. 1998. “Detailed Energetic Interactions of Adsorbed Si Dimers on Si(001).” *Surf. Sci.* **411**: L828.

3502.320

Exploiting LENS Technology Through Novel Materials

J. A. Brooks

Laser-Engineered Net Shaping (LENS™) is a direct fabrication process in which metal powders are deposited into a laser-melted pool, with succeeding layers deposited to build up complex engineering shapes. This process is a rapid, low-cost, low-footprint, direct fabrication technique that lends itself to the concept for advanced manufacturing. However, previous work developed LENS™ as an advanced manufacturing tool rather than exploiting its potentially unique attributes. These attributes include real-time control of microstructure, tailored material properties at different locations in the same part, the production of graded thermal expansion parts, etc. This project seeks to develop a science–based approach to utilize LENS™ to process for properties in a controlled fashion, or for the production of components that cannot be made using other methods. Three materials—a tool steel with an optimized structure/property mix, a graded structure based on stainless-steel compositions, and a ceramic-to-metal transition—are novel material systems through which we will investigate and exploit LENS™.

We will achieve this goal by first developing a thorough understanding of the process in terms of how it impacts solidification and solid-state microstructure development. Additionally, we will study and understand the unique attributes and capabilities of the LENS™ process. From this knowledge base, we will design and produce a suite of experimental materials and structures that optimally exploit the LENS™ process and demonstrate its unique potential. We will develop an understanding of the residual stresses in LENS™ parts and what mitigation techniques may be available.

We used a tool steel to determine critical metallurgical-related aspects of the LENS™ process that are required to exploit the technology in the development of novel structures. We determined the parameter space in which good-quality structures could be fabricated, and we measured the thermal cycles associated with these parameters using thermocouple techniques. These (first-ever) thermal measurements showed that high cooling rates on the order of 10^{3}°–10^{4}°K/s are developed and are critical to the development of many novel microstructures. We also evaluated other noninvasive thermal measurement techniques that appear promising for process and microstructure control. We determined the range in scan speeds and subsequent solidification velocities and thermal gradients that can be achieved and that are required input parameters to the solidification and microstructural models. We developed a microstructural, carbide-coarsening model that we are integrating with process thermal models, validating with the experimental results, and using to predict hardness and tensile strength of H13 tool steel. We conducted characterization of the H13 microstructure and properties for model development and comparison with model prediction. We also evaluated experimental techniques to determine the magnitude of residual stresses that can lead to part distortion. We used a holographic hole-drilling technique to show that the residual stresses in 316 stainless steels were close to yield-strength values. An outstanding feature of this technique is its ease of data collection in time and effort. We also measured residual stresses as a function of process parameters in a series of H13 tool steel samples, which will serve as a comparison to future finite-element model predictions.

Publications

Refereed

Griffith, M. L., M. E. Schlienger, L. D. Harwell, M. S. Oliver, M. D. Baldwin, M. T. Ensz, J. E. Smugeresky, M. Essien, J. A. Brooks, C. V. Robino, W. H. Hofmeister, M. J. Wert, and D. V. Nelson. 1998. "Thermal Behavior in the LENS Process." *Proc. Solid Freeform Fabrication Symp.* (Austin, TX, 10–12 August).

Schlienger, M. E., D. Dimos, M. Griffith, J. Michael, M. Oliver, T. Romero, and J. E. Smugeresky. 1998. "Near Net-Shape Production of Metal Components Using LENS." *Proc. 9th Solid Freeform Fabrication Symp.* (Honolulu, HI, 12–16 July).

Schlienger, M. E., J. Brooks, M. Griffith, M. Oliver, T. Romero, and J. E. Smugeresky. 1998. "Laser-Engineered Net Shaping." Paper presented to the Automotive Applications of Thermal Spray Technology Conference, Romulus, MI, 3 June.

THIS PAGE
INTENTIONALLY BLANK

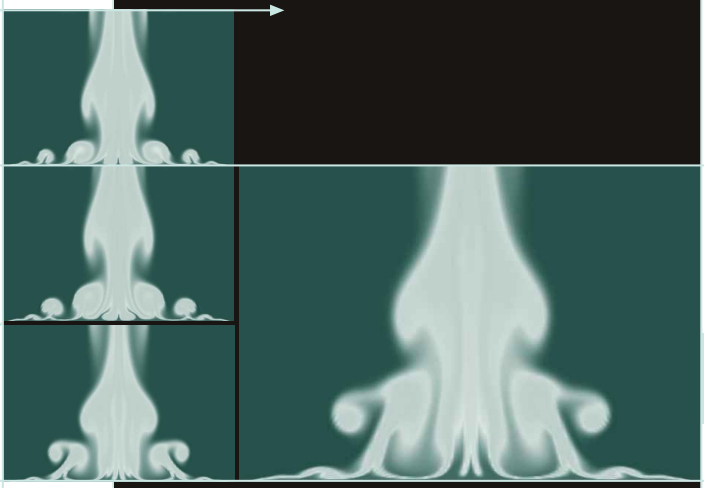

COMPUTER SCIENCES

Computer Sciences projects seek to develop revolutionary capabilities in high-performance computing and simulation technologies that work at systems levels. Computer Sciences consists of three research areas: (1) development of distributed computing technologies that will enable computing at the 30- to 100-teraflop scale; (2) development of technologies that address key science and engineering challenges related to massively parallel (MP) computing, algorithms, systems software, virtual environments, and advanced simulations; and (3) the encouragement of the development of revolutionary ideas in computational and computer sciences and mathematics. The DOE Accelerated Strategic Computing Initiative (ASCI) is also an important area of emphasis.

The advent of large, MP supercomputers led to modeling more complex problems, particularly turbulent, chemically reacting flows, but the process became mired in thousands of equations, preventing focusing on the real issues. Aztec, an MP software library that grew out of a chemically reacting flow project called MPSalsa, made the modeling easier. It helped solve very large, chemically reacting flow problems, now containing tens of millions of unknowns, on large-scale parallel machines. Engineers use MP supercomputers to solve scientific computing problems that previously were nearly unsolvable. Aztec was ported to the new Sandia-Intel Teraflop Computer, which has achieved applications of over 200 gigaflops. Aztec has helped to make parallel computing the standard platform for large-scale simulations and design codes.

Industry and universities use Aztec for groundwater flow with toxic-waste transport modeling, heat-transfer modeling for manufacturing processes, nuclear material nonproliferation studies, cardiac defibrillation simulations, compressible-flow calculations for hypersonic vehicles, automotive tire manufacturing design calculations, fire simulations, and more. There are now over 400 external research licenses for the Aztec library.

The Aztec library is part of Sandia's leading-edge scientific simulation capabilities. The Aztec project won an R&D 100 Award, and the MPSalsa code was a finalist in the Gordon Bell Competition for high-performance scientific simulation on parallel supercomputers. This technology has had a huge impact on ASCI and on parallel computing technology

THIS PAGE
INTENTIONALLY BLANK

3504.090

Gradient-Driven Diffusion of Multi-Atom Molecules Through Macromolecules and Membranes

G. S. Heffelfinger, A. P. Thompson, D. J. Hobbs, D. M. Ford

The goals of this work are threefold: (1) to develop a method for modeling diffusion of multi-atom molecules through macromolecules under conditions of a chemical potential gradient, (2) to develop a companion parallel algorithm, and (3) to apply the new method to three sample problems. Currently, no such method exists. Therefore, many important industrial and technological materials problems where gradient-driven diffusion of multi-atom molecules is the predominant phenomenon are beyond the reach of today's molecular simulation, including the three that we plan to study. These are (1) diffusion in polymers, (2) chiral polymer membranes for separating racemic mixtures, and (3) the permeation of drug analogs through lipid bilayers.

We finished extending the method to model gradient-driven diffusion through bonded (macromolecular) systems. Other work included enabling the insertion and deletion of small multi-atomic species. This will allow steady-state gradients to be established for small multi-atomics (e.g., O_2) diffusing through polymers (e.g., isobutylene). We investigated this system (O_2 diffusing in isobutylene) with the method.

We also developed and prototyped a method of establishing chemical potential gradients of larger multi-atomic species without carrying out insertions and deletions. We accomplished this by adding two pistons to the system to control the pressure on each end of the system. We then prototyped the method on a binary atomic system.

Publications

Refereed

Ford, D. M., and G. S. Heffelfinger. 1998. "Massively Parallel Dual-Control Volume–Grand Canonical Molecular Dynamics with LADERA. II. Gradient-Driven Diffusion Through Polymers." *Molecular Phys.* **94** (15 July): 673.

Heffelfinger, G. S., and D. M. Ford. 1998. "Massively Parallel Dual-Control Volume–Grand Canonical Molecular Dynamics with LADERA. I. Gradient-Driven Diffusion in Lennard-Jones Fluids." *Molecular Phys.* **94** (15 July): 659.

Thompson, A. P., D. M. Ford, and G. S. Heffelfinger. 1998. "Direct Molecular Simulation of Gradient-Driven Diffusion." *J. Chem. Phys.* **109** (15 October): 1.

Thompson, A. P., D. M. Ford, and G. S. Heffelfinger. 1998. "Direct Molecular Simulation of Gradient-Driven Diffusion." *Proc. 9th CIMTEC–World Congress and Forum on New Mater.* (July) (Florence, Italy, 14–19 June).

Van Swol, F., and G. S. Heffelfinger. 1996. "Gradient-Driven Diffusion Using Dual-Control Volume–Grand Canonical Molecular Dynamics (DCV–GCMD)." *Proc. Mater. Res. Soc. Symp.* **408** (Boston, MA, November): 299.

Other

Ford, D. M., and G. S. Heffelfinger. 1997. "Gradient-Driven Diffusion of Small Penetrants in Polymers Using Dual-Control Volume–Grand Canonical Molecular Dynamics (DCV–GCMD)." Paper presented to the Spring Meeting of the American Physical Society, Kansas City, MO, 17–21 March.

Ford, D. M., and G. S. Heffelfinger. 1997. "Modeling Gradient-Driven Diffusion of Small Molecules in Polymers with Dual-Control Volume–Grand Canonical Molecular Dynamics (DCV–GCMD)." Paper presented to the American Institute of Chemical Engineers Conference, Los Angeles, CA, 17–21 November.

Ford, D. M., A. M. Thompson, P. I. Pohl, and G. S. Heffelfinger. 1998. "Gradient-Driven Diffusion of Liquids and Adsorbed Fluids Using Dual-Control Volume–Grand Canonical Molecular Dynamics." Paper presented to the 5th LIBLICE Conference on the Statistical Mechanics of Liquids, Zelzna Ruda, Czech Republic, 7–12 June.

Heffelfinger, G. S. 1996. "Dual-Control Volume–Grand Canonical Molecular Dynamics." Paper presented to the 4th Joint Conference on Computational Mathematics, Chelyabinsk, Russia, 20–24 May.

Heffelfinger, G. S., and F. van Swol. 1995. "Diffusion in Non-Ideal Mixtures Using Dual-Control Volume–Grand Canonical Molecular Dynamics." Paper presented to the American Institute of Chemical Engineers Conference, Miami Beach, FL, 13–17 November.

Thompson, A. P., and G. S. Heffelfinger. 1998. "Molecular Dynamics Simulation of Gradient-Driven Diffusion in Binary Mixtures: Comparison of Chemical Potential and Osmotic Pressure Approaches." Paper presented to the American Institute of Chemical Engineers Conference, Miami Beach, FL, 15–20 November.

Thompson, A. P., M. G. Martin, and G. S. Heffelfinger. 1998. "Molecular Simulation of Nonequilibrium Gradient-Driven Transport Processes: Gas Permeation in Rubber Polymers." Paper presented to the American Institute of Chemical Engineers Conference, Miami Beach, FL, 15–20 November.

3504.010

Parallel Quantum Chemistry for Material Aging and Synthesis

C. F. Melius, E. J. Friedman-Hill, E. T. Seidl, J. L. Durant, Jr.

Computer simulations must increase their role in design, certification, and maintenance of weapons systems as budgets shrink, yet design cycles shorten. Massively parallel (MP) computers offer the promise of predicting the aging of materials and optimizing the synthesis of new materials. Sandia is developing a new hybrid quantum chemistry (QC) procedure for accurately calculating the thermochemical properties of these materials. The procedure will incorporate a combination of density-functional–based (DFT) methods and Hartree-Fock–based methods (HF, MP2), using various basis sets for each calculation step. We will implement all methods to run on the MP machines as well as on distributed shared-memory machines. We will employ intelligent agents to balance the workload between machines and methods.

This project will have a major impact on the Accelerated Strategic Computing Initiative (ASCI) program. It will provide the computational QC methods necessary to treat the chemical degradation process occurring in the aging of the nuclear stockpile, including polymers, energetic materials, adhesion, and corrosion. The developed procedures will aid in the processing of new materials, such as semiconductors, protective coatings, and ceramics, coupling the molecular level to equipment design and process optimization. The thermochemistry will also aid in the areas of chemical warfare agent destruction, environmental cleanup, and waste minimization. This project will enable the MP machines to be effectively harnessed by QC applications. Furthermore, the resulting process for implementing multiple coupled codes, using intelligent agents to maximize the effectiveness of MP machines, will have spin-offs to other Sandia applications requiring complex computer simulation modeling.

We successfully developed a bond-additivity-correction (BAC) procedure that can be applied to a variety of QC methods that will provide accurate thermochemical properties. The procedure includes atomic and spin–based corrections in addition to the bond–based corrections. The procedure works on the DFT methods as well as on the Möller-Plesset perturbation theory methods at second order and fourth order. We also showed that it works on the G2 method, itself a composite of QC methods. The key to the correction is the use of a correction for an electron geminal (or electron pairing). This would occur not only when a chemical bond is formed, but also when a negative ion is formed. Thus, the procedure will work for charged as well as neutral species. We found that the corrections are very basis-set-dependent. For the large basis sets, the correction can be negative, particularly for ionic bonds. For quantum chemical methods that are already quite accurate, we found that the correction parameters need only depend on the atom types involved, rather than on the bonds themselves. This provides a bootstrapping procedure for obtaining the correction factors for lower levels of theory, using the higher levels of theory as references.

3504.020

Modeling Complex Turbulent Chemically Reacting Flows on Massively Parallel Supercomputers

J. N. Shadid, T. M. Smith, S. P. Burns, A. G. Salinger, A. R. Kerstein, R. C. Schmidt, R. J. Cochran, K. D. Devine

This project will develop a massively parallel (MP), adaptive, unstructured finite-element (FE) code for simulating 3-D high-Reynolds-number and turbulent chemically reacting flows in complex geometries. Important applications of such flows include the "crash-and-burn" scenario for safety calculations for nuclear weapons transport and storage (Accelerated Strategic Computing Initiative [ASCI]-related); jet-mixed chemical reactor design; internal combustion engine analysis; high-performance compact heat-exchanger design for aircraft, automobiles, and chemical process plants; and high-temperature combustion process modeling for the destruction of hazardous waste. Currently, these large, multiple length- and time-scale problems can be solved only in 2-D for a limited number of species because of the required computational resources. These difficult problems strongly couple turbulent momentum, thermal energy, and mass transfer with chemical reaction kinetics, making current 2-D models unsuitable. We constructed the simulation code on the foundation of an existing, successful, 3-D MP chemically reacting flow-simulation code (MPSalsa). State-of-the-art engineering models for reaction kinetics in turbulent flow, thermal radiation in participating media, and advanced turbulence models for fluid flow and heat and mass transfer will be added to MPSalsa. We will also add MP adaptive mesh methods, dynamic load-balancing techniques, high-order convection stabilization methods, and subgrid turbulent reaction models to enable the sharp resolution of steep gradients and multiple length scales in the flow. With the proposed code development, MPSalsa will be capable of solving very large, strongly

coupled multiphysics turbulence problems with multiple time and length scales. This tool will be immediately useful for Sandia's weapons program responsibilities (ASCI) as well as many advanced engineering technology problems for U.S. industry. As a result, Sandia's recognized leadership role in large-scale multiphysics complex system simulation will be greatly strengthened, as will the capabilities of other interested federal agencies (DOE, DoD) and U.S. industry.

We successfully completed the following: (1) the implementation in MPSalsa of the participating media radiation model—a discrete ordinates method capable of treating variable property flows, (2) the implementation in MPSalsa and testing of the higher-order hydrodynamic turbulence model—this is a large eddy simulation (LES) model with both a Smagorinski and a *k*-equation-type subgrid model, (3) the calculation of a benchmark participating media radiation problem, and (4) the implementation of a dynamic equal order refinement and a general solution/grid transfer capability into MPSalsa.

The implementation of a higher-order turbulent species mixing and reaction model (the linear eddy model) is nearing completion and will soon be ready for testing. We will also soon complete local mesh adaptivity (*h*-refinement) and the associated dynamic load-balancing capability.

Publications

Refereed

Devine, K. D., J. N. Shadid, A. G. Salinger, S. A. Hutchinson, and G. L. Hennigan. 1997. "Parallel, Adaptive Finite-Element Methods for Chemically Reacting Flow Simulations." *Proc. ACM/IEEE SC '97 Conf.* (San Jose, CA, 15–21 November).

Devine, K. D., J. N. Shadid, A. G. Salinger, S. A. Hutchinson, and G. L. Hennigan. 1998. "Toward Parallel Adaptive Mesh Refinement for Chemically Reacting Flow Simulations." *Proc. 10th Internat. Conf. on Finite Elements in Fluids* **1** (Tucson, AZ, 5–8 January): 285–290.

3504.050

Automated Geometric Model Builder Using Range Image Sensor Data

C. F. Diegert, L. M. Doran, J. T. Sackos

Sandia's goal is to develop algorithms that automatically construct realistic 3-D models of physical environments based on range and optical reflectance information collected with Sandia's scannerless range imager (SRI). We will design algorithms to analyze and reduce the complexity of the data collected from multiple range images taken from different perspectives, recognize and eliminate redundancies in the images, and integrate them into a simplified geometric model. The resulting model will be compatible with virtual reality (VR) and computer-aided design (CAD) software. The algorithms will be flexible enough to accommodate massively parallel processing (MPP) for national security applications involving large volumes of data. The SRI is a unique camera system invented and patented by Sandia that provides distance and reflected light intensity to each pixel in a field of view (FOV). It has no moving parts and is built with off-the-shelf (OTS) components. The resulting capabilities could be used to rapidly survey unknown terrain or hazardous environments, monitor remote sites for security, plan clandestine activity, and enhance the ability of robotic systems to move about an environment based on a 3-D model.

Our field experimentation work demonstrates our greatly improved SRI instrument and visualization algorithms, and our new ability to achieve a quick-turnaround 3-D data rendering on a transportable system. The 0.1-inch-range accuracy we established in this experiment generated a lot of excitement and outside interest, and in the context of reaching our automatic model-building goals, it demonstrated our new statistical fitting capabilities. We could not have established the 0.1-inch accuracy without first fitting the planar surface models of the test calibration targets. Beyond simple fitting tasks are the automatic model-building capabilities we obtain by applying fitting and segmentation algorithms together. We produced both fitted plane models and trimming curves. While the considerable extra trouble of obtaining trimmed models was unnecessary for establishing a simple accuracy measure, it did allow us to present computer-generated imaging of the fitted models and of the residuals about the model. That is, adding the trimming summarizes the raw range-imaging information in a manner that helps us obtain insight from these data. We need the trimming information to produce fully formed models that load into a CAD or VR system. During the past year we also added the capability to write summary models to DXF-format files.

3504.060

A Massively Parallel Sparse Eigensolver for Structural Dynamics Finite Element

G. M. Reese, D. M. Day, R. S. Tuminaro

Structural dynamics finite-element (FE) analysis is critical to applications in weapons, nonproliferation, space sensors, and computational manufacturing. Sandia recently accepted stringent new requirements essential to meet DOE obligations for stockpile stewardship without nuclear testing. These applications require modeling and simulation with unprecedented fidelity and accuracy. Such capabilities are building blocks for design optimization, model validation, nondeterministic design, and virtual testing for weapons and other defense programs. While Sandia developed several codes for nonlinear structural mechanics, we are developing for the first time a structural dynamics FE code with both frequency and time-domain solution capabilities for vibration and late-time shock-response problems. This code requires an essential component: a massively parallel (MP) eigensolver. This eigensolver will enable the solution of high-fidelity structural dynamics models, as well as minimize the number of engineering approximations (which are prone to error, time-consuming, and difficult to automate). We developed an initial version of an MP structural dynamics eigensolver. A major hurdle in building this eigensolver was the integration of a sophisticated multilevel preconditioner needed to solve the extremely ill-conditioned linear subproblems required by the eigensolver. A new parallel FE code, SALINAS, is a direct outgrowth of this project. We integrated the new MP eigensolver into SALINAS. The combined code represents a fundamental advance in Sandia's structural dynamics FE analysis capabilities. Simple all-hex-element models have been solved in parallel with up to 800,000 equations (requiring one-half hour of computation) and confirm the scalability of the overall algorithm. The largest eigen-solution previously performed at Sandia involved fewer than 200,000 equations. Our project addressed two critical tasks: improvement (robustness, memory, computation time) of kernel algorithms within the iterative linear solver, and extension/application of the overall iterative algorithm to more realistic structural dynamics problems containing both constraint equations and more complex discretization schemes.

• We developed a sophisticated structural dynamics linear and eigensolver based on the Finite-Element Tearing and Interconnecting (FETI) parallel multilevel linear system solution method and the PARPACK parallel Krylov-subspace–based eigensolver. FETI methods are multilevel iterative methods developed for structural dynamics, an application area in which iterative methods have not previously been successful. We explored reorthogonalization methods leading to increased robustness. We incorporated this solver into the SALINAS parallel FE/structural dynamics code developed separately at Sandia and improved the combined solver. We addressed domain decomposition issues related to convergence and robustness. We developed a new graph partitioner that eliminates spurious subdomain mechanisms and aligns subdomain boundaries with critical material interfaces. Similar functionality will be available in future versions of the CHACO graph partitioning package that is widely available. These enhancements make possible robust subdomain pseudo-inverse calculation and substantially enhance the scalability of the FETI linear solver. We modified the coarse grid solver so an approximation of the operator is solved on the coarse space. We now accomplish the coarse solve by forming the sparse coarse linear system and applying a sparse direct linear solver. We also developed a prototype code that handles multipoint constraints in two ways: Intersubdomain constraints are reduced out, and intrasubdomain constraints are included in the second level of the multilevel solver.

• We solved representative model structures problems (2 million unknowns). This includes both solving static problems and computing a few of the lowest modes. We developed a strategy to determine missed modes and will include it in a future release of PARPACK. We have developed the functionality to analyze floating substructures in a prototype code only.

Publications

Refereed

Day, D. 1996. "A Basic Parallel Sparse Eigensolver for Structural Dynamics." Paper presented to the SIAM National Conference, Palo Alto, CA, November.

3504.070

Density-Functional Theory for Classical Fluids at Complex Interfaces

L. J. D. Frink, E. R. Lindgren, K. D. Devine, A. G. Salinger

The primary objectives of this project were to develop a code for modeling inhomogeneous fluid systems in 2-D and 3-D geometries and to demonstrate the utility of the code. Sandia used the first two years to identify and solve several test problems with an initial 1-D code, develop the computational strategies for several types of model systems, and implement an initial parallel 2-D/3-D capability. Final-year efforts focused on improving the algorithms to achieve up to one–two orders-of-magnitude speed-up, applying the code to problems in 2-D with more complex surfaces than have ever been studied with a nonlocal density-functional theory (DFT), and cultivating application areas including corrosion

(Accelerated Strategic Computing Initiative [ASCI]), competitive adsorption in zeolites, sensors, self-assembly, colloidal systems, surface forces/adhesion, and emerging threats/computational biology. As a result of this project, Sandia now has a unique capability for modeling inhomogeneous fluids for applications ranging from processing of nanoscopically tailored materials to materials aging to emerging threats/biological warfare (BW).

In the first year of this project, accomplishments centered on developing a 1-D code and applying that code to a variety of materials problems. In year two, the applications work continued, but code development efforts shifted to a new 3-D code (called TRAMONTO), and we completed an initial parallelization. In the final year, applications work focused on systems that need a 2-D code. We made several improvements to the algorithms to achieve very efficient parallel 2-D solves. In addition, we completely rewrote the previous year's parallelization to improve memory handling and code scaling for 3-D applications. By the end of the year, focus had shifted to 3-D applications. These capabilities are having a great impact both inside and outside of Sandia.

While we initially developed a 2-D/3-D parallel code, the outlook for the code was uncertain because of the complexity of the needed Jacobian fill. To demonstrate a viable method, it was therefore necessary to improve the performance of the fill algorithm. We achieved this by implementing nonuniform meshes, coarsened Jacobians, and approximate Jacobians. The result was that the fill can now be performed 10–100 times faster (depending on the particulars of the underlying mesh) than was possible with the earlier algorithms. These improvements provided immediate access to a wide range of 2-D problems. Two systems previously studied extensively as test cases were cylindrical polyelectrolytes in electrolyte solutions, and wetting and self-assembly at chemically heterogeneous (striped) surfaces.

Even with the improved Jacobian fill routines, all but the simplest 3-D applications remained out of reach due to a non-optimal initial parallelization. As a result, we rewrote the parallelization. The latest version of the code scales linearly with the number of processors, and real 3-D applications are within reach.

In addition to working on improved algorithms for TRAMONTO, we also cultivated application areas for future work with this code. Those application areas of most interest to Sandia include corrosion (ASCI), competitive adsorption in zeolites, sensors, self-assembly, colloidal systems, surface forces/adhesion, and emerging threats/computational biology. The impact of this work is being felt outside as well as inside Sandia. Inquiries from many sources have focused on these modeling capabilities, including modeling gas adsorption, modeling disk drive performance, modeling adsorption in random porous media, modeling drying of porous materials, and modeling ion-channel proteins. As a result of this project, Sandia now has a unique capability for modeling inhomogeneous fluids for applications ranging from processing of nanoscopically tailored materials to materials aging to emerging threats/BW.

Copyright and licensing for TRAMONTO were begun by the end of calendar year 1998.

Publications

Refereed

Frink, L. J. D., and A. G. Salinger. 1998. "Wetting of a Chemically Heterogeneous Surface." *J. Chem. Phys.*, submitted.

Frink, L. J. D., and F. van Swol. 1998. "A Common Theoretical Basis for Surface Forces Apparatus, Osmotic Stress, and Beam Bending Measurements of Surface Forces." *Colloids and Surf. A*, submitted.

Frink, L. J. D., and F. van Swol. 1998. "Solvation Forces Between Rough Surfaces." *J. Chem. Phys.* **108** (1 April): 5588–5598.

Samuel, J., C. J. Brinker, L. J. D. Frink, and F. van Swol. 1998. "Direct Measurement of Solvation Forces in Complex Microporous Media: A New Characterization Tool." *Langmuir* **14** (22 April): 2602–2605.

Other

Frink, L. J. D. 1997. "Capillary Condensation and Adhesive Pull-Off Forces." Paper presented to the Annual Fall Meeting of the American Institute of Chemical Engineers, Los Angeles, CA, 20 November.

Frink, L. J. D., and A. G. Salinger. 1998. "Calculating Solvation Forces and Adsorption in Complex Geometries with a Finite Element–Nonlocal Density-Functional Theory." Paper presented to CIMTEC '98, World Ceramics Congress and Forum on New Materials, Florence, Italy, June.

Frink, L. J. D., and A. G. Salinger. 1998. "Solving Nonlocal Density-Functional Theories in Geometries Without Convenient Symmetries." Paper presented to the LIBLICE Conference on the Statistical Mechanics of Liquids, Zelzna Ruda, Czech Republic, 7–12 June.

Frink, L. J. D., A. G. Salinger, and F. van Swol. 1997. "Beyond DLVO Theory and the Yukawa Potential for Simulation of Colloidal Systems." Paper presented to the Annual Fall Meeting of the American Institute of Chemical Engineers, Los Angeles, CA, 18 November.

Frink, L. J. D., A. G. Salinger, and F. van Swol. 1997. "Density-Functional Theory for Classical Fluids on Parallel Computers." Paper presented to the Annual Fall Meeting of the American Institute of Chemical Engineers, Los Angeles, CA, 18 November.

3504.120

Fast and Easy Parallel I/O for Efficient Scientific Computing

J. E. Sturtevant, M. L. Barnaby, D. N. Sands, R. A. Haynes

The performance of input/output (I/O) subsystems on massively parallel (MP) computers lags the computational power of these machines. I/O includes data transfer to and from disks, archival storage, and networks. New algorithms and approaches to I/O are necessary to compensate for the imbalance between I/O and computational performance. In this project, Sandia will develop new tools and algorithms that allow applications programmers to use I/O resources easily and efficiently and will work with the ALEGRA and PRONTO groups to test these ideas in important Sandia applications on the Teraflop machine. Deliverables will include (1) an I/O research platform on which new application interfaces, libraries, and algorithms for I/O can be incorporated and tested, (2) an I/O library with a simple, general-purpose interface for application programmers, (3) a higher-level I/O library for finite-element (FE) applications, and (4) optimal data layouts for efficient data retrieval based on common or user-specified access patterns.

We will focus on collective I/O, i.e., coordinated requests from many processors, because of the increased potential for efficient use of disk and tape systems. Programs that require out-of-core computation or frequent checkpointing should see significant performance improvement due to lower I/O overhead. Moreover, new I/O capabilities developed in this project will allow larger simulations to be run, reduce the computer time required for these simulations, eliminate the long file-recombination processor prior to visualization, and reduce the programming time to develop new applications. In sum, the Accelerated Strategic Computing Initiative (ASCI), model simulation–based life-cycle engineering (MSBLCE), and warhead protection program (WPP) codes will be able to solve bigger problems than would otherwise be possible, and they will run faster while doing so.

We progressed toward the ultimate goal of having a scalable parallel I/O (PIO) library that simulation and visualization applications can use to transfer massive amounts of data among memory, disks, and tape archive. The research done by this project has affected both ASCI problem-solving environment (PSE) and DisCom plans.

We established a solid software infrastructure, delivering a usable, high-performance PIO library for Sandia unstructured-grid FE applications. We continue to improve the low-level collective disk I/O library that supports efficient transfers of locally permutable data arrays with minimal buffering requirements and the mid-level parallel data set (PDS) management library that supports collective, random access of primitive FE data arrays.

Specifically, we accomplished the following:

(1) Designed and implemented an additional library, PXI (Parallel eXodus Interface), to provide a higher level of abstraction for both simulation and visualization applications. Based on our initial experience integrating PDS/PIO into simulation and visualization applications, we identified the need for a higher level of abstraction. Applications using the eXodus II data format expected a high-level application programming interface (API) and thus can be more easily transitioned to PXI.

(2) Integrated the PIO library, PXI/PDS/PIO (Parallel eXodus Interface/Parallel Data Set/Parallel I/O) into ALEGRA and PRONTO. Initial observations from ALEGRA using the current parallel file system (PFS) on the Teraflop indicate at least a fourfold speedup in I/O.

(3) Adapted two visualization packages, MUSTAFA (a Sandia-specific AVS/Express project) and EnSight (a commercial visualization tool) to read the new file format, PXI (PDS).

(4) Instrumented the PIO library to measure performance of the lowest-level I/O functions.

(5) Improved the PDS interface based on experience with PXI.

Publications

Refereed

Sturtevant, J., M. Christon, P. D. Heermann, and P. C. Chen. 1998. "PDS/PIO: Lightweight Libraries for Collective Parallel I/O." *Proc. Supercomputing 1998*, accepted.

3504.130

Novel Load-Balancing for Scalable, Parallel Electromagnetic and Plasma Physics Simulation Software

M. L. Kiefer, R. S. Coats, L. P. Mix, Jr., M. F. Pasik, D. J. Riley, D. B. Seidel, S. J. Plimpton

Electromagnetic particle-in-cell (EM-PIC) simulation techniques are used to address many Sandia National Security (NS) areas and Accelerated Strategic Computing Initiative (ASCI) applications. These include simulation of neutron generators, weapon response to hostile x-ray environments, Z-pinch (x-ray) accelerators, radiography

systems for weapon primaries, and high-power microwave devices. EM-PIC simulates the time-response of EM fields and low-density plasmas in a self-*consistent manner (the fields push the plasma, and the plasma self-current modifies the fields). We currently use the Sandia QUICKSILVER/VOLMAX code suite for these applications, but it does not yet have the scalability required to perform full system-level simulations on thousands of nodes as required for ASCI applications. The chief obstacles are load-balancing the computations due to the nonuniform, time-dependent density of particles on the grid and the use of different numerical algorithms and cell types in various grid regions. We will test and implement novel methods to achieve a fully parallelized scalable code and have devised two potential candidates. The first is a static method that divides the grid into many more subdomains than nodes and assigns them to nodes so that, on the average, each node has nearly equal amounts of computation per time-step. The second is a dynamic method where weighted subdomains will migrate as needed between nodes to address the changing workload due to particle motion. We will also automate setup for parallel execution as well as parallelize diagnostics.*

Both QUICKSILVER and VOLMAX are now running. We implemented the full static decomposition method in QUICKSILVER for both pure EM and EM-PIC plasma simulation using hundreds of processors. This represents a significant advancement over the previous year's accomplishment, where only a subset of QUICKSILVER's full capabilities was available for the parallel version. Our testing showed that this version will work at the tera-scale level (thousands of processors), but difficulties in getting such simulations through the queues in a timely manner have delayed performing them. We believe this version of QUICKSILVER is capable of EM and EM-PIC simulations well beyond any other such codes.

The QUICKSILVER preprocessor performs static 3-D decompositions of multiple-block rectilinear grids into general rectangular subdomains. Detailed studies of this decomposition scheme show that parallel efficiency on the Red machine is acceptable for very small subdomain sizes. Sizes as few as 3000 for the sum of the cells and particles work well. These results demonstrate that over-partitioning techniques (many more subdomains than nodes) will not fail because of excessive communication time. Testing also showed that communication overhead is acceptable with eight partitions per node on 64 nodes. Our next step is to implement and test in QUICKSILVER a dynamic load-balancing technique. This will extend the general static method to a dynamic method that migrates subdomains when load imbalances appear.

We parallelized a significant portion of QUICKSILVER's extensive diagnostic capabilities this year while retaining our efficient data file format. This allows us to use our sophisticated data analysis tools. Now the code can be used for massively parallel (MP) production-level simulation and analysis. This parallel file creation capability uses Sandia's parallel data set/parallel input/output (PDS/PIO) library and has proven to be robust and easy to use.

Many spin-offs of this research have improved the general state of QUICKSILVER. First, we discovered a new PIC data-handling method that increases computational speed by making better use of central processor unit (CPU) caches. Second, we found that as the subdomain size is reduced, we reach the point where data for an entire subdomain fits in the CPU cache, resulting in a sharp increase in performance. This occurs well before the subdomain size reaches the point where communication overhead begins to significantly reduce performance. Third, the new message-passing algorithms for repairing data on the surface of each subdomain with data from the interior of another subdomain have proven to date to be more straightforward than those used for the shared-memory processing (SMP) version.

The unstructured grid portion of the VOLMAX code, where each node has exactly one subdomain, is now parallelized for EM simulation, and hundreds of processors have been used. We accomplished the grid decomposition into subdomains, using grids generated by the commercial I-DEAS software, using Sandia's CHACO/NEMESIS tools. The decomposition itself is performed in a parallel manner and is quite efficient. We will soon parallelize VOLMAX for hybrid grids (where portions of the grid are unstructured, others are rectilinear, and different time-step values are used in each type) for EM simulation with one subdomain per node.

In both QUICKSILVER and VOLMAX, extensive tests revealed subtle algorithmic sensitivities to parallel connection schemes for both rectilinear-grid particle-related data and unstructured-grid EM field data. We are currently investigating these problems. These sensitivities cause the simulation to become unstable. It is thought that the cause may be a small difference, possibly only the least significant difference, in data that are duplicated on different subdomains. We think that minor changes to the connection schemes will eliminate the problem; however, a complete understanding of these sensitivities is required.

3504.140

Parallel Computational Chemistry Using Constraints

T. D. Plantenga, C. F. Melius, S. J. Plimpton

Accurate computer estimation of material properties requires solving force-field equations for systems of up to a million covalently connected atoms. Covalent bonds are usually modeled as stiff harmonic potentials in the force fields. Our research shows they are the primary source of numerical difficulties in the computation of structures with minimum potential energy.

This project will develop advanced optimization algorithms for fast, robust computation of the local energy minima of large molecules. We will implement and test algorithms in three Sandia computational chemistry codes: LAMMPS (Large-Scale Atomic/Molecular Massively Parallel Simulator), CCEMD (Center for Computational Engineering Molecular Dynamics), and DEMoS (Distributed Extensible Molecular Simulation). Two of these, LAMMPS and DEMoS, require that the algorithms exploit distributed computing environments. An implicit Hessian method utilizing modified conjugate gradient will provide the basis for an unconstrained algorithm. A novel constrained optimization approach will aim to eliminate numerical ill-conditioning by substituting quadratic distance constraints for the stiff harmonic potentials. This technique is known to speed up molecular dynamics (MD) calculations by a factor of three, but has never been applied on a large scale to calculate energy minima.

We succeeded in adding minimization algorithms to LAMMPS, CCEMD, and DEMoS. The algorithms have already proved useful in Accelerated Strategic Computing Initiative (ASCI) work on estimating O-ring diffusion coefficients.

We implemented minimization algorithms and are already using them in LAMMPS to estimate O-ring diffusion coefficients. The research effort also expanded beyond original goals to pursue promising new ideas.

We upgraded the unconstrained implicit Hessian conjugate gradient–based algorithm to support version 4.0 of LAMMPS. We recast the same algorithm in object-oriented Java code for incorporation in the new DEMoS project. In collaboration with the Optimization Technology Center (OTC) of Northwestern University and Argonne National Laboratory, we tested a new preconditioner based on limited-memory BFGS concepts with the unconstrained algorithm. The preconditioner performed well, but needs more fine-tuning.

We implemented the Newton–based constrained minimization algorithm and tested it with the Sandia code CCEMD. We significantly enhanced performance by choosing constraints in a preprocessing step based on QR factorizations, and by utilizing sparse Cholesky factorizations during minimization. We had hoped that the constrained algorithm could be converted to a massively parallel (MP) format for integration into LAMMPS. We distributed vector and matrix objects and replaced the sparse Cholesky factorization with the Sandia AZTEC solver code. However, distribution of the constraints did not match the distribution of atoms chosen by LAMMPS, thus creating high communications costs on the Teraflop machine. Investigations with the preprocessing formula demonstrated that the constraint set cannot be altered without causing dramatic ill-conditioning. It is hoped that the more general distributed computing approach taken by DEMoS will allow unmatched atom and constraint distributions to communicate without high overhead costs.

We also tested remote optimization, in which we executed the computational chemistry and optimization algorithm codes on separate networks, linked only by occasional data transfers. This computing model provides security partitioning and some fault tolerance.

Publications

Other

Plantenga, T. D. 1998. "Fast Energy Minimization of Large Polymers Using Constrained Optimization." Sandia Technical Report SAND98-8251 (October). Sandia National Laboratories, Albuquerque, NM.

Plantenga, T. D. 1998. "Molecular Energy Minimization in Parallel Using Constraints." Paper presented to the American Mathematics Society Fall Western Sectional Meeting, Albuquerque, NM, November.

Plantenga, T. D. 1998. "Parallel Unconstrained Minimization of Potential Energy in LAMMPS." Sandia Technical Report SAND98-8201 (October). Sandia National Laboratories, Livermore, CA.

3504.160

Massively Parallel *Ab Initio* Validation for ASCI Materials Aging

C. F. Melius, C. L. Janssen, C. H. Tong

Sandia is undergoing a revolutionary transition from being a lab based on experimental testing to a lab based on predictive computational modeling. A central part of the Accelerated Strategic Computing Initiative (ASCI) is a detailed model–based understanding of the aging of weapon components. Such an understanding will require the simulation of molecular systems larger than have ever been studied at accuracies beyond the state-of-the-art, even for small chemicals. Currently, large-scale ab initio *quantum chemistry (QC) simulations are possible using the massively parallel (MP) Hartree-Fock (HF) and density-functional methods developed at Sandia. Unfortunately, these workhorse QC techniques do not have predictive accuracy for many of the chemical species formed in the aging of polymers and energetic materials (e.g., the peroxyl radicals formed in the aging of PETN). Chemically accurate predic-*

tions are possible with these methods if they are calibrated and if systematic corrections are developed that depend on the chemical system being modeled. Historically, these computer simulations were accurate QC methods, such as coupled-cluster theory, which approach the exact result with increased computational effort. The goal of the project is to provide methods for calibrating the workhorse simulation methods for the ASCI project and other Sandia programs by developing MP versions of more accurate, highly electron-correlated quantum chemical methods.

Also during this project, we will apply these parallel methods to several problems related to the chemical aging of high-energy weapon components. These benchmark calibrations will constitute some of the largest highly correlated QC calculations ever performed and will take full advantage of teraflop-scale parallel computing.

We implemented a program for the parallel computation of coupled-cluster singles and doubles with perturbative triples correction (CCSD[T]) in the C++ language. This is the first CCSD(T) program that uses a distributed data representation for all of the large coupled-cluster intermediates. We validated the program with a series of small molecules, including the PETN fragment CH3ONO2. In the course of our work, we discovered a serious flaw in the size-scaling of all currently used coupled-cluster diagnostics that causes the value of the diagnostics to be meaningless for most large chemical systems. We proposed an alternative diagnostic for the closed-shell case that shows the correct size-scaling, and demonstrated that the value of the diagnostic is indeed correlated with the accuracy of physical properties. We collaborated with the University of California–Berkeley to develop local-correlation methods. We developed the atoms-in-molecules (AIM) approach to local-correlation, applied it to the second-order Möller-Plesset framework, and carefully examined its convergence to the exact nonlocal methods.

3504.190

Integrated Quantum/ Classical Modeling of Hydrogenic Materials

J. G. Curro, R. M. Fye, F. B. Van Swol

This project concerns the modeling of quantum fluids with the path integral (PI) formalism. In the PI approach, Sandia will map quantum particles onto classical ring polymers that consist of beads connected by harmonic springs. The key observation is that ring polymers can be modeled by molecular simulation methods as well as by integral equation approaches, both of which are actively pursued in this effort. The molecular simulation methods focus hydrogen adsorption at single substrates, graphite slit pores, and nanotubes. We are also studying quantum sieving of tritium from a mixture of hydrogen. The integral equation methods consist of a self-consistent field theoretic extension of Polymer Reference Interaction Site Model (PRISM) theory to ring polymer fluids.

(1) *Single surfaces*. We made several comparisons between simulation and experiments for the adsorption of hydrogen isotopes onto a graphite substrate.

(2) *Confined fluids*. We performed a detailed study of hydrogen isotopes adsorbed into porous materials and found that quantum effects lead to a suppression of the capillary condensation transition.

(3) *Nanotubes*. We explored the hydrogen storage potential of nanotubes. In particular, we quantified the storage capabilities for hydrogen in porous graphite (using slit pores) and a variety of single-walled nanotubules (SWNTs). We can improve the latter's storage capability by exploiting the outer surface, as in arrays of SWNTs.

(4) We performed simulations on quantum sieving of tritium from tritium/hydrogen mixtures. Preliminary results confirm the existence of quantum sieving, whereby quantum effects can preclude the adsorption of the lighter isotopes.

(5) *PRISM calculations*. We wrote a computer code to treat polymer rings with PRISM theory. The program uses a self-consistent solvation potential to describe the correlations between different rings.

Publications

Refereed

Wang, Q., and J. K. Johnson. 1998. "Adsorption of Hydrogen in Graphite Slit Pores." *Internat. J. Thermophys., accepted*.

Wang, Q., and J. K. Johnson. 1998. "Hydrogen Adsorption on Graphite and in Carbon Slit Pores from Path Integral Simulations." *Molecular Phys.*, accepted.

Wang, Q., J. K. Johnson, and J. Q. Broughton. 1998. "Path Integral Grand Canonical Monte Carlo." *J. Chem. Phys.* **107** (1 January): 5108.

Yethiraj, A. 1997. "Conformational Properties and Static Structure Factor of Polyelectrolyte Solutions." *Phys. Rev. Lett.* **78** (1 January): 3789.

3504.170

Computational Methods for Coupling Microstructural and Micromechanical Materials Response Simulations

E. A. Holm, G. A. Knorovsky, C. C. Battaile, V. R. Vedula, M. D. Rintoul, T. E. Buchheit, R. M. Fye, G. W. Wellman, M. K. Neilsen, S. J. Glass, H. E. Fang

Computational materials simulations have traditionally focused on individual phenomena: grain growth, crack propagation, plastic flow, etc. However, real materials behavior results from a complex interplay between phenomena. Sandia will explore methods for coupling mesoscale simulations of microstructural evolution and micromechanical response. In one case, we will dynamically couple massively parallel (MP) simulations for grain evolution and microcracking in brittle materials. In the other, MP codes for domain coarsening and plastic deformation will be iteratively linked. This project will provide the first comparison of two promising ways to couple mesoscale computer codes. We will extend Sandia's MP PARGRAIN code to simulate microstructural evolution. To overcome the computational limitations of resolving crack-tip singularities, we take a three-tiered risk approach to fracture modeling. Initially, PARGRAIN will couple with the parametric GLAD model; later, with a more costly finite-element (FE) model with death elements; and finally, with a newly developed Element-Free Galerkin (EFG) model. Plastic flow is amenable to a conventional FE modeling approach. We will extend the constitutive relations used in the JAS3D–based crystal plasticity model to incorporate the appropriate flow mechanisms. Coupling microstructure and mechanics codes will require time synchronization, mesh matching, and information-passing algorithms appropriate to each case. We will experimentally validate the computer simulations on stockpile materials. We will study microcracking in brittle materials in the context of alumina used in stronglinks. We will study plastic deformation response in a silver-copper (Ag-Cu) eutectic braze alloy used in weapon components. This project will achieve the first experimentally validated model for plastic deformation and fracture in realistic, evolving microstructures. Moreover, this project provides the first full spatial and dynamic integration of computational models for coupled materials response phenomena. The mesh linkage and time-step synchronization techniques developed here will have applications in various simulation methods and will support Sandia's stockpile stewardship mission.

We extended the Monte Carlo Potts model (MCPM) to include a new strain-dependent coarsening model and a mesh-independent sphere-of-influence local energy calculation. We developed a new, order-of-magnitude-faster Potts algorithm and implemented it in PARGRAIN. This algorithm allows more straightforward extension to important physical problems. We developed, tested, and parallelized the first fully 3-D GLAD model. We directly coupled the 2-D MP GLAD code to 2-D PARGRAIN and resolved meshing, time-step matching, data transfer, and physical issues. PARGRAIN/MP GLAD is the first and only simulation code capable of modeling simultaneous microstructural evolution and inter- and transgranular cracking under thermomechanical deformations. Results show complex dependencies between grain growth and fracture. We extended EFG 2-D to simulate microcracking in ceramic materials due to residual thermal stresses and to perform tensile tests of microcracked polycrystals. We incorporated an improved work-hardening law into the JAS3D polycrystalline plasticity model. We successfully modeled a single polycrystalline Cu fatigue loop, solid solution-strengthened Cu and Ag alloys, and a two-phase microstructure. We implemented the first coupled PARGRAIN/JAS3D simulations using a data-passing approach. Computational issues addressed include mesh matching, update frequency, and element state adjustment when a boundary moves through. PARGRAIN/JAS3D is the first model that allows microstructural-scale resolution of grain evolution and stress state. Preliminary results for a short tensile hold test of pure Cu show previously unobserved features, including strain-inhibited grain growth. We overcame logistical difficulties in the ceramic experiments. We quantified growth and coarsening parameters in the Ag-Cu alloys. We performed fatigue tests and nanoindentation studies that led to a new experimental approach for studying the microstructure/micromechanics relationship.

Publications

Refereed

Battaile, C. C., and E. A. Holm. 1998. "Evolution of 2-D Potts Model Grain Microstructures from an Initial Hillert Size Distribution." *Proc. Internat. Conf. on Grain Growth*, accepted.

Buchheit, T. E., G. W. Wellman, M. K. Neilsen, and R. J. Bourcier. 1997. "3-D Deformation Simulations of Polycrystalline FCC Metals." Paper presented to the 2nd Biennial Tri-Laboratory Engineering Conference on Modeling and Simulation, Santa Fe, NM, November.

Fang, H. E. 1997. "A Multilevel Computational Model for Predicting Thermomechanical Fatigue in Solder Joints." Paper presented to SC '97, San Jose, CA, November.

Fang, H. E. 1998. "Microstructural Evolution and Mesoscale Fracture." Paper presented to the ER/SSI Materials Group Meeting, Oak Ridge, TN, May.

Fang, H. E. 1998. "Multilevel Modeling of Thermomechanical Fatigue in Solder Joints." Paper presented to the ASCI PI Meeting, Los Alamos, NM, July.

Fang, H. E. 1998. "Thermomechanical Fatigue of Solder Joints." Paper presented to the Center 9200 External Review, Santa Fe, NM, June.

Fang, H. E., V. L. Porter, R. M. Fye, and E. A. Holm. 1997. "Multi-Level Modeling of Thermomechanical Fatigue in Solder Joints." Paper presented to the 2nd Biennial Tri-Laboratory Engineering Conference on Modeling and Simulation, Los Alamos, NM, November.

Fang, H. E., V. L. Porter, R. M. Fye, and E. A. Holm. 1997. "Simulation of

Thermomechanical Fatigue in Solder Joints." Paper presented to the 5th Joint Conference on Computational Mathematics, Albuquerque, NM, September.

Fye, R. M. 1998. "Fast Algorithm for Potts Model Simulations of Grain Growth." Paper presented to the DOE/AMS Workshop on Mathematical Aspects of Materials Science Modeling, Gatlinburg, TN, April.

Fye, R. M. 1998. "Fast Algorithm for Simulating Grain Growth Using the Potts Model." Paper presented to the 1998 Conference on Computational Physics, Granada, Spain, September.

Holm, E. A. 1997. "Applications of Mesoscale Materials Models at Sandia." Paper presented to the Caterpillar Research Group Seminar, Peoria, IL, September.

Holm, E. A. 1997. "Computers in Materials Science: Processing, Performance, and Reliability Modeling." Paper presented to the ASM International Peoria Chapter Meeting, Peoria, IL, September.

Holm, E. A. 1998. "Modeling of Microstructure-Property Relationships." Paper presented to the Gordon Research Conference on Physical Metallurgy, Holderness, NH, June.

Holm, E. A. 1998. "The Surface Formation Energy for Intergranular Fracture in Two-Dimensional Polycrystal." *J. Amer. Ceram. Soc.* **81** (March): 455–459.

Holm, E. A., C. C. Battaile, M. D. Rintoul, and H. E. Fang. 1998. "Applications of Grain Growth Modeling." Paper presented to the 3rd International Conference on Grain Growth, Pittsburgh, PA, June.

Rollett, A. D., W. W. Mullins, M. D. Rintoul, and E. A. Holm. 1998. "The Link Between Kinetics and Configurational Statistics in Two-Dimensional Grain Growth: Comparison of Theory and Simulation." *Proc. Internat. Conf. on Grain Growth*, accepted.

Tikare, V., and E. A. Holm. 1998. "Simulation of Grain Growth and Pore Migration in a Thermal Gradient." *J. Amer. Ceram. Soc.* **81** (March): 480–484.

3504.250

From Atom-Picoseconds to Centimeter-Years in Simulation and Experiment

J. C. Hamilton, M. F. Horstemeyer, J. M. Faulon

The understanding of aging phenomena is a critical aspect of stockpile stewardship. Accelerated aging tests and examinations of stockpile components play an important role, but both have their limitations. Accelerated aging tests at elevated temperatures skew the relative probabilities of various reactions. Examination of stockpile components provides a limited database and tends to leave us in a reactive rather than proactive position; we may learn about a problem only when it is almost too late to do anything about it. Consequently, it is a vital part of stockpile stewardship to develop simulation techniques that are accurate and valid over much greater time and length scales than those presently available. Most importantly the simulation techniques should be tested by experiment at various length and time scales so they can be validated and improved.

In the past year Sandia made rapid progress toward this goal. Our success is due in part to highly productive collaborations with the originators of a state-of-the-art first-principles code (VASP) and of the hypermolecular dynamics (HMD) method. Both of these techniques are likely to become important to Sandia modeling efforts. We also developed a massively parallel (MP) transition state theory (TST) code to calculate hopping rates of penetrant molecules in microporous media. We will use this code for studies of zeolites used as weapons desiccants.

(1) Sandia now has a highly efficient MP first-principles code (VASP) incorporating the chain-of-states method for finding transition states. As part of this project, we installed, tested, and corrected the chain-of-states methods in VASP in collaboration with a colleague in Vienna, Austria. VASP and the chain-of-states method are now fully integrated in a locally developed graphical user interface (GUI) that allows a number of Sandia users to run VASP on multiple processor computer clusters at Sandia.

(2) Sandia now has a preliminary version of a code that performs parallel-replica variable-boost HMD. We demonstrated that this code can perform HMD even in the presence of dramatically varying barrier heights. Dramatically varying barrier heights will exist in most physical systems, so this is an important result. This code is running in a developmental mode.

(3) We completed an efficient parallel code that identifies cavities in polymer samples and calculates transition rates between cavities. For tests on simple cubic lattices, the code correctly identifies interstitial cavities, evaluates surface and volume integrals, and calculates intercavity hopping rates. In addition, we initiated a study of multicomponent diffusion in zeolites using TST.

(4) We performed calculations of planar simple shear for single-crystal nickel slabs with two orientations ranging in size from 46 to 9546 atoms. We plotted the simulated yield stress as a function of the surface-to-volume ratio and showed a definite correlation.

3504.180

An Investigation of Wavelet Bases for Multiscale, Grid–Based Simulation

M. A. Christon, D. W. Roach, S. P. Burns, D. E. Womble, T. E. Voth, R. S. Baty

The primary objective for this project is to establish a rigorous foundation for grid–based hierarchical/wavelet simulation methods based on numerical performance, computational efficiency, parallelism, and the ability to exploit the hierarchical adaptive nature of wavelets. Wavelets are a new mathematical tool that dissects data, functions, and differential operators into components of different frequency and wave number with a resolution matched to the scale of each component. Wavelet bases constitute a significant shift from traditional grid–based simulation methods because the multiresolution character of wavelets enables the development of hierarchical solutions—a critical requirement for simulation–based design. Compactly supported wavelets are localized in space, permitting the solution to be refined without local or global remeshing to resolve regions of high gradients and without causing overshoot phenomena (ringing) in adjacent regions where the solution is smooth. In addition, preliminary studies indicated that wavelet formulations can deliver spatial convergence rates superior to finite-element (FE) and finite-difference (FD) methods. This effort seeks to develop a rigorous technical framework for the evaluation and application of wavelet bases to the solution of wave propagation, advection, and diffusion problems. These physical processes are characteristic of complicated problems such as turbulent flow where the solution accuracy and computational requirements depend on the numerical errors (e.g., numerical dispersion) associated with the computational method. The algorithms developed as a result of this research will find direct application in multiple Accelerated Strategic Computing Initiative (ASCI) codes in addition to wave propagation for problems that demand accurate far-field solutions such as counterproliferation and environmental characterization.

Research activities this year focused on the four areas associated with the primary project milestones: performing 1-D computational experiments and numerical analyses of wavelet–based formulations, down-selecting the most successful formulations, and extending the work to two spatial dimensions. One of the primary considerations in the down-selection process was the ability to directly use wavelets in a solution strategy for hyperbolic, parabolic, and elliptic partial differential equations (PDEs). The down-selection process relied directly on experiences with the Donovan-Geronimo-Hardin-Massopust (DGHM) multiwavelets in the context of a Galerkin FE framework. Numerical analysis determined that the DGHM wavelets yield an FE that has the cost of a quadratic FE with the convergence rate of a linear FE and inferior dispersive behavior for hyperbolic problems. However, work with the DGHM element led to the conclusion that the strict orthogonality imposed for classical wavelets, although popular in the mathematics community, is neither required nor desirable for an efficient multiscale basis and, in fact, led to the development of a hierarchical basis that is orthogonal in the energy norm for elliptic PDEs. This is consistent with other research in the field where strict orthogonality has been relaxed in favor of bases where bi-orthogonality and semi-orthogonality are imposed. This result led to the development of the multiscale FE basis that relies on a coarse-grid linear FE and injects multiscale degrees-of-freedom as dictated by the solution. A nodal change-of-basis in the multiscale element yields condition numbers that are independent of mesh resolution in one dimension, and scale approximately as the mesh resolution in multidimensions. Although the multiscale element is attractive for elliptic problems, we also selected the reproducing kernel (RK) method for further investigation. The numerical analysis demonstrated that reproducing kernel particle method (RKPM) delivers excellent dispersive properties for hyperbolic problems for the entire discrete spectrum representable by a grid or particle distribution. In addition, RKPM provides a natural framework for multiscale decomposition of discrete fields according to a prescribed scale and can make use of pre-wavelets for adaptive computations. RKPM is based on a flexible space-frequency window function that results in spatial filters compatible with commutative filtering operations for large-eddy simulation (LES). In addition, we demonstrated RKPM to be effective for large-deformation Lagrangian computations where extreme mesh distortions lead to premature termination using traditional methods. At this point, we are beginning to apply both the multiscale element and RKPM to applications ranging from thermal transport with phase transformation to LES of turbulent flow fields.

Publications

Refereed

Christon, M. A., and T. E. Voth. 1998. "Results of von Neumann Analyses for Reproducing Kernel Semi-Discretizations." *Internat. J. Numer. Meth. in Engin.* (special issue), accepted.

Christon, M. A., D. W. Roach, and T. E. Voth. 1998. "The Numerical Performance of Wavelets for PDEs." *Computational Mechanics* (special issue), in press.

Roach, D. W., and D. Hardin. 1998. "Semi-Orthogonal Wavelets for Elliptic Variational Problems." *Proc. Internat. Wavelets Conf.—Wavelets and Multiscale Meth.* (Morocco, Tangier, 13–17 April).

Voth, T. E., M. A. Christon, and S. P. Burns. 1998. "Truncation and Dispersive Errors Associated with Reproducing Kernel Methods." *Computer Meth. in Appl. Mechanics and Engin.*, in press.

Other

Christon, M. A., D. W. Roach, and T. E. Voth. 1998. "The Numerical Performance of Wavelets and Reproducing Kernels for PDEs." *Proc. Internat. Conf. on Computational Engin. Sci.* **1** (Atlanta, GA, 6–9 October): 29–34.

Christon, M. A., R. S. Baty, S. P. Burns, D. W. Roach, T. G. Trucano, T. E. Voth, J. R. Weatherby, and D. Womble. 1998. "An Investigation of Wavelet Bases for Grid–Based Multiscale Simulations—Final Report." Sandia Technical Report SAND98-2456 (November). Sandia National Laboratories, Albuquerque, NM.

Roach, D. W., M. A. Christon, D. Womble, T. E. Voth, S. P. Burns, R. S. Baty, D. Hardin, and P. Massopust. 1998. "Semi-Orthogonal Wavelets for Elliptic Variational Problems." Paper presented to the University of New Mexico Colloquium, Albuquerque, NM, 24 April.

Roach, D. W., P. Massopust, M. A. Christon, and D. Womble. 1998. "A Wavelet-Galerkin Multilevel Method with Level Independent Convergence and No Preconditioning." Paper presented to the 9th International Conference on Approximation Theory, Nashville, TN, 3–6 January.

Voth, T. E., and M. A. Christon. 1998. "Results of von Neumann Analyses for Reproducing Kernel Semi-Discretizations." *Proc. 4th World Congress on Computational Mechanics CDROM* (Buenos Aires, Argentina, 29 June–2 July).

3504.210

The Next Generation of Teraflop Density-Functional Electronic Structure Codes

M. P. Sears, K. Leung, N. A. Modine, S. J. Plimpton, E. B. Stechel, P. A. Schultz, A. F. Wright

Sandia will develop a next-generation massively parallel (MP) electronic structure code, going well beyond Sandia's current capabilities with a focus on large systems and making direct connections with experimental spectroscopic observables. First-principles methods based on density-functional theory (DFT) offer a well-developed methodology for such a code. Experimental observables such as vibrational, optical, and electron spectroscopies are amenable to calculation by linear response theory within DFT. A competitive next-generation code must scale linearly with system size (for both energy/force and linear response calculations), must have an efficient MP implementation, and must be thoroughly tested. We plan to develop a parallel linear response code that is independent of representation that accurately calculates second and third derivatives of the energy with respect to relatively arbitrary perturbations. We plan to create a linear scaling serial version of our linear combination of atomic orbitals (LCAO) code. We plan also to combine a real-space variable grid method with our own innovative linear scaling algorithms, testing the resulting code against existing codes and against experiment. The result will be a production tool useful for a wide variety of materials research applications and will keep Sandia in the forefront of this area.

Work is proceeding simultaneously on several fronts: (1) linear response (second- and third-order perturbation theory) to applied perturbations ultimately with an algorithm that scales as Order N, (2) solution for the electronic structure in a curvilinear (variable grid in real space, regular grid in curvilinear space) coordinate system, including new ways to solve for the optimum coordinate system, (3) the determination of advantages and disadvantages of various linear scaling algorithms in the literature, including variational Green's function approaches, (4) solution for the electronic structure numerically on a fully real-space grid (no fast Fourier transforms [FFTs]), and (5) development of a linear scaling version of LCAO-LDA (local density approximation) serial code. Our most significant accomplishments this year involve the linear response. We have a fully operational variational linear response code that can calculate the full phonon spectrum of a solid as well as the dielectric response. When used in conjunction with occupied stationary states, this new algorithm, like others, scales as N3 for each perturbation, and therefore as N4 for vibrational modes. However, our new algorithm is invariant to linear transformations and therefore not only works with localized nonstationary occupied states but also will scale linearly. We also derived, coded, and debugged an efficient method for third-order perturbation theory within the same formalism. Further progress on the variable grid includes showing that the Pulay-like forces vanish identically and that the basis-set-dependent change in the energy with moving atoms is entirely due to the change in the Hilbert space. This is undesirable and similar to basis-set-superposition error in LCAO calculations. We are devising possibilities to eliminate this error.

Publications

Refereed

Leung, K., and E. B. Stechel. 1998. "Occupied Subspace Invariant Linear Response." Paper presented to the American Physical Society Meeting, Los Angeles, CA, March.

Stechel, E. B. 1997. "Linear Scaling, Linear Response and Distorted Grids in Density-Functional Algorithms." Paper presented to the 213th American Chemical Society National Meeting, San Francisco, CA, 10 April.

Stechel, E. B. 1998. "Occupied Subspace Invariant Variational Kohn-Sham DFT Through Third Derivatives (Linear Response)." Paper presented to the CECAM Workshop: Local Orbital Methods for Large-Scale Atomistic Simulations, Lyon, France, 22–25 July.

Stechel, E. B. 1998. "Occupied Subspace Invariant Variational Kohn-Sham DFT Through Second Derivatives (Linear Response)." Paper presented to the Workshop on Materials Theory, Davis, CA, 20–22 March.

3504.220

Methodology for Characterizing Modeling and Discretization Uncertainties in Computational Simulation

K. F. Alvin, K. V. Diegert, W. L. Oberkampf, B. M. Rutherford

To meet the goals of the scientifically–based stockpile stewardship program, significant confidence must be built into a variety of numerical simulations. The goal of these simulations is to accurately characterize the response of complete systems with high-fidelity, 3-D, unsteady, coupled physics, together with uncertainty bounds on the responses. Quantifying uncertainties in computational physics–based simulations is also critical to verification and validation of these simulations; without uncertainty quantification, validation is highly subjective. Nondeterministic methods seek to quantify response uncertainties by propagating uncertainties due to stochastic inputs and variability or uncertainty in geometric, constitutive, and manufacturing parameters through the computational simulation. There remains a pressing need, however, to address the question of whether the proper physics have been modeled, both mathematically and numerically. The objective of this research is to develop methods to quantitatively estimate the errors or uncertainties due to the mathematical form of the partial differential equations (PDEs) and errors due to the discretization of the equations. Thus, this work complements, but is distinct from, nondeterministic methods for numerical simulations.

Sandia is developing a methodology for characterizing the effects of modeling on computational simulation. This methodology is intended to apply in all numerical simulations of continuum mechanics, assuming the mathematical formulation of the physical model is given by PDEs that are solved by discretization methods. The research effort focuses on three strategies for characterizing computational simulation errors and uncertainties: (1) identification of error sources and interactions, (2) parameterization of the model structure, and (3) methods for evaluating model uncertainty and its contribution to global uncertainty. We will study two application areas, evolving from linear problems dominated by physical modeling considerations to nonlinear problems dominated by numerical discretization errors. The methodology will be applicable to applications being developed for the Accelerated Strategic Computing Initiative (ASCI), as well as other computational mechanics disciplines.

We developed a methodology for combining discretization error estimation with propagation of continuous parameter variabilities (i.e., nondeterministic analysis). This technique involves estimating the parameters of a response surface that predicts the analysis output over a range of parameter values. This response surface is extended to include mesh spacing as a parameter. We performed code analyses with variations in both the uncertain continuous parameters of the model and the characteristic mesh length. The resulting response surface could then be used to propagate parameter uncertainties while also identifying the discretization error. As part of this work, we developed and tested a simple experiment design for combining discretization error and parameter variabilities. We also worked with researchers at the University of Wisconsin to implement a metamodeling approach with discrete qualitative model form parameters. We identified a framework for combining model forms with inconsistent parameter sets, which is important when considering different model forms in a model uncertainty analysis, and for decomposing conceptual model probabilities into mathematical and discrete model probabilities. We identified limitations of sampling methods for certain classes of stochastic differential equations, in particular where the statistics of the input variables are time-dependent. Finally, we made further progress on example problems in flight dynamics and structural dynamics.

Publications

Refereed

Alvin, K. F. 1998. “Treatment of Discretization Error in Nondeterministic Analysis.” *1999 AIAA Forum on Non-Deterministic Approaches* (Washington, DC: AIAA), submitted.

Oberkampf, W. L., K. V. Diegert, K. F. Alvin, and B. M. Rutherford. 1998. “Variability, Uncertainty, and Error in Computational Simulation.” *J. Fluids Engin.* (New York), submitted.

Oberkampf, W. L., K. V. Diegert, K. F. Alvin, and B. M. Rutherford. 1998. “Variability, Uncertainty, and Error in Computational Simulation.” *Proc. 1998 ASME/AIAA Joint Thermophys. and Heat Trans. Conf.* (Albuquerque, NM, 15–18 June).

Oberkampf, W. L., S. M. DeLand, B. M. Rutherford, K. V. Diegert, and K. F. Alvin (U.S. Army). 1998. “A New Methodology for the Estimation of Total Uncertainty in Computational Simulation.” *1999 AIAA Forum on Non-Deterministic Approaches* (Washington, DC: AIAA), submitted.

Other

Alvin, K. F., W. L. Oberkampf, K. V. Diegert, and B. M. Rutherford. 1998. “Uncertainty Quantification in Computational Structural Dynamics: A New Paradigm for Model Validation.” *Proc. 16th Internat. Modal Anal. Conf. II* (Santa Barbara, CA, 2–5 February): 1191–1198.

3504.260

Emergent Behavior of Large Swarms of Intelligent Agents

R. J. Pryor, J. E. Hurtado, B. L. Spletzer

This research focused on investigating and developing new methods of analyzing, predicting, and manipulating the emergent behavior of large swarms of cooperating agents. Sandia developed new simulation and analysis tools and used existing particle physics simulation concepts and codes. We also developed and documented a genetic algorithm learning strategy. We used traditional continuum and statistical mechanics methods to model a large swarm of agents, and in other work we developed a distributed sensing and cooperative control method that allows a swarm of agents to share information as they each locate a set of targets. We developed preliminary statistical nonlinear control methods to analyze the overall behavior of a swarm of agents.

This year's accomplishments can be divided into four general categories:

(1) *Co-evolutionary learning methods*. We developed a strategy for co-evolutionary learning and used these learning methods to develop genetic algorithm learning strategies that are specific to swarms of agents. We developed these learning strategies on Sandia's massively parallel (MP) computer, the Paragon—an ideal testbed for this phase of the research. We also developed a simulation code for investigating the resulting swarm behavior.

(2) *Applying continuum and statistical mechanics methods to modeling the overall behavior of swarms of intelligent agents*. We lifted the theories behind traditional continuum and statistical mechanics and applied these methods to swarms of intelligent agents. Using continuum and statistical mechanics analogies, we can now design group behavior. That is, we accomplished obstacle and collision avoidance by assigning repulsive potential functions to objects; we used attractive potential functions to locate targets and mimic flocking or schooling patterns of swarms of animals.

Using low-level attraction and repulsion rules, we were able to create very high-level behavior. In particular, we created some striking results by paying close attention to surface tension analogies. For example, we manipulated a group of robots so they behave very much like a fluid. The group can cluster, move forward and tag targets, and even separate as they encounter an obstacle, then regroup later. We folded these ideas into particle physics simulation codes. This is a new application for particle physics simulation concepts and codes, and we have benefited from the fact that particle physics simulation is a mature subject that is well understood.

(3) *A new approach to distributed sensing and cooperative control*. We developed a novel approach to distributed sensing and cooperative control that has its roots in function minimization (i.e., traditional optimization). This approach works extremely well for inexpensive function evaluations. We used nonlinear estimation and nonlinear adaptive control methods within the optimization routine to tune the update procedure.

Two remarkable features of this approach are that (a) one-dimensional search methods are not employed, but rather gradient information is inferred from neighboring agents, and (b) the update of all agents requires only one sensor (or function) evaluation per agent. This technique is ideally suited for controlling a swarm of autonomous robots in search and surveillance tasks. In this application, distributed sensing is achieved through each agent sampling and sharing his information with others. Cooperative control is accomplished by each agent using his neighbors to approximate the function surface that leads to a control (or update) strategy for that particular agent. The true function is approximated with a quadratic model, and we use a least-squares routine to determine the model coefficients that best match the actual data. Each agent then uses the quadratic model to generate a position update.

(4) *Nonlinear control design*. We developed preliminary statistical Lyapunov control methods and alpha-beta coordination algorithms to manipulate and analyze the overall behavior of a swarm of agents. These are new approaches to choose the focus for controlling the overall behavior of a swarm of agents rather than the behavior of each individual agent. Using these methods we are able to statistically guarantee that the swarm of agents will conduct desired group behaviors.

Publications

Refereed

Pryor, R. J. 1998. "Developing Robotic Behavior Using a Genetic Programming Model." Sandia Technical Report SAND98-0074. Sandia National Laboratories, Albuquerque, NM.

3504.230

Global Optimization for Engineering Science Problems

W. E. Hart, K. O. Hunter, J. S. Wagner, C. A. Phillips

A wide variety of scientific and engineering problems can be posed as optimization problems in which the desired solution to the problem corresponds to an optimal set of parameters for an objective function that measures a solution's quality. Sandia is developing a library of robust and efficient optimization algorithms that can be used to find globally optimal solutions to complex optimization problems. Our work will lead to a critical evaluation of standard global optimization algorithms (e.g., genetic algorithms, simulated annealing) as well as new, innovative methods that are inspired by our analysis. This analysis will focus on a variety of algorithmic factors that fundamentally affect the practical application of these methods, including (1) the combination of global sampling and local optimization, (2) termination rules that provide practical confidence guarantees, (3) the appropriate design of constrained optimization methods, (4) the effective use of all function evaluations, and (5) the role of parallelism (for large-scale optimization problems). Our research will have immediate impact on three application domains—problems relating to scheduling, system design optimization, and chemical, biological, and warfare (CBW) defense (counterproliferation). This effort will develop new expertise in global optimization techniques as well as build on Sandia's current expertise in parallel algorithms.

We integrated eight new global optimization methods into stochastic global optimization (SGOPT) and evaluated their effectiveness on test problems and real-world applications. We noted problems with current implementations of these methods on high-dimensional problems. We extended the architecture of SGOPT to allow constrained and mixed-integer optimization. We made a variety of algorithmic advances:

(1) Developed new hybrid genetic algorithms for continuous search spaces. Particularly, we analyzed how the initial step size of the local search method needs to be initialized to improve the efficiency of the entire optimization process.

(2) Extended a convergence analysis for evolutionary pattern search to the most general case, thereby eliminating many artificial constraints that were imposed by earlier versions of this analysis.

(3) Developed an empirical analysis for GAs optimizing noisy functions, which suggests weaknesses in current theoretical models.

(4) Developed a method for adapting the step size in GAs based on a novel hybridization with simulated annealing.

We submitted one technical advance licensed for SGOPT 1.0 to a consortium of companies.

Publications

Refereed

Eldred, M., and W. E. Hart. 1998. "Design and Implementation of Multilevel Parallel Optimization on the Intel Teraflops." *Proc. AIAA Symp. Multidisciplinary Anal. and Optimization* **1** (St Louis, MO, September).

Greenberg, D., W. Hart, and C. Phillips. 1998. "Architecting Department-Scale Simulation." *Algorithms for Parallel Processing*, accepted.

Hart, W. E. 1997. "A Generalized Stationary Point Convergence Theory for Evolutionary Algorithms." *Proc. Internat. Conf. on Genetic Algorithms* **1** (Lansing, MI, 19–23 July): 127.

Hart, W. E. 1998. "On the Application of Evolutionary Pattern Search Algorithms." *Proc. Evolutionary Programming VII* **1** (San Diego, CA, 3 March): 303.

Morris, C., *et al.* 1998. "Autodock 3.0: Automating Docking Using a Laramckian Genetic Algorithm and an Empirical Binding Free-Energy Function." *J. Comp. Chem.*, accepted.

Rosin, C. D., R. S. Halliday, W. E. Hart, and R. K. Belew. 1997. "A Comparison of Global and Local Search Methods in Drug Docking." *Proc. Internat. Conf. on Genetic Algorithms* **1** (Lansing, MI, 19–23 July): 221.

Trahan, M., J. Wagner, K. Stantz, P. Gray, and R. Robinett. 1998. "Swarms of UAVs and Fighter Aircraft." *Proc. 2nd Internat. Conf. on Nonlinear Problems in Aviation and Aerospace*, accepted.

Wagner, J. 1998. "Computationally Intelligent Algorithms for Design, Control, Analysis and Optimization." *Proc. AIPA 1998 Symp.* **1** (Tysons Corner, VA, 17–18 March).

Other

Anderson, M., and W. Hart. 1998. "Optimizing Noisy Functions with an Adaptive GA." In preparation.

Gray, P., C. Wehlburg, J. Wagner, G. Tisone, and H. Chan. 1998. "Dense Multispectral UV Fluorescence Detection of a Dilute Constituent in an Optically Dense Matrix." *Appl. Optics*, submitted.

Gray, P., M. Trahan, and J. Wagner. 1998. "Hybrid Simulated Annealing Evolutionary Algorithms." In preparation.

Hart, W. E. 1998. "Methods for Parallel Optimization." Presentation at Oak Ridge National Laboratory, Oak Ridge, TN, February.

Hart, W. E. 1997. "On the Convergence of Evolutionary Pattern Search Algorithms." Paper presented to the AMS Fall Western Section Meeting, Albuquerque, NM, November.

Hart, W. E. 1997. "On the Dynamics of Hybrid Genetic Algorithms that Use Local Search." Paper presented to the UC–San Diego, San Diego, CA, October.

Hart, W. E. 1997. "SGOPT: A C++ Library of Global Optimization Meth-

ods." Paper presented to the International Symposium on Mathematical Programming, Lausanne, Switzerland, 29 August.

Hart, W. 1998. "Stochastic Pattern Search and Evolutionary Algorithms." *J. Artificial Intelligence and Mathematics*, submitted.

Stantz, K., M. Trahan, P. Gray, and J. Wagner. 1998. "Genetic Optimization of Recurrent Neural Networks." In preparation.

Wagner, J. 1998. "On Neural Network Analysis of Mass Spectral Data." Paper presented to Los Alamos National Laboratory, Los Alamos, NM, May.

Wagner, J. 1998. "On Neural Network Analysis of Mass Spectral Data." Paper presented to the ASMS Meeting, Orlando, FL, June.

Wagner, J. 1998. "Real-Time Analysis of Mass Spectral Data." Paper presented to the ASMS Meeting, Orlando, FL, June.

Wagner, J. 1997. "Status Report of the Joint Sandia–ERDEC Multispectral UV Fluorescence Measurement Analysis Using Computationally Intelligent Algorithms." *Proc. MASINT Biological Def. Sci. and Tech. Symp.* **1** (Patrick AFB, FL, January).

Wagner, J. 1998. "Using GAs and Neural Networks to Analyze Mass Spec Data." Paper presented to Oak Ridge National Laboratory, Oak Ridge, TN, May.

3504.240

Dynamic Simulation of Mechanical Systems with Intermittent Contacts

C. L. Lewis, R. A. Lafarge

Sandia is developing an efficient dynamic simulator to accurately predict probabilistic distributions of motions for arbitrary numbers of bodies experiencing multiple applied forces and intermittent contacts. Current simulators employ either weak or computationally expensive contact models and frequently cannot handle complex time-varying contacts. Our approach utilizes a compliant surface model. We are verifying our simulation results through comparison to physical data.

To prove the viability of our contact analysis and collision-detection scheme, we integrated our software into ADAMS using the standard interface library developed by Mechanical Dynamics, Inc. (MDI). We used the mature user interface and advanced numerical integration tools in ADAMS to demonstrate the capabilities of our collision-detection software and contact model. MDI had implemented a constraint–based contact model, but then discovered problems due to the rigid contact approach. Consequently, they removed automatic contact modeling from the latest release.

The basic capability to automatically analyze intermittent contacts will now enable the development of software modules specific to Sandia applications. We are developing modules to predict the statistical robustness of mechanisms such as stronglinks, weapons, and small smart machines, as well as the robustness of the assembly, disassembly, and maintenance procedures for those mechanisms. Our simulation software will provide force histories for critical tasks and predict the success of inherently stochastic processes.

Our first task was to complete a model for contact analysis. There were two ways for us to model contacts: hard or soft. In a hard contact model, the bodies are rigid; in a soft contact model, the bodies are compliant. After extensive research, we felt there were too many limitations to a hard contact approach. To avoid this fundamental limitation with the rigid-body formulation of contact dynamics and to capture phenomena like wedging and press fits, we chose the soft contact approach with nonlinear lumped elements.

To take advantage of MDI's fully developed computer-aided design (CAD) interface and robust numerical integration codes, we integrated our collision-detection software and contact analysis into ADAMS by using callable ADAMS, the standard software interface. With the implementation of our contact model within ADAMS, we were able to simulate intermittent contacts between mechanisms composed of non-convex bodies rigidly jointed together.

By using Latin Hypercube Sampling (LHS) for the generation of random numbers, our implementation of the design of experiment (DOE) option should be significantly faster than that currently available. We are developing a statistical analysis package based on the LHS and our advanced simulation capabilities. This package requires that we modify a standard input file to identify the random variables. Using the modified input file, we created multiple files with variations in the random parameters. We then executed the individual files to ascertain the effects of the variations.

We are currently in the process of verifying our contact models. Using our simulation, we will produce a simulation system that automatically generates and solves the equations of motion for systems of bodies undergoing transitions in multiple contacts. We will then thoroughly test our system, considering the whole spectrum of contact transitions.

Publications

Refereed

LaFarge, R. A., and C. L. Lewis. 1998. "Contact Force Modeling Between Non-Convex Objects Using a Nonlinear Damping Model." *Proc. 1998 Internat. ADAMS Users Conf.* **1** (Ann Arbor, MI, 8–10 June): 19–25.

LaFarge, R. A., and C. L. Lewis. 1998. "Contact Modeling for Robotics Applications." *Proc. IASTED Internat. Conf. on Control and Applic.* **1** (Honolulu, HI, 12–14 August): 254–299.

Tenaglia, C. A., D. E. Orin, R. A. LaFarge, and C. L. Lewis. 1998. "Toward Development of a Generalized Contact Algorithm for Polyhedral Objects." *Proc. 1999 IEEE Internat. Conf. on Robotics and Automation* (Detroit, MI, May 1999), accepted.

3504.270

Parallel Combinatorial Optimization for Scheduling Problems

C. A. Phillips, R. D. Carr, D. A. Jones, E. A. Kjeldgaard, W. E. Hart

Sandia will develop a state-of-the-art massively parallel (MP) combinatorial optimization engine. This will be the first fully general mixed-integer programming (MIP) code scalable to thousands of processors. We will develop two general search strategies for MIP: branch-and-bound and branch-and-cut. We will study the feasibility of an MP version of a third strategy: branch-and-price. The engine will be able to adaptively incorporate application-specific methods (combinatorial approximation algorithms and genetic algorithms), for both lower and upper bounds, to limit the search space explored by the MIP engine. We will use this exact method in a statistically rigorous performance analysis of sequential heuristics.

We will use the MIP engine to solve scheduling of stockpile evaluation activities, neutron-generator manufacturing at Sandia, and related scheduling problems for the Product Realization Program, Stockpile Life Extension Program, Revolution in Engineering (formerly ADaPT), and the computational plant. However, MIP is a core optimization technology, and this capability can be applied in other areas consistent with Sandia's mission: nonproliferation, transportation, infrastructure analysis and design, manufacturing, energy, environment, and tools for MP computation such as meshing and scheduling heterogeneous supercomputers.

Management of multiple, loosely coupled threads, each distributed and largely asynchronous, may require the development of new systems-level tools. Implementation of the search engine alone will require solution of novel global and semi-global distributed resource-management problems.

We implemented parallel branch-and-bound for both master-slave and more general distributed job management. Code for parallel MIP is in place and working under message passing interface (MPI) for multiple processes. We have run the code on a network of workstations for up to seven machines. The code can now use any of three linear-programming solvers for the general lower-bounding procedure: CPLEX, XPRESS (DASH associates), and SoPlex. The latter is public domain. CPLEX has agreed to give us research licenses for the Accelerated Strategic Computing Initiative (ASCI) machine and will install the code as soon as accounts are established.

We implemented a new branching method. We used pseudo-cost (gradient) information, which indicts effects on bounds from previous branches on each integer variable. Since early branching choices can have a profound effect on performance, the code now initializes these gradients via an artificial branch the first time it encounters each variable. Hooks are in place for hybridization. We implemented load-balancing. We have preprocessing code but have not yet integrated it into the full system. These features represent the state-of-the-art in MIP.

We modeled a scheduling/production-planning problem from Pantex. We formulated the problem as an MIP, taking care to ensure that our output will be comparable with the output of the current on-site code (the Pantex Processing Model, or PPM). We modified the PPM to provide data. We developed an interface between this raw data and the MIP engine. We acquired the data for a challenging test problem and have partially run this problem in serial to verify that the problem will fit on a single processor. We believe we will be able to solve this problem in the near future using massive parallelism, improved lower-bounding techniques, better memory management, and more careful branching.

Publications

Other

Carr, R. D., J. Eckstein, W. E. Hart, V. J. Leung, and C. A. Phillips. 1997. "Massively Parallel Integer and Combinatorial Optimization with National Security Applications." Presentation to Los Alamos National Laboratory (Invited), Los Alamos, NM, 8 December.

3504.280

Programming Paradigms for Massively Parallel Computers

W. E. Hart, M. P. Sears, R. E. Riesen, S. J. Plimpton, R. B. Brightwell

The goal of this project is to enable applications to take full advantage of the hardware available on Sandia's current and future supercomputers. Currently, nearly all Sandia codes on existing massively parallel processing (MPP) systems use only a single thread of execution. On the commodity–based machines, this approach will not allow us to achieve maximal performance. More generally, the future of high-end computing appears to be clusters of shared-memory processing (SMPs); i.e., a mixture of distributed and shared-memory hierarchies is exposed to the user. Learning how to program such machines effectively to achieve maximum impact, both inside and outside Sandia, with simulations is a must. The best model for each of the different types of applications will be discovered through implementation and exploration of several programming models from both the system and application perspectives.

Sandia purchased large SMP boxes from DEC and SGI and gained access to SMP IBM boxes. We worked to understand the nature and peculiarities of both the architecture and the programming models of the SMP boxes from DEC, SGI, and IBM. Further, we surveyed parallelization methodologies that are appropriate for SMP

clusters and developed conclusions concerning where our research efforts would be productively spent. Based on this survey, we evaluated four programming models and noted the need for a general programming environment within which users can tailor their application to a particular machine's hardware. We also evaluated thread implementations in Linux and identified a new scheduling method that seems appropriate for scientific computing applications. We are working on a thread-aware implementation of message passing interface (MPI) that can take advantage of the extended capabilities that threads provide. Finally, we began to explore how we can leverage the application programming interface and constructs of MPI to provide the functionality needed by a hybrid cluster environment. We expanded the expertise by collaborating with SGI/Cray and the University of Maryland to provide hybrid SMP libraries, models, and applications codes.

3504.290

Multilevel Techniques for Unstructured Grid Problems on Massively Parallel Computers

C. H. Tong, A. B. Williams, P. R. Schunk, A. C. Robinson, C. D. Moen, J. N. Shadid, R. S. Tuminaro

Robust and efficient linear system solution techniques are critical to Sandia's leading-edge scientific simulation capabilities. Current parallel iterative techniques suffer deteriorating performance and even failure as mesh sizes increase and geometric complexity grows (a significant problem for ALEGRA, GOMA, FUEGO, and MPSalsa). These difficulties are even more pronounced on larger, massively parallel (MP) systems such as Sandia's Computational Plant (Cplant). Without significant advances, convergence limitations will hinder next-generation simulations.

This project proposes a fundamental change in linear system solution strategy at Sandia by providing tools that facilitate the use of multilevel (ML) techniques. ML methods offer the best promise for overcoming convergence difficulties with iterative solvers. Unfortunately, ML methods are rarely used at Sandia due in part to MP implementation difficulties for unstructured grids. In this project, we will focus on two distinct tasks to address these difficulties and facilitate the use of ML preconditioners. The first corresponds to the development and analysis of automatic coarsening techniques (e.g., agglomeration) to construct mesh hierarchies. The second task is to define multigrid operators and ML preconditioners that utilize a given sequence of grids. In this second case we will specifically consider mesh hierarchies coming from adaptive meshes (important for MPSALSA and ALEGRA), as well as those arising from automatic coarse grid generation techniques (important for MPSalsa, FUEGO, and GOMA). We will develop these techniques and integrate them in Sandia's parallel iterative solver library AZTEC and incorporate them into Sandia's applications, including, but not limited to, ALEGRA, GOMA, FUEGO, and MPSalsa.

We emphasized four aspects: (1) designed a finite-element (FE) to ML interface, (2) implemented the Newton-Krylov-Schwarz (NKS) algorithm for nested grids, (3) implemented NKS for independently generated coarse grids, and (4) studied automatic coarsening algorithms.

We designed an application-FE interface to support ML computations and fully implemented this extension to the SIERRA finite-element interface (FEI). We also designed and implemented a first-version FE-to-ML interface.

Implementation of the FE-to-ML interface expends over ten thousand lines of C code using object-oriented techniques. Current implementation works not only for nested grids, but also for user-provided non-nested coarse grids. We also completed and tested integration with AZTEC. We will incorporate the new features in AZTEC to support ML in the AZTEC 2.0 release.

We completed integration with MPSalsa and tested it using the NKS algorithm. The new preconditioner not only gives two to three times improvement in solution times on our Paragon and Tflop machines, but it also is more robust than the local incomplete LU preconditioner on our test problems (2-D thermal convection problem on structured and unstructured grids).

We also began to study efficient coarsening algorithms in the event that neither nested nor non-nested coarse grids are available. We performed a literature search and selected a few candidate algorithms for further investigation. In addition, we collaborated with UCLA Mathematics Department on agglomerated ML methods.

Publications

Other

Tong, C. H., R. S. Tuminaro, K. D. Devine, and J. N. Shadid. 1998. "A Framework for Parallel Multilevel Preconditioners on Unstructured Grids." Paper presented to the ASCI Tri-Lab Linear System Meeting, Livermore, CA, 13 October.

Tong, C. H., R. S. Tuminaro, K. D. Devine, and J. N. Shadid. 1998. "Design of a Multilevel Preconditioning Module for Unstructured Calculations: Two-Level Schwarz." Sandia Internal Report, in preparation.

Tong, C. H., R. S. Tuminaro, K. D. Devine, and J. N. Shadid. 1998. "Software Design and Implementation of Multilevel Techniques for Unstructured Finite Element Calculations." Paper presented to the SIAM Annual Meeting, Toronto, Ontario, Canada, 13 July.

3504.310

Scalable Tools for Massively Parallel Distributed Computing

R. C. Armstrong, L. A. Fisk, A. C. Gentile

Platforms for parallel computing that harness thousands of independent commodity machines, such as Sandia's Computational Plant (Cplant), will require robust, efficient, scalable, secure, and easy-to-use tools for system and user management. Both hard-coded tools, traditionally used on specialized massively parallel processor (MPP) machines, and high-level tools, exploiting features of commodity operating systems, will be effective for these systems. Both types are designed to manage MP distributed systems: an analogy would be the difference between PERL and C for creating common UNIX tools—both have their place. Generally, trade-offs in these types of tools involve development time, efficiency, and ease of use. Hard-coded tools can be specifically designed for efficiency, but innately take longer to develop than less efficient, but easier-to-produce, high-level tools. Hard-coded and high-level tools need not exist independently, however. High-level tools can be prototypes for hard-wired tools, decreasing overall development time.

Utilizing the resources in the development of Cplant, Sandia will identify tools whose creation would enhance the ability to use and maintain large platforms (e.g., controlling user processes, monitoring system status). We will develop tools whose performance is critical in a hard-coded fashion. Tools whose performance is not an issue, or tools expected to be used infrequently, will be developed via a high-level framework. High-level tools will also serve as prototypes for hard-coded tools.

(1) We identified and developed six tools and utilities (both high-level and hard-coded) for the use, maintenance, and monitoring of large distributed clusters.

(2) We developed a Server Library for the hard-coded tools that provides common services and exports a well-defined application programming interface (API). This library allows the hard-coded tools to interact and speeds overall development of the tools.

(3) We are in the process of designing and implementing the security infrastructure for the Lilith framework. This infrastructure will provide flexible, scalable security for the Lilith–based tools. This work is ahead of schedule.

(4) We have tentatively identified a tool to take through the entire development cycle of high-level tools serving as a prototype for a hard-coded tool. Under consideration is a flexible, scalable status monitor for highly parallel distributed systems. This tool will capitalize on some of the infrastructure of one of the high-level tools developed during this first year.

Publications

Refereed

Evensky, D. A., A. C. Gentile, and P. Wyckoff. 1998. "A Visualization Tool for Parallel and Distributed Computing Developed via the Lilith Framework." Paper presented to the 2nd SIGMETRICS Symposium on Parallel and Distributed Tools, Welches, OR, August.

Gentile, A. C., D. A. Evensky, and R. C. Armstrong. 1998. "Lilith: A Software Framework for the Rapid Development of Scalable Tools for Distributed Computing." *Proc. 7th IEEE Internat. Symp. on High-Perf. Distributed Computing* **1** (Chicago, IL, 28–31 July): 360.

Other

Evensky, D. A., A. C. Gentile, and R. C. Armstrong. 1997. "Lilith: Software Infrastructure for Scalable Tools." Paper presented to SC '97: High-Performance Networking and Computing, San Jose, CA, November.

3504.320

Massively Parallel Methods for Simulating the Phase Field Model

R. M. Fye, S. J. Plimpton, D. Fan, V. Tikare

Prediction of the evolution of microstructures in weapons systems is critical for meeting the objectives of stockpile stewardship. For example, accurate simulation of microstructural evolution in solder joints, cermets, lead zirconate titanate (PZT) power generators, etc., is necessary for predicting the performance, aging, and reliability both of individual components and of entire weapons systems. A recently developed but promising approach called the phase field model *(PFM) has the potential of allowing the accurate quantitative prediction of microstructural evolution, with all the spatial and thermodynamic complexity of a real microstructure. Simulating the PFM requires solving a set of coupled nonlinear differential equations, one for each material variable (e.g., grain orientation, phase, composition, stresses, anisotropy, etc.). While the PFM is versatile and is able to incorporate the necessary complexity for modeling real material systems, it is very computationally intensive, and it has been a difficult and major challenge to formulate an efficient algorithmic implementation of the approach. Sandia will develop and implement numerically efficient techniques for performing large-scale massively parallel (MP) simulations of the PFM. This involves exploring, e.g., different discretizations or other alternative implementation approaches, with issues of accuracy, numerical stability, locality, dissipativity, and parallel efficiency; possible reductions in the number of required differential equations; generalizations to certain coupled or more complicated physical processes; comparison with experiment, etc.*

In microstructural simulation, using the phase field approach, a different field is associated with each possible feature. In grain-growth simulations, one wishes the number Q of possible grain orientations and hence of fields to be as large as possible, since Q is actually physically infinite. Since the computational time of grain-growth simulations scales linearly with Q, and since grain growth is an important general component of microstructural evolution, this can lead to a bottleneck in microstructural simulations. We developed a much faster algorithmic approach that replaces the multiple (Q) grain-growth phase fields by a single field.

We also investigated a variety of implementation issues. For example, we developed a speed-up technique that selectively ignores the (dynamically changing) less active grain interiors. In addition we investigated various discretization approaches. The standard alternating direction implicit (ADI) approach involves tridiagonal solves across the entire length of the simulated region. We first found a completely local and hence more efficient alternative to ADI that nonetheless retains ADI accuracy; however, this alternative did not have as good stability and dissipativity properties as ADI. We did, however, find a way to increase the time-step size while still maintaining stability and dissipativity. We are in the process of implementing these and other algorithmic speed-ups in a phase field grain-growth code, and have installed capabilities for varying kinetics and variable diffusion.

In addition to making the PFM implementation more efficient, we also began validating the ability of the PFM to simulate microstructural evolution by comparing to other models and to experimental data. For example, we compared the results of two well-understood coarsening processes using the Potts model and the PFM, confirming that the two approaches gave quantitatively similar results. We also simulated a more complex microstructural evolution problem of simultaneous grain growth and diffusion. Among other results, this latter work underscored the challenge in determining physically appropriate, free-energy functionals that do not have undesired numerical artifacts.

3504.330

Visual Explanation and Insight

B. N. Wylie, K. W. Boyack, D. K. Johnson, B. A. Hendrickson, M. H. Koller

With the current trend of information collection and storage, the quantity of information far exceeds the analyst's ability to comprehend it. Conventional tools exist for exploring small amounts of data, such as key-word search or text-matching techniques, but these approaches break down when trying to decipher emerging trends and relationships within large data sets. Sandia's knowledge-mining and -management tool, VxInsight™, explores new methods for visually presenting the structural context of large sets of relational data. Preliminary use of the tool demonstrated a powerful capability of enabling analysts to discover information through their interaction within the visual environment. Through exploration, users can detect emerging trends over time, observe interactions of scientific fields, and grasp the overall structure of large data sets. With the use of encapsulated data techniques, VxInsight™ has a broad range of applications. Currently within Sandia, VxInsight™ is being used to explore transaction data for intelligence agencies, track competitive research using patent data, and follow research trends in published articles.

Currently, we have not fully explored the potential of this tool, and verification of the structures, clustering, and techniques used by VxInsight™ need to be addressed. We need further research to begin to understand how this and other tools will become the basis for a 21st-century knowledge–based society.

• We developed some rudimentary verification and validation techniques for use with the ordination algorithm used in the VxOrd tool. Ordination is defined as the process of giving 2-D coordinates to a group of objects with a user-defined similarity metric between objects. These initial validation techniques include both quantitative measurements of Euclidean distances between similar objects and repeatability tests with different random seeds.

• We conducted research on other knowledge-management tools, including SGI's Mineset (3-D visual relationship tool) and Pacific Northwest National Laboratory's Spire (text–based clustering on documents).

• We explored alternate ordination approaches and developed an interactive application that allows the user to define the similarity metric and control the forces guiding the ordination.

• We applied VxInsight™ to new fields, including transactions and patent analysis, and are working on fraud, waste, and abuse (FWA).

• We applied VxInsight™ to real-world problems, including strategic alliance research and weapon parts transaction analysis.

Publications

Refereed

Davidson, G. S., B. Hendrickson, D. K. Johnson, C. E. Meyers, and B. N. Wylie. 1998. "Knowledge Mining with VxInsight™: Discovery Through Interaction." *J. Intel. Inform. Sys.* **11** (November/December).

THIS PAGE
INTENTIONALLY BLANK

ELECTRONICS & PHOTONICS

Electronics and Photonics solicits research that ensures the supply of Sandia components supporting the DOE mission of stockpile stewardship. This area emphasizes concepts that will enable the realization of small, low-power, highly integrated electronics packages.

Electronics and Photonics projects are represented by two categories of effort: (1) silicon–based microdevices for defense, energy, and industrial uses, seeking new concepts for microelectronics, photonics, microelectromechanical systems (MEMS), and sensors; and (2) integration solutions suitable for high-yield, high-reliability microsystems, including integrated packages capable of communication, self-authentication, and encryption.

Because of the potential devastation of losing huge amounts of information during a power outage or when a computer freezes up, the development of a method to preserve this information could have a revolutionary impact on society, whether in a commercial, scientific, or home environment. Such a development would be especially helpful in defense systems that work in harsh environments, such as those associated with satellites and nuclear weapons, where a radiation-hardened, low-voltage chip would be invaluable.

Information is lost because electrons, which are not stable, do much of the memory work in electronic devices. Attempts to create circuits that save the information on a computer screen use high voltages, which quickly wear down computer electronic components, and they are expensive.

In a project titled "A Novel Nondestructive Silicon-on-Insulator Nonvolatile Memory," Sandia researchers sought to design, fabricate, characterize, and optimize simple circuits to create a novel, low-power, nonvolatile memory. They were successful in developing techniques that could lead to an inexpensive, low-powered, memory-retaining device that may keep computer data from being lost during a power outage. The technique is simple and requires only a few extra processing steps over those currently used in creating microchips. This R&D 100 award-winning memory-retentive computer chip uses hydrogen ions as the primary carriers of information.

Sandia and its partner in this project have applied for a patent on a prototype memory-retention device that is inexpensive, low-powered, and simple to fabricate.

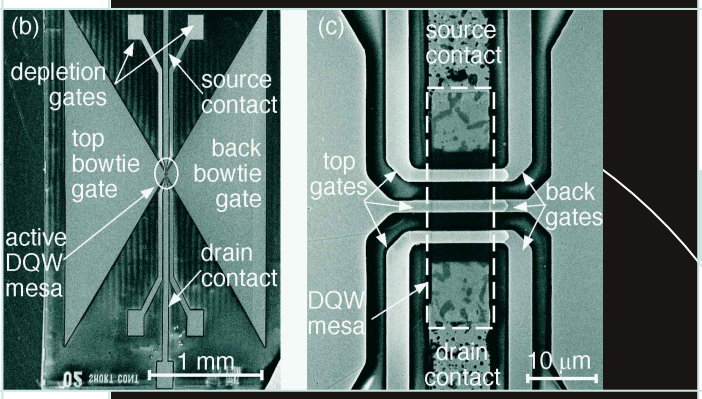

THIS PAGE
INTENTIONALLY BLANK

3506.190

Advanced Concepts for High-Power VCSELs and VCSEL Arrays

K. D. Choquette, G. R. Hadley, A. A. Allerman, W. W. Chow

Sandia designed, fabricated, and characterized high-power, single- and multimode, vertical-cavity surface-emitting lasers (VCSELs). We fabricated VCSELs emitting into a single-transverse mode using two approaches: (1) designed novel buried-oxide apertures to overlap the longitudinal field null, and (2) designed leaky-mode VCSELs using lateral modification of the cavity resonance to provide the lateral refractive index difference. Using the first approach, we demonstrated single-mode operation to 3.5 mW for 850 nm VCSELs. The second approach resulted in single-mode VCSEL operation to 13 times threshold producing 1 mW. Further efforts continue for the second approach. For high-power continuous-wave (CW) operation, we leveraged 2-D VCSEL arrays. We showed output powers as high as 0.6 W, which were limited by thermal management issues. We achieved pulsed output power as great as 1 W using large-area selectively oxidized VCSELs. We achieved the overall project objective to develop high-power, single-mode and multimode sources appropriate for many applications leveraging the many inherent advantages of VCSELs.

We demonstrated high-power single- and multimode VCSELs and accomplished the following:

(1) Fabricated and packaged 8x8 selectively oxidized VCSEL arrays for high-power operation. Using an advanced ceramic pin grid-array package, we demonstrated greater than 0.6 W of CW output. The maximum output power is limited by the package heat sinking.

(2) Characterized the effects of thermal crosstalk in 2-D VCSEL arrays.

(3) Found that individual large-area VCSELs producing greater than 15 mW maximum output exhibited unchanged laser characteristics at room temperature for greater than 300 hours.

(4) Demonstrated leaky-mode VCSELs employing transverse cavity modifications to produce antiguided optical confinement for the first time. The leaky-mode VCSELs showed single-mode operation to 13 times threshold and fivefold improvement over conventional VCSELs. Single-mode output power was limited to 1 mW due to the output mirror coupling. Further studies continue for this technology.

(5) Characterized single-mode VCSELs using thin and thick buried-oxide layers. Although the thin-oxide devices exhibited lower optical loss and greater mode size, the thick-oxide VCSELs exhibited higher single-mode output due to greater modal discrimination.

Publications

Refereed

Choquette, K. D. 1998. "Optical Confinement in Selectively Oxidized Vertical-Cavity Lasers." Paper presented to the Semiconductor Science and Technology Conference, La Jolla, CA, September.

Choquette, K. D., and H. Q. Hou. 1997. "Vertical-Cavity Surface-Emitting Lasers: Moving from Research to Manufacturing." *Proc. IEEE* (Invited) **85** (October): 1730–1741.

Choquette, K. D., A. A. Allerman, H. Q. Hou, G. R. Hadley, K. M. Geib, and B. E. Hammons. 1998. "Improved Efficiency of Small-Area Selectively Oxidized VCSELs." *Proc. 16th Internat. Semiconductor Laser Conf.* (Nara, Japan, October): 237–238.

Choquette, K. D., A. A. Allerman, H. Q. Hou, K. M. Geib, and B. E. Hammons. 1998. "Applications and Performance of VCSELs." Paper presented to the 1998 GaAs IC Symposium (plenary), Atlanta, GA, November.

Choquette, K. D., A. A. Allerman, K. M. Geib, B. E. Hammons, D. Mathes, and R. Hull. 1998. "Design of Oxide Aperture Profile Within Selectively Oxidized VCSELs." Paper presented to the 1998 LEOS Annual Meeting, Orlando, FL, December.

Choquette, K. D., G. R. Hadley, H. Q. Hou, K. M. Geib, and B. E. Hammons. 1998. "Leaky-Mode Vertical-Cavity Lasers Using Cavity Resonance Modifications." *Electron. Lett.* **34** (June): 991–992.

Choquette, K. D., G. R. Hadley, H. Q. Hou, K. M. Geib, and B. E. Hammons. 1998. "Leaky-Mode Vertical-Cavity Lasers Using Cavity Resonance Modifications." *Proc. Conf. Lasers and Electro-Optics (CLEO '98)* (San Francisco, CA, May): 587.

Choquette, K. D., H. Q. Hou, G. R. Hadley, K. M. Geib, and B. E. Hammons. 1997. "Thick-Oxide Aperture Single-Mode Vertical-Cavity Lasers." *Proc. 1997 OSA Ann. Mtg.* (Long Beach, CA, October): 245.

Choquette, K. D., H. Q. Hou, K. M. Geib, M. H. Crawford, and B. E. Hammons. 1997. "High-Performance Selectively Oxidized Vertical-Cavity Laser Arrays." *Proc. 44th Nat. Symp.—Amer. Vac. Soc.* (Invited) (San Jose, CA, October): 456.

Hegarty, S. P., G. Huyet, J. G. McInerney, K. D. Choquette, K. M. Geib, and H. Q. Hou. 1998. "Size Dependence of Transverse Mode Structure in Oxide-Confined Vertical-Cavity Lasers Diodes." *Appl. Phys. Lett.* **73** (July): 596–598.

Other

Choquette, K. D., W. W. Chow, G. R. Hadley, H. Q. Hou, K. M. Geib, and B. E. Hammons. 1997. "Engineering the Optical Properties of Selectively Oxidized Vertical-Cavity Lasers." *OSA Trends in Optics and Photonics* **15** (June): 125–129.

3506.110

Wafer Fusion for Integration of Semiconductor Materials and Devices

K. D. Choquette, S. H. Kravitz, A. A. Allerman, M. H. Crawford, D. M. Follstaedt

Sandia developed a low-temperature wafer-fusion process to achieve integration of semiconductor materials and heterostructures with widely disparate lattice parameters, electronic properties, and/or optical properties for novel devices not possible on any one substrate. As a baseline fabrication technology applicable to many semiconductor systems, wafer fusion has enabled novel device configurations not possible by epitaxial growth. Using our simple process, we developed appropriate wafer-fusion techniques for GaAs on AlGaAs, GaAs on GaP, and InP on Si. We demonstrated the viability of this technology by integrating infrared (IR) vertical-cavity surface-emitting lasers (VCSELs) on transparent AlGaAs and GaP substrates. Thus, we have achieved substrate-emitting, short-wavelength, high-performance laser sources for the first time.

We optimized the fusion process for device technology integration onto dissimilar substrates. We fabricated and characterized bottom-emitting short-wavelength VCSELs. Specific accomplishments include the following:

(1) Examined the fused interface between VCSELs bonded on AlGaAs and GaP transparent substrates by transmission electron microscopy (TEM). We observed a disordered interface region without evidence of extended defects and did not detect oxygen at the bonded interface.

(2) We achieved reliability tests of IR VCSELs bonded to transparent AlGaAs. The preliminary results indicate that the VCSELs exhibit no degradation over 300 hours of continuous-wave operation at room temperature.

(3) We optimized the fusion process for bonding VCSELs to GaP and improved the fabrication sequence for bottom-emitting VCSELs, resulting in high-performance, bottom-emitting, 850 nm VCSELs. For IR VCSELs bonded to GaP, we achieved a threshold voltage reduction of 3 volts by bonding at 600°C and using appropriate ohmic contacts.

Publications

Refereed

Choquette, K. D., B. E. Roberds, K. M. Geib, H. Q. Hou, R. D. Twesten, K. L. Lear, and B. E. Hammons. 1997. "Bottom-Emitting 850 nm Selectively Oxidized VCSELs Fabricated Using Wafer Bonding." *Proc. 1997 LEOS Ann. Mtg.* (San Francisco, CA, November): 687–688.

Choquette, K. D., H. Q. Hou, M. E. Warren, M. H. Crawford, K. M. Geib, and B. E. Hammons. 1998. "Performance and Applications of Selectively Oxidized Vertical-Cavity Lasers." *Proc. 1998 IEEE Aerospace Conf.* (Snowmass, CO, March).

Choquette, K. D., K. M. Geib, B. E. Roberds, H. Q. Hou, and B. E. Hammons. 1998. "Short-Wavelength Bottom-Emitting Vertical-Cavity Lasers Fabricated Using Wafer Bonding." *Electron. Lett.* **34** (June): 1404.

3506.120

Highly Parallel, Low-Power, Photonic Interconnects for Inter-Board Signal Distribution

P. J. Robertson, L. E. Shea, V. M. Hietala, K. D. Choquette, L. G. Pierson, M. E. Warren, C. J. Helms

The transmission of digital signals has become ubiquitous in Sandia applications, which range from weapons interconnections to secure parallel computing and signal processing. Many of these digital interconnects occur at the board or connector level and require low-power communication of data in formats that allow for (1) electromagnetic interference (EMI) immunity, (2) scalability to large numbers of parallel channels, and (3) large data throughputs over serial links at moderate (< 3 m) distances. In almost all of these cases, separability of links is required to allow for separately yielded boards that are field-interchangeable. The separability requirement, in particular, causes problems for traditional electrical edge-card and cable connectors. In cases where a large EMI is present, these connectors must provide filtering, which greatly limits their potential data rates. If scalability is needed, the board-level electrical connectors are limited in data-throughput density. This is because such connectors are limited by crosstalk and electrical impedance matching, and must have a certain area of the metal-to-metal contact to function reliably through repeated mating and de-mating steps. Another factor that limits data-throughput density is the need for equal numbers of signal and ground lines to prevent crosstalk and ground-bounce effects. These difficulties can be alleviated with photonic interconnections that provide noncontacting separable connections, if the photonic interconnections can be realized at a sufficiently low-power consumption. Here, Sandia's high-efficiency vertical-

cavity surface-emitting laser (VCSEL) technology can be brought to bear, as it can be combined with appropriate optics or optical fibers and optimized photoreceivers to produce high-density, scalable interconnections that are separable, but consume much less power than previous optical links using light-emitting diodes (LEDs) or edge-emitting laser sources. Possible implementations include low-power links that provide ultra-high isolation of signals and limited power transmission and parallel free-space board-to-board interconnections for protocol processing applications.

We focused on enabling technologies and demonstration of operating links. We developed a demonstration of the high isolation power and data transmission connector. In this design, high-power, fiber-coupled lasers illuminate multiple center-tapped photovoltaic (PV) cells for power transfer to remote modules. Detectors, VCSELs, and optical fibers are held in alignment by submounts within the connector body, and light passes between the two sides of the connector through windows that contain collimating optics. We designed and fabricated applicable drive and receiver circuitry. We designed and fabricated a 64-element integrated receiver array and showed that individual elements operate at 850 nm up to 100 Mbps. We fabricated a flex-circuit optical board holding both the VCSEL array and the receiver array. We developed a unique method of automatically aligning the two free-space optical interconnect boards. This method involved the use of an infrared digital assistant (IrDA) link (common on laptop computers) as the reverse channel that can operate without exact alignment. We accomplished the mechanical movement of the boards using unique Rainbow piezoelectric actuators. We built and will use these actuators to align two optical boards.

Publications

Other

Robertson, P. J., L. Shea, C. Sullivan, K. D. Choquette, L. G. Pierson, K. Gass, and T. Hardin. 1998. "Final Report and Documentation for the Highly Parallel, Low-Power, Photonic Interconnects for Inter-Board Signal Distribution." Sandia Technical Report, in preparation.

3506.140

Virtual Reactor for the Semiconductor Manufacturing Plant of the Future

M. E. Coltrin, K. M. Horn, H. K. Moffat, J. F. Klem, K. C. Baucom, C. P. Tigges, T. J. Drummond

This project will develop a sophisticated system to enable model–based agile manufacturing in the critical metalorganic chemical vapor deposition (MOCVD) and molecular beam epitaxy (MBE) materials growth processes essential to high-speed microelectronics and optoelectronic components. This effort is founded on a modular and configurable process automation system that will serve as a backbone allowing integration of process-specific models and sensors. Sandia will develop and integrate both MOCVD- and MBE-specific models in this system and demonstrate the effectiveness of both model–based and sensor–based real-time feedback control in improving the accuracy and reproducibility of semiconductor heterostructure growth on MOCVD and MBE systems. In addition, within this framework we will construct virtual reactor models for both growth processes and will show how we can use these models to greatly shorten the epitaxial growth process development cycle.

We applied *in situ* reflectance and a simple real-time feedback control algorithm in our MBE growth system. We used this approach to reproducibly grow a complex indium aluminum gallium arsenide (InAlGaAs) resonant-cavity reflectance modulator structure with a resonance wavelength position error of approximately ± 0.3%.

We demonstrated the generality and predictive nature of the reflectance monitor and feedback algorithm described above by applying them to a substantially modified modulator structure with nearly identical results, without adjusting any model parameters.

We generalized our analytical virtual reactor model of a rotating-disk MOCVD reactor to consider forced-flow situations, i.e., when the reactor is operated with inlet flow velocities in excess of the flow required by the ideal rotating disk's natural drawing velocity. The model can now be used for pure stagnation flows, i.e., zero rotation rate or pure rotating disk flows, and for any case between the two pure limits. We found a simple scaling relationship to characterize the mass transport limited growth rate as a function of two Reynolds numbers, one based on rotation rate and the other based on inlet velocity.

Publications

Refereed

Breiland, W. G., H. Q. Hou, B. E. Hammons, and J. F. Klem. 1998. "*In Situ* Reflectance and Virtual Interface Analysis for Compound Semiconductor Process Control." *Proc. 1998 Electrochem. Soc. Nat. Mtg.*

3506.160

Selective Oxidation Technology and Its Applications Toward Electronic and Optoelectronic Devices

O. B. Spahn, A. V. Smith, C. I. H. Ashby, J. P. Sullivan, C. T. Sullivan, J. F. Klem, G. A. Vawter, K. D. Choquette, A. A. Allerman

Selective oxidation of aluminum gallium arsenide (AlGaAs) compounds has facilitated dramatic improvements in the performance of near-infrared (IR) vertical-cavity surface-emitting lasers (VCSELs). Sandia will (1) expand our understanding of both the strengths and the limitations of this technology, (2) explore its applicability to other Al-bearing materials, (3) utilize this technology base to demonstrate a variety of new electronic and optoelectronic devices, and (4) establish the reliability and manufacturability of oxidized devices such as VCSELs. Specifically, we will investigate conditions required to maximize control of the oxidation process as well as those required to facilitate/inhibit etching of the resultant oxide. Concurrently, we will perform preliminary studies to extend the technology to other Al-bearing compounds such as Al(Ga)AsSb, InAl(Ga)P, and Al(Ga)N. We will consider several new devices utilizing the selective oxidation technology of AlGaAs, as well as of Al(Ga)AsSb. On a separate front, we will also explore the possibility of using oxidized AlGaAs and InAl(Ga)P to form GaAs/AlGaAs field-effect transistors (FETs). Finally, we will address reliability and manufacturability issues of the high-performance VCSELs fabricated using selective oxidation technology.

We established a robust, manufacturable oxidation process that resulted in the design, fabrication, and testing of high-power, high-speed, oxide-confined VCSEL structures. Furthermore, extended lifetime tests prove that reliability of the oxidized VCSELs is comparable to commercial implanted devices.

We oxidized AlGaAs and evaluated it as a waveguide material. We obtained significantly lower losses with oxidized layers embedded in the waveguide than reported by others in the literature. We observed anomalous polarization behavior, however, with launch polarization appearing to rotate upon propagation of some distance in the oxidized waveguide.

We modeled how the production of large amounts of elemental As during the oxidation and its diffusion into adjacent regions can modify the properties of these regions in ways that impact device design, fabrication, and performance. The oxidation rate is determined primarily by the Al mole fraction, but the close proximity of a faster-oxidizing layer can produce a several-fold increase in oxidation rate for a layer of a given Al composition over the rate obtained with an isolated layer of the same composition. Injection of As interstitials into adjacent layers and the resulting development of defects, such as As antisite defects and Group-III vacancies and interstitials, can alter the oxidation rate for nearby regions. Observed rate accelerations are consistent with the diffusion of As-generated defects from the fast-reaction layer to the slower-reaction layer. Our model, based on the role of elemental As in such behavior as enhanced oxidation rates in close proximity to faster-oxidizing layers, the effect of relative layer thicknesses, and dependence of oxidation rate on position within the total structure, provides a semi-quantitative prediction of oxidation profile for complex structures.

We explored an alternative strategy for reducing the interface state density of insulator-GaAs interfaces. We applied a sulfur–based wet-chemical surface passivation treatment to freshly etched GaAs surfaces prior to formation of the insulator layer. Early testing involved the use of a low-temperature–deposited insulator, silicon oxynitride, which we chose to reduce the possibility of sulfur migration from the interface during insulator formation.

Publications

Refereed

Ashby, C. I. H. 1998. “Compound Semiconductor Surface Passivation and Novel Device Processing.” Paper presented to the Spring MRS Meeting (Invited), San Francisco, April.

Ashby, C. I. H. 1998. “Device/IC Processing Challenges for Commercial Applications: Dynamics of Wet Oxidation of High-Al-Content III–V Materials.” Paper presented to the 1998 Fall MRS Symposium I: III–V and SiGe Group IV (Invited), Boston, MA, December.

Ashby, C. I. H. 1998. “Material Science of Oxidation.” Paper to be presented to the Gordon Conference Electronic Materials: Chemistry, Excitations, and Processing (Invited), Henniker, NH, July 1999.

Ashby, C. I. H. 1998. “The Critical Role of Arsenic in Wet Oxidation of AlGaAs.” Paper to be presented to PCSI-26: 26th Conference on the Physics and Chemistry of Semiconductor Interfaces (Invited), San Diego, CA, January 1999.

Ashby, C. I. H., R. D. Twesten, K. D. Choquette, D. M. Follstaedt, K. M. Geib, O. Blum, and H. Q. Hou. 1998. “Wet Oxidation of AlGaAs: Elemental Arsenic and Its Influence on the Oxidation Process.” Paper presented to the 1998 Electronic Materials Conference, Charlottesville, VA, June.

Ashby, C. I. H., R. D. Twesten, K. D. Choquette, D. M. Follstaedt, K. M. Geib, O. Blum, and H. Q. Hou. 1998. “Wet Oxidation of AlGaAs: The Influence of Elemental Arsenic on the Oxidation Process.” Paper presented to the 1998 Annual Symposium of the New Mexico Chapter of the American Vacuum Society, Albuquerque, NM, May.

Choquette, K. D. 1998. “Optical Confinement in Selectively Oxidized Vertical-Cavity Lasers.” Paper presented to the Semiconductor Science and Technology Conference, La Jolla Institute, La Jolla, CA, September.

Choquette, K. D. 1998. “The Technology and Applications of Selective Oxidation of AlGaAs.” Paper presented

to the 10th Conference on Semiconducting and Insulating Materials (SIMC-X), Berkeley, CA, June.

Choquette, K. D., and H. Q. Hou. 1997. "Vertical-Cavity Surface-Emitting Lasers: Moving from Research to Manufacturing." *Proc. IEEE*. **85** (November): 1730.

Choquette, K. D., A. A. Allerman, H. Q. Hou, G. R. Hadley, K. M. Geib, and B. E. Hammons. 1998. "Improved Efficiency of Small-Area Selectively Oxidized VCSELs." Paper presented to the 16th International Semiconductor Laser Conference, Nara, Japan, October.

Choquette, K. D., A. A. Allerman, K. M. Geib, B. E. Hammons, D. Mathes, and R. Hull. 1998. "Design of Oxide Aperture Profile Within Selectively Oxidized VCSELs." Paper presented to the 1998 LEOS Annual Meeting, Orlando, FL, December.

Choquette, K. D., H. Q. Hou, K. M. Geib, and B. E. Hammons. 1997. "Uniform Selectively Oxidized Two-Dimensional VCSEL Arrays for VLSI Photonics." Paper presented to the 1997 LEOS Annual Meeting, San Francisco, CA, November.

Choquette, K. D., H. Q. Hou, K. M. Geib, M. H. Crawford, and B. E. Hammons. 1998. "High-Performance Selectively Oxidized Vertical-Cavity Laser Arrays." Paper presented to the 44th National Symposium American Vacuum Society, San Jose, CA, October.

Crawford, M. H., K. D. Choquette, R. J. Hickman, and K. M. Geib. 1997. "Performance of Selectively Oxidized AlGaInP–Based Visible VCSELs." *OSA Trends in Optics and Photonics* **15**: 112.

Hegarty, S. P., G. Huyet, J. G. McInerney, K. D. Choquette, K. M. Geib, and H. Q. Hou. 1998. "Size Dependence of Transverse Mode Structure in Oxide-Confined Vertical-Cavity Lasers Diodes." *Appl. Phys. Lett.* **73** (August): 569.

Li, H., A. Hohl, A. Gavrielides, H. Q. Hou, and K. D. Choquette. 1998. "Stable Polarization Self-Modulation in Vertical-Cavity Surface-Emitting Lasers." *Appl. Phys. Lett.* **72** (July): 2355.

Other

Choquette, K. D. 1998. "Technology of Selectively Oxidized Vertical-Cavity Lasers." *Vertical-Cavity Surface-Emitting Lasers—New Technologies and Applications*, accepted.

Choquette, K. D., H. Q. Hou, G. R. Hadley, K. M. Geib, and B. E. Hammons. 1997. "Thick-Oxide Aperture Single-Mode Vertical-Cavity Lasers." Paper presented to the 1997 OSA Annual Meeting, Long Beach, CA, October.

Choquette, K. D., H. Q. Hou, K. M. Geib, and B. E. Hammons. 1997. "Low-Threshold InGaAs Selectively Oxidized Vertical-Cavity Lasers." Paper presented to the 1997 OSA Annual Meeting, Long Beach, CA, October.

Choquette, K. D., W. W. Chow, G. R. Hadley, H. Q. Hou, K. M. Geib, and B. E. Hammons. 1997. "Engineering the Optical Properties of Selectively Oxidized Vertical-Cavity Lasers." *OSA Trends in Optics and Photonics* **15**.

3506.180

Agile Prototyping of Microelectromechanical Systems (MEMS)

H. K. Schriner, C. L. Henderson, K. Current, E. J. Garcia, J. J. Sniegowski, M. S. Rodgers

Under this project Sandia is developing an agile prototyping capability for microelectromechanical sensors (MEMS) and actuators based on Sandia's state-of-the-art tri-level polysilicon micromachining process (Sandia Ultra-planar Multi-level MEMS Technology [SUMMiT]).

Making Sandia's state-of-the-art surface-micromachining technology more widely available will vastly increase its impact. The agile prototyping capability will make available to a variety of both Defense Programs (DP) and non-DP the ability to test new concepts in this advanced manufacturing technology in a relatively short period of time. Sandia's capability to manufacture MEMS structures with three structural levels of polysilicon and integrated electronics will be unique among micromachining facilities.

We are ahead of schedule on our stated milestones, having already successfully completed several lots of wafers in SUMMiT using a reticle that includes designs by designers both inside and outside Sandia. We made the manufacturing process more robust and have begun correlating performance data with process control data. We also made good progress on design tool development—this year we integrated design-rule checking into our computer-aided design (CAD) environment. Finally, we far exceeded our goals in developing training materials for new designers.

We successfully implemented an advanced design course specifically geared toward educating designers on the intricacies in designing in our complex three-layer technology. We further improved our standard components library, design rules, and design rule checker, and incorporated a cross-sectional visualization tool and prototyped a 3-D visualizer tool. We also successfully fabricated twelve multi-user reticle sets using designs both internal and external to Sandia.

Publications

Refereed

Barron, C. C., B. R. Davies, J. J. Sniegowski, M. S. Rodgers, J. H. Comtois, and M. A. Michalicek. 1997. "SAMPLE (Sandia Agile MEMS Prototyping, Layout Tools, and Education)." *Proc. SPIE Micromachining and Microfabrication Process Technol. III* **3223** (Austin, TX, 29 September): 10–16.

Schriner, H. K., B. R. Davies, J. J. Sniegowski, M. S. Rodgers, J. J. Allen, and C. Shepard. 1998. "Sandia Agile MEMS Prototyping, Layout Tools, Education and Services Program." *Proc. 2nd Internat. Conf. Engin. Design and Automation CD* (EDA '98, Wailea, HI, 9–12 August).

3506.210

Midwave-Infrared (2–6 µm) Emitter–Based Chemical Sensor Systems

S. R. Kurtz, A. A. Allerman, R. M. Biefeld, A. J. Ricco

Long-wavelength (2–6 µm) diode emitters are desirable for many applications, including monitoring of chemical species in the environment and manufacturing, long-wavelength fiber-optic communications, lidar, and infrared (IR) detector countermeasures. No practical diode lasers are available for any of these applications because the band structure of bulk III–V, II–VI, and IV–VI semiconductor alloys results in large Auger recombination rates at these wavelengths. Experimental and theoretical work at Sandia resulted in new understanding of the electronic properties of narrow-bandgap III–V heterostructures, and we found methods to reduce the Auger rates in certain indium arsenide antimony (InAsSb) superlattices and quantum wells (QWs). These devices enable us to begin chemical-sensing demonstrations of important species such as CO–CO_2 and numerous other compounds. This project will involve developing chemical-sensing systems and determining the sensitivity and limitations of these systems. Concurrently, we will improve on IR emitters used in these systems.

We demonstrated the first cascaded lasers and light-emitting diodes (LEDs) with type I InAsSb QW active regions using the Sandia-designed reactor. Also, these were the first cascaded devices grown by metalorganic chemical vapor deposition (MOCVD). The broadband LEDs produced high average powers, > 2 mW (@ 80°K, 3.7 µm) and > 0.1 mW (@ 300°K, 4.3 µm). The 10-stage, 3.8–3.9 µm laser operated up to 180°K. At 80°K, we observed peak laser power > 100 mW and a slope efficiency of 48% (4.8% per stage). Slope-efficiency was strongly dependent on cavity length, and analysis of efficiency data suggests an internal quantum efficiency > 1 and a loss coefficient * 100 cm^{-1}. We are optimistic that advances in material quality and device design will improve carrier confinement and reduce loss, leading to higher efficiencies and higher-temperature operation of cascaded InAsSb lasers.

We examined by optical pumping several laser structures grown in the Sandia MOCVD reactor. These structures consisted of an InAs substrate with a 2.5 µm-thick AlAsSb lower cladding, a 1.0 µm-thick InAsSb/InAs (83^3 / 87^3) strained-layer superlattice (SLS) active region and several different top terminations. We pumped the SLS laser with a Q-switched Nd:YAG (1.06 µm, 20 Hz, 10 ns pulse, focused to a 200 µm-wide line) and detected emission with a Fourier transform infrared (FTIR) operated in a step-scan mode. We observed laser emission from cleaved bars, 1000 µm wide, with uncoated facets. We saw a lasing threshold and spectrally narrowed laser emission from 80°K through 240°K, the maximum temperature where lasing occurred. At 80°K, we could obtain peak powers > 100 mW. The temperature dependence of the SLS laser threshold is described by a characteristic temperature, T_0 = 33°K, over the entire range. Similar experiments on structures containing 2000^3 InAs top and bottom wave-guiding regions resulted in improved power (> 650 mW) at 80°K and 3.8 µm. We obtained this result using an 808 nm diode stack pump laser with a 2% duty cycle and 50 µs pulses in collaboration with Phillips Laboratory.

Publications

Refereed

Allerman, A. A., S. R. Kurtz, R. M. Biefeld, and K. C. Baucom. 1998. "10-Stage, Cascaded InAsSb Quantum-Well Lasers at 3.9 µm." *Electron. Lett.* **34** (19 February): 369–370.

Kurtz, S. R., A. A. Allerman, R. M. Biefeld, and K. C. Baucom. 1998. "High Slope Efficiency, Cascaded Mid-Infrared Lasers with Type I InAsSb Quantum Wells." *Appl. Phys. Lett.* **72** (27 April): 2093–2095.

3506.230

A Novel Nondestructive Silicon-on-Insulator Nonvolatile Memory

J. R. Schwank, M. R. Shaneyfelt, D. M. Fleetwood, J. R. Murray, B. L. Draper, W. L. Warren

Radiation-hardened nonvolatile memories are used in several Sandia, other DOE, and DoD systems for both program and critical data storage. This project will design, fabricate, and characterize a novel nondestructive, low-power, nonvolatile memory based on protonic transport in the buried oxides of silicon-on-insulator (SOI) transistors. SOI technology offers advantages over bulk-silicon (Si) technology for high-speed/lower-power and radiation-hardened (single-event upset [SEU] and high dose rate) applications. We performed previous laboratory work that shows that the most common techniques used to fabricate SOI substrates cause many oxygen vacancies in the buried oxide. If these oxides are exposed to hydrogen at moderate temperatures (600°C to 800°C), mobile protons can be generated. These protons can be made to move from the top to bottom oxide/Si interface by application of an electric field. The motion of the protons forms the basis for a nonvolatile memory. In the first two years of this project, we examined methods for optimizing protonation effects in capacitors. We developed a circuit architecture for fabricating an SOI–based nonvolatile memory. One of the key goals of this work was to demonstrate that mobile protons could be generated in a state-of-the-art processing facility. In addition, we performed experiments to better understand the mechanisms for proton incorporation and the effects of ionizing

irradiation on protonic transport and memory retention. We will investigate protonic transport in transistors and build a simple one-cell nonvolatile memory. We will characterize transistor test structures for their electrical, radiation, fatigue, and retention properties. We will also demonstrate at the transistor and integrated circuit (IC) level the feasibility of an SOI nonvolatile memory based on proton motion in the buried oxide.

Previously, we expended considerable effort at optimizing anneal conditions for maximizing voltage hysteresis on capacitors. Previous device structures used aluminum (Al) metallization and, consequently, we could not perform repeated anneal/measurements. Because the turnaround time for fabricating capacitor lots was normally more than two months, this severely limited the number of anneal variations. To greatly enhance the number of variations of anneal cycles, we developed a process flow that uses TaSi instead of AlSi for this work. The TaSi metallization contacts can withstand post-annealing treatments up to 900°C, and repeated anneal/measurement cycles can be performed. We performed several different types of hydrogen anneals, including standard furnace anneals, rapid thermal anneals (RTA), and vacuum anneals. We obtained the best results from samples using RTA with a fast ramp-up to temperature and a fast ramp-down. We obtained the maximum hysteresis voltage shifts around 3 V for a 700°C, 15-minute RTA anneal on small pieces of wafers (< 1 in.^{2}). These shifts are sufficient to fabricate a nonvolatile memory. Unfortunately, the uniformity across the sample was poor (1 to 3 V, typical). We developed two memory architectures for the SOI nonvolatile field-effect transistor (NVFET). The first is an electrically erasable programmable read-only memory (EEPROM) cell that consists of an NVFET and an *n*-channel metal-oxide semiconductor (NMOS) access transistor. During a read mode, we ground the gate so there is no risk of upsetting the data in the cell. We do not use the gate to select which cell to read, so we require an access transistor. The second option is a Flash architecture. The advantage of this approach is that we require only one NVFET per cell and no access transistor. The disadvantage is that the gate of the NVFET is biased during read operations.

Publications

Refereed

Vanheusden, K., D. M. Fleetwood, J. R. Schwank, M. R. Shaneyfelt, T. L. Meisenheimer, and B. L. Draper. 1998. "The Effect of Irradiation and Proton Implantation on the Density of Mobile Protons in SiO_2 Films." *IEEE Trans. Nucl. Sci.*, accepted.

Vanheusden, K., J. R. Schwank, W. L. Warren, D. M. Fleetwood, and R. A. B. Devine. 1977. "Radiation-Induced H+ Trapping in Buried SiO_2." *J. Microelectron.Engin.* **36** (June): 241–244.

Vanheusden, K., R. A. B. Devine, J. R. Schwank, D. M. Fleetwood, R. G. Polcawich, W. L. Warren, S. P. Karna, and R. D. Pugh. 1997. "Irradiation Response of Mobile Protons in Buried SiO_2." *IEEE Trans. Nucl. Sci.* **44** (December): 2087–2094.

Vanheusden, K., W. L. Warren, D. M. Fleetwood, J. R. Schwank, M. R. Shaneyfelt, B. L. Draper, P. S. Winokur, R. A. B. Devine, L. B. Archer, G. A. Brown, and R. M. Wallace. 1998. "Chemical Kinetics of Mobile-Proton Generation and Annihilation in SiO_2 Thin Films." *Appl. Phys. Lett.* **73** (August): 674–676.

Vanheusden, K., W. L. Warren, R. A. B. Devine, D. M. Fleetwood, J. R. Schwank, M. R. Shaneyfelt, P. S. Winokur, and Z. J. Lemnios. 1987. "Nonvolatile Memory Device Based on Mobile Protons in SiO_2 Thin Films." *Nature* **386** (April): 587–589.

Warren, W. L., D. M. Fleetwood, J. R. Schwank, M. R. Shaneyfelt, B. L. Draper, P. S. Winokur, M. J. Knoll, K. Vanheusden, R. A. B. Devine, L. B. Archer, and R. M. Wallace. 1997. "Nonvolatile Field-Effect Transistors Based on Protons in Si/SiO_2/Si Structures." *IEEE Trans. in Nucl. Sci.* **44** (December): 1798–1797.

Warren, W. L., K. Vanheusden, D. M. Fleetwood, J. R. Schwank, M. R. Shaneyfelt, P. S. Winokur, and R. A. B. Devine. 1996. "Proposed Model for Positive Charge in SiO_2 Thin Films: Over-Coordinated Oxygen Centers." *IEEE Trans. on Nucl. Sci.* **43** (December): 2617–2626.

Other

Schwank, J. R., M. J. Anc, M. R. Shaneyfelt, B. L. Draper, T. L. Meisenheimer, W. L. Warren, K. Vanheusden, D. M. Fleetwood, and L. P. Schanwald. 1997. "Improving ITOX Conditions for Low Defect Density and BOX Breakdown." *Proc. 1997 IEEE Internat. SOI Conf.* (Yosemite, CA, October): 14–15.

Vanheusden, K., W. L. Warren, W. M. Shedd, R. D. Pugh, D. M. Fleetwood, J. R. Schwank, and R. A. B. Devine. 1997. "Characterization of Interface Traps in SOI Material." *Proc. 1997 IEEE Internat. SOI Conf.* (Yosemite, CA, October): 64–65.

3506.240

Integration of Optoelectronics and MEMS by Free-Space Microoptics

M. E. Warren, F. M. Hosking, A. A. Allerman, G. A. Vawter, J. R. Wendt, O. B. Spahn, R. E. Asbill, J. H. Smith

Combining microelectromechanical systems (MEMS) with optoelectronic components is a means of realizing compact optomechanical subsystems. Some examples are laser beam scanning, switching and routing and active focusing, and spectral filtering or shuttering of optical sources. A major obstacle to realizing these types of systems is the difficulty of integrating the two technologies. The devices use dissimilar materials with significant problems for a common process line. Another major difficulty with direct integration is providing the optical path for the MEMS components to interact with the light source. Simply stacking one device on top of another is not compatible with many optical wavelengths. Sandia will use folded optical paths in a transparent substrate to provide the interconnection route between the components of the system. The components will be surface-mounted by flip-chip bonding the substrate. Microoptics can be fabricated into the substrate to reflect and refocus the light at precise angles so that it can propagate from one device to another and be directed out of the substrate into free space. The MEMS components do not require the development of transparent optics and can be completely compatible with the current three-level polysilicon process. The optoelectronics devices will be vertical-cavity surface-emitting laser (VCSEL) arrays that are ideally suited for surface-mounting. This technology will enable the combination of two very successful activities—silicon MEMS and III–V optoelectronics—to address applications in weapons systems, sensor systems, and other areas. Optical systems that can be miniaturized include beam scanning for sensing, communications or displays, active focusing for motion sensing or tracking, and 2-D arrays of phase shifters for real-time reconfiguration of optical systems or miniature displays.

This year's work emphasized postprocessing MEMS components fabricated at Sandia. These postprocessing techniques include metallization of MEMS devices either before or after release, deep via etches, and complete release processing, including self-assembled monolayer coatings and sublimation drying. Prerelease metallization consists of gold coatings, which can survive the subsequent release etch and are patterned by conventional lithography; postrelease coatings are applied by shadow masking. The coatings allow for high-reflectivity polysilicon mirrors and for metallic bondpads for improved wire bonding and flip-chip bonding. The deep via etch process allows for transmission of light through the MEMS substrate that would otherwise be absorbed. The process allows vias to be etched all the way to the first oxide layer in the MEMS process from the back of the wafer. In addition to optical access, the vias are useful to improve the release of large structures and for advanced packaging and electrical interconnect concepts. The other area of process development is flip-chip bonding processes that can be used to mechanically and electrically interconnect MEMS and optoelectronic devices. Continued improvement in the gold thermocompression flip-chip bonding process includes destructive testing to investigate ways to improve the bond strength, and preliminary investigation of possible underfill adhesives that would improve bond strength while compatible with optical applications. We developed solder-bump bonding based on a solder-plating capability. We demonstrated good reproducibility of the solder plating and fluxless reflow of the solder and bonded some devices with this technique. We also developed an alternative to electroplating of solder, using an automated dispensing system for solder pastes. We developed optical designs for a scanning system incorporating moving MEMS mirrors and VCSEL arrays and will submit these designs for fabrication soon. We performed a number of functional demonstrations of optical systems with MEMS structures.

Publications

Other

Blum, O., M. E. Warren, H. Q. Hou, R. F. Carson, K. D. Choquette, M. S. Rodgers, and J. J. Sniegowski. 1998. "Combined Photonics and MEMS Function Demonstration." *Proc. SPIE Photonics West* **3286** (San Jose, CA, 25 January): 57–61.

Warren, M. E., O. Blum, C. T. Sullivan, R. J. Shul, M. S. Rodgers, and J. J. Sniegowski. 1998. "The Integration of Surface-Micromachined Devices with Optoelectronics: Technology and Applications." Paper presented to the Topical Meeting on Optical MEMS, Monterey, CA, 20–22 July.

3506.250

Advanced Laser Structures for Short-Pulsed Power in Active Optical Sensor Systems

G. A. Vawter, A. A. Allerman, F. J. Zutavern, W. W. Chow, G. R. Hadley, A. Mar

To address the technological needs of Sandia customers in DOE and DoD for high-power, low-cost, reliable, pulsed lasers in the 0.01–100.0 ns regime, we will develop diode lasers for short-pulse duration and high-peak pulse power. Our goal is up to 10 W, while maintaining good far-field beam quality and ease of manufacturability for low cost. We will achieve high-peak-power picosecond pulses by gain switching flared-geometry waveguide lasers and amplifiers. In the longer pulse-length regime, we will obtain 1 to 100 ns pulses using conventionally pumped ridge waveguide lasers of unique design. We will use novel very large optical cavity (VLOC) lasers to achieve high-saturated-output power.

A second, far-reaching aspect of pulsed diode lasers is their unique ability to generate very high repetition rate optical pulses in the microwave and millimeter-wave regime. We will explore experimentally all-optical monolithic integrated microsystems for direct generation of radio-frequency (RF) and millimeter-wave frequencies. Based on our successful demonstration of 90 GHz power generation from mode-locked ring diode lasers, we will explore new techniques to reduce noise in the output signal and actually tune the output frequency by adjusting bias currents within the laser.

• *Flared output lasers*. We (1) redesigned the flared lasers for reliability, yield, and power extraction, (2) activated a photoconductive semiconductor switch (PCSS) using a gain-switched laser, (3) demonstrated greater than 14 W peak output power from a flared laser in a 30 ps pulse, (4) fabricated, packaged, and tested flared lasers appropriate for use as pump sources for optical frequency conversion, (5) designed and built master-oscillator-power-amplifier (MOPA) lasers, which we will test next year for evaluation of output couplers, and (6) completed the gain-switched laser model.

• *LOC nonflared lasers*. We (1) improved the process technology for higher yield and output power, (2) demonstrated 560 mW peak output power from a VLOC laser using 1 µs drive pulses, (3) observed the predicted large, two-dimensionally expanded optical mode, (4) identified power limitations arising from the strong coupling of material refractive index to temperatures wherein significant deviation of the internal temperature from the simulated value causes loss of oscillation of the desired fundamental optical mode, and (5) proposed a new type of VLOC laser using vertically stacked waveguides with an antiguide-type coupling region to obtain the desired large optical mode without the temperature sensitivity observed in previous designs.

• *Mode-locked ring lasers for RF generation*. We (1) designed a wide range of ring-cavity lasers with integrated amplifiers and photodetectors for investigation of linewidth, noise, and frequency tuning, (2) designed both single-lateral-mode and multilateral-mode devices for exploration of reduced linewidth under single-mode operation, (3) developed robust process technologies for oxygen implantation and dielectric isolation, and (4) began fabricating mode-locked ring lasers.

Publications

Refereed

Vawter, G. A., C. T. Sullivan, J. R. Wendt, R. E. Smith, H. Q. Hou, and J. F. Klem. 1997. "Tapered-Rib Adiabatic-Following Fiber Couplers in Etched GaAs Materials for Monolithic Spot-Size Transformation." *IEEE J. Selected Topics in Quantum Electron.* (Invited) **3**(6) (December): 1361–1371.

Vawter, G. A., C. T. Sullivan, J. R. Wendt, R. E. Smith, H. Q. Hou, and J. F. Klem. 1998. "Tapered-Waveguide Mode Expansion in Etched GaAs Materials for Low-Loss Coupling of Photonic Structures to Optical Fiber." Paper presented to the 1998 OSA Annual Meeting/ILS-XIV (Invited), Baltimore, MD, 4–9 October.

3506.260

Metal Micro-Heat-Pipe Substrates for High-Power-Density Electronics

D. A. Benson, S. H. Kravitz, C. V. Robino, S. N. Burchett

Sandia will develop a new efficient substrate for cooling microelectronic systems. As electronic system requirements move toward higher processing speeds and ever-smaller weight and volume requirements, electronic cooling capabilities increase in importance. Sandia found that a major advance in cooling is now possible using an efficient Sandia micro-heat-pipe design combined with a metal substrate. A metal substrate such as Kovar matches the coefficient of thermal expansion of semiconductor die while the micro-heat-pipe gives very high effective thermal conductivity. The result is a robust, potentially low-cost and efficient cooling technology. First we developed processes and made and tested an initial prototype. Next we optimized prototypes for improved performance. We made new wicks with low-drag radial features, with multilayer patterns and overplated capped designs. We developed a model of the heat-pipe to allow us to assess the devices for new applications and to predict the heat-pipe behavior for new substrate geometries.

We developed a finite-element (FE) model of the substrate for the substrate and support structure to meet design needs. The results defined a substrate design with sufficiently low stress levels in the die attach layer for a prototype application. We developed processes for the photo-mask production of a wick structure on metal substrates. We defined laser weld schedules for the assembly and sealing of the substrate. We used a simple developmental fill-and-seal process to complete the first prototype. Finally, we developed an infrared (IR) thermal test system and measured the first results for heat-transfer properties of the prototype design. The initial heat-pipe substrate prototype showed a twofold improvement of effective conductivity over a similar geometry with only Kovar. We completed the computational model of stresses in the die and Kovar wall material. The results of the model analysis show no major design limits in die attach stresses. We improved weld-and-fill tube designs for future applications. We tested new prototypes with radial, multilayer, and capped features of the wicks. Heat-transfer results can now be expressed with a 3-D numerically solved heat-pipe model, which allows us to compare performance with existing cooling technologies for specific application designs. Discussions on Defense Programs (DP) and industry–based applications are being pursued to use this technology in new electronic designs.

Publications

Refereed

Benson, D. A., *et al.* 1998. "Substrate Keeps Today's Hot Chips Cooler." *OE Reports, SPIE Internat. Soc. for Optical Eng.* **178** (October): 16.

Benson, D. A., R. T. Mitchell, M. R. Tuck, D. W. Palmer, and G. P. Peterson. 1998. "Ultra–High-Capacity Micromachined Heat Spreaders." *Microscale Thermophys. Engin.* **2** (February): 21–30.

Other

Benson, D. A., C. V. Robino, D. W. Palmer, and S. H. Kravitz. 1997. "Heat Pipe with Improved Wick Structures." U.S. Patent Application based on Disclosure SD-6089 S-89,239 (Washington, DC, 10 December).

Benson, D. A., R. T. Mitchell, M. R. Tuck, D. R. Adkins, D. Shen, and D. W. Palmer. 1997. "Micromachined Heat Pipes in Silicon MCM Substrates." Sandia Technical Report SAND97-0100 (January). Sandia National Laboratories, Albuquerque, NM.

3506.280

Vacuum Encapsulation of MEMS Structures

S. Montague, J. G. Fleming, A. J. Farino, J. J. Sniegowski, B. D. Staple

The monolithic integration of microelectromechanical systems (MEMS) with driving, controlling, and signal-processing electronics on a single chip have enabled the recent development of a new class of high-performance inertial and other sensors. Development of on-chip vacuum encapsulation is a critical enabler for many of these new MEMS sensors. The commercial interest in this area is extremely high. A reliable, on-chip vacuum encapsulation technology is critical. Vacuum encapsulation of MEMS sensors will lower their cost, size, and operating voltages while increasing their sensitivities. In addition, vacuum encapsulation facilitates wafer-scale MEMS release and electrical testing and greatly simplifies the packaging process.

We accomplished the following tasks:

(1) Designed a complete reticle set of various resonant sensors and vacuum-encapsulated test structures. This included analyzing the deflection of the 4-micron vacuum lids for various geometries and sizes, investigating the use of different-spaced polysilicon columns for supporting large-vacuum areas, and interconnecting the MEMS sensors with the complementary metallic oxide semiconductor (CMOS) electronics.

(2) Developed an extensive integrated circuit (IC) fabrication process for fabricating the MEMS sensors with on-chip vacuum encapsulation and started two wafer lots to manufacture the integrated devices.

(3) Ran a short-loop lot to analyze the feasibility of using evaporated versus sputtered aluminum (Al) in the final vacuum-sealing process. The results indicate that evaporated Al has the potential of providing a good seal. Evaluations of the final sealing process are ongoing.

3506.290

Massively Parallel Sensor Arrays for Volatile Organic Detection

A. J. Ricco, A. W. Staton, W. G. Yelton, J. W. Bartholomew

Sandia will develop a flexible chemical sensor microlab (µlab) for detecting volatile organic compounds (VOCs) with high chemical selectivity based on large (~ 20 sensors) arrays of sorption–based resistors and surface acoustic-wave (SAW) devices. This µlab will comprise a massively parallel (MP) microsensor array using inexpensive, easily fabricated, polymer-coated, planar interdigitated resistors/polymers that are rendered conductive through admixture of conductive colloidal particles. Using chip–based electronics, sensor-array resistance changes due to VOC exposure can be monitored inexpensively in real time. The response of each sensor is rapid, reversible, and repeatable; hundreds of polymers with distinct sorptive characteristics are commercially available. Limits of detection (LODs) can reach ppb (parts-per-billion) levels; for high-volatility species, this is likely to require adding a preconcentrator as a front-end for this µlab. In contrast to separations–based µlab concepts, this approach is analogous to spectroscopy: The rich spectrum of resistor responses enables high chemical selectivity through multivariate analyses without separations; sensor redundancy provides improved system robustness.

The detection of VOCs is a key national security concern—detection of the proliferation of weapons of mass destruction (WMD). Particular combinations of chemical precursors, solvents, and by-products signal the production of nuclear, chemical, and biological WMD. We will determine system performance for WMD compounds, including various multicomponent VOC mixtures and their relevant LODs. In addition, DOE environmental monitoring and remediation applications, as well as industrial-waste minimization, require the development of effective, inexpensive VOC µlabs; we will address key species, as well, many of which are potential interferants for WMD detection and must therefore be included in any case.

Previously we focused on 20 polymer/colloid film combinations. We are using primarily 40%-by-weight loading of the polymer matrix with graphitized carbon (27–30 nm particle size). To date, we have run step-injection and isotherm (0.05–20% P/Psat.) analyses using 20 WMD analytes and interferants, as well as 5 binary chemical mixtures. We tested both dip-deposited coatings (thicker films) and high-speed spin-cast films (3000 rpm for 30s, producing ~ 200 nm-thick films). Promising results indicate the ability to unambiguously detect a range of organics.

We are working to improve the colloidal distribution of carbon in polymers that are lyophobic. To date, we have studied five commercial surfactants (dispersing agents), resulting in five kinetically stable polymer/sol solutions with particle agglomerates less than 5 mm. Finally, we are studying a promising polymer/carbon composite based on PEVA (polyethylene vinyl acetate) at carbon loadings of 15%, 20%, 25%, 30%, and 40% by weight to determine its percolation threshold, where sensitivity may be greatest.

We made and tested films using four ratios (7:1, 8:1, 9:1, and 10:1) of poly(ethyleneoxide) (PEO) to lithium perchlorate ($LiClO_4$). Though conceptually similar to the electronically conductive carbon-loaded polymer composites, these materials differ in their fundamental mechanism of detection: The principal conductivity mechanism is the motion of ions. Tests to date have focused on step-injection analyses with 11 analytes and included impedance and phase analyses with frequencies from 100 mHz to 1 MHz.

We microdispensed five films (~ 20 by 400 mm) on fabricated, chemically sensitive field-effect transistors (chemFETs), which allow resistance and work function measurements on a single chemically sensitive layer. Leveraging SAW sensor array work, we are assembling results from a large library of SAW coatings (ca. 30) to evaluate and refine visually empirical region of influence (VERI) pattern recognition (PR) methods for very large coating arrays.

We were able to stabilize 10 more polymer/sol solutions with commercial surfactants, for a total of 15 kinetically stabilized films. We studied over 160 samples to address the stability problem.

We completed the fourth training data set from a 12-chemiresistor array. Each training set is the combination of 18 analytes.

We completed a flow system hardware to provide low-ppb concentration of key analytes and are adding a spectrometer to the output to verify ppb-level concentrations.

We are near completion of the hardware for the first prototype µlab system. This hybrid system will have a seven-sensor SAW array with five classes of films. The system will be capable of detecting and identifying key analytes from the built-in PR algorithms and training library. Work continues in developing the microdispensing of 20+ chemiresistor solutions onto a platform array suitable for the µlab system.

3506.270

Integration of Microsensor Technology into a Miniature Robotic Vehicle

R. H. Byrne, C. Anderson, E. J. Heller

The goal of this work is to develop a miniature robotic vehicle capable of deploying environmental sensors (like Sandia-invented radiation field-effect transistors [RadFETs], volatile organic compounds [VOCs], hydrogen sensors, etc.) and navigation sensors (like Sandia's three-axis accelerometer). We will fabricate the sensor, signal processing, communications, power, and control electronics using surface-micromachining techniques. We will fabricate the vehicle chassis and drive mechanism using various precision-machining technologies developed at Sandia. We will use electromagnetic (EM), optical, or other signals to power and communicate with the vehicle. A base station will transmit command signals to the vehicle, which will direct the vehicle to reposition itself, take sensor readings, or transmit sensor readings. We will determine the location of the vehicle in two ways, first by measuring the time of flight (TOF) between multiple base-station transmission and reception signals, and second, via navigation sensors. Combining vehicle position and environmental sensor information will make it possible for multiple vehicles to map out the location and characteristics of radioactive, chemical, military, or other entities. While the ultimate goal of this project is to fabricate working prototype units, this project will also focus on developing the integration technologies (including integrating control and sensing electronics with sensors in single dies) necessary to design, build, and test future intelligent miniature systems for DOE and DoD applications. This process will assess current internal and external capabilities, specify the design and analysis tools, develop a prototype manufacturing and testing environment, and design and fabricate prototype vehicles and sensors.

We developed a 0.5-cubic-inch prototype robotic vehicle propelled by two miniature brushless dc motors that drive small wheels. We achieved two-way communications with an infrared (IR) link. We used a hand-held operator control unit to send commands to the vehicle. The vehicle electronics consist of an 8051-compatible microprocessor, motor commutation electronics, and the IR communications module. A six-layer 0.75-by-0.79-inch printed circuit board contains all of the surface-mount vehicle electronics. The printed circuit board is also the main component of the robotic vehicle. The robot is powered by a battery pack that consists of four NiCd or nickel metal hydride batteries in series that provide 11 mAh of capacity.

Battery energy density and the power requirements for mobility and sensing are critical items that must be tackled to develop a smaller robotic vehicle. The motors currently employed for mobility draw a significant amount of current relative to the other electronics on the vehicle. To meet the ultimate size goal of 0.25 cubic inch, we are exploring more efficient mobility methods that require less power and are smaller than the brushless dc motors currently used. Piezoelectric materials are promising and are being investigated. In an effort to reduce the size of the robot further, we are also exploring wafer-scale integration or having a commercial application-specific integrated circuit (ASIC) company design a single-chip version of our current design.

The hand-held operator control unit uses the same Atmel processor as the robotic vehicle. The range of the IR remote is proportional to the square root of the light-emitting diode (LED) transmit current. We are investigating increasing the range further using Sandia-developed vertical-cavity surface-emitting laser (VCSEL) technology to replace the discrete LEDs.

Publications

Refereed

Byrne, R. H., and C. Anderson. 1998. "Design of a Miniature Robotic Vehicle." IASTED '99 Conference, submitted.

3506.320

Precision-Formed Micromagnets

T. R. Christenson, E. L. Venturini, T. J. Garino

The feature of permanent magnets, and in particular rare-earth (RE)–based permanent magnets, that makes their use compelling in the microdomain is that their magnetization remains independent of scale. This situation is in contrast to electromagnetic (EM) coils, where constraints due to current density limits do not allow one to maintain a given magnetic field with a particular scaled coil. Even superconductors suffer the same limitation. Many uses of permanent magnets on the microscale, however, require that they be fabricated to small dimensions and corresponding tolerances. Fabricating permanent magnet materials is not only difficult

and expensive, but in situations where microsize multipole magnets are needed, it is not practical: Establishing multi-oriented high magnetic fields in a small volume is prohibited by coil scaling, which is the means used to magnetize magnetic material. The implementation of microsized permanent magnets, however, will yield device firsts such as novel static microdevices and more efficient magnetic micromotors. The primary technique being pursued to fabricate micromagnets is derived from bonded RE permanent magnet fabrication and precision molding achieved with the use of deep x-ray lithography-patterned mold forms. Sandia used resulting prismatic molds with dimensions down to 5 microns, thicknesses up to several millimeters, and tolerances less than 0.5 micron to incorporate permanent magnet powder mixed with a binder material. A subsequent batch-magnetizing step results in an array of permanent magnets batch-fabricated on a substrate with maximum energy products of 10 MGOe (Mega-Gauss-Oersted). We are investigating methods to increase the energy product by using anisotropic powder as well as incorporating a fully dense sintered RE magnet. A current method proposed to implement higher-density permanent magnets uses an intermediate mold obtained by accurately molding ceramics into the Plexiglas deep x-ray lithography mold as used previously.

The bonded NdFeB micromagnet process has become nearly routine. We fabricated bonded micromagnets using deep x-ray lithography-defined molds in a geometry suitable for 5 mm-diameter four- and eight-pole rotors to be used in an 8 mm-diameter by 1 mm-thick brushless dc motor that we are constructing. We fabricated many other shapes of interest, including ring sections that, when assembled, constitute miniature Halbach arrays (magic cylinders) that create magnified uniform static fields.

We characterized the trade-off between maximum energy product of bonded NdFeB micromagnets versus mechanical strength for various percent composition of binder material. At 20% by volume of an epoxy binder, we achieved a maximum energy product of 10 MGOe with a mechanical strength sufficient to allow manipulation and assembly of individual micromagnets. We also pursued an anisotropic form of powder, which allows for a potential energy product of 19 MGOe. Commercial interest has pushed the fabrication of miniature permanent magnets down to 20-micron linewidth with 30-micron thickness and vertical sidewall definition.

To improve the maximum energy product further, we investigated methods to achieve higher-density sintered magnets, including hot-pressing. We found that directly pressing and sintering NdFeB powders in the precision PMMA (polymethylmethaculate) (Plexiglas) mold did not transfer precision nor yield good magnet properties. Using an intermediate mold of electroformed copper was also unsuccessful due to the high sintering temperatures, which causes yielding of the copper. Therefore, a mold material that will not deform due to the temperatures and pressures of hot-pressing is required that has prompted the possibility of using alumina to replicate the PMMA mold. The technique that we demonstrated is to press a ceramic (alumina) powder into a complementary PMMA mold. After burnout of the PMMA, the ceramic is sintered in such a way that it develops the required amount of strength for hot-press molds without undergoing any significant densification. In this way, the precision of the mold is maintained. We obtained increased strength without any shrinkage by sintering the alumina at a relatively low sintering temperature where the dominant sintering mechanism is surface diffusion, which causes interparticle necks to grow. We found these alumina molds to be strong enough to hot-press ferrite powder to full density at 1000°C and 15,000 psi without breaking. Sintered MnZn-ferrite and NiZn-ferrite materials were micromolded in this manner and have applications on the microscale for high-frequency magnetic devices. We successfully molded ferrite parts with dimensions down to 30 microns. We have started to use this alumina mold coated with a thin sacrificial metal to fabricate fully dense RE permanent micromagnets in batch. The achievement of a precision ceramic mold used in conjunction with a suitable sacrificial release layer has an added benefit, which is that molding microminiature precision powder metallurgy–based components with a large number of materials is possible, thereby dramatically increasing the number of materials available over the currently available electroplatable metals.

Publications

Other

Christenson, T. R., T. J. Garino, and E. L. Venturini. 1998. "Deep X-Ray Lithography–Based Fabrication of Rare-Earth Permanent Magnets and Their Application to Microactuators." *Proc. 5th Internat. Symp. on Magnetic Mater., Processes and Devices (1998 ECE Meeting)* (Invited).

3506.310

Agile Dry Etching of Compound Semiconductors for Science–Based Manufacturing Using *In Situ* Process Control

C. I. H. Ashby, G. A. Vawter, J. R. Woodworth, W. G. Breiland

Compound semiconductor–based electronic and photonic devices are and will continue to be critical to the fabrication of robust, versatile sensing and communications systems. These devices are dependent on sophisticated bandgap and optical-index engineering, in both the vertical and horizontal dimensions. Because of its versatility, critical dimension control, and anisotropy, the enabling tool to provide horizontal and vertical pattern formation for these devices is dry plasma etching.

To make full use of the richness of compound semiconductors, however, device structures are typically constructed of a complex sequence of layers, each with its own composition (semiconductors, metals, and insulators) and etch chemistry. Control of the etch chemistry (and its impact on etch rates, feature profile, and morphology), both within a device structure and from one device structure to the next, is a major technical challenge and has been the focus of an enormous amount of trial-and-error engineering.

In this project, Sandia will combine advanced in situ *diagnostics with fundamental understanding of plasma physics and chemistry to achieve an unprecedented degree of control and reproducibility over the etching process.*

(1) *In Situ Optical Diagnostics*

(a) *Patterned surface reflectance modeling.* We constructed a model for reflectance from a rough surface. The new model departs significantly from standard roughness models and more closely describes a patterned wafer. We included interference effects between surface features and substrate. We identified limitations of the ADVISOR (Analysis of Deposition Using Virtual Interfaces and Spectroscopic Optical Reflectance) method for rough surfaces.

(b) *Reflectance installations on inductively coupled plasma (ICP) and reactive ion beam etch (RIBE) machines.* We made monochromatic reflectance installations, including software, on two etch tools to allow direct comparison between etched and as-grown structures, thereby allowing more precise stopping on specific device layers. Room-temperature wavelength-dependence studies of the reflectance of gallium arsenide (GaAs) substrates revealed unexpected behavior that was consistent with the evolution of thin surface films, most likely oxides. We analyzed the consequence for the determination of surface temperature with spectroscopic reflectance.

(c) *New methods of analysis using digital filter techniques.* We developed digital filtering methods to use the qualitative features in the reflectance data to determine precise endpoints.

The first digital filter helps identify kinks in the reflectance spectra that occur when the optical properties change abruptly as a new layer is reached during etching. This change is emphasized by displaying the second derivative of the reflectance, which reveals layer changes as delta-function spikes.

The second digital filter is necessary for etching samples patterned with photoresist when the resist-to-exposed-semiconductor ratio is high. The strong resist signal overwhelms the smaller semiconductor signal, obscuring the etch endpoint. Low-frequency oscillations resulting from slow etching of the photoresist and high-frequency oscillations resulting from etching of the semiconductor can be separated using high-pass and low-pass digital filters.

(2) *Ion Beam Diagnostics*

We used an apparatus of gridded ion analyzers to measure mean ion energies, ion energy distributions, ion fluxes, and ion angular distributions at different positions at the wafer location.

3506.330

Time-Resolved Ion-Beam–Induced Charge-Collection (TRIBICC) Imaging

F. W. Sexton, D. S. Walsh, P. E. Dodd, R. S. Flores, J. F. Aurand

With the continuing shrinkage of microelectronic device dimensions, single-event upset (SEU) is a reliability concern for space–based electronics due to naturally occurring energetic heavy ions, and for avionics and ground–based systems due to terrestrial cosmic rays. SEU-imaging, a technique developed at Sandia's nuclear microbeam facility, provides in situ *observation of upset location as a function of device operational parameters. A companion technique, ion-beam–induced charge collection (IBICC), measures the amount of charge arising from heavy-ion strikes as a function of position across a device. However, the rate at which charge is collected determines upset in static circuits. Under this project, Sandia is developing the capability to measure the charge transients resulting from heavy-ion strikes using time-resolved IBICC (TRIBICC). TRIBICC measurements are a key to validating device-level 3-D SEU modeling tools. This will lead to a refined understanding of charge-collection processes and an improved estimate of the SEU sensitive volume. Improved charge-collection models will result in increased simulation accuracy, reducing our reliance on empirical studies of the design space for hardening devices to SEU. Empirical studies require variations in processing and design that are both expensive and time-consuming. Model–based design trade-off studies can easily be one to two orders-of-magnitude cheaper, with months-to-years-shorter development times. Also, SEU-hardened devices can*

be made more manufacturable by clearly understanding the trade-offs between SEU sensitivity, performance, and process complexity. Developing accurate device-level simulation tools is a key element of Sandia's stockpile stewardship mission.

We measured TRIBICC images on complementary metallic oxide semiconductor 6R (CMOS6R) test structures with several different ion species and compared results to predictions of 3-D simulations. We observed good agreement for fast-charge transients arising from 12 MeV C, but we observed a large difference in the delayed component of charge. This indicates a need to adjust minority carrier lifetimes in the model. We observed a significant discrepancy for 28 MeV Si ions. We predicted a 2x increase in the amplitude of fast transients, but observed only a 0.4x increase. We subsequently determined that the high-frequency preamplifiers are saturating at levels 2x lower than specified by the manufacturer and identified technical solutions to this problem. Transients due to 5 MeV He could not be captured with the present system because of a minimum 120 mV triggering level for the SCD5000 transient digitizer.

We improved and simplified the hardware and software. The system now uses the internal front-edge triggering capability of the SCD5000 transient digitizer, rather than the original constant-fraction-discriminator/delay-line system. The result is a more reliable and user-friendly system. We added a fast beam blanking capability, which gives the system a true single-ion strike capability. This is essential to eliminate the effects of displacement damage on charge-collection transients. Calibration of the test apparatus to extend its capability to 15 GHz will be completed this year.

Measurement of TRIBICC signals from a multiple-bit memory test structure was delayed because of problems with test structure design and damage to the test structure during assembly.

Publications

Refereed

Schone, H., D. S. Walsh, F. W. Sexton, B. L. Doyle, P. E. Dodd, J. F. Aurand, R. S. Flores, and N. Wing. 1998. "Time-Resolved Ion-Beam–Induced Charge Collection (TRIBICC) in Microelectronics." *IEEE Trans. on Nucl. Sci.*, accepted.

Other

Sexton, F. W., D. S. Walsh, H. Schone, P. E. Dodd, R. S. Flores, and J. Aurand. 1998. "Time-Resolved Ion-Beam–Induced Charge Collection (TRIBICC)." *Proc. 11th Biennial Single-Event Effects (SEE) Symp.* (Manhattan Beach, CA, 20–23 March): 514–528.

3506.430

Compliant Substrates for Epitaxial Integration of Dissimilar Materials

J. A. Floro, J. Y. Tsao, D. M. Follstaedt, S. R. Lee, J. F. Klem

This project will explore a promising approach to a substrate with a continuously variable lattice constant, the so-called compliant substrate. *In collaboration with Cornell University, Sandia is focused on demonstrating and understanding the nature of compliancy effects in novel twist bicrystal compliant substrates. These substrates differ from the bulk only in the presence of a twist homointerface (created by wafer fusion) located just below the growth interface. Sandia's capabilities combining novel* in situ *diagnostics with advanced growth reactors and our expertise in heterostructure processing and properties uniquely position us for success in this area.*

Preliminary growth and analysis of $Si_{1-x}Ge_x$ alloys on silicon (Si) bicrystal compliant substrates indicate that a reduction in defect density may be associated with growth on the bicrystal, if the twist overlayer is sufficiently thin. $Si_{1-x}Ge_x$ alloys grown on thicker Si bicrystals exhibit stress-relaxation kinetics that are identical to alloys grown on monocrystal Si substrates. We fabricated patterned Si bicrystal compliant substrates to further evaluate the mechanisms for compliancy. We demonstrated the abilities and limitations of x-ray reciprocal space mapping to characterize the thickness and strain distribution of as-prepared twist bicrystal compliant substrates. We installed and are testing a Multibeam Optical Stress Sensor (MOSS) in our III–V molecular beam epitaxy (MBE) chamber for real-time stress-relaxation measurements during indium-gallium-arsenide (InGaAs) and indium-arsenide-antimony (InAsSb) growth on GaAs twist bicrystal compliant substrates. Our overall progress was significantly hindered by an inability to obtain consistent, high-quality bicrystal substrates of either Si or GaAs. To partially offset this problem, we are attempting to fabricate our own GaAs twist bicrystals.

3506.370

Double Quantum-Well Long-Wavelength Optoelectronic Devices

J. A. Simmons, J. R. Wendt, S. K. Lyo, J. L. Reno, S. R. Kurtz, S. Y. Lin

Sandia will research and develop long-wavelength emitters and detectors based on intrasubband transitions in semiconductor-coupled quantum wells (QWs). Present work on long-wavelength optoelectronics is largely based on optical transitions across the intrinsic bandgap in the more exotic semiconductors. In contrast, the unipolar quantum structures on which we will work can be fabricated in the mature aluminum gallium arsenide (AlGaAs) system. Transition energies and thus wavelength and other properties can be tailored across a wide range by appropriately engineering the QWs and intervening barriers. The structures can also be electronically tuned. Bell Labs recently demonstrated semiconductor laser diodes operating at 5–9 microns using intrasubband transitions.

Our approach leverages Sandia's innovative processing technology, initially developed for fundamental quantum transport experiments, to realize similar light emitters but with certain features that should enable superior performance. In addition to the application of novel processing technology, we will explore alternative intrasubband transitions.

Because the nature of light emission and detection in these devices is substantially different from that in conventional lasers and detectors, this research provides rich opportunities for investigating fundamental phenomena, including tunneling, phonon-mediated relaxation processes, and electronic states in artificially structured materials. The knowledge gained will be valuable for both quantum and classical microelectronics and photonics. The work also exercises existing compound semiconductor fabrication techniques and drives the development of new capabilities for processing long-wavelength waveguide geometry devices.

The primary goal of this project is to develop room-temperature, long-wavelength, semiconductor emitters and/or detectors that will be directly relevant to requirements for sensing and other applications. Semiconductor lasers should offer a variety of benefits for systems in terms of functionality. Mid-infrared (mid-IR) lasers and detectors can be used for chemical analysis and thermal detection. Electronic tunability and narrowband operation are particularly attractive for spectroscopic systems.

We performed extensive photoresponse measurements of double quantum-well (DQW) detectors in a free-electron laser. We observed a narrowband photoresponse and also saw indications of gate tunability. We determined that we needed new samples with smaller, electron-beam-written gates and faster resistance-capacitance (RC) response times, and also larger energy subband offsets, which we designed, grew, and fabricated. Electrical measurements showed excellent behavior, with large resonances visible at 77°K. These samples are now being optically measured in the free-electron laser. We also developed a gate insulation processing technique that greatly increased our yield by preventing the shorting of backgates to frontgates, a failure mode that appeared in more than half of our samples. We designed, grew, and measured laterally contacted triple QW light emitters and measured their electrical characteristics quite extensively. We are currently measuring the emission of these structures in a spectrometer, and have grown and are fabricating a new generation of similar triple-well emitters having thicker tunneling barriers to make the gate-induced energy subband lineups easier, and also some new four-well emitter structures. Finally, we initiated a collaboration with researchers at MIT on stacked triple-well terahertz emitters. MIT has already seen narrowband emission at 14 meV and has performed extensive transition-rate calculations. We plan new structures using our epoxy-bond-and-stop-etch (EBASE) flip-chip technique to achieve better mode confinement by surface metal on both sides, in the hopes of achieving lasing, and are looking at shorter-wavelength single-cell structures that would be electrically tunable via surface gates.

Publications

Refereed

Peralta, X. G., S. J. Allen, S. Y. Lin, J. A. Simmons, M. A. Blount, and W. E. Baca. 1998. "Photoconductive Response of Double Layer Quantum Wells in Intense Terahertz Electric Fields." Paper presented to the 20th International Free Electron Laser Conference, Williamsburg, VA, 16–21 August.

Simmons, J. A., J. S. Moon, M. A. Blount, J. L. Reno, X. G. Peralta, and S. J. Allen. 1998. "The Double Electron Layer Tunneling Transistor (DELTT)." Paper presented to the Future Trends in Microelectronics Workshop, Ile des Embiez, France, 31 May–5 June.

Simmons, J. A., J. S. Moon, M. A. Blount, S. K. Lyo, V. M. Hietala, J. L. Reno, R. Lake, X. G. Peralta, S. J. Allen, P. J. Burke, and J. P. Eisenstein. 1998. "Development of the Double Electron Layer Tunneling Transistor (DELTT) for Electronics and Optical Applications." Paper presented to the DARPA Ultra Electronics Program Review, Estes Park, CO, 18–21 October.

Other

Peralta, X. G., S. J. Allen, S. Y. Lin, J. A. Simmons, M. A. Blount, and W. E. Baca. 1998. "Photon-Assisted Resonant Tunneling and 2-D Plasmon Modes in Double Quantum Wells in Intense Terahertz Electric Fields." *Bulletin of the Amer. Phys. Soc.* **43** (Los Angeles, CA, 16–20 March): 554.

3506.350

Role of Defects in III-Nitride–Based Electronics

J. Han, S. M. Myers, Jr., A. F. Wright, R. J. Shul, C. H. Seager, M. H. Crawford, A. G. Baca

Wide-bandgap III-nitride semiconductors are extremely promising materials for the compact, high-power, high-frequency amplifiers required for future satellite cross- and up-/downlinks, and for the robust microelectronics required for future severe-environment national security applications. In addition, they have the potential to enable a new generation of optoelectronic devices in the visible and ultraviolet (UV) spectral regions. The ultimate realization of high-performance GaN–based devices is presently limited by the high density of defects and the complex microstructure of the gallium nitride (GaN) materials, both of which interfere with the intrinsic materials properties. This project is intended to provide a scientific base for understanding the role of defects in GaN. Our approach can be categorized into three parts: (1) establishing a strong metalorganic chemical vapor deposition (MOCVD) growth capability for III-nitride materials that we will apply to study and control microstructural evolution and growth parameter-dependent defect formation, (2) applying various microscopic probes (some unique to Sandia) and bulk characterization techniques to study defects in GaN and determine their effects on electronic and optical properties, and (3) performing state-of-the art first-principles calculations of the energetics of defects and defect complexes in III-nitride alloys.

We significantly enhanced the MOCVD growth capability. Starting from the growth of GaN films, we explored and demonstrated both *n*-type and *p*-type doping of GaN as well as aluminum gallium nitride (AlGaN) alloys. We demonstrated an electron concentration of up to 5e18 cm^{-3} for AL0.25Ga0.75N. We reproducibly achieved free-hole concentrations exceeding 5e17 cm^{-3}. We characterized these materials using low-temperature photoluminescence (PL), high-resolution x-ray diffraction, x-ray reciprocal mapping, and Hall measurements. These materials growth advances were critical to enable our studies on the interaction of defects with dopants as well as the microstructure and defects of AlGaN alloys. We thoroughly examined the role of hydrogen (H) in GaN, including the state, transport, and microstructural effects of H, through post-growth ion-implantation studies. We found strong attachment of H to nitrogen (N) dangling orbitals, which is favorable for passivation of defects. In addition, we determined the permeability of H in GaN for the first time. In the area of theoretical modeling, we went beyond single-point defect calculations and performed first-principles calculations of the energetics of various structural defects, including stacking faults and dislocations in GaN and AlN. The calculations revealed that the core structure of an edge dislocation in GaN depends critically on the Fermi level in the material and would therefore be different for *n*-type and *p*-type GaN. Furthermore we used density-functional theory (DFT) to determine the solution sites for hydrogen in a perfect crystal (without defects) as a prerequisite for studying its interaction with defects.

Publications

Refereed

Han, J., J. J. Figiel, M. H. Crawford, M. A. Banas, M. E. Bartram, and R. M. Biefeld. 1998. "MOVPE Growth and Gas-Phase Reactions of AlGaN." Paper presented to the 9th International Conference on MOVPE, LaJolla, CA, 4 June.

Han, J., J. J. Figiel, M. H. Crawford, M. A. Banas, M. E. Bartram, and R. M. Biefeld. 1998. "MOVPE Growth and Gas-Phase Reactions of AlGaN for UV Emitters." *J. Crystal Growth*, accepted.

Han, J., T. B. Ng, R. M. Biefeld, M. H. Crawford, and D. M. Follstaedt. 1997. "The Effect of H_2 on Morphology Evolution During GaN MOCVD." *Appl. Phys. Lett.* **71** (24 November): 3114.

Myers, S. M., J. Han, T. J. Headley, C. R. Hills, G. A. Petersen, C. H. Seager, and W. R. Wampler. 1998. "Ion-Implanted Hydrogen in Gallium Nitride." *Nucl. Instr. and Meth. in Phys. Res. B*, accepted.

Ng, T. B., J. Han, R. M. Biefeld, J. C. Zolper, M. H. Crawford, and D. M. Follstaedt. 1998. "The Effect of H_2 Carrier Gas on the Morphological Evolution and Material Properties of GaN on Sapphire." *Proc. Mater. Res. Soc. Symp.* **482** (May) (Boston, MA, 1 December 1997): 143.

Seager, C. H., S. M. Myers, G. A. Petersen, and J. Han. 1998. "Trapping of H in Ion-Implanted GaN." Paper presented to the Spring MRS Meeting, San Francisco, CA, 13 April.

Seager, C. H., S. M. Myers, G. A. Petersen, J. Han, and T. Headley. 1998. "Infrared Studies of Ion-Implanted H in GaN." *J. Appl. Phys.*

Wright, A. F. 1997. "Theoretical Investigation of Extended Defects in Group-III Nitrides." *Proc. Mater. Res. Soc. Symp.* **482** (Boston, MA, 4 December): 795.

Wright, A. F., and U. Grossner. 1998. "The Effect of Doping and Growth Stoichiometry on the Core Structure of a Threading Edge Dislocation in GaN." *Appl. Phys. Lett.* (9 November).

3506.340

Composite-Resonator Surface-Emitting Lasers

K. D. Choquette, B. E. Hammons, K. M. Geib, A. A. Allerman, W. W. Chow

Applications of vertical-cavity surface-emitting lasers (VCSELs) have requirements ranging from amplitude modulation, frequency tunability, and amplitude or frequency stability, to high output power. The present single-resonator VCSEL lacks the agility to readily perform many of the above functions. Sandia will use composite resonators to control spectral and temporal properties of VCSELs. This structure in effect is a coupled-resonator vertical-cavity laser (CRVCL). Using composite resonators opens up new possibilities because of their unique ability to (1) tailor the coupling between the monolithic cavities, (2) dynamically modify the cavity interaction, and (3) incorporate passive or active resonators that are spectrally degenerate or detuned. Composite resonators can be utilized to influence the spectral and temporal properties within a VCL. The composite resonator will consist of a primary resonator containing the gain section and an active or passive secondary resonator. Separate contacts provide independent current injection into the resonators. The coupling between the resonators is controlled by the transmission of the shared distributed Bragg reflector (DBR). We will use different configurations of a monolithic composite-resonator surface-emitting laser structure to demonstrate (1) amplitude modulation, (2) gain-switching, and (3) frequency tuning. The latter will allow fine-tuning of the mode/gain alignment after growth to compensate for temperature and injection current fluctuations. Successful demonstration of the above functions will be a major step toward making VCSEL technology viable for many defense and commercial applications.

Our accomplishments this year include the following:

(1) Developed detailed coupled resonator optical model and identified cavity length tuning and mode-locking as two viable methods of amplitude modulation.

(2) Demonstrated large single modulation up to 50 MHz (apparatus limited) using cavity length tuning via current injection into the passive cavity. Using current injection into the passive cavity depresses the index and thus optical path length in the passive cavity, leading to a decrease in light output. We determined that the most efficient modulation using forward injection current into the passive cavity is achieved when the active cavity is biased at its maximum output power.

(3) Demonstrated large single modulation up to 50 MHz (apparatus limited) using mode-locking by reverse-biasing the passive cavity.

(4) Developed many-body analysis of quantum-well (QW) gain region and are incorporating this into optical coupled-resonator model to analyze gain-switching.

(5) Are developing short-pulse characterization based in an optical streak camera system to probe the gain-switching of coupled-resonator VCSELs on the picosecond time scale.

(6) Are developing a suitable device topology and required masks to fabricate coupled-cavity VCSELs for short-pulse and high-speed modulation characterization.

Publications

Refereed

Choquette, K. D., H. Q. Hou, W. W. Chow, K. M. Geib, and B. E. Hammons. 1998. "Composite-Resonator Vertical-Cavity Laser Diode." *Proc. Conf. on Lasers and Electro Optics* '98 (*CLEO '98)* (San Francisco, CA, May): 567.

Choquette, K. D., W. W. Chow, H. Q. Hou, K. M. Geib, and B. E. Hammons. 1998. "Vertical Coupled-Cavity Surface-Emitting Laser Diodes." *Proc. Device Res. Conf. '98* (Charlottesville, VA, June): 67.

Other

Choquette, K. D., W. W. Chow, H. Q. Hou, K. M. Geib, and B. E. Hammons. 1998. "Coupled-Resonator Vertical-Cavity Laser." *Proc. SPIE, Vertical-Cavity Surface-Emitting Lasers II* **3286** (San Jose, CA, January): 45–49.

3506.360

Ultra–Low-Power Sensors for Microtelemetry Systems

R. C. Hughes

Sandia will design, fabricate, and test ultra–low-power sensors that are capable of being powered and read out by analog circuits that are, in turn, capable of coupling the sensor information to radio frequency (RF) telemetry. The microelectrochemical cell (MEC) is a key enabling technology for a wide variety of chemical sensors in the sensor/tag combination and opens the door to new applications in sensing for counterproliferation, weapon monitoring, and many other areas. The current state of electronic tagging circuits is effective for grain-of-rice– to jelly-bean–sized chips that can be remotely powered, programmed, and read out. The first new sensors to be used in this project are polymer film composites with metal powders. They conduct by percolation, and swelling of the polymer causes an increase in film resistance. A second kind of chemiresistor film involves the conductivity of ions and how that is affected by various analytes. A considerable literature on electroactive chemically sensitive films has developed over the last few years, and Sandia has the technology to combine the tagging electronics with these low-power electrochemical sensors. Issues to be resolved include the quality and type of data to be transmitted, how to handle analog data from the sensor as well as ultra–low-power management, and the range of operation. Other technical issues would involve the levels of voltage and charge required to obtain a reliable read-out. We also envisage ultra-small versions of the radioactive field-effect transistor (radFET) and hydrogen sensor that require only a small number of coulombs.

A matchbox-sized telemetry system using commercial RF components with voltage input from one of our chemiresistors allowed the sensing of a volatile organic chemical (VOC) to be transmitted through the building walls to an office computer some 50 feet away. We fabricated many new

chemiresistors from a variety of polymer/metal powder composites and measured their response to a variety of VOCs. We developed the concept of a universal solvent sensor array using the solubility parameter approach for both polymers and solvents. Because our sensor array gives signals for solvents representing the extremes of solubility parameters, we believe that no solvent will go undetected by this array. In addition to detecting solvent vapors, we showed that the individual vapors can be identified by the array, independent of their concentration, by using pattern recognition (PR) techniques. We also made progress in identifying the two components in binary mixtures of unknown concentration. This is particularly important in field use when one of the unknowns is water vapor. We also used impedance spectroscopy to gain new insight into mechanisms of response of solid electrolyte sensors. The low-frequency impedance is dominated by polarization effects that depend in detail on the analyte molecules. We filed a technical advance for using this technique to identify analytes. We also fabricated a new substrate with electrodes for four chemiresistors (four terminal), two heaters, and a Pt/Ti temperature sensor. This array is about 1 square centimeter and fits in a standard 16-pin dual in-line package (DIP). We demonstrated that a chemiresistor on one set of electrodes works along with the heater and temperature sensor. This chip, along with a signal-processing chip, will form the goals of next year's work, demonstrating an extremely small, low-power sensor system.

Publications

Refereed

Hughes, R. C., M. P. Eastman, W. G. Yelton, A. J. Ricco, S. V. Patel, and M. W. Jenkins. 1998. "Application of the Solubility Parameter Concept to the Design of Chemiresistor Arrays." *Tech. Digest 1998 Solid-State Sensors and Actuators* (Hilton Head, SC, June): 379–382.

3506.380

The Development of Integrated Chemical Microsensors in GaAs

S. A. Casalnuovo, S. L. Hietala, A. G. Baca, V. M. Hietala, J. L. Reno, R. J. Kottenstette, G. C. Frye-Mason, E. J. Heller

By taking advantage of both the piezoelectric and semiconducting properties of gallium arsenide (GaAs), Sandia will fabricate arrays of acoustic-wave chemical microsensors integrated with microelectronic drive and output circuitry on a single GaAs substrate, resulting in a compact, extremely low-power, highly sensitive chemical-detection system capable of discriminating among large numbers of liquid and gaseous chemicals. GaAs has several advantages in this application. Its piezoelectric coefficient is comparable to that of quartz, the standard material for acoustic resonator chemical sensors. High-frequency (nominally 1 GHz) resonator microelectronics are easily fabricated in GaAs using existing GaAs microfabrication technology and are process-compatible with GaAs acoustic devices. Selective etching of GaAs and aluminum gallium arsenide (AlGaAs) epitaxial films makes possible the fabrication of thin (typically 1 to 10 microns) piezoelectric membranes, nominally 100 microns in diameter, capable of high-sensitivity (1 femtogram) detection. No other piezoelectric material can support the integrated microelectronics nor produce the thin-film resonators. No other semiconductor, particularly silicon (Si), is piezoelectric, and fabrication process incompatibilities make the integration of Si and piezoelectrics difficult.

We produced the first functional monolithically integrated GaAs surface acoustic-wave (SAW) delay line oscillators for chemical-sensing applications. This device comprises a GaAs integrated circuit (IC) amplifier and a GaAs SAW delay line fabricated on the same substrate. It is small (2 mm^2) and low power (60 mW, operating at 3 V). We also fabricated a hybrid GaAs SAW oscillator using a Sandia-designed, commercially fabricated IC amplifier and a Sandia-fabricated GaAs SAW delay line. We demonstrated chemical detection with this device. We designed, fabricated, and tested functional phase comparator ICs. When integrated with the oscillators, this will produce a complete dc-in, dc-out chemical microsensor.

We demonstrated the first GaAs membrane flexural plate-wave (FPW) acoustic delay lines, using micromachining techniques we developed previously. These devices have potentially higher sensitivity than conventional SAW sensors and have the additional advantage of operation in liquids.

We developed multi-element arrays of SAW delay lines on a single GaAs chip, making possible the detection of numerous chemical species with a single sensor.

We demonstrated a temperature-compensated GaAs SAW delay line, thereby eliminating one of the principal disadvantages of GaAs sensors when compared to conventional quartz sensors.

We fabricated and tested a GaAs IC phase comparator that converts the high-frequency output of the GaAs SAW oscillator sensor to a dc signal. This device has a sensitivity of 6 mV/degree at 500 MHz, operates at 3 V, and draws 27 mW.

Publications

Other

Casalnuovo, S. A., E. J. Heller, V. M. Hietala, A. G. Baca, R. Kottenstette, S. L. Hietala, J. L. Reno, and G. C. Frye-Mason. 1998. "Acoustic-Wave Chemical Microsensors in GaAs." *Proc. SPIE, Micromachined Devices and Components IV, Micromachining and Microfabrication Symp.* **3514** (Santa Clara, CA, 21–22 September): 103–110.

3506.410

Monolithic Integration of VCSELs and Detectors for Microsystems

K. D. Choquette, B. E. Hammons, J. A. Nevers, K. M. Geib, A. A. Allerman, M. E. Warren

Vertical-cavity surface-emitting lasers (VCSELs) are high-efficiency light sources appropriate for microsystem applications that will benefit from monolithic integration with compatible photodetectors. Such an integration of functions has applications ranging from near-term use in monitors for surety devices to longer-term enabling of on-chip photonic interconnects and advanced microsystems for sensing, surety, data storage, data routing, communication, and image manipulation, processing, and transmission. Moreover, 2-D arrays are an important extension of VCSEL technology, and intermeshed VCSEL/detector arrays will enable numerous advanced applications. Approaches for VCSEL/photodetector integration include the application of metal-semiconductor-metal (MSM) detectors on the laser substrate and the creation of resonant-cavity photodetectors (RCPDs) using the VCSEL epitaxial layers. Note that the detectors could be the same as the VCSEL wavelength, or be designed at different wavelengths using wafer-bonded detector material. An array of the latter would provide the means of image intensification or image conversion, e.g., for infrared viewing. This project will address the basic enabling technologies for these approaches and will use combinations of these approaches to create example prototypes that are designed to demonstrate the ability to enable new applications. In addition, this project will include environmental testing (radiation and high temperature) of these devices under conditions appropriate for internal DOE applications as well as external applications, such as opto-couplers in spacecraft targeted for outer planetary systems.

We made the following accomplishments this year:

(1) Developed integrated VCSELs and RCPDs. This required the design of suitable masks and an appropriate device fabrication process. We laid out numerous different RCPD structures and geometries and characterized them for high-temperature and high-radiation environments that are of interest to internal programs and to the Jet Propulsion Laboratory for space opto-couplers.

(2) Characterized the photocurrent response of RCPD illuminated by neighboring VCSEL. In this experiment, we suspended a mirror over the chip to reflect the output from the monolithic VCSEL into the neighboring detector. The laser threshold was clearly exhibited in the photodetector current. As the VCSEL became multimoded, the detector response showed some structure above threshold due to changes in the reflected far-field VCSEL beam. In addition, the photocurrent fell off faster than the laser output because of the spectral shift of the laser emission beyond the spectral acceptance of the photodetector.

(3) Characterized the spectral responsivity of RCPDs. We achieved a peak responsivity of 0.8 W/A using a 9 V reverse bias. We also identified key material issues for improved photodetector response.

(4) Used preliminary characterization of VCSELs under high-energy charged-particle radiation to demonstrate self-repair during post-radiation laser operation. Thus the radiation hardness of VCSELs appears very promising.

(5) Constructed a 16-board (128-device) automated VCSEL lifetime testing system.

(6) Operated eight selectively oxidized VCSELs at 1 mW output power over 20,000 hours at 80°C with only a single device failure.

Publications

Refereed

Choquette, K. D., and H. Q. Hou. 1998. "Vertical-Cavity Surface-Emitting Lasers: Moving from Research to Manufacturing." *Proc. IEEE* (Invited) **85** (October): 1730–1741.

Choquette, K. D., A. A. Allerman, H. Q. Hou, K. M. Geib, and B. E. Hammons. 1998. "Applications and Performance of VCSELs." Paper presented to the 1998 GaAs IC Symposium (Plenary), Atlanta, Georgia, November.

Choquette, K. D., H. Q. Hou, K. M. Geib, and B. E. Hammons. 1997. "Uniform Selectively Oxidized Two-Dimensional VCSEL Arrays for VLSI Photonics." *Proc. 1997 Lasers and Electro Optics (LEOS) Ann. Mtg.* (San Francisco, CA, November): 335.

Choquette, K. D., H. Q. Hou, K. M. Geib, M. H. Crawford, and B. E. Hammons. 1997. "High-Performance Selectively Oxidized Vertical-Cavity Laser Arrays." *Proc. 44th Nat. Symp. Amer. Vac. Soc.* (Invited) (San Jose, CA, October): 246.

Paxton, A. H., R. F. Carson, H. Schone, E. W. Taylor, K. D. Choquette, H. Q. Hou, K. L. Lear, and M. E. Warren. 1997. "Damage from Proton Irradiation of Vertical-Cavity Surface-Emitting Lasers." *IEEE Trans. Nucl. Sci.* **44** (December): 999.

Pu, R. E. M. Hayes, C. W. Wilmsen, K. D. Choquette, H. Q. Hou, and K. M. Geib. 1997. "VCSELs Bonded Directly to Foundry-Fabricated GaAs Smart Pixel Arrays." *IEEE Photon. Tech. Lett.* **9** (March): 1622–1624.

Other

Choquette, K. D., H. Q. Hou, K. M. Geib, and B. E. Hammons. 1997. "Low-Threshold InGaAs Selectively Oxidized Vertical-Cavity Lasers." *Proc. 1997 OSA Ann. Mtg.* (Long Beach, CA, October): 423.

3506.420

AlGaN Materials Engineering for Integrated Multifunction Systems

J. Han, M. H. Crawford, D. M. Follstaedt, R. J. Shul, S. A. Casalnuovo, J. G. Fleming, S. R. Lee, T. J. Drummond

In response to a world-wide interest in wide-bandgap III-nitride devices and the recent progress in the development of metalorganic chemical vapor deposition (MOCVD) growth of aluminum gallium nitride ([Al,Ga]N) materials at Sandia, we are exploring the multifunctional usage of these semiconductor alloys to meet various mission requirements and to position Sandia at the technological forefront of this strategically important material family. Over a wide range of possible applications, we identified the development of compact ultraviolet (UV) optoelectronic devices (emitters and detectors), piezoelectric devices (surface acoustic-wave [SAW] sensors), and the integration of GaN with silicon (Si) as the initial thrust areas. All of these areas have thus far remained relatively unexplored and yet are well aligned with Sandia's mission objectives. In addition to maintaining a broad portfolio, this project will explore the full potential of the ceramic-like nature of the III-nitride materials (namely, the physical robustness, chemical inertness, and tolerance to structural defects) to achieve chip-level integration into microsystems containing various nitride devices and possibly between nitride devices and Si–based electronics. Our work in the first year included the demonstration of UV GaN/AlGaN quantum-well (QW) light-emitting diodes (LEDs) at 354 nm, initial demonstration of the first 200 MHz GaN SAW delay lines, and substantial progress in the integration of GaN with Si(111) substrates as well as Si(100) surfaces through the use of silicon-on-insulator (SOI) structures.

We laid down a solid foundation in the growth and application of (Al,Ga)N alloys. The MOCVD growth operation evolved from the initial phase of materials exploration into a stage where both device demonstrations and scientific investigations can be routinely supported. In terms of the growth of III-nitride materials, we demonstrated both *n*-type and *p*-type doping of GaN. We grew and characterized up to 45% Al-containing AlGaN alloys and GaN/AlGaN QW heterostructures. We successfully combined our new ability to achieve bipolar doping and GaN/AlGaN heterostructures to achieve the further demonstration of GaN/AlGaN multiquantum-well LEDs emitting at 354 nm. We believe this device result to be quite significant, as we believe it is the shortest-wavelength QW LED reported to date, and the UV emission can be applied to a number of sensor and illumination applications. We filed a technical advance on the UV LED design and performance.

We also investigated the growth of GaN on different Si surfaces ([111], [100], and Si dioxide). In particular, we verified the unique and crucial role of the Si(111) surface in providing a hexagonal template for the growth of GaN. We prepared novel SOI structures to investigate the feasibility of integrated GaN with (100)Si surfaces. Initial evidence suggests that the insertion of a thermal oxide layer tends to alleviate the tensile stress and reduce the cracking density in Si wafers. Finally, we successfully fabricated the first 200 MHz GaN SAW delay lines.

Publications

Refereed

Han, J., J. G. Fleming, and D. M. Follstaedt. 1998. "MOCVD Growth of GaN on Silicon and Related Surfaces." *Proc. Mater. Res. Soc. Symp.* **512** (San Francisco, CA, 31 March–4 April): 53–58.

Han, J., J. J Figiel, M. H. Crawford, M. A. Banas, M. E. Bartram, and R. M. Biefeld. 1998. "MOVPE Growth and Gas-Phase Reactions of AlGaN for UV Emitters." Paper presented to the 9th International Conference of Metal Organic Vapor Phase Epitaxy, La Jolla, CA, 30 May–4 June.

Han, J., J. J Figiel, R. M. Biefeld, and M. H. Crawford. 1998. "Gas-Phase Reactions During MOCVD Growth AlGaN." Paper presented to the 40th Electronic Materials Conference, Charlottesville, VA, 23–26 June.

Han, J., M. H. Crawford, R. J. Shul, J. J. Figiel, M. Banas, L. Zhang, Y. K. Song, H. Zhou, and A. V. Nurmikko. 1998. "AlGaN/GaN Quantum-Well Ultraviolet Light-Emitting Diodes." *Appl. Phys. Lett.* **73** (September): 1688–1690.

3506.440

Post-Processed Integrated Microsystems

R. J. Shul, K. O. Wessendorf, W. K. Schubert, S. A. Casalnuovo, S. H. Kravitz, T. R. Christenson

Sandia will develop a low-cost platform for integrated microsystems that is easily configured to meet a wide variety of specific applications-driven needs. Once developed, this platform, which incorporates many of the elements that are common to numerous microsystems, will provide integrated microsystem users with access to this technology without paying the high upfront development costs that are now required. The process starts with the fabrication or acquisition of wafers of sparsely placed device or circuit components fabricated in any foundried technology (silicon [Si] complementary metal oxide semiconductor [CMOS] or bipolar technologies, high-frequency gallium-arsenide (GaAs) technologies, microelectromechanical systems [MEMS], etc.). We call these smart substrates. *Using Sandia's diverse processing capabilities, we then intend to post-process high-value components in open areas on the front or the back of the wafers and microelectronically integrate the added components with the preplaced circuitry. Examples of post-processed components include sensors, antennas, surface acoustic-wave (SAW) devices, passive elements, microoptics, and surface-mounted hybrids. The combination of preplaced electronics and post-processed components will enable the development of many new types of integrated microsystems. Targeted applications include integrated sensored systems, tags, and electromechanical systems.*

(1) We developed and integrated several microelectronic fabrication processes into the post-processing of smart substrates. Processes include thin-film metallization, low-stress silicon nitride (SiN), thermal oxide, front- and backside contact lithography, and a deep high-aspect-ratio Si etch (HARSE).

(2) We developed and optimized a HARSE process, which enabled the fabrication of a variety of Si structures where deep trench etching is necessary. We demonstrated high Si etch rates, ranging from 1 to 3.5 µm/minute, with highly anisotropic profiles and smooth etch morphologies. The HARSE process operates at room temperature and yields etch selectivities of Si to resist > 100:1 (eliminating the need for hard masks), Si to Si dioxide (SiO_2) ~ 275:1, and Si to SiN ~ 85:1, thus enabling the fabrication of membrane–based devices.

(3) We demonstrated the HARSE process for many device applications, including a fundamental mode mag-flexural plate-wave (FPW) device, micromachined heater, device locator, post-processing of MEMS devices, and a locating assembly to support and align corresponding LIGA (German for lithography, electroforming, and molding)-fabricated mechanical components. LIGA gear trains used an array of 150-micron-diameter by 320±micron-tall pins, which were etched into a Si wafer using the HARSE process. In addition, we successfully demonstrated an FPW–based transmitter/receiver at atmospheric pressure with a 1 mm-diameter SiN membrane.

(4) We demonstrated post-processing capability on an integrated GaAs chemical microsensor that monolithically integrates a SAW sensor, a high-frequency amplifier, and a frequency-converter output stage. We also demonstrated post-processing on MEMS discriminator wheels and pop-up mirrors. We aligned vias to the frontside structures and etched using the HARSE process.

(5) We demonstrated post-processing capability on a MEMS counter-meshing gear discriminator. Unreleased MEMS structures were post-processed using the HARSE process to etch vias through 400 to 600 microns of Si. We then released the MEMS structures and used them to transmit light through the Si substrate.

Publications

Refereed

Shul, R. J. 1998. "Selective, Deep Si Etching with Dimensional Control." *Proc. SPIE, Micromachining and Microfabrication Process Technol. IV* **3511** (Santa Clara, CA, 21–22 September): 252–261.

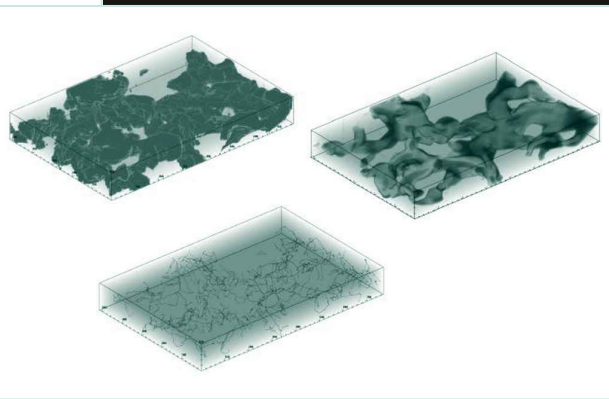

PHENOMENOLOGICAL MODELING & ENGINEERING SIMULATION

The driving force for this area is the Revolution in Engineering, a vision in which the life-cycle engineering process occurs within a pervasive, validated simulation environment. Research seeks to develop computer models that predict if and why a component will fail, projects that describe how a product will perform under various operating conditions, and projects that enhance or expand use of the Sandia teraflops computer. Success in this vision will require unprecedented levels of confidence in computer simulation.

Six key research areas support this effort: (1) increased model fidelity that requires the development of a computer model that will contain sufficient resolution to allow for predictions of product failure, (2) improved high-performance computing solutions that operate across platforms, (3) performance of uncertainty quantification rigorous enough to quantify the validity of the simulation, (4) experimental discovery to enable high-fidelity models, (5) validation of the computer algorithms and codes by experimentation, and (6) development of diagnostics necessary to ensure the success of the experiments.

Comprehending the behavior of a material requires understanding the process of heat and mass transfer. These transfers, or flows, can be studied for either fluid or thermal events. Fluid material flows include the movement of fluids such as water and oil, or of molten solids such as liquid metals. Thermal flow studies examine the way heat is transferred through a specific material. A Sandia project developed an advanced computational framework for investigating the fundamental phenomena characterizing complex 3-D flows.

Lattice Boltzmann (LB) is a kinetic theory–based method that forms the basis for this research. Because LB methods are explicit in time and space, they are ideally suited for modeling these complex heat- and mass-transfer processes.

This research will make it possible to use computer modeling to understand and predict heat and mass transport in complex materials such as porous media. Sandia developed a distributed computational platform based on commercial off-the-shelf computer components that is capable of production-scale LB simulations. Applications for this product abound in the geosciences, materials science, and chemical, thermal, and mechanical engineering.

THIS PAGE
INTENTIONALLY BLANK

3508.060

Enhanced Vapor-Phase Diffusion in Porous Media

S. W. Webb, C. K. Ho

Vapor-phase diffusion in porous media may significantly impact many important applications. Examples include the drying of sol-gel coatings and textiles, agricultural processes, and the transport of chemicals such as TNT from buried landmines. Vapor-phase diffusion may also be important in gas transport at high-level nuclear-waste repositories. In addition, in many environmental-remediation and waste-isolation applications, such as the removal of nonaqueous phase liquid (NAPL) contaminants from low-permeability layers in the subsurface, vapor-phase diffusion is the limiting transport mechanism. Enhancement of vapor-phase diffusion by up to several orders of magnitude has been postulated, but not directly measured, in the presence of its liquid through local pore-scale condensation and evaporation at vapor-liquid interfaces. The objective of the present work is to resolve critical processes and questions associated with postulated enhanced vapor-phase diffusion mechanisms. The approach taken in the present research is to perform modeling and experimental investigations of enhanced vapor-phase diffusion in porous media at various length scales, including the pore scale and the laboratory scale.

Results of this investigation include the first direct measurements of significant enhancement of vapor-phase diffusion at the pore scale and at the laboratory scale. We developed the first mechanistic pore-scale model of enhanced vapor-phase diffusion. The results from this model and the pore-scale experiments are in agreement with each other. Therefore, we have definitively answered the question concerning the existence of enhanced vapor diffusion (EVD). EVD does exist as directly measured and mechanistically modeled for the first time.

Our accomplishments in this project included the completion of the modeling and experimental investigations.

(1) *Modeling*

• We calculated pore-scale modeling results for numerous situations. We investigated transient drying conditions; the results are similar to steady-state conditions if the proper scaling is employed. We calculated the effect of concentration and temperature gradients on EVD. EVD is predominantly driven by concentration gradients; any temperature gradient is a secondary factor. These results are supported in a collaboration with New Mexico Tech and are contrary to the standard model of Philip and deVries, who assumed that a temperature gradient was the only driving force. Therefore, the Philip and deVries model needs to be modified to reflect these findings.

• Continuum modeling results show that EVD is necessary to predict the vapor diffusion rate in a partially saturated packed bed. If EVD is ignored, the model predictions do not agree with the data.

(2) *Experiments*

• Innovative pore-scale experiments were designed and conducted at New Mexico Tech. These experiments show significant enhancement of vapor diffusion due to pore-scale liquid island processes, in agreement with pore-scale modeling studies.

• Porous media experiments using a bed of glass beads were completed at Washington State University. These results also confirm the existence of EVD.

(3) *Overall*

We performed the first direct measurements of EVD and developed the first mechanistic pore-scale model of EVD. Both of these efforts demonstrate conclusively that EVD exists and is a potentially important transport mechanism in porous media.

Publications

Refereed

Gu, L., C. K. Ho, O. A. Plumb, and S. W. Webb. 1998. "Diffusion with Condensation and Evaporation in Porous Media." *Proc. 7th AIAA/ASME Joint Thermophys. and Heat Trans. Conf.* **357-2** (Albuquerque, NM, 14–18 June): 213–220.

Gu, L., C. K. Ho, O. A. Plumb, and S. W. Webb. 1998. "Vapor Diffusion in Partially Saturated Packed Beds." *Proc. 1999 ASME/JSME Thermal Engin. Joint Conf.*, accepted.

Ho, C. K., and S. W. Webb. 1998. "Review of Porous Media Enhanced Vapor-Phase Diffusion Mechanisms, Models, and Data—Does Enhanced Vapor-Phase Diffusion Exist?" *J. Porous Media* **1** (January): 71–92.

Webb, S. W. 1998. "Gas-Phase Diffusion in Porous Media—Evaluation of an Advective-Dispersive Formulation and the Dusty-Gas Model for Binary Mixtures." *J. Porous Media* **1** (March): 187–199.

Webb, S. W. 1998. "Pore-Scale Modeling of Transient and Steady-State Vapor Diffusion in Partially-Saturated Porous Media." *Proc. 7th AIAA/ASME Joint Thermophys. and Heat Trans. Conf.* **357-2** (Albuquerque, NM, 14–18 June): 221–231.

Webb, S. W. 1998. "Temperature Gradient Effects on Vapor Diffusion in Partially-Saturated Porous Media." 1999 ASME/JSME Thermal Engineering Joint Conference, accepted.

Webb, S. W., and C. K. Ho. 1997. "Pore-Scale Modeling of Enhanced Vapor Diffusion in Porous Media." *Proc. ASME Fluids Engin. Div.* **244** (Dallas, TX, 16–21 November): 457–468.

Other

Webb, S. W. 1998. "Gas-Phase Diffusion in Porous Media: Comparison of Models." *Proc. TOUGH Workshop '98* **LBNL-41995** (Berkeley, CA, 4–6 May): 269–274.

Webb, S. W., and C. K. Ho. 1998. "Pore-Scale Modeling Using TOUGH2." *Proc. TOUGH Workshop '98* **LBNL-41995** (Berkeley, CA, 4–6 May): 288–293.

Webb, S. W., and C. K. Ho. 1998. "Review of Enhanced Vapor Diffusion in Porous Media." *Proc. TOUGH Workshop '98* **LBNL-41995** (Berkeley, CA, 4–6 May): 257–262.

3508.110

Stress Evaluation and Model Validation Using Laser Ultrasonics

W. Lu, L. W. Peng, J. J. Dike

The evaluation of mechanical stress has been, and continues to be, an area of active research due to its effect on the performance and reliability of mechanical hardware. Of particular interest to Sandia is the ability to predict and experimentally verify stress fields in engineering components resulting from both their intended operation (external loading) and fabrication process (residual stress). Noncontact stress-measurement techniques are needed for in situ *experimental evaluation of stresses for validation of constitutive models and structural analyses to enable model–based design.*

Based on the acoustoelastic behavior of material, which refers to the fact that elastic wave velocities vary with stress, stress can be evaluated from ultrasonic-wave velocities. We demonstrated the capability of laser ultrasonic (LU) crystallographic texture measurements over a path length of a few millimeters, an improvement in spatial resolution of at least an order of magnitude over conventional methods. LU is a novel method for the optical generation and detection of ultrasound. These advances will allow us to analytically and numerically model, as well as experimentally validate, the acoustoelastic behavior of candidate materials, thus qualifying this stress-measurement technique.

In the previous year, we demonstrated acoustoelastic techniques in stress and stress-gradient evaluations and the applicability of LU. We also developed and validated finite-element models (FEMs) for simulating thermal and mechanical responses due to heating by a laser pulse. FEMs are viable tools for guiding LU experimental techniques.

This year's main focus was to apply LU techniques to evaluate stresses in engineering components. We compared experimental results and model predictions. Throughout the investigation we continuously undertook theoretical and experimental study of effects of texture (preferred orientation of material) on acoustoelastic behaviors, FEM simulations (or numerical experiments) of Rayleigh-wave propagation under various conditions, and LU experimental techniques (such as narrowband wave generation).

This year's accomplishments were in four areas: acoustoelasticity, FEM, LU techniques, and demonstrations.

• *Acoustoelasticity*. We developed a model to include texture effects on acoustoelastic constants of aluminum alloys, which are functions of seven texture coefficients (W_{400}, W_{420}, W_{440}, W_{600}, W_{620}, W_{640}, and W_{660}). We experimentally measured acoustoelastic constants and texture coefficients of two AA6061-T6 samples. Model-predicted acoustoelastic constants from texture coefficients are in accordance with experimental values. This explains why inconsistent values were reported in the literature.

• *FEM*. We validated FEMs by comparing with analytical results, which we further improved to include temperature-dependent thermal and mechanical (elastic and plastic) properties of the material. Temperature-dependent properties significantly decreased the peak magnitudes in waveform; including plasticity affected the shape of the waveform. We used FEM to simulate several experimental scenarios. The purpose was to guide experiments to generate desired waveforms, broadband or narrowband signal, for stress-gradient evaluation. We investigated the effect of pulsed-laser spot size. It shows that frequency content of signal increases as source diameter decreases. We simulated narrowband generation by using multiple exciting sources. Increasing the number of sources with source-spacing fixed narrows the bandwidth of the received waveform. We also used FEM for structural analysis for validation purposes. We calculated the stress distributions of a compressed ring and a welded tube, which we can use to compare with measured values.

• *LU techniques*. We demonstrated ultrasonic stress-gradient measurement last year by using a piezoelectric transducer for excitation and LU for receiving. To have a fully LU system, the critical task was to generate desired waveforms using a laser. From the guidance of FEM, we successfully developed the technique to generate narrowband signals. Unfortunately, there are still a few problems to overcome to meet the consistency and accuracy required for velocity measurements.

We designed and performed three experiments to demonstrate the applicability of LU techniques. First, an annular ring made of AA6061-T6 was compressed diametrically beyond yield. We measured the residual stress distribution at the horizontal section, which was in agreement with analytical predictions. Second, we made LU measurements on a bend beam. We had evaluated the residual stress by several different techniques such as neutron diffraction, x-ray, etc. LU results matched other results qualitatively since the acoustoelastic constants of the material were not available. The third experiment was the welded tube. We made LU measurements but were not able to obtain consistent and accurate velocity versus frequency relations.

• *Demonstrations*. We developed and demonstrated an LU technique in stress measurement and a partial LU method in stress-gradient measurement. The spatial resolution of the technique is about 1 centimeter; the stress and stress-gradient resolutions are about 40 MPa and 40 MPa/mm, respectively.

Publications

Refereed

Dike, J. J. 1998. "Finite Element Modeling of Ultrasonic Waves Produced by a Pulse Laser." *Rev. of Progress in Quantitative Nondestructive Eval.* **17** (San Diego, CA, 27 July–1 August): 667–674.

Dike, J. J., and T. M. Sanderson. 1998. "Simulations of Surface Waves Gener-

ated Using Laser Ultrasonics." Paper presented to the 25th Annual Review of Progress in Quantitative Nondestructive Evaluation, Snowbird, UT, 14–19 July.

Dike, J. J., and T. M. Sanderson. 1998. "Simulations of Surface Waves Generated Using Laser Ultrasonics." *Rev. of Progress in Quantitative Nondestructive Eval.* (New York), submitted.

Lu, W., L. W. Peng, and P. Holland. 1998. "Measurement of Acoustoelastic Effect of Rayleigh Waves Using Laser Ultrasonics." *Rev. of Progress in Quantitative Nondestructive Eval.* **17** (San Diego, CA, 27 July–1 August): 1643–1648.

Man, C. S., W. Lu, and J. Li. 1998. "Effects of Crystallographic Texture on the Acoustoelastic Coefficients for Rayleigh Waves in Aluminum." Paper presented to the 25th Annual Review of Progress in Quantitative Nondestructive Evaluation, Snowbird, UT, 14–19 July.

Man, C. S., W. Lu, and J. Li. 1998. "Effects of Crystallographic Texture on the Acoustoelastic Coefficients for Rayleigh Waves in Aluminum." *Rev. of Progress in Quantitative Nondestructive Eval.* (New York), submitted.

3508.040

Using Higher-Order Gradients to Modeling Localization Phenomena

D. J. Bammann, D. A. Mosher, N. R. Moody, D. A. Hughes

Prediction of structural failure in components due to void growth and ductile crack propagation requires a constitutive model based on the physics of these processes. As a result, much research is currently directed toward bridging the micro- to macroscales in mechanics of materials to bring better descriptions of material response into our finite-element (FE) calculations. In many cases, an attempt to include micromechanical phenomena into a macroscale model results in mesh dependency when implemented into an FE code. Sandia demonstrated this, in particular, for problems such as damage or crack propagation and strain localization. Attempts to describe this by local continuum damage models leads to the unacceptable condition that any refinement of the FE mesh results in a change in the result. This mesh dependency results from the lack of a length scale in the formulation of the local continuum theory. Currently, Sandia's most accurate FE model (FEM) constitutive models use a state-variable approach but still do not contain a length scale. In this project we are taking the next step in extending these models by embedding a length scale into the continuum by introducing higher-order spatial gradients into the evolution of the state variables. Utilizing this in the evolution of the dislocation density, both void coalescence and ductile failure can be accurately modeled while eliminating the mesh dependency of the solution. This will also allow a more accurate description of shear bands, including the stress and strain level, and an understanding of when shear bands lead to failure and when they are acceptable for a particular design. We plan an experimental program to help guide the appropriate choice of a length scale as well as provide insight into appropriate boundary conditions (BCs). Another important part of this project will be an attempt to develop a better model of friction by accurately describing the steep gradients in hardness that occur near the surface at interfaces.

We modified BCs, motivated by solutions of image forces on dislocations at free surfaces. This was necessary to describe the experimental observation that the stress depends on the diameter in torsion of very thin wires. We developed and conducted an experimental program to isolate a physical length scale. This involved the tensile testing of a series of self-similar thin foils containing an array of holes. The smallest-hole diameters were on the order of 8.5 mm. While the tests provided useful information on the structure of the localized zone, we discovered that the dependence of the mechanical response on changing dimensions would have been better modeled using foils consisting of single crystals. We developed and implemented a gradient theory for dislocations in a single crystal and used it to model cyclic response. The model predicts the formation of persistent slip bands in larger-grained materials, consistent with existing experimental observations. We performed calculations to model dislocation substructures resulting from frictional loading of steel plates sliding on copper. Local models underpredict both the depth of deformation into the material and the increased hardness of the deformed copper near the surface. The gradient model captured both of these effects with reasonable accuracy.

Publications

Other

Bammann, D. J. 1998. "A Gradient Model of Dislocation–Based Plasticity." Invited seminar, CalTech, Pasadena, CA, January.

Bammann, D. J. 1998. "A Gradient Model of Dislocation–Based Plasticity." Invited seminar, University of Illinois, Department of Theoretical and Applied Mechanics, Urbana-Champaigne, IL, January.

Bammann, D. J. 1998. "A Gradient Model of Plasticity." Paper presented to the U.S. National Congress of Applied Mechanics, Gainesville, FL, June.

Bammann, D. J., and P. R. Dawson. 1997. "Effects of Gradients in Hardening on Strain Localization." *Plasticity '97, Finite Plastic and Viscoplastic Deformation* **1** (Juneau, AK, July): 123.

Bammann, D. J., and P. R. Dawson. 1997. "Nonlocal Aspects of Localization and Failure." *Proc. IUTAM Symp. on Plasticity and Microplasticity* **1** (Bochum, Germany, August): 125.

Dawson, P. R., D. J Bammann, and D. R. Mosher. 1997. "Modeling the Influence of Gradients on the Evolution of Damage in Metals." *Proc. 3rd Internat. Conf. Mater. Processing Defects* **1** (Paris, France, July): 223.

3508.120

Altered Simulation Properties for Tetrahedral Finite Elements for Use in Engineering Simulation

S. W. Key, K. H. Brown, C. R. Dohrmann, M. W. Heinstein, C. M. Stone

In 3-D numerical simulations in solid mechanics, the current finite element (FE) of choice for spatial discretization is some form of eight-node brick hexahedron. In spite of a multiyear quest, an automatic all-hexahedron mesh-generation scheme for general geometries has not been forthcoming. The alternative is tetrahedral FEs, for which a number of automatic mesh generators exist. However, four-node tetrahedral FEs, while attractive for their computational simplicity, result in numerical predictions of abysmal quality. Sandia will develop a tetrahedral element with numerical properties competitive with the eight-node brick hexahedron FEs extant today. If the effort is successful, existing automatic tetrahedral mesh generators can be used, and the time- and manpower-intensive efforts currently used to build all-hexahedral meshes by hand can be avoided.

Theoretical developments led to the generation of discrete gradient and divergence operators. We applied a number of standard numerical tests that generated very positive outcomes. It is clear that the concepts employed were fruitful.

We pursued two separate studies: (1) We studied a number of alternative tetrahedral FE (the FE method is a technique for spatial discretization for field equations, in this case solids) formulations (spectral enrichments and different nodalizations) to ensure that our final tetrahedral FE selection could be expected to meet or exceed our simulation–based design requirements for a new FE for 3-D solids. (2) Detailed studies of the numerical requirements for interactions between independently meshed 3-D solids via contact algorithms led to new understandings of how the new tetrahedral FE will fit into existing simulation software. Both of these studies successfully produced larger understandings of the issues.

Publications

Refereed

Dohrmann, C. R., and S. W. Key. 1998. "A Transition Element for Uniform Strain Hexahedral and Tetrahedral Finite Elements." *Internat. J. Numer. Meth. in Engineering,* accepted.

Dohrmann, C. R., and S. W. Key. 1998. "Enhanced Uniform Strain Triangular and Tetrahedral Finite Elements." *Internat. J. Numer. Meth. in Engin.,* submitted.

Dohrmann, C. R., S. W. Key, and M. W. Heinstein. 1998. "A Method for Connecting Dissimilar Finite Element Meshes in Two Dimensions." *Internat. J. Numer. Meth. in Engin.,* submitted.

Dohrmann, C. R., S. W. Key, M. W. Heinstein, and J. Jung. 1998. "A Least Squares Approach for Uniform Strain Triangular and Tetrahedral Finite Elements." *Internat. J. Numer. Meth. in Engin.* **42**: 1181–1197.

3508.130

Development, Implementation, and Experimental Validation of the Lattice Boltzmann Method for Modeling Three-Dimensional Complex Flows

J. T. Fredrich, D. R. Noble, R. M. O'Connor, C. E. Hickox, Jr., H. W. Stockman

This project (1) developed codes based on the Lattice Boltzmann (LB) method for modeling nonreactive and reactive transport in complex geometries, including implementing scalable, distributed algorithms, (2) developed methods and computational algorithms to extract quantitative statistical descriptions of the microgeometry of porous media, and (3) validated the numerical codes by comparison with both laboratory transport and flow experiments, as well as calculations based on other numerical methods. The LB method shows exceptional promise for modeling both phenomena at intermediate scales where neither continuum models nor molecular dynamics (MD) methods are practical, and also for modeling very large-scale continuum flows where conventional computational fluid dynamics (CFD) methods suffer severe difficulties. This project coupled innovative experimental approaches, physical and chemical theory, novel algorithms, and advanced computing techniques and capabilities, and developed an advanced computational framework in which to investigate the fundamental phenomena characterizing micro- and macroscale complex flows.

Work in the second year focused on two areas: (1) development of an advanced capability to model geo-

metrically complex 3-D flows using the LB method, and (2) experimental validation.

Under the first task area we (a) developed single- and multiple-component 3-D LB codes, (b) optimized a distributed single-component 3-D LB code including parallel I/O and visualization, (c) developed LB code to enable simulation of other complex flow phenomena such as heat conduction, melting, and moving boundary problems, (d) developed code specific to the solution of initial value problems, (e) investigated variable grid resolution, and (f) developed a distributed computational platform based on Pentium Pro and Pentium II processors and a high-bandwidth switch for efficient message passing, for use both in code prototyping for the Accelerated Strategic Computing Initiative (ASCI) supercomputer and in production-scale runs.

Accomplishments under the second task area included (a) experimental characterization of the 3-D microgeometry and transport properties of complex porous media, (b) code development for image processing and binarization of volumetric confocal image data, and (c) quantitative comparison of numerical LB simulations with laboratory experiments and analytic test problems.

Publications

Refereed

Fredrich, J. T. 1998. "3-D Imaging of Porous Media and Application to Microscale Flow Modeling." *Phys. and Chem. of the Earth*, submitted.

Lindquist, W. B., and A. Venkatarangan. 1998. "Investigating Three-Dimensional Geometry of Porous Media from High-Resolution Images." *Physics and Chem. of the Earth*, submitted.

Noble, D. R. 1998. "A Lattice Boltzmann Method for Partially Saturated Computational Cells." *Internat. J. Modern Phys. C*, submitted.

Oh, W., and W. B. Lindquist. 1998. "Image Thresholding by Indicator Krigging." *IEEE Trans. Patt. Anal. and Mach. Intel.*, submitted.

Stockman, H. W. 1998. "Accuracy and Computational Efficiency in 3-D Dispersion via Lattice Boltzmann: Models for Double-Diffusive Fingering and Dispersion in Rough Fractures." *Internat. J. Modern Phys. C*, submitted.

Stockman, H. W. 1998. "Practical Application of Lattice-Gas and Lattice Boltzmann Methods to Dispersion Problems." *Internat. J. Complex Sys.*, submitted.

Other

Fredrich, J. T. 1998. "3-D Imaging of Porous Media and Application to Microscale Modeling of Transport." *Annales Geophysicae, Proc. XXIII General Assembly of the European Geophysical Society* **16** (Nice, France, 19–24 April): C254.

Fredrich, J. T. 1997. "3-D Imaging of Porous Media and Application to Microscale Modeling of Transport Properties." Paper presented to Los Alamos National Laboratory, Los Alamos, NM, 18 September.

Fredrich, J. T. 1998. "Microgeometry and Fluid Flow in Porous Media." Lecture at the GeoForschungsZentrum (Invited), Berlin, Germany, 30 April.

Fredrich, J. T. 1998. "Microgeometry and Fluid-Flow Processes in Porous Media." Lecture at SUNY Stony Brook (Invited), Stony Brook, NY, 19 February.

Fredrich, J. T. 1998. "Microgeometry of Porous Media and Fluid Flow." Lecture at University of Edinburgh (Invited), Edinburgh, Scotland, 3 July.

Fredrich, J. T. 1998. "Microscale Flow Modeling in Reconstructed Porous Media." Lecture to be given at New Mexico Tech (Invited), Socorro, NM, 4 February 1999.

Fredrich, J. T., and R. M. O'Connor. 1998. "Microscale Flow Modeling in Reconstructed Porous Media." *EOS Trans. Amer. Geophys. Union* (San Francisco, CA, 6–10 December).

Holdych, D., and D. R. Noble. 1998. "Lattice Boltzmann Model for Second-Order-Accurate Simulation of Initial Value Problems." Paper presented to the 1998 APS Meeting, Philadelphia, PA, November.

Lindquist, W. B. 1998. "Investigating Three-Dimensional Geometry of Porous Media from High-Resolution Images." *Annales Geophysicae, Proc. XXIII General Assembly of the European Geophysical Society* **16** (Nice, France, 19–24 April): C255.

Noble, D. R. 1998. "Mixed Convection Over a Backward-Facing Step in a Vertical Channel by the Lattice Boltzmann Method." *Proc. ASME HTD, ASME/AIAA Thermophys. Conf.* **357-2** (Albuquerque, NM, June): 167.

O'Connor, R. M., and J. T. Fredrich. 1997. "ARANEAE—A Scalable System for Distributed Computing." Paper presented to the Scalable Cluster Workshop, Monterey, CA, 21–22 November.

O'Connor, R. M., J. T. Fredrich, and H. W. Stockman. 1998. "Microscale Flow Modeling in Geologic Materials." *Annales Geophysicae, XXIII General Assembly of the European Geophysical Society* **16** (Nice, France, 19–24 April): C255.

3508.140

Capturing Recrystallization of Metals with a Multiscale Material Model

D. A. Hughes, M. A. Miodownik, A. W. Godfrey, E. A. Holm, S. M. Foiles, D. J. Bammann

The goal of this project is to develop a predictive continuum model that incorporates essential mechanisms from the atomic, dislocation substructure, and grain-size length scales. Sandia will accomplish this by developing a nonlinear nonequilibrium thermodynamic gradient theory that provides the mathematical framework to incorporate key microstructural processes. We will predict the physics at each length scale from experimental discovery and theoretical calculations, and the bridges between each length scale and the continuum level will be established by their contribution to the thermodynamic process. Although the framework we are developing is often more general, we chose to apply this formulation to the prediction of recrystallization processes in metals. Recrystallization (or annealing) occurs when cold-worked metals are heated. Above approximately 60% of the melt temperature, new strain-free grains nucleate and grow to consume all the cold-worked metal. This drastically changes the dislocation density, grain size, hardness, and ductility of the material. Recrystallization often occurs during manufacturing, during high-rate deformation, and in high-temperature environments. The continuum-level material model will evolve macroscale material response based on models at lower-length scales incorporating dislocation structure evolution, grain nucleation, and grain changes due to recrystallization. Specifically, a mesoscale recrystallization model based on a Monte Carlo Potts model will embody the local dislocation structure, grain orientation, and strain energy, which we will correlate with the variables in the continuum model. Automated microstructural analyses in the transmission electron microscope (TEM) supplemented by atomic-scale simulations will provide experimental discovery of dislocation structure evolution and nucleation in selected bicrystals. Quantitative statistical data of dislocation and boundary properties combined with results of atomic-scale simulations and scaling theory will provide relevant parameters for models at the mesoscale. These parameters will enter new kinetic equations for dislocation structure evolution and a multicrystal model of local orientation evolution.

Accomplishments at the continuum-level material constitutive law include the following:

(1) At the macroscale, in collaboration with Georgia Tech, we added an additional state variable to the rate- and temperature-dependent BCJ (Bammann Chiesa Johnson) plasticity model (nongradient version) to crudely describe dynamic recrystallization. The evolution of the variable depends on a critical function of the existing state variables, strain rate, and temperature. The model compares reasonably well with data on copper compression specimens.

(2) We incorporated the kinematics of finite deformation plasticity into the thermodynamic approach of Gurtin and Fried. We extended this formulation to endow the continuum with an extra rotational degree of freedom by decomposing the deformation gradient into elastic, plastic, and rotational parts. We used this same approach of Gurtin and Fried to develop a phase-field theory for use in modeling grain growth and recrystallization from a continuum perspective.

At the mesoscale we incorporated 3-D dislocation substructures determined by experiment and Monte Carlo modeling into the mesoscale recrystallization model. The mesoscale modeling effort focused on determining how strain-free nuclei form from the subgrain network. To convert the 2-D to a 3-D subgrain structure, we developed a new Monte Carlo algorithm that adjusts subgrain orientations to reflect the experimentally observed scaling laws for misorientation angles. Using this method, we generated realistic microstructures in 3-D that match all geometric and orientational parameters determined from experiments. We implemented the Read-Shockley model for grain boundary energy as a function of misorientation in the subgrain model. We performed the first 3-D simulations of grain growth with anisotropic grain boundary energy, and they showed behavior consistent with the thermodynamic analyses.

At the atomistic to grain scale, the deformation characteristics and resulting dislocation structure of the deformed bicrystal are important to the nucleation study. We grew, deformed, and characterized bicrystals with Laue x-ray diffraction and TEM. We observed and measured the dislocation structure of a compressed [421] bicrystal in the TEM. This characterization revealed a very heterogeneous microstructure with large rotations. These heterogeneities are important in characterizing potential nucleation sites.

Experimental observations of universal scaling for deformation microstructure evolution provide constraints on the continuum mechanics finite-element (FE) treatments. To be consistent with the observed scaling, we reduced the scaling properties to three constraining equations. We will incorporate these constraining equations into FE models.

Publications

Refereed

Campbell, G. H., S. F. Foiles, H. Huang, D. A. Hughes, W. E. King, D. H. Lassila, D. J. Nikkel, T. D. de la Rubia, J. Y. Shu, and V. P. Smyshlyaer. 1998. "Multiscale Modeling of Polycrystal Plasticity: A Workshop Report." *Mater. Sci. Eng. A*, accepted.

Grach, G., M. T. Lusk, and D. J. Bammann. 1998. "A Modulated Energy Function for Modeling Dislocation–Based Plasticity: Part 1 Production." *Internat. J. Plasticity*, submitted.

Gurtin, M. E., and M. T. Lusk. 1997. "Sharp-Interface and Phase-Field Theories of Recrystallization in the Plane." *Physica D*, submitted.

Hughes, D. A., D. C. Chrzan, Q. Liu, and N. Hansen. 1998. "Scaling of Misorientation Angle Distributions." *Phys. Rev. Lett.*, accepted.

Lusk, M. T. 1998. "A Phase-Field Paradigm for Recrystallization and Grain Growth." *Proc. Royal Society of London A*, accepted.

Lusk, M. T. 1998. "On a Modulated Energy Function for Simulating Grain Growth and Recrystallization." *Phys. Rev. B*, submitted.

Other

Battaile, C. C., and E. A. Holm. 1998. "Evolution of 2-D Potts Model Grain Microstructures for an Initial Hillert Size Distribution." *Proc. Internat. Conf. on Grain Growth*, submitted.

Chrzan, D. C. 1997. "Toward a Dislocation–Based Theory of Cell Formation." Paper presented to the 4th U.S. Congress on Computational Mechanics, San Francisco, CA, 6–8 August.

Godfrey, A., and D. A. Hughes. 1998. "Characterization of Dislocation Wall Spacing Distributions." *Solidification 1998*, in press, ed. S. P., Marsh, *et al.*

Hansen, N., and D. A. Hughes. 1998. "Structural Parameters and Strength." Paper presented to the Joint ASME, ASCE, SES Summer Meeting, Evanston, IL, 29 June–2 July.

Holm, E. A. 1997. "Applications of Mesoscale Materials Models at Sandia." Paper presented to the Caterpillar Research Group Seminar, Peoria, IL, September.

Holm, E. A. 1998. "Modeling of Microstructure-Property Relationships." Paper presented to the Gordon Research Conference in Physical Metallurgy, Plymouth, NH, June.

Holm, E. A., C. C. Battaile, M. D. Rintoul, and H. E. Fang. 1998. "Applications of Grain Growth Modeling." Paper presented to the 3rd International Conference on Grain Growth, Pittsburgh, PA, June.

Hughes, D. A. 1997. "Scaling of Deformation Microstructures." Presentation to Northwestern University, Evanston, IL, June.

Hughes, D. A. 1998. "Scaling of Dislocation Structure Evolution." Paper presented to the NIST Workshop on Work Hardening and Dislocation Patterning in Metals, Pleasanton, CA, June.

Hughes, D. A. 1997. "The Effect of Dislocation Microstructures and Grain Subdivision on Crystal Plasticity." Paper presented to the Finite Plastic and Viscoplastic Deformation, 6th International Conference on Plasticity and Its Current Application, Juneau, AK, July.

Lusk, M. T. 1998. "A Modulated Energy Function for Grain Growth of Recrystallization." Paper presented to the Colorado School of the Mines, Golden, CO, January.

Lusk, M. T. 1997. "A New Phase-Field Model for Grain Growth and Recrystallization." Paper presented to the 2nd Euroconference and International Symposium on Material in Deformation and Fracture, Thessaloniki, Greece, September.

Lusk, M. T. 1997. "A Phase-Field Paradigm for Grain Growth and Recrystallization." Presentation to the University of Colorado, Golden, CO, November.

Lusk, M. T. 1998. "Modulated Energy Functions and Recrystallization." Paper presented to the Materials Research Society, Symposium L: Interaction of Phase and Defect Microstructures in Metallic Alloys, Boston, MA, 2–6 December.

Lusk, M. T. 1998. "On Phase-Field Paradigms for Grain Growth and Recrystallization." Paper presented to the California Institute of Technology, Pasadena, CA, May.

Rollett, D., W. W. Mullins, M. D. Rintoul, and E. A. Holm. 1998. "The Link Between Kinetics and Configurational Statistics in Two-Dimensional Grain Growth: Comparison of Theory and Simulation." *Proc. Internat. Conf. on Grain Growth*, submitted.

3508.150

Nondeterministic Modeling in Engineering Science

J. R. Red-Horse, D. G. Robinson, L. P. Swiler, V. J. Romero, T. L. Paez

Physical processes that are the subject of engineering analyses invariably contain parametric entities that can, at most, be specified to within some level of uncertainty. The ability to evaluate the nature of the predicted system response in the face of this inevitability is a vital risk-reducing capability made necessary by the new model–based weapons-design initiative. The subject approach is to use approximate analytical methods to estimate response uncertainty using probabilistic measures. These approximation schemes will require only that point analysis results be available through which analytically complete probabilistic descriptions will result. Thus, not only can the methodologies be easily wrapped around existing analysis codes, but significant reductions in computational requirements, relative to Monte Carlo methods, also are often realized without a reduction in probabilistic information. The objectives of this research effort are to develop a suite of viable, computationally feasible, analytical approaches that can characterize (1) certain classes of input uncertainty, (2) the propagation of statistical uncertainty through analytical models to response quantities of interest, and (3) the proportion that particular physical model primitives contribute to that propagation process; that is, we will develop a means for performing probabilistic sensitivity analyses. The goal is to provide Sandia with new methodologies and computational tools for assessing the results of predictions in the face of approximation and uncertainty that are inherent to the processes being modeled.

This fiscal year, efforts included (1) establishing a technique, based on a method known as *bootstrap sampling,* for assessing the accuracy of probability approximations made with the Advanced Mean Value (AMV/AMV+) techniques over a broad range of applications, (2) examining the accuracy of AMV/AMV+ techniques as a function of properties of the response surfaces themselves, (3) developing a simplified version of the stochastic finite-element method (FEM), specific to linear analytical models, and running it externally around a local, general, FE code on a structural mechanics application, (4) investigating three alternative transformation methods that possess the potential to overcome weaknesses in AMV: a coordinate change using stereographic mapping, the likelihood method, and the maximum likelihood, (5) completing the development of the finite-element/lattice-sampling (FE/LS) progressive response surface construction algorithm and subsequently testing it on nondeterministic and optimization sample test problems, and (6) developing a methodology for building univariate probabilistic models of input parameters using measurement data as the basis.

Publications

Other

Red-Horse, J. R., and T. L. Paez. 1998. "Assessment of Probability Models Using the Bootstrap Method." *Proc. 39th Structures, Structural Dynamics, and Mater. Conf.* **1** (Long Beach, CA, 20–23 April): 1001–1008.

Red-Horse, J. R., and T. L. Paez. 1998. "Uncertainty Evaluation in Dynamic System Response." *Proc. 16th Internat. Modal Anal. Conf.* **4** (Santa Barbara, CA, February): 1206–1212.

3508.160

Lagrangian Modeling of Radiative Transport

L. A. Gritzo, P. E. Desjardin, J. H. Strickland

Many complex multiphysics, multiscaled, time-dependent processes include radiative heat transfer in turbulent flow. Conventional grid–based models are not well suited for such problems due to the complexity of gridding domains, which are very large relative to the scale required to resolve the important transport phenomena. A logical alternative is the gridless, Lagrangian–based approach employed in vortex methods that have been used successfully to simulate turbulence dynamics in internal and external flows, mixing flows, and buoyant jets and plumes. The same strategy was employed at M.I.T. to formulate the transport element method, which is used with the vortex method, to solve the species transport equation and the energy equation in nonreacting and reacting flows. The development of a compatible approach to simulate radiative transport, which exploits fast solvers developed at Sandia, is the objective of this effort. We are using massively parallel (MP) architectures to enhance computational tractability.

We developed a gridless technique (compatible with numerical simulation of the flow and temperature field by gridless vortex and transport element methods, respectively) for the solution of the integral form of the radiative transfer equation for an emitting and absorbing medium with uniform properties. We obtained the solution by representing the medium by Lagrangian elements whose strength depends on the absolute value and/or gradients of local temperature. We compared results to established and newly developed closed-form solutions for a planar media. We illustrated significant errors in other techniques that include simplifications of the governing equations by direct comparison with the present solutions. We also devel-

oped a fast-solver algorithm, based on the expansion of the Green's function in terms of a convergent separable series, for radiative transfer in a planar media. We investigated axisymmetric forms of the radiative transfer equation and showed them not to be conducive to the favorable form of equations obtained in planar or 3-D media. We developed an accurate, approximate solution strategy that includes near- and far-field formulations and are presently coupling it to the transport element method code to provide combined solutions of reacting flow and radiative transport. We are also updating the coupled axisymmetric code to include fast solvers for the fluid-flow field and message-passing constructs for MP computing. We developed a 3-D direct solver and are verifying the results using closed-form solutions for planar media. We developed a 3-D fast solver and are presently exercising and benchmarking it. Fast solvers for both planar and 3-D media show order-of-magnitude decreases in computational expense for reasonable amounts of elements and are amenable to use in a parallelization framework recently developed at Sandia. We developed and are implementing and testing a formulation for nonuniform radiative properties. We also defined conceptual treatments of solid boundaries.

Publications

Refereed

Gritzo, L. A., and J. A. Strickland. 1998. "A Vortex and Transport Element Method Compatible Technique for Solving 1-D and 3-D Radiative Heat Transfer." *Proc. 3rd Internat. Workshop on Vortex Flows and Relat. Numer. Meth.* (Toulouse, France, 24–27 August).

Gritzo, L. A., and J. A. Strickland. 1998. "Gridless Solution of the Radiative Transfer Equation for Fire and Combustion Calculations." *Combustion Theory and Modeling*, accepted.

Strickland, J. H., R. S. Baty, L. A. Gritzo, and G. F. Homicz. 1998. "Fast Multipole Solvers for Three-Dimensional Vortex and Radiation Problems." *Proc. 3rd Internat. Workshop on Vortex Flows and Rel. Numer. Meth.* (Toulouse, France, 24–27 August).

3508.170

High-Resolution Modeling of Multiscale Transient Phenomena in Turbulent Boundary Layers

A. R. Kerstein, T. Echekki, S. E. Wunsch, V. Nilsen, T. D. Dreeben, R. C. Schmidt

Modeling of transient multiphysics phenomena in turbulence is especially difficult near walls, where the enhanced role of molecular transport introduces length scales far smaller than scales resolvable by 3-D computational models. Present-day empirical wall treatments are not applicable to strongly coupled multiphysics environments.

One-dimensional turbulence (ODT), the novel modeling approach adopted in this project, addresses this difficulty by capturing relevant length and time scales in an unsteady 1-D simulation. In this research effort, Sandia is coupling the coupled effects of transient applied shear, buoyancy, exothermic chemical reactions, and heat and mass transfer, with attendant property variations, into ODT. We will use this formulation to perform parametric studies to support the development of improved wall treatments for steady-state flow solvers, with emphasis on the needs of the FUEGO fire-model development effort.

We formulated an ODT–based wall submodel for large-eddy simulation (LES). We will implement it first within an LES code suitable for testing and direct comparison with existing wall submodels. Subsequently, we will implement it within a code architecture that is compatible with Sandia software integration objectives. The implementation of this code will demonstrate new capabilities needed to simulate combustion, heat transfer, and related multiphysics phenomena in turbulent flows with wall geometries relevant to programmatic applications.

We formulated ODT as a suite of utility modules within Sandia's CHEMKIN gas-phase chemistry/transport/thermodynamics code framework. This formulation calls CHEMKIN subroutines to compute molecular-level subprocesses. This information is fed back to the ODT driver to serve as input for the ODT computations of thermal expansion and viscous effects on the turbulence evolution. Within this framework, we implemented two formulations of ODT: the original boundary-layer formulation and an impinging-flow formulation. We performed verification tests of these formulations.

We also incorporated and verified the code modifications needed to simulate buoyancy-driven flow along a vertical wall. We performed a validation study demonstrating the predictive capabilities of this formulation, involving comparisons to laboratory data and to data from fully resolved 3-D flow solutions. The ODT simulations reproduced previously observed flow-structure and heat-transfer parameter dependencies and extrapolated them to larger-scale flows. These scalings have not yet been explained theoretically. ODT is currently the only available method for extrapolation from the regime that is accessible by 3-D simulation to larger-scale flows of programmatic interest.

We developed and are testing a formulation of ODT configured for use as a wall submodel for LES. We based this formulation on a novel concept for representing the time evolution of a 3-D velocity vector on a linear (1-D) spatial domain. In contrast, ODT as implemented in the effort to date represents the time evolution of a single velocity component on a linear spatial domain.

We identified an LES formulation suitable for incorporation of this wall submodel. It is based on an LES code being used by a Stanford University group to test a class of wall submodels that couple to the LES in the same manner as required for the ODT wall submodel.

3508.180

Dispersive Measurements of Velocity in Heterogeneous Materials

L. C. Chhabildas, J. B. Aidun, M. R. Baer, W. M. Trott

To provide real-time data to validate 3-D numerical simulations of heterogeneous materials subjected to impact loading, Sandia adapted an optically recording velocity interferometer system (ORVIS) to a line-imaging instrument capable of generating precise measurements of spatially resolved velocity variations during dynamic deformation. Combining independently variable target image magnification and interferometer fringe spacing, this instrument can provide spatial resolution of a few millimeters along a line segment together with a temporal resolution of < 0.2 ns. As a complementary development, we also demonstrated a simultaneous stop-motion imaging of the complete fringe field (using a fast-gating intensifier/charge-coupled device [CCD] system). This additional capability can be used to generate a complete 2-D map showing velocity variations in a moving surface at one point in time. These novel diagnostic methods for examining the mesoscopic-scale dynamic response of heterogeneous materials have been packaged for use in well-controlled, well-characterized impact-loading experiments at a gas-gun facility, and we designed and assembled the optical interface with the gun target chamber. Candidate substances for examination include such programmatically interesting materials as pressed granular explosives, ferroelectric ceramics, and ALOX (alumina-filled epoxy). We will use observed spatially resolved velocity profiles to evaluate critically corresponding 3-D computer simulations on the selected materials. Validation of computer predictions at the mesoscopic scale is designed to encourage development of internal state continuum models that will also be validated at the macroscopic level using conventional shock-wave profile techniques. Validation of material response at these two different material response levels will provide an unprecedented capability for developing and validating physics–based models directed at better predictive modeling as a replacement for extensive experimental testing of weapons systems and subcomponents.

The principal focus of our research involved evaluation and optimization of optical designs for adapting line-imaging ORVIS to provide real-time measurements of spatially resolved (mesoscopic scale) velocity variations in impact-loaded heterogeneous materials. We performed initial testing of these designs on laser-driven flyer plates that exhibit fine-scale nonplanarity and Rayleigh-Taylor perturbations, depending on exact launch conditions. We then packaged these designs in a portable configuration for use in well-controlled experiments on heterogeneous materials at a gas-gun facility.

Characterization of target-imaging optics in ORVIS demonstrated that precise control of image magnification is achievable over a wide range (x10–x200); fringe spacing is independently and widely variable as well. Moreover, we determined that image magnification can be made to be relatively insensitive to target distance. These features enable the study of different heterogeneous materials having varying characteristic scale lengths (< 10 mm to > 1 mm) and permit location of the interferometer system at a safe, variable distance from a gas-gun target chamber.

Free-surface velocity measurements on laser-accelerated flyers and wave profile measurements of flyers impacting a lithium-fluoride (LiF) window verified the ability of line-imaging ORVIS to discern fine-scale phenomena at temporal and spatial resolutions of < 0.2 ns and < 10 mm, respectively. We also developed a new complementary technique utilizing a redundant set of image/fringe data. We used a fast-gating, intensifier/CCD system to obtain stop-motion images of the complete fringe field that can be used to generate detailed maps of the target surface velocity.

We assembled a fully functioning line ORVIS setup, including source laser, streak camera, intensifier, and CCD detector, on a 2 x 6 optical breadboard, and transported it to a gas-gun site at Sandia. In addition, we designed, assembled, and tested the optical interface to the gas-gun target chamber. We assembled hardware for the initial set of experiments consisting of fused silica targets (both optically flat and wedged samples) designed for planar impact by fused silica. The experimental design supports simultaneous line ORVIS and conventional single-point velocity interferometer system for any reflector (VISAR) measurements. Preparations for the initial set of gas-gun experiments were nearly complete as the first year of the project came to a close.

Finally, in concert with experimental progress, we developed a robust method for individual-line fringe analysis (based on push-pull VISAR concepts) for line-imaging ORVIS. In reducing records of numerous flyer tests, we showed that this powerful approach can generate remarkably clean velocity-time profiles from noisy image data. We generated and are currently testing an automated analysis routine. This routine includes ORVIS image import and pre-processing (e.g., image rotation, determination of fringe separation, background subtraction, etc.), followed by export to an existing VISAR analysis platform.

3508.190

A Physically–Based Computational Method for Predicting Generalized Fracture

P. A. Klein, E. S. Alber

Fracture is an important mode of failure, and computational methods for its simulation are essential to failure prediction. Yet an efficient, exhaustive computational method for accurate fracture prediction does not exist at this time. Attempts at combining classical

(or continuum) fracture mechanics with the standard finite-element method (FEM) or with the element-free Galerkin (EFG) method offer a good first step; however, FEM has inherent difficulties in resolving arbitrary crack trajectories, and the current development of EFG is limited to the growth of predefined, existing cracks. Furthermore, both approaches are subject to the limitations of classical fracture mechanics, which deals with preexisting cracks and with crack growth criteria that have not been confirmed under generalized conditions.

This project will develop a new computational tool based on EFG in conjunction with embedded traction-separation (or cohesion) relations. EFG provides an automatic resolution of new surfaces as they develop during the solution process (this avoids the remeshing and remapping required in FEM), and the traction-separation relation provides a physically–based resistance to fracture. This tool is capable of solving the entire specter of fracture, which encompasses crack nucleation, crack growth, crack interaction, and crack branching (fragmentation). This provides a high-fidelity capability for predicting generalized fracture with application to a wide range of problems, including polymer aging, thermally induced cracking of encapsulants, glass fragmentation, and weapon slap-down.

We developed a new 2-D code (written in FORTRAN-90) based on the EFG method with emphasis on cohesive fracture. The code can be used for transient-dynamic or quasi-static analysis and represents a computational method that resolves cracks as they appear during the solution process, without any changes to the initial discrete model. We validated the code by solving several simple test problems. Currently, we are using it to simulate intergranular-fracture in ceramic materials and interaggregate-fracture in concrete. The code allows for crack initiation (i.e., nucleation), crack growth (including branching or kinking), and crack arrest to emerge as a natural outcome of the analysis (i.e., there is no need for an *a priori* criterion to identify the onset of such phenomena even in the presence of widespread dissipative deformations). We developed and are currently validating a 3-D version of the code; preliminary results are encouraging. We also plan to combine the current approach with the virtual internal bound model to treat crack initiation and growth.

3508.220

Micromechanical Failure Analyses for Finite-Element Polymer Modeling

R. S. Chambers, T. R. Guess, D. B. Adolf, E. D. Reedy, Jr., C. S. Lo

Accurate failure models are needed in analyses to predict margins of safety to determine whether encapsulated components meet life-cycle requirements. Using recently developed and validated viscoelastic models for epoxy encapsulants, the stress concentrations in fracture process zones near failure-prone corners and material interfaces now can be computed accurately as functions of time and temperature. This technology enables us to consider a novel approach for developing a micromechanics–based cohesive failure criterion that includes nonlinear viscoelastic (NLVE) behavior.

Linear elastic fracture mechanics adopts a macro approach and ignores the details of the material behavior at the crack tip. Alternatively, Sandia will model the details of the stress/strain behavior within the process zone surrounding a crack tip to pursue microscopic mechanisms. Using a proven NLVE material model for epoxy encapsulants, we will analyze crack-tip deformation histories in fracture samples that are loaded to failure. We then will look for correlations between the local crack-tip behavior and new as well as traditional fracture parameters. This approach will scrutinize failure criteria based on such things as finite extensibility of the polymer network, shear banding, cavitation, or subcritical crack growth. This project also provides a way for studying the dependencies of macrofracture parameters on temperature and aging and may offer a more general approach to predicting failure that works in situations where traditional fracture mechanics does not.

A key aspect of this project was to design and manufacture test samples and perform fracture experiments to collect data for use both in model validation and in defining an NLVE material–based cohesive failure criterion. We selected a three-point bending test on a pre-cracked beam to experimentally measure fracture toughness (KIc). We made samples and conducted tests at three different temperatures (–60°, 23°, and 50°C) and three different loading rates (.01, .1, and 1 mm/s). Similar test data collected on partially cured samples showed that toughness is much more sensitive to the degree of cure. We also designed and fabricated a second test geometry representative of cracking around an encapsulated sharp-cornered inclusion. We performed a novel fracture analysis of an encapsulated inclusion test sample extending traditional linear elastic fracture mechanics to discontinuities other than cracks. This macro approach seeks to relate failure to the stress intensity factor characterizing the inclusion corner. Cracks observed during thermal cooling on different shaped inclusions with different interface adhesion have thus far been consistent with expectations.

We added the NLVE constitutive equation to the JAS3D finite-element code and validated it in tension, compression, and torsion over a 50° temperature range by analyzing tests and comparing predictions to measurements. The higher-temperature tests showed that better relaxation spectra definitions are needed to capture the post-yield softening. We showed the formalism, strain measure, and clock mechanism to be qualitatively correct. We are now resolving parameter sensitivities. To begin addressing modeling issues, we meshed the cracked, three-point bending sample and analyzed it elastically and viscoelastically. We identified two refinement schemes to resolve crack-tip stresses.

3508.210

Development of *In Situ* Diagnostics for Simultaneous Measurement of Transient Gas Species and Soot in Large Fires

C. R. Shaddix, P. D. Ludowise, L. R. Thorne, J. R. Ross, H. A. Johnsen, D. K. Ottesen, S. W. Allendorf, L. A. Gritzo

The thermal hazard posed by a fire to a weapon or other engineered system is a consequence of combined radiation and convection from high-temperature soot and gases. The development of advanced, predictive models of this hazard requires detailed knowledge of the transient chemical structure and soot distributions within real-scale fires. At present, there are no measurements, and hence no understanding, of transient gaseous species generation and transport in large, fully turbulent fires.

In this project Sandia is applying tunable diode laser absorption spectroscopy (TDLAS) to perform in situ, *temporally and spatially resolved measurements of gas species and soot in discovery and validation experiments in real-scale fires. We identified chemical species that are most likely to be detected and that are characteristic of the hydrocarbon fuel, combustion intermediates, and combustion products. We are combining TDL measurements of these species with absorption/emission measurements of soot concentration and temperature. In addition, we are exploring the possibility of detecting acetylene because of its importance in soot formation.*

Success of this project depends on the ability to develop and apply TDLAS in a hot, transiently attenuating environment, with several TDL lasers (to access several gas species). We constructed a buoyant flame facility to evaluate multipass techniques for improving the system sensitivity and other probe design issues. In addition, we conducted evaluations of several different possible approaches for laser multiplexing. We are performing experiments in a low-pressure, flat-flame, Fourier transform infrared (FTIR) facility to identify and quantify the strongest absorption lines for the target species.

We completed background research and design work that are critical to the successful implementation of the TDL gas species measurement technique in fires during the first year of this project. These efforts may be grouped according to the following considerations: assessment of the best detectable gas species to measure in fires and the optimal spectral locations for their measurement, development of a suitable laser multiplexing approach, and design of a sensitive, fast TDL data-acquisition system.

Analysis of spectral considerations, expected species concentrations, and predicted absorption line strengths at high temperatures resulted in tentative identification of methane, carbon monoxide, carbon dioxide, and water as good candidates for detection in fires. We extensively analyzed and compared the HiTran96 and HiTemp spectral databases with recent measurements reported in the literature to identify the most promising spectral regions for high-temperature transitions of target molecules and to provide estimates of the absorption line strengths at high temperatures. In addition, we identified and acquired detailed chemical kinetic mechanisms for aviation fuel and similar transport fuels. We are performing calculations of the expected chemical compositions for different stoichiometries and residence times. Work is continuing in evaluating acetylene and ethylene as potential target species and in identifying interfering carbon dioxide and water absorption features, using a low-pressure, flat-flame, high-resolution FTIR facility. The potential detection of oxygen together with the other species does not appear promising due to the need to use separate fiber optics and detector for the short wavelength (760 nm) of these transitions.

We evaluated several approaches to combining (or multiplexing) several TDLs that have been suggested in the literature for their applicability within the constraints of this project. The use of either injection-current staggering or high-frequency multiplexing, or perhaps even a hybrid approach combining these two concepts, appears to be the most promising possibility. We initiated experiments in a buoyant flame facility with variable soot concentrations to evaluate the feasibility of these concepts.

To achieve the rapid response (> 100 Hz) and short measurement length (2–5 cm) desired for grid-level fire measurements, improvements must be made in the sensitivity of the TDL system. We performed experiments assessing the noise characteristics of fiber–based TDL systems, and an analysis of existing soot data from a pool fire suggests that an optimal path length for species measurements in this environment is 20–30 cm. Consequently, we are designing a parallel-mirror, off-axis multipass sampling system for the fire probe. Also, we specified and acquired a fast A/D (analog-to-digital) converter and computer system for TDL data acquisition.

Publications

Other

Shaddix, C. R., S. W. Allendorf, D. K. Ottesen, H. Johnsen, and K. Hencken. 1997. “Species Measurements with Near-IR Tunable Diode Lasers in Demanding Environments (including Fires).” Presentation to the National Institute of Standards, Building and Fire Research Laboratory (Invited), Gaithersburg, MD, 15 December.

3508.240

A Phenomenological Model for Multicomponent Transport with Electrochemical Reactions in Concentrated Solutions

K. S. Chen, M. E. Coltrin, F. M. Rupley, R. S. Larson, G. H. Evans

Liquid-phase electrochemical processes play important roles in Sandia's missions (e.g., thermal batteries, stockpile metal corrosion, fuel cells, and electroless and electrolytic plating as in LIGA [German for lithography, electroforming, molding] fabrication of microelectromechanical systems [MEMS] devices); the processes can involve multicomponent transport of charged species with simultaneous electrochemical reactions in concentrated solutions. For example, in a thermal battery cell, an interacting molten mixture of electrolytes is transported between electrode surfaces where reactions take place; consumption of the electrode results in moving boundaries. Accurate prediction of battery performance (e.g., discharge voltage) requires proper description of diffusion of charged species (driven by concentration and electrical-potential gradients), convection due to volume changes, energy transport, electrochemical reactions, and thermodynamic potentials. Classical dilute-solution framework based on Fick's first law is generally valid only for non-interacting species diffusing in dilute solutions. In short, a predictive capability is lacking at Sandia for modeling electrochemical processes such as thermal batteries.

Sandia will develop a phenomenological model for multicomponent transport of charged species with simultaneous electrochemical reactions in concentrated solutions using a state-of-the-art framework, accounting for interactions between multiple diffusing species. The new framework will utilize the Stefan-Maxwell equations, which describe multicomponent diffusion of interacting species using composition-insensitive binary diffusion coefficients. We will validate the phenomenological model, based on conservation of mass, momentum, energy, and species, as well as the law of mass action, using data available at Sandia for thermal batteries. We also will develop a liquid-phase electrochemistry package and a liquid-phase transport package for computing reaction rates and thermodynamic and transport properties. The coupling of the GOMA–based computer model with the liquid-phase electrochemistry and liquid-phase transport packages will provide Sandia a unique predictive capability for modeling electrochemical processes such as thermal batteries.

We completed conceptual designs of the liquid-phase electrochemistry and liquid-phase transport packages and theoretical developments for the two packages. In addition, we modified the existing Surface CHEMKIN Interpreter and rate routine to allow for the specification of Butler-Volmer kinetics. We developed a general theoretical framework for describing multicomponent transport of ionic (i.e., charged) species with simultaneous electrochemical reactions in concentrated solutions. We formulated equations that govern the phenomena of species diffusion and convection, electrochemical reactions, energy transport, and electrode-pore evolution in a Li(Si)/FeS^2 thermal-battery cell. We made sample predictions using a 1-D computer model based on that developed at UC–Berkeley. We made substantial progress toward developing a multidimensional GOMA–based computer code for modeling multicomponent transport of charged species with simultaneous electrochemical reactions in concentrated solutions as in thermal batteries. (GOMA is a multidimensional, multiphysics, finite-element code being developed at Sandia.) Specifically, we implemented in GOMA the Stefan-Maxwell flux model for describing transport of multiple species (neutral or charged). We modified the existing GOMA framework to allow the solution of the species mass conservation equations for systems involving multiple species. Moreover, we began implementing the needed framework in GOMA for solving the pair of Poisson equations that describe the electrical potentials in the molten electrolyte and the solid electrode. In short, we accomplished significant code development work in both GOMA and the condensed-phase version of CHEMKIN. This sets the stage for developing an integrated capability based on GOMA and CHEMKIN for modeling the complex chemical/physical phenomena involved in thermal batteries.

3508.230

Methodology Optimal Selection of Test and Simulation Levels for Problems Involving Computational Simulation

B. M. Rutherford, K. F. Alvin, V. J. Romero, T. G. Trucano

The investigation of a complex system is often performed using data from system and component test results supplemented by computer-generated responses that are based on conceptual and mathematical models of the physical system and its environment. Analysts rely on an efficient use of limited experimental resources to test the physical system, evaluate the models, and ensure (to the extent possible) that the models accurately simulate the system under investigation. The general problem considered here is one where only a restricted number of physical tests and/or system simulations can be performed to provide the data necessary to accomplish the project objectives. The levels of variables used for defining input scenarios, for setting system parameters, and for initializing other experimental options must be selected in an efficient way. Sandia developed a resampling–based approach for performing this selection. The methodology is applicable to the design of variable levels for physical testing and/or system simulation.

(1) During the first year of this project we completed a literature review of material related to experimental design for large-scale systems analysis. This review led to a more formal framework for defining desirable features of an algorithmic approach to these types of problems. A review of our results solidified our view that the proposed methodology was a promising and original approach.

(2) Our initial proposal included several components that we considered tactical aspects of the approach, in that while they were integral parts of the strategic methodology, their perfection was not required to demonstrate the potential of the algorithm. We investigated these components to a limited extent where we are satisfied that they function satisfactorily for the purpose of demonstrating the approach. They include (a) the methodology for ensuring that the representation of system knowledge is consistent with that knowledge; (b) specific parametric methods for constructing response surfaces that are useful in engineering applications; (c) metrics that can be used to measure the potential information provided by a candidate experimental design; and (d) a tuned evolutionary algorithm to be used for selecting candidate designs.

(3) We began the development of software that we will use to demonstrate the approach for small- and medium-scale problems.

Publications

Refereed

Rutherford, B. M. 1998. “A Methodology for Selecting an Optimal Experimental Design for the Analysis of a Complex System.” *Technometrics*, submitted.

Rutherford, B. M. 1998. “Important Considerations in Experimental Design for Large-Scale Simulation Analyses.” *Proc. Lockheed Martin Sys. Engin. and Software Symp.* (May).

MANUFACTURING SCIENCE & TECHNOLOGY

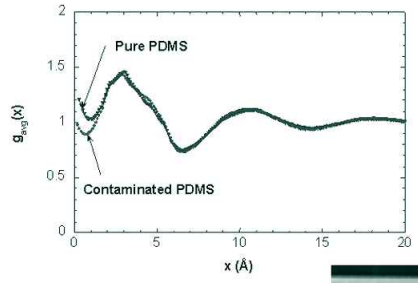

$$W_a = \sum_i \int_0^\infty v_i(z)\rho_i(z)dz$$

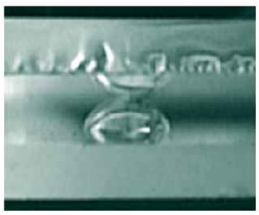

The Manufacturing Science and Technology investment area develops advanced manufacturing and production technologies with an emphasis on moving the product from the design stage to accepted hardware. Projects that reduce cost, shorten the design and manufacturing cycle, and improve predictability of products are encouraged. Projects must have a potential to impact the Nuclear Weapons Program.

Activity areas include two main thrusts: (1) develop processes that enable defect and cost reduction, or that enable the manufacture of emerging product technologies, and (2) provide new processes that reduce product fabrication or service defects. This will reduce product development time and expense.

About 75% of critical process steps for weapons manufacture involve surface cleaning or preparation, making surface cleaning the most common process step in DOE manufacturing operations. When an engineer qualifies a new solvent for weapons manufacture, he must rely on cumbersome laboratory tests that are expensive, repetitious, and time-consuming. After machining metals, an engineer must remove the lubricants used in the machining process, but many cleaners that were once used are now banned because of ozone problems. Frequently the engineer will put the dirty part into a cleaner and measure the strength of the joint, yet the part will still come to failure. In addition, overcleaning is a concern because it may introduce contaminants into the waste stream.

Sandia is applying their computer-modeling expertise, fracture mechanics understanding, and cleaning experience in a project titled “Investigation of the Impact of Cleaning on Adhesive Bond and the Process Implications” to find out how clean a material must be to achieve a good adhesive bond. Understanding the link between surface preparation and adhesion will result in reduced cleaning development time and testing, improved bonds, and improved manufacturability, which can be applied to agile manufacturing tools and will help advance product realization for encapsulated components. Developing a validated model for cleaning and surface preparation in adhesive bonding, coating, encapsulation, or painting processes would complete Sandia’s capability for a process that ensures efficient, low-cost production of small lots.

THIS PAGE
INTENTIONALLY BLANK

3510.540

Ultra-Precise Assembly of Microelectromechanical Systems (MEMS)

J. T. Feddema, M. X. Tan, M. A. Polosky, T. R. Christenson

Sandia is currently developing processes to make surface-machined silicon (Si) and LIGA (Lithographie Galvanoformung Abformung, German for lithography, electroforming, molding) parts with 100-micron outside dimensions (OD) and submicron tolerances for use in weapons surety devices. LIGA parts are of special interest because they are thicker than typical surface-machined parts; they can be made of metals, which makes them stronger (in tension) than surface-machined Si; and, when assembled, the components are not restricted to the plane. This last advantage is also a disadvantage. Today, most microcomponents are assembled manually using microscopes and teleoperated precision mechanisms—a time-consuming and tedious task. An automated assembly system is needed.

The goal of this project is to develop a visual feedback and robotic control system that improves positioning accuracy and eliminates the manual assembly of LIGA components. One possibility is to develop fixtures for the LIGA parts and teach points to a robotic system to perform a repetitive motion. Unfortunately, it is difficult to build fixtures with submicron tolerances, and it is not effective to teach points in an agile environment with a variety of parts. Therefore, this project uses vision and force sensing in the feedback loop to pick up and assemble randomly placed LIGA parts. Both the vision and force sensing allow for the assembly operations to be performed using relative position information rather than absolute. We used computer-aided design (CAD) information about the parts to generate an augmented assembly plan that accounts for uncertainties and microscale effects such as electrostatics, surface tension, and van der Waals forces.

We investigated the assembly of massively parallel (MP) LIGA parts and the use of multiple cameras for visual feedback. For LIGA to be profitable, a means of assembling multiple parts at one time is needed. For example, imagine 1000 gears attached to a wafer. By picking up the wafer and all 1000 gears, aligning them with 1000 shafts, and performing the insertion operation, the throughput of the assembly is increased 1000-fold. We designed, fabricated, and tested a system that presses 375-micron-diameter pins in a LIGA substrate and places a 3-inch-diameter wafer of 100 LIGA gears on the pins. We used a two-camera vision system to locate holes in the LIGA substrate, the location of the pins, the location of the pin insertion tool, and the location of the gears. We demonstrated that the vision system can locate parts within 1-micron standard deviation. Our positioning system can then place the parts within 0.4-micron accuracy.

In addition, we did a short theoretical study and published a paper on the effects of van der Waals and electrostatics on the grasping of 1–10-micron-diameter spheres. We concluded that it is possible to generate a fine-motion assembly planner that accounted for these effects during the pick-up and release of the parts. This is important since parts this size typically stick to most all surfaces. We also implemented a 2-D version of the assembly planner, but a more general 3-D version would require substantially more work.

Publications

Refereed

Feddema, J. T., and R. W. Simon. 1998. "CAD-Driven Microassembly and Visual Servoing." *Proc. 1998 IEEE Internat. Conf. on Robotics and Automation* (Leuven, Belgium, 16–20 May): 1212–1219.

Feddema, J. T., and R. W. Simon. 1998. "Visual Servoing and CAD-Driven Microassembly." *IEEE Robotics and Automation Magazine* (December).

Feddema, J. T., C. G. Keller, and R. T. Howe. 1997. "Experiments in Micromanipulation and CAD-Driven Microassembly." *Proc. SPIE, Microrobotics and Microsystem Fabrication* **3202** (Pittsburgh, PA, 16–17 October): 98–107.

Feddema, J. T., M. Polosky, T. Christenson, B. L. Spletzer, and R. W. Simon. 1998. "Micro-Gripper for Assembly of LIGA Parts." *Proc. World Automation Congress '98 ISORA* (Anchorage, AK, 10–14 May): 045.1–045.8.

Other

Feddema, J. T. 1997. "Microassembly of Microelectromechanical Systems (MEMS) Using Visual Servoing." *The Confluence of Vision and Control, Block Island Workshop on Vision and Control* (Block Island, RI, 23–25 June).

Feddema, J. T., P. G. Xavier, and R. G. Brown. 1998. "Assembly Planning at the Micro Scale." *Proc. Workshop on Precision Manipulation at the Micro and Nano Scales, IEEE Internat. Conf. on Robotics and Automation* (Leuven, Belgium, 16 May): 56–69.

3510.460

Laser-Spray Fabrication for Net-Shape Rapid Product Realization

M. E. Schlienger, M. L. Griffith, C. L. Atwood, J. E. Smugeresky

The primary purpose of this project is to characterize the laser-deposition process and determine the feasibility of fabricating complex near net shapes directly from a computer-aided design (CAD) solid model. Although Sandia demonstrated that the laser-spray fabrication process (laser-engineered net-shaping [LENS™]) is compatible with metal deposition for simple geometries, using this process to produce net-shape high-performance metal, ceramic, and composite components in a controllable fashion is not yet feasible. Process characterization results from the feasibility study will provide direction in developing a system to fabricate complex shapes directly from a CAD solid model. Our goal is to develop a system that is robust and that provides a significant advancement in existing technology. Sensors must be identified, developed (where necessary), and implemented to provide closed-loop process control. We must identify closed-loop powder-feed techniques to stabilize the process. It is also necessary to develop methodologies to slice CAD solid models to directly drive the motion control. We must develop the interfaces to be interactive with sensor inputs from the process. Development of this process will allow design engineers to produce functional models of their designs directly from CAD files. The turnaround time for complex geometrical shaped parts will be hours instead of days and days instead of months. With the reduced turnaround time, more time can be spent on the product design phase to ensure that the best component design is achieved. Maturation of this technology will revolutionize the way the world produces structural components.

We used the LENS™ process to produce trial forming dies, triclad joints, and tab attachments for neutron-generator tubes.

Over the course of this project, the time to produce a cubic inch of material decreased from 8 hours to under 3 hours with no loss of quality. Nozzle design improved such that the development and drop-in of metal deposits on the nozzle were largely eliminated.

We shifted sensor development efforts from sensing the thermal environment to more fully characterizing the process for enhanced repeatability. As a result of these efforts, we implemented coriolis flow-meter technologies for powder mass flow determination. This new sensing capability allowed a fuller characterization of the powder feed and resulted in new insights into control methodologies for controlling powder feed.

We designed and built a new powder feeder. Typical designs use screws or other moving parts in contact with the powder, an arrangement that results in clogging. We based the new design on an hourglass principle. Powder falls onto a ramp where it spreads out, and a diverter selects a portion of the resultant flow. The desired powder stream is then entrained in a carrier gas, whereas the excess powder is recirculated to the hopper. In this fashion there are no moving parts other than powder.

We linked the new powder feeder with the coriolis mass flow meter and an argon mass flow controller, which we use for the carrier gas. The gas flow is subtracted from the total mass flow, leaving powder mass flow only. We then compare this signal against a setpoint and use the difference to adjust the powder feeder diverter. The powder feeder/sensor setup allows the powder flow to be held stable over time.

We made substantial progress in the processing of titanium (Ti). Ti is a reactive metal that, when in the molten state, attacks most refractory mold materials. As a result, Ti is difficult to investment-cast. Direct fabrication techniques offer significant opportunities for the production of Ti components. Work with Ti revealed that very good properties can be obtained.

We produced graded materials, but before we had the ability to achieve good control of the powder feeders, it was challenging. To date, we have had to build graded parts by layering material in the powder hopper. This technique was successful, and we produced a part that transitioned from a stainless-steel to a nickel–based alloy. The new powder feeders will allow the mass flow of constituent powders to be specified and, as a result, graded materials will be much easier to produce.

Research into sensor utilization revealed that the best way to control the overall process is to control the size of the melt pool. Since the deposition width and thickness are directly related to the melt pool geometry, controlling this parameter will stabilize the build process. Presently, changes in part geometry, distance from the substrate, powder flow, traverse speed, and laser power all affect the bead morphology. By monitoring the pool size, then employing appropriate techniques to keep it constant, we will remove variability from the process. Work at Vanderbilt University revealed that by using video cameras to monitor the emissivity of the pool at two wavelengths, we can determine a material-independent measure of the molten pool size. Once we know this parameter, we can stabilize the process.

Publications

Refereed

Ensz, M. T., L. D Harwell, and M. L. Griffith. 1998. “Software Development for LENS.” *Proc. 9th Solid Freeform Fabrication Symp.* **9** (Austin, TX, 10–12 August).

Griffith, M. L., M. E. Schlienger, J. A. Brooks, L. D. Harwell, M. Essien, D. Nelson and W. Hofmeister. 1998. "Thermal Behavior in the LENS Process." *Proc. 9th Solid Freeform Fabrication Symp.* **9** (Austin, TX, 10–12 August).

Maziasz, P. J., E. A. Payzant, M. E. Schlienger, and K. M. McHugh. 1998. "Residual Stresses and Microstructure of H13 Steel Formed by Combining Two Different Direct Fabrication Methods." *Scripta Materialia*, accepted.

Schlienger, M. E., D. Dimos, M. Griffith, J. Michael, M. Oliver, T. Romero, and J. Smugeresky. 1998. "Near Net-Shape Production of Metal Components Using LENS." *Proc. 3rd Pacific Rim Internat. Conf. on Adv. Mater. and Processing* **3** (Honolulu, HI, 12–16 July).

Schlienger, M. E., M. Griffith, M. Oliver, T. Romero, and J. E. Smugeresky. 1998. "Sacrificial Materials for Complex Geometry Fabrication." *Proc. 9th Solid Freeform Fabrication Symp.* **9** (Austin, TX, 10–12 August).

Other

Schlienger, E. M., M. Griffith, M. Oliver, and T. Romero. 1998. "Laser-Engineered Net Shaping." Paper presented to the Automotive Applications of Thermal Spray Technology Conference, Romulus, MI, 3 June.

Schlienger, E. M., M. Griffith, M. Oliver, T. Romero, and J. E. Smugeresky. 1998. "Recent Advances in Direct Fabrication of Metal Components." Paper presented to the Materials Solutions Conference, Rosemont, IL, 12–15 October.

3510.510

Solution Synthesis and Processing of PZT Materials for Neutron-Generator Applications

J. A. Voigt, T. V. Montoya, D. L. Sipola, R. H. Moore, S. J. Lockwood, B. A. Tuttle, T. W. Scofield, J. D. Keck

Neutron-generator power supplies require two unique ferroelectric materials, specifically lead zirconate titanate (PZT) with a zirconium-to-titanate (Zr-to-Ti) ratio of 95:5 (PZT 95/5) and PZT 95/5 with a partial substitution of tin for zirconia (PSZT). These PZT formulations are unique to neutron generators, and there are no current U.S. suppliers of the material. Sandia has about a 5-year supply of the materials prepared commercially using a traditional multistep mixed-oxide processing route. There are several concerns about acquisition of qualified PZT and PSZT when the current supply runs out: (1) Will U.S. industry be willing to produce these difficult-to-process materials in the limited quantities required, and, if so, can they produce qualified material? (2) Past experience has shown that the success of the current mixed-oxide process is highly dependent on the source of raw materials used—will the required raw materials be available? (3) The current preparation process has many powder-handling and -processing steps that are of an environmental, safety, and health (ES&H) concern because of the PbO used in their synthesis. (4) The current process is extremely labor-intensive and requires extensive in-process testing and tweaking to produce qualified material. (5) Finally, the lack of scientific understanding of the mixed-oxide process makes it difficult to address problems when they occur. Based on our past experience in which we successfully developed and transferred to industry chemical preparation processes, we will develop an alternate process based on solution chemistry to prepare the PZT powders. We developed a process that satisfactorily addresses these concerns. We emphasized the underlying fundamentals of system solution chemistry and how these fundamentals relate to the ceramic material properties that are critical to neutron-generator applications.

Our major accomplishment was to develop a new process for preparing PZT (ratio of zirconium to titanium of 95:5, PZT 95/5) powders using the solution synthesis approach. When these powders were processed and machined into voltage bar components, we also demonstrated that the components would meet neutron-generator power supply requirements when explosively functionally tested. We filed a patent for the process we developed. We fabricated voltage bars from several powder lots of material this year. Explosive functional test results from several of these lots passed all neutron-generator power supply output requirements.

We also demonstrated that our PZT 95/5 powder synthesis process was highly reproducible with respect to powder properties, including particle size distribution and surface area and powder processability.

Publications

Refereed

Tuttle, B. A., J. A. Voigt, D. L. Sipola, W. R. Olson, and D. M. Goy. 1998. "Chemically Prepared Lead Magnesium Niobate Dielectrics." *Proc. Mater. Res. Soc. Symp.* **495** (June) (Boston, MA, 1–5 December 1997): 185–195.

Other

Tuttle, B. A., J. A. Voigt, J. Cesarano, B. H. King, and W. R. Olsen. 1998. "Chemically Prepared $Pb(Mg,Nb)O_3$ and $Pb(Zr,Ti)O_3$ Ferroelectrics." Paper presented to the Annual Meeting of the American Ceramic Society, Cincinnati, OH, 5 May.

3510.570

Finite-Element Meshing Approached as a Global Minimization Process

W. R. Witkowski, V. J. Leung, J. Jung, C. R. Dohrmann

The ability to generate a finite-element (FE) mesh in an automatic fashion is becoming the key to being able to automate the entire engineering analysis process. However, placing an all-hexahedron mesh on a general 3-D body continues to be an elusive goal.

Sandia's approach is fundamentally different from any other that we know of. We started from the premise that the problem of placing an all-hexahedron mesh on an arbitrary 3-D geometry needs to be addressed from a global perspective. We employed a physical analogy for the actual meshing problem that allowed us to construct a global mathematical description of the problem. The physical analogy that we substituted for the meshing problem was that of minimizing the electrical potential for a system of charged particles within a charged domain (the particles could represent either the nodes or the elements). Our work in two dimensions showed that very reasonable meshes can be obtained by using this method with a mesh closure rate of 99% of geometries tested. Furthermore, the method is directly extendible to 3-D domains.

The goal of this work is to develop the technology in three dimensions to an adequate point, then pass it to the meshing groups to complete the implementation. To do this we need to transfer our understanding of this process for 2-D problems to the 2-D problem. This involves understanding how to describe and place particles in three dimensions and how to establish connectivity and achieve mesh-density transitions.

We focused on maturing the 2-D meshing work and starting the extension of the technique in three dimensions. We rewrote the 2-D prototype code in C++ and integrated it with CoMeT to produce a more production-like code. This provided a more efficient environment for discovery and code testing. With improved hole-closing algorithms and reformulation of the objective function, the scheme is currently able to close 99% of the tested geometries without intervention. We tested both convex and concave geometries. We also implemented a mathematical combinatorial approach to perform the particle connectivity step, and it performed quite successfully. This provides another scheme to perform the difficult connectivity step and is believed to be more robust and more easily extendible in three dimensions.

We are prototyping the scheme for meshing 3-D geometries. Although we could not spend much time in developing the 3-D code, we met our milestones, formulated an initial functional, and completed the particle description. Simple cubes can be successfully meshed with hexagonal duals. The meshing of more difficult geometries may require reworking the functional, which we are currently investigating.

Publications

Refereed

Wolfenbarger, P., J. Jung, C. Dohrmann, W. Witkowski, M. Panthaki, and W. Gerstle. 1998. "A Global Minimization–Based, Automatic Quadrilateral Meshing Algorithm." *Proc. 7th Internat. Meshing Roundtable '98* **1** (Dearborn, MI, 26 October): 1.

3510.590

Investigation of the Impact of Cleaning on Adhesive Bond and the Process Implications

J. A. Emerson, E. D. Reedy, Jr., J. G. Curro, E. P. Lopez

Surface cleaning is the most common process step in DOE manufacturing operations—approximately 75% of AlliedSignal/Federal Manufacturing & Technologies' (AS/FM&Ts') critical process steps for weapons manufacture involve surface cleaning or preparation. We do not understand the link between a successful adhesive bond and the surface clean performed prior to adhesion. When qualifying a new solvent for weapons manufacture, the cleaning engineer must rely on cumbersome laboratory tests, which are expensive, repetitious, and time-consuming. For many years, the cleaning community has called for an understanding of "how clean is clean?" Very little work has been done in this area since it requires a fundamental understanding of the process following the clean. This project, applying Sandia's computer-modeling expertise, fracture mechanics understanding, and cleaning experience, is truly innovative in that we are addressing the issue: "How do we achieve a good adhesive bond?" Modeling has not been commonly used to deal with cleaning processes in the past. Understanding the link between surface preparation and adhesion would result in reduced cleaning development time and testing, improved bonds, and improved manufacturability, and may also result in an understanding that leads to improved aging. This capability can ultimately be applied to agile manufacturing tools. This project will help advance product realization for encapsulated components. Developing a validated model for cleaning and surface preparation in adhesive bonding, coating, encapsulation, or painting processes would complete Sandia's capability for a process that ensures efficient, low-cost production of small lots.

We are developing tools, involving the convergence of several expert areas across Sandia, that allow the robust manufacture of bonded structures. These tools include models and test techniques that can be applied to adhesively bonded components (structural joints, weapon subassemblies) and to encapsulated components (neutron generators, electronic packaging). By establishing a fundamental understanding of the effect of known contaminants on the bond interface for both adhesives and encapsulants, we will enable the manufacturing complex to make it easier for a cleaning engineer to apply this technology to weapons development, and make the work of private industry easier and more efficient. The first year of this project had specific requirements: develop fracture-test methodology, characterize contamination, and develop modeling techniques. The second year built on these requirements by utilizing the methods to address the issue of gaining an *a priori* understanding of cleaning.

A simulation modeling technique, Polymer Reference Interaction Site Model applied near wall (Wall PRISM), provided the capability to include contaminants on the surface. The process requires a molecular description of polymer and contaminants as input, and the results are critically dependent on its accuracy. We performed preliminary calculations on the effect of contamination for 1% ethanol contamination on the structure of a silicone adhesive near a substrate. This change in the PDMS (polydimethylsiloxane) structure leads to approximately an 8% reduction in the work of adhesion.

We based repeatable coatings and quantitative analysis of the surface for deposition of controlled amounts of contamination on three deposition methods. Hexadecane is less difficult to model, whereas mineral oil represents a typical contaminant used for machining. We varied deposition times in a closed environment for different times and temperatures. Time-of-flight mass spectrometry (TOF-MS) determined the uniformity and thickness of the contaminant deposited. The contaminant was not distributed uniformly, and it took approximately 48 hours for the contaminant to saturate, or come to equilibrium. The film thickness for hexadecane after 48 hours (TOF-MS) is approximately 15–20[3] (1 monolayer). Because we performed the analysis in a high vacuum, the contaminant may be partially volatized during analysis. We analyzed sputtered aluminum (Al) glass slides after 48-hour exposure to hexadecane in a closed environment and dipping into hexadecane followed by blowing the visible film off. Atomic force microscopy (AFM) images for the 48-hour hexadecane exposure indicated that the contaminant deposition was in the form of islands or puddles; i.e., the film was not continuous. This discontinuous film was further supported through contact-angle hysteresis measurements. The hexadecane coating was discontinuous.

We determined the effect of the cleaning process used on interface toughness by measuring the toughness of an Al/epoxy interface. The toughness using an asymmetric double cantilever beam (ADCB) specimen with a Brulin-cleaned Al surface is significantly greater than that with a trichloroethane (TCE)-cleaned Al surface (~ 50% greater). Because Brulin is an alkaline cleaner, etching on the microscopic level of Al may play a role in bond toughness.

The sensitivity of measured fracture toughness to various test conditions ensured reliability of the measurement. Interfacial toughness (measured using ADCB sample) depends on strong function of surface roughness; increasing by a factor of five, the surface roughness increases from 1 to 5 microns. Interface corner toughness (butt joint) is also strongly dependent on surface roughness. Surface roughening is a common technique used by adhesion experts to improve the chances of achieving good adhesion. We also investigated the effect of bond thickness on interfacial toughness. The dependence of butt joint strength on bond thickness is predictable, and the interface corner toughness is independent of bond thickness.

We determined the work of adhesion value for silicone/silicone interface by a contact mechanics technique known as the JKR (Johnson, Kendall, Roberts) method. These values compare within experimental error with recent theory and other experimental techniques. The interaction between silicone and a clean stainless-steel surface shows a dependence on surface roughness and chemical interaction. We are synthesizing new silicones to study this effect in more detail.

Publications

Refereed

Curro, J. G., J. D. Weinhold, J. D. McCoy, and A. Yethiraj. 1998. "The Structure of Amorphous Polymers Near Surfaces: Athermal Systems Computational and Theoretical." *Polymer Sci.* **8**: 159.

Reedy, Jr., E. D., and T. R. Guess. 1998. "Interface Corner Failure Analysis of Joint Strength: Effect of Adherent Stiffness." *Internat. J. Fracture*, accepted.

Other

Emerson, J. A., E. O'Toole, D. Zamora, and B. Poon. 1998. "Comparison of Three Works of Adhesion Measurements." *Proc. 21st Ann. Mtg. of the Adhesion Soc.* (Savannah, GA, 22–25 February): 238–239.

Reedy, Jr., E. D., and T. R. Guess. 1998. "Use of Interface Corner Stress Intensity Factors to Predict the Failure of Butt Joints." *Proc. 21st Ann. Mtg. of the Adhesion Soc.* (Savannah, GA, 22–25 February): 192–193.

3510.580

Application of Parallel Mechanism Technology to Manufacturing

L. F. Bieg, V. De Sapio, D. M. Kozlowski, D. L. Plymale, G. L. Benavides, D. J. Schmitt, C. King

The goal of this project is to apply human-like motion to the fabrication of Sandia components. Currently, Defense Program (DP) products are realized by processes and tools based on orthogonal motion. However, the constraints of orthogonal systems have become more apparent as component designs increased in complexity. In an orthogonal world, the fabrication of complex parts requires multiple manufacturing processes and setups, resulting in numerous fixture transitions. Aside from cost, time, and quality disadvantages, orthogonal manufacturing processes also lead to orthogonal designs. Freeing designers from this bias will allow new and innovative designs to be developed based purely on component and assembly functionality.

The overall challenge is to develop, control, and apply human-like motion to manufacturing. Non-orthogonal parallel motion (NOPM) devices must be developed and evaluated. We evaluated the scalability and accessibility of NOPM devices for fabrication, microassembly, and micropackaging applications. The power of this paradigm cuts across the spectrum of Sandia's design and fabrication requirements, and applies equally well to the micro and macro environments.

Because of this project, Sandia has become the U.S. leader in NOPM technology development, employing a number of mechanisms to evaluate future applications. We will apply two hexapods to evaluate metal-removal applications, a MicroDexterity System for automated assembly, a prototype Rotopod for research evaluation, and other NOPM-like devices for workpiece holding and alignment.

(1) *Evaluated and selected micro and macro candidate applications*. We emphasized application areas of high impact to Sandia's missions. The candidate areas are micro-assembly, micro-inspection, coordinate measurement, automated assembly, automated joining, and various forms of metal removal. We performed our evaluation by using the commercially available NOPM systems, the Sandia-fabricated hardware, and the kinematic and dynamic models previously developed at Sandia, National Institute of Standards (NIST), and in industry. Sandia alone had four platforms available for applications development by the end of FY98.

(2) *Developed and applied seamless process to NOPM prototype device*. We have the capability to seamlessly move from a computer-aided design (CAD) model to an NOPM application. The tool paths for machining are automatically generated with enhanced algorithms, which take into account the multiple degree-of-freedom (DOF) control possible with NOPM devices. We can select individual cutting tools for each part feature, and calculate feeds and speeds based on tool geometry, material selection, and a cutting-science database. Software graphically depicts the fabrication process to pre-verify the actual manufacturing process.

(3) *Designed and built an NOPM device*. We performed the design of this device using the kinematic and dynamic analysis tools previously developed, as well as the information learned from the evaluation of the previously constructed prototype. Our NOPM device, called a Rotopod, is fully motorized and can be moved in six-DOF space under PC-computer control, using U.S.-made motion-control technology. Sandia also developed the motion-control software for a commercially available NOPM device from MicroDexterity Systems, and evaluated the pros and cons of both mechanisms.

(4) *Developed industrial and university partnerships and user facilities*. Sandia is a user's facility for performing research to complement and enhance our work.

(5) *Demonstrated and quantified benefits of micro and macro applications*. Based on test results, we compared the performance of Sandia NOPM prototypes to commercially available systems. We demonstrated on the existing NOPM hardware specific applications that established the benefits of this technology. This project resulted in five individual patent applications. In support of quantifying benefits of NOPM devices over orthogonal systems, we actively interacted with NOPM builders, users, and researchers on a national and international level. This included hosting the 4th Hexapod Users Group Meeting at Sandia.

3510.610

Standard Cells for Microelectromechanical Systems (MEMS)

M. S. Rodgers, J. J. Allen, M. P. De Boer, V. R. Yarberry

Microelectromechanical systems (MEMS) design tends to take place by a trial-and-error approach resulting in the necessity for several iterated fabrication runs before working MEMS devices are achieved. This precludes the devices from being integrated together in a single fabrication run or, even more importantly, into a single monolithically integrated system design (micromachines with microelectronics). Typically, each design starts from scratch since no standard part definitions exist. This lack of standardization and compatibility in both manufacturing processes and device designs is a major factor preventing MEMS from attaining the same level of success as that achieved by microelectronics. The focus of this project effort is to amass a set of verified, useful, diverse, standardized MEMS parts that can all be fabricated in the same process technology (Sandia's multilevel polysilicon surface-micromachining process). These parts will provide an appropriate range of actuation, sensing, energy storage, and

functionality. By creating a set of diverse modules that can be fabricated together on the same chip, we will create a library of standard cells similar to those common in the highly successful integrated circuit (IC) manufacturing industry. We will distribute the standard cells on a compact disc (CD) that will include the drawing, description, photo, and video (where appropriate) of each standard cell along with other information and tools relevant to designing systems in Sandia's multilevel MEMS technologies.

Sandia's internal customers used several of the first-generation components for developing test vehicles to study friction, tribology, and reliability, and to successfully demonstrate advanced weapons surety concepts. We continued to refine these first-generation standard cells for ease of use, functionality, and robustness, based on input from the early Sandia customers and evaluation of multiple runs. One of the actuation systems that resulted from this work was featured in the news briefs of several magazines, including *Mechanical Engineering*, *Popular Science*, *Popular Mechanics*, and *Discover*.

The most significant accomplishment is that we implemented on CD a core set of standard components and a method for checking for proper usage and/or modification of these components via the Internet from remote customer sites, along with our short-course materials. We designed these tools to fully integrate with the customers' existing layout software. In addition to the computer-aided design (CAD) definition of each component, the software includes a description, scanning electron microscope image, and in some cases a video clip of the part in operation. This CD is now in its second beta undergoing evaluation by graduate students at the University of California at Berkeley and the University of Wisconsin.

We also designed and submitted for fabrication many other candidates for the standard parts library. Some of these have already emerged.

Publications

Refereed

Allen, J. J., and H. K. Schriner. 1998. "Micromachine Wedge Stepping Motor." *Proc. 1998 ASME Internat. Mechanical Engin. Congress and Expositions*, accepted.

Rodgers, M. S., and J. J. Sniegowski. 1998. "Five-Level Polysilicon Surface-Micromachining Technology: Application to Complex Mechanical Systems." *Tech. Digest Solid-State Sensor and Actuator Workshop* (Hilton Head Island, SC, 10 June): 144–149.

Rodgers, M. S., J. J. Sniegowski, S. L. Miller, and G. F. LaVigne. 1998. "Designing and Operation of Electrostatically Driven Microengines." *Proc. 44th Internat. Instrumentation Symp.* (Reno, NV, 5 May): 56–65.

3510.660

Scripting for Video Inspection

J. T. Feddema, C. Q. Little, J. J. Carlson

Sandia's primary mission of ensuring a safe, secure, and reliable nuclear deterrent depends critically on the reliability of deployed components. Visual inspection of these components serves as the last chance to prevent a defective part from entering the stockpile. Most of these parts are subjected to manual visual inspection, which raises questions of consistency and accuracy. Even state-of-the-art commercial visual inspection systems are inadequate, because they require skilled engineers to artfully adjust camera parameters, lens settings, lighting, and processing, which is prohibitively expensive for small-lot manufacturing. In this project, we fill this research gap in visual inspection by developing technology to automatically inspect parts with a video camera. Using a computer-aided design (CAD) model of the part, our system will automatically determine camera locations, lens settings, and illumination to make good images. We refer to this combination of imaging parameters as a script, *and it will result in a movie of the part highlighting the sections that need to be inspected. These images will be automatically compared to CAD renderings of the part, with differences marked as defects. We will enhance the system with specialized inspection routines that cannot be accomplished with the CAD model. The result of this work will be a system for automatically inspecting parts such as neutron generators, printed wiring boards, semiconductor wafers, and machined parts.*

We reordered several of the tasks to assess the feasibility of the inspection routines. Instead of automatically generating inspection paths from CAD data, we developed a robotic inspection workcell and inspection routines for the neutron-generator header and frame. Using image differencing, we successfully showed that we can find voids in the braze fillets as well as braze splatter on the ceramic insulators. The image inspection results along with electronic images of the subassemblies can be transferred to the project database via the Internet. We will combine these image inspection results with other information of the brazing process (e.g., the furnace temperature profiles) to aid the engineers who are responsible for the design and manufacturing of the subassemblies. We archived the stored images for future comparison when the parts are tested.

Plans are currently under way to put a production version of this system in Sandia's neutron-generator production facility. The initial part to be inspected is the screen; with future development, the same workcell will inspect the header, source, and frame subassemblies.

3510.620

Laser Wire Deposition for Fully Dense Shapes

L. D. Harwell, D. O. MacCallum, M. T. Ensz, T. E. Buchheit, M. L. Griffith, V. Tikare

The purpose of this project is to characterize the laser wire deposition process (WireFeed) and develop the technology to fabricate complex near-net shapes directly from a computer-aided design (CAD) solid model. This additive process will fabricate solid metal parts directly from the software representation, thereby saving numerous steps and time compared to current methods and technologies. The initial intent of this work is to understand the processing conditions (laser power, wire feed rate, traverse velocity) and the materials properties, and to model the solidification behavior of the weld pool in the WireFeed process. By understanding the experimental and theoretical aspects for laser wire deposition, it will be possible to fabricate metal parts with appropriate material properties.

Secondly, Sandia's goal is to develop a system that rapidly fabricates accurate, complex parts. We will develop software to translate CAD data into process commands for complex geometry fabrication. We will determine procedures to selectively deposit material for controlled geometry fabrication. Development of this process will allow engineers to produce functional parts of their designs directly from CAD files. The turnaround time will be hours instead of days, and days instead of months. With reduced turnaround time, more time can be spent on the product design phase to ensure that the best component design is achieved. Maturation of this technology will revolutionize the way the world produces structural components.

At the beginning of the fiscal year, it became apparent that the current hardware design of the WireFeed system would not allow for complex geometry fabrication. This is because the laser beam is brought perpendicular to the substrate, and the wire is fed from the side. This configuration does not maintain the same wire insertion direction with respect to the scanning direction. We determined a novel (patent submitted) engineering concept to allow for complex geometry fabrication. The new design splits the laser beam into three beams that reconverge to one focal point, and the wire is fed into the middle of the weld pool (e.g., perpendicular to the substrate). We completed development of the new system, including design, fabrication, and assembly, in approximately 8 months. This produced a system with full 360-degree XY plane contouring capability. We completed initial testing of the system and fabricated simple cylindrical shapes.

We extended the predictive model to a 3-D model to understand microstructural evolution in the WireFeed process. The model predicts the relative 3-D grain size and shape. We are investigating potential coarsening of microstructures by subsequent layer deposition. This model also incorporates a new thermal weld pool temperature model for rastering the laser beam. We developed the weld pool temperature model for understanding laser metal deposition behavior (e.g., laser-engineered net shaping [LENS™], WireFeed). We have begun initial work to obtain experimental thermal data, near and far from the weld pool. We accomplish this by using an infrared camera focused on the part. Current, qualitative measurements reveal large thermal trails during fabrication. We will incorporate these data into the weld pool and microstructural models.

Publications

Refereed

Griffith, M. L., L. D. Harwell, D. L. Greene, J. A. Romero, T. E. Buchheit, T. B. Crenshaw, and V. Tikare. 1998. "Materials and Properties of Components Formed Using the 3DWire Process." *Advanced Materials and Processing, Proc. 3rd Pacific Rim Internat. Conf. on Adv. Mater. and Processing* **I** (Honolulu, HI, 12–16 June): 3074.

Other

Griffith, M. L., L. D. Harwell, D. L. Greene, J. A. Romero, T. E. Buchheit, T. B. Crenshaw, and V. Tikare. 1998. "Free-Form Fabrication of Metallic Components Using the WireFeed Process." Paper presented to the TMS Annual Meeting, San Antonio, TX, 16–19 February.

Tikare, V., M. L. Griffith, L. D. Harwell, and M. E. Schlienger. 1998. "Simulation of the Effect of Variable Temperature History on Three-Dimensional Grain Growth During WireFeed Processing." Paper presented to the TMS Annual Meeting, San Antonio, TX, 16–19 February.

3510.630

High-Throughput Dry Processes for Large-Area Devices

D. S. Ruby, B. L. Silva, C. I. H. Ashby, P. A. Miller, R. J. Buss, D. J. Rieger, P. Yang, G. A. Hebner

The goal of this work is to develop guidelines for high-throughput dry processes that can effectively replace wet processes used in manufacturing of large-area devices and/or batches of moderate-area devices. Wet processes generally increase worker exposure to toxic and hazardous chemicals and tend to generate large volumes of liquid hazardous waste. Successful development of high-throughput dry processing could eliminate much of the waste stream while minimizing worker exposure. This interdisciplinary project utilizes Sandia's expertise in photovoltaics, plasma processing, sensor–based controls, and process modeling to develop environmentally benign processes that can reduce costs, improve product performance, and shorten product realization times. We will use large-area commercial silicon solar cells as the test vehicle in this program. We will develop a sequence of dry processes for selective etching of the emitter, defect passivation, and deposition of the antireflection coating. Successful completion of this project will provide validated process models that can be used in a variety of applications for surface cleaning, selective etching, and thin-film deposition, which are necessary for reliable small-lot product realization systems for Defense Programs (DP). The models will provide guidance for development of the next generation of plasma reactors and new applications.

Langmuir probe and mass spectroscopy measurements have been performed in a SF_6 etching discharge to provide a database for understanding the chemical mechanisms and validating the model predictions. We measured the electron density, electron temperature, ion saturation current, ion density, and neutral radical density for a range of plasma conditions identified as optimum by a statistically designed multiparameter experiment on the solar cell etch and passivation processes. Our measurements show a large number of radical species as well as etch products.

Based on a survey of the literature, we proposed a chemical mechanism to model the SiH_4 / NH_3 deposition process and the SF_6 etch process. Comparison of the SF_6 etching model with experimental data for etching conditions shows similar trends for several of the dominant plasma radical species. However, in some cases the agreement is not very good, indicating that the preliminary chemical mechanisms incorporated into the models must be refined. We are currently reexamining the literature and our experiments to improve our models.

Empirical optimization of the SF_6 etch process using a new Plasmatherm reactor resulted in finding a set of parameters that resulted in better uniformity over larger areas and less surface damage than obtained previously. A three-step nitride deposition process was found to provide better surface passivation than a simple one-step deposition. We conducted a statistically designed multifactor experiment to find process parameters that would optimize surface passivation. Use of the optimum parameters resulted in a significant 7% increase in solar cell output power.

Publications

Other

Ruby, D. S., C. B. Fleddermann, M. Roy, and S. Narayanan. 1997. "Self-Aligned Selective-Emitter Plasma-Etchback and Passivation Process for Screen-Printed Silicon Solar Cells." *Solar Energy Mater. and Solar Cells* **48** (November): 255–260.

Ruby, D. S., P. Yang, S. Zaidi, S. Brueck, M. Roy, and S. Narayanan. 1998. "Improved Performance of Self-Aligned, Selective-Emitter Silicon Solar Cells." *Conf. Rec. of 2nd World Conf. on PV Energy Conversion* **1** (Vienna, Austria, July 6–10).

3510.640

Assuring High Reliability and Production Readiness in Low-Volume Manufacturing

S. V. Crowder, M. F. Martin, K. S. Marlman, E. W. Collins, J. T. Spooner, A. J. Johnson

Manufacturing philosophy in the nuclear weapons complex has shifted dramatically from the regular production and delivery of significant orders to infrequent small orders. New weapons components are produced less frequently and in smaller quantities. The challenge is to build much smaller lot sizes while maintaining the same high-reliability standards. For Sandia to meet this challenge, specific areas need more attention, including process development and characterization with small-sample experiments, low-volume statistical process monitoring and control, and small-lot reliability, given few actual performance tests of the product. The first year of the work focused primarily on the development of methods for low-volume statistical process control (SPC). We also began our study of small-sample design and repair of experiments. In the second year we completed the low-volume SPC study and applied the methodology to a battery cathode data set as well as neutron-tube performance data. We also completed the study of small-sample design and repair of experiments and applied the methodology to the repair of an ion-source experiment. In the third year of the study we focused on a methodology for small-lot reliability assessment and applied the methodology to the production of neutron tubes.

This year's efforts focused primarily in the areas of small-sample design of experiment and low-volume SPC. We also proposed a new reliability assessment methodology.

We developed a design optimality criterion for constructing and repairing small-sample experiments. The design optimality approach uses a metric called *maximum prediction variance* (MPV), a quantitative measure of the amount of information contained in an experiment. The metric can be used to appropriately size an experiment. This approach leads to experiment plans that are often much smaller than traditional experiment plans, so the technique is ideal for small-lot production environments, often resulting in great cost savings. We identified a statistical software package, STATISTICA, to construct these nonstandard designs and used the approach to repair a small-sample ion-source experiment.

The second major accomplishment was in the area of low-volume SPC. We completed our research into sample size requirements for the SPC algorithm that we developed. We were able to show that the algorithm can be applied to as few as 25–50 samples, compared to 100–200 samples recommended for traditional SPC. We wrote the statistical software required to implement the algorithm in FORTRAN, C, and MATLAB code. We applied the technique to battery-cathode data as well as neutron-tube performance data.

Publications

Refereed

Crowder, S. V., and L. Eshleman. 1998. "Small-Sample Properties of an Adaptive Filter with Application to Low-Volume Statistical Process Control." *J. Quality Technol.*, submitted.

3510.670

Advanced Machining Processes for Microfabrication

G. L. Benavides, A. N. Campbell, B. L. Doyle, P. Yang, D. P. Adams, D. L. Plymale

An important product realization goal for Sandia is to reduce the volume of weapon components by 50%. Sandia is a national leader in microfabrication technologies such as silicon–based microelectromechanical systems (MEMS) and electroformable metal–based LIGA (German for lithography, electroforming, molding). However, there are micromachining technology voids that need to be filled to meet the volume reduction goal. Sandia must attain capabilities unavailable through LIGA, i.e., to fabricate subminiature parts from nonelectroformable metals or ceramics and to micromachine nonplanar features. We will augment our microfabrication technologies by researching novel applications of excimer laser and focused ion beam (FIB) machines. The process of micromachining by material removal is new to both Sandia and industry and, as such, presents opportunities for the creation of intellectual property.

We will use the Sandia FIB to fabricate microsize features in desirable materials and to fabricate steel microtools for use in conventional processes such as drilling, milling, and sinker electro-discharge machining (EDM). The FIB beam width of 100 nanometers can create 0.5-micron-size features in high-strength/high-temperature metals and ceramics. We plan to collaborate with Louisiana Tech University (LTU) on FIB/micromachining research.

We will use the excimer laser to fabricate microsize features in materials including ceramics, magnetic materials, and polymers. This ultraviolet (UV) laser ablation process removes material without sample melting, providing the precision essential to fabricate high-aspect-ratio microstructures. We directly machine thin sheet materials into 3-D structures. Unlike LIGA, this process will not require a synchrotron, wet chemical process, or planarization.

We accomplished the following in FY98:

(1) Prepared the excimer laser for the micromachining of materials.

(2) Prepared the FIB machine for micromachining.

(3) Identified microtools for fabrication.

(4) Collaborated with LTU on the development of microtools.

(5) Fabricated the microtools identified above using an ion source.

(6) Machined holes in polymers and ceramics using the excimer laser.

(7) Characterized microhole dimensions and surface quality.

We made two major breakthroughs:

(1) Acquired an FIB machine through our collaboration with LTU, which gives us a micromachining capability we did not have.

(2) Successfully machined acrylic, aluminum, and brass with a .001-inch-diameter end mill. This is the first time that a .001-inch hexagon end mill has been used to machine metal. Prior to using the .001-inch end mill, the smallest end mill used at Sandia was .005-inch diameter.

We also purchased a new micro-EDM. Because of the success of micromilling with the .001-inch end mill, we will fabricate channels for the Micro-Chem-Lab-on-a-Chip technology. There is interest in our capability to micromachine microholes with our excimer laser.

3510.680

Fusion of Product and Process Data Using Real-Time Streaming Visualization

V. De Sapio, G. K. Hicken, J. M. Baldwin, R. G. Hillaire, T. R. Walker, D. A. Sheaffer, Jr., C. M. Leonard, Jr.

This work will involve the use of socket input/output (I/O) to communicate in-process data from a machine tool, welding system, or coordinate measuring machine (CMM) in real-time to a simulation package. For example, Sandia will send machining data streams associated with force or acoustic emission sensors, as well as positional data, in process to a simulation software package. We will fuse these data streams in real-time to part geometry that constantly changes as material is removed. In addition to sensor data streams, process and machine models running in software external to the main simulation engine will be able to feed model–based data in real time to the simulation environment. The process models will address the physics of the specific unit process. The machine models will address the kinematic behavior of the machine(s) involved in the process. We will capture the resulting dynamic process overlay and export the motion paths as parametric kinematic data. We will then disseminate the VRML 2.0 data files representing this information via an electronic traveler (PRIME) client. We are proposing an additional approach to client-side access to the simulations and process data representations. This uses object-oriented behavioral components called Simlets, as well as a number of existing technologies including Open Inventor/VRML (virtual reality modeling language) for graphics rendering, Java Applets, and ActiveX.

We developed file parsers to process raw data from both inspection reports and milling machine and welder data-acquisition systems.

We developed custom applications using the Express development environment for visualization applications. The metrology application incorporates custom file readers for importing the metrology data files (.met) and the feature files (.fet). The milling and welding applications incorporate custom file readers for importing the scalar hyperpoint data files (.shd). We incorporated a DXF import module and a VRML export module into all of the process visualization applications.

We developed ActiveX Web-browser components for the metrology, milling, and welding visualization applications.

A Web interface is complete for the metrology application. We wrote CGI (common gateway interface) PERL scripts to automate the retrieval and parsing of raw inspection data. We are writing the hypertext markup language (HTML) templates and CGI scripts for all applications to automate the retrieval of overlaid process-model data (in VRML format) via the Web.

We will complete the integration of the Web–based process visualization front end with the PRIME electronic traveler. This is still in process but will be completed concurrently with early second-year activities.

3510.690

Advanced Production Planning Models

D. A. Jones, W. E. Hart, C. A. Phillips

Advanced production planning and scheduling tools are vital for the Nuclear Weapons Complex (NWC) to satisfy its mission with increasingly constrained resources. In addition, stockpile life-extension program managers and weapons designers need to be able to see how their new designs will affect production, especially resource requirements and logistics. To address these issues, Sandia is developing advanced production planning and scheduling tools focused on task–based operations at NWC sites; i.e., operations that require a series of tasks to be performed in a particular sequence, and where various sets of tasks compete for common resources. The underlying mathematical problem addressed in this project is extremely complicated, and our objective is to develop effective heuristics; i.e., methods to obtain approximately optimal plans/schedules quickly. Our technical approach involves four major steps: (1) identify ways to model important site-specific elements of production planning and scheduling, (2) develop a mathematical formulation of enhanced planning/scheduling models, (3) develop exact solutions to planning/scheduling problems for several sets of test data to create benchmarks, and (4) develop effective heuristics for achieving rapid approximate solutions, and compare their performance to the exact solutions. The end product from this project will be a suite of solvers that will provide advanced production planning and scheduling capability for many different sites within the NWC.

We developed a highly innovative modeling approach for task–based production planning and scheduling problems. This formulation has direct application to planning of stockpile evaluation activities at Pantex, as well as future stockpile life-extension program activities.

The new formulation is an optimization model that uses only continuous variables, avoiding the use of integer variables. From a conceptual standpoint, three main features distinguish this formulation from previous approaches. First, its time periods can have variable lengths. This means that monthly (weekly or other) boundaries can be matched precisely. Second, the principal choice variables are the starting times for each task, rather than using a period index for a start time, as is done in integer programming approaches. Third, the assignment of tasks to resources (facilities and technicians) accurately reflects the character of feasible assignments at production facilities in the NWC.

Test results based on actual data are very encouraging that this new approach to task–based production scheduling will be a major breakthrough for large-scale, realistic scheduling problems in a variety of production settings. We created a fundamentally different way of viewing and formulating math programs for this class of problems, and we believe this approach (after further testing and development in conjunction with advanced computation on parallel computers) will be the basis for a new generation of advanced production planning and scheduling models.

Publications

Other

Kjeldgaard, E. A. 1998. “Advanced Production Planning Models.” Brochure, Sandia National Laboratories (12 December).

LIFE-CYCLE SYSTEMS ENGINEERING

Life-Cycle Systems Engineering studies trace the entire life cycle of a product, considering affordability, performance, design, testing, production, field operation and maintenance, and product retirement, and encourage development of modeling and simulation prototypes that support life-cycle studies. Studies may involve collaboration with other LDRD areas and with national security programs.

This activity comprises projects in five areas: (1) developing single systems that engineers at all stages of product development can use; (2) deepening the understanding of how production technology affects product performance, cost, and usefulness; (3) adding knowledge and capabilities to product development; (4) creating technologies that allow workers to focus on innovation by relieving them of activities that can be automated; and (5) developing innovative collaborative arrangements to create long-distance work environments as productive as those where all workers share the same site.

Any design or production system requires complete, realistic, easy-to-understand documentation so manufacturers can design and produce a consistent, high-quality product cost-effectively, but the cost of high-quality documentation is staggering, and the necessary skills are not always available. Sandia is developing automatic tools to help engineers develop and refine design concepts and generate information that others can use to produce the design and to incorporate design changes faster and more easily. The Internet is especially suited to sharing the graphical, multilayered design used with computer-aided design and engineering (CAD/CAE).

Sandia's work in automated multimedia document creation began with its award-winning assembly planning and visualization software tool called Archimedes. Engineers use Archimedes to automatically determine optimal assembly sequences for mechanical devices. Sandia's first multimedia tools automatically turned Archimedes' output into Web-ready multimedia documents that included movies of each assembly step. Sandia applied these document-creation techniques to both commercial and in-house robotic simulation software packages, letting engineers quickly turn simulations, from robots to entire factories, into Web-ready 3-D animations and movies.

Sandia now uses these tools to relay design simulations via the Internet to customers outside Sandia, and customers are spending less time and money traveling to Sandia while getting better answers more quickly and less expensively via the Internet.

THIS PAGE
INTENTIONALLY BLANK

3511.080

Enabling Human Skills with Cooperative Automation

D. J. Schmitt, T. S. Gladwell, R. J. Anderson

This project is developing the sensing and intelligent controls technologies required to create cooperative automated assistants. Sandia is doing this by developing workspace sensor systems to dynamically track moving objects such that an automated system can be continuously aware of the location of the human within the workspace. We are using data from the sensing systems to allow the automated system to not only safely co-exist with the human, but also to cooperate to perform tasks. This project is producing, for the first time, the ability of humans and automated systems to cooperate to perform tasks within the same workspace. The intent is to enable efficient task execution by simultaneously utilizing the best skills of the human and machine to perform a required task. This cooperative automation frees the human from mundane and hazardous tasks and allows the human to perform the more insightful operations such as task supervision. This technology will offer the potential for reducing personnel requirements in battlefield and battleship operations by providing cooperative automated assistants, and by allowing multiple cooperative systems to be directed by a single individual.

We are focusing on developing the sensor systems and control architectures required for human and robot interaction. Three modes of interaction are important: tracking, engagement, and guidance. *Tracking* involves dynamically following the location of a human as he approaches the robot's workspace. *Engagement* involves intersecting the workspace of the human and robot so that interaction can occur. *Guidance* involves the human physically directing the motion of the robot. We are developing a vision–based system for tracking, electromagnetic sensors for engagement, and a force sensor for guidance. We are now interfacing these sensor systems to a pedestal-style robot to demonstrate each of these interaction modes. The pedestal robot we chose has two separate computer controllers, which are providing flexibility in the control architecture development. One system uses the native controller and provides human/robot cooperation capabilities suitable to the large installed base of these robots. The other controller is a PC–based, open-architecture controller, and is providing the capability to utilize the SMART architecture developed at Sandia. SMART provides a more sophisticated and flexible control system that allows us to implement higher-level human/robot interactions, and provides a means to implement these behaviors on other automated systems. We implemented demonstrations of each of these capabilities. One demonstration uses the vision system to track and engage a human such that an object can be exchanged with the robot. This demonstration also includes a structured lighting system to map the location of critical objects in the workcell. The second demonstration shows the capability of the Polhemus sensor to finely resolve the location of a person's hand for more precise engagement. A third demonstration shows the use of the force sensor such that a person can guide the robot to a location for task execution.

The architecture for enabling the human/robot cooperative behavior in the vision–based demonstration utilizes a supervisory control computer to control data flow between the vision system and the robot. We defined a series of states that are based on the human's location within the monitored workspace (e.g., automatic motion, track human, engage human, inspect object, emergency stop). The supervisor monitors the incoming vision data, determines the state the robot should be in, and communicates the state and vision data to the robot. The robot interprets and acts on the communicated vision data differently based on the state. The supervisor ensures that the states are implemented in the proper order for a safe interaction. The robot's transition through different behavior states establishes a dialog between robot and human. When no humans are in proximity to a robot, the robot can operate at high speed along optimal paths. When a human approaches the workcell, the robot stops its current task, slows its speed, and responds to the human presence in a nonthreatening manner. For example, in a material hand-off operation, the robot may mirror the operator's position, tracking the operator's position across the workcell and approaching the operator only when the operator approaches the robot. Once the operator passes into a transition zone, the robot comes to a complete stop.

We reviewed the recent literature related to human and robot interactions. Trends in this research include studying and modeling human behavior such that the behavior can be emulated in automated systems, and co-manipulation of objects by a human and robot.

3511.010

Automatic Generation of Multimedia Documentation for Assembly Operations

M. J. McDonald

Realistic, easy-to-understand, and complete documentation greatly facilitates designing and manufacturing of consistent, high-quality products. This is especially true in Sandia's high-consequence, low-volume design and production environments. Unfortunately, document production costs often limit the amount of documentation produced. This project built new technologies to reduce those costs.

The World Wide Web provides effective solutions for efficiently distributing high-quality, multilayered graphical information typical in engineering. Importantly, Web movies have become more accessible than videos, and modern virtual reality modeling language (VRML) viewing software can now support many 3-D visualization needs.

A first step in reducing documentation costs is to harness computer-aided design (CAD) and Web technologies to efficiently produce the needed documents. This project first leveraged Sandia's automated assembly-planning technology, called Archimedes, to develop a software tool that converts CAD models of devices being manufactured into multimedia documents of the steps required to assemble the products. The project then developed translators that could produce digital movies and 3-D VRML animations from Sandia (Umbra) and commercial (Denebs Envision) simulation tools. Now, engineers can generate multimedia documents of assembly processes, robotic manufacturing processes, and small smart machine motions whenever they run a simulation.

The second step was to develop electronic document review mechanisms to integrate peer and customer review with Web-served digital documentation. This effort developed three multimedia feedback systems. Each system allows people to make context-sensitive comments about specific Web content and electronically ties the comments back to the Web content being referenced. The first ties comments to specific Web pages, the second ties the comments to specific frames of digital movies, and the third ties the comments to specific times and viewpoints within 3-D animations.

To validate the tools, this project tested these technologies against real-world applications in neutron-generator production and robotic system design. We found that the tools reduced multimedia documentation costs and provided effective support for reviewing Web reports, movies, and VRML animations.

We researched existing multimedia, assembly, and engineering documentation software tools and concluded that Web–based documentation approaches held the most promise as delivery tools. To better ground this work, we established relationships with potential multimedia assembly and engineering documentation authors at Sandia in the neutron-generator fabrication and tied development to their problems. We then prototyped example multimedia assembly documents and socialized the processes and results. We extended the Archimedes system to directly output Web-viewable movie files that we used in Web and Microsoft Word documents. These results led to a team effort to produce a second-generation prototype tied into the product data management (PDM) document control system. We developed a prototype extension to Archimedes to directly generate basic Web-viewable documentation including text, still graphics, and movies. We developed an addition, a VRML 1.0 (static model) translator for viewing Archimedes outputs. We established relationships with neutron-generator production personnel at Sandia and a related effort at Pantex. We published Archimedes and multimedia efforts in the form of Web–based reports and examples.

This work showed that multimedia documents had broad use in both production and engineering, and we identified the need to support a broader range of simulation and analytical tools. To address these issues, we identified and tested existing technologies, including modern hypertext markup language (HTML) editors, commercial CAD-to-movie and VRML 1.0 translators, imaging tools, and portable document format (PDF) documents for use in engineering documentation. At the same time, we found good static scene generation but a lack of development or research in animated VRML models.

Through this evaluation we identified that the then-emerging VRML 2.0 standard could support the 3-D graphic animation needs in engineering and production. By leveraging past graphic file translation work done at Sandia, and intimate knowledge of the in-core memory structure of two simulators, we developed in-core translators for one commercial (Denebs Envision) and one Sandia-developed (Umbra) simulator. We can run the resulting software works in the background to automatically generate animation information while running simulations. Later, we translate this information and save it into a VRML file that we can then run on any VRML viewer, publish it on a Web site, or e-mail it to a customer. In addition, we can run the file within Internet Explorer and in conjunction with a Java–based applet that we developed to provide VCR-like animation control.

We socialized these results and practices by installing and training engineers in its use and by applying the tools against systems-engineering projects, including one for automated radioactive source unpacking. In addition, we used materials generated early in this effort in collaboration with New Mexico Tech.

Through these applications, we identified the further need to tie detailed comments back to the specific Web pages, movie frames, or VRML animation viewpoints to which they referred. Unfortunately, the existing method for tying comments to Web views was by e-mailing Web pages or

screen copies of animations. While Internet discussion groups could provide appropriate distribution mechanisms, we needed better solutions.

To address these review needs, we developed three multimedia feedback systems. Each system allows people to make context-sensitive comments about specific Web content and electronically ties the comments back to the Web content being referenced. The first system ties comments to specific Web pages, the second system ties the comments to specific frames of digital movies, and the third ties the comments to specific times and viewpoints within 3-D animations.

The result of this work is a new approach for building documentation into the design process. These tools are already in use in a variety of projects and will be extended to meet the evolving opportunities of multimedia technologies.

Publications

Refereed

McDonald, M., E. Gottlieb, C. Slutter, and S. Gladwell. 1998. "Multimedia Feedback Systems for Robot Systems Engineering." *Proc. ANS 8th Topical on Robotics and Remote Systems*, accepted.

3511.020

Distributed Life-Cycle Models in Enterprise Simulations to Answer System Questions

M. M. Johnson, H. R. Ammerlahn, A. S. Yoshimura, T. D. Plantenga, E. K. Lemen

The goal of this project is to pull together an integrated Sandia systems story about enterprise modeling and simulation. This requires development of a distributed computing software framework that can integrate various Sandia planning models into a single discrete-event simulation. The framework must address special issues important to potential Sandia customers, including the definition of software interfaces, distributed operation on multiple heterogeneous platforms, enforcement of multilevel access restrictions that derive from differing user classes, and coordination of local planning/scheduling models into a unified enterprise-wide life-cycle simulation. The software framework and associated interfaces will be a general-purpose package suitable for many different customers.

The project will also construct a classified life-cycle model of the DOE nuclear weapons complex (NWC) and populate it with enough real information to demonstrate the capabilities of an enterprise simulation. A fully populated enterprise model will provide stockpile managers with an important tool for planning and decision analysis.

We completed a general-purpose, distributed, discrete-event simulation software package called IDES (Infrastructure for Distributed Enterprise Simulations). We wrote IDES in Java for platform independence and tested it on a variety of heterogeneous computer networks. The IDES framework follows a philosophy of open extensibility: Diverse participants in an enterprise simulation contribute their expertise through individual software "confederate models." Each confederate plans/simulates its portion of the enterprise through a simple application programming interface (API). IDES links the confederates into a consistent, unified, discrete-event simulation for answering enterprise system questions. The IDES framework also exports user inputs and outputs, authenticates database queries, coordinates multiple interactive users, and supports computational load-balancing across an arbitrary network of machines.

The simulation framework provides multilevel authentication through a novel, secure, computing environment developed under this project. We extended conventional role–based access control (RBAC) to provide a distributed implementation (D-RBAC). The D-RBAC model allows each confederate to control how much information is exported to each user logged into an enterprise simulation. A confederate submodel can participate privately (exporting only minimal transaction-level data), publicly (allowing external control of internal model parameters), or at any level in between. Confederates also determine their visual appearance to other enterprise participants through a general Java API. This API provides a high degree of flexibility to confederate designers, but integrates the output with a consistent look and feel to provide a friendly interface for all users.

IDES provides a test-bed and simple examples for simulation developers. The project also helped support creation of a detailed enterprise simulation of the DOE NWC called CoMPASS (Confederation of Models to Perform Assessments in Stockpile Stewardship). CoMPASS brings together stockpile surveillance databases and production planning models from Pantex, Y-12, AlliedSignal at Kansas City, Sandia, and other sources. Each of these is a confederate with specific security and authentication requirements addressed by the D-RBAC model. We wrapped and integrated confederate software models according to the IDES API. The IDES–based CoMPASS simulation will answer stockpile life-cycle questions from different perspectives, utilizing different confederate inputs. The prototype product has already been successful in developing related business for individual weapons system programs.

Publications

Refereed

Johnson, M. M., A. S. Yoshimura, and D. M. Nicol. 1997. "The IDES Framework: A Case Study in Development of a Parallel Discrete-Event Simulation System." *Proc. 1997 Winter Simulation Conf.* **1** (Atlanta, GA, December): 93–99.

3511.040

Immersive CAD

A. L. Ames, J. L. Brazee, E. A. Peña, C. Q. Little, D. Hickerson

Recent widespread acceptance of solid modeling in product realization is largely due to improved user interfaces. While these interfaces are sufficient for detailed design, they are proving inadequate for conceptual design. The "back-of-the-envelope" is still the concept modeler of choice. Current solid modelers require complete specification of product geometry, which is awkward in early stages of design. Engineers want to see, feel, and manipulate their designs, but are frustrated by overwhelming data complexity (the "hairball effect").

This project will develop a prototype immersive computer-aided design (CAD) environment. The work involves four fundamental concerns: (1) developing a set of interaction mechanisms that provide easy, natural product model editing, (2) providing a means for supporting design constraints, (3) managing the wealth of product information, and (4) dealing with the radical difference in time scales between rendering rates and solid modeler speeds to permit real-time model manipulation. Editing operations that work in multiple tightly coupled representations (design features, constraints, boundary representation, and facets) on a parallel architecture address performance requirements, while Sandia will use virtual reality (VR) techniques to address interface concerns. This work steps beyond any current VR CAD system by producing constrained feature–based boundary-representation solid models. This project has the potential to impact every Sandia project involving the design of mechanical parts and assemblies. The ability to more easily synthesize and visualize design concepts, without complete detailing, will encourage more concepts to be evaluated, yielding better product. Including analyzability and manufacturability constraints in the interface will deliver better products to market faster.

(1) We developed a mechanism for detecting topology change during solid-model editing operations using C-Space Toolkit and Gilbert's algorithm.

(2) We developed mechanisms for performing topology-invariant editing of solids. Such editing permits rotation, translation, and scaling of faces within the solid model with only very minimal local recomputation. The approach permits real-time editing.

(3) We demonstrated feature–based topology editing. Such editing permits topology-changing edits to be performed, but exacts a penalty similar to current CAD systems. Use of topology-change-detection algorithms minimizes impact of this algorithm to relatively infrequent occurrences.

(4) We partially developed algorithms for topology-changing operations. Fast topology changes are possible with minimal time penalty through the use of persistent data structures. We can minimize geometric operations again through the use of C-Space Toolkit distance computations. We showed it is possible for solid-modeling operations to occur in time proportional to the magnitude of the change, rather than in time proportional to the complexity of the entire model.

(5) We developed object selection and manipulation algorithms to permit immersive editing of solid objects.

(6) We demonstrated usefulness of this technology compared to legacy CAD systems and showed profound speed improvements.

Publications

Other

Ames, A. L., E. Peña, J. Brazee, and D. Hickerson. 1998. "Immersive CAD." Sandia Technical Report, in preparation.

3511.050

Automatic Planning of Life-Cycle Assembly Processes

T. L. Calton, G. A. Laguna, J. C. Trinkle, R. R. Peters, E. A. Mitchell, R. G. Brown

Sandia today expends more effort on upgrade and maintenance projects than on clean-slate designs. However, commercial computer-aided design (CAD) tools are better suited to initial product design. Computer-aided analysis, optimization, and visualization of life-cycle assembly processes based on the product CAD data can help ensure accuracy and reduce effort expended in planning these processes for existing products and provide design-for-lifecycle analysis for new designs. We will adapt and apply Sandia's automated assembly-planning and design-for-assembly capabilities to later life-cycle assembly processes of a system, including service, field repair, and upgrade. The system will support replacing one or several subassemblies, gaining access for inspections, and optimizing disassembly costs.

Automated simulation and analysis tools resulting from this project can provide expert advice to field personnel needing to (remotely) disassemble a terrorist device and can have significant impact in the reduction of physical mock-ups required for training personnel in maintenance operations and depot repair.

We made significant achievements in each of the work areas: (1) improvement in the Design for Lifecycle (DFLC) cost module, (2) research and development of specific optimization algorithms addressing both nondestructive and destructive (dis)assembly planning, (3) code efficiencies, (4) publications, and (5) business development.

• *Upgrades to DFLC module*. Last year we developed a prototype module that could calculate the cost, in dollars or other units, for remove-and-replace

assembly operations. This is a powerful tool for comparing costs of competing designs, upgrade versus new product. We expanded the capabilities to (1) include input from generic databases, (2) store and retrieve previously defined assembly, disassembly, and cost-analysis information simultaneously, and (3) allow the user to edit cost on the fly. Upgrades allow users to optimize sequences based on real dollars and time.

• *Automated disassembly R&D.* We made substantial progress in both nondestructive and destructive areas for automatically planning sequences. We added an optimizing algorithm for part-removal by implementing a special-purpose search strategy for partial disassembly tasks. The algorithm uses a simulated-annealing-like process to distill locally shortest disassembly plans from the longer plans provided by the general-purpose planner. This planner enables Archimedes to find optimal partial disassembly/service plans in a few minutes in most cases, for assemblies much larger than the 20–25-part limit that was the previous limit, and brings this kind of planning into the realm of possibility for assembling hundreds of parts.

In some applications, operations that destroy parts, such as cutting, tearing, or melting, are acceptable in disassembly. Destructive operations have complex and sometimes unpredictable geometric effects, but in many cases they are the most effective methods of disassembly. We are in the process of developing algorithms that can automatically identify assembly operations requiring destructive disassembly. We are currently incorporating additional manufacturing processes into the code.

We are presently working to extend the core planning capabilities to include compound linear remove-and-replace trajectories. However, due to the difficulties associated with both the geometric complexity and the planning complexity, we expect only minimal progress this year. The difficulties occur with the recognition of convergence for a series of linear movements that will allow a component to be removed. Since the number of interactions between any pair of parts (with reasonable complexity) is limited, the number of simple linear trajectories that need to be considered to determine whether one exists for removal of a particular part from an assembly is effectively finite. These interactions (simple linear trajectories) are understood, and the current Archimedes planner approximates the set of possible trajectories. However, for a given class of compound trajectories we need to formulate finite sets of equivalent trajectories so that it is not necessary to consider an infinite set of possibilities.

As a result of last year's data, translation capabilities, and the promise of an effective cost module, more than 35 companies have expressed interest in the life-cycle planning capabilities.

Publications

Refereed

Calton, T. L., R. G. Brown, and R. R. Peters. 1998. "Automated Analysis for Lifecycle Assembly Processes." *Proc. 2nd Internat. Conf. on Engin. Design and Automation* **1** (December) (Maui, HI, August): 1–10.

Calton, T. L., R. Jones, and R. Wilson. 1998. "On Constraints and Quality Measures in Assembly Planning." *IEEE Trans. on Robotics and Automation*, accepted.

Calton, T. L., R. R. Peters, and R. Jones. 1997. "Automated Assembly and Fixture Planning at Sandia National Laboratories." *Assembly Automation, Internat. J. Assembly Technol. and Management* **17** (November): 201–205.

Other

Calton, T. L. 1998. "Archimedes Consortium Workshop." Presentation to the Archimedes Consortium Workshop, Albuquerque, NM, 2–3 March.

Calton, T. L. 1998. "Automated Assembly Planning—The Archimedes Tool." Invited talk/demonstration to the International Tour of Hexapod Users, Albuquerque, NM, 19 June.

Calton, T. L. 1998. "Automated Assembly Planning—The Archimedes Tool." Invited talk to be presented to Redstone Arsenal, Huntsville, AL, 1999.

Calton, T. L. 1998. "Automated Assembly Planning—The Archimedes Tool." Invited talk to the Ford Expo, Detroit, MI, 3 November.

Calton, T. L. 1998. "Automated Assembly Planning—The Archimedes Tool." Paper presented to the Joint Unmanned Systems Technology Workshop, Panama City, FL, 22–23 September.

Calton, T. L. 1998. "Automated Assembly Planning—The Archimedes Tool." Presentation to meeting at Raytheon Systems Company, Tucson, AZ, 3 February.

Calton, T. L. 1998. "International Trip Report." Trip report on 1998 IEEE International Conference on Robotics and Automation (May).

Calton, T. L., R. E. Jones, M. McDonald, P. Bennett, B. Anderson, R. G. Brown, R. R. Peters, Y. Hwang, F. Oppel, R. Lafarge, and A. Ames. 1997. "Simulation and Off-line Programming at Sandia's Intelligent Systems and Robotics Center." *Proc. RIA Workshop* (Detroit, MI, 21–23 October).

3511.070

Analysis of Very Large Assemblies

R. G. Brown

Sandia's Archimedes automated assembly analysis system has now been applied successfully to several large industrial and weapon assemblies. While Archimedes represents the state-of-the-art in automated assembly-planning software, these applications show the limitations of the system and the need for extensive modifications to support practical analysis of assemblies with several hundred to a few thousand parts. We believe that there is substantial potential for enhancing Archimedes to routinely handle much larger models and/or to handle more modestly sized assemblies much faster. Such a mature assembly analysis capability is needed to support routine application to industrial assemblies that now overstress the system, such as full nuclear weapon assemblies or full-scale aerospace or military vehicles.

Two arenas in which Archimedes might prove to be of interest are that of automating shipboard maintenance tasks and that of battlefield-condition custom assembly of autonomous and teleoperated vehicular robots. In the case of automated shipboard maintenance tasks, Archimedes could be invaluable for evaluating the feasibility and efficiency of various designs for shipboard systems, relative to the cost and difficulty of automating maintenance and service tasks on those systems. In the case of battlefield robotic vehicles, again the evaluation of designs and design strategies could be quite valuable, as would the ability to generate multimedia training documentation for the soldiers working with the robots. Since the shipboard systems and likely the vehicular robots tend to be quite complex, Archimedes needs to be able to handle large systems quickly and efficiently.

We made significant progress in reducing all of the three main resources identified as barriers to application of the Archimedes assembly-planning system to very large assemblies: memory utilization, contact analysis computation time, and planning time. Furthermore, we added capabilities enabling the user to more quickly and easily interact with large assemblies, in terms of providing mating and manufacturing overrides, and assembly constraints. The user can now interact with an assembly at the subassembly level, establishing appropriate constraints and overrides, and have those constraints and overrides show up at the full assembly level. Additionally, the user was previously restricted to specifying mating and manufacturing overrides on single parts and pairs of parts. The user can now specify most mating and manufacturing overrides on larger sets of parts, making it faster to specify and modify those overrides, and also easier to keep track of them. We added faceting control to speed up certain aspects of analysis and playback.

3511.090

Cloud To CAD

A. L. Ames, P. G. Xavier, C. Q. Little

Sandia is developing algorithms that recognize engineering shapes from scanned data. The algorithms partition points into groups that represent engineering surfaces, trim and extend surfaces, and adjust representations to achieve model closure. The algorithms will integrate geometry from multiple views and suggest surfaces based on engineering expectations to account for occlusions. The result of this processing is a computer-aided design (CAD) solid model. This representation is suitable for a wider variety of applications than any other geometric representation.

The benefits of generating engineering representations of a scanned object include tremendous data compression and object reasoning. The shape of an object can be stored, transmitted, and reasoned about in an appropriate language (e.g., radius and height of a cylinder), rather than in the verbose terms of thousands of points. An object in the field can be compared to known designs in engineering terms. This reduces communication requirements for battlefield reconnaissance and surveillance.

All of our automatic engineering algorithms can be directly applied to the engineering representation of an acquired object in the following applications: identifying targets, analyzing a competitor's products, designing fixtures, planning operations for demilitarizing

old ordnance, and archiving the as-built geometry of a stockpile component.

(1) We evaluated commercial and academic approaches for importing scanned data into CAD as facets and curved surfaces. Such models are useful for visualization, but are insufficient for many important applications. They exhibit insufficient or extraneous topology and are typically expressed using inappropriate surface geometry. This search leads to the requirement of producing models in engineering terms, with minimally complex topology and geometry.

(2) We developed an algorithm that connects facets into a closed boundary representation model. The model thus produced is sufficient for performing Boolean operations, and for computation of volume and mass properties. This capability proved interesting to a commercial funding source.

(3) We developed routines for fitting planes, cylinders, spheres, and ellipsoids to raw cloud data, for previously segmented data and nonsegmented data. We can extend and trim surfaces to close holes in the model.

(4) We developed code to knit together overlapping surfaces from 3-D range data. We can combine surfaces from separate scans to form a more complete model.

(5) We began investigating methods for integrating multiple views into a single solid model. We considered and tested a sweep/Boolean approach; other approaches are under development.

3511.120

Feature Reduction of Geometric Solid Models for Analysis Tools

P. A. Watterberg, R. G. Brown

Sandia's goal is to facilitate task-specific simplification of solid geometric models for interaction with sensing, design, analysis, planning, and execution tools. We will design and implement algorithms that will streamline the design-to-analysis progression, thereby increasing the capabilities of Sandia's existing and analysis tools under development (e.g., Archimedes, CTH, and CUBIT applications, SANDROS applications) by eliminating complexity, which is unnecessary for specific applications. These algorithms will also provide support for the automatic creation of simplified geometric representations that would be appropriate for use with real-time planning and execution systems, such as might be used on autonomous insectoid or vehicular robots. Example simplifications include elimination of purely internal features from subassemblies in an assembly-planning scenario, eliminating small holes from an obstacle in a motion-planning scenario, and simplification or removal of complex fillets for fixturing analysis. We would also incorporate some ability to simplify and refine faceted models. Preliminary experiments indicate that these capabilities would enable our analysis tools to tackle problems an order-of-magnitude larger than they can currently handle and would greatly facilitate seamless integration of Sandia's many analysis tools with the variety of solid-modeling packages currently used both within the weapons complex and within U.S. industry. The ability to simplify geometric models is becoming vital, as it will become increasingly difficult for the tools used to plan manufacturing and service operations to handle the complexity of the modeling systems used to represent parts and assemblies. Thus, any design or execution code used to deal with large, complex geometries in either the manufacturing or the robotic vehicle realms would benefit from inclusion of this technology into its core.

• *Assessing specific user needs.* We carried on discussions with Sandians working on several projects making use of geometric solid models to assess simplification needs.

• *Prototype interactive viewing/interaction tool.* We built a Motif– and GL (SGI's graphical language)–based, mouse-driven viewing/visualization tool that allows a user to view an ACIS (Applications of Collectively Intelligent Systems, a geometry modeling package from Parametric Technologies Corporation) object dynamically, from multiple directions and magnitudes, and to interact with certain classes of geometric features using the mouse. We enhanced the viewing tool to highlight specific face types and allow the selection of a single face.

• *Faceted data.* We implemented stereolithography (STL) (faceted) to planar-ACIS-body conversion and cylindrical approximation detector. We can now replace many cylindrical surface approximations by an actual cylindrical surface.

We implemented several different feature-removal heuristics. We removed holes less than a specified size, slots and voids in planar surfaces, and chamfers and fillets. We applied these heuristics to several sample objects yielding mostly modest results. Some objects yielded dramatic results. Continued refinement of the algorithms should yield satisfactory results on most objects.

3511.110

Ergonomics in Life-Cycle Assembly Processes

T. L. Calton, T. S. Gladwell, J. C. Trinkle, R. J. Anderson, R. R. Peters

To meet the design-to-costs of Sandia's operation/sustainment, we need to identify, develop, and integrate improved, affordable manufacturing technologies that must allow for design and assembly at a lower cost with greater flexibility. All automated assembly-planning software tools assume that the individual components fly into their assembly positions; in reality they have to be moved with human hands rather than mechanical devices. Automatic assembly sequencing and visualization tools are valuable in determining the best (dis)assembly sequences/plans for weapons and other military and industrial system components and subassemblies, but without Human Factors and Figure Models (HFFMs) it is difficult to evaluate or visualize human interaction. HFFMs allow engineers to verify that maintenance is possible and see ways to make the design even better.

The goals of this project are in direct alignment with Sandia's Applications of Collectively Intelligent Systems (ACIS) business focus; war-fighting operations, both military logistics and automated ship functions, are areas of this project that can have significant impacts in reducing physical mock-ups required for training personnel in maintenance operations, reducing depot repair and logistical footprints, and providing repair-on-demand services. Already a cooperative research and development program initiated by the U.S. Army's Aviation Applied Technology Directorate (AATD), Sikorsky Aircraft Corporation conducted a nine-month study and identified our assembly planner as a technology that could help overcome critical barriers that are preventing airframes from being truly affordable. They concluded that to accurately verify assemblability/maintainability, it is necessary to include HFFMs.

Our first-year work included (1) surveying human modeling software, surveying the research in human factors and manufacturing, surveying human factors that are of interest to both the public and private communities, and selecting a commercially available human modeling software package, (2) integrating the human figure model with Sandia's collision-detection software system, (3) defining hand grasps for tools in the Archimedes Tool Library, (4) developing a routine to compute sweep volumes of the hand and tool(s), (5) implementing inverse kinematic routines for the human arm, (6) developing a motion planner for tool/hand and arm, and (7) implementing the first prototype. We focused on the geometric and kinematic representations of humans.

(1) *Surveys.* We completed a survey of commercially available human modeling software packages and identified two appropriate candidates: Jack by Transom and ErgoMan by Deneb. The direct integration of a noncommercial model increases the marketability of the resulting product by reducing the cost to a user. This activity will occur next year.

Each of these two commercial human figure models offers various levels of sophistication and features. Jack is differentiated from ErgoMan by a number of features. (a) *Stature models*: The models in Jack have much greater sophistication allowing scaling in stature and corpulence, with appropriate models of children as well as adults. They also maintain extensive demographics information for different cultures. (b) *Sophistication of model*: Jack is a 17-degree-of-freedom (DOF) torso model. (c) *Behavioral models*: Jack utilizes a PATNET (Parallel Transition Network) to define behavior changes. Jack can implement behaviors such as maintain balance while executing a given task, take a step forward if needed, keep one hand on a table while reaching, or keep his eyes on a target object at all times. ErgoMan has no such capability. Although the Jack model is anthropomorphically more appealing, we are currently developing algorithms based on the ErgoMan model and will use Jack next year.

We assimilated an extensive collection of research and development documents and Web sites identifying current trends in human figure modeling and on human factors. They range from scientific applications in ergonomics to gait analysis of athletes to physical rehabilitation.

(2) We selected Sandia's collision-detection software package, C-Space Toolkit (CSTK), for integration with both ErgoMan and Jack. CSTK provides a library that makes it easier to program motion-planning, simulation, robotics, and virtual reality codes using the configuration space abstrac-

tion. We integrated the CSTK with Deneb's Telegrip package.

(3) We defined hand grasps for tools in the Archimedes Tool Library. For each of those tools we defined a discrete set of standard positions, torques, and tool-offsets. The importance of establishing a variety of hand grasps for each tool is that a wider class of humans may be assessed, thus offering greater flexibility in the system.

(4) For each of the hand grasps defined, we predefined an upper bound on the space required to apply it; such volume represents a sufficient condition for tool applications. Next year we will implement a more flexible approach using the motion planner to find approach and removal paths for tool/hand and arm wielder.

(5) We implemented a 7-DOF inverse kinematic numerical solution and a straight-line motion planner to compute the arm joint angles that are necessary to move the tool and hand along a desired path.

(6) We developed a motion planner for tool/hand and arm. Here we planned to integrate SANDROS Path Planner and the SMART motion-planning algorithms. We canceled this activity because of scheduling conflicts.

(7) We began the initial phases of integration with the Archimedes Assembly Planner. Archimedes generated a script containing the sequence of (dis)assembly, tool selection, and trajectories of motions. We then used this script within IGRIP's simulation package to demonstrate the feasibility of the operations.

3511.130

System Surety Life-Cycle Engineering

R. A. Sarfaty, W. F. Young, R. L. Hutchinson, S. V. Spires, G. E. Rivord, S. Y. Goldsmith

System surety modeling currently lacks formalized overarching methods that scrutinize the engineering lifecycle commencing with abstraction and requirements-gathering. Object-oriented methodologies evolved to yield, inter alia, *encapsulation, polymorphism, and inheritance. However, surety's security and availability balance are obviated by the object-oriented Unified Method (UM) modeling technique dynamic model, particularly user authentication, confidentiality, and nonrepudiation. UM also lacks cost/risk information, assessed through consequence modeling, thereby failing to address the system as a whole.*

This research will expand each of UM's three models (object, dynamic, and functional) under systems engineering lifecycle, to include surety's components (reliability, user-authentication, data integrity, confidentiality, nonrepudiation) and incorporate the consequence model yielding bi-directional temporal cost analyses complemented with stochastic probabilistic risk assessment (PRA), or similar techniques.

The meta-modeling techniques (enhanced UM) would include object–based technology to ensure validation and cross-referencing among the four models. Surety objects would gain cognition through a dynamic knowledge-base such as secure network segments, encryption algorithms, and vulnerability assessments resulting from natural and anthropogenic threats. Most knowledge-base repositories are static, requiring triggers for updates; conversely, surety objects would augment their knowledge dynamically (emergent behavior) based on empirical outcomes, hence serving as the filters to coalesce surety elements into the system's lifecycle.

Subsequently a tool development effort would deliver a modeling engine with graphical interfaces accessible to a systems/surety engineer. The engine that transparently performs system constraint validations to the user facilitates the modeling process. This allows for systems surety modeling without the UM expert knowledge while yielding robust and valid system designs throughout the lifecycle.

• We conducted a fairly extensive investigation into the meta-modeling language and the three models of the Unified Modeling Language (UML).

• We established interdependencies among the object, dynamic, and consequence models.

• We formulated the information surety modeling methodology by selecting an example problem (i.e., the infrastructure surety problem).

• We began adding object model elements based on the UML to support the augmented methodology.

• We established a use-case scenario that will test the interdependencies of various critical infrastructures from a critical node perspective and assess the impact of each efferent and afferent link to the object model. The underlying meta-language is under development and uses both Boolean logic and predicate calculus. We created several nominal models to test the impact of classes on critical nodes (e.g., energy, capital, information) and defined the first-order rules to conduct forward transformations.

THIS PAGE
INTENTIONALLY BLANK

INFORMATION SYSTEMS

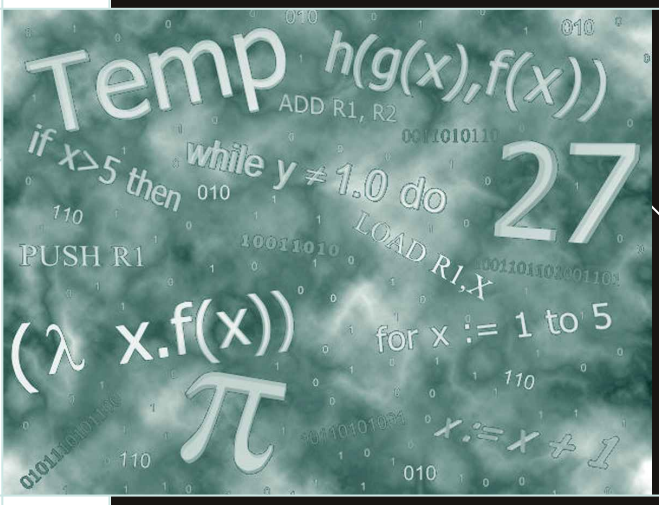

Information technology provides support to mission-critical Sandia activities. Information Systems research ensures that Sandia engineers and scientists can reduce time and costs associated with stockpile stewardship and other, related goals. Information surety is important to certifying critical infrastructures and mitigating emerging threats.

Desirable projects include developing secure, high-speed computer networks and location-insensitive computing, converting data to information, and developing the science of information.

Sandia is developing a technology to manage ambiguous data, called *mission surety*, that is critical for large-scale, real-time information systems. Military and defense applications must deal with ambiguous information and/or data with errors, creating the need for a technology that monitors decisions based on incomplete or inconsistent data. This concept allows researchers to design systems that compensate for erroneous decisions by enabling the algorithm to backtrack and recover when errors are detected. Before, systems would ignore the errors or eventually throw out the results and start over when it became clear the system had made a big mistake.

Mission surety technology allows the software to detect the wrong turn as soon as possible, figure out how far back the decision-making process has to go, return to that point, then continue down the correct path.

Benefits include greatly reducing development costs for certain information-intensive defense systems. In collaboration with the University of New Mexico, Sandia is adapting this technology to make less expensive, more accurate models of roads and other large components of the nation's infrastructures.

THIS PAGE
INTENTIONALLY BLANK

3512.160

Content–Based Search of Geometric Databases

P. G. Xavier, L. Meirans, T. R. Henry, L. P. Ray, Y. K. Hwang, R. A. Lafarge

Unlike textual or numerical data, geometry currently cannot be indexed or searched. Consequently, users of geometric data, such as designers, are at a considerable disadvantage when attempting to benefit from past experience. The impact of textual search systems such as SMART and Alta Vista hint at the potential if geometric data were to be successfully indexed and made available online. Sandia is developing algorithms and a prototype system for efficiently searching databases of 3-D geometric data by content.

Our main achievement is a prototype system for searching databases of geometric models such as AutoCAD. In addition to use in design, the underlying technology is suitable for autonomously identifying and estimating the pose of singulated objects that have been scanned to produce a renderable 3-D model. In addition, we completed software for automatically recognizing and characterizing holes and pockets in computer-assisted design (CAD) models. However, we finished this work too late to integrate it into our index-building code and interactive query system.

Our main achievement this year was a prototype system for searching databases of geometric models, such as AutoCAD. Mode of use is simple: The user loads a 3-D query object into the system, selects a view, and the system searches for objects in the database most similar in overall shape. Objects may be searched for based on any view, but some views may be nondistinguishing. While geometric models can be added to the database index incrementally, speed and storage space can be optimized in a global post-process. Models can be added after this post-processing, but if the domain sample is not adequate, speed and accuracy may be affected. In addition to use in design, the underlying technology is suitable for autonomously identifying and estimating the pose of singulated objects that have been scanned to produce a renderable 3-D model.

We tested the system with a database of over 200 CAD models, and it performed accurately and intuitively. Preliminary testing with 32 models and using randomly selected views yielded over 99% accuracy. We will include quantitative results based on the larger data set in the final report.

We also completed software for automatically recognizing and characterizing holes and pockets in CAD models, but we finished this work too late to integrate it into our index-building code and interactive query system.

Publications

Other

Xavier, P. G., L. P. Ray, T. R. Henry, R. A. Lafarge, and L. Meirans. 1998. "Content–Based Search on a Database of Geometric Models: Identifying Objects of Similar Shape." Sandia Technical Report SAND98-2684 (November). Sandia National Laboratories, Albuquerque, NM.

3512.190

Mission Surety for Large-Scale Real-Time Information Systems

S. J. Bespalko, H. L. Dison

This project will develop a new capability, termed mission surety, *that will enable the designers of large-scale, real-time systems to guarantee the correctness of results. Complexity of a system, and thus the propensity for error, is best characterized by the number of states the system can encounter. In general, the number of states grows exponentially as data sources are added. It is unlikely that current* ad hoc *methods of developing systems will be able to handle this increasing complexity.*

Two technologies will provide the basis for establishing mission surety. Over the past two years Sandia analyzed the problematical modules in an operational defense system and developed extensions to existing formal language techniques. These new methods provide a comprehensive and compact method for specifying, and subsequently automatically generating, error-free implementations.

We performed an analysis on ICADS (a Sandia-developed groundstation application) that concluded that the source of most errors in the development process resulted from the inadequacy of the design methodology.

We completed the second of three activities to demonstrate formal languages application. The algorithm is a new method of deducing which triggers are associated with a single event. This new algorithm makes no heuristic steps and is completely defined in terms of nonlinear optimization steps and formal language.

The project resulted in a new mission-critical algorithm for a deployed war-fighting system developed at Sandia. The algorithm beat two other algorithms based on heuristics, and also beat the current algorithm by making nearly two-orders-of-magnitude fewer errors. This demonstrates in no uncertain terms the power of rigorous design in mission-critical software.

Publications

Refereed

Bespalko, S. J., D. L. Sulsky, M. M. Wyman, and H. L. Dison. 1998. "A Nonlinear Correction for GPS Data." *Federal Research Record*, accepted.

Bespalko, S. J., D. L. Sulsky, M. M. Wyman, and H. L. Dison. 1998. "A Nonlinear Correction for GPS Data." *Proc. 1999 Winter Mtg. of the Transportation Res. Board* **1** (Washington, DC, 10 January 1999).

3512.170

Integrated Service Provisioning in an "IPv6 over ATM" Research Network

H. Y. Chen, D. W. Palmer, P. J. Robertson, J. A. Friesen, R. P. Tsang, J. M. Brandt

During the past few years the worldwide Internet has grown at a phenomenal rate, which has spurred the proposal of innovative network technologies to support the fast, efficient, and low-latency transport of a wide spectrum of multimedia traffic types. Existing network infrastructures have been plagued by their inability to provide for real-time application traffic, as well as their general lack of resources and resilience to congestion. This work addresses these issues by implementing a prototype high-speed network infrastructure consisting of Internet Protocol Version 6 (IPv6) on top of an asynchronous transfer mode (ATM) transport medium. Since ATM is connection-oriented while IP uses a connectionless paradigm, the efficient integration of IPv6 over ATM is especially challenging and has generated much interest in the research community. Sandia will, in collaboration with an industry partner, implement IPv6 over ATM using a unique approach that integrates IP over fast ATM hardware while still preserving IP's connectionless paradigm. We will achieve this by replacing ATM's control software with IP's routing code and by caching IP's forwarding decisions in ATM's virtual path identifier/virtual circuit identifier (VPI/VCI) translation tables. We will also develop prototype virtual reality (VR) and distributed-parallel-computing applications to exercise the real-time capability of our IPv6 over ATM network.

(1) *The integrated service network test-bed*. While IPv6 is defined to address the exhaustion and routing-table explosion issues caused by the exponential growth of today's global Internet, the sheer size of the IPv4 Internet complicates its transition process to IPv6. Like most vendors, our research partner, Ipsilon, also chose to take the path of least resistance and embrace the intermediate solution, the Classless Inter Domain Routing (CIDR), which offers temporary relief to these symptoms. Additionally, switched Gigabit Ethernet is the new technology trend for local area networks (LANs), which has influenced Ipsilon's business decision on future product directions. Accordingly, we also changed our research direction to one that implements Differentiated Services (DiffServ) on IPv4 networks that support CIDR. The fundamental elements of DiffServ include per-hop forwarding behaviors, packet classification functions, and traffic conditioning (traffic metering, marking, shaping, and policing). We built a test-bed that consists of five PC–based nodes with kernel modified to support the DiffServ functions. We plan to become a member of the ESnet DiffServ workshop to gain global experience.

(2) *The mission-critical visualization applications*. Because of the geographical distribution of its two sites, scientists and engineers at Sandia are especially sensitive to performance issues in distant computing. In particular, the ability to provide efficient visualization of scientific data over local- and wide-area networks (LANs/WANs) is of major concern. In the past year, we characterized the traffic pattern of two mission-critical visualization applications at Sandia, the client-server–based Ensight, and the remote-x–based CTH code. We modeled the applications traffic using measured statistics. These models can generate traffic for simulation and experimental studies to understand resource allocation mechanisms and the performance metrics in terms of their ability to deliver the contracted quality of services (QoS).

(3) *The digital video transport system*. Several experimental studies at Sandia strive to improve the performance of remote visualization over WAN by taking advantage of the remote graphic server's hardware speed, and by eliminating cumulative round-trip delays caused by the X and GL (SGI's graphical language) commands exchanged during interactive sessions. These experiments use a scan converter that takes the analog signal of the server's display and converts it to NTSC (National Television System Committee) frames. The NTSC frames are then digitized, compressed, and streamed over the network using an MPEG2/JPEG (Moving Picture Expert Group2/Joint Picture Expert Group) encoder. At the receiving end, a decoder reverses the process and sends the recovered analog signal to the monitor of a desktop. Meanwhile, a software utility is used to transfer the control of mouse and keyboard from the server to the desktop, thereby allowing the remote user to manipulate the server's display as if it were local.

While video compression preserves the precious wide-area bandwidth, it degrades video quality because of the lossy JPEG/MPEG compression and the conversion from the display (1280x1024) to NTSC (~ 640x480) signal. Therefore, we will build a high-resolution digital video transport system, without compression, for large campus environments where bandwidth is plentiful. This system takes the high-resolution (1280x1024x24) digital video signal directly from the graphics server's frame buffer, via a parallel digital interface (DVP2), and then direct memory accesses (DMAs) it to a Gigabit Ethernet or ATM interface over the system's PCI (peripheral component interconnect) bus. The system will then distribute the digital video signal to remote desktops around campus. We can adjust its bandwidth requirements by varying the transmission frame rates, which can range between 11 and 30 fps. We finished the design phase with complete schematic drawings.

These two video applications will provide real-time, constant, and variable-bit-rate traffic streams for our DiffServ study.

Publications

Other

Chen, H. Y. 1997. "A User's Perspective on the IP over ATM Approaches." Paper presented to the 22nd IEEE Local Computer Network, Expert Panel Session 2 (Invited panelist), Minneapolis, MN, 5 November.

Chen, H. Y. 1998. "Data Flow Modeling of ASCI Remote Visualization." Presentation to the JOWOG Meeting (Invited), Livermore, CA, 18 June.

3512.180

Virtual Desktop Engineering with Integrated Multimedia Data

J. A. Friesen, J. Schwegel, J. N. Jortner

The growth of the Internet has spurred the development of innovative technologies that support the fusion of a wide spectrum of multimedia data types. Those technologies have made it possible to provide an environment in which engineers can design, prototype, and test components in a virtual space while integrating actual data into the process.

Sandia will insert multimedia streams such as video into a desktop virtual reality (VR) environment. We will store compressed audio, video, animation, scientific visualization, and text streams in a distributed database and deliver it in real time over the network to desktop computers. Using leading-edge World Wide Web (WWW) technology such as Java and Virtual Reality Modeling Language (VRML), we will build an integrated VR environment unlike any currently available on high-end visualization servers.

For example, an engineer using ProEngineer to design a mechanical part could call up similar products from a multimedia part database that displays part behavior from a 3-D perspective. In addition, audio/video clips of engineering advisors, test data, and computer simulations could be displayed interactively. After designing the part, the engineer can virtually manufacture the part to predict actual part performance.

Engineers can quickly evaluate the quality of a design in an interactive environment. Using collaboration tools, they will be able to virtually design, manufacture, and test a part before resorting to stereolithography (STL). That will result in significant reduction of cycle time and cost. In addition, they can archive the design process in multimedia form for future use.

Sandia has made substantial investments in a number of technologies to support concurrent engineering and integrated manufacturing. The appropriate integration of these component technologies is essential to realize the full potential of these investments. This project will integrate a number of leading-edge technologies into a collaborative environment to facilitate rapid product realization.

Specifically, we designed and created an environment and facility where engineers can design, prototype, and test components in a virtual space, and analysts can explore the results of their large-scale simulations. The environment is composed of the latest interface and display technology and is backed up by the highest-performance networking and storage systems available.

Technologies brought together to implement this design facility include graphical supercomputers, advanced visual projection systems, leading-edge audio/video switching systems, and state-of-the-art interactive modeling and analysis software. Using this collaborative environment, we demonstrated the following design and analysis functions:

(1) Interactive viewing and manipulation of scientific data in a 3-D environment.

(2) Application of kinematic motion data and telemetry data to simulations.

(3) Integration of flight-test data with visualization packages to produce physically correct simulations.

(4) Animation of mechanical assemblies for training, assembly, and archive purposes.

(5) Conversion of solid-model assemblies into Web-friendly formats for presentation purposes.

(6) Delivery of simulation results over the network to customers.

(7) Archival of graphical results in multimedia databases for future use.

Based on experiences with our pilot project, we decided not to wrap our applications. At the start of this project, critical software methods used for wrapping applications were in their fledgling state and therefore not integrated into this project. This approach should be reevaluated once the software methods become more developed and stable. The decision to implement a collaborative co-located environment rather than a distributed environment, shifting focus from individual to team environments, was also based on lessons learned with our pilot project. Engineers and analysts are more comfortable using local computers to handle their day-to-day tasks and needed more assistance attacking larger computational problems. We deemed high-resolution, large-scale group viewing facilities more critical to customers' operational needs than individual desktop solutions.

The integration of real data with visualization provides valuable insight into the behavior of test situations that cannot be witnessed directly. Using this collaborative environment, Sandians will improve their engineering process, thus facilitating more rapid product realization.

3512.220

Scaled ATM End-to-End Encryption

L. G. Pierson, P. J. Robertson, T. D. Tarman, L. B. Dean, E. L. Witzke

This project will position Sandia to influence and accelerate the deployment of scalable, variable-bit-rate (VBR) asynchronous transfer mode (ATM) encryption equipment needed to satisfy DOE/ASCI (Accelerated Strategic Computing Initiative) requirements for communication security. The Microelectronics Center of North Carolina (MCNC) "Attila" prototype ATM end-to-end encryptor is the fastest known, operating at 622 Mb/s. Sandia's Scalable ATM Encryptor Prototype is the second fastest, operating at 155 Mb/s. The NSA (National Security Agency) "Milkbush" prototype encryptor is the third fastest, operating at about 100 Mb/s. NSA's efforts have evolved into plans to make commercially available ATM end-to-end encryptors that operate at up to 0.6 Gb/s, yet little work is ongoing to deliver ATM encryptors for the higher data rates (2 to 10 Gb/s) expected to soon be required to meet ASCI objectives.

This research integrated innovative methods of key management, crypto synchronization, and key agility while scaling encryption speed. We identified encryption modes of operation that are scalable, yet interoperable with dissimilarly scaled implementations, and developed prototype encryptor designs. We simulated and/or prototyped major portions of these designs for performance assessment. We showed viability of these methods for encryption of ATM cell payloads at the SONET (Synchronous Optical Network) OC-192 data rate (10 Gb/s), and for operation at OC-48 rates (2.5 Gb/s).

We established collaboration with academia, NSA, GTE, Motorola, Secant Networking, Fore Systems, and elements of the telecommunications industry. We co-developed an algorithm-agile and key-agile architecture with NSA/R22. As a result of Sandia's participation in the Security Working Group of the ATM Forum, a scalable and interoperable encryption method was incorporated into the ATM Forum's Security Specification version 1.0. We identified authentication mechanisms for key management implementation. We selected encryption mechanisms for prototype implementation at high speeds. We developed and simulated a 16-stage pipelined implementation of the Data Encryption Standard (DES). The simulations show that this design will operate at 1.3 Gb/s in reconfigurable logic, and implementation in the form of an Applications of Collectively Intelligent Systems (ASIC) is expected to yield over 5 Gb/s in complementary metallic oxide semiconductor (CMOS) or 40 Gb/s in GaAs. We designed an electronic circuit board containing eleven high-density programmable logic devices and fabricated it for prototype implementation of the encryption mechanisms. This circuit board won the 1998 VeriBest Superior Systems Award for the most unusual circuit board design.

This effort integrated innovative methods of key management, crypto synchronization, and key agility while scaling encryption speed. We identified encryption modes of operation, which are scalable and yet interoperable with dissimilarly scaled implementations, and developed prototype encryptor designs. We simulated major portions of these designs and/or prototyped them for performance assessment. We showed viability of these methods for encryption of ATM cell payloads at the SONET OC-192 data rate (10 Gb/s), and for operation at OC-48 rates (2.5 Gb/s).

This effort positioned Sandia to influence and accelerate the deployment of scalable, VBR ATM encryption equipment needed to satisfy DOE/ASCI requirements for communication security. Through collaborations with NSA, this research demonstrated the viability of these techniques for scaling encryption speed. Because of the expertise developed in this area, project personnel have been invited to participate in the ongoing design reviews for the development of the production GTE 10 Gb/s encryptor to further ensure that the delivered encryption equipment will meet DOE needs.

Publications

Refereed

Tarman, T. D., R. L. Hutchinson, L. G. Pierson, P. E. Scholander, and E. L. Witzke. 1998. "Algorithm-Agile Encryption in ATM Networks." *IEEE Computer* **31** (9) (September): 57–64.

3512.250

Ten-to-One-Hundred-Gigabit/Second Network Enabling R&D

L. B. Dean, M. A. Ngujo, T. D. Tarman, L. G. Pierson, P. L. Campbell, R. L. Hutchinson, P. J. Robertson, J. G. Peña

The next major performance plateau for high-speed, long-haul networks is at 10 Gbps (OC-192). Data visualization, high-performance network storage, and distributed massively parallel processing (MPP) all demand these (and higher) communication rates. Previous research and Accelerated Strategic Computing Initiative (ASCI) needs show that MPP-to-MPP distributed processing applications and MPP-to-Network File Store applications already require single-conversation communication rates in the range of 10 to 100 Gbps.

MPP-to-visualization station applications are ready now to utilize communication rates of 1 to 10 Gbps. The ASCI roadmap specifies 100 Gbps interconnects for 100-teraflop computers.

We conducted theoretical examinations, based on Lambda calculus, of the foundations of MP computing and interconnects to create models of computing communications traffic. We are considering these models for implementation as traffic sources for communication system models. The Lambda calculus work seeded other proposals and new research collaborations.

Finally, we developed a scalable implementation of the Internet Protocol (IP), including IP switching and multiprotocol over ATM (MPOA), a method for providing cut-through routing for IP datagrams. We also described alternative mechanisms for providing application data services in excess of 10 Gbps, including emerging operating-system bypass technologies, like the virtual interface architecture (VIA) and scheduled transfer (ST) protocols. The model led to several new and refined project internal milestones.

We completed an internal white paper on the architecture design, development, and technology selection rationale for this research. It describes a high-level architectural model for our effort that shows how a variety of protocols and components can fit together to provide the desired 10–100 Gbps research results we seek. At the lowest level of this model are the physical layer technologies, including the SONET and wave division multiplexing (WDM) technologies. Above the physical layer, we described switching and interface technologies, including ATM switching, UTOPIA, and AAL mechanisms. Finally, we investigated methods for the scalable implementation of the IP, including IP switching and MPOA. We also described alternative mechanisms for providing application data services in excess of 10 Gbps, including emerging operating-system (OS) bypass technologies, especially the VIA and ST protocols. As a direct result of the model architecture work, we developed and refined several new project internal milestones.

We completed a detailed project plan and an initial literature survey, both of which are now living documents to keep up with the rapid changes in the field. Based on these, we decided to pursue doped optical fiber amplifiers rather than superconducting Josephson junctions (SJJ). The erbium-doped, and the related emerging neodymium and praseodymium rare-earth (RE)-doped, optical fiber amplifier technologies are mature and will likely be a mainstay of future long-haul communications. SJJs are still too immature for our use and have the considerable operational overhead of needing cooling.

We completed the implementation of the PLD-11 flexible prototyping board, with which we will evaluate methods of processing communications protocol functions in parallel at high speed. We selected and purchased our major network simulation tool, OPNET Modeler, and completed staff training on it. We developed communication system models in collaboration with the Nanosat team. We began the detailed study of WDM and of optical computing (OC). Emerging evidence indicates that full OC will most likely drop out as a viable technology for our work, being too immature for use in our time frame. However, we will be able to use some emerging, purely optical processing for a few critical communications functions.

We completed a number of viable designs for scalable UTOPIA interfaces, including an innovative separation of header from payload in processing streams yielding higher-throughput 64- and 128-bit-wide data paths. This led to new designs that scale UTOPIA across the whole range from 1 to 424 bits (full cell) width. We completed first benchmark feasibility designs for framing ATM cells into SONET and for interfacing SONET framers to ATM devices using UTOPIA. We will test and evaluate these results on the PLD-11 board.

We initiated a study of the OS bypasses: the Virtual Interface Architecture (VIA), Scheduled Transfer, the Data Link Providers Interface, and the Advanced Graphics Port protocols. We completed initial investigation of the scalability of the ATM adaptation layer and the IP. We initiated a study of the Inverse Multiplexing of ATM, to be used in matching rates to processes and available circuits.

We completed theoretical studies on the feasibility of developing Lambda calculus–based models for generating computer traffic statistics and mapping MP computations to processors. We are considering these models for implementation as traffic sources for communication system models. We filed a Sandia Technical Advance on a portion of this work. It appears to allow great advances in mapping computer applications to MP and distributed processors, including *ad hoc* collections of processors. This Lambda calculus work seeded other proposals and new research collaborations.

3512.230

Network Surety Modeling for Wireless ATM Networks

B. P. Van Leeuwen, P. E. Sholander, L. F. Tolendino, L. G. Martinez, Jr., B. A. Mah, J. Espinoza

In general, there are four types of network elements: fixed systems that are tracked by the routing protocol, fixed systems that participate in the routing protocol, mobile systems that are tracked by the routing protocol, and mobile systems that participate in the routing protocol. The fourth type, movable asynchronous transfer mode (ATM) switches, is a research focus of this project.

There are two areas of interest. The first area is integrating mobile ATM switches into a mainly fixed infrastructure that uses a link-state routing protocol such as the ATM Forum's Private Network–Network Interface (PNNI) protocol. The second area is ad hoc *network topologies wherein most network elements have some switching functionality. Standard link-state routing protocols may not work well in dynamic,* ad hoc *networks. This mobile switch work addressing the problem of mobility management and routing is important to various government and commercial users, such as DOE, DoD, and Boeing.*

Proposed wireless asynchronous transfer mode (WATM) systems present several interesting problems. The first problem is quality of service (QoS). ATM is optimized for optical fiber channels that have both low error rates and low latency. In contrast, wireless channels may have much higher latency and/or error rates. Mobility introduces other QoS impairments. For example, handoffs between wireless-cells may require ATM-cell buffering during the network path rearrangement. This buffering may increase the cell loss rate.

This research investigated various approaches and protocols used for routing information through dynamic network topologies or networks that have mobile nodes. We focused on issues that mostly reside in the network and data link layers of the OSI (open system interconnection) network architecture model. We addressed network organization, link scheduling, and routing in the protocols. One known effect is that transmission control protocol (TCP) will interpret any increased ATM-cell loss as congestion. This may significantly reduce the TCP throughput..

We developed extensions for ATM's PNNI protocol that would support mobility. We identified a number of specific mobility impairment issues and proposed extensions for these impairments.

We identified a new network impairment for proposed WATM systems—namely, the effects of user mobility on usage parameter control (UPC)—that is not present in existing ATM networks and cellular networks.

We extended the outside nodal hierarchy list (ONHL) procedures. These extensions allow multiple mobile networks to form either an *ad hoc* network or an extension of a fixed PNNI infrastructure.

We examined methods of mobile communications with an emphasis on mobile computing and wireless communications. Many of the advances in communications involve the use of Internet Protocol (IP), ATM, and *ad hoc* network protocols. Recently we directed our focus on advancing communication technology in the area of mobile wireless networks. We looked at various protocols used in mobile communications and a number of extensions to existing protocols, desirable protocol characteristics and evaluation criteria, and several network simulation tools that may be used to evaluate network protocols.

Publications

Refereed

Sholander, P., L. Martinez, L. Tolendino, and B. Mah. 1998. "The Effects of User Mobility on Usage Parameter Control in Wireless ATM Systems." *Proc. 1998 IEEE Internat. Perf. Computing and Commun. Conf.*, accepted.

Other

Sholander, P., L. Martinez, and L. Tolendino. 1997. "PNNI Routing Support for *Ad Hoc* Mobile Networking: A Flat Architecture." Paper presented to the ATM Forum, Singapore, Malaysia, 29 November.

Sholander, P., L. Martinez, and L. Tolendino. 1998. "PNNI Routing Support for *Ad Hoc* Mobile Networking: The Multilevel Case." Paper presented to the ATM Forum, Anaheim, CA, 8 February.

Sholander, P., L. Martinez, and L. Tolendino. 1997. "The Effects of Mobile ATM Switches on PNNI Peer Group Operation." Paper presented to the ATM Forum, Chicago, IL, 28 April.

3512.280

Algorithm–Based Fault Tolerance on Heterogeneous Massively Parallel Computers

P. D. Hough, M. M. Johnson, C. H. Tong

Sandia will do research and development of fault-tolerance strategies (e.g., in redundancy design, fault detection, fault recovery) and the implementation of a fault-tolerant software environment for massively parallel (MP) heterogeneous systems such as Sandia's Computational Plant (Cplant). Such systems are more vulnerable to failures than homogeneous systems, like Sandia's Tflop machine, due to the diverse subsystem and network architectures, the need for multiple operating-system (OS) support, and the decentralized computing and storage platforms. These unique features mandate a fundamental change in fault-tolerance strategies. We will develop an algorithm-dependent fault-tolerance methodology based on a combination of disk–based and diskless checkpointing. This hybrid approach offers low overhead and allows fine-tuning for efficient performance of individual applications. We will encapsulate the techniques in a Java–based object-oriented framework and apply it to a number of Sandia applications, including linear system solvers in AZTEC, numerical optimization methods in OPT++, and enterprise simulations (IDES [Infrastructure for Distributed Enterprise Simulations]). In addition, we will develop failure models to assess the effectiveness of and to suggest refinements for the fault-tolerance strategies. The effort will enhance the robustness of Sandia's distributed computing applications, especially on heterogeneous platforms such as the Cplant. It will have an immediate impact on problems in enterprise modeling, optimal design, and DOE2000 projects. Moreover, the fault-recovery techniques to be developed for the software environment will include strategies for process migration, processor reconfiguration, and reclamation, thus contributing to the advancement of location-insensitive heterogeneous computing technology at Sandia.

We compiled a list of fault scenarios and determined which of those are most likely to occur. Development focuses on covering the more common failures while allowing the flexibility to incorporate others. We also determined fault scenarios particular to Cplant.

We designed a framework for implementing fault tolerance. The basic components include a fault detector, a fault handler, and a machine description. We will incorporate basic tools for recovery in a library accessible by the application.

We are currently using Pentium–based PC clusters for development. These clusters have message-passing interface (MPI) and Java available for use. Cplant clusters of DEC Alphas are now available for use and will be incorporated.

We designed fault-detection schemes for two common machine topologies. These are simple algorithms that are incorporated into a hierarchical structure to allow for scalability. We implemented these schemes in Java and completed incorporation into the hierarchy. In addition to detecting faults, this code allows resources to be reclaimed if the failure is intermittent.

We prototyped a fault-tolerant version of an unconstrained parallel direct search optimization algorithm. This is based on a master-slave formulation, and the algorithm itself can tolerate some loss of information. We currently use checkpointing to handle the failure of the master, but we are investigating alternate techniques.

We implemented a fault-tolerant version of a statistical sampling tool intended for use in the validation and verification of large Accelerated Strategic Computing Initiative (ASCI) codes. The implementation is similar to that for the optimization algorithm except that all information is recovered in the event of a failure.

We are collaborating with researchers at the University of Florida. They are developing simulation tools useful for our study of various fault scenarios and evaluation of fault-tolerance tools.

3512.260

High-Performance Commodity Interconnects for Clustered Scientific and Engineering Computing

L. Stans, T. D. Tarman, T. C. Hu, R. C. Armstrong, P. S. Wyckoff, H. Y. Chen

The Computational Plant (Cplant) runs distributed parallel applications on a large cluster of commodity PCs. Because properly load-balanced distributed parallel applications tend to send messages synchronously, minimal blocking is as crucial a requirement as high bandwidth and low latency. Therefore, the following factors are important network design considerations: (1) the selection of an optimal commodity interconnect network technology and topology to provide both high bandwidth and congestion control, and (2) the development of an efficient local-area communication layer to minimize per-packet processing latency in compute and input/output (I/O) nodes.

The goal of this project is to develop and demonstrate a design methodology for constructing high-performance interconnects using high-bandwidth, low-latency, local-area network (LAN) technologies such as Myrinet, asynchronous transfer mode (ATM), switched Gigabit Ethernet, and the emerging operating-system (OS) bypass Virtual Interface Architecture (VIA). An important element of the research is the pursuit of an emerging communication model that decouples I/O support from the OS and allows individual applications to directly control their own I/O processing. This approach will eliminate the large delay introduced by the per-packet Transmission Control Protocol/Internet Protocol (TCP/IP) processing overhead.

Since our network design goal is to facilitate the performance of real applications, Sandia will evaluate the above LAN technologies in the context of working applications on a small test-bed. We will evaluate performance of very large networks with thousands of interconnections using modeling and simulation tools developed in this project. These modeling and simulation tools will be invaluable in designing the next-generation interconnect for a large Cplant system and its associated applications. In addition, we will evaluate the ability of techniques such as priority queuing, enhanced message-passing algorithms, network–based multicast/broadcast, and cut-through routing to increase throughput and reduce latency and congestion.

During the previous year we completed studies on LAN interconnect technology trends, procured and gained experience with MIL3 OPNET modeling and simulation tool, and designed and implemented four simulation models: (1) VIA network model, (2) layer-2 and -3 Gigabit Ethernet model, (3) Myrinet model, and (4) a 2-D mesh and a smooth-particle hydrodynamic parallel algorithm model. We developed the models to provide us with a flexible method to predict network performance for large-scale systems (thousands of nodes). The developed VIA model provides the foundation for testing and evaluating various OS bypass strategies. There are currently two leading contenders: VIA and scheduled transmission (ST). The Gigabit Ethernet, Myrinet, and Giganet hardware technology models provide the foundation for predicting the performance of different networking technologies and the effect on system performance when these technologies are combined. The two applications models will be critical tools in evaluating how representative applications will perform on large-scale multiprocessor systems.

On the hardware side, we developed and implemented a small, four-node cluster and installed VIA-compliant hardware. We obtained, debugged, and implemented a complementary set of initial VIA software drivers. We conducted initial VIA performance testing to obtain baseline metrics to be applied to the design of a more complex test-bed. These initial test results provided the foundation for the development of a larger test that is currently under construction.

Publications

Other

Canady, C., and P. Wyckoff. 1998. "Bobnet: High-Performance Message Passing for Commodity Networking Components." *Proc. 2nd IASTED Internat. Conf., Parallel and Distributed Computing and Networks (PDCN '98)* (Brisbane, Australia, 14–16 December).

3512.240

Low-Power, Reduced-Computation, Public-Key Protocols

V. A. Hamilton, E. V. Thomas, R. A. Gonzales, T. J. Draelos, A. M. Johnston

Public-key cryptography can be used to provide privacy, data authentication, and nonrepudiation. The advantage of public-key cryptography is the ease of key management in terms of the amount of data that must be protected (i.e., private keys). For instance, a single authenticated message can be verified by multiple parties, each of whom requires access only to the appropriate public key. This feature is advantageous in remote monitoring applications in support of multilateral treaties, in critical infrastructure applications, and in the area of emerging threats. In addition, investigators on this project currently support nuclear weapons applications in which lower resource public-key authentication mechanisms would be very valuable. No solutions to the problem of computational intensity exist, and while key management issues are minimized in public-key applications, they are not inconsequential. System developers will often use symmetric or private-key techniques where power or computational capabilities are limited and then re-encrypt or re-authenticate at some intermediate system. We authenticate the data (in the case of authentication) only from the intermediate system, not from the data originator. Therefore, source-to-sink data authentication, while desirable, is often difficult to achieve. Sandia can enhance its current cryptographic capabilities and leadership in

defense and industry by developing an innovative solution(s) to these problems. This project will research and develop mechanisms that will enable the use of public-key cryptography in low-power and/or reduced-computation environments by investigations in several technical areas, including number theoretic, one-time, probabilistic, and polynomial techniques, thereby enhancing the chances of project success.

• We researched and documented candidates for baseline public-key protocols/algorithms. Three classes of algorithms appeared promising: number theoretic, one-time, and probabilistic algorithms.

• We documented proposed modifications of existing baseline public-key protocol/algorithm candidates and/or new protocols/algorithms. Modifications to the baseline algorithms include performance enhancements to the number theoretic schemes, conversion of one-time schemes to multiple-use schemes, and conversion of probabilistic identification protocols to authentication protocols.

• We researched and documented candidates for baseline key management techniques. Converted one-time protocols require significantly modified key management methods primarily to include authentication trees. We researched and documented these requirements along with methods to optimize these data structures. Probabilistic protocols require slight modifications to standard mechanisms since these types of algorithms have never been considered by developers of the standard techniques.

• We surveyed and documented hardware candidates, smart card, custom, and general purpose. We developed proposed changes in design capability. We performed a survey of the computing platform and segmented the evaluation into two major categories: (1) general-purpose commercial devices, and (2) special-purpose/custom platforms.

We also investigated polynomial algorithms.

3512.270

AVATAR—Navigating and Mining in Massive Data

W. P. Kegelmeyer

The sheer scale of modern data sets defeats attempts to understand that data. Even when coupled with advanced visualization systems, the volume is such that all data can no longer be available at a glance. Thorough inspection is impossible, and yet inspection is necessary, especially when the phenomena of interest are easier to recognize than to describe.

This project will develop an advanced tool for data "understanding," one that supports exploration, easy collaboration, and knowledge encapsulation. The core idea is to exploit massive parallelism and robust pattern recognition (PR) to manipulate derived properties of the data sets. This approach is called AVATAR (Adaptive Visualization Aid for Touring and Recovery) and will produce avatars, sophisticated user profiles that are attached to data. These, in turn, are exploited by the visualization tool, permitting the data to be understood in a fashion uniquely adapted to a particular user.

Sandia developed a powerful and robust PR method known as dense feature maps *(DFM). We previously applied DFM methods to a similarly difficult problem, detection of cancer in mammograms, with noted success (two patents, a commercial software license). We will use DFM here, as well, to extract the avatars by invisibly watching how a user interacts with the data.*

The end result will be prototype AVATAR software, integrated with a 3-D physics visualization application already in active use at Sandia with full documentation. We will also report on performance, treating both objective measures of classification accuracy and subjective feedback from interviews with users.

• *Parallel classification*. We completed a full literature search into the field of classifier parallelization.

We ported three mature parallelized classification algorithms to the Accelerated Strategic Computing Initiative (ASCI) machine.

We made substantial improvements to the ScalParC parallel classification algorithm, to include adapting it to handle continuous valued features and improving its load-balancing and communication overhead.

We also developed and implemented a promising and intriguingly counter-intuitive approach. This new method grows trees on disjoint subsets of data, then merges the trees at the end.

We acquired real data sets ranging up to 10 Mbytes, along with a generator that can create synthetic data sets of any size.

• *Human factors*. We evaluated MeshTV, IBM DX, and MUSTAFA, and selected and installed MUSTAFA as the base visualization tool.

We conducted user interviews; those results shifted saliency measures away from time spent investigating a region to number and nature of operations applied to a region.

We developed methods for extracting initial saliency figures from human operators, as these are needed to create realistic training data sets.

We implemented initial saliency detection measures and inserted them into the MUSTAFA user interface and data model.

Publications

Refereed

Hall, L., N. Chawla, and K. Bowyer. 1998. "Combining Decision Trees Learned in Parallel." *Proc. 1998 Distributed Data Mining Workshop* (New York, NY, 27–28 August).

Hall, L., N. Chawla, and K. Bowyer. 1998. "Decision Tree Learning on Very Large Data Sets." *Proc. 1998 IEEE Conf. on Systems, Man, and Cybernetics* (San Diego, CA, 11–14 October).

THIS PAGE
INTENTIONALLY BLANK

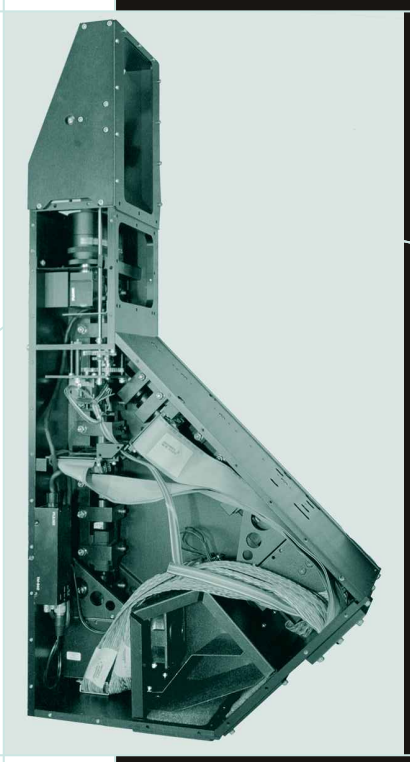

PRECISION SENSING & ANALYSIS

Sensing technologies are being used to solve more and more complex problems. Uses for sensors range from battlefield applications to underground facility detection to environmental cleanup. LDRD supports development of sensors to measure and help researchers understand phenomena that in the past had been unobservable.

There are six objectives in Precision Sensing and Analysis: (1) develop physical imaging techniques to view concealed or difficult-to-view objects; (2) develop distributed sensor systems that will monitor complex systems such as battlefields or manufacturing processes; (3) develop a distributed command-and-control system for diverse military assets; (4) develop algorithms and sensing capabilities for autonomous navigation in complex environments; (5) develop precise, dexterous robotic manipulation capabilities; and (6) develop advanced chemical and biological sensors that can detect minute quantities of specific chemicals in a field environment and in real time.

There are many military applications where fast, efficient spectral imaging is necessary. Hyperspectral imaging (HSI) is a remote-sensing technique that is gaining significant attention for its unique ability to allow passive identification of materials in a scene. To achieve this, HSI systems acquire high-resolution simultaneous images in hundreds of spectral bands, generating a significant volume of data for a single image. This makes data acquisition and processing difficult and limits the ability to do real-time target detection with HSI. Information-efficient spectral imaging sensor (ISIS) is an optical system concept designed to significantly reduce data rates compared to HSI systems, and it allows on-the-fly target discrimination while retaining similar spectral detail. Most applications experience at least a factor of fifty reductions in data rate and signal-to-noise improvements of a factor of ten over traditional HSI systems with similar specifications.

ISIS also offers opportunities for advances in manufacturing and medical imaging. Large volumes of data are examined in counting cancerous cells or looking for semiconductor defects. Faster, more efficient data analysis would benefit many diverse fields.

THIS PAGE
INTENTIONALLY BLANK

3516.080

Sampling and Sensing Systems for High-Priority Analytes

G. C. Frye-Mason, D. Y. Sasaki, A. Sellinger, R. J. Kottenstette, C. J. Brinker, G. C. Osbourn, P. R. Lewis

This project focused on redesigning current array–based sensing systems to optimize them for detecting high-priority analytes (HPAs) such as chemical warfare (CW) agents, CW precursors, and explosives in the presence of common interferants. Since the target HPAs have either low volatility or high reactivity, their analysis will require modifications in adsorbent materials and surface acoustic-wave (SAW) sensor-array coatings. The team of investigators assembled to perform this project demonstrated leadership in the areas of SAW sensor systems, thin-film adsorbents and coating materials, pattern recognition (PR) analysis, and chemical microanalysis, which makes this team uniquely qualified to take on this task. The materials and system optimization performed will facilitate development of low-power, microanalytical systems (chemistry laboratory-on-a-chip) that could provide rapid, sensitive, and selective detection of these HPAs in truly miniaturized field-deployable units. Spin-off applications in environmental monitoring and industrial process control are likely for other classes of semivolatile chemicals (e.g., pesticides, sludges) that are notoriously difficult to monitor.

Accomplishments included synthesis and testing of new derivatized sol-gel and reactive polymer coatings for SAWs. The sol-gel coatings continue to show very high uptakes of the semivolatile analytes such as dimethylmethylphosphonate (DMMP). Because of the high activity of these materials, they require large sample volumes at low concentrations to accumulate enough analyte to equilibrate the surfaces. In addition, the release at room temperature is slow. However, tests using these materials on thermal desorption platforms verified rapid release with pulsewidths of under 200 ms upon rapid heating to 200°C. This verifies the utility of these materials for sample preconcentration. In addition, we demonstrated reversible responses on SAW sensors at elevated temperatures (80°–100°C). At these temperatures, uptake of potentially interfering compounds should be low, enhancing the selectivity of these materials.

Another highlight was the demonstration of a material for detecting reactive species such as phosphorous oxychloride. These compounds are used in the production of CW agents and could be useful targets for detection. The challenge for an SAW sensor is that these compounds have high volatility, making them hard to collect on the sensor surfaces, and they are reactive, so they may not survive for long on the sensor. We decided to look at the use of materials that would irreversibly react with these compounds so we could form a dosimetric sensor with the potential for trace detection of these reactive precursors. We successfully demonstrated this concept using a polyacrylic acid/polyacrylamide copolymer that exhibited an 80 mdeg/min response when exposed to 100 ppb of phosphorous oxychloride. In contrast, a polyvinylalcohol-coated device exhibited no detectable response. This demonstrated proof-of-principle for sensitive and selective detection of these types of compounds. With further optimization, this new capability will enable us to develop systems for detecting a broader range of compounds relevant for nonproliferation of CW agents.

Publications

Refereed

Frye-Mason, G. C., R. J. Kottenstette, E. J. Heller, C. M. Matzke, S. A. Casalnuovo, P. R. Lewis, R. P. Manginell, W. K. Schubert, and V. M. Hietala. 1998. “Integrated Chemical Analysis Systems for Gas-Phase CW Agent Detection.” *Proc. Micro Total Analyt. Systems Conf.* (Banff, Canada, 12–16 October): 477–481.

Lewis, P. R., G. C. Frye-Mason, R. J. Kottenstette, and J. Vitko, Jr. 1998. “MicroChemLab: An Update on the Integrated Chemical Analysis System for CW Agent Detection.” *Proc. MASINT Chemical Def. Sci. & Tech. Symp*. (Aberdeen, MD, 9–11 June).

3516.050

Electrokinetic Immunoaffinity Chemical Sensors

J. S. Schoeniger, J. V. Volponi, D. H. Thomas, D. S. Anex, V. A. Vandernoot, D. W. Neyer

The purpose of this project is to establish the feasibility of capillary affinity electrochromatography (CAEC) with laser-induced fluorescence (LIF) detection as a portable means for the detection of trace quantities of toxins in liquid samples. The project focuses on the detection of analytes for which there is currently no portable sensor capability with adequate sensitivity and specificity, e.g., potential biological warfare (BW) agents (bacterial toxins). In CAEC, the chromatographic matrix consists of immobilized molecular recognition materials (MRMs), (e.g., antibodies [Abs] or receptors) that bind selectively to the target analyte, surpassing the specificity of capillary electrochromatography (CEC). A sensor based on CAEC has the potential to combine the versatility of CEC, the high sensitivity of LIF, and the exquisite selectivity of molecular recognition. We obtained new results regarding both the scientific basis of CAEC and the technology required to implement effective, field-portable CAEC–LIF units for toxin detection.

We demonstrated the first-ever implementation of CAEC. In this second year, we completed a more thorough scientific investigation of the fundamental processes involved in, and the practical measures necessary to implement, CAEC–LIF for measurement of biological toxins. To understand the similarities and differences between CAEC and traditional affinity chromatography, we successfully quantitatively modeled and compared to experiment CAEC of small analytes.

Building on this work, we also implemented affinity chromatography on macromolecular analytes. Initially, attempts at CEC on proteins using traditional nanoporous silica chromatographic supports were unsuccessful. Further investigation revealed a previously unknown, but potentially extremely useful, size-dependent reversible electrokinetic (EK) trapping effect. We showed that this effect can be used to concentrate protein analytes by factors greater than 1000 and are presently completing a technical disclosure based on such systems.

We also showed that we may avoid trapping by using nonporous silica microspheres as chromatographic supports. We therefore synthesized nonporous affinity phases. To meet stability and sensitivity requirements for fieldable/portable toxin detection systems, we focused on synthesizing non-Ab–based affinity phases because we wanted to use affinity ligands with enhanced stability. This required the development of methods for immobilizing carbohydrate or synthetic peptide toxin receptors on silica supports. Using both pressure-driven and EK flow, we are currently characterizing the retention and elution of affinity phases for the toxic protein ricin, and peptide–based affinity systems for model proteins.

Finally, we constructed and evaluated a prototype field-portable LIF apparatus with photon-counting detection. We demonstrated concentration sensitivity with this apparatus down to subnanomolar levels.

Publications

Refereed

Thomas, D. H., J. S. Schoeniger, D. L. Rakestraw, V. Lopez-Avilla, and J. M. Van Emon. 1998. “Selective Trace Enrichment by Immunoaffinity Capillary Electrochromatography.” *Electrophoresis*, accepted.

3516.060

Information-Efficient Spectral Imaging System (ISIS)

S. M. Gentry, W. C. Sweatt, J. W. Daniels, R. J. Blake, M. K. Hinckley, L. J. Krumel, B. R. Stallard, D. A. Smith

Hyperspectral imaging (HSI) is a remote sensing technique that is gaining significant attention for its unique ability to allow passive identification of materials in a scene. To achieve this, HSI systems acquire high-resolution simultaneous images in hundreds of spectral bands, generating a significant volume of data for a single image. This makes data acquisition and processing difficult and limits the ability to do real-time target detection with HSI. In addition, signal-to-noise ratio is compromised by parsing the photons among a large number of spectral bins. Information-Efficient Spectral Imaging Sensor (ISIS) is an optical system concept designed to significantly reduce data rates compared to HSI systems, and it allows on-the-fly target discrimination with minimal processing overhead, while retaining similar spectral specificity. ISIS allows the optical selection and mixing of key spectral image components into a small number of outputs related to target identification. Most applications experience at least a factor-of-fifty reduction in data rate and signal-to-noise improvements of a factor of ten over traditional HSI systems with similar specifications.

The project was successful in developing an imaging instrument operating in the silicon (Si) spectral region (0.45–1.05 µm) that is able to discriminate between a camouflaged HUMVEE and natural desert scrub background scenery. We conducted field tests at Coyote Canyon on Kirtland Air Force Base.

(1) We designed, fabricated, and tested an ISIS field-test instrument operating in the Si spectral region. The instrument is capable of achieving 5 nm spectral resolution over 0.45–1.05

µm and can resolve 500 spatial samples over a 5-degree field.

(2) We utilized the ISIS field-test instrument at Sandia's Coyote Canyon test site to evaluate the ability to discriminate a camouflaged National Guard HUMVEE from the natural vegetative background. Tests were successful when the HUMVEE was under camouflage, but the material variability of the uncovered HUMVEE made it more difficult to discern. We expect different spectral regions and the use of more complex filter vector settings to remedy this difficulty.

(3) We developed a variety of methods for synthesizing filter vector programs utilizing source spectral data collected with the instrument.

(4) We developed a potential Work for Others (WFO) customer to carry the ISIS research forward to operational stages.

Publications

Other

Gentry, S. M., and B. R. Stallard. 1998. "Theoretical Analysis of the Sensitivity and Speed Improvement of ISIS over a Comparable Traditional Hyperspectral Imager." Sandia Technical Report SAND98-1887 (September). Sandia National Laboratories, Albuquerque, NM.

Stallard, B. R., and S. M. Gentry. 1998. "Construction of Filter Vectors for the Information-Efficient Spectral Imaging Sensor." *Proc. SPIE*, accepted.

Stallard, B. R., S. M. Gentry, W. C. Sweatt, S. E. Motomatsu, and C. A. Boye. 1997. "Principles and Satellite Applications of the Information-Efficient Spectral Imaging Sensor." Sandia Technical Report SAND97-1493 (June). Sandia National Laboratories, Albuquerque, NM.

Sweatt, W. C., C. A. Boye, S. M. Gentry, M. R. Descour, B. R. Stallard, and C. L. Grotbeck. 1998. "ISIS: An Information-Efficient Spectral Imaging System." *Proc. SPIE*, accepted.

3516.070

Imaging of Moving Targets Using Simultaneous Synthetic Aperture Radar (SAR) and Moving Target Indicator (MTI) Radar

J. T. Cordaro, C. V. Jakowatz, Jr., J. A. Hollowell

Sandia will combine two well-known radar techniques and an adaptation of an existing algorithm to image moving targets. Synthetic aperture radar (SAR) images objects at known velocities relative to the SAR platform. In SAR the motion relative to objects that are fixed on the Earth is accomplished by using inertial measurement systems and the global positioning system (GPS). Targets that move over the Earth are displaced and defocused because of unknown motion components. This fact obscures information about the target in the SAR image. Moving target indicator (MTI) radars measure the relative position and velocity of objects that are moving over the Earth, but they do not produce an image of the moving target. While traditional MTI radars measure the average radial velocity of the target, higher-order motion components are not measured. This prevents formation of a good-quality, fine-resolution image of the moving target. Even the straightforward combination of these two radar techniques will have significant limitations. The information necessary to form the image of the moving target is contained in the raw data; however, it must be extracted by a suitable algorithm.

In SAR, inaccuracies in inertial measurement systems typically result in unsensed radar platform motion. Generation of well-focused, fine-resolution SAR images requires compensation for this unsensed motion. We demonstrated great success at estimating the unknown radar platform motion using phase-gradient autofocus (PGA). This type of algorithm should also have success in estimating the higher-order motions of a moving target. Our approach will be to combine the information from an MTI radar with an algorithm similar to PGA to estimate the phase errors in the moving target data, compensate for those errors, produce an image of the moving target, and place the image of the moving target in the proper place in the SAR image.

Our work consisted of two algorithm-development efforts plus a Twin-Otter-radar data collection. The first algorithm effort aims at focusing moving targets after they have been detected in SAR data. We successfully tested the method on data collected at the end of FY97. For this initial test, the targets were traveling at constant velocity along straight roads. We modeled target motion in terms of range and cross-range velocities. A contrast optimization technique searches over the resulting 2-D space to achieve the best focus.

The second algorithm effort implements simultaneous SAR/MTI to detect moving targets and to then reposition them in an image. Slow-moving targets remain in the clutter (endoclutter targets) and must be distinguished from stationary objects. We developed a method to use SAR data from two antenna phase centers to reduce stationary clutter for detection and measure target angle for relocation. We successfully tested the algorithm on data from the FY97 collection.

We recently completed a second data collection. For this test, the moving targets executed a variety of motions. On straight roads, the targets accelerated to different velocities. Three vehicles did start-stop-passing drills; one vehicle moved in a circle. All this will provide challenging data for our algorithms.

3516.090

Automated Vegetation Height Measurement for Automatic Terrain Mapping

J. R. Fellerhoff, D. L. Bickel, M. L. Yee

Sandia demonstrated that interferometric synthetic aperture radar (IFSAR) accurately measures the tops of vegetation. A map of the tops of vegetation is sufficient for airborne users of terrain elevation information; however, troops or personnel in ground vehicles need to know the terrain below the vegetation. Many commercial and civilian map users require ground-level information rather than vegetation-top information, as well. A proof-of-principle of under-tree, ground-level terrain mapping is the primary goal of the project. Research from Sandia's High-Altitude Doppler Radar Altimeter (HIDRA) work shows that in many forested areas, radar altimeters receive a significant return from the top of the trees as well as the terrain underneath. We are studying the combination of these two radar techniques to measure not only the elevation of tree tops but the terrain underneath. IFSAR is a technology that has the potential to satisfy the high demand for accurate and timely terrain data from both government and commercial entities. It is likely to become a necessary feature on most future imaging radar systems. Solving this problem could help keep Sandia in technological leadership in this extremely important area. A second goal of the project is the understanding of the exact relationship between IFSAR and HIDRA data in vegetated areas, as this is also an important problem for the new generation of weapon guidance systems based on imaging altimeter technology. This study will provide much insight into that relationship. A third important result from this study will be the ability to detect, classify, and quantify vegetation regions in IFSAR elevation models. This could be important to automatic target recognition (ATR) in cueing the algorithms to use different recognition methods, depending on the vegetation type and height.

In the first year we collected and processed IFSAR data from the bosque where I-25 crosses the Rio Grande near Black Mesa, south of Albuquerque, NM. We also processed existing HIDRA data from the same flight path taken in September 1995. (HIDRA was unavailable in the first half of 1997.) Mapping the HIDRA data onto the IFSAR data showed there were a large number of HIDRA ground returns in areas covered by trees. In a number of areas where the IFSAR data measured the tree profile, the HIDRA data provided a measurement of the underlying ground profile. We can then determine vegetation height by taking the difference of the IFSAR tree profile and the HIDRA ground profile. This demonstrated the basic capability of combined IFSAR and HIDRA data to measure both vegetation height and the terrain height underneath the vegetation.

In the second year we collected new data from a newly developed HIDRA sensor. This HIDRA is optimized for the down-looking mode of operation and is more representative of an operation sensor. The results from this year clearly show that terrain features (significant ditches, sloped terrain) beneath the trees are visible to this sensor.

Publications

Other

Fellerhoff, R. 1998. "Bald Earth Mapping Research." Formal briefings of results to DARPA, AF RMAG, and JPSD, Washington, DC, May.

3516.110

Sparse Geophysical Networks for Monitoring Deep Targets

G. E. Sleefe, A. A. Yee, L. C. Bartel, M. D. Ladd, H. D. Garbin, J. P. Claassen, G. J. Elbring

Facilities for the manufacture and storage of weapons of mass destruction (WMD) are often contained within deeply buried structures or tunnels. The ability to detect, characterize, and monitor these deep underground production and storage sites is critical to the defeat of these threats to our national defense. The intent of this project is to focus on the key technology issues required to bring a deep-target unattended ground sensor system to fruition. In particular, the use of a sparse seismic network is very desirable for this application since it represents a practical field-deployable configuration. However, the application of sparse networks for accurately determining the 3-D location of underground activities has never been addressed. As such, Sandia will design, develop, and test an advanced algorithm that uses sparse seismic networks to accurately determine the 3-D location of underground activity, especially activities of a continuous nature. The algorithm will incorporate several novel elements to address the sparse network problem: (1) the use of enhanced 3-D geophysical modeling to optimize sensor layout and distribution, (2) the isolation of local soil effects by using both velocity inversion and spectral ratio methods, (3) the use of modified array processing methods to handle the spatially aliased network data set, (4) the incorporation of an active calibration source to remove geophysical biases, and (5) resonance-extraction techniques to infer underground cavity dimensions. To validate these advanced geophysical and signal-processing methods, we will

process data previously acquired at the Nevada Test Site (NTS) P-tunnel using the novel algorithms. Additionally, we will collect a small data set at the P-tunnel to confirm the optimized sparse network approach.

We made significant progress in the development of a novel algorithm for locating underground target activity using sparse seismic networks. We formalized the framework of the algorithm, which includes 3-D forward seismic modeling, geologic medium estimation, and model–based seismic signal processing. Within this framework, we made significant technical progress on each aspect of the algorithm. In the modeling area, we developed a fully elastic seismic 3-D finite-difference model and implemented it on an engineering workstation. We optimized the code to run efficiently; it can handle complex underground seismic sources including rotary torque and shear motions. We tested the model and successfully generated synthetic surface seismograms resulting from a source in an underground void. We successfully completed the second aspect of the algorithm: geologic estimation. A spectral ratio algorithm, based on the Haskell-Thompson formulation, enables the estimation of subsurface geology from passive surface seismic observations. We successfully applied this geologic estimation method using data from the P-tunnel. We also made substantial progress in developing model–based seismic signal-processing techniques to perform underground source localization. The signal-processing techniques under investigation include advanced array processing for bearing estimation, cross-correlation for continuous source timing estimates, and improving the LOCSAT (software package) location estimator, to include 3-D ray tracing and optimized use of both bearing and time-of-arrival inputs.

3516.120

Miniature Bioaerosol Concentrator

K. Wally, D. J. Rader, S. H. Kravitz, R. F. Renzi, M. X. Tan

To be most effective, biological warfare agent (BWA) sensors must detect BWA bioaerosols at concentrations as diffuse as one pathogen particle per liter of air. The most capable portable miniature BWA detectors under development employ techniques of biological or chemical detection in aqueous or solvent solution. These techniques, miniaturized to the microfluidic level, typically require an influent concentration of ten bioparticles per microliter of solvent. Demonstrably, therefore, there is a pressing need for a device to couple these conditions, i.e., to collect highly diffuse bioaerosols and concentrate them into microfluidic volumes for further analysis. For hand-portable detectors, such a device must be both battery-operable and miniature—only one or two cubic inches in volume. Unlike existing miniature aerosol collectors, which fall short in one area or another, Sandia's miniature bioaerosol concentrator satisfies all these requirements. A unique integration of science, process, and engineering is the key. First, ours will be a true bioaerosol collector in that bioaffinity detection techniques require that surface proteins on collected particles be unscathed by collection processes. Therefore, our collector uses only benign techniques of inertial separation and virtual impingement into aqueous solvent to collect particles. Second, our device concentrates bioaerosol particles into a mere microliter of aqueous solvent. This is a concentration several orders of magnitude greater than the best currently achieved in miniature aerosol collectors. We can achieve this through development of microseparator and microimpinger stages employing the principles of aerodynamic particle lenses and electrokinetic (EK) fluid flow, all realized through techniques of miniature fabrication (i.e., LIGA [German for lithography, electroforming, and molding] or Bosch deep-etched silicon). Third, in our concentrator the sampling fan and its motor are miniaturized, integral to the device, and accounted in its tiny package volume. Existing miniature collector/concentrators achieve miniaturization only by depending on external apparatus for sample air flow.

The scope of first-year work concentrated on refining issues of technical feasibility. As a result, two key uncertainties appear on the way to resolution. The first was whether the required volume of air could be drawn through the proposed microseparator by a miniature high-speed fan of conventional design. We developed a computer model for separation and collection of bioaerosol particles (i.e., particles 1 to 5 microns in size) using the FIDAP 7.60 commercial finite-element (FE) gas dynamics code to mesh the selected geometry and calculate air flow and particle trajectories. We identified a promising geometry that exploits the concept of the aerodynamic lens. Preliminary results suggest that the aerodynamic lens may enable collection of 1- to 5-micron bioaerosol particles directly in one single-stage inertial separation rather than the two stages postulated in our original proposal. The second uncertainty was whether microfluidic EK pumping could generate the flow rates needed to transport particles collected in open microchannels. We recently completed design and fabrication of an EK pump that preliminarily demonstrated the feasibility of achieving high flow rates. The EK pumping mechanism consists of thin wafers of microporous alumina. These dielectric structures, comprising short, massively parallel (MP) microchannels (each under 20 microns in diameter), produce relatively high EK flows (substantially greater than tens of nanoliters/second) roughly proportional to the face area of the wafer, but producing little hydraulic head due to the wafer's overall thinness. This is precisely the pump characteristic we desire for open channel flow, where high flow rate is needed to transport particles, but excessive hydraulic head risks overflowing channels.

3516.130

Recognizing Partially Obscured Targets by Combining Multiple Data Sources Using Evidential Reasoning

M. W. Koch, D. A. Yocky, J. S. Salazar, M. M. Moya

Military commanders in the battlefield need accurate, reliable target information. Yet any single sensor has necessarily limited detection capability and inherent sensitivities to some false targets. Multiple sensors, particularly those with different sensing modalities, can provide complementary target information. However, even small increases in amounts of sensor data can quickly overwhelm a human analyst. Automating the target recognition process by combining data from multiple sensors to produce a single likelihood for each target's existence/location can assist analysts in identifying significant threats.

Sensor evidence is typically uncertain; it allows for multiple interpretations, which can be incomplete (i.e., a sensor rarely has a full view of the situation) and/or conflicting (e.g., a sensor may be partially incorrect). Because of these characteristics, Sandia combined evidence from multiple sensors using an evidential reasoning engine. First, we extracted evidence from the different sensors by applying image-processing and pattern recognition (PR) algorithms to identify target subparts or chunks. Each of these feature-level chunk detectors functions as a separate knowledge source, which provides evidence to the reasoning engine. Since we could tailor the algorithms to exploit each sensor's unique characteristics, we maximized the relevance of each sensor's information.

The reasoning engine represents its knowledge of the target as multiple-level frames of discernment, where each sensor target template comprises a spatially registered combination of chunks. The engine updates contextual evidence for the presence of target chunks by examining the similarity and compatibility evidence from other chunks. It updates evidence for the presence of target templates based on information from individual chunks, where missing chunks can provide negative evidence. Thus, the evidential reasoning engine provides a formalized methodology for combining incomplete and uncertain evidence from feature-level sensor chunks to allow recognition of partially obscured targets.

We developed an evidential reasoning engine that combines evidence from multiple synthetic aperture radar (SAR) chunks. We also developed and implemented algorithms for matching SAR target chunks with test images. For each chunk, we measured a chunk's intrinsic and contextual support by computing the mean square error between a chunk or chunk pairs and a possible location in an image. The evidential reasoning approach represents the evidence in frames. Each frame specifies a set of possible situations, and basic probability assignments represent evidence relative to the frames. Relationships between the frames and Dempster's rule allow the gathering of contextual evidence for a chunk and evidence for a set of chunky templates. Using actual SAR data of a SCUD target, we determined the detection and false-alarm rate characteristics for the chunky evidential reasoning algorithm. We also collected multisensor data from seven target vehicles at Kirtland Air Force Base and urban clutter from Albuquerque using the Otter SAR and the Remote Sensing Lab Daedalus multispectral (MS) sensor. We developed MS target material detection algorithms, which detect single-pixel MS chunks, for future incorporation into the evidential reasoning.

Publications

Other

Koch, M. W., J. S. Salazar, M. M. Moya, and D. A. Yocky. 1998. "Recognizing Partially Obscured Targets by Combining Multiple Data Sources Using Evidential Reasoning." Presentation at DIA Meeting, Sandia National Laboratories, Albuquerque, NM, 23 June.

Koch, M. W., J. S. Salazar, M. M. Moya, and D. A. Yocky. 1998. "Recognizing Partially Obscured Targets by Combining Multiple Data Sources Using Evidential Reasoning." Presentation at meeting with Captain Paul Schultz and Lt. Dan Sunvolt, U.S. Navy, at Sandia National Laboratories, Albuquerque, NM, 2 March.

Koch, M. W., J. S. Salazar, M. M. Moya, and D. A. Yocky. 1998. "Recognizing Partially Obscured Targets by Combining Multiple Data Sources Using Evidential Reasoning." Presentation at meeting with Gary Beeler, VP of Org. 2500, Sandia National Laboratories, Albuquerque, NM, 8 April.

3516.140

Computational Engineering of Sensor Materials and Integration with a Novel Biological Weapon Detection System

D. C. Roe, J. S. Schoeniger, S. Istrail

This project will develop the computational tools to efficiently design combinatorial peptides (CPs) for use as sensor materials in the detection of bioagents. A necessary step in sensor design is to discover a material that binds and molecularly recognizes a target biomolecule. CPs are a new class of molecular recognition materials (MRMs) based on small molecules that can be engineered to bind tightly and specifically to a target analyte. They have a significant advantage over antibodies and enzymes in that they are much more rugged, cheaper, and more versatile. However, identifying highly selective CPs can be time-consuming, since potentially 1012 CPs may be possible, but only 105 compounds can be tested at a time. Sandia used computational modeling of molecular recognition and developed a unique software algorithm, shuffle-and-screen, that will greatly enhance the efficiency of the sorting process to discover highly select CPs. In our approach, we generated CP MRMs in a simplified three-step process. First, we used bead synthesis to create and evaluate an initial set of CPs specific for a target analyte. Second, we applied a novel computational molecular recognition (CMR) shuffle-and screen algorithm to abstract the key interaction properties of the most promising candidates of the initial bead synthesis, and searched a virtual library of all possible CPs for ones that contain those recognition features and thus may have improved detection properties. Third, we generated and tested these designed CPs in a second bead assay. The final result is CPs that are highly selective for a target analyte. The successful completion of this project will have several important impacts. The methodology developed will enable rapid generation for a broad range of other biological warfare (BW) targets. The computational methods developed will be generally useful tools for all areas of molecular recognition.

We chose an initial set of test cases from a combinatorial library of potentially 10^{15} compounds to develop our shuffle-and-screen algorithm. We developed a prototype algorithm that analyzes the key molecular recognition features of the top binders from an initial bead assay. It searches a virtual library of all possible CPs for ones that contain the same molecular recognition features and therefore may have improved detection properties. The key molecular recognition features we analyzed are a 2-D topological index called the *Wiener index* that can be used to describe the similarity between two chemical structures. Approaches in the literature using this index usually employ genetic algorithms (whose results vary, depending on the starting conditions) since it would take roughly 37 years to exhaustively examine all 10^{15} possible compounds. Our algorithm takes advantage of inherent redundancies in the combinatorial compounds, reducing the search time to examine all possibilities from 37 years to less than a day. Experimentally we initiated a collaboration with North Carolina State University to (1) perform initial bead assays on ovalbumin (as a test system) and then either SEB (*Staphylococcal enterotoxin B*) or C-fragment of botulinum toxin, and (2) perform selectivity, competition, and sequencing tests of 20 or so top candidates for each analyte. We completed a preliminary assay and currently are running a full-scale bead assay to search for CPs specific to ovalbumin. So far, we have found seven CPs with better than one micromolar binding that we showed to be selective for ovalbumin. We are sequencing these compounds.

Publications

Refereed

Goldman, D., S. Istrail, G. Lancia, A. Piccolboni, D. Roe, and B. Walenz. 1998. “Efficient Algorithms for Designing Combinatorial Peptides.” Poster presentation for Pacific Symposium on Biocomputing ’99, Kapalua, Maui, HI, 4–9 January 1999, submitted.

3516.150

Biological Weapon Detector Using Bioaffinity Array Impedance Analysis with Chemical Amplification Through Redox Recycling

A. W. Flounders, R. P. Janek, D. D. Chu, S. H. Kravitz, A. J. Ricco, R. C. Hughes, K. Wally, J. S. Schoeniger

Sandia will develop a novel structure for ultra-sensitive detection (1 particle per liter of air) of biological warfare (BW) agents, e.g., anthrax, to the sensor prototype stage. Surface-attached specific affinity components (antibodies, combinatorial peptides [CPs], or glycolipids) will capture a particle on one element of a microelectrode array monitored via impedance analysis transduction, chemically amplified through disruption of redox recycling. We monitored Faradaic impedance using a reversible redox couple (e.g., Fe[(CN)6]-3/-4) recycled between its oxidation states by each microelectrode and a shared counter electrode. Capture of a single pathogen blocked one microelectrode, disrupting the redox cycle at that electrode. An array of pathogen-sized, individually monitored, small-area (2x2 μm^2) microelectrodes enables single-particle detection. Many identically coated array elements (100s–1000) covering one surface of the flow cell enhances the probability of single-particle capture and provides interferant discrimination by spatio-temporal tracking of the capture/release of each particle traversing the cell. Small capture area is key to single-particle detection; a multi-element array is key to rapid response, realistic sample volume, and improved discrimination. Because of large particle size, diffusion alone may not be sufficient for particle movement through the flow cell. We will also investigate electrophoretic or dielectrophoretic movement of particles through the flow cell.

We made significant progress toward a proof-of-principle demonstration of the sensor concept. We selected surrogate capture and analyte materials, identified the preferred electrode material, and verified system compatibility of the redox couple. We maintained the parallel approach outlined in the original proposal of working with commercially available single electrodes while designing and fabricating a simple multi-element array. We investigated impedance characterization of surrogate binding at a single electrode and found that it supports the proposed sensor concept. We performed these measurements with a large electrode, and signal represents binding of many surrogate particles. We designed and fabricated a 20-element microelectrode array. We packaged, encapsulated, and tested array chips. Microelectrode currents are reproducible, correspond well with exposed electrode area, and are of suitable magnitude (nanoamp) to be monitored without additional on-chip amplification. We functionalized the microelectrode array with affinity capture material (biotin), and surrogate particles (latex beads) with corresponding affinity recognition material (streptavidin). Particle capture in the electrode capture well led to a significant current decrease. Response was an abrupt (1-second), digital-like current decrease and preferable to a gradual current decay. We have not yet demonstrated specific recognition of surrogate materials. Because of the large (1–2-micrometer) diameter of the target particles, particle movement to the electrode surface can not rely on diffusion alone. We are currently investigating techniques to electrophoretically move particles to the electrode surface.

3516.160

ATR / Exploitation Utilizing Ultra–High-Resolution, Complex SAR Imaging

D. W. Harmony, P. H. Eichel, W. J. Bow, K. M. Simonson

The goal of this project is to develop novel automatic target recognition (ATR) and exploitation techniques utilizing ultra–high-resolution as well as complex (magnitude, phase) synthetic aperture radar (SAR) imagery. Current ATR techniques utilize classification metrics applied only to high-resolution magnitude images. Sandia will research and develop new classification metrics and algorithms designed to take advantage of the increased information content of the complex and ultra–high-resolution SAR imagery. The existing major DoD program developing next-generation algorithms reported results three orders of magnitude short of their probability of detection (Pd) and false-alarm rate (FAR) goals. Analyses show that significant increases in the number of resolved scatterers as well as improvements in the ability to localize them are necessary before ATR can successfully handle the extended operating conditions of partial obscuration, articulation, camouflage, etc. This is particularly true for small tactical targets where the number of image resolution elements on target is limited. Our research will provide these needed improvements and then some. Not only will we take advantage of the enhanced information content coming from increased signature bandwidth, but also this improved resolution will now separate the underlying scatters enough to allow us to utilize the additional information carried in the phase of the complex-image pixels. Other DoD efforts are under way, struggling to improve performance by modifying their current

algorithms without upgrading the sensors. We believe, from a system perspective, that our combination of sensor resolution enhancements coupled with new complex-image ATR algorithms will significantly outperform these other approaches.

We completed a large ultra–high-resolution SAR data collection with over 1400 images, including approximately 9500 target images. In addition to six target vehicles, we collected a number of radar primitives as well as a small amount of urban clutter. We believe that this collection gives Sandia the largest database of ultra–high-resolution SAR target imagery in the world.

We modified existing recognition algorithms to handle ultra–high-resolution data. These changes involved accounting for rotational effects so that estimation of signature statistics could be done accurately, even with the relatively sparse data set we had for training.

We showed that sub-aperture processing can be used to determine which features in a single complex SAR image are stable throughout the aperture flown to collect the scene. This processing technique will be of great value in determining which features are flat-plate flashes and which are behaving like true point returns.

We analyzed data generated with a popular synthetic data-generation tool (XPatch) to evaluate the possibility of using synthetic data to augment measured data. High computational cost of signature generation and poor accuracy of the signature phase and amplitude produced with the available facet target models lead us to recommend dropping this tool's use for now.

Finally, work on a new stability metric–based feature extraction and matching technique is under way.

THIS PAGE
INTENTIONALLY BLANK

ENVIRONMENTAL SCIENCES

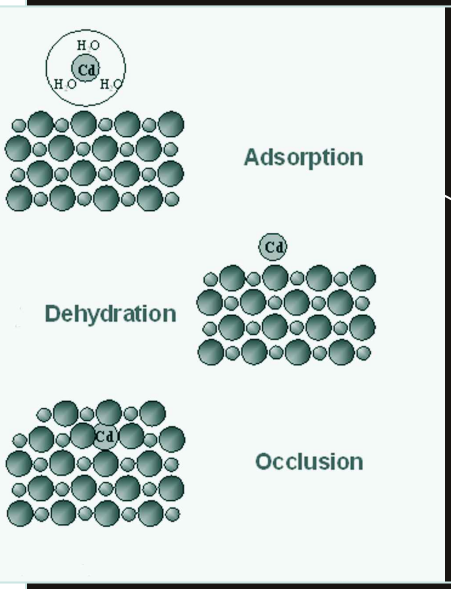

Finding technical solutions to environmental issues is the thrust of this investment area. Three categories of study are supported: (1) site characterization projects that typically use sensors to monitor several aspects of one environment, such as the air, water, and soil at a site; (2) industrial ecology projects that reduce waste and harmful industrial by-products as well as increase energy efficiently without sacrificing quality, reliability, and performance of a product; and (3) environmental science projects consisting of basic research that supports breakthroughs in nuclear stockpile stewardship.

Over the years, many thousands of areas across the country have been contaminated; DOE is responsible for 10,000 of those sites and has allocated $60 billion for cleanup. The staggering costs of cleanup mean that only a fraction of the contaminated sites will undergo active remediation. In some cases, nature will be able to gradually attenuate the contaminants, particularly organic contaminants. In others, soil and groundwater are contaminated with inorganic materials that will require remediation. DOE currently has no established protocol by which to tell whether nature will be able to attenuate the contamination. DOE has asked Sandia Labs to take the lead in developing a DOE complex-wide natural attenuation protocol.

Researchers in the project titled “Mechanistic Models for Radionuclide Desorption from Soils” are looking for a way for site managers to answer the question, “Which ones do we have to clean up?” Sandia will write the guidelines that DOE will follow in site

Sandia has developed the MNAtoolbox for site managers to use to screen sites for the potential implementation of MNA (monitored natural attenuation). MNA refers to the reliance on natural attenuation processes under a carefully controlled and monitored site cleanup approach. The Web–based MNAtoolbox assesses the data about a particular site and allows the site manager to make a decision about whether or not to spend funds to clean up that site. By identifying and collecting the specific natural mechanisms that remove contaminants from the subsurface, Sandia researchers will make it possible for DOE to much more rapidly screen contaminated sites than was previously possible. This will lead to huge potential cost savings, in the millions of dollars.

THIS PAGE
INTENTIONALLY BLANK

3518.030

Designed Molecular Recognition Materials for Chiral Sensors, Separations, and Catalytic Materials

T. M. Nenoff, J. A. Shelnutt

The goal of this project is to develop materials that are highly sensitive and selective for chiral chemicals and biochemicals (such as insecticides, herbicides, proteins, and nerve agents) to be used as sensors, catalysts, and separation membranes. Sandia is using molecular modeling methods to tailor chiral molecular recognition (CMR) sites with high affinity and selectivity for specified agents. The work focuses on both silicate and nonsilicate materials modified with chirally pure functional groups for the catalysis or separations of enantiomerically pure molecules. We are using surfactant and quaternary amine templating to synthesize porous frameworks containing mesopores of 30 to 100 angstroms. We are using computer molecular modeling methods in the design of these materials, especially in the chiral surface-modifying agents. We are also using molecular modeling to predict the catalytic and separations selectivities of the modified mesoporous materials. The ability to design and synthesize tailored asymmetric molecular recognition sites for sensor coatings allows a broader range of chemicals to be sensed with the desired high sensitivity and selectivity. Initial experiments target the selective sensing of small-molecule gases and nontoxic model neural compounds. Further efforts will address designing sensors that greatly extend the variety of resolvable chemical species and forming a predictive, model–based method for developing advanced sensors.

In this project we synthesized and characterized both new chiral porphyrins and molecular sieves.

The chiral porphyrins include a computer-designed and then synthesized Ni(II) tetra(cyclopropyl) porphyrin (known as the "Venus fly trap" porphyrin) and the Zn(II) heptabromo-mono-2-methoxyphenyl-tetraphenylporphyrin. These molecules are unique because they were designed, synthesized, and characterized specifically for CMR. We coupled these materials to silicate and sol-gel support materials by surface modification. We characterized them by Raman spectroscopy, x-ray, and magic-angle opening nuclear magnetic resonance (MAS NMR), and showed them to retain their chirality; this is important for future use as a chiral separations material.

We also synthesized and characterized completely novel, chirally templated, inorganic (Zn/P) crystalline phases for separations. These phases include 2-D layered phases and a 3-D mesoporous phase. We showed these phases to be very pH- and concentration-dependent. Characterization techniques include transmission electron microscopy (TEM), x-ray diffraction, and thermal and elemental analyses. Furthermore, we grew these new phases successfully as inorganic thin-film membranes. Permeation modeling through the phases predicted the type of separations capable with these materials.

These important results led to a technical advance.

Publication

Refereed

Drain, C. M., S. Gentemann, J. A. Roberts, N. Y. Nelson, C. J. Medforth, S. L. Jia, M. C. Simpson, K. M. Smith, J. Fajer, J. A. Shelnutt, and D. Holten. 1998. "Picosecond to Microsecond Photodynamics of a Nonplanar Nickel Porphyrin: Solvent Dielectric and Temperature Effects." *J. Amer. Chem. Soc.* **120** (June): 3781.

Jia, S. L., J. Zhang, J. Ema, N. Nelson, C. J. Medforth, K. M. Smith, J. G. Ma, and J. A. Shelnutt. 1998. "Axial Ligand Affinity Variation Induced by Nonplanar Distortion." *Abstracts of Papers of the Amer. Chem. Soc.* **310** (Dallas, TX, March).

Jia, S. L., W. Jentzen, M. Shang, X. Z. Song, J. G. Ma, W. R. Scheidt, and J. A. Shelnutt. 1998. "Axial Coordination and Conformational Heterogeneity of Nickel(II) Tetraphenylporphyrin Complexes with Nitrogenous Bases." *Inorg. Chem.* **37** (July): 4402.

Lemke, C., J. A. Shelnutt, J. M. E. Quirke, R. Schweitzer-Stenner, and W. Dreybrodt. 1998. "The Effect of Meso-Nitro-Substitution on Nickel(II) Porphyrins." Paper presented to the Biophysical Society Meeting, Kansas City, MO, February.

Ma, J. G., M. Laberge, J. Zhang, S. L. Jia, J. M. Vanderkooi, and J. A. Shelnutt. 1998. "Raman Spectroscopic Investigation of Nickel Microperoxidase-11." *Biochemistry*, accepted.

Nenoff, T. M., A. Chavez, S. G. Thoma, P. Provencio, and R. S. Maxwell. 1998. "Templated Inorganic Thin Films." *Proc. Mater. Res. Soc. Symp.* (San Francisco, CA, April).

Nenoff, T. M., J. A. Shelnutt, S. G. Thoma, S. L. Jia, and P. Provencio. 1998. "Chiral Templating and Modeling for Separations and Catalysis." *Mater. Res. Bulletin*, accepted.

Nenoff, T. M., S. G. Thoma, P. Provencio, and R. S. Maxwell. 1998. "Zinc Phosphate Phases Templated with the Chiral Molecule d-Glucosamine." *Chemistry of Mater.*, accepted.

Shelnutt, J. A., A. L. Jia, T. M. Nenoff, C. M. Muzzi, C. J. Medforth, and K. M. Smith. 1998. "Computational Design of Chiral Catalysts Based on Novel Nonplanar Chiroporphyrins." *Abstracts of Papers of the Amer. Chem. Soc. 216* **21** (Boston, MA, August).

3518.050

Rapid Screening of Complex Chemical Samples Via Capillary Array Analysis

D. S. Anex, D. W. Neyer, D. M. Haaland, M. K. Alam, J. S. Schoeniger

Complete characterization of complex chemical samples often requires a series of time-consuming analyses. A carefully designed parallel analysis scheme can rapidly obtain and interpret a unique chemical signature from a complex sample. Toward this goal, Sandia developed a novel instrument and approach to sample analysis based on simultaneous separations in a parallel array of capillary columns. Each column in the array is individually optimized to probe a particular broad chemical characteristic of the sample. The array of columns is bundled in an instrument designed for simultaneous detection of the signals generated at each column. Since a particular component of a sample will migrate through each column in a different characteristic time, the chemical signature for a particular sample consists of migration times for all components in each column and individual component detector responses. Chemometrics can be used to interpret this complex signature and maximize the information obtained.

The project combined and exploited Sandia's strengths in capillary separations and parallel data collection (demonstrated previously in development of a multiple-capillary DNA sequencer) and was augmented by expertise in molecular recognition and chemometrics. The array instrument also serves as a platform for demonstrating concepts for powerful microfabricated devices, where highly parallel analyses can be naturally implemented. A low-cost, compact parallel analysis approach, enabled by this project, will lead to fieldable devices with capabilities that are not possible using current laboratory instrumentation. This new capability will lead to rapid screening and exacting molecular-level characterization of complex chemical samples encountered in environmental site characterization and monitoring. It will also advance industrial process control capabilities, as well as contribute to wider DOE and DoD national security missions.

The accomplishments of this year concentrated on the experimental aspects of refining the eight-capillary instrument, characterizing its performance, and analyzing real-world samples. Instrument refinement emphasized reproducibility (column-to-column and run-to-run) and robustness, especially when running real-world samples. Although it is still deemed important to the ultimate use of the array instrument, we did not use statistical analysis in the second year to the extent anticipated at the beginning of the project.

Through collaboration with the Environmental Sciences Division of the U.S. Environmental Protection Agency's National Exposure Research Laboratory, we identified a test sample consisting of polycyclic aromatic hydrocarbons and nitrogen-containing aromatic compounds. We also obtained a number of extracts of creosote-contaminated soil, which we expected to contain compounds present in the test sample. We designed an analysis method for this sample using a variety of mobile phase compositions in the different capillary columns in the array and laser-induced fluorescence detection.

We successfully demonstrated the instrument performance using the test sample. With respect to migration times through the column, column-to-column reproducibility was better than 5 percent, and the run-to-run reproducibility was better than 1 percent. We also successfully ran the real-world test sample and identified several targeted compounds.

Publications

Other

Anex, D. S. 1997. "Packed-Column Electrochromatography: Advances in Single-Column and Multiple-Column Techniques." Paper presented to the Departmental Seminar, Chemistry Department, Lehigh University, Lehigh, PA, 19 November.

Anex, D. S., D. W. Neyer, H. Zhao, R. Dadoo, R. N. Zare, and C. Yan. 1997. "Selectivity and Efficiency in Capillary Electrochromatography." Paper presented to the 36th Annual Eastern Analytical Symposium, Somerset, NJ, 16–21 November.

Anex, D. S., D. W. Neyer, R. N. Zare, and H. Zhao. 1997. "Packed-Column Electrochromatography: Advances in Single-Column and Multiple-Column Techniques." Paper presented to the 214th National Meeting of the American Chemical Society, Las Vegas, NV, 7–11 September.

Zhao, H., D. S. Anex, D. W. Neyer, and R. N. Zare. 1998. "Capillary Electrochromatography Using Arrays of Packed Columns." Paper presented to HPCE '98: The 11th International Symposium on High-Performance Capillary Electrophoresis and Related Microscale Techniques, Orlando, FL, 1–5 February.

Zhao, H., D. W. Neyer, R. N. Zare, and D. S. Anex. 1998. "Analysis of Complex Chemical Samples by Capillary Array Electrochromatography." Paper presented to HPLC '98: The 22nd International Symposium on High-Performance Liquid Phase Separations and Related Techniques, St. Louis, MO, 2–8 May.

3518.060

Designed Synthesis of Controlled Degradative Materials

T. A. Ulibarri, D. A. Loy, M. J. Carr, S. H. Scott, R. S. Saunders, J. G. Curro, T. R. Guess, D. R. Wheeler

Sandia will develop polymeric materials containing weak links for degradation capabilities that are activated only by specific keys. Weak links are specific functionalities that are susceptible to degradation and are placed within the polymer to provide readily cleavable sites. Placement of the weak links can occur randomly or at regular spacing. We will generate materials for three general applications:

(1) nonlethal deterrents, (2) removable encapsulants, and (3) readily recyclable/environmentally friendly polymers for structural and thin-film applications. In all three applications, a great benefit would result from the successful development of materials that can be controllably degraded into smaller components, thus providing facile removability and recyclability. In addition, we use commercial–based polymer formulations to create another class of readily degradable systems. While these systems may not provide as intricate a key system for degradation, they should provide workable materials for large-scale applications in a more timely manner than the weak-link systems. In addition, the development of these commercial–based polymer systems will provide further insight into useful degradation pathways that can be built into weak-link polymers. To understand the possible property changes manifested due to the weak-link incorporation, we will combine classical density-functional theory (DFT) with PRISM (Polymer Reference Interaction Site Model) calculations. We will correlate the information on polymer structure and thermodynamic properties generated through these modeling efforts with experimental mechanical characterization. Through this correlation, we will utilize a feedback loop for the synthetic effort to optimize the production of super-slick materials, as well as structurally similar weak link-containing polymers suitable for structural and thin-film applications. The ultimate goal of this project is to generate families of degradable materials that can be applied anywhere from in nonlethal deterrent systems to removable encapsulants and recyclable materials for the commercial market.

We used new linear and branched synthesis methods to generate high-molecular-weight, weak link-containing polymers. We chemically and mechanically characterized the most successful polymer system, a series of branched polyacrylamide/polyethylene oxide (PEO) copolymers. We achieved lubricity values approaching high-molecular-weight PEO with this copolymer system. We developed a bench-top screening method to assess lubricity using a MINIMAT Miniature Materials Tester and custom fixturing. Using this testing technique, we identified and characterized a commercial–based system using PEO and ascorbic acid (vitamin C) as a potentially deployable system for near future use. We identified viscosity measurements of polymer solutions as another method of evaluating the effectiveness of degradation processes. Since we proposed lubricity to be related to surface tension, we performed a series of DFT calculations on a polymer chain near a surface to identify the factors that are important in controlling surface tension. Surface tension appears insensitive to both polymer density and backbone stiffness; however, cohesive forces play a critical role.

3518.120

Adaptive 3-D Sensing

C. Q. Little, D. J. Schmitt, J. J. Carlson, D. E. Small, C. L. Nelson

The purpose of this project is to create sensing, reasoning, and control technologies that will allow the safe and effective cooperation of humans and intelligent machines in a variety of operations. This will rely heavily on real-time 3-D sensing and interpretation of the 3-D data. The results of this research will include a new adaptive 3-D sensing system as well as new research into dynamic object modeling, behavior recognition, and sensor–based control. The 3-D sensing system will combine two existing sensing technologies in a new way to create a site-monitoring system that can continuously maintain an accurate 3-D model of the site and real-time estimates of the shape, location, and motion of humans and machines. A key strength of this system will be the ability to monitor simultaneous activities, such as several robots and humans working independently, while also detecting unexpected entry into the workspace. We will use data from this sensing system to allow automated systems, such as robots, to not only safely co-exist with humans within the workspace but to also cooperate in performing tasks. This will improve the practicality and efficiency of many operations by simultaneously using the best skills of both humans and machines.

We set up a lab with a Fanuc robot, 3-D sensors, and a supervisory system to perform experiments in human-machine cooperation. The 3-D sensors include a laser-mapping system and a dynamic 3-D motion-detection system. We updated both 3-D sensor systems to operate on PC/NT platforms to maintain state-of-the-art computing, and improved performance on both systems. We selected a target application to demonstrate a human and robot working cooperatively to perform a task. We developed a control methodology to implement the cooperative behavior. Several safety systems are included to ensure safe operations at all times, including the robot, the supervisor software, an independent check for illegal entry into robot workspace, and the activated live-man switch the operator carries. We performed image segmentation work to aid in object recognition. We developed adaptive sensing to dynamically update the 3-D model as new data are collected.

We gave a human-machine cooperative demonstration with the system to the review team and a number of potential customers. In this demonstration, the robot system performs an automated task until a human walks into an area close to the robot. The robot becomes aware of the human through the sensor systems and tracks the human's movements. The human can then approach the robot and hand off a part. When the human backs away, the robot moves to identify the part and places it accordingly.

3518.070

Mechanistic Models for Radionuclide Desorption from Soils

P. V. Brady, P. Zhang, M. D. Siegel, D. J. Borns

The objective of this project is to develop and implement a procedure for relying on natural processes (monitored natural attenuation [MNA]) to clean up contaminated soils and groundwaters in the DOE complex. Sandia believes that complex-wide implementation of the technical protocol will result in the savings of several billion dollars in clean-up costs. The first two years of the project involved development of the technical protocol. In this time we collaborated with the U.S. Environmental Protection Agency (EPA), the New Mexico Environmental Department (NMED), and several of the national labs. Moreover, EM-43 began funding spin-off efforts.

We completed all experimental work on desorption (U-FeOOH; Sr-$CaCO_3$; Cs-Clays; Pb-FeOOH/Basalt) and published our book on natural attenuation. We developed a field–based technique for demonstrating natural attenuation of metals and radionuclides to regulators. We also completed the first versions of our technical protocol for natural attenuation of metals and radionuclides.

Above and beyond our milestones, the following happened as a result of this project:

(1) We were invited to present the MNA protocol to HQ DOE (Washington, DC, Las Vegas), the U.S. EPA, the Hanford Site, Lawrence Livermore National Laboratory, and the European Science Foundation (Crete).

(2) HQ DOE asked us to generate a completely general (including organic contaminants) version of the protocol for review by the National Academy of Sciences (NAS) and subsequent DOE complex-wide implementation. The NAS panel is reviewing all of the MNA protocols being used nationwide. Our contribution is the only DOE entry, as we have been chosen as the lead lab for complex-wide implementation.

(3) We were asked to help develop monitoring guidelines for HQ DOE.

(4) We evaluated the trends of the EPA's MNA implementation efforts.

Publications

Refereed

Brady, P. V. 1998. "Natural Attenuation of Inorganic Contaminants." Paper presented to the National Academy of Sciences Panel on Intrinsic Remediation, Washington, DC, September.

Brady, P. V. 1998. "Natural Attenuation of Metals and Radionuclides." Paper presented to the National Stakeholders Forum on Natural Attenuation, San Francisco, CA, August.

Brady, P. V., B. P. Spalding, K. M. Krupka, R. D. Waters, P. Zhang, and D. J. Borns. 1998. "Site Screening for Monitored Natural Attenuation with MNAtoolbox." Sandia Technical Report, in review.

Brady, P. V., B. P. Spalding, K. M. Krupka, R. D. Waters, P. Zhang, D. J. Borns, and W. D. Brady. 1998. "Site Screening and Technical Guidance for Monitored Natural Attenuation at DOE Sites." Sandia Technical Report, in review.

Brady, P. V., D. A. Lucero, and H. W. Papenguth. 1998. "Adsorption/Desorption of Sr from Calcite." *Proc. 8th Ann. Goldschmidt Conf.* (Toulouse, France, 7–12 August).

Eick, M. J., J. D. Peak, P. V. Brady, and J. D. Pesek. 1998. "Kinetics of Lead Adsorption/Desorption on Geothite: Residence Time Effect." *Soil Sci. Soc. of Amer.* (Rancho Mirage, CA, June), accepted.

3518.080

Development of Innovative Combustion Processes for a Direct-Injection Diesel Engine

J. E. Dec, P. C. Miles, D. L. Siebers

The engine for the Partnership for New Generation Vehicle (PNGV) is one of the most critical components for meeting the goal of 80 miles per gallon. In FY96, PNGV selected a small-bore, high-speed, direct-injection (HSDI) diesel as the best engine candidate. These engines offer high thermal efficiency, reliability, and compatibility with the existing fuel infrastructure and with projected PNGV vehicle designs. Despite the significant advantages of these engines, meeting PNGV's goals will require major technological advances that improve their efficiency, power density, and emissions. These advances include improvements in controlling fuel injection, in-cylinder air motion, combustion, and emissions formation. The current state-of-the-art, small-bore diesels (found in Europe) utilize two valves per cylinder and an angled, off-center, speed-dependent fuel injector. PNGV recently determined that this is not adequate and that the base engine configuration must have four valves per cylinder, variable swirl, and a vertical, center-mounted, high-pressure, common-rail fuel injector. In addition, advanced fuel-injection and combustion strategies are needed. Some promising new techniques are fuel injection-rate

modulation, water injection, enhanced-swirl combustion chambers, exhaust-gas recirculation (EGR), and modified fuels. This project will evaluate these technologies, down-select to the most promising, develop a research engine, and conduct research to determine the viability of the most promising technologies.

We completed installation and testing of the engine, but the engine and laboratory infrastructure are not yet operational. We investigated the ignition delay and locations in the optical research engine using pressure analysis and chemiluminescent imaging. We found that ignition delay measurements based on combustion luminosity and natural chemiluminescence are more sensitive than pressure measurements. We completed corresponding measurements, employing split-injection strategies.

We expanded investigations of fuel-water emulsions for simultaneously reducing the production of both NO_x and soot. The expanded data sets include three emulsion concentrations and parametric variations of engine operating conditions (top dead center [TDC] temperature, TDC density, and fuel loading) for some emulsion mixtures. We also implemented an additional diagnostic capability to quantitatively measure the changes in in-cylinder soot levels. This diagnostic involves a line-of-sight (LOS) extinction measurement through the operating diesel engine, which allows more rapid quantitative measurements of the relative soot concentration than previous laser-induced incandescence (LII) imaging measurements. We conducted several tests:

(1) We measured the straight fuel and an emulsion with 10% water in the fuel with the new diagnostic. For the base condition, the LOS extinction measurement showed that the emulsion reduced the in-cylinder soot levels by about a factor of two, which is in good agreement with previous measurements using LII imaging reported last year.

(2) We made parametric variations to the TDC temperature, TDC density, and fuel loading for both the straight fuel and the 10% emulsion. For both fuels, soot levels changed considerably across the parameter space. However, the 10% emulsion consistently produced lower soot levels for all conditions (approximately a factor of two lower).

(3) We increased the water concentration in the emulsion to 20%. This resulted in a further reduction of in-cylinder soot levels. Although the reduction varied with operating conditions, it was on the order of two-thirds of the level with the 10% emulsion, or about one-third of the soot level for the straight fuel.

(4) We further increased the water concentration to 30%. This produced even lower soot levels, but the drop was less significant, being only about 15% less than for the 20% emulsion. This indicates that we were reaching a point beyond which additional water would not offer further improvement.

These investigations show that water added to diesel combustion has a strong potential for reducing in-cylinder soot levels. Since water addition is well known to reduce NO_x emissions through its cooling effect on the combustion process, these studies show that fuel-water emulsions or dual fuel-water injectors have a strong potential for reducing diesel-engine emissions.

We presented results from the research and implications for design parameters to the U.S. engine manufacturers through three meetings associated with the DOE-funded Cooperative Research and Development Agreement (CRADA).

Publications

Other

Canaan, R. E., and J. E. Dec. 1997. “The Effect of Fuel-Water Emulsions on In-Cylinder Soot Levels.” Paper presented to the Diesel Combustion Review Meeting, Southfield, MI, 19 August.

Dec, J. E. 1998. “Report on the Line-of-Sight Diagnostic and Results with Diesel Fuel.” Paper presented to the Diesel Combustion Review Meeting, Dearborn, MI, 12 May.

Miles, P. C. 1998. “Small-Bore Diesel Update.” Paper presented to the Diesel Combustion Review Meeting, Dearborn, MI, 13 May.

3518.090

Hydrogen Production for Fuel Cells by Selective Dehydrogenation of Alkanes in Catalytic Membrane Reactors

T. J. Gardner, C. J. Brinker, A. G. Sault

Hydrogen-powered polymer electrolyte membrane (PEM) fuel cells, fueled by on-board H_2 generation from liquid fuels, represent an important technology for all-electric or hybrid-electric vehicles. Much current effort has been devoted to the use of steam-reforming or partial oxidation of liquid fuels for on-board H_2 generation, but these technologies generate large amounts of CO and CO_2, which can poison PEM fuel cells. Sandia will develop a catalytic membrane reactor system for the generation of pure H_2 via selective dehydrogenation of liquid fuels. We will achieve separation of H_2 from hydrocarbons and other potential contaminants (e.g., CO, CO_2, etc.) by modifying commercial alumina membrane tubes with size-selective microporous ceramic membranes. We will also use hydrous metal oxide (HMO)–based ion-exchanger technology to prepare novel bulk and coated dehydrogenation catalysts. These HMO materials are superior to conventional oxide supports, such as titania and silica, in that they can be synthesized to contain high concentrations of sodium ions, which can be ion-exchanged with transition-metal ions that are catalytically active for selective dehydrogenation. By using HMO–based catalysts, we hope to increase conversions achievable with a conventional catalyst inside the membrane tube. This overall scheme offers a potential method for increasing H_2 production rates without increasing reactor size, an important consideration for transportation applications or for remote electricity generation for civilian or military applications.

Previous membrane reactor studies identified a problem with low H_2 generation rates due to insufficient catalyst activity and selectivity combined with significant catalyst deactivation over time. Although HMO–based catalyst development identified Cr/silica-doped hydrous titanium oxide (HTO:Si) catalysts with high heptane dehydrocyclization activity on an active metal basis, increased metal loading did not result in the required improvement in catalyst activity or selectivity relative to commercial Cr–based catalyst (7.5 wt.% Cr/Al2O3). We also investigated Pt (and Pt-Sn or Pt-Re/HTO:Si)HTO:Si catalysts as an alternative to the Cr–based catalysts. We observed significant catalyst activity for the lower metal loading (~ 1 wt.% metal) Pt/HTO:Si catalysts; however, we encountered significant catalyst deactivation problems, and overall catalyst performance again fell short of the results obtained for the commercial 7.5 wt.% Cr/Al2O3 catalyst. Our catalyst development efforts were unable to identify an improved catalytic membrane reactor catalyst material relative to the commercial Cr/Al2O3 catalyst.

We pursued microporous ceramic membrane development in parallel with the catalyst development efforts. We developed a range of SiO_2–based membranes that offer the promise of superior H_2 separation performance combined with increased H_2 permeance. Various synthesis routes can be used individually or in combination to fabricate these membranes, including surface derivatization, fugitive organic templating, and surfactant templating. This past year, efforts concentrated on membrane fabrication via surfactant templating combined with surface derivatization techniques.

We developed a new process to form a highly selective membrane capable of discriminating H_2 (2.89^3) from N_2 (3.64^3), CO_2 (3.3^3), CH_4 (3.8^3), and CO (3.76^3) for fuel-cell applications. In practice, membrane formation is very sensitive to the quality of the support surface and the film-coating environment. Therefore, we first deposited a C_6-surfactant (triethylhexylammonium bromide)-templated silica intermediate layer on top of a commercial *g*-alumina support to both improve surface finish and prevent the subsequently deposited sol from penetrating into the support. Second, we dip-coated membranes under class 100 clean-room conditions to avoid dust contamination and vacuum-calcined them to promote further pore shrinkage. The vacuum calcination procedure apparently also resulted in the decomposition of surface ethoxy groups; therefore, a hydrophobic inner pore surface was formed to avoid water attack. This new procedure resulted in both high flux and selectivity for the asymmetric membranes with gradual changes of pore size from 50^3 (*g*-alumina support layer) to $10–12^3$ (surfactant-templated silica sublayer), and then to $3–4^3$ (ultra-microporous silica top-layer). For a pure gas-permeation experiment, H_2 flux reached $1x10^{-3}$ cm^3 (STP)/s/cm^2/cmHg with a H_2/CO selectivity of 200. The membrane also showed a high H_2 flux (5.4×10^{-4} cm^3 (STP)/s/cm^2/cmHg) at 80° C in the separation of hydrogen from a simulated fuel-cell feed stream (compositions: 33.98% N_2, 15.00% CO_2, 0.997% CO, balance H_2) as evidenced by a high concentration of hydrogen (92 mol.%) recovered in the permeate side stream. The CO concentration (CO is a fuel-cell poison) in the permeate was 193 ppm in a one-throughput feed condition.

Publications

Refereed

Lu, Y., G. Cao, R. P. Kale, S. Prabakar, G. P. Lopez, and C. J. Brinker. 1998. "Microporous Silica Prepared by Organic Templating: Relationship Between the Molecular Template and Pore Structure." *Chemistry of Mater.*, accepted.

Lu, Y., R. Ganguli, C. A. Drewien, M. T. Anderson, C. J. Brinker, W. Gong, Y.

Guo, H. Soyez, B. Dunn, M. H. Huang, and J. I. Zink. 1997. "Continuous Formation of Supported Cubic and Hexagonal Mesoporous Films by Sol-Gel Dip Coating." *Nature* **389** (25 September): 364–368.

Tsai, A. C., and C. J. Brinker. 1998. "Silica Gas Separation Membranes Prepared with Surfactant-Templated Sublayers." *Proc. 5th Internat. Conf. on Inorg. Membranes* **1** (Nagoya, Japan, 22–26 June): 180–183.

3518.110

Hybrid Vehicle Engine Development

P. Van Blarigan, K. L. Wu, N. J. Paradiso, Jr., S. S. Goldsborough, J. Wu, D. V. Zanini

An attractive approach to increasing the fuel efficiency and lowering the emissions of motor vehicles is the hybrid drive train. In the series-type hybrid, the engine drives only an electrical generator; electric motors power the drive wheels. With electrical energy storage this allows the engine to run at constant speed and power with the engine at maximum efficiency at all times. The concept of a variable compression ratio free-piston internal-combustion electrical generator subsidizes mechanical simplicity with electronic sophistication, resulting in a one-moving-part engine. The one moving part is a double-ended piston that oscillates in a cylinder that is closed on each end. Ports are placed in the cylinder walls to allow venting of the burned gases and introduction of a fresh fuel/air mixture in the two-stroke-cycle scavenging mode. Electrical output is generated directly from piston motion by fixing magnets on the piston, which moves through magnet steel and generates a time-varying current in fixed coils. Ignition is by compression heating of the homogeneous fuel/air charge, with timing accomplished by electronically controlling the compression ratio.

Several advantages ensue: (1) The compression is developed inertially and is not fixed. Thus, it can be controlled by kinetic energy management by the engine controller. (2) Homogeneous charge compression ignition (HCCI) can combust lean mixtures of hydrocarbon fuels, impossible with spark ignition, greatly reducing NO_x production. (3) All moving engine parts except the piston and inlet blower are eliminated. (4) Ideal Otto cycle performance is approached more closely than in a conventional engine due to rapid combustion and reduced heat transfer, a consequence of the velocity profile of the free piston. Coupled with the high-compression ratio of compression ignition, we anticipate that this engine will produce electricity with 40% less fuel than existing low-emissions designs. The goal of this project is to design, build, and demonstrate the performance of a prototype engine.

(1) We demonstrated substantial improvements in the efficiency of the HCCI combustion system over conventional combustion processes through the use of a free-piston, single-stroke, combustion experiment burning hydrogen, propane, natural gas, methanol, and dimethyl ether, and through computational investigations of the same. We noted the following findings:

(a) High-compression ratio (30:1) can be achieved at the time of combustion.

(b) A high rate of combustion for propane, natural gas, hydrogen, and methanol approaches that of constant volume combustion.

(c) While NO_x emissions do increase with increasing compression ratio, they can be controlled by decreasing the equivalence ratio since the problem of sparks igniting ultra-lean mixtures is not a concern in the HCCI combustion process.

(d) The autoignition characteristics of the fuels tested varied widely. The data showed that some fuels react in two stages and not completely. Generally higher initial temperatures and higher compression ratios burn more of these fuels. An additional factor that may affect the burning process, especially for the two-stage fuels, is the rate of piston oscillation. This variable should be investigated in the future.

(2) We tested the performance potential of hydrogen, propane, natural gas, methanol, unleaded gasoline, dimethyl ether, ethanol, isooctane, pentane, hexane, and heptane.

(3) We established important criteria regarding the design and construction of the linear alternator components of the electrical generator.

(4) We constructed a full-scale linear alternator tester.

(5) We developed a preliminary design for a linear alternator.

Publications

Refereed

Goldsborough, S. S. 1998. "A Numerical Study of a Free-Piston, Internal-Combustion Engine." *J. Soc. of Automotive Engin.* (Spring 1999).

Van Blarigan, P. 1998. "Advanced Hydrogen-Fueled Internal-Combustion Engines." *Energy and Fuels* (January).

Van Blarigan, P. 1998. "A Hydrogen-Fueled Internal-Combustion Engine Designed for Single-Speed/-Power Operation." *Internat. Assoc. H_2 Energy* **23** (7) (May): 603–609.

Van Blarigan, P., S. Goldsborough, and N. Paradiso. 1998. "Homogeneous Charge Compression Ignition with a Free Piston: A New Approach to Ideal Otto Cycle Performance." *J. Soc. Automotive Engin.* (Spring 1999).

Other

Goldsborough, S. S. 1998. "A Numerical Investigation of a Two-Stroke Cycle, Hydrogen-Fueled, Free-Piston Internal-Combustion Engine." MSME Thesis, Colorado State University, Fort Collins, CO (Summer).

3518.130

Aqueous Organic Sensor

D. S. Blair, W. C. Sweatt, M. J. Kelly, K. J. Kasunic, S. A. Kemme

Currently regulated drinking water standards dictate that concentrations of specific chemical compounds known as aromatic hydrocarbons *not exceed 5 parts per billion (ppb). However, detection and quantitation of compounds in water at these concentrations are extremely complex and are typically performed using purge-and-trap analytical methods. This approach has inherently long analysis times and, for field-deployable instrumentation, high device maintenance requirements and equipment failure rates. Sandia will build a new, unique sensor that has the potential to measure aromatic hydrocarbons in aqueous solutions at ppb concentrations. This technology uses spectroelectrochemistry as its fundamental transduction mechanism. Significant advances have been made in the past two decades in studies of metal/solution interfaces by spectroelectrochemical methods. Here, the detection and quantitation of analytes in water typically rely on monitoring the electrochemical generation of an optically detectable compound. However, in strongly protonating solutions (e.g., water), detection of a strongly absorbing ionic species, such as the benzo anion, can be problematic. This work recognizes and addresses that problem by modulating the electrode potential such that protonation does not occur on the time scale of the spectroelectrochemical measurement. The spectroscopic method that we are combining with electrochemistry is known as* Grating Light Reflection Spectroscopy *(GLRS). A new, emerging technology, it noninvasively provides information about the dielectric function (i.e., both the real and imaginary parts of the refractive index) of the sample. This can then be translated into quantitative chemical information. The goal of this research is to produce a field-deployable aqueous organic sensor that is compact, rugged, and simple to use.*

We designed, fabricated, and assembled all components of the optical spectroscopy system and the spectroelectrochemical cell. We then initiated the evaluation of the laboratory-prototype GLRS aqueous sensor. The key components of the GLRS experiment are the grating, the spectroelectrochemical cell, and the optical spectroscopy system. We evaluated gratings with 1.6-micron chromium metal lines deposited on glass. The spectroelectrochemical cell uses the metallized grating lines as the working electrode and incorporates a platinum mesh counter electrode and a silver wire quasi-reference electrode. Finally, we designed and fabricated two optical spectroscopy systems. The first system exploits the wavelength dependence of the angle of diffracted light from the grating. The second GLRS system scans the light source across the spectral singularity via the angle of the incident light. Our experiments to date show that the second system provides tremendous improvements in signal-to-noise (S/N) ratio compared to the first system. Further, it reduces cost, complexity, and size, all of which are extremely important when it comes to turning the laboratory prototype into a rugged, fieldable sensor. This system will work with a medium-power (5–10 mW), single-mode, frequency-stabilized laser source, which allows interferometric means for aligning the grating. This will further improve the quality of the GLRS data. The second system is simple and elegant, as are a number of planned improvements, all of which are projected to provide quantum, order-of-magnitude leaps in the sensitivity and detection limits of the GLRS aqueous organic sensor.

3518.140

Designed Ionophores for Liquid-Membrane Separation and Extraction of Metal Ions

J. A. Shelnutt, G. E. Bujewski, J. E. Miller, A. Martino

Sandia is developing new materials and processes for metal-ion separation and extraction based on selective transport of ions across membranes. Using molecular simulations, we are designing a new group of porphyrin–based ionophores (molecular ion-carriers) for selectivity in complexing and transporting metal ions by controlling basicity, shape, and size of the ionophores. Using the initial design results, we will design sandwich/clamshell ionophores specifically for extraction of heavy metals and radionuclides. We will synthesize and test promising ionophores for application in two different membrane systems. The first is a supported liquid membrane that separates two liquid phases—one

containing waste and the other a liquid from which the specified metal ions are extracted. The ionophores selectively transport a specified metal ion through the intervening liquid layer to give a pure solution of the metal ion that is easily concentrated. In the second, we are developing metal-ion transport and entrapment in surfactant vesicles using the new ionophores. Separation of the vesicles leaves a pure metal-ion solution. These extraction technologies offer convenient new means of separation and extraction for processing Mo^{99}, decontamination and decommissioning, radioactive-waste remediation, and heavy-metal waste stream treatment. The initial focus area is high-level waste tank remediation of heat and gamma emitters (^{137}Cs and ^{90}Sr), long-lived radionuclides (^{99}Tc), and other metal ions contained in high- and low-level waste. Ion-extraction technologies using designed ionophores lead to increased sustainability and lower cost and complexity of manufacturing processes. Adaptation to pump/treat methods for use at sites such as the White Sands Experimental Test Station and Tuba City is also considered. The technology is differentiated from other efforts (1) by using molecular simulation to engineer high-performance ionophores, (2) by applying Sandia's recognized expertise in computer-aided molecular design of unexplored ionophore types, and (3) by using two new membrane systems.

We synthesized more than ten potential free-base porphyrin ionophores and evaluated them for their ion-transport properties. We used both supported-liquid membranes and bulk-liquid membranes in the transport testing protocols. The ionophores included some porphyrins that are highly nonplanar and therefore expected to be good carriers. The ionophores tested exhibited a wide range of ion-transfer rates, varying from almost no transport to some that are comparable to or better than currently used ion carriers. As expected, the planar porphyrins are poor carriers, consistent with our initial hypothesis and also our molecular simulations of the porphyrin-ion complexes. We suspected that out-of-plane saddling of the porphyrin would be necessary to expose the lone pairs on the nitrogens so they could interact with the ion. The perceived requirement for saddling of the porphyrin structure turned out to be not so important, however. The reason is that many nonplanar free-base porphyrins are highly flexible and thus easily become saddled due to H-bonding and ionic interactions with the porphyrin core. This unexpected outcome effectively broadens the base of possible porphyrins suitable for computer design and synthesis as new ionophores. We structurally characterized many of the designed ionophores with UV-visible absorption, nuclear magnetic resonance (NMR), x-ray crystallography, and resonance Raman spectroscopy. We found relationships between porphyrin conformational and electronic properties and their ion-transport rates and will incorporate this information into the molecular design procedures. For example, the presence of electron-withdrawing substituents on the porphyrin is desirable because they apparently increase ion-transport rates. Because of the successes in liquid-membrane extraction methods, we focused less on the vesicle-extraction methods.

Publications

Refereed

Kadish, K. M., E. Van Caemelbecke, F. D Souza, M. Lin, D. J. Nurco, C. J. Medforth, T. P. Forsyth, B. Krattinger, K. M. Smith, S. Fukuzumi, I. Nakanishi, and J. A. Shelnutt. 1998. "Fluorinated Dodecaphenylporphyrins: Synthetic and Electrochemical Studies Including the First Evidence of Intramolecular Electron Transfer Between an Fe(II) Porphyrin p-Anion Radical and an Fe(I) Porphyrin." *Inorg. Chem.*, submitted.

Other

Qiu, Y., A. Martino, J. Kawola, and J. A. Shelnutt. 1998. "Porphyrins as Ionophores for Liquid-Membrane Metal Ion Extraction." *Abstracts of Papers of the Amer. Chem. Soc.* **215** (Dallas, TX, 29 March): 228.

3518.150

An Electromagnetic Imaging System for Environmental Site Reconnaissance

G. M. Loubriel, G. J. Denison, A. G. Baca, G. L. Peace

The advantages of time-domain, ultra-wideband transmitters for ground-penetrating radar (GPR) are many and well known: GPR has the potential for high-resolution subsurface imaging unmatched by any other subsurface sensing method. With GPR there are large contrasts between contaminated and noncontaminated regions. Thus GPR may detect man-made buried objects and detect and define the extent of contaminated soil. This project seeks to develop a GPR system that can be utilized for environmental site reconnaissance and, in particular, for (1) detecting disrupted soil layers where there is a potential for buried waste, (2) finding buried metallic objects such as 55-gallon drums at depths of up to 10 m (and other man-made objects at various depths), and (3) detecting contaminated soil. Because of the simplicity of the time-domain technique, the system will be fast enough to evaluate extensive land areas that may be contaminated. The primary disadvantages of GPR have been low penetration depth and low signal-to-clutter. This project is designed to minimize both of these problems. Sandia will augment the penetration depth by using (1) high-peak-power, high-repetition-rate operation for high average power, (2) low center frequencies that better penetrate the ground, and (3) short-duration impulses. The latter allow for the use of low platforms that increase the power on target relative to a high flying platform (due to the R4 *term in the radar equation, where* R *is the range to the target). We minimize clutter by time-gating the surface clutter return and using low frequencies (since natural objects are smaller than the wavelengths used here, and their cross-section is smaller than for higher-frequency systems). The factor that makes this work unique is that we will utilize direct time-domain radar at low frequency and high average power.*

We accomplished our major objectives: to model the problem, build an impulse transmitter for GPR field tests, and design a variable center frequency transmitter that we will build in the upcoming year. We also added a new task, to measure switch jitter and longevity. Three major efforts were required to meet the FY98 objectives: to theoretically model ground penetration to guide the transmitter development (carried out in collaboration with Duke University), perform pulser construction at fixed frequency (but higher than attempted previously), design a variable frequency system, and develop a switch. We started tests of the system in transmit/receive mode and of reflection from targets in air. The biggest challenge this year was to increase the operating frequency of the transmitter; this forced us to design and test different pulser designs that were variants of the original design. Because of the introduction of the new pulser designs, we wanted to assess the effect of the different designs on switch longevity. We added a new task, to measure switch jitter and longevity with the original pulser design.

Publications

Other

Loubriel, G. M., F. J. Zutavern, A. Mar, A. G. Baca, H. P. Hjalmarson, M. W. O'Malley, G. J. Denison, W. D. Helgeson, D. J. Brown, R. L. Thornton, and R. M. Donaldson. 1998. "High-Gain GaAs Photoconductive Semiconductor Switches: Switch Longevity." *Proc. 23rd Internat. Power Modulator Symp.*

RISK & RELIABILITY

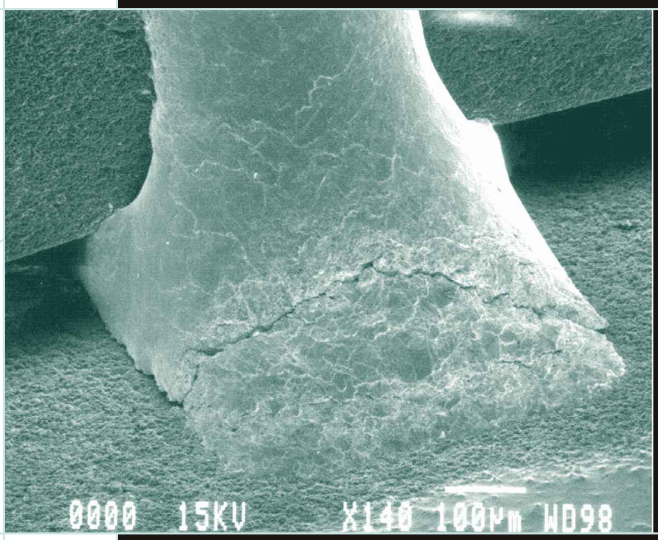

Sandia's primary mission of stockpile stewardship requires a superior understanding of how to manage the risks and to ensure the reliability of nuclear weapons and waste and other high-value assets. This area sponsors development of methods and tools as well as new components and systems to support the Sandia mission.

The Risk and Reliability investment area encompasses four categories of study: (1) predicting risk and reliability for systems and components; (2) studying how products and technologies age; (3) developing methods, techniques, and tools to evaluate how design changes affect reliability; and (4) developing approaches and tools to detect potential problems and to maintain equipment and systems.

Traditional reliability methods depend on the collection of a large number of samples or observations to characterize the existing condition of the weapons stockpile. A major objective of this research is to develop mathematical techniques and computer analysis tools to anticipate stockpile problems before they become critical issues. This approach permits a more efficient use of limited test resources and also assists design engineers in planning for new materials and manufacturing techniques. This is particularly important as Sandia moves toward commercial off-the-shelf replacement components.

This research focused on developing mathematical methods for incorporating uncertainty in traditional modeling, in particular, the advanced phenomenological modeling and simulation techniques used to characterize the physics of the underlying failure processes. The overall objective of the research is to statistically characterize how the performance characteristics of the system change as a function of system age.

We are currently using the analysis tools developed under this project to characterize the reliability of the national electrical power grid. These new reliability and uncertainty analysis methods could easily be integrated into the Product Realization Environment (PRE) framework. The PRE framework has been designed and developed in support of Sandia's Product Realization backbone with the goal of providing new and improved information tools to help reduce the time and cost for realizing nuclear weapons components.

THIS PAGE
INTENTIONALLY BLANK

3520.220

Integrated Approach to Develop Microelectromechanical (MEMS) Reliability Tools

D. M. Tanner, L. W. Irwin, N. F. Smith, K. A. Peterson, W. P. Eaton, P. Tangyunyong

The burgeoning new technology of microelectromechanical systems (MEMS) shows great promise in the weapons arena. We can now conceive of microgyros, microsurety systems, and micronavigators that are extremely small and inexpensive. Do we want to use this new technology in critical applications such as nuclear weapons? The answer to this question drives us to understand the reliability and presently unknown failure mechanisms of MEMS.

Sandia assembled an interdisciplinary team that integrated the individual research areas of failure and performance analysis, reliability characterization, and wafer-level reliability. This work has not been attempted before and will produce the knowledge that is essential for maintaining world-class MEMS status at Sandia. The overall goals of this work are (1) to perform statistical characterization, (2) to identify failure modes, (3) to develop reliability test structures, (4) to develop reliability models that account for temperature, humidity, cycles, operating speed, etc., and (5) to develop failure analysis tools for MEMS.

In meeting our goal of statistical characterization, we successfully used SHiMMeR (Sandia High-Volume Measurement of Micromachine Reliability) to acquire data on microengines driving loads at different stress frequencies. We observed wear as the main failure mode in this experiment. We developed a reliability model that predicts the failure as a function of number of revolutions and stress frequency. We based the model on the fundamental physics of wear coupled to mechanical resonance effects. We effectively used the basic wear model to describe failures in different MEMS devices.

Since many of the critical applications for MEMS require that the part lie dormant, then work when needed, we started several storage-life experiments. The experiments are ongoing; preliminary results indicate a failure of 10% in 8 months, implying that this is an area that needs further investigation.

We built up an incredible amount of infrastructure needed to perform the reliability experiments. We now have a super microdriver computer code that can drive any MEMS device; an environmentally controlled chamber to perform experiments; automated wafer-probing capability; and SHiMMeR Lite, a smaller data-acquisition station that allows small fast experiments to follow up on promising ideas.

To facilitate the understanding of fundamental failure modes, we designed several reliability test structures to measure friction and wear of rubbing surfaces and are currently fabricating them.

Publications

Refereed

Tanner, D. M., W. M. Miller, K. A. Peterson, M. T. Dugger, W. P. Eaton, L. W. Irwin, D. C. Senft, N. F. Smith, P. Tangyunyong, and S. L. Miller. 1998. "Frequency Dependence of the Lifetime of a Surface-Micromachined Microengine Driving a Load." *J. Microelectron. Reliability*, submitted. SAND98-1968J.

Other

Eaton, W. P., N. F. Smith, L. Irwin, D. M. Tanner, J. J. Allen, S. L. Miller, and W. M. Miller. 1998. "Characterization Techniques for Surface-Micromachined Microengines." *Proc. SPIE, 1998 Symp. Micromachining and Microfabrication* **3514** (Santa Clara, CA, September): 171–178.

Miller, S. L., M. S. Rodgers, G. LaVigne, J. J. Sniegowski, P. Clews, D. M. Tanner, and K. A. Peterson. 1998. "Failure Modes in Surface-Micromachined Microelectromechanical Actuators." *1998 Proc. IEEE Internat. Reliability Phys. Symp.* (Reno, NV, March): 17–25.

Peterson, K. A., P. Tangyunyong, and A. A. Pimentel. 1998. "Failure Analysis of a Surface-Micromachined Microengine." *Proc. SPIE, 1998 Symp. on Micromachining and Microfabrication* **3512** (Santa Clara, CA, September): 190–200.

Tanner, D. M. 1998. "Reliability of Surface-Micromachined MEMS Actuators." Paper to be presented to the IEEE 22nd International Conference on Microelectronics (Invited keynote), Nis, Yugoslavia, 19–22 September 1999.

Tanner, D. M., L. W. Irwin, W. P. Eaton, N. F. Smith, K. A. Peterson, and W. M. Miller. 1998. "Linkage Design Effect on the Reliability of Surface-Micromachined Microengines Driving an Inertial Load." *Proc. SPIE, 1998 Symp. Micromachining and Microfabrication* **3512** (Santa Clara, CA, September): 215–226.

Tanner, D. M., W. M. Miller, W. P. Eaton, L. W. Irwin, K. A. Peterson, M. T. Dugger, D. C. Senft, N. F. Smith, P. Tangyunyong, and S. L. Miller. 1998. "The Effect of Frequency on the Lifetime of a Surface-Micromachined Microengine Driving a Load." *1998 IEEE Proc. Internat. Reliability Phys. Symp.* (Reno, NV, March): 26–35.

3520.210

Reliability Degradation Due to Stockpile Aging

D. G. Robinson, P. C. Butler

This research involves the development of a new method for characterizing the reliability of systems with the time-dependent failure modes associated with stockpile aging. Current stockpile reliability assessment techniques do not consider time-dependent degradation of components, but instead view system operation as a go/no-go situation. Fundamental to the approach being investigated here is the hypothesis that, by monitoring system performance through testing in conjunction with science–based modeling, it is possible to characterize time-dependent changes in material properties and identify aging-related problems earlier, with fewer test resources. This requires the coupling of the actual physics associated with degradation with uncertainties in material properties, storage environment, etc. The potential applications to be addressed involve stress-voiding of electronic interconnects, thermo-mechanical fatigue of integrated circuit (IC) packaging, and the corrosion of electronic components, all of which we identified as high-consequence, high-likelihood stockpile issues. Of particular concern was the need to assess the reliability of submicron interconnects common in ICs as they are affected by a failure mechanism known as stress-voiding. *Stress gradients in the metallization are caused by a mismatch of thermal expansion coefficients. These gradients are known to drive mass transport and void growth. The original thrust of this research was to construct a reliability model for this process. However, as this research progressed, various design and analysis groups identified the potential of this new approach, and other applications were investigated.*

A number of probabilistic methods could potentially be applied, at least in part, to this problem. The emphasis of the research was on the documentation and software coding of the existing techniques, applying these techniques to existing stockpile problems, and identifying weakness in the existing probability and reliability methods. We applied the methods to provide insight into not only the stress-voiding problem, but also the time-dependent electronic component failure due to atmospheric corrosion. As we investigated each of the techniques, we coded a software routine, incorporated it into a general uncertainty analysis package (CRAX), and evaluated it relative to computational efficiency and accuracy. We will complete a survey of the predominant probabilistic methods. This document discusses each method in technical detail and is applied to a simple working example. (The example involves the stress-voiding of electronic interconnects.) We also present a summary of the computational requirements along with the technical limitations of each approach.

Publications

Refereed

Mahadevan, S., D. Robinson, and Z. Guo. 1998. "Probabilistic Analysis of Stress-Voiding Problem in Aluminum Interconnection Lines." *IEEE Trans. on Reliability*, submitted.

Robinson, D., S. Mahadevan, and Z. Guo. 1998. "Time-Dependent Stress-Voiding Reliability of Electronic Circuits." *Proc. 3rd Internat. Conf. on Computational Stochastic Mechanics* **1** (Santorini, Greece, 14–17 June): 100–124.

Other

Robinson, D. G. 1998. "A Survey of Probabilistic Methods Used in Reliability and Uncertainty Analysis: Analytical Techniques I." Sandia Technical Report SAND98-1189 (June). Sandia National Laboratories, Albuquerque, NM.

3520.230

Precursors to Failure of Oxides and Metal Lines in CMOS Technology

W. F. Filter, W. L. Larson, L. W. Irwin, S. H. Yazzie

Sandia originally proposed a paradigm shift away from statistical reliability toward individual part reliability. Historically, reliability engineers conducted long-term, expensive, large-sample lifetime tests to predict the reliability of electrical components. Sandia and the integrated circuit (IC) industry have since implemented a model–based methodology that uses test structures to predict the reliability of components as a group. However, both of these strategies treat component reliability statistically and are valid only for large numbers of parts. This is not a complete methodology in a world of low-volume production and use. We will use electrical-failure precursors to tell when individual devices are going to catastrophically fail.

An electrical-failure precursor is any electrical signal that gives warning of a component's impending demise. People are already familiar with other precursors in their everyday lives: the creak of a wooden board about to break, or the cracks that appear in an ice-covered pond just before it gives way. Likewise, electrical precursor signals from failing microelectronics would provide similar warnings of failure, if only we were able to recognize and model them. This would result in major benefits: (1) ability to characterize individual component reliability, thereby allowing small numbers of parts to be

used, (2) ability to use components until near the end of life with sufficient warning to procure replacements (such as through block upgrades), and (3) ability to automate reliability surveillance, possibly resulting in components that monitor themselves or ICs that monitor system or subsystem reliability. In a world of increasing lifetime expectations from a smaller stockpile, the understanding and implementation of a science–based reliability precursor detection and characterization scheme might allow us to have longer-lived parts with better-characterized reliability. Therefore, our overall goal is to gain an understanding of electrical-failure precursors for insulators and conductors in ICs, to model these precursors, and to create a method for predicting failure times based on these models.

After redirection by the review panel, we focused our investigation of electrical precursor signals in ICs on electromigration experiments on metal conductors; we dropped the investigation of dielectric breakdown. Programmatically, this redirection occurred because of a perceived greater importance of metal breakdown in weapons systems over dielectric breakdown. Technically, the dielectric breakdown studies that were dropped may have been the more promising of the two, being based on a firmer theoretical and modeling foundation.

In performing new electromigration testing, we discovered that our current electromigration testing methodology, termed *isothermal*, probably created breakdown that we would not expect to occur in normal use. This meant that the precursor signals observed in these experiments would not necessarily manifest themselves under normal wearout, leaving the quantification and interpretation of the precursors in doubt. The isothermal test method is based on joule-heating a metal test stripe with a high-current density and adjusting the current to a target stress temperature until catastrophic failure. The problem with this method is that, when a metal stripe develops a void as failure occurs, the temperature of the nonvoided section of the stripe can drop significantly in an unknown way. Temperature is a key parameter in this testing, yet control of temperature was lost at this point. A simpler, low constant-current stress test, where temperature was not determined by the stripe current, was put in place to get rid of the uncertainty.

We observed that precursor signals still occurred at a low-stress current; however, the failure signatures did not occur at the times predicted by extrapolating the highly accelerated isothermal stress data using a well-established time-to-failure equation (Black's equation). This discovery caused us to question and review our department's long-established electromigration testing methods and procedures. The low-current testing performed as part of this year's activities resulted in precursor signatures occurring very quickly. Warning times were very short, less than 5% of the remaining test-stripe lifetime. Data acquired the previous year using the isothermal method had resulted in precursors at approximately 10%–15% of remaining stripe lifetime. Obviously, the time of occurrence of the precursor depended on the test conditions to the extent of obscuring any fundamental physical triggering, and any study of what the best test methodology should be would go far beyond the work and budget established for this project.

This year we also questioned whether or not the standard electromigration test equipment used to detect precursor signals had sufficient bandwidth. To answer this question, and to analyze precursor characteristics in the frequency domain, we prototyped a higher-bandwidth test system to capture and measure the electrical signatures. Data from this test system indicated evidence of faster precursor spikes that could perhaps be used to understand the basic physics of precursors. However, understanding the basic physics is well beyond the scope of the current project. A much less noisy high-bandwidth test system than the prototype needs to be built. With this accomplished and a careful correlation of precursor events to transmission electron microscopy (TEM) analysis of changes in the test-stripe microstructure, we may discover a physics–based understanding of these electrical precursors caused by electromigration. In the original provision for this project, we lacked an understanding of the complexity of the problem—the importance, complexity, and wide variance of metal microstructure; the sensitivity of test equipment required; and the need for realistic electromigration testing. We could probably develop a predictive methodology for component end-of-life reliability using precursors as impending failure warnings, given a realistic appreciation of the complexity of such a task and a correspondingly appropriate allocation of funds.

3520.240

An Extensible Object-Oriented Framework for Risk and Reliability Analysis

G. D. Wyss, D. R. Funkhouser, R. L. Vandewart, R. L. Craft

To assess a system's risks, an analyst must understand the system's dynamics and structure and have expert domain knowledge (particularly in viable faults and attacks). The large volume of information required can obscure the system-wide effects of changes in a given system element. This project developed a demonstration prototype for an extensible tool to support risk assessment of multi-disciplinary systems. The project established the requisite theoretical basis for an object-oriented risk analysis approach. In this approach, each system element is represented by a risk object that contains a knowledge base about the element's failure modes, support requirements, and spatial and temporal characteristics. In addition, each object contains pieces of generic risk models that can be automatically assembled to form system risk models. Through a blend of object-oriented system modeling, simulation, and expert decision aids, the tool provides a framework for the capture and presentation of current and future expert risk knowledge. As every risk analysis model is currently hand-tooled, encapsulating domain-specific knowledge into risk objects enables risk analysts to generate studies more quickly and with greater confidence that they have not omitted important risk sources, thus spending less to obtain a better product.

We demonstrated that concepts derived from object-oriented analysis form an excellent common language for the information required by system designers, simulators, and surety analysts, and that this language can form the basis for a knowledge repository that is common to all of these disciplines. We also demonstrated that the models required to perform surety analyses (especially risk and reliability analysis models) can be derived from the object-oriented analysis methodology provided that the concepts embodied in the object models support both inductive and deductive qualitative reasoning. We also demonstrated that all major elements of this modeling methodology will be representable in a standardized language once the Universal Modeling Language (UML) is extended to incorporate data-flow diagrams. Commercial off-the-shelf software to implement UML is already available. We also developed systematic rules by which one can automate the derivation of many surety analysis models from a single common object model. Derivable analysis types include failure modes and effects analysis, HAZOP (hazards and operability study), event trees and fault trees, and discrete simulation analyses. We implemented the fault tree methodology in a simple demonstration program that made use of JAVA programs coupled to the ROSE commercial computer-aided software engineering tool. The fact that we were able to generate these rules and implement them in software means that we were able to prove the major portion of our hypothesis: namely, that it is possible to construct a single object–based model to represent the behavior of a system, and to automatically extract from that object model a wide variety of types of risk and reliability analysis models. Another point that we verified under this project was the ability to construct generic object models for individual components that can be assembled and customized rapidly to build the common object model. This stands in stark contrast to traditional risk and reliability model development techniques, which require a human analyst to construct each individual model by hand. Thus, the methodology developed under this project can dramatically reduce the amount of time required to develop risk and reliability models for complex systems.

Publications

Refereed

Craft, R. L., G. D. Wyss, R. L. Vandewart, and D. R. Funkhouser. 1998. "An Open Framework for Risk Management." *Proc. 21st Nat. Inform. Sys. Scty. Conf.* **1** (Arlington, VA, 5–8 October): 291–302.

Wyss, G. D., R. L. Craft, R. L. Vandewart, and D. R. Funkhouser. 1998. "Recasting Risk Analysis Methods in Terms of Object-Oriented Modeling Techniques." *Sys. Safety: The Total Solution, Proc. 16th Internat. Sys. Safety Conf.* **1** (Seattle, WA, 14–19 September): 198–207.

3520.270

Simulation/Optimization Tools for System Variability Analysis

J. E. Campbell, B. M. Thompson, K. D. Marx

Sandia has used electrical system simulation successfully over the past decade. Two common applications are (1) supporting the electrical system design process and (2) analyzing anomalies detected in the fielded product. Simulation also has a future role in helping to predict failures when degradation precursors are identified. In short, electrical simulation is a tool that can be used during the entire product lifecycle to develop an understanding of the system over the range of expected conditions.

Electrical simulation typically treats a single data point in the very large input space of component properties. For electrical simulation to reach its full potential as a design tool, it must be able to address the unavoidable variability and uncertainty in component properties. Component variability is strongly related to reliability of the end product. This project addresses a set of problems that hinder effective use of simulation, especially in the context of understanding variability.

The first goal of this effort was to create a novel linkage of disparate variability analysis approaches to greatly reduce the overall analysis time. There is an associated need for methodologies to effectively apply this toolset to a range of problem types. The second goal is to develop an approach to quantify the reliability impacts of variability, especially for time-dependent issues. Ultimately, we will explore the benefits and limitations of the developed tools and methodologies, including a consideration of the uncertainties and underlying assumptions.

In pursuing this project, it became apparent that there are two complementary paths to be explored: variability analysis and optimization. Each has its role in the product lifecycle, and each poses a unique set of challenges.

I. *Selection of Analysis Issues*

• Identify specific stockpile problems of interest to analyze (aging and nonaging).

(1) We identified and analyzed a simple filter problem to test the variability analysis toolset.

(2) After an initial parameter screening study, we may use the tools developed in this project to analyze variability for both aging and nonaging parameter sets.

(3) We are developing an attributes data (pass/fail) contour for a firing set high-voltage breakdown issue. We are examining three parameters (breakdown resistance, inductance, and time) using the project tools.

II. *Tool Linkage*

• Develop software for linked input vector generation and net list formulation.

This software is currently in two pieces. The first converts an input vector file into a form that can be parsed and combined with a circuit file; this is a combination of SUNS (Sensitivity and Uncertainty Analysis Shell), which creates an input vector file of sample values, and some additional code that converts an input vector file into a form that can be parsed. The second actually parses the input vector and builds the circuit net lists.

• Explore means for MPACTR (Massively Parallel Computer Resource) program management and input/output (I/O) management.

(1) We selected a newer version of SPICE (Simulation Program with Integrated Circuit Emphasis) (3f5) that has more capability and will also run on the MPACTR machine.

(2) In conjunction with another project, we implemented the MPACTR Distributed Queuing System (DQS) to allow for program and I/O management of multiple SPICE jobs.

• Formulate a set of software routines to automate extraction of response variable values from output data (include such variables as rise/fall times, peak values, pulsewidths, etc.).

We implemented one custom data-extraction routine (selection of a 3 dB cutoff frequency).

• Link software elements for the end-to-end tool package.

We made significant progress in coupling the tools for variability analysis.

(1) The kernel of the variability analysis toolset, SUNS, is now running under Windows, and we completed a draft user's manual.

(2) The kernel of the optimization analysis toolset, GO (Genetic Optimization), is now running under Windows, and we completed a draft user's manual.

(3) We developed a script that takes an input vector and converts it into a set of net lists that are then automatically executed on the MPACTR machine.

(4) Another script extracts outputs from the SPICE files and consolidates them for analysis.

III. *Tool Use Methodology*

• Identify issues and caveats for top-down and bottom-up approaches.

We have explored two methodologies for SUNS to date:

(1) Determining the impact of input parameter variability on system output and system output variability (R/C [resistor/capacitor] circuit cutoff frequency example).

(2) Using a state-space examination to generate an attributes (pass/fail) contour. This is a first step in mapping variability to reliability. Other methodologies (particularly top-down approaches) remain to be developed, including (a) parameter screening, (b) attributes contours in the presence of variability, and (c) optimization for design-for-reliability.

• Work selected problems with unlinked tools and validate.

The firing-set high-voltage breakdown problem is in progress. We will complete the variability analysis of the W80 firing set.

IV. *Reliability Methodology*

• Identify issues and caveats for top-down and bottom-up approaches.

We have explored two methodologies for SUNS to date:

(1) Determining the impact of input parameter variability on system output and system output variability (R/C circuit cutoff frequency example).

(2) Using a state-space examination to generate an attributes (pass/fail) contour. This is a first step in mapping variability to reliability.

• Work selected problems with unlinked tools and validate.

The firing-set high-voltage breakdown problem is in progress.

3520.280

A Massively Parallel Microsimulation Model of Infrastructure Interdependency

D. C. Marozas, R. J. Pryor, D. L. Harris

The U.S. infrastructure is a complex system of interdependent elements whose continued operation is vital to the security of the United States. These interdependencies create tremendous vulnerabilities that must be understood and managed to minimize the impact of deliberate disruptions, human error, or natural disasters to the surety of the infrastructure system. We are utilizing Sandia's unique microsimulation approach to develop a model of critical infrastructure interdependencies. This simulation technology capitalizes on recent technological advances in evolutionary learning algorithms and massively parallel (MP) computing. We model interactions individually among infrastructure elements by intelligent agents—one for each interaction. This modeling protocol can utilize thousands of agents to model very complex systems and offers several advantages over traditional modeling techniques for modeling infrastructure interdependencies. For example, unlike analytic models, functional forms of the model's endogenous relationships are not required. For problems where macroscale information is sparse or nonexistent, as is the case for infrastructure interdependencies, microsimulation models are differentiated in their capacity to utilize existing rich sources of microlevel data to develop interaction forecasts.

Extending Sandia's ASPEN microsimulation model of the economy to include rules and interactive agents for additional infrastructures will improve ASPEN's capabilities to the study of extremely complex, interconnected networks. In addition, we are using ENERGY 2020, an existing agent–based, regionalized, interdependency-focused energy model as the prototype for a microsimulation model of the energy infrastructure. This combination will provide a powerful framework for quickly delivering a credible model of three infrastructures (i.e., telecommunications, banking and finance, and power) most critical to the nation's economy and security.

We modified Sandia's ASPEN program to incorporate the effects of telecommunication disruptions. We also improved simulation methods to account for shocks resulting from communication disruptions. To test coding changes, we modified ASPEN's prototype model and analyzed several calculations of disruptions of varying degrees. We created a single processor version of the code to run on a fast workstation to improve testing speed and to provide a version of the code that could be delivered to customers for direct use. We also developed a user interface for the Internet, where outside users can set up and run simulation problems in ASPEN that include telecommunication disruptions. Results from the telecommunication prototype indicate that infrastructure disruptions can be modeled with ASPEN. We identified and are incorporating software changes into the development model. We collected data on wide-area telecommunication outages to provide information for calibration and to identify agent behavior during disruptions.

To rapidly build a model capable of addressing multi-infrastructures, we evaluated a well-established planning and policy analysis model, ENERGY 2020, for its potential to be combined with ASPEN and to provide a prototype for the electric and gas/oil infrastructure. Like ASPEN, ENERGY 2020 is an agent–based simulation model, but is focused on energy infrastructure interactions and thus provides agent definitions for electric and gas utilities. Like ASPEN, it models fundamental infrastructure system feedback loops, critical to understanding and predicting responses to unexpected perturbation or shocks. The ENERGY 2020 code is written in a dynamic simulation language called PROMULA that is not transferable to Sandia's multiple processor computer platforms. To develop a combined economic/energy infrastructure model, we wrote a translator that reads PROMULA and converts the code to C++, which is compatible with Sandia's high-performance computing platforms. We successfully converted a simplified version of ENERGY 2020 to C++ and inserted message-passing interface (MPI) calls in the code to allow it to be executed on the DEC 8400 multiprocessors. We parallelized ENERGY 2020 in several ways: (1) ran a different scenario on each processor, (2) ran a different state, economic category, and electric company on a separate processor, and (3) ran parts of each procedure on each processor.

We modified the PC version of ENERGY 2020 to simulate daily dispatch of the power plants and track unserved power load due to outages. We revised the seasonal dispatch to simulate twelve time periods (Monday through Friday for the summer and winter, plus a dispatch for the rest of the summer and the rest of winter). We ran this model with a one-day outage to several generating units and transmission lines both with and without any gaming. In this case, gaming means generators who adjust their prices to increase their revenues. We are using results to evaluate the ENERGY 2020 model for estimating the impact of power outages and to develop a strategy for incorporating power disruptions in a combined ASPEN/ENERGY 2020 model in the next fiscal year.

Developing the behavioral algorithms for individual agents in a multi-agent model is one of the challenges of producing useful models.

We investigated both genetic algorithms and genetic programming approaches for developing price-setting strategies for industrial agents in ASPEN. We developed a JAVA toolkit of genetic algorithms for use on Sandia's MP DEC8400 computer.

Publications

Other

Pryor, R. J., D. Marozas, M. Allen, O. Paanen, K. Hiebert-Dodd, and R. K. Reinert. 1998. "Modeling Requirements for Simulating the Effects of Extreme Acts of Terrorism: A White Paper." Sandia Technical Report SAND98-2289 (October). Sandia National Laboratories, Albuquerque, NM.

3520.320

Reliability Predictions for Advanced Electronics in Smoke Environments

T. J. Tanaka, S. P. Nowlen, V. F. Nicolette, C. R. Shaddix, J. E. Brockmann, D. J. Anderson, C. W. Bogdan, L. A. Gritzo

Smoke causes disruption and failure of advanced electronics by increasing conductivity. The conductivity is highest while the smoke is in the air and decreases as the smoke settles or is vented away. Video recordings show that delicate soot chains form on high-potential surfaces and may create solid soot bridges. Air movement breaks the soot bridges and reduces conductivity if the smoke concentration drops. This project will model smoke effects on electronics as a function of the type of smoke by measuring real-time electrical parameters. This model can be used to include the effects of smoke in fire-risk assessments.

The real-time measurements include smoke conductivity for different dc voltages, and conductance and susceptance for a range of ac frequencies. Sandia will use the conductivity information in conjunction with an electrical circuit modeling program, Simulation Program with Integrated Circuit Emphasis (SPICE), to determine the smoke concentration that should cause failure. We will test the model using memory chips and other equipment contributed by outside sponsors. The failure of the electronics will then be linked with fire models that calculate smoke production and transport.

Our goal was to measure the parameters that are important in causing failure in electronics. Using a small-scale smoke-exposure chamber developed for the U.S. Nuclear Regulatory Commission, we developed, purchased, or borrowed hardware and software to measure these parameters. The measurements include conductivity between parallel plates, conductivity on surfaces, dielectric constant, smoke mass density, smoke optical density, soot deposition, and digital-signal error rate.

Three significant improvements to the smoke research include two new computers, a modern program to control the smoke exposure and measurements, and a new multimeter. Because of these improvements, the measurement cycle time decreased from 1 minute to 10 seconds. We upgraded the smoke optical density to a laser beam and built a manifold to obtain multiple filter samples. We upgraded the computer system, developed a new program to control the system, and began the tests, which are proceeding rapidly. We burned polyvinylchloride cable insulation, JP-8 aviation fuel, and douglas fir to produce the smoke.

Our measurements show that conductivity between the parallel plates increases when soot, attracted to high-voltage surfaces, collects as long chains and forms bridges between the surfaces of opposite polarity. The soot collects on high-voltage surfaces just as dust collects on electrostatic precipitators. The soot chains are fragile and can be broken by air movement, but can rebuild if the smoke concentration is high. The chains are best produced by soot from flaming fires. Smoldering fires produce conductivity on surfaces, but do not bridge air gaps. High conductivity on parallel plates occurs for JP-8 and cable insulation.

The conductivity increases with the amount of fuel burned and can remain significantly high if little air movement is induced in the smoke chamber, even if the smoke concentration drops. Because of the solid nature of the soot bridges, the conductivity is not directly proportional to the smoke concentration as measured by optical density. We assume that the conductivity of the soot is dependent on the chemicals present and the humidity, and we plan to measure the conductivity per mass or volume of soot collected on high-potential surfaces.

The multiple air filter samples show that the optical density is proportional to the mass density. These measurements are comparable to results of other researchers at the National Institute of Standards (NIST). This research has increased interest in smoke effects during fires.

Publications

Refereed

Tanaka, T. J., and J. T. Chapin. 1998. "The Effect of Smoke from Plastics on Digital Communications." Paper presented to the Plastics in Telecommunications Conference VIII, London, UK, 14–16 September.

3520.290

Physical Models for Predicting the Effect of Atmospheric Corrosion on Microelectronic Reliability

J. W. Braithwaite, D. G. Robinson, J. N. Sweet, D. W. Peterson, N. R. Sorensen

Atmospheric corrosion is the leading age-related degradation mode observed in the weapon stockpile. Of particular interest is corrosion-induced failure of electronic components (including microelectronics) because of the direct consequence to function and therefore reliability. Sandia is now addressing the probable insertion of plastic-encapsulated microelectronic (PEM) devices in future weapon systems and upgrades. These devices use plastic-molding materials that make many of the metallization features susceptible to corrosion. In nuclear weapon components, the failure rate due to corrosion may dramatically increase during long-term dormant (unpowered) periods when the die surface is not dried out due to internal ohmic heating. This failure mode is currently being ignored by industry. Analytical tools that can effectively assess the reliability of PEM devices must be based on a physical understanding of the moisture-related phenomena relevant to metallization failure. The objectives of this project are to provide this needed physical basis along with an associated mathematical model of the degradation process of primary interest: bondpad corrosion. We are following a phased inside-out approach: (1) intrinsic bondpad corrosion behavior as a function of physical configuration and environmental parameters, (2) extrinsic effects of encapsulant materials, and (3) integration and refinement of a corrosion-process model. We are applying computational reliability techniques to permit the uncertainties inherent in the degradation, the transport processes, and the storage environments to be efficiently addressed. Two important initial outcomes will include a quantitative assessment of the validity of the PEM storage concern and a demonstration of the attractiveness of using computational reliability to model materials-degradation processes.

We made important progress in four key areas related to corrosion in PEM devices: (1) development of characterization/monitoring techniques, (2) measurement of intrinsic kinetic parameters, (3) identification of the factors that affect corrosion, and (4) reliability simulation using a preliminary mathematical model.

• *Corrosion monitoring.* We characterized corrosion and monitored it quantitatively as a function of environmental and device-configuration variables using two test structures: a Sandia-developed test chip and transparent quartz slides onto which gold/aluminum (Au/Al) wirebonds were deposited. We used the chip device primarily to monitor bondpad resistance (a measure of the extent of corrosion), and the quartz–based structure was attractive for characterizing corrosion initiation and propagation behavior. A good correlation exists between time–based resistance measurements, visual/optical observations, and expected environmental effects (e.g., increased rate at higher temperature and humidity). These results validated the use of change in resistance as a measure of the extent of corrosion. Relative to contamination, we used two techniques to simulate potential exposures: contamination during manufacture and contamination due to exposure to industrial pollutants.

• *Kinetic property measurement.* Typical kinetic results obtained from the test chip device showed that under the constant environmental conditions, a linear kinetic relationship existed between bondpad resistance and time. Considerable scatter existed in these rate data between individual bondpads on the same test device, a situation that was probably due to physical configuration effects (bond location, water condensation, presence of intermetallic compounds, galvanic coupling), or possibly the stochastic nature of the Al corrosion process.

• *Mechanism identification.* We used thin-film Al test structures to identify how Al bondpads actually corrode in microelectronics. Using backlit optical microscopy, we showed the density and size of the corroded areas to increase with increasing time. Digital image analysis enabled the corrosion initiation and propagation rates to be quantified. Importantly, we observed corrosion only in the area of the Au/Al couple where the Au was thin enough to be porous. This observation, combined with the lack of any observable corrosion on nonbonded Al pads or Al/Al wirebonds (in either NaCl or chlorine gas), clearly demonstrated the critical function of the Au/Al galvanic couple. The corrosion that did exist on the test-chip bondpads appeared to be general rather than localized and was probably associated with the intermetallic compounds that formed during ultrasonic bonding. Cross-sectioned bondpads identified the existence of a physical crevice under the periphery of bond that could function as a site for capillary condensation.

• *Mathematical modeling.* Although a number of physical processes have yet to be completely characterized, we developed and exercised a preliminary PEM corrosion model to improve the efficiency of the experimental activities and to provide a focal point for achieving the ultimate project objective. We based this model primarily on the ongoing experimental studies; it consisted of a governing equation that described the rate of relative increase in bondpad resistance. This simple equation contained three distributed parameters: a surface reaction-rate constant that included the previously discussed stochastics of corrosion propagation in Al, and two environmental parameters (temperature and relative humidity) that vary with time and incorporate a specific time–based uncertainty. As a vehicle for the model development and capability demonstration, we then successfully performed a numerical reliability simulation in which we aged LM185 voltage reference devices in

desert, Gulf Coast, and arctic environments. Chlorine gas was the only contaminant considered. We calculated values for the kinetic parameters (and their variability) using averaged kinetic-rate constants. Because of the presence of the nondeterministic parameters and the knowledge that much more complicated chemical and physical processes must be incorporated in the future, we used the computational reliability techniques (i.e., CRAX) being developed to numerically solve this equation.

Publications

Other

Braithwaite, J. W., and N. R. Sorensen. 1998. "Physical Models for Predicting the Effect of Corrosion on Microelectronics Reliability." Paper presented to the Gordon Research Conference on Aqueous Corrosion, New London, NH, 8 July.

3520.310

Backside Localization of Open and Shorted IC (Integrated Circuit) Interconnections

E. I. Cole, Jr., D. A. Benson, P. Tangyunyong, D. L. Barton

Integrated circuits (ICs) are critical components of virtually every Sandia system. Open and shorted internal IC interconnections are major reliability concerns and have been significant in stockpile systems. These failures occur as a result of processing defects and/or stress during operation and use. Both failure mechanisms have been significant in stockpile components. Localization of these defects has been extremely difficult due to decreasing feature sizes and increasing levels of interconnections. Concurrently, the implementation of flip-chip packaging (as in Sandia's Warhead Protection Program [WPP] and MicroNavigator Program) has made backside analysis the only feasible examination method in many cases. Most active circuit elements in these ICs are accessible only from the backside and, to date, there are no effective backside techniques to directly localize open and shorted interconnections.

We will continue our development of two new imaging techniques for IC backside open and short localization: Seebeck Effect Imaging (SEI) for localizing open interconnections, and Short Localization (SL) for localizing short-circuited sites. The imaging modes use constant current biasing to make defect activation by an outside stimulus more readily detected. Our detection method uses thermal gradients produced by a scanned infrared (IR) laser. On open interconnections, thermal gradients induce voltage gradients (Seebeck effect). Thermal gradients change the resistivity of electrical shorts. Both effects are used to localize defects.

SEI and SL have the potential to revolutionize backside IC analysis in the same way Sandia's charge-induced voltage alternation (CIVA) technique has for frontside open interconnection localization. Backside SEI and SL, for which there are presently no alternatives, could have greater benefits by providing critically needed missing links in analysis capabilities. Sandia's development of SEI and SL will also further the Nuclear Weapons Strategic Management goals of reducing the time and cost of analyses.

First-year work demonstrated the feasibility of SEI and SL. We acquired SEI and SL images on complex devices from the front and backside of the IC. We localized open interconnections produced by focused ion beam (FIB) modification and design errors using SEI. The image data clearly define the defect site. The SEI images produced are the only known method to directly detect and localize open interconnections from the backside of an IC. Examination of devices from the backside required development of sample preparation techniques that have maintained electrically active, packaged ICs with polished die backsides for observation.

We used SL to localize interconnection short sites resulting from FIB modifications and stainless-steel particle contaminants. Through metal probing, we demonstrated detecting a defect covered by an interconnection layer with both SEI and SL, showing a wider range of applicability than originally expected.

We filed a patent for SEI and SL. Although still under development, SL has already been used successfully in a Sandia and an external customer failure analysis. An existing Cooperative Research and Development Agreement (CRADA) partner has expressed interest in seeing if SEI and SL would be applicable to their product.

Although we have demonstrated feasibility, the SEI and SL signal strength is presently weak compared to other analysis techniques. The small signals can make image acquisition very difficult. Exploring methods of improving the sensitivity is the goal of the FY99 project.

Publications

Refereed

Cole, Jr., E. I., P. Tangyunyong, and D. L. Barton. 1998. "Backside Localization of Open and Shorted IC Interconnections." *Proc. IEEE Internat. Reliability Phys. Symp.* **1** (Reno, NV, 31 March–2 April): 129–136.

Cole, Jr., E. I., P. Tangyunyong, and D. L. Barton. 1998. "Local Thermal Probing to Detect Open and Shorted IC Interconnections." *Microelectron. Reliability* (Invited). Oxford, UK: Pergamon (Elsevier Science).

Other

Cole, Jr., E. I. 1998. "Rapid Localization of Interconnect Defects Through Recent Advances in Failure Analysis." Paper presented to the 1998 Advanced Metallization Conference, Seminar on Future Technology (Invited), Colorado Springs, CO, 5 October.

3520.330

Security of Bulk Power Systems

D. G. Robinson, P. C. Butler

The electrical grids of North America are an extremely large and complex set of interconnected networks vital to the economic lifeblood and safety of over 380 million people. These networks are dynamic and constantly changing systems whose surety (safety, security, and reliability) is vulnerable to significant disruptions due to evolving energy policies as well as from natural and man-made sources. The President's Commission on Critical Infrastructure Protection identified electric power as a critical infrastructure sector, of which these networks are essential components. Furthermore, electric-power utilities are transitioning from a regulated, rate–based mode of operation in which utilities provide service to areas and customers on an exclusive franchise basis to a mode of competitive energy markets. It is inevitable that the transition to competitive energy markets will impact electric service reliability. Therefore, there is a need for models and methods to assess the likely reliability impacts of utility deregulation and to provide guidance to energy providers, regulatory agencies and other government agencies, and the public during this process. In addition, there exists an increasing problem of potential physical and cyber sabotage of key power-grid elements. There is already a complex interaction between infrastructure elements (communications, power, transportation, etc.), and under restructuring, these interactions will increase in scope to a national level. Existing reliability assessment models are not capable of accurately reflecting and assessing critical reliability issues, so improved, more comprehensive models are needed.

We focused on three major research areas:

(1) To deal with power flow analyses at a national level, we started developing a new approach to network modeling. Current transportation and dc load flow models can be used to characterize large areas but lack the accuracy to address voltage stability issues. However, the necessary ac flow models are too computationally cumbersome for even moderate-size power grids. Preliminary research conducted in this area involved the development of a hierarchical modeling scheme with increasing model fidelity driven by increasing network sensitivity.

(2) We looked at the probabilistic characterization of network stability. To address stability issues, we developed a new probabilistic load flow methodology that is supported by the reliability analysis software tools (Cassandra). We applied a prefatory integration of the Cassandra software and the ac load flow model to the Modified IEEE (Institute of Electrical and Electronics Engineers) Reliability Test System and had encouraging results.

(3) In addition to addressing the adequacy and stability issues associated with power-grid reliability, we undertook preliminary investigations to characterize and model advanced technologies to determine their suitability for addressing surety issues. Renewable generation, storage, and high-speed power electronics and switches are candidates for solving many of the problems identified above and are areas of expertise in the organizations involved with this research.

NATIONAL GRAND CHALLENGES

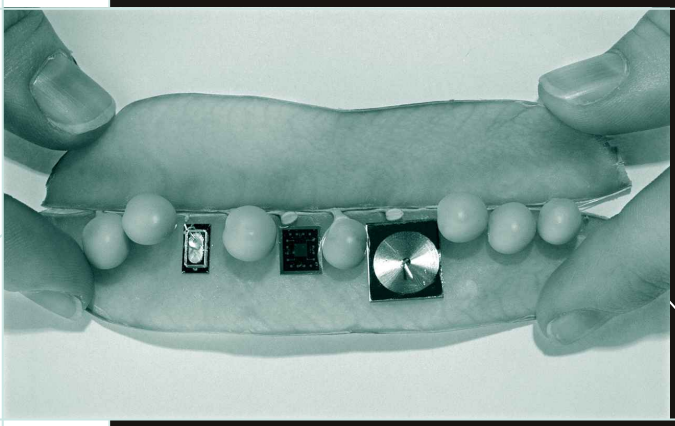

Projects that promise dramatic impact by at least a factor of two on national concerns—such as health care, transportation, and counterterrorism—comprise the National Grand Challenges. High-risk, potentially outrageously successful ideas in all areas are encouraged.

This activity includes a number of possible areas of interest: research projects that could facilitate cutting nonfossil energy prices in half, major reductions in health-care costs with concurrent improvements in quality and availability, reducing the cost of pulsed power substantially below one dollar per megawatt of radiated power, and developing petaflop computing capabilities and applications. All proposals must support achieving Sandia's business goals.

The current National Grand Challenge involves development of an autonomous microchemistry laboratory. Imagine bands of tiny vehicles that cooperatively canvass the countryside, sniffing out suspicious or threatening chemicals, or even landmines buried beneath the soil. About 40 scientists and engineers at Sandia National Laboratories have been researching how to create such technology over the past year in the largest project of its type ever funded by the Department of Energy. At the end of three years, they hope to demonstrate a device about the size of a palm-top computer that can sniff explosives and chemical warfare agents. In 5 to 10 years, devices should be able to simultaneously identify hundreds of liquids and gases.

Arrays of these chemistry-labs-on-a-chip could be sent onto battlefields or mounted near factories to provide chemical reconnaissance. The same technology might also provide quick diagnostic screening at a patient's bedside. Inexpensive mass fabrication, based on existing microchip manufacturing techniques, could spur widespread use of microChemLabs. Potential national security applications range from detecting weapons of mass destruction to monitoring the state of the nuclear stockpile. Everyday items employing similar technology might also become available one day in neighborhood stores to test water and food, or perhaps in other areas to monitor the course of an illness or to determine the safety of the immediate environment.

THIS PAGE
INTENTIONALLY BLANK

3522.010

Science on the Microdomain

T. A. Michalske, G. C. Osbourn, C. C. Wong, W. Wolfer, J. L. Dohner, M. H. Crawford, M. E. Warren

The ability to shrink sophisticated chemistry laboratories to pocket-calculator size and smaller will revolutionize chemical detection in a manner similar to the way that integrated circuits (ICs) revolutionized information technology. Sandia can lead this field because we have the science and technology base to address all aspects of complex microsystems. We demonstrated our expertise in silicon (Si) micromachining, microsensors, and photonics, and are receiving significant external recognition for our accomplishments. However, as our recently completed Integrated Microsystems Roadmap points out, several critical scientific frontiers must be tamed before we can capitalize on the substantial military and intelligence–based business opportunities offered by this rapidly developing technology. The goal of this project is to provide the technical focus needed to ensure Sandia's leadership in the invention and application of the MicroChemLab (µChemLab). We will demonstrate the world's first mobile, autonomous µChemLab for explosives chemical detection.

We proposed a focused laboratory thrust on the science of the microdomain. This regime of very small sizes (roughly 0.1 mm and below) is new territory for machines where normal intuition and standard engineering models cannot be scaled to predict performance, reliability, aging, or manufacturing. This project will develop the scientific basis to understand and predict microscale processes involving micromechanics, transport, microoptics and sensing, and multivariate analysis that lead not only to the invention of a mobile, autonomous µChemLab, but also provide the engineering foundation to address the key technical objectives of reliability, performance, and manufacturability in future microdevice applications.

The Science of the Microdomain project within the µChemLab Grand Challenge is organized into five technical focus areas: (1) integrated optics, (2) on-board data analysis, (3) microscale transport, (4) micromechanical actuators, and (5) *in situ* diagnostics. In the integrated optics area we successfully demonstrated the spectrometer on a chip; produced a blue-and-green-emitting, doubled, vertical-cavity surface-emitting laser (VCSEL); demonstrated ultraviolet (UV) emission from a GaN diode; and conducted the first flow experiments in microcavity sensors. In the on-board data analysis area we developed a pseudo-floating-point library for the on-chip processor and analyzed first continuous-wave (CW) simulant data from integrated preconcentrator and surface acoustic-wave (SAW) array. In the microscale transport area we developed a liquid-flow model to describe electrokinetic transport in packed columns and used gas-flow modeling to optimize the micromachined gas chromatography (GC). In the micromechanical actuators we modeled the magnitude of acoustic streaming as a gas-pumping approach. In the *in situ* diagnostics we designed and manufactured a membrane deflection–based pressure sensor using piezoelectric transducer films. We also fabricated and packaged it and began performance testing. We completed the design of a thermocouple–based bridge-type flow detector, and fabricated and are testing the prototype device.

3522.030

Cooperative, Distributed Sensing and Action Using Microminiature, Intelligent Agents

B. L. Spletzer, P. C. Bennett, T. M. Weber, C. L. Lewis, P. G. Xavier, P. R. Klarer

This project will complete the development of a strong technical base for modeling, simulating, designing, evaluating, developing, and deploying microminiature intelligent machines. The main thrust of the project is to build hardware-verified simulation tools and to develop control systems for cooperating intelligent agents. Sandia will demonstrate the achievement of this main thrust by deploying multiple autonomous microChemLabs (µChemLabs) in a cooperative sensing environment. We will produce the world's first mobile autonomous cooperative µChemLab as part of the hardware verification to perform detection and localization of a chemical source. This project will position Sandia as a leader in the community of researchers in computer science and mathematics regarding cooperative behavior and as a supplier of microminiature intelligent systems and technology.

(1) We completed the simulation to the extent of providing a powerful tool for investigating and observing cooperative behavior of both large and small groups. We simulated as many as 100 vehicles in real time. In addition, the simulation provides the capability to run multiple control and behavior algorithms simultaneously to simplify direct comparison between competing schemes.

(2) We procured and are evaluating the first advanced power supply, a fuel cell, for integration into the Robotic All-Terrain Lunar Exploration Rover (RATLER) test-bed vehicles.

(3) We conducted preliminary demonstrations with the swarm of RATLER vehicles, demonstrating the usefulness of cooperative behavior.

(4) The integration of the RATLER test-bed vehicles with the surrogate µChemLab sensor is under way. Until the µChemLab is available, we will use corona discharge sensors to detect the presence of SF6 in the atmosphere. As long as the plume species can be selected, simple gas detectors are adequate for demonstrating the usefulness of cooperative behavior.

(5) We developed several very promising control and behavior strategies that demonstrated that in real-world problems, cooperative behavior can effectively localize a chemical source where similar agents lacking cooperation are unable to complete the task.

3522.020

Autonomous MicroChem Laboratory (µChemLab)

G. C. Frye-Mason, S. A. Wright, S. A. Carichner, W. B. Chambers, S. H. Kravitz, D. J. Rakestraw, G. N. Ryba

*This project will lead to a new generation of field-ready, compact, chemical analysis devices that will have unprecedented capabilities for measuring and deciphering detailed chemical signatures. At the end of three years, we will demonstrate an autonomous microscale chemical laboratory (µChemLab) that will establish Sandia as a leader in this field. This project will position Sandia to support increasing demands for detailed chemical information by current national security customers and is essential for developing new customers in nonproliferation, counterterrorism, and critical infrastructures. The µChemLab, formed by miniaturizing and integrating sensing capabilities, sampling and separation systems, power sources, and systems architecture, would meet the needs of applications in Defense Programs (DP) (nuclear material monitoring, material aging), NN (National Security and Nonproliferation Office) (nonproliferation, cooperative monitoring), intelligence agencies (covert sensing), DoD (landmine detection, battlefield chemical warfare/biological warfare [CW/BW] monitors), and energy and environment (E&E) (*in situ *probes).*

• *System design and integration.* We developed the preliminary system design for the µChemLab together with requirements for major systems and subsystem components and presented it to the External Advisory Committee and µChemLab team. We partitioned the design to the product teams, defined interfaces, and agreed on a schedule. We completed mechanical integration design concepts and are prototyping detailed designs. We completed electronic integration design architecture, selected components, and conducted feasibility studies on power supplies and microprocessors.

• *Liquid-phase analysis.* We established three rapid separation methods for parallel analysis of explosives. We demonstrated detection limits of < 100 ppb for explosives in a high-speed micellar electrokinetic (EK) separation using indirect laser-induced fluorescence (LIF) detection. We demonstrated microelectrochemical detection of explosives in flow injection at < 10 ppb. We demonstrated insulation of silicon (Si) using layered Si_2N_3 and SiO_2 up to 3,000 volts. We developed a patterned polyimide sealing technique for microchannels and fabricated patterned chromatographic supports in Si and crystalline quartz. We packed microfabricated channels with SiO_2 particles for chromatography. We characterized EK pumping in detail with various materials and solvents.

• *Gas-phase analysis.* We fabricated and tested prototype devices for the three gas-phase components and established baseline designs for these components. We demonstrated the first functional integrated gallium arsenide (GaAs) surface acoustic-wave (SAW) oscillators this year. We also produced discrete GaAs amplifier integrated circuits (ICs) suitable for hybrid integration with GaAs SAW delay lines. The packaging and interconnection of the gas-phase components made significant progress. We successfully demonstrated techniques for attaching lids and microcapillary tubing to all three components. The most successful techniques include anodic bonding of Pyrex to Si and the use of ultraviolet (UV)-curing epoxies. Regarding chemically selective materials, we developed techniques for spray-casting through masks to deposit polymers and sol-gels into selected regions of miniature preconcentrators and acoustic-wave detectors. We established an automated vapor-generation system in conjunction with other programs that can provide ppb levels of CW agent simulants with up to 100 ppm levels of interferant vapors.

• *Sampling, fate, and transport.* We evaluated the TOUGH2 series of codes, and the modifications considered are currently in progress. The physicochemical constants being evaluated include water solubility, soil-water partition coefficients, and soil-vapor partition coefficients. We completed the water solubility work using the generator column method under dynamic conditions on TNT, DNT, and RDX. Development of solid-phase microextraction techniques for *in situ* soil and water analysis resulted in a technical advance and patent application for landmines and buried unexploded ordnance (UXO) detection. Similar success was demonstrated for water analysis with applications to sea mines and submerged UXO.

• *Micro-fuel-cell-on-a-chip power source.* We demonstrated platinum (Pt)-coated porous Si to electrolyze water. We also demonstrated 1 cm-diameter porous Si membranes under routine fabrication in 3-inch and 4-inch wafers. We developed process steps and Si membrane backing. We masked electrode structures and vapor-deposited them on catalyzed porous Si. We constructed a test stand for testing anode and cathode structures. We developed a plasma-derived Si carbide mask (replaces SiN). We also developed high-aspect-ratio Si shadow masks made with Bosch process to enable photoresist patterning on porous Si.

Publications

Refereed

Arnold, D. W. 1998. "Capillary Electrochromatography." Paper presented to the High-Performance Capillary Electrophoresis Conference, Orlando, FL, January.

Arnold, D. W. 1998. "Laser Applications to Chemical and Environmental Analysis." Paper presented to the OSA Topical Meeting, Orlando, FL, 9–11 March.

Bailey, C. G. 1997. "Capillary Electrochromatography." Paper presented to the Gordon Conference on Illicit Substance Detection, Oxford, England, August.

Bailey, C. G. 1998. "Capillary Electrochromatography." Paper presented to the High-Performance Capillary Electrophoresis Conference, Orlando, FL, January.

Bailey, C. G., and C. Yan. 1998. "Separation of Explosives Using Capillary Electrochromatography." *Anal. Chem*.

Casalnuovo, S. A., E. J. Heller, V. M. Hietala, A. G. Baca, R. J. Kottenstette, S. L. Hietala, and G. C. Frye-Mason. 1998. "Acoustic-Wave Chemical Microsensors in GaAs." *Proc. 1998 SPIE Micromachining and Microfabrication Symp*. (Santa Clara, CA, 20–22 September).

Casalnuovo, S. A., G. C. Frye-Mason, and S. L. Hietala. 1998. "Surface and Bulk Micromachining of Thin GaAs Membranes for Acoustic-Wave Chemical Microsensor Applications." *Proc. 1998 Solid-State Sensor and Actuator Workshop* (Hilton Head, SC, 3–8 May).

Chambers, W. B., J. M. Phelan, R. J. Rodacy, and S. W. Webb. 1998. "Chemical Detection of Buried, Unexploded Ordnance." Paper presented to the UXO Forum '98, Anaheim, CA, 4–7 May.

Chambers, W. B., R. J. Rodacy, E. E. Jones, B. J. Gomez, and R. L. Woodfin. 1998. "Chemical-Sensing System for Classification of Mine-Like Objects by Explosives Detection." Paper presented to the International Symposium on Aerospace/Defense Sensing, Simulation, and Controls, Orlando, FL, 13–17 April.

Chambers, W. B., S. F. A. Bender, and P. J. Rodacy. 1997. "Analysis of Semivolatile Nitroaromatic Compounds by Headspace SPME." Paper presented to the 37th ORNL-DOE Conference on Analytical Chemistry, Gatlinburg, TN, 7–9 October.

Dadoo, R., C. Yan, R. N. Zare, D. S. Anex, D. J. Rakestraw, and G. A. Hux. 1997. "Advances Toward the Routine Use of Capillary Electrochromatography." *LC GC-Magazine of Separation Sci.* **15**: 630.

Frye-Mason, G. C., R. J. Kottenstette, E. J. Heller, C. M. Matzke, S. A. Casalnuovo, P. R. Lewis, R. P. Manginell, W. K. Schubert, and V. M. Hietala. 1998. "Integrated Chemical Analysis Systems for Gas-Phase CW Agent Detection." *Proc. Micro Total Analytic. Sys. (µTAS) Conf.* (Banff, Alberta, Canada, 13–16 October).

Frye-Mason, G. C., S. A. Casalnuovo, E. J. Heller, R. J. Kottenstette, W. K. Schubert, C. M. Matzke, S. H. Kravitz, and M. C. Oborny. 1998. "Fabrication and Packaging of Integrated Chemical Analysis Systems." *Proc. IMAPS Sensor Packaging Workshop* (Ojai, CA, 26–28 January).

Garguilo, M. G., P. H. Paul, and D. J. Rakestraw. 1998. "Imaging of Pressure and Electrokinetically-Driven Flows Through Open Capillaries." *Anal. Chem*.

Heller, E. J., S. A. Casalnuovo, G. C. Frye-Mason, R. J. Kottenstette, A. G. Baca, and V. M. Hietala. 1998. "Optimization of GaAs Surface Acoustic-Wave Delay Lines for Chemical Microsensor Applications." *Proc. IEEE Freq. Control Symp*. (Orlando, FL, 27–29 May): 43.

Kottenstette, R., G. Frye-Mason, C. Colburn, E. Heller, J. Roark, M. Wilhelm, D. Newby, and M. la Grone. 1998. "A Hand-Held SAW Array for Volatile Organic Compounds." Paper presented to the 193rd Electrochemical Society Meeting, San Diego, CA, 6 May.

Lewis, P. R., G. C. Frye-Mason, R. J. Kottenstette, and J. Vitko, Jr. 1998. "µChemLab: An Update on the Integrated Chemical Analysis System for CW Agent Detection." Paper presented to the MASINT Chemical Defense Science & Technology Symposium, Aberdeen, MD, 11 June.

Manginell, R. P., G. C. Frye-Mason, R. J. Shul, and C. G. Willison. 1998. "Microfabrication of Membrane–Based Devices by HARSE and Combined HARSE/Wet Etching." Paper presented to the SPIE Micromachining Microfabrication Conference, Santa Clara, CA, 20–22 September.

Manginell, R. P., G. C. Frye-Mason, W. K. Schubert, R. J. Shul, and C. G. Willison. 1998. "Microfabrication of Membrane–Based Devices by Deep Reactive Ion Etching (DRIE) of Silicon." Paper presented to the Electrochemical Society Conference, Boston, MA, 1–6 November.

Matzke, C. M., S. A. Casalnuovo, G. C. Frye, R. P. Manginell, D. Y. Sasaki, and C. C. Wong. 1998. "Integrated Silicon Gas Chromatographic Microchannel Fabrication and Performance." Paper presented to the SPIE Micromachining Microfabrication Conference, Santa Clara, CA, 20–22 September.

Paul, P. H., D. W. Arnold, J. J. Scherer, and D. J. Rakestraw. 1998. "High-Pressure Electrokinetic Liquid Micropumps." *Science*.

Phelan, J. M., and S. W. Webb. 1998. "Chemical Detection of Buried Landmines." Paper presented to the 3rd International Symposium on Technology and the Mine Problem, Monterey, CA, 6–9 April.

Phelan, J. M., and S. W. Webb. 1998. "Simulation of the Environmental Fate and Transport of Chemical Signatures from Buried Landmines." Paper presented to the International Symposium on Aerospace/Defense Sensing, Simulation, and Controls, Orlando, FL, 13–17 April.

Rakestraw, D. J. 1998. "Capillary Electrochromatography." Paper presented to the American Chemical Society National Meeting, New Orleans, LA, 2–5 March.

Rakestraw, D. J. 1998. "Capillary Electrochromatography." Paper presented to the MASINT Chemical and Biological Defense Symposium, Aberdeen, MD, 11 June.

Rakestraw, D. J. 1998. "Capillary Electrochromatography." Paper presented to the MASINT Chemical Defense Science and Technology Symposium, Wright Patrick AFB, FL, 12–15 January.

Webb, S. W., S. A. Finsterle, K. Pruess, and J. Phelan. 1998. "Prediction of the TNT Signature from Buried Landmines." Paper presented to the TOUGH Workshop '98, Berkeley, CA, 4–6 May.

THIS PAGE
INTENTIONALLY BLANK

INITIATIVES

Initiatives supports studies in areas of urgent concern to the DOE and Sandia. Energy production is a vital national concern. Sandia developed a technology at least two orders of magnitude better than current technology to monitor drill parameters. Surface area modulation telemetry was designed for oil production in a cased well. LDRD is proving Sandia's monitoring technology in more complex environments such as petroleum, geothermal, and environmental industries.

In defense, developers need a powerful fabrication tool to allow low-volume production of the complex shapes and materials found in highly specialized weapons components. Sandia developed a technology called Laser-Engineered Net Shaping (LENS™), using computer-controlled lasers that can weld air-blown streams of metallic powders into custom parts and manufacturing molds. LENS™ can fabricate 3-D metallic components directly from CAD solid models, showing potential to revolutionize the production of metal parts such as complex prototypes, tooling, and small-lot production parts.

Resulting materials have outstanding mechanical properties—very high strength and high ductility—and can mix powder streams of different materials. Engineers will eventually make intricate material combinations in complex geometries out of hard-to-machine materials. An early industrial application of LENS™ to produce injection-molding dies saved more than 50 percent in both time and cost over conventional methods.

Other benefits include fabricating hardware with complex features and producing functionally gradient structures made of multiple materials. As a material additive process, increased material utilization will create additional cost savings over a bulk removal process. LENS™ technology can also modify or repair existing hardware. Microscopy studies show the LENS™ parts to be fully dense with no compositional degradation. Tests of several structural metal alloys reveal outstanding as-fabricated mechanical properties.

University and industry collaboration provides enhancement of laboratory capabilities through an inflow of knowledge and skills from selected researchers who are leaders in their fields. Sandia recognizes that much of the scientific expertise for these emerging technical fields lies with universities and industry. These activities support the world-class, external sources of cutting-edge knowledge development that Sandia requires to develop critically needed technical capabilities for the future.

THIS PAGE
INTENTIONALLY BLANK

3530.030

Computational Methods for Predicting the Response of Critical As-Built Infrastructure to Dynamic Loads (Architectural Surety)

R. V. Matalucci, S. W. Attaway

Sandia enhanced the PRONTO3D structural dynamics code to enable it to model the response of concrete, steel beams and rebars, reinforced concrete, and reinforced and unreinforced masonry structural components. We added two major enhancements: (1) a concrete material model, and (2) a beam/truss element to model the rebars used in reinforced concrete and masonry. We developed the beam element formulation and used the existing concrete and rebar material models and properties to implement the enhancements in PRONTO3D. To verify the implementation of the rebar and concrete models, we defined several benchmark problems and ran them through PRONTO3D. To demonstrate the new capabilities (i.e., rebar and concrete models), we also ran application problems with PRONTO3D.

Adding the capability of modeling reinforced concrete to PRONTO3D helped us develop an advanced capability that would also provide airblast and structural calculations within a single coupled calculation. Other typical design issues and tradeoffs to be answered using this coupled analysis are whether increasing cladding or window strength is likely to put more load on columns and perhaps reduce the lethality for some explosive attacks. Determining the cost of upgrades versus their effectiveness, comparison of design options vis-à-vis terrorist bombs, and establishing effective standoffs for perimeter barriers are also capabilities resulting from this effort. Coupling allows the airblast and response predictions to be performed together so they may interact. The coupled capability uses two existing Sandia codes: CTH for predicting the blast environment and PRONTO3D for the structural response. These codes are linked into a single integrated analysis with the ZAPOTEC code.

The combined airblast and structural response calculation is especially relevant to the analysis of conventional buildings subjected to terrorist bombs because airblast pressures in those problems are often affected by the structural failures they cause. The capability is particularly useful in predicting damage to the building interior, determining cladding effects on column failure, and applying the load in the correct spatial distribution. Having a coupled code allows a straightforward, convenient means to simulate the actual loadings because the pressure history and arrival time of the loading are unique at every point in the building.

To verify the implementation of the material model, we ran several benchmark problems for the rebar (steel) and concrete materials. These results indicated that both material models satisfactorily match the measured data. To illustrate the structural response that PRONTO3D can determine, we developed several models of reinforced concrete structures and components from which we carried out analyses of response to various loadings. We developed a 3-D building model of a four-story structure constructed by a DoD program at White Sands, NM, using concrete continuum elements and explicitly modeled reinforcing steel. The model calculations can be used to validate the code against the upcoming DoD Divine Buffalo test series of the structure at White Sands.

As a result of the work performed under this project, PRONT3D now has the capability to analyze reinforced-concrete structures subjected to blast loading. Combined with the massively parallel (MP) JANUS computer, complete buildings can be modeled in three dimensions at an unprecedented level of detail to more accurately predict the response. Additional work should focus on continued development of the coupled code (ZAPOTEC) capability for airblast/structure interaction problems in general and validation of the codes against test data and the implementation of additional enhancements to the modeling of reinforced-concrete structures, such as gravity preloading and cyclic material response.

We drafted a report describing the PRONTO3D enhancements that discusses the measured data related to the behaviors of concrete and rebar, the concrete model, and the element and material models used to simulate the response of the reinforcement. It provides studies verifying the implementation of the rebar and concrete models, as well as examples of the application of these models. The enhanced capabilities of the coupled airblast/response code that we developed are also presented. Several appendices provide further detail for using the coupled PRONTO3D finite-element (FE) code and the models for predictive purposes, such as input instructions, sample inputs and calculations, benchmark information, and structural design drawings.

Publications

Other

Attaway, S. W., K. B. Morrill, L. J. Malvar, J. E. Crawford, and R. V. Matalucci. 1998. “Enhancements to PRONTO3D to Predict Structural Response to Blast.” Sandia Technical Report, in preparation.

Preece, D. S., J. R. Weatherby, S. W. Attaway, J. W. Swegle, and R. V. Matalucci. 1998. “Computational Methods for Predicting the Response of Critical As-Built Infrastructure to Dynamic Loads (Architectural Surety).” Sandia Technical Report SAND98-1240 (June). Sandia National Laboratories, Albuquerque, NM.

3530.050

Background Radiation Anisotropy Measurement Sensor (BRAMS)

M. J. Adriaans, R. D. Moyer, P. D. Thacher

The Cosmic Background Explorer (COBE) was launched on November 18, 1989, to measure the effective temperature and the anisotropy of the cosmic background radiation (CBR). COBE was a great success, posing many more astrophysical questions than it answered. Another mission with much higher temperature resolution, flown much farther away from the Earth and sun to avoid noise associated with diffuse solar scattering, is needed. High-resolution thermometer (HRT) technology offers a unique opportunity for astrophysical radiometry. COBE observed the large-scale (distance) temperature anisotropy of the CBR and the microwave background quadrupole moment of the Universe. These measurements, however, were very near the limits on their thermometry and hence have large uncertainties. One of the next-generation missions, PLANCK, a European Space Agency (ESA) mission expected to launch in 2005, will improve the temperature resolution to approximately 3 mK, an improvement of about a factor of 30 over COBE. The temperature resolution and stability of the current, space-proven HRTs is 0.1 nK. These HRTs have already flown on the space shuttle in the Lambda Point Experiment (STS-52) and will fly again on the Confined Helium Experiment and DYNAMX.

The goal of the BRAMS project is to make use of this very precise thermometry in two key areas in astrophysical instrumentation: (1) the development of a radiometer for detecting the CBR with a sensitivity of at least 10 nK near 2.7°K, and (2) the development of an ultra-stable blackbody calibrator. We will test both the radiometer and the calibrator in a stable, low-temperature laboratory instrument. During the development and testing of these instruments, we will also complete a phase A scientific definition study of a possible mission.

Programmatically, we completed initial studies of technical issues that would be important in implementing this project on a deep space probe, and we studied previous flight experiments in this class to determine our market potential.

On the technical side, we developed both PdFe and PdMn metallic alloys and studied how their Curie temperature varies with magnetic concentration. We measured the thermal sensitivity of these new devices that utilize these new alloys as their thermometric elements. We studied these sensitivities as a function of charging magnetic field and as a function of the metallic ion concentration. We demonstrated a thermal resolution of 0.4 nK in a 1 Hz bandwidth and at a nominal temperature of 2.2°K. This device displayed a drift rate of less than 0.1 pK/second, with a time constant faster than 0.6 second. These devices are robust enough to readily survive launch, and they are easily manufactured.

Publications

Other

Moyer, R. D. 1998. “Proposal of Techniques for Coupling Millimeter-Wave Energy Into Palladium-Iron Thermometer Rods.” Internal report, Sandia National Laboratories (February).

3530.090

Exploitation of Satellite Communications Systems and Networks for Intelligence Applications

J. E. Heustess

There exists a subset of the intelligence community that is involved in covert ground–based intelligence applications worldwide. These applications are based on small, battery-powered systems that are placed in the field for long periods of time. These systems require both one-way and two-way world-wide communications support that cannot be supplied by available ground–based long-lines communications networks. These systems require that the communications links be both low-probability-of-detection (LPD) and low-probability-of-interception (LPI).

These applications include the use of covertly installed electronic sensor/receiver units that collect, process, and exfiltrate intelligence data for analysis and processing. There also exists a class of problems that require data to be both exfiltrated and delivered to equipment and systems remotely located world-wide. These systems can include overt and covert tagging and tracking applications, and overt and covert remote monitoring systems such as unattended ground sensors and remote control applications. There are also remote systems that can interrupt operation of specific systems and subsystems at critical times during national conflicts.

The intelligence community involved in covert, ground–based intelligence data-collection applications worldwide has continued to show interest in this area.

We based the applications studied in this project on small, battery-powered systems that can be placed in the field for long periods of time. The system defined and designed in the project provides both one-way and two-way world-wide communications support that cannot be supplied by available ground–based long-lines communications networks. The project

shows that the communications links that can be implemented have both LPD and LPI.

This application includes the design of a system to support covertly installed electronic sensor/receiver units that collect, process, and exfiltrate intelligence data for analysis and processing. The project also discusses the class of problems that require data to be both exfiltrated and delivered to equipment and systems remotely located worldwide. The technology developed in the report can be used to support overt and covert tagging and tracking applications, and overt and covert remote monitoring systems such as unattended ground sensors and remote control applications. This technology can also support the implementation of remote systems that can interrupt operation of specific systems and subsystems at critical times during national conflicts.

3530.110

Microcode Evaluation

J. W. Walkup, G. L. Smithberger, E. I. Cole, Jr., J. S. Williams, D. C. Carlson, T. H. Desiena, R. P. Fleming

Having discovered a technique for breaking or bypassing the cryptography involved in updating microcode for a selected microprocessor, Sandia will modify the information one bit at a time and use the in-circuit emulator (ICE) equipment to evaluate any effects on processor operation. Although tedious, this will provide a map of the relationship between microcode bits and functions. With that map, we can select functions that will have the desired effect on the overall operation of the processor.

We will continue to physically evaluate the processor in an attempt to find the encryption circuitry and the microcode read-only memory (ROM), random-access memory (RAM), and associated registers. The technique will again require ICE, which will repeatedly load a microcode update. During the download, a backside light-induced voltage alteration (LIVA) image should allow isolation of the active section(s) of the processor.

We selected a central processor unit (CPU) type, bought appropriate ICE equipment, and investigated the microcode download techniques, and have a tool to perform the download at will rather than simply upon power-up. The tool will also identify the processor and can modify the microcode being downloaded to test the effects of bits being modified.

We characterized and compared various microcode download packages and can isolate interesting sections of the code. We have a working hypothesis about the encryption used and believe we can bypass the encryption by using a brute force technique. A demonstration of this technique will be available as a result of the first year of this effort.

We are also deprocessing and characterizing the silicon die of the CPU to gain an understanding of how the microcode download works. This has not been fruitful because of the extensive metallization on the front of the die and will require running tests from the back side of the die.

3530.120

Real-Time Image Analysis Using Field-Programmable Gate Arrays

K. J. Jefferson, J. C. Wehlburg, K. R. Lanes, C. L. Grotbeck, A. R. Baeza

Performance and target discrimination requirements for the next-generation remote sensors are driving designs into the hyperspectral regime. Although the mission payoffs for going hyperspectral are significant, the bandwidth requirements imposed by additional sensing dimensions are impossible to meet with available ground links. In addition, the transformation of data into knowledge requires increased speed in data processing. These requirements will force next-generation payloads to support on-board processing and event detection. In addition, the processing is computationally intensive, and for many types of algorithms, batch processing is the current choice for mode of operation.

Sandia developed a unique concept for a hyperspectral fast-transient staring sensor. We will develop a hardware/software solution that will allow us to process imagery in real time using a combination of adaptive algorithms and distributed processing arrays.

Two important problems that need to be addressed in the processing of the data are geo-location and the extraction of small, moving-target signatures.

We acquired and brought into operation a basic field-programmable gate array (FPGA) development system. We developed a simple trial microscan algorithm and implemented it in C code as a test for FPGA processing. The conversion from C code to VHDL (very high speed integrated circuit [VHSIC]) is in process. Collaborations are in place with researchers from the U.S. Air Force. The implementation of a subset of matrix manipulations required for the chromotomography is in progress.

We supported a field test recording transient spectral data from actual munitions of interest. We recorded the data with the prototype chromotomography system. These data will be an ideal test data set for our algorithm implementation in FPGAs. That algorithm development is in process now. The architecture for a fast-throughput system is emerging. We expect that it will be a combination of FPGAs and digital signal processors (DSPs). We anticipate demonstration of an FPGA microscan algorithm applied to an 8x8 array by the end of the year and expect to have the appropriate pieces of a chromotomographic algorithm embedded in an FPGA.

Publications

Other

Jefferson, K. J., J. C. Wehlburg, and A. R. Baeza. 1998. “Real-Time Image Processing Using Reconfigurable Logic.” *Proc. Mil. and Aerospace Applic. of Programmable Devices and Technol. Conf.*, accepted.

3530.130

Advanced 3-D Sensing and Visualization System for Unattended Monitoring

J. J. Carlson, D. E. Small, C. Q. Little, J. J. Harrington, C. L. Nelson

The purpose of this project is to create a reliable 3-D sensing and visualization system for unattended monitoring. The system will benefit several of Sandia's initiatives, including nonproliferation, treaty verification, national security, and critical infrastructure surety. The robust qualities of the system will make it suitable for both interior and exterior monitoring applications. The 3-D sensing system will combine two existing sensing technologies in a new way to continuously maintain accurate 3-D models of both static and dynamic components of monitored areas (e.g., portions of buildings, roads, and secured perimeters in addition to real-time estimates of the shape, location, and motion of humans and moving objects). A key strength of this system will be the ability to monitor simultaneous activities on a continuous basis, such as several humans working independently within a controlled workspace, while also detecting unauthorized entry into the workspace. We will use data from the sensing system to identify activities or conditions that could signify potential surety (safety, security, and reliability) threats. The system could alert a security operator of potential threats or could be used to cue other detection, inspection, or warning systems. We will also develop an interactive, Web–based, 3-D visualization capability using Internet technologies, Virtual Reality Modeling Language (VRML), and JAVA. This will allow remote, interactive inspection of a monitored area (via the Internet or satellite links) using a 3-D computer model of the area that is rendered from actual sensor data.

Our accomplishments included developments in 3-D sensing, automated sensor calibration, intrusion detection and monitoring using 3-D data, and remote visualization of 3-D sensor data.

We integrated and modified two existing 3-D sensor technologies for an interior monitoring application. We developed intrusion-detection algorithms to monitor the 3-D characteristics of both static and dynamic components. We monitored static components, including barrels and other physical structures, using Sandia's Laser Mapper (LAMA) technology. We monitored dynamic components, including humans and other moving objects, by Sandia's 3-D Video Motion Detection (3DVMD) technology. We developed a robust sensor calibration procedure to facilitate setup and application of the 3-D sensor technologies. The integration of the LAMA and 3DVMD sensor technologies allowed us to accurately detect changes in the location, shape, and size of both static and moving objects. We also developed a Web–based, 3-D visualization capability based on the VRML. This Internet–based, 3-D graphical user interface (GUI) allowed remote, interactive inspection of the monitored area using a computer model of the area that was rendered from actual sensor data.

3531.020

System-of-Labs Direct Fabrication Technology

M. E. Schlienger

This project is a cooperative effort between Sandia National Laboratories, Oak Ridge National Laboratory (ORNL), and the Idaho National Engineering and Environmental Laboratory (INEEL). The goal of this project is to integrate the direct fabrication capability at Sandia in laser-engineered net shaping (LENS™) with the capability at INEEL in spray-forming and the expertise at ORNL in novel materials fabrication and analysis.

LENS™ is a laser–based direct manufacturing process that starts with a computer-aided design (CAD) solid model. The model is decomposed into a series of layers. Each layer is broken up into a series of raster lines. We use a three-axis system to raster a laser beam along the resultant lines. We focus the laser on a substrate, and a molten pool forms. We inject powder into this molten pool, forming a bead. An X-Y table moves the substrate under the LENS™ head, and the bead is pulled across the evolving part, resulting in controlled deposition of metal. As the part builds up, the LENS™ head is raised one layer in height.

The INEEL spray-forming process sprays molten metal onto a shaped substrate to build a part. In the INEEL process, an RTV negative (a latex negative) is made from a master part. This mold is used to cast a ceramic form. The ceramic is cured and placed into the spray-forming device. Molten metal is sprayed on the ceramic form, and a deposition builds up. Once spraying is completed, the part is removed and excess material is cut off. This process is much faster than LENS™, but shadowing of the metal spray makes the process unsuitable for high-aspect-ratio features.

The intent of this project is to investigate combining these two processes to jointly exploit their advantages. ORNL will provide evaluation and ultimately custom alloy development in support of this effort.

In the first year, we produced a sample part via the spray-form process and added LENS™ features to the part. However, metallographic analysis yielded some interesting data. Perhaps most important was the fact that the parts from the two processes are very different with regard to their thermal histories and solidification structure. While LENS™ exhibits a fully dense, rapidly solidified structure, the spray-formed parts were coarser and more porous. These structures are consistent with process observations that reveal that the entire spray-formed part glows quite hot for an extended period of time, while the LENS™-produced material glows hot only for a fraction of a second. These empirical observations clearly indicate a very different cooling rate, as exhibited by the microstructure. Further, the spray-formed material exhibits droplet boundaries and porosity, where the LENS™ material is fully dense, with no prior powder boundaries. However, in LENS™ the path of the molten pool during the deposition process is indicated by a variation in grain morphology that occurs along the prior molten pool boundaries.

Examination of the interface between the two types of deposits revealed the presence of cracking. We did not pinpoint the exact source; however, two theories arose. We based the first possibility on the observation of a surface layer on the spray-formed material. The possibility was raised that perhaps a contaminant was embrittling the interface between the two deposits. The second possibility was that the effect was entirely thermal in nature and that preheating the spray-formed part prior to the addition of the LENS™ deposit could eliminate the cracking.

These analyses indicated that alloy development suitable for both processes might be challenging, as the solidification behavior of the two is very different. In addition, we decided that some further investigation into the interfacial area between the two deposits and the mechanism responsible for the cracking was warranted.

In the second year, INEEL dropped out of the project. Although we obtained no further spray-formed substrates, we identified solidification shrinkage at the substrate/LENS™ interface as being at least partially responsible for the cracks we observed at this interface. The final proof will require experiments wherein identical LENS™ deposits are placed on room-temperature and preheated substrates. Once such deposits have been produced, we will evaluate both the interface and substrate deformation. We assumed that the cracking will be greatly minimized. We installed a high-temperature platen on the new LENS™ machine and on the machine that has just entered initial stages of operation. The experiments indicated by the results of this System-of-Labs (SOL) project are still of significant interest and will be completed sometime in the next few months.

The alloy studies revealed that LENS™-processed H13 had excellent properties as deposited. The use of LENS™ as a process for the production of tooling makes good metallurgical sense. Further, there appears to be an opportunity to fine-tune the composition of H13 tool steel to take advantage of the rapid solidification environment available within LENS™.

Although no special H13 powder compositions were produced, ORNL did provide some nickel aluminide powder of a proprietary composition. This alloy is a hard, high-strength material that is difficult to work using conventional processes. However, with the LENS™ process, near-net-shape objects were produced, and subsequent testing at ORNL revealed excellent properties.

Although this project was not as successful as we had hoped, we obtained significant useful information at both ORNL and Sandia as a result of this collaboration. This project contributed to the substantial progress achieved by the LENS™ process, resulting in current commercialization efforts and implementation of the LENS™ process in the production of neutron generators.

Publications

Refereed

Griffith, M., M. E. Schlienger, J. Brooks, L. D. Harwell, M. Essien, D. Nelson, and W. Hofmeister. 1998. "Thermal Behavior in the LENS Process." *Proc. 9th Solid Freeform Fabrication Symposium* **9** (Austin, TX, 10–12 August).

Maziasz, P. J., E. A. Payzant, M. E. Schlienger, and K. M. McHugh. 1998. "Residual Stresses and Microstructure of H13 Steel Formed by Combining Two Different Direct Fabrication Methods." *Scripta Materialia*, accepted.

Schlienger, M. E., D. Dimos, M. Griffith, J. Michael, M. Oliver, T. Romero, and J. Smugeresky. 1998. "Near Net-Shape Production of Metal Components Using LENS." Proc. *3rd Pacific Rim Internat. Conf. on Adv. Mater. and Processing* **3** (Honolulu, HI, 12–16 July).

Schlienger, M. E., M. Oliver, and T. Romero. 1998. "Sacrificial Materials for Complex Geometry Fabrication." *Proc. 9th Solid Freeform Fabrication Symp.* **9** (Austin, TX, 10–12 August).

Other

Schlienger, M. E., M. Griffith, M. Oliver, and T. Romero. 1998. "Laser-Engineered Net Shaping." Paper presented to the Automotive Applications of Thermal Spray Technology Conference, Romulus, MI, 3 June.

3531.140

Poco Switch Tubes

G. E. Boettcher

This project will explore design variations in Poco switch tubes to provide improved reliability, performance, and ease of fabrication. Some of the initial design features that Sandia will explore more fully include the following: (1) Probe design: eliminate the present 6 mil mo nail-head trigger wire, with either cermet or active braze material, and evaluate sapphire versus 96% alumina trigger ceramics with smaller inner dimensions (IDs) for enhanced electric field at trigger electrode, and (2) envelope construction: determine minimum thickness envelope height with metallizing both sides for smaller tubes and provide more self-fixturing features in trigger-cathode design.

(1) We obtained sapphire trigger probes and evaluated them with dimension, 10 mil outer dimension (OD), 60 mil length, and 3 mil ID, and found them to be similar in performance to ceramic probes twice as large. We evaluated these small probes in one-kilovolt sprytrons. We fabricated five tubes and tested them 100%, and pulse-life–tested two units out to two-thousand operations to show similarity to previous standard design tubes.

(2) We successfully fabricated and tested 20 mil-thick ceramic envelopes for a 1000 V dc sprytron tube. We fabricated three tubes; two good sealed units were 100% tested and pulse-life–tested to failure. The anode-cathode spacing was 20 mils. Both anode and cathode were palco flat-facing electrodes with no recess at anode-to-cathode ceramic wall, i.e., 20 mil straight-line breakdown path. One tube failed at 407 operations, and the other failed at 76 operations. Short pulse life is due to the extremely small envelope ceramic that is the tradeoff for the smaller size.

(3) We successfully fabricated and tested a 0.214 OD sprytron, which is approximately one-third the size of the previous smallest sprytron design.

(4) We successfully fabricated and tested a probe/cathode sprytron design that is self-fixturing.

(5) We showed feasibility for brazing niobium to sapphire and ceramic without metallization required and without the use of active braze material.

3531.150

Chemiresistors Based on Metal-Loaded Polymers for Solvent Spill Detection

R. C. Hughes

Sandia discovered that small, planar microsensors for solvents can be fabricated by mixing common, commercial polymers with metal powders like graphite. Thin films of these composites can be deposited on interdigitated electrodes on an insulating substrate. An example of such a film is fabricated from polyisobutylene mixed with 40% by weight of carbon powder. The resistance of such a film appears to be dominated by percolation of charge through the conducting carbon particles. The resistance depends on the number of such contacts and thus on the volume fraction of the carbon particles. Vapors of some solvents can cause the polymer to swell and thus decrease the volume fraction of conducting particles. The electrical resistance thus increases with increasing solvent vapor pressure. We will study this phenomenon. We are particularly interested in the reproducibility of the sensor signals, as well as long-term drift in the base (dry) resistance. Temperature-dependence of the signals is also important for an understanding of the thermodynamics of the polymer swelling. We wish to understand the role of entropy and heat of mixing the solvent vapors in the sensor output. It may turn out that different polymers will have a sufficiently different response to various vapors, that arrays of sensors can be used to identify an unknown vapor by pattern recognition.

We successfully fabricated a number of chemiresistor sensors based on the principle of solvent swelling of polymers. We made these normally insulating polymers conductive by mixing them with a large volume of conducting powder, often carbon. The conduction is by percolation paths through chains of the powdered conductor, and swelling of the polymer increases resistance by breaking some of the chains. The polymer that showed the best behavior in terms of speed of response, baseline stability, and reproducibility of signal over time to many different analytes was a copolymer of polyethylene and polyvinylacetate (PEVA). We were excited to see that signals from some volatile organic chemicals (VOCs) like toluene could be seen with only a few ppm of partial pressure. The baseline stability was so good that changes in resistance due to low levels of analyte of less than 0.1% could be reliably measured over many hours. Other polymers included polyisobutylene (PIB), polydiphenoxyphosphazine (DPPZ), syndiotactic polybutadiene (PBS), polyvinylalcohol (PVA), and poly-N-vinylpyrrolidone (PNVP). When we plotted signals from these polymer sensors versus the solubility parameter of a wide variety of solvents, we found that no solvent goes undetected by at least one of the sensors. These results confirm our hypothesis that a four- or five-sensor array can be used as a universal solvent sensor.

3531.160

Advanced Neutron-Tube Design and Producibility

J. P. Brainard, R. S. Goeke

This work has two goals: (1) to develop doped insulators to replace an uncontrolled coating process now used to reduce wall-charging in neutron tubes, and (2) to apply integrated circuit (IC) technology to the production of more reproducible ion sources.

Neutron-tube ion sources contain a patterned metal hydride thin film. The current fabrication technique uses a physical mask that is placed in intimate contact with the source assembly. Correct registration of the mask to the source substrate is critical. An operator assembles the source substrate, mask, and fixturing with the aid of an optical microscope. The assembly process is time-consuming and highly dependent on the skill of the operator.

An alternative technique is to replace the physical contact mask definition of the patterned film with photolithographical processing. Photolithography is used in the IC industries to define features smaller than those on an ion source. In this process, we deposited the film over the entire source assembly face. We then spun photoresist onto the film and defined a pattern by exposure to ultraviolet (UV) light through a chrome glass mask. Once the pattern was developed, we could etch away the metal film in the exposed regions, leaving the patterned metal film. We then removed the photoresist.

We found that hydrided metal films etch very poorly. The MHx material apparently is stable and resists dissolution. We performed further experiments on pure metal films with the understanding that the films would be post-hydrided. We varied etchant concentrations and determined etch rates for the metals of interest.

Initial results of patterned metal etching showed severe undercutting of the resist pattern by the etchant. We believe this to be due to poor adhesion of the resist film to the metal. We are currently trying to improve the quality of this adhesion.

We began research into the use of IC technology to produce ion sources. This research was slated to determine if standard semiconductor processing techniques can be effectively applied to reliably produce hydrided metal film patterns for neutron-tube applications. Initial evaluation showed that hydrided metal films etch very poorly. The MHx material apparently is stable and resists dissolution. We pursued a second approach involving further experimentation on pure metal films with the understanding that the films would be hydrided after formation by the etching technique. We conducted a parametric evaluation using several variables: etchant concentrations and etch rates as applied against various metals of interest.

The initial results of the second approach, patterned metal etching, showed severe undercutting of the resist pattern by the etchant. Subsequent evaluation led us to believe that poor adhesion of the resist film to the metal is the cause of this unacceptable undercut. We are presently evaluating additional techniques to improve the quality of the film adhesion to yield our desired pattern.

3531.170

Surface Hardening by Nanoparticle Precipitation and Atomic Clustering in Ni(Al,O)

S. M. Myers, Jr.

This project explores strengthening of the near surface of nickel (Ni) by dense dispersions of hard oxide particles and atomic clusters in the size range from ~ 1 nm downward. These dispersions are formed by various combinations of aluminum (Al) and oxygen (O) ion-implantation and Al and O ion-diffusion from surface sources in conjunction with heat treatments to manipulate particle microstructure. Mechanical properties are quantified by nanoindentation coupled with finite-element (FE) modeling, and microstructures are characterized by transmission electron microscopy (TEM). Theory predicts that the extremely small sizes and separations of the hard particles in such metal matrices should give rise to new highs of strength with retention of ductility. Specific objectives of the project are (1) to probe the limits of strengthening that can be reached at the extremes of small particle size and high particle density, (2) to extend such hardening to the technologically important iron-nickel (Fe-Ni) class of materials, and in particular to Ni because of its anticipated use in defense-related microelectromechanical systems (MEMS), and (3) to explore diffusion as an alternative to implantation for nanoparticle-hardening in metal matrices where the alloying additions are soluble.

Ion-implantation of O into Ni at a concentration of 8 atomic percent produced a yield strength of 5 GPa and a hardness of 14 GPa within the treated layer, as shown by nanoindentation testing combined with FE modeling. Corresponding values for hard bearing steels extend only to about one-half of the above, so that the implantation treatment has, in fact, achieved a new level of strength in the Ni-Fe system. Moreover, the treated layers were ductile and adherent during severe deformation of the specimen surface.

TEM of the above material revealed a dense distribution of Al2O3 particles with an average size of about 2 nm and a volume fraction near 13% within the implanted layer. Application of dispersion-hardening theory to this microstructure gives a predicted yield strength of 5 GPa, in good agreement with the above experimental result. This serves to validate the theory in the regime of extreme particle refinement and density.

Initial mechanical testing of Ni(Al,O) alloys formed by ion-diffusion of Al and O at elevated temperatures revealed strengthening that was significant but substantially less than that achieved by ion-implantation of Al and O at room temperature. This difference is provisionally attributed to a lesser degree of microstructural refinement in the diffused alloy.

3531.180

Dynamical Properties of Polymers: Computational Modeling

J. G. Curro

The Polymer Reference Interaction Site Model (PRISM) theory has been extremely successful in modeling the equilibrium structure and physical properties of bulk, amorphous polymers. In this investigation, Sandia will attempt to also use PRISM theory to extract information regarding nonequilibrium properties. In the past, dynamical properties such as the glass transition and viscoelasticity have been correlated with the static, equilibrium structure of the polymer through the free-volume distribution. Although the free-volume concept has long been useful from a qualitative viewpoint, it has not had a precise statistical mechanical interpretation. PRISM theory has the ability not only to provide this fundamental interpretation, but also to provide a computationally tractable modeling tool to compute the free-volume distribution for polymers at the atomistic level. In this project, we would use the PRISM theory to extract the free-volume distribution of a range of polyolefin polymers to test its ability to predict glass-transition temperatures, diffusion constants, and viscoelastic shift factors. If this approach is successful, the modeling capabilities of PRISM theory will be greatly extended.

We developed a computational technique that allows one to compute the free-volume distribution of a polymer material from PRISM theory. The cumulative free-volume distribution is defined to be the probability of inserting a spherical cavity of a given diameter *s* into an already-existing polymer liquid. We found this probability function by integrating the radial distribution function *g(r)*, obtained from PRISM theory, as the cavity size was systematically increased from *0* to *s*. We wrote a computer code to implement this computational strategy and successfully demonstrated it for an idealized, freely jointed chain model of a polymer. We also wrote a computer code to compute the free-volume distribution of semiflexible chains with a variable chain stiffness. We performed calculations on both freely jointed and semiflexible chain melts as a function of chain length and chain stiffness. We found that as the chain stiffness increases, the free-volume distribution becomes narrower and more sharply peaked at low free volume.

3531.210

Calculation and Interpretation of the Energies that Underlie Transition-Metal Surface Structure

P. J. Feibelman

Recent advances in computer power and in algorithms for first-principles, electronic structure calculation make it possible to evaluate energy versus atomic arrangement for essentially any bonding geometry of any combination of atomic species. Sandia will use this power in a systematic effort to uncover basic laws of surface energetics. Using state-of-the-art electronic-structure methods, we will determine the energies and geometries of fundamental atomic configurations at transition-metal surfaces to a well-defined level of numerical convergence. The results will serve as a standard systematic foundation for the discovery and explanation of trends in adatom and vacancy formation energetics, diffusion mechanisms, vibration spectra, molecular-fragment stability, surface stress effects, work functions, etc. They will also provide a reference by which to judge the range of accuracy of the basic physical approximations used to represent the effects of electron exchange and correlation, that is, the local density and generalized gradient approximations.

Surface diffusion by concerted substitution (CS) implants adsorbed atoms into a metal's outermost layer at low temperatures. Knowing when this process will occur is therefore vital to controlling growth morphology. To learn the rules that determine the low-T self-diffusion mechanism on transition-metal (100) surfaces, and particularly to assess the relevance of tensile surface stress, we performed extensive *ab initio* calculations. The results for Rh (rhodium), Ir (iridium), Pd (palladium), and Pt (platinum) show that the barrier to surface self-diffusion by CS is lower on surfaces where the substrate relaxation around an adatom and the corresponding energy gain are greater. For example, on Ir(100) and Pt(100), where CS is known to be the low-barrier self-diffusion process, lattice relaxation reduces the adatom formation energy by at least 16%. On Pd(100) and Rh(100), which favor self-diffusion by hopping, the reduction is 10% or less. On the other hand, the calculations contradict the notions discussed in the published literature that lower-barrier CS corresponds to larger clean-surface excess tensile stress or to tensile stress reduction in the CS-barrier geometry.

Publications

Refereed

Feibelman, P. J., and R. Stumpf. 1998. "Adsorption-Induced Lattice Relaxation and Diffusion by Concerted Substitution." *Phys. Rev. B*, submitted.

Other

Feibelman, P. J. 1998. "Are There Laws of Surface Stress?" Paper presented to the Conference on Atomic Origins of Stress and Strain at Surfaces, Halle, Germany, 6 June.

3531.220

Interfacial Reactions in Ceramic Systems

R. E. Loehman

Understanding and control of interfacial reactions are important to many applications of ceramics. Such reactions can determine the processing and performance of multilayer electronic devices, sensors, cermets, composites, and ceramic-metal seals. This research seeks to develop a fundamental understanding of reaction mechanisms by performing controlled wetting and reaction experiments in a high-temperature vacuum furnace equipped with a quadrupole mass spectrometer for atmosphere analysis. Sandia will study reacted specimens by scanning and transmission electron microscopy (SEM/TEM) and electron-probe microanalysis. We will model thermochemistry using the MTData Gibbs energy-minimization code and databases.

We studied reactions between aluminum (Al) and monazite (LaPO4). We are actively developing monazite as a protective coating for ceramic fibers used in advanced composites. Some proposed compositions use reactive metals such as Al as a matrix component. We studied wetting and reaction of bulk LaPO4 by Al at 1200°C. Al reacts by a redox mechanism, creating a reaction layer of Al2O3. Lanthanum (La) formed in the reaction diffuses into the residual Al and precipitates on the grain boundaries on cooling. The phosphorus (P) formed in the reaction is either gaseous P or AlP that forms porous structures at the interface. Our present analysis cannot tell which is the case. We concluded that LaPO4 cannot be used to make composites that contain elemental Al.

In another result we did some wetting and reaction experiments for a yttrium (Y)-Al-silicate glass on aluminum nitride (AlN). We are developing AlN for components in chemical vapor deposition (CVD) chambers in the semiconductor industry because of its excellent thermal conductivity. However, suitable high-temperature joining techniques are not available. Our experiments suggest that the Y-Al-silicate glass may be useful to join AlN.

We also evaluated a refractory $Y2O_3$-Al2O3-SiO_2 glass and a gold-palladium-vanadium (Au-Pd-V) alloy for joining silicon-carbide (SiC) composites. Those continuous-fiber ceramic composites (CFCCs) comprise SiC fibers embedded in a SiC matrix. We measured contact angles for samples of the glass or alloy heated on composite coupons from 1200° to 1500°C in argon (Ar) or N_2. We inferred reactions from analyses of polished cross-sections of cooled specimens. We joined other specimens for strength measurements using process conditions determined from the reaction studies. The Au-Pd-V alloy wet all the composites and reacted with them to give a complex interfacial microstructure. Wetting by the glass differed strongly with the source of the composite, and reaction was less than with the alloy. Strengths measured in four-point bending are about 50 MPa, which is much lower than strengths obtained for these joining materials on other ceramics.

Finally, although preceramic polymers are finding uses in many applications, their interactions with ceramic powders and surfaces are not well understood. Previous work indicated that crystallization of Si3N4 from a polymer is affected significantly by the presence of sintering additives. We studied the effects of temperature on the interactions between polysilazane, ceramic powders, and additives. We coated SiN coupons by dipping them in slurries of ceramic powders, polycyclomethylsilazane, and solvent. After drying, we heated the coupons from 1000°C to 1750°C for 2 hours to pyrolyze the polymer and crystallize the derived ceramic materials to form a ceramic coating. We examined the resulting microstructures and compositions of the coatings by electron analytical techniques to determine mechanisms of pyrolysis reactions and subsequent conversion to the ceramic. In the next phase we will study interfaces to determine the relation between processing conditions, microstructure, and adhesion of the coating to the SiN.

Publications

Refereed

Loehman, R. E.; W. G. Fahrenholtz, and J. J. Walker (University of New Mexico); and J. B. Davis, J. R. Porter, and P. E. D. Morgan (Rockwell Science Center). 1998. “Wetting and Reaction of Monazite by Al.” Paper presented to the American Ceramic Society Conference, Cincinnati, OH, 6 May.

Other

Loehman, R. E., S. J. Glass, and B. E. Staley (University of New Mexico). 1998. “Interfacial Reactions in the Joining of SiC Fiber-Reinforced Ceramic Composites.” Paper presented to the American Ceramic Society Conference, Irvine, CA, 22 October.

3531.230

Direct Fabrication of Multi-functional Nanocomposites Via Supramolecular Self-Assembly

C. J. Brinker

The ability to efficiently organize molecular components at the nanometer scale will greatly influence the future of advanced materials in applications for electronics, catalysis, magnetism, sensors, and mechanical design. This stems from the fact that interplay of structure, organization, and dynamics at the molecular level are all vital in determining a functional response. Based on this premise, Sandia successfully developed an efficient, continuous process to form ordered nanocomposite thin films and particles via evaporation-induced self-assembly. We prepared thin films by spin- or dip-coating a homogeneous sol containing alcohol, silica precursors, organic monomers, initiators, and surfactant (at an initial concentration [co] below the critical micelle concentration [cmc]). Evaporation of the alcohol induces the formation of micellar structures that co-organize with silica to form cubic, hexagonal, or lamellar mesophases. We solvated the organic monomers and initiators within the hydrophobic micellar interiors. Subsequent photo or thermal polymerization and washing resulted in a silica/polymer thin-film nanocomposite. We demonstrated extension of this evaporation-induced nanocomposite self-assembly process to the preparation of particles with ordered (vesicular) structures via aerosol processing of related sols. Finally we initiated synthesis of polythiophene/silica nanocomposites in an attempt to develop conductive nanowires isolated in a dielectric medium.

We developed an efficient, continuous process to form ordered polymer containing nanocomposite thin films and particles via evaporation-induced self-assembly. The process starts with a homogeneous solution of soluble silicates, coupling agent, surfactant, organic monomers, and initiators prepared in ethanol/water solvent with an initial surfactant co below the cmc. During dip-coating, preferential evaporation of ethanol progressively enriches the concentrations of water, hydrochloric acid (HCl), and the nonvolatile solution constituents within the depositing film. As cmc is exceeded, micelles form, causing the spontaneous organization of inorganic precursors around the hydrophilic micellar exteriors and partitioning of alcohol-soluble monomer(s) and initiators into the hydrophobic micellar interiors. Continued evaporation promotes cooperative assembly of these (silica-surfactant-monomer) micellar species into interfacially organized liquid crystalline mesophases, thereby simultaneously organizing both the inorganic and organic precursors into the desired laminated structure in a rapid (~ 10 s), continuous process. Photo- or thermally-induced organic polymerization combined with continued inorganic polymerization locks in the nanocomposite architecture and covalently bonds the organic-inorganic interface. Through variation of the surfactant type or its initial co, we can exploit evaporation-induced self-assembly to arrive at other nanocomposite constructions. We can extend the process to particles with ordered (vesicular) structures via aerosol processing of related sols. Characterization of these materials showed that the resultant structure can be tuned, depending on variables such as surfactant type and concentration, humidity during dip-/spin-coating, and substrate preparation. Mechanical testing of the layered thin films via nanoindentation measurements quickly demonstrated the added value provided by such nanolaminated constructions. For example, nanoindentation performed on poly(4-methylstyrene)/silica nanolaminated thin films prepared with ~ 50 wt.% polymer showed a threefold increase in indentation hardness (from 0.3 GPa to 1.0 GPa) due to combined organic/inorganic polymerization. We noted that 1 GPa is the indentation hardness measured for rather dense sol-gel silica films. Hence, this material, containing 50 wt.% soft polymer, has a similar hardness value to that of pure silica films. This enhancement in mechanical properties achieved by the nanolaminated construction is similar to that observed for seashell nacre, composed of alternating layers of calcium carbonate and biopolymer. We measured nacre to be two times harder and 1000 times tougher than its constituent phases. We believe this nanocomposite self-assembly process will be important for applications requiring hardness and toughness combined with optical transparency. In addition, by confining polymers to small dimensions and reinforcing them on a molecular scale with silica, we anticipate achieving totally new materials properties.

Publications

Refereed

Sellinger, A., P. M. Weiss, A. Nguyen, Y. Lu, R. A. Assink, W. Gong, and C. J. Brinker. 1998. "Continuous Self-Assembly of Organic-Inorganic Nanocomposite Coatings that Mimic Nacre." *Nature* **394** (16 July): 256–260.

Other

Sellinger, A., P. M. Weiss, Y. Lu, and C. J. Brinker. 1998. "Self-Assembly of Organic-Inorganic Nanocomposite Coatings that Mimic the Structure of Shell." *Hybrid Materials, Proc. MRS* **519** (San Francisco, CA, 13–17 April): 95–102.

3531.240

Biophotonic Materials for Optical Encryption and Noncomputing

J. A. Shelnutt

The photosynthetic protein bacteriorhodopsin uses light energy to pump protons across a membrane in some photosynthetic bacteria. The protein contains a retinal molecule that experiences a large-scale, photo-induced, conformational switching that functions as the light-activated proton pump. An analogous optical molecular switch composed of a more robust nonbiological molecule like a porphyrin has obvious importance in photonics, microelectromechanical systems (MEMS) devices, and chemLab chip integration. Sandia demonstrated such a new type of light-activated molecular switch. We will engineer these new biophotonic materials to the point where optical encryption devices can be fabricated using vertical-cavity surface-emitting laser/charge-coupled device (VCSEL/CCD) technologies. We will enhance the optoelectronic properties (lifetimes and light-absorption characteristics) of the molecular switch using computer-guided synthesis of new analogs. In addition, we will support the molecular switches in polymers for use in photonic and encryption devices. We will demonstrate the potential of these biophotonic materials for many defense-related and commercial applications (including ultra–high-density [> 1 Gbyte/cm^2] optical memory, ultra-fast [1 ps] optical switching, optical limiting, Q*-switching, cavity dumping, mode locking, monolithic optoelectronic integration, sensor arrays, displays, verification and encryption, and noncomputing).*

We previously demonstrated a novel optical switching method in a nickel (Ni) porphyrin. However, the lifetime of the optically switched state was only 50 nanoseconds at room temperature and 6 microseconds at liquid nitrogen temperatures. Our goal was to utilize the conformational trapping mechanism by which the optical switch works to design a Ni-porphyrin analog in which the switched-state lifetime is in the seconds-to-years time regime. We designed such a molecule, nickel octabromo-tetra(trifluoromethyl)-porphyrin, using molecular simulations methods and synthesized it. By the addition of electron-withdrawing groups, we introduced a new mechanism (axial ligation) for extending the lifetime along with conformational trapping. We investigated the properties of the new optical switch by optical absorption, fluorine nuclear magnetic resonance (NMR), and resonance Raman spectroscopy, and by x-ray crystallography. Electron spin resonance and femtosecond time-resolved ultraviolet (UV)-visible absorption measurements are in progress. These results indicate that we have an optical switch with an apparent switched-state lifetime of minutes to months, depending on the type of molecular support or solvent. We filed a patent on the mechanisms and specific switching materials.

Publications

Refereed

Ma, J. G., M. Laberge, X. Z. Song, W. Jentzen, S. L. Jia, J. M. Vanderkooi, and J. A. Shelnutt. 1998. "Protein-Induced Changes in the Nonplanarity of the Porphyrin in Nickel Cytochrome c Probed by Resonance Raman Spectroscopy." *Biochemistry* **37** (1 February): 5118–5128.

Other

Ma, J. G., J. Zhang, R. Franco, S. L. Jia, and J. A. Shelnutt. 1998. "Resonance Raman Spectroscopy and Normal-Coordinate Structural Decomposition of the Hemes in Cytochromes c3." *Biophysical J.* **74** (Kansas City, MO, 22–26 February): A113.

Ma, J. G., R. Franco, S. L. Jia, and J. A. Shelnutt. 1998. "Conformational Differences of the Hemes in Cytochromes c3 Probed by Resonance Raman Spectroscopy." *Bulletin APS* (Los Angeles, CA, 16 March).

Zhang, J., J. G. Ma, M. Laberge, J. M. Vanderkooi, S. L. Jia, and J. A. Shelnutt. 1998. "Nonplanarity of the Porphyrin in Nickel Cytochrome c Probed by Resonance Raman Spectroscopy." *Bulletin APS* (Los Angeles, CA, 16 March).

3531.190

Broadening Mechanism in 2-D Excitonic and Electron Gases

E. D. Jones

This research will investigate the origins for the broadening mechanisms leading to the Gaussian photoluminescence (PL) lineshapes observed in doped and undoped quantum-well (QW) structures. All homogeneous broadening mechanisms predict a Lorentzian (lifetime) broadened lineshape, while inhomogeneous effects lead to Gaussian lineshapes. Experimentally, Sandia will observe Gaussian PL lineshapes for all samples, ranging from nearly free exciton (undoped) systems to doped structures exhibiting band-to-band transitions at high magnetic fields. The latter result is surprising because it is generally believed that electron screening in doped systems will smooth out the effects of varying internal electric fields arising from QW fluctuations.

This study will consider the effects of artificially (or controlled) induced fluctuations. We will generate fluctuations due to varying QW widths by growing self-aligned islands indium gallium arsenide (InGaAs) alloys in InGaAs single-strained-layer QW structures or by placing InAs quantum dots on the GaAs QWs in GaAs/AlGaAs systems. We can then study the effect of randomness by also growing nonaligned (random) islands or quantum dots. We will make the same kinds of studies for the doping layer thickness for modulation-doped QWs. The PL lineshape contribution from deformation potential fluctuations vis-à-vis the electron-phonon interactions can also be made by deliberately growing InGaAs alloy clusters formed by low-temperature growth.

We collaborated with researchers at Emory University in Atlanta, GA, to write an analysis program for studying the magnetoexciton energy, linewidth, and binding energy for a series of GaAs QW structures. This study considered the contributions to the exciton linewidth in a series of (411)A GaAs/AlGaAs QWs. We also collaborated with researchers at the University of California–San Diego for scanning-tunneling microscope (STM) measurements of QW-size fluctuations. We successfully applied our theoretical modeling to experimental data of GaAs/AlGaAs QWs ranging in widths from 0.6 to 1.2 nm. We performed the measurements at 1.2 K, and the magnetic fields ranged between 0 and 13 tesla. We had to modify the theory to account for conduction-band mass nonparabolicity and also a QW width-dependent exciton binding energy. After we made these corrections, we found good agreement with binding energies and magnetoexciton diamagnetic shifts.

3531.250

Low-Stress Amorphous Diamond: A New Material for Sensors

J. P. Sullivan, T. A. Friedmann

The purpose of this project is to create new types of sensors with greatly enhanced performance using a new material that Sandia recently discovered: stress-free amorphous diamond (a-D). Stress-free a-D is a unique material that has some of the best properties of crystalline diamond (extreme high hardness and elastic modulus, low coefficient of friction, high wear resistance, high toughness, and chemical inertness) together with some of the best properties of thin-film materials (low and tunable film stress, extreme surface smoothness, ease of synthesis, low-deposition temperature, and a robust process for deposition). By taking advantage of these unique properties, we fabricated flexural plate-wave (FPW) devices that employ a thin membrane of a-D (1000 to 1500 angstroms thick) as the working element. We also developed a simple, reliable processing sequence for the creation of these devices, using photolithographically patterned aluminum (Al) lines and a high-density-plasma deep-etch tool (a Bosch etcher). The FPW devices realized from this process were easier to synthesize than conventional silicon-nitride (SiN) FPW devices and offer greater promise of achieving high sensitivity and low resonant frequency (important both for controlling the ultimate detection limit and for enabling alternative sensor concepts, such as acoustic sensors that work in the audible range).

We created and tested a working sensor, the FPW device, that uses a new material, stress-free a-D. This new material—developed at Sandia—has many of the mechanical properties of crystalline diamond but the processing advantages of a thin-film material. We demonstrated that it is possible to create ultra-thin, free-standing membranes in this material that are at least one inch in diameter and only six-hundred angstroms (approximately 300 to 400 atomic layers) thick. We used several processing sequences to create the FPW device. For one processing sequence, an Al meander line was photolithographically patterned onto an a-D film on Si. We then created a membrane out of the a-D material by etching the Si in an anisotropic chemical etch (potassium hydroxide and water). The second processing approach also used

photolithographically patterned Al lines, but we achieved the etching of the Si using a deep-etch tool (a Bosch etcher). We found that this second approach easily and reproducibly creates the FPW device. We discovered that the extreme inertness of a-D results in a selectivity to the Bosch etch process of 1 in 1000 (in the time it takes to etch one unit of Si, only 1/1000th of a unit of a-D would be etched). This selectivity is far better than SiN (about 1 in 75), and thus enables a-D membranes to be synthesized that are both far thinner than SiN membranes and that also are far easier to create. We are developing a technical advance on the use of a-D films as an etch-stop layer for deep-etching.

The FPW devices that we synthesized have a-D membrane thicknesses of 1000 to 1500 angstroms, which is considerably thinner than comparable SiN FPW devices (5000 to 10000 angstroms thick). These devices have performance that is as good as or better than the best SiN devices of the same geometry but with the promise of far exceeding SiN devices (with small additional processing improvements). Furthermore, the ease with which it is possible to create sensors using ultra-thin a-D membranes enables new future sensor concepts, such as miniature acoustic sensors with good response in the low audio-frequency range.

Publications

Other

Sullivan, J. P., T. A. Friedmann, A. J. Magerkurth, M. P. de Boer, M. M. Bridges, and C. I. H. Ashby. 1998. "Amorphous Diamond Micromechanical Structures." *Mater. Sci. of Microelectromechanical Sys. (MEMS) Devices, Proc. MRS* (Boston, MA, 2 December).

3531.260

Nanoengineered Cu-Al Defects in Al: A Prototype System for Corrosion

N. A. Missert, J. P. Sullivan

The modeling and prediction of corrosion, particularly in metals that undergo localized corrosion, has remained elusive despite centuries of investigation. This project will isolate one potential corrosion mechanism in aluminum (Al) alloys by intentionally fabricating nanoscopic aluminum-copper (Al-Cu) defects in Al with well-defined spatial and chemical properties, then systematically identifying which properties of the defect led to the onset of localized corrosion. This is the first step in enabling the development of computational codes that can accurately model and predict.

The fundamental scientific question to be explored is: How does an Al-Cu precipitate in Al act to initiate localized corrosion? Surprisingly, even for this one simple defect structure, several mechanisms may be occurring to initiate corrosion: (1) the Al-Cu particle is more noble than the matrix, (2) the Al oxide that forms over the A1-Cu particle may be defective, and (3) the existence of Cu impurities in the Al oxide may enable high-leakage currents locally in the oxide. We hope to learn (1) which corrosion mechanism(s) is/are operative, (2) over what size scales this/these mechanism/s is/are operative, and (3) what are the electrochemical signatures of this specific defect (so that the action of this defect can be recognized in a real alloy system). This will ultimately help lead to the development of a computational model of corrosion.

We achieved arrays of nanoengineered Cu-Al defects on Al thin films that dominate the electrochemical response. Optimized Al templates for growth of isolated Al-Cu defects are deposited by electron beam evaporation. Small-grained, random-orientation films provide a low-leakage-current, high-pitting-potential surface for nanofabrication of the Cu defects. We used photolithography to define defect sizes of 2–50 microns with spacings ranging from 10–100 microns. Residual oxide is removed by argon (Ar) ion plasma prior to the Cu deposition to allow a clean Cu-Al interface as observed by x-ray photoelectron spectroscopy. Electron beam evaporation of Cu results in large arrays of identical defects, which we then subject to electrochemical testing.

Our initial results indicated that the nanoengineered defects are extremely active relative to the surrounding Al matrix. Under free corrosion conditions, metastable events that may be associated with Al dissolution in the vicinity of the defects dominate the response for time scales up to 4000 seconds. At longer times, the events cease and the system achieves a constant potential. The final state of the sample shows that the Al is dissolved down to the silicon (Si) substrate in the vicinity of the Cu defect for each defect in the array structure. In addition, Cu is dissolved and redeposited in a halo surrounding the region of Al dissolution. Clearly the nanoengineered defects are governing the electrochemical response.

3531.270

Novel Energy-Conversion Devices of Icosahedral Borides

T. L. Aselage

Solid-state devices are commonly used to generate electrical power from radiant energy sources. These devices rely on the incident radiation to generate electrons and holes in semiconductors. The power obtained from such devices is proportional to the rate of carrier generation and to the efficiency with which generated carriers are collected. The rate of generation increases as the energies of incident particles increase. Radioactive decay processes yield particles with very high energies: 105 to 108 eV. Furthermore, radioactive materials are reliable, continuous energy sources. Unfortunately, solid-state devices that directly convert nuclear energy to electrical energy using conventional semiconductors are not feasible since these solids do not survive bombardment with high-energy particles. Icosahedral borides, however, have been shown to be especially resistant to radiation damage. In particular, vacancies and interstitials induced by bombardment of icosahedral borides appear to spontaneously recombine with one another—self-healing. Thus, bombardment fluxes that would severely damage or amorphize conventional semiconductors produce no observable defects in icosahedral borides. This remarkable observation of self-healing in icosahedral borides makes plausible the successful operation of a device based on these materials to directly convert the energies of nuclear particles into electrical power.

This project explores capitalizing on the self-healing of radiation-induced damage in icosahedral borides to develop novel power sources that directly convert the energies of nuclear particles into electrical power. The goal of the project is to evaluate the advantages and disadvantages of various radioisotopes for use in such devices. We identified several attractive radioisotopes.

There are abundant radioactive sources with potential for our devices. These sources differ in the particles they emit: *a*-particles, *b*-particles, and *g*-rays. We found *b*-particle emitters to be the most promising for direct energy conversion using icosahedral borides. Among radioisotopes that emit *b*-particles, differences occur in intensities, half-lives, and the required shielding. The source chosen for each application should optimize these factors.

a particles are doubly charged, energetic, and penetrate only short distances in solids. Despite these attractive features for direct energy-conversion devices, their accumulation within bombarded solids would ultimately damage the material. Furthermore, *a*-particle bombardment of light elements, such as boron (B), generates high-energy neutrons that pose a substantial hazard. Because of their weak interactions, neutrons penetrate long distances through solids. For this reason, sources that generate energetic neutrons require extensive shielding: about 25 cm of paraffin is required to shield a 1 W *a*-particle/*b*-source.

Even though *g*-rays create electron-hole pairs in solids, they are not attractive for our energy-conversion devices because the energy they deposit per unit distance is very small. Attempting to capture a response from *g*-rays would require a very large device.

b particles offer the greatest potential for our energy-conversion devices. Unlike *a*-particles, stopping *b*-particles within a solid does not directly introduce large strain fields. However, some degree of shielding is required to attenuate energetic photons that accompany *b*-particle emissions. These energetic photons arise from two sources. First, some *b*-emitters radiate *g*-rays from nuclear processes. Second, a small fraction of energy of the *b*-particles is converted to radiation as they are decelerated in a solid, Bremsstrahlung. Since the intensity of Bremsstrahlung increases with the atomic number of the bombarded solid, the low atomic number of B is advantageous.

Most attractive *b*-particle emitters are readily available in the waste of power reactors. Others may be produced intentionally in nuclear reactors. The nuclear energy available from selected *b*-emitters is very large. These capacities range from 1.1 MW per hour per mole of ^{147}Pm (promethium) to 25 MW per hour per mole of ^{144}Ce (cerium). The half-lives of attractive radioisotopes vary from 0.35 to 30 years. Energy-conversion devices based on these sources thus offer the potential to produce significant, continuous power over extended time periods.

Some illustrate examples of particular *b*-decay sources, and their choices for specific applications follow. In these illustrations, the lifetime of a device is taken to be the half-life of the isotope, and the power listed is the initial power available from the nuclear decay of the pure isotope.

^{147}Pm is appropriate for a minimally shielded, lightweight source when moderate lifetime (2.6 years) and power (0.05 kW/mole) are sufficient. ^{170}Tm (thulium) is appropriate for a high-power device (2.2 kW/mole) that can tolerate a short lifetime (0.35 years) and moderate shielding. ^{144}Ce is appropriate for a high-power device (3.6 kW/mole) that can tolerate a moderate lifetime (0.78 years) and extensive shielding. ^{90}Sr (strontium) is appropriate for a long-lived device (28 years) that delivers moderate power (0.08 kW/mole) and can tolerate significant shielding.

Publications

Other

Aselage, T. L., and D. Emin. 1998. “Novel Energy Conversion Devices of Icosahedral Borides.” Paper presented to the JASON Summer Study, San Diego, CA, 15 July.

3531.280

Ion-Mobility Spectroscopy of Biological Materials

P. J. Rodacy, M. A. Butler

The military has used ion-mobility spectrometers (IMS) to detect chemical agents for over ten years. Sandia developed IMS for the Federal Aviation Administration (FAA) portal detector and is using IMS for the detection of landmines, sea mines, and unexploded ordnance. The only area of IMS that has not been pursued is in the detection of large molecules such as biological agents. To the best of our knowledge, no preliminary data exist. In addition, the increasing use of biological agents by terrorist groups mandates better detection techniques for these materials, and IMS appears to be one of the prime candidates. This project will allow Sandia to maintain our position as a world leader in all areas of IMS and to begin responding to an international need for a sensitive, specific biological agent detector.

This project demonstrated that we could successfully introduce biological materials into an IMS using an electrospray inlet system and see a response. Poor resolution prevented the identification of individual species.

We designed and built a small IMS and fabricated appropriate control electronics. We performed a series of tests to optimize the system to respond to the long drift times (60 to 80 milliseconds versus 5 to 20 milliseconds normally used) expected of these large molecules. By using innocuous viruses, we demonstrated that the IMS responded. However, we observed a large proportion of this response in the reactant ion behavior, with only a small (indistinct) signal resulting from the parent virus. We believed the most likely reason for this poor response to be (1) poor ionization efficiency, (2) poor transfer of the viruses through the drift tube, or (3) instability of the viruses when exposed to the high electrical fields in the electrospray apparatus. To improve the IMS response, we used various electro-phillic solvents to maximize the ionization efficiency, examined the transfer efficiency through the drift tube, and verified that bacteria (used instead of viruses for this test because of our ability to grow a culture) showed that the large biological molecules can survive electrospraying without decomposition.

Publications

Refereed

Rodacy, P. J., M. Butler, and J. Sterling. 1998. “Analysis of Biological Materials Using Ion Mobility Spectroscopy.” Sandia Technical Report, in progress.

3531.310

Direct Fabrication of Planar Solid-Oxide Fuel Cells

J. Cesarano, III

Solid-oxide fuel cells (SOFCs) are efficient power sources that are capable of both using a wide range of fuels and avoiding the problems associated with liquid electrolytes. The solid-state character of all the components also means that there are no intrinsic restrictions on the cell configuration. However, current manufacturing of SOFCs is very complicated and requires many processing steps, which has limited SOFC fabrication to relatively large shapes with simple cylindrical or planar geometries. Therefore, for SOFCs to be used on a widespread basis and have their inherent design capabilities fully exploited, the fabrication methods must be simplified and be versatile enough to process the various component materials into precise structures.

Sandia will adapt techniques currently being developed for direct fabrication of ceramics to the fabrication of advanced SOFCs, which could hence be used for rapid fuel-cell manufacturing and inexpensive fabrication of miniature fuel cells. We based the fabrication technique on technology for computer-controlled extrusion of powder slurries and used this project to demonstrate feasibility for the direct fabrication of highly concentrated yttria-stabilized zirconia slurries.

We completed this project to determine the feasibility of using robocasting technology for the direct fabrication of solid-oxide fuel cells. Robocasting is the moldless fabrication of materials by computer-controlled deposition of highly concentrated powder slurries. We have already demonstrated the technique for aluminum oxide fabrication. An important material for solid-oxide fuel cells is yttria-stabilized zirconia. Therefore, the objective of this work was to develop highly concentrated yttria-stabilized zirconia slurries that could be directly fabricated into dense parts with robocasting technology. We accomplished this objective, which is the first step in creating a capability at Sandia for the complete fabrication of multimaterial fuel cells in one robocasting operation.

We made highly concentrated yttria-stabilized zirconia slurries with powders supplied by Tosoh, Inc. We wet-milled the powders with polyelectrolyte dispersants to eventually achieve a solids loading that was 54 vol.% zirconia. The slurries were relatively stable with respect to settling and exhibited a rheology useful for robocasting with a syringe. We fabricated solid samples approximately 2 cm x 1 cm x .7 cm thick in a moldless layer-wise fashion. We deposited the slurry through an orifice .8 mm in diameter. After complete drying, the samples were 58% of theoretical density. After sintering, the samples were completely dense and translucent. The measured average density was 99.9% of theoretical.

3531.290

Visualization Tools for MEMS Designs in a Virtual 3-D World

S. L. Miller, G. F. Lavigne, V. R. Yarberry, J. H. Smith

The field of microelectromechanical systems (MEMS) is growing rapidly, with great potential to benefit applications to Defense Programs (DP) as well as commercial partnerships. The market for MEMS is anticipated to reach $14 billion by the year 2000. One of the key barriers to product realization and commercialization is the lack of design and visualization tools available to MEMS designers. This barrier was identified by both the Sandia Microsystems Roadmap and the Commercialization of Microsystems Workshop. This project will overcome this barrier by developing a visualization tool that enables designers to see their designs realized in a virtual 3-D space before they commit their designs to fabrication.

Presently, Sandia uses AutoCAD as a design and layout tool for MEMS. This product is an accepted standard for mechanical design and includes some visualization features appropriate for simple macro structures, but does not include the complex features needed for a designer to visualize the intricacies of components fabricated with MEMS. Imagine a designer being able to explore the subtle design issues of a MEMS part in the same way that a dust mite can presently explore a MEMS microengine.

The result of this work will be increased visualization capabilities for the designer, which will overcome one of the key barriers to the commercialization of MEMS and the realization of products in MEMS for DP applications.

We developed a system for 3-D visualization of MEMS devices for use with the Sandia four-layer polysilicon SUMMiT (Sandia Ultra-planar Multilevel MEMS Technology) process. This system consists of an AutoCAD user interface and the visualizer code. These codes execute under the Windows NT 4.0 operating environment.

The AutoCAD user interface, written in LISP, provides the MEMS designer with a button to initiate the visualizer. The MEMS designer can select the initial viewing area. The code extracts the mask geometry formed by circles and closed polygons, then creates a hierarchical 2-D geometry file.

The 2-D geometry file provides input to the visualizer. The visualizer, which runs on a PC, converts the 2-D geometry to 3-D surfaces based on an extrusion model. This model extrudes the 2-D geometry using nominal dimensions specified for the SUMMiT process. The result is a 3-D surface model that can be viewed by the MEMS designer. The designer reviews the structures using a joystick to control elevation and azimuth. Control of panning and zooming allows the designer to fly through the geometry to inspect the simulated structure. This navigation process occurs in real time.

We translated the standard Sandia library of MEMS components using this system. This provides recallable views of over 40 MEMS components. The 3-D visualizer is currently available for use in the MEMS Design Lab.

We expect that this new capability will dramatically increase the MEMS designers' understanding of the SUMMiT design process, reduce design errors, and improve design turnaround time, significantly reducing cost. The creation of this design tool will greatly improve access to MEMS technology by both national laboratory and commercial designers.

3531.320

Micromachining with Ultra-Short Pulsewidth Lasers

D. P. Adams, G. L. Benavides, D. E. Bliss, S. M. Cameron

Numerous technologies critical to Sandia require components having micron-size features patterned over large areas. This includes subminiature stronglinks, neutron-tube micro-mechanical screens, switch tube triggers, and the microChem laboratory-on-a-chip (µChemLab). However, existing microfabrication techniques are limited in their ability to pattern a diverse set of materials. For example, LIGA (German for lithography, electroforming, molding) is useful for patterning unique 2-D structures but is restricted to electroformable metals. In this work, we intend to research ultra–short-pulse laser ablation as a tool for drilling and milling high-aspect-ratio features. Specifically, we will determine the feasibility of micromachining a variety of structural materials, such as non-electroformable metals and their alloys.

This work will explore the use of lasers having pico- to femtosecond pulsewidths. Recent research involving single-pulse drilling demonstrates that these lasers are amenable to precise micromachining of metals, compared with conventional industrial lasers. The quality of ablated patterns improves with decreased pulsewidth, in part because the thermal diffusion length is reduced. As a result, material is removed more efficiently with little damage to the volume surrounding a feature (i.e., no large melt zone). Also, the destructive effects of plasmas,

formed over machined holes during conventional laser drilling, are reduced when using ultra-short pulses.

We demonstrated that femtosecond-pulse lasers are useful for precise micromachining of metal alloys. We prepared a Ti:sapphire laser system for this project. The apparatus allows for sample ablation at atmospheric pressure and under vacuum and incorporates an *x,y* stage for accurate positioning of target samples. The optics provide small spot diameters of < 20 microns. We ablated samples of Kovar using femtosecond pulses of light. In particular, we drilled multiple holes to different depths to probe the evolution of hole shape, the morphology surrounding a hole, and their dependence on laser fluence. In general, the material removal rate depends on fluence and the pressure surrounding the target. The experiments determine that the ablation threshold for this metal alloy is 100 mJ/cm^2. Samples drilled in vacuum show a smoother-edge morphology compared with samples ablated in air. In this report we also analyze the morphology surrounding holes drilled by other femtosecond-pulse lasers. In collaboration with the University of Arkansas, we drilled holes in Kovar using a femtosecond excimer laser.

Publications

Other

Bliss, D. E., D. P. Adams, and S. M. Cameron. 1998. "Laser Machining with Ultrashort Pulses." Paper presented to the Materials Research Society Fall Symposium, Boston, MA, December.

3531.330

Molecular Characterization of Energetic Material Initiation

A. M. Renlund, A. S. Tappan, J. C. Miller

Sandia has responsibility for a diverse mix of energetic materials and components. Initiation, reactive wave growth, and ultimately deflagration or detonation depend on chemical and physical processes at the microscale. The high-explosive HMX (1,3,5,7-tetranitro-1,3,5,7-tetraazacyclooctane) is an energetic material used in many applications, from actuators to main charge explosives. Additionally, it is often used in propellant formulations. We recently discovered that its high-temperature polymorph (designated the delta-phase*) appears to control reaction progress for thermal initiation. Understanding the rate of phase transition as functions of temperature, particle size, pellet density, and confinement are critical to predicting cookoff response for components and systems. We will develop an* in situ *probe that can investigate the HMX phase in confined geometries and at elevated temperatures. We will rely on both Raman spectroscopy and second-harmonic generation (SHG) that appear possible with the delta-HMX. To access confined geometries, we will use optical fibers to deliver and return light from the sample. Optimizing the Raman scattering and simultaneous detection of SHG will be the main focus of the probe development. Following development of the experimental probe, we will examine the phase behavior of HMX in temperature ranges and confinement pressures relevant to component and system cookoff environments. In particular, we will apply this to monitor the kinetics of the phase transition and subsequent decomposition reactions that lead to explosive initiation.*

In previous work on Raman spectroscopy of HMX, we observed a curious phenomenon that appeared to be frequency-doubling of incident laser light when HMX underwent the beta-delta phase transition. We encountered a variety of problems quantifying the results, as there appeared to be both particle size and density effects. Recently, investigators at Los Alamos National Laboratory (LANL) independently observed this phenomenon. In the past two months we discussed these results and will try to investigate this method of tracking the phase transition jointly with LANL. Of primary importance is the simultaneous monitoring of the Raman spectrum and the frequency-doubling. We began literature surveys on SHG accompanying phase transitions or heating. Indications are that processes other than phase transitions could account for the experimental observations to date.

Publications

Refereed

Renlund, A. M., J. C. Miller, W. M. Trott, K. L. Erickson, M. L. Hobbs, R. G. Schmitt, G. W. Wellman, and M. R. Baer. 1998. "Characterization of Thermally Degraded Energetic Materials." *Proc. 11th Internat. Detonation Symp.* **11** (Snowmass, CO, 31 August), in press.

3532.070

Engineering Complex Distributed Systems

S. Y. Goldsmith, T. M. Berg, L. M. Napolitano, R. J. Pryor, G. C. Osbourn, B. L. Spletzer, J. T. Feddema, H. E. Link, L. R. Gilliom, S. V. Spires, L. R. Phillips

In this project, Sandia will develop a comprehensive design environment for the synthesis and analysis of complex distributed systems—in particular, engineered collectives. We will develop the initial fundamental theory for modeling, simulating, and designing systems composed of distributed autonomous actors with distributed decision making and control. Such systems will be capable of predictably realizing important systems-level behaviors. The resulting technology base will provide the basis for controlling the behavior of tens to millions of intelligent actors, especially robots inhabiting the physical world and software agents inhabiting large-scale networks. Through abstract models and the corresponding simulations, we will identify the critical parameters that influence collective behavior. We will use the models and simulations to evaluate relationships among those parameters and tradeoffs that enable the development of principled design methods. This project will establish Sandia as the engineering leader in emergent and cooperative behavior and will enable us to become an important supplier of advanced solutions to evolving national security needs. We will distinguish ourselves by focusing on the development of this new engineering discipline to enable the synthesis of sure solutions to real-world problems in complex distributed systems. As such, this project represents an investment in innovative systems engineering.

We gained initial insights into collective behavior and engineered collectives. We conducted extensive literature surveys in the fields of multi-agent systems, distributed artificial intelligence, statistical physics, information theory, agent architectures, communications, and intelligent systems. We conducted theoretical investigations of collective behaviors, developed models and computer simulations of agent collectives, and developed engineering prototypes of advanced software–based network agents.

Specific accomplishments include the following:

• Identified the canonical problem taxonomy and core technical challenges. Explored the congruence between the physical and cyber worlds within the canonical problem space.

• Developed the Alpha-Beta Coordination Algorithm for coordinating teams of mobile robot (alpha-beta).

• Developed a simulator for collective robotics.

• Developed a multi-agent optimization algorithm, a new paradigm in optimization.

• Invented a deliberative mechanism for software agents.

• Invented an adaptive sensory mechanism for software agents.

• Invented cloning and mating software agents.

• Established collaborations with the Santa Fe Institute (SFI), University of Southern California (USC), Carnegie-Mellon University (CMU), University of New Mexico (UNM), and Caltech.

• Completed an initial market assessment that provided strong support for this project.

• Wrote and presented numerous papers on collective robotics, optimization, agent development systems, and agent theory.

• Submitted three technical advances; eleven others are in preparation or identified for preparation.

• *Canonical problem articulation*. Our principal emphasis was on the source localization problem. We invented and tested in the collective robotics simulator a new coordination algorithm for controlling a team of mobile robots, called the *alpha-beta algorithm*. Simulated robots, controlled by this algorithm, effectively localize at the source of a measurable gradient. This algorithm is novel and represents a new approach to collective coordination of robot teams.

We initiated work related to the exploration and mapping problem. We developed a search strategy for mobile robots operating in information-poor environments that utilizes space-filling curves to ensure exhaustive search of geographic regions. We also initiated work on exploration and mapping in the purely cyber domain.

We made progress on the adaptive configuration canonical problem. We investigated concepts from pattern recognition and classification to attempt to give individual agents a means to recognize and represent emerging global configurations in a collective.

In understanding the collective problem class, we conceived a lattice model of communicating agents based on statistical mechanics concepts. Our interactions with others confirm the value of this approach.

• *Modeling and simulation environment*. We investigated several different approaches to simulating the

behavior of autonomous agent collectives: (1) an object-oriented simulator for a team of Robotic All-Terrain Lunar Exploration Rover (RATLER) robots, (2) an object-oriented simulator for collective robotics studies of teams of up to 500 actors in two dimensions, and (3) a simulator of abstract agents based on principals of molecular dynamics.

• *Individual intelligent agent life-cycle engineering capability*. We developed a second-generation software agent development framework that is based on design reusable patterns so that its applicability to multi-agent systems is enhanced. We developed a second-generation agent with significant meta-reasoning and control functions that enhance the agent's abilities to learn and adapt to changing environments. We incorporated new agent-reasoning functions into the development framework. We developed an initial approach to software agent cloning based on meta-object programming and cryptographic digital signature technology.

• *System surety approaches*. We identified and are pursuing four approaches to system surety: (1) first-principles design approaches that seek to provide architectural features to enable system surety, (2) formal methods, (3) risk-management approaches, and (4) principled design methods based on complexity theory.

Publications

Refereed

Feddema, J. T., and B. J. Dreissen. 1997. "Cooperative Target Convergence Using Multiple Algorithms." *Proc. SPIE Conf. on Decentralized Control in Autonomous Robotic Sys.* **3209** (Pittsburgh, PA, 14–17 October): 67–77.

Feddema, J. T., R. D. Robinett, III, and B. J. Dreissen. 1998. "Designing Stable Finite-State Machine Behaviors Using Phase Plane Analysis and Variable Structure Control." *Proc. 1998 IEEE Internat. Conf. on Robotics and Automation* (Leuven, Belgium, 16–20 May): 1134–1141.

Feddema, J. T., R. D. Robinett, III, and B. J. Dreissen. 1997. "Explaining Finite-State Machine Characteristics Using Variable Structure Control." *Proc. SPIE Conf. Decentralized Control in Autonomous Robotic Sys.* **3209** (Pittsburgh, PA, 14–17 October): 46–54.

Goldsmith, S. Y., and H. Link. 1998. "Using KQML to Communicate Mutual Beliefs and Shared Goals." *Proc. HICSS '99, Agents Track* (Maui, HI, September), accepted.

Goldsmith, S. Y., and R. D. Robinett, III. 1998. "Collective Search by Mobile Robots Using Alpha-Beta Coordination." *Lecture Notes on Artificial Intelligence, Proc. Collective Robotics World 1998 Workshop* **1456** (Paris, France, July): 135–146. Springer-Verlag.

Goldsmith, S. Y., L. R. Phillips, and S. V. Spires. 1998. "A Multi-Agent System for Coordinating International Shipping." *Proc. Agents '98* (Minneapolis, MN, May): in press.

Goldsmith, S. Y., S. V. Spires, and L. R. Phillips. 1998. "Object Frameworks for Agent System Development." *Proc. Amer. Assoc. for Artificial Intelligence* (Madison, WI, June).

Interrante, L. D., and S. Y. Goldsmith. 1998. "Emergent Agent–Based Scheduling of Manufacturing Systems." *Proc. Agents '98* (Minneapolis, MN, May).

Kwok, K. W., B. J. Dreissen, and C. A. Phillips. 1997. "Analyzing the Multiple-Target–Multiple-Agent Scenario Using Optimal Assignment Algorithms." *Proc. SPIE Conf. Decentralized Control in Autonomous Robotic Sys.* **3209** (Pittsburgh, PA, 14–17 October): 111–123.

Spires, S. V., and S. Y. Goldsmith. 1998. "Exhaustive Geographic Searching with Mobile Robots Along Space-Filling Curves." *Lecture Notes on Artificial Intelligence, Proc. Collectives Robotics World* **1456** (Paris, France, July): 1–12. Springer-Verlag

Other

Dreissen, B. J., J. T. Feddema, and K. S. Kwok. 1998. "Decentralized Fuzzy Control of Multiple Nonholonomic Vehicles." Paper presented to the 1998 American Control Conference, Philadelphia, PA, 24–26 June.

Hurtado, J. E., R. D. Robinett, III, C. R. Dohrmann, and S. Y. Goldsmith. 1998. "Cooperative Distributed Agents for Optimization." Paper presented to the IASTED International Conference on Controls and Applications, Maui, HI, August.

Pryor, R. J. 1998. "Developing Robotic Behavior Using a Genetic Programming Modal." Sandia Technical Report SAND98-0074 (January). Sandia National Laboratories, Albuquerque, NM.

Robinett, III, R. D., and S. Y. Goldsmith. 1997. "Critical Technologies Institute Presentation: Engineering the Behavior of Complex, Distributed Systems." Presentation to the Critical Technologies Institute, White House, Washington, DC, November.

3532.030

Global Approaches to Infrastructural Analysis (GAIA)

D. Engi, T. E. Drennen, K. L. Hiebert-Dodd, D. L. Harris

Our country (and, in fact, the global community) is vulnerable to significant costs (in both dollars and human lives) associated with stresses arising from sources that are both manmade (e.g., war, terrorism, and political disruptions) and natural (e.g., hurricanes, tornadoes, earthquakes, droughts, and floods). There is currently a need for a comprehensive, integrated suite of information that would be of value in helping identify opportunities for technological responses to these stresses. This project is directed toward the development and deployment of a decision support system (DSS) that will provide timely, accurate, and high-impact information. The context for this information is the international arena with an emphasis on the technological aspects of responses to these stresses.

This project is motivated by Sandia's recognition that enhancing our nation's ability to manage vulnerabilities of global infrastructures is necessary to maintain our national security. We recognize the technical challenges of creating an integrated infrastructure DSS and will use a strategy consisting of architecture, process, and metrics to address these challenges. We will create an architectural framework to support the system, methods for specifying modeling and analysis and for integrating new commodities into the system, and metrics for measuring the utility of the knowledge provided. Integrating the computer modeling and simulations of diverse commodities, explicitly considering the international arena as the system, and combining the judgment of international subject matter experts are innovations now possible due to the advent of high-performance computers and the global information infrastructure. This project will require and extend the expertise from several Sandia core competencies and directly addresses Sandia Strategic Objectives.

We accomplished three major tasks and produced significant analytic results. We developed dynamic simulation models of three significant policy options that may be implemented to decrease their overall emissions of greenhouse gases, primarily carbon dioxide. We then integrated these models into a single dynamic simulation model allowing us to execute the model with various subsets of these policies and their respective related policy implementation activities. We were thus able to more accurately model impacts from policy activities on greenhouse gas productions and their impacts on factors that influence the policy community. We decomposed the energy and greenhouse gas model, which we completed as part of the FY97 work, into a provincial-level model. We executed the provincial model to project the provincial energy-use patterns, thus providing a more detailed description of the anticipated energy use. The results of the integrated infrastructure model were cited by other sources. We continued to execute model scenarios and to refine the model components, primarily in the policy model subsection.

3532.010

Chemical Feedstocks for the Future: Oxidative Dehydrogenation

N. B. Jackson, J. E. Miller, A. G. Sault

Oxidative dehydrogenation (ODH) is a potential chemical process for producing olefins such as ethylene and propylene—the organic chemicals with the largest production from alkanes in the U.S. Alkanes are readily available from nature, natural gas, and petroleum, and as major by-products from refinery operations. ODH offers the advantage of energy efficiency and financial savings over traditional processes. Before ODH can be used commercially, an active and selective ODH catalyst must first be developed. Sandia is developing an understanding of the chemical nature of the active surface site that is necessary to make an economically feasible ODH catalyst. We focused on the mixed metal-oxide system of molybdenum-magnesium (Mo-Mg) oxide. We prepared over 20 different pure and mixed-phase magnesium molybdate catalysts and extensively characterized them for propane ODH activity/selectivity, phase composition, surface area, surface composition, and reducibility. Exciting results emerged regarding phase synergies of these materials. We identified a phase or species in the Mo-Mg oxide catalytic system that has an active site particularly suited to active and selective ODH of propane. We believe there is a high likelihood that we will be able to generalize our observations regarding the genesis of phase synergies to several other systems. This discovery could be crucial in understanding how to

make an active and selective ODH catalyst. Since 26 billion pounds of propene is synthesized from propane annually in the U.S. alone, this could have a profound impact on the industry as well as propel Sandia forward in the field of catalysis.

We prepared and extensively characterized over 20 different pure and mixed-phase Mo-Mg catalysts for propane ODH activity/selectivity, phase composition, surface area, surface composition, and reducibility. The activity and selectivity of these materials were very sensitive to the stoichiometry and method of preparation. Exciting results emerged tracing this sensitivity to phase synergies of these materials. Mixtures of phases (primarily MoO_3, $MgMoO_4$, and $MgMo_2O_7$) that are poorly active and selective by themselves interacted to produce active and selective catalysts when combined. Heating the combinations was often required to bring about the interactions leading to improved performance. The catalysts exhibiting superior activity and selectivity were characterized by a unique temperature-programmed reduction (TPR) peak, centered at about 650°C, that was not present for the poorly active or selective catalysts. Our results suggest that the beneficial synergism results from the formation of a new phase or species rather than through the remote communication between phases (e.g., by oxygen spillover), as is often claimed in the literature for systems of this type.

Results from an x-ray photoelectron spectroscopy (XPS)/atmospheric pressure reactor system were in excellent agreement with the TPR results. The Mo on the surface of active catalysts could be substantially reduced from Mo(VI) to Mo(IV) by pure propane at temperatures above 500°C, while we observed little or no reduction for inactive catalysts. However, when propane and oxygen were co-fed at typical reaction conditions (i.e., 108 Torr propane, 54 Torr oxygen at 450°–600°C), we did not observe Mo reduction for any catalysts. This result suggests that ODH occurs via a Mars–Van Krevelen mechanism on the active Mo-Mg catalysts. That is, oxygen for the dehydrogenation reaction is provided by the oxide surface (reducing the Mo), which is then reoxidized by gas-phase oxygen.

Finally, we observed a previously unreported phenomenon for ODH wherein low selectivities occur at very low conversions, but increase rapidly as conversion is increased. At the highest conversions, we observed the more typical ODH behavior of decreasing selectivity with conversion. Further studies are required to determine the cause of this unexpected behavior.

In conclusion, we developed a "fingerprint" of a phase or species in the Mo-Mg oxide catalytic system that has an active site particularly suited to active and selective ODH of propane. We believe there is a high likelihood that we will be able to generalize our observations to several other systems. This discovery could be crucial in understanding how to create an optimal active and selective ODH catalyst. In fact, our experience with ODH resulted in two collaborative efforts with industry being funded by DOE's Office of Industrial Technology.

Publications

Refereed

Miller, J. E., N. B. Jackson, L. Evans, A. G. Sault, and M. M. Gonzales. 1998. "The Formation of Active Species for Oxidative Dehydrogenation of Propane on Magnesium Molybdates." *Catalysis Lett.*, submitted.

Nenoff, T. M., N. B. Jackson, J. E. Miller, A. G. Sault, and D. E. Trudell. 1997. "Structure-Property Relationships of BaCeO Perovskites for the Oxidative Dehydrogenation of Alkanes." *MRS Symp. Series* **497** (Boston, MA, 1 December): 100.

Other

Jackson, N. B., J. E. Miller, and A. G. Sault. 1998. "Oxidative Dehydrogenation of Propane Using Mixed Phases of Magnesium Molybdate." Paper to be presented to the Spring National Meeting of ACS, Anaheim, CA, March 1999.

Miller, J. E., A. G. Sault, and N. B. Jackson. 1998. "Studies of Magnesium Molybdates for Oxidative Dehydrogenation of Propane." Paper presented to the Fall National Meeting of AIChE, Miami, FL, November.

3532.080

Laser Communication Nanosatellites

J. P. Kern, H. Chang, L. G. Pierson, L. B. Dean, M. D. Baldwin, A. A. Allerman, J. M. Gee, D. Ingersoll, C. T. Sullivan, S. M. Cameron, J. L. Schoeneman

Affordable, reliable, high-bandwidth global communications will contribute to increasing, by orders of magnitude, the volume of information available for such diverse applications as surveillance, missile threat warning, delivering data from unattended ground sensors, and delivery of intelligence information to military field commanders. DOE has numerous applications for which versatile, global, and very high bandwidth communications may be employed, including monitoring of materials, delivering hyperspectral surveillance data of potential proliferant or chemical warfare/biological warfare (CW/BW) production facilities, and linking DOE laboratories, facilities, and computing resources into an integrated environment, to name a few. Fiber-optic wide-area communications are limited to terrestrial application and constrained by geographical availability. Low Earth-orbiting (LEO) communications satellites can overcome these limitations. Furthermore, they can overcome the physical limitations of optical fiber and, with fewer nodes between geographical locations, reduce switching delays that further limit available capacity. Finally, the utilization of space–based lasers, rather than radio frequency (RF), as the communication media has the advantage of superior bandwidth availability.

Dozens, even hundreds, of satellites are required for global coverage at low Earth altitudes. For such a system to be affordable and reliable, the cost of satellites and launches must be drastically reduced, and challenges in the control and exploitation of this highly distributed communication satellite network must be overcome. Miniaturization and mass production of highly integrated nanosatellites will be key to reducing satellite costs. Miniaturization will also allow mass launches of a dozen or more satellites, further reducing system costs. The problem of numerous cooperating mobile communications nodes will require the principles of distributed processing and distributed network architectures to be adapted and applied.

• *Laser communication/photonics/optics*. The laser communications and photonics task developed the Optical Phased-Array Steering System (OPASS) concept, which can enable fine-pointing accuracy for laser intersatellite crosslinks, with the potential for substantially reducing gimbal weight needed for beam steering, and can correct for system defocus caused by unavoidable solar and thermal-loading effects. We designed and are currently fabricating OPASS devices for a 4X4 2-D steering proof-of-concept using Sandia's photonic integrated circuit (PIC) technology.

We also applied state-of-the-art microfabrication technology to the problem of dramatically reducing the volume needed to hybrid-package dissimilar materials (silicon [Si], gallium-arsenide [GaAs], indium-phosphorus [InP]) in a high-density, wafer-scale, stacked multichip module; we achieved passively self-aligned interlocking Si die with ± 5-micron tolerance and accurately positioned microlasers into etched Si wells.

• *Satellite power systems*. Satellite power subsystems traditionally consist of three elements: (a) energy conversion (photovoltaics), (b) energy storage (batteries), and (c) power management and distribution. In current satellite systems the power subsystem alone can constitute up to one-third of the overall weight of the satellite; hence, it can be a key limiting element in any space mission, and in fact is one of the main limiting elements confronting implementation of the nanosatellite concept. To overcome these limitations, we initiated development work in three areas.

(1) A four-junction solar cell having a theoretical efficiency of 40%. Work toward the four-junction solar cell focused on developing a novel compound semiconductor material (InGaAsN) that is essential in realizing the high theoretical efficiency. We demonstrated the other materials required for the four-junction cell.

(2) Advanced Si microstructures (diffractive optics) that could significantly enhance end-of-life performance of Si solar cells. We demonstrated creation of enhanced optical absorption diffractive optical structures in Si using reactive ion etching.

(3) Advanced lithium-ion battery that will increase specific energy and energy densities. We designed and fabricated a 28 V battery pack with an energy density of 115 W h/kg and specific energy of 221 W h/l.

• *Advanced manufacturing technologies*. An alternative casting technique is under development in which a filled hollow mold is withdrawn from a molten pot of metal to fabricate complex thin-walled structures. We developed a high-thermal-conductivity shell system; designed, assembled, and tested a withdrawal system for the 500-pound vacuum-induction melting (VIM) furnace; prepared initial bar molds; established initial casting parameters; and generated and tested mechanical test samples. Finally, we fabricated a complex part to demonstrate the viability of the process.

• *Satellite constellations/networking*. We conducted theoretical and simulation studies of possible Nanosat constellation geometries. This resulted in four unique new concepts varying in complexity and amount of coverage/redundancy. We also completed studies for power-saving designs as a passive up-/downlink and a unidirectional laser link. To simplify on-satellite complexity, we completed and documented development of a geographical addressing and simple routing protocol concept. Further exploration provided the uniqueness of minimum latency communications in LEO constellations as a critical national security asset to be further cultivated. We studied 64-byte datagrams for asynchronous transfer mode/interface

protocol (ATM/IP) regarding source–based routing concepts for use in satellite constellation networking.

• *Laser communications through Earth's atmosphere*. Laser optical communication potentially offers significant advantages for remote coordination and covert data exfiltration from distributed ground-sensing networks. A major weakness limiting the operational utility of nonideal optical communication channels propagating in atmosphere, however, has been adverse effects of extinction (loss), scattering (dispersion), turbulence (degraded coherency), and fade, which degrade realizable transmission bandwidth and gain aperture for acceptable bit error rate. For this task, we investigated the use of a previously developed active imaging technique based on optical parametric amplification (OPA) to enhance detector sensitivity and error rate performance for unguided communication links affected by clouds and turbulence. Using an eyesafe kilohertz repetition rate femtosecond laser system, we evaluated the role of signal-spontaneous OPA beat noise, amplified spontaneous emission (s-ASE) on amplified signal, noise figure, bit error rate, and channel-sampling capacity for various modulation formats in both direct and coherent detection modes to establish fundamental limitations on realizable transmission bandwidth as a function of turbidity.

Publications

Refereed

Chen, H. Y., J. Hutchins, B. Mah, and J. Naegle. 1998. "A Lightweight, Link-Layer, Source–Based Routing Protocol for LEO Satellite Networks." *Proc. NanoSpace '98 Conf.*, accepted.

Other

Dean, L. B., J. G. Peña, L. G. Pierson, and H. T. Chang. 1998. "Nanosat Communications Network Development." Internal Quarterly Review for Center 5700 (24 August).

3532.130

Accelerator Technologies for Emerging Threats

B. N. Turman, S. M. Cameron, J. C. Wehlburg, J. F. Wagner, G. M. Loubriel, C. L. Olson, M. G. Mazarakis, S. L. Shope, J. A. Jacobs

Pulsed-power accelerator technologies offer the potential for high-energy projection at great distances, with the possibility of use for direct destruction, disruption, and decontamination on the conventional battlefield or the nonconventional urban environments of terrorist attacks. With recent accelerator and pulsed-power technical developments (such as the Collective Ion Accelerator, compact high-intensity pulsed-RF sources), this capability may now be brought to bear on the problems of newly emerging threats of the 21st century, such as biological agent attack and detection of terrorist bombs, mines, and unexploded ordnance (UXO). Of particular interest and importance is the use of high-energy, high-intensity beams for projecting energy and radiation over extended ranges for neutralization of biological weapons. Based on the current U.S. standards for commercial radiation sterilization of medical products, the dose level required for neutralizing biological organisms is about 1 Megarad. These radiation levels can be produced with state-of-the-art pulsed-power accelerators, as well as commercial industrial accelerators. Accelerator systems are shown to be feasible for mobile ground–based decontamination. Locating and eliminating UXO and combating terrorism are possible using MeV-energy backscatter x-ray imaging (BXI) to detect buried UXO. Sandia identified key technologies and development requirements, including compact accelerators, compact lightweight power sources, and beam propagation and control.

This study identified a number of future emerging-threat military requirements and capabilities that could be met effectively with accelerators and pulsed-power technology. The threat of biological warfare, and particularly the threat posed by terrorist attack, is an area of high priority for the nation and the world today, and this is a problem in which an accelerator–based radiation source could be of immense importance. The result of our preliminary analysis shows that we could use commercial accelerator technology to develop a radiation-producing system that would provide large-area decontamination from biological agent release. The example system would be based on RF Linac or Rhodatron accelerator design, with an average beam power of 50 kW. The radiation generated by the beam upon impact with target surfaces would be the decontaminating/neutralizing effect. We would accomplish beam scanning by conventional magnetic scanning techniques. We envision a remotely operated system. Demilitarization of stockpiled weapons is also a possibility with a high-energy electron beam and x-ray converter. We evaluated the concept of an accelerator–based system for intercepting and decontaminating an incoming warhead. While this application has potential, the technology is not currently available and will require significant future development.

Also of importance for future military and environmental applications is use of low-energy backscattered x-rays for location of buried objects. Extension of this technique to MeV level energy, and combined with ground-penetrating radar (GPR), could give significant enhanced capability for mine detection and location of UXO. The x-ray system, scaled at 6 MeV energy level, could give excellent detection and imaging of the near-surface environment, down to a depth of about 0.5 m. The GPR would give deeper subsurface imaging for deeply buried ordnance. The two systems would be relatively easy to integrate and merge imaging data. Therefore, this hybrid detection system is worthy of further development and demonstration.

3532.090

Collection and Data Synthesis of Atmospheric Explosion Ground Truth for Global Monitoring Systems

M. B. Boslough

Sandia is in the process of collecting and interpreting ground truth data for the October 9, 1997, superbolide explosion over El Paso. Comprehensive Test Ban Treaty (CTBT) infrasound instruments observed the event from Los Alamos, at the correct azimuth and with a preliminary yield estimate of about 0.5 kiloton. This energy release corresponds to a magnitude that recurs only once every few years in North America. The frequency of occurrence over a major city like El Paso–Juarez is therefore quite low, and we hope to extract as much useful information as we can from this circumstance. The location of this event near a city provides an opportunity to independently assess the accuracy and precision of the CTBT monitoring system.

We collected seismic, videotape, still photo, and other data on a field expedition to El Paso. The burst location that we constructed based on ground data is several kilometers away from the point on the satellite trajectory, both vertically and in the horizontal plane. We expect to confirm the final ground–based trajectory by the recovery of meteorites

The primary reason for us to continue and follow up our field work is the apparent discrepancy between satellite and ground truth. The CTBT community needs to know the limitations of the satellite data, and the difference needs to be explained.

Our project was twofold: to (1) characterize the October 9, 1997, El Paso bolide and compare to CTBT data, and (2) prepare to collect ground truth for future events.

On October 9, 1997, at ~ 18:47:15 UT (local noon), a large fireball detonated east of El Paso. Most residents of El Paso and Ciudad Juarez heard the blast, and many watched the resulting dust clouds. The fireball cast discernible shadows on this cloudless, clear day; it was bright enough to be observed by persons inside curtained rooms. The flash exceeded - 20 magnitude, making it a superbolide (> million times brighter than a normal fireball). Witnesses under the burst location described the landscape turning red. A security camera system recorded the secondary shadow cast by the event.

The terminal explosion was 31.80 N, 106.06 W at ~ 28.5 km altitude, well located by eyewitness reports, videos, and photographs of the dust cloud and seismic records. We analyzed 18 photographs and 6 video recordings, one that includes the sound. The fireball was visible and audible for several hundred kilometers. Visual records were taken between 2 and ~ 20 minutes after the event; the cloud was perceptible for ~ 40 minutes. The disintegration of the projectile resulted in a chain of puffs between 35 and 28.5 km altitude with a near ~ 1 km spherical cloud from the terminal blast. Streamers continued past the terminal explosion, but photographs suggest that most of the projectile was pulverized. Wind shearing of the puffs destroyed their linearity within ~ 5 minutes. The shearing is consistent with upper wind data recorded nearby earlier that day, confirming the derived altitude for the terminal burst.

Infrared (IR) satellite systems, seismographs, and infrasound detectors recorded the event, allowing intercalibration to atmospheric explosions. The satellite detection fixed five active stations. The provisional calibration of energy released to induced ground motion (3.3 X 1010 J/nm for 58 km distance) derived for the St. Robert (Quebec) fireball is supported by preliminary data. Seismic solutions from the El Paso region indicate average velocities of ~ 305 m/second for the loudest audible arrivals. Although a single relatively compact ground-shaking boom dominated the sound, the audible energy lasted ~ 20 seconds (for observers within ~ 40 km), and the subaudible signal ~ 35 seconds. At Los Alamos National Laboratory (LANL), two infrasound arrays maintained as part of the CTBT monitoring system recorded the event. The signal lasted ~ 4 minutes at this ~ 450 km distance with a 0.2–0.8 Hz frequency range and maximum amplitude of 21 microbars. An energy release equivalent to ~ 0.5 kilotons was indicated.

The trajectory was within 20° of an S-N azimuth, with an elevation angle of ~ 65°. Radiants within this range require entry velocities of ~ 25 km/s for objects from the middle of the asteroid belt (~ 2.5 AU) consistent with a projectile having an initial mass of 5 to 10 tons for the observed energy release. The deep atmospheric penetration suggests a strong stony object, but the large entry velocity resulted in disintegration of most of the projectile, thereby suppressing meteorite delivery. Any meteorites fell in terrain that is relatively favorable for meteorite recovery. This fall occurred 11 hours prior to the node crossing for the fifth anniversary of the Peekskill H6 chondrite fall on October 9, 1992, but the trajectory is well enough known to exclude a Peekskill radiant.

We developed and built about a dozen all-sky video cameras and are in the process of deploying them in several arrays. The primary pilot arrays are in the Albuquerque area and the Pacific Northwest. Several small fireballs have already been recorded, and we are in the process of developing software tools to determine the trajectories of fireballs recorded on more than one camera.

Publications

Other

Hildebrand, A. R., P. Brown, D. Crawford, M. Boslough, E. Chael, D. Revelle, D. Doser, E. Tagliaferri, D. Rathbun, D. Cooke, C. Adcock, and J. Karner. 1998. “The El Paso Superbolide of October 9, 1997.” Paper presented to the 1998 Hypervelocity Impact Symposia (Extended abstract), Huntsville, AL, 16–19 November.

3532.110

Advanced Radiation Sources: Rayleigh-Taylor Mitigation Via Perturbation Reduction

R. B. Spielman, M. R. Douglas

Sandia will increase the overall efficiency of z-pinch plasma radiation sources by reducing the effect of the dominant magnetohydrodynamic (MHD) instability, the Rayleigh-Taylor (RT) instability. In particular, we plan to investigate the source and the magnitude of the density perturbations in the initial plasma sheath both experimentally and computationally. These perturbations seed the RT instability. Calculations suggest that modest reductions in the level of the initial perturbations (2.5% to 1.25%) could increase the radiated x-ray power from z-pinches by 2X or equivalently allow the present level of performance from longer implosion times, thereby reducing pulsed-power driver requirements.

We plan experiments to study the evolution of plasmas in z-pinch configurations. The measured evolution of the plasma will be modeled at Sandia using two- and three-MHD codes and the latest resistivity and equation-of-state (EOS) models.

We divided tasks into two parts: the experimental portion and the related computational tasks. The experimental work is being carried out in collaboration with the University of Nevada–Reno.

We are building up the experimental capability to explore the evolution of *z*-pinch plasmas from the initially cold, solid-state condition. This means that we must have a large current delivered to the load in ~ 100 ns and sufficiently accurate plasma diagnostics to measure the density and temperature with spatial and temporal resolution.

We designed and built optical and x-ray plasma diagnostics.

The computational and modeling work is under development. We developed tungsten, copper, and steel resistivities models and are tabulating them for ALEGRA and MACH2. These resistivity and EOS models are critical for any *z*-pinch calculations. We are taking great care to ensure the maximum accuracy of the models.

ALEGRA 2-D MHD with radiation transport is now up and running, and we have begun 2-D ALEGRA calculations. Single-wire calculations using the tabular SESAME resistivities and EOSs have started. We tested the 3-D ALEGRA capabilities without radiation transport and are testing this modeling capability with single- and multiple-wire configurations.

3532.120

Microfluidic Engineering

P. H. Paul

A new class of microfluid devices has been uncovered that offers a unique opportunity to develop new microscale actuation, control, and thermofluid devices. Sandia determined that electroosmotically driven flow of an electrolytic fluid as contained in a microporous medium can yield very high pressures (hundreds of atmospheres) at flow velocities of mm/s. This ability to transform electrical power into high-specific-force mechanical motion in a microscale device offers the ability to create microscale actuators at the wafer scale. Traditionally, microelectromechanical systems (MEMS) have employed electrostatic motors (or linear displacement engines) that provide rapid deflection rates but at a very low force. To achieve force levels required for useful actuation, electrostatic drivers require a large gear train to convert this motion to small displacement at high force. The electrokinetic pump (EKP) provides a means to convert electrical power directly to force levels suitable for actuation. An EK system is essentially a microhydraulic device that allows the EKP action to be delivered at a distance using capillary interconnects, hence the name fiber hydraulic system *(FHS). The FHS is the work analog of a fiber-optic system, i.e., the communication of work (information) at a distance through a fused silica capillary (fiber-optic) link. The ability to pump fluids efficiently and at high pressure in microscale systems also offers the opportunity to develop microscale liquid-cycle heat pumps that would be capable of operating at much higher heat fluxes than conventional Peltier devices.*

We experimentally characterized the basic physical properties and responses of an EKP and developed a predictive model. Parametric testing included responses to variations in the working fluid (permittivity and viscosity); electrolyte pH, composition, and conductivity; and pump host microgeometry, pore size, and material. We measured general engineering performance characteristics, including pressure generation, flow rate, and power-conversion efficiency. We created a set of basic engineering design rules. The demonstrated performance of these devices suggests that EK fluidic systems can contribute to a broad range of areas. EK actuators can provide microvalves, pumps, and mixers; robotic systems, where EKPs can be employed to drive miniature linear and rotary motors; new methods of vehicle drag reduction, where arrays of EK pumps in the skin of the vehicle can be used to modify the laminar sublayer; surety devices, where EKPs offer the high specific force required to drive miniaturized strong links; and advanced miniature passive and active heat-transfer systems.

3532.150

InGaAsN: A Novel Material for High-Efficiency Solar Cells and Advanced Photonic Devices

A. A. Allerman, D. S. Walsh, D. M. Follstaedt, S. R. Lee, S. R. Kurtz, J. M. Gee, J. F. Klem

Increased deployment of satellites for communications and surveillance applications has led to explosive growth in the demand for high-efficiency solar cells to power these platforms. Today's satellites are increasingly power-hungry, since on-board power capacity directly translates to mission capability. In response to this demand, compound semiconductors have revolutionized the space photovoltaic (PV) business over the last five years by offering higher-efficiency solar cells than achievable by competing technologies. Their success comes through the use of bandgap engineering to build multilayer structures tailored to efficiently convert photons from different bands of the solar spectrum into electricity. While this approach led to two- and three-junction tandem solar cells with efficiencies of 22%–24%, further advances were limited by the range of bandgaps obtainable with conventional III–V compound semiconductor alloys composed of aluminum, gallium indium, arsenide, and phosphorus (Al, Ga, In, As, and P). In a recently applied-for joint patent from Sandia and the Air Force Research Laboratory (AFRL), we identified a way to introduce small amounts of nitrogen into the Group-V mix to create a new class of compound semiconductors of the type InGaAsN. The small percentage of N, with a correspondingly small percentage of In added to maintain lattice-matching, significantly lowers the materials bandgap, thereby opening up considerable new flexibility for bandgap engineering of new photonic devices in addition to higher-efficiency PV.

We are developing multijunction tandem solar cells as power sources for satellite systems operating in air mass zero (AM0) solar radiation. The InGaAsN alloy system appears ideal for this application. Nitrogen incorporation has proven problematic and a challenge to demonstrate high-quality InGaAsN (N > 0.02) epilayers needed for solar cells. We report on properties, growth, and performance of InGaAsN solar cells. We demonstrated internal quantum efficiencies > 70% for 1.0eV bandgap solar cells.

We grew InGaAsN films by metalorganic chemical vapor deposition (MOCVD). Unintentionally doped InGaAsN was *p*-type. We achieved *n*-type material using SiCl4. We grew lattice-matched films at 600°C and 60 Torr using a V/III ratio of 97, a DMHy/V ratio of 0.97, and a TMIn/V ratio of 0.12.

We observed a significant increase in photoluminescence (PL) intensity from these films following a post-growth anneal. The PL intensity was a maximum for samples annealed for either 700°C for 2 minutes or 650°C for 30 minutes.

The optical properties of the InGaAsN films were extremely sensitive to N content, *ex situ* annealing, and doping. In addition to the bandgap reduction, there was PL quenching in InGaAsN films with increasing N content. We did not observe a band-edge PL peak in as-grown In0.07Ga0.93As0.98N0.02 films at 300°K. After the *ex situ* annealing process, we observed a band-edge PL peak, approximately 60 meV linewidth, in our *p*-type films. Annealing had negligible effect on the absorption spectra of the *p*-type films. Deep-level transient spectroscopy (DLTS) results show that annealing eliminates a midgap defect state present in our as-grown material. *N*-type doping with Si appears to introduce yet another defect. With Si doping, the band-edge PL was weak both before and after *ex situ* annealing. Also, the absorption spectrum for the Si-doped material displayed a low-energy tail.

The solar cell described in this work consisted of a 1.0 µm-thick, *n*-type (2x10e17cm^{-3}, Si-doped) In0.07Ga0.93As0.98N0.02 emitter grown on a 1.0 µm-thick, *p*-type (4x10e16cm^{-3}) base. A 50 nm-thick, Al0.8Ga0.2As window layer and a 0.15 µm-thick GaAs cap/contact layer (both *n*-type, 5x10e18cm^{-3}) were grown on top of the solar-cell emitter. We applied no antireflection coatings to the 0.25cm^2 cell.

Solar cell spectral response extended out to the band-edge of the InGaAsN at 1.2 µm. We obtained peak internal quantum efficiencies of > 70% for the annealed cell. Annealing improved the quantum efficiency by roughly a factor of five over as-grown cells. Comparing the performance of our thick *n*-type emitter solar cell with thin *n*-type emitter cells, we found that negligible electron diffusion is occurring in the 1.0 eV *p*-type material (annealed or as-grown). To date, we have obtained high quantum efficiencies only with cell designs utilizing hole diffusion in *n*-type material.

Previously, InGaAsN solar cells displayed short minority carrier diffusion lengths, and their photocurrents were dominated by electron-hole pairs generated in the depletion region. The highest internal quantum efficiency reported for an InGaAsN solar cell was = 60% (@ 1.1 µm), achieved with a compensation-doped *p-i-n* device. Conventional *p-n* InGaAsN solar cells displayed internal quantum efficiencies typically < 25% (@1.1 µm).

To estimate the minority carrier diffusion length in our cells, we measured the photocurrent response versus bias. The photocurrents of the annealed and as-grown cells displayed roughly the same dependence on depletion width, although the photo-

current was much larger for the annealed cell. From our modeling and absorption data, we estimate that the hole diffusion lengths are 0.6–0.8 µm (annealed) and 0.2–0.3 µm (as-grown). The improved efficiency of our annealed InGaAsN cell was due to diffusion of holes in the *n*-type emitter.

Annealing decreased the saturation current from 1.1x10e-6A/cm^2 (as-grown) to 8.3x10e-7A/cm^2 (annealed). Similarly, the diode ideality factor (*n*) approached unity with annealing. (n=1.21 annealed versus n=1.33 as-grown). As bandgap energy increased, we found that the open-circuit voltage rapidly increased.

We grew and designed an InGaAsN solar cell with improved performance. Unlike previous cells, we demonstrated viable minority carrier diffusion and realized > 70% internal quantum efficiency.

Publications

Refereed

Jones, E. D., A. A. Allerman, and S. R. Kurtz. 1998. "Photoluminescence Studies of InGaAsN/GaAs Single Quantum Wells." Oral presentation to the 4CF98 Meeting of the American Physical Society, Los Angeles, CA, March.

Kurtz, S. R., A. A. Allerman, E. D. Jones, J. M. Gee, J. J. Banas, and B. E. Hammons. 1998. "InGaAsN Solar Cells with 1.0 eV Bandgap, Lattice Matched to GaAs." *Appl. Phys. Lett.*, submitted.

Other

Allerman, A. A., S. R. Kurtz, E. D. Jones, J. M. Gee, J. C. Banks, P. C. Chang, J. J. Banks, and B. E. Hammons. 1998. "InGaAsN for High-Efficiency Multiple-Junction Solar Cells." Presentation to the DOE/BES Next-Generation Team Meeting, Denver, CO, 11 September.

3532.160

Technologies for Countering C/B Terrorism

G. A. Thomas, B. L. Haroldsen, W. Einfeld, D. C. Roe, R. G. Schmitt, P. K. Falcone

The threat of chemical/biological (C/B) terrorism is as diverse as the technologies required to combat it. The problem space spans from initial detection of the threat through predicting the consequences to mitigating the consequences. The thrusts of this effort address all three facets of the problem:

(1) Development of an ultraviolet (UV)-microchip laser for application in compact biodetection systems. One critical component in any practical, fieldable sensor for bio-agents is the UV excitation source. In this project, Sandia seeks to design, build, and test diode-laser–pumped, passively Q-switched microlasers with nonlinear frequency conversion to produce UV wavelengths needed to build a fieldable biomaterial sensor.

(2) Innovative physical validation techniques for C/B transport and fate models. The development of computer simulation tools must be accompanied by model validation efforts. In this project we intend to explore the ability of recent developments in synthetic aperture radar (SAR) to produce high-resolution, subscale, physical models of typical U.S. urban locales, such as the Washington, DC, mall or downtown Chicago, and, in a wind or water tunnel, generate a set of data that describes how toxic agents disperse throughout the city landscape. These data will be directly applicable to numerical code validation.

(3) Computational molecular recognition (CMR) tools for antiviral/antitoxin development. The ability to develop highly effective drugs for mass treatment of casualties following a domestic biological warfare (BW) release can be significantly enhanced by the use of computational tools. We will develop CMR tools in this effort.

(4) In situ *destruction of C/B agents before release. The ability to neutralize terrorist devices* in situ *before agent release is of prime concern to the domestic response community. We will develop a percolating hydrothermal oxidizer, a.k.a. batch incinerator, as a portable system for on-site device neutralization.*

• *Development of a UV-microchip laser for application in compact biodetection systems*. We developed and characterized a microchip laser that produced UV light in the correct wavelength region (260–360 nm), had acceptable output energy (50–100 microjoules), and was capable of pulsed operation in the desired frequency range (100 Hz).

• *Innovative physical validation techniques for C/B transport and fate models*. We completed a survey of available wind tunnel testing facilities and the sensors required for model validation. We constructed a simple model using available SAR data.

• *CMR tools for antiviral/antitoxin development*. We developed a functional framework for the CMR tools that incorporated several model domains from physical interactions including electrostatic and van der Waals forces, molecular dynamics interactions involving conformational folding, to quantum effects. We integrated some simple chemical/physical models.

• In situ *destruction of C/B agents before release*. We developed a scale prototype percolating hydrothermal oxidizer and initial tests to evaluate potential performance.

A supplemental task to evaluate strategic threats to U.S. targets from C/B terrorism resulted in an initial study being completed.

3532.140

Technologies for System-Level Innovations in Ballistic Missile Defense

C. T. Sullivan, S. M. Cameron, R. K. King, W. W. Tarbell, S. Y. Goldsmith

The proliferation of ballistic missiles is an emerging threat to U.S. national security; rogue nations are rapidly acquiring ballistic missile systems that can potentially deliver weapons of mass destruction (WMD) (such as nuclear, chemical, or biological weapons) against U.S. allies and military forces. The U.S. is faced with responding to this crisis on several levels. The military needs better sensors (typically hidden in protective sanctuaries such as tunnels, bunkers, etc.) that see or detect the presence of ballistic missiles. After weapon detection, military planners need better methods to help them quickly formulate a battle management plan (gleaning information from multiple sources) to deal with the threat. Finally, the military needs the most effective means to destroy the missile assets, preferably while they are still in their protective structures or the boost phase of launch. Early destruction significantly reduces the burden of terminal missile defense.

• *High-sensitivity lightwave modulation for enhanced satellite–based sensing.* We measured an on-chip loss of about 9 dB and a Vp of about 3 V, compared to the predicted values and goals of 3 dB and 1.2 V, respectively. Neither packaged fiber-to-fiber insertion loss nor electrooptical bandwidth was measured because the basic unpackaged Mach-Zehnder modulation (MZM) did not meet our expectations. We believe two effects may have compromised the device performance. First, an intermittent electrical contact along the electrical-optical interaction length can cause lower sensitivity than predicted and higher optical loss by scattering. A thin dielectric scum that formed under our Schottky contact during the dielectric isolation step may have caused this. Second, we observed anomalously high losses in the signal arm of the MZM for sample EA0300, which degraded our extinction ratio to practically zero and increased our loss by > 6 dB. Numerical modeling for the somewhat idealized device geometry does not adequately explain this effect as yet, and it may not be able to do so if the source of the loss is a layer resulting from chemical reactions between the semiconductor and its contact metals. Changing or even eliminating the dielectric isolation step and increasing upper cladding thickness in the waveguide can solve both problems.

• *Atmospherically compensated laser vibrometry for remote detection of ground motion.* This work establishes the viability of an optical parametric amplifier (OPA)–based, self-referencing, laser speckle shearing interferometer as a sensitive means to detect surface vibrations, even in the presence of an intervening scattering layer. The instrumental sensitivity to surface displacements overlaps with the predicted range for vibrations due to heavy machinery operated in an underground structure. The OPA technology can be integrated with a standard lidar platform and is compatible with active multispectral sources.

• *Agent–based C^2 systems.* Military C^2 places requirements on an agent architecture that cannot be met with current technology. Significant investments in R&D are required to enable agent–based C^2 on a scale that addresses real C^2 problems. This chapter provides a technical vision and the technical elements of agent–based C^2. We did not complete development of a prototype system.

• *Development of a detonator for hard-target fuze applications.* This work shows promise for improving the shock survivability of HNS (hexinitrostilbene) using inert binder materials. The candidates considered demonstrated a marked increase in the static crush strength over pellets made from the raw material. We expended considerable effort in developing a viable design to incorporate the semiconductor bridge (SCB) slapper into a configuration capable of surviving the harsh environment associated with hard target penetration. Future work will study the effects of high-intensity shock loading on the candidate binder-HNS compositions. We will perform a series of threshold determination tests to assess the degradation in sensitivity incurred as a result of using the binder formulations. We will compare these results to similar data from the untreated HNS material.

• *Technologies for suppression of enemy ballistic missiles through boost-phase intercept (BPI).* Based on this work, it is unlikely that any technology investment in sensors or interceptors will ever turn these concepts into long-range (> 100 km) systems. Having reached this conclusion, there are still investments that can make these systems all that they can be for short- to medium-range intercepts.

Publications

Refereed

Cameron, S. M., S. Y. Goldsmith, R. K. King, J. L. McDowell, C. T. Sullivan, and W. T. Tarbell. 1998. “Innovations in Ballistic Missile Defense (BMD).” Sandia Technical Report SAND98-2328 (October). Sandia National Laboratories, Albuquerque, NM.

3532.170

Aerosol Stand-Off Detection Test-Bed

R. P. Toth

A validated requirement exists for port and airbase survivability under biological warfare (BW) attack. The basis of this survivability is early indication and warning (I&W) from sensors for BW agents. Two concepts are possible: (1) an array of point sensors, or (2) a stand-off sensor. The first option has many defects, e.g., data communications and pattern analysis are needed to confirm BW attack. This means a significant area is subject to unprotected attack before a valid I&W is issued. Stand-off sensors clearly provide an attractive alternative.

Our radio-frequency (RF) dispersion analysis concept is attractive because of near-real-time reporting, viability determination, detection of microencapsulation, and potential to classify BW threat at the level of Genus.

We collected pilot data for vector network detection of aerosol in various RF regimes in the aerosol test-bed. The aerosol has a narrow dispersion around a nominal 1 micron. We confirmed the hypothesis that phase of scattering parameter S21 parallels aerosol production in the transmission electron microscopy (TEM) cell. Thus, measurement of electrical path length is the indicator of sensitivity. As predicted, the magnitude of S21 is insensitive, as are both real and imaginary components of S11. We are now confident that a bistatic configuration of the stand-off sensor is the only workable method.

With respect to sensitivity, we are limited by the 0.25-degree phase resolution of the vector network analyzer plus the physical path length of the TEM cell. These set the sensitivity of the test-bed. We note that at 345 MHz for the first 100 ml of aerosol in the TEM cell, phase shift is about 0.75 degrees. We detected a 1.8 mm change in electrical path length. This is an impressive result! To scale to 30 MHz, the TEM cell would need to be about 12 times longer. This suggests that a small-scale, free-space experiment may be the next step before dispersion analysis for microcapsules.

We produced the following key results:

(1) Confirmed the stand-off sensor system design concept as a bistatic RF sensor.

(2) Confirmed the hypothesis that the phase of complex scattering parameter S21 is the most sensitive measurement method.

(3) Confirmed the hypothesis that the time course of change in complex scattering parameter S21 is linearly related to the time course of aerosol production at three frequencies.

(4) Demonstrated aerosol detection sensitivity in the test-bed by detection of as little as 1.8 mm change in electrical path length.

Publications

Refereed

Larsen, L. E., and R. P. Toth. 1998. “Stand-off Sensor for Microencapsulated Micro-Organisms.” Aerosol Detection Test-Bed Report to Sandia and DOE (January).

Other

Larsen, L. E., and R. P. Toth. 1998. “Stand-off Sensor for Microencapsulated Micro-Organisms.” Invited presentation to CBDCOM, Albuquerque, NM, January.

Larsen, L. E., and R. P. Toth. 1998. “Stand-off Sensor for Microencapsulated Micro-Organisms.” Invited presentation to DSWA, Arlington, VA, January.

3532.180

Design and Optimization of High-Power Electromagnetic Source Systems and Engagement Scenarios for Achieving Functional Upset or Damage in Specific Target Electronic Systems

R. C. Pate, J. F. Aurand, L. F. Rinehart, P. E. Patterson, P. J. Federico, S. B. Dron, P. D. Coleman, D. J. Riley

Modern electronic systems are vulnerable to upset or damage from electromagnetic (EM) attack, especially in the form of narrowband and short-pulse wideband, high-power microwave (HPM) radiation. It is in the best interest of both the DOE and DoD to be aware of our national vulnerabilities to HPM as a threat and, at the same time, to better understand and optimize the capability of HPM technology as the basis for effective nonlethal weapons systems for use against specific classes of tactical and strategic targets. Key to the assessment of HPM both as a threat to national assets and as the basis for useful weapon systems for specific applications is the development and validation of quantitative models and methodologies for systems characterization, engineering analyses, and optimization, taking into consideration the entire ensemble of target set configuration and susceptibilities, HPM source system design and performance, engagement scenarios, and defensive countermeasures.

This project seeks to integrate the best available target susceptibility data, HPM weapon system modeling, and mission planning to conduct first-order design and optimization of HPM weapon system configurations, operational requirements, and target engagement scenarios to achieve successful target upset or damage in two specific hypothetical cases of interest. This will provide an initial framework and methodology to more systematically evaluate the HPM threat to national assets, design and optimize HPM sources and engagement scenarios for use against specific selected targets, evaluate the effectiveness of defensive countermeasures, assess the completeness and consistency of available database information, and identify specific key areas where further work is needed.

This project focused on establishing analysis procedures and conducting classified systems engineering feasibility and design/performance trade-off studies involving the application of candidate high-power EM source technology options against selected specific electrically vulnerable target systems.

Our approach was to first select specific targets of particular interest and assess their effects on a susceptibility threshold. We then chose an appropriate and practical range of candidate source technologies, basing mode, and engagement scenario parameter space for use in conducting source system design and performance trade-off studies to achieve a desired effect in conjunction with each specific target selected. The candidate source technologies, basing mode, and range of engagement parameters selected also resulted in the imposition of certain practical constraints on allowable source system size, weight, and physical configuration. Constraints on source size and weight subsequently impact the estimated capability and performance available from each candidate source system design.

We based target system vulnerabilities to a candidate EM source threat based on the specific engagement scenario under consideration, the radiated output pulse spectrum expected for the candidate source technology, the dominant energy-coupling paths/mechanisms expected into the target, and the identification of critical target system component(s) expected to have the greatest susceptibility. We undertook specific target component vulnerability threshold analyses that made use of existing available information and some additional experimental data acquired during the project on damage susceptibility thresholds for key component(s). We then combined component susceptibility thresholds with expected EM coupling path attenuation to yield estimates of the incident EM-pulse field strength, or effective radiated power density, for a given duration required on-target to achieve the desired effect.

Estimates of the power density on-target (Pt) required to achieve desired effects, combined with engagement scenario information on the range (R) from the source to the target, allows one to calculate the effective isotropic radiated power (ERP) output required of the source. The basic relationship is ERP = (4*PI*R**2)* Pt, where R is the range in meters, Pt is the on-target power density in watts per square meter, and ERP is in watts. For a given operating frequency, the ERP is simply related to actual source parameters by ERP = Ps * G, where Ps is source output power in watts and G is the total effective source antenna gain (dimensionless quantity).

For a given operating frequency, the total effective antenna gain term (G) is proportional to the cross-sectional area of the radiating antenna structure. Conversely, the output beamwidth (which dictates the pointing accuracy required) of the source for a given frequency is approximately inversely proportional to the linear dimensions (e.g., width or diameter) of the antenna structure. The output power of the source (Ps) depends on the output stage operating voltage, impedance, and effective radiation output efficiency for the particular type of source technology under consideration. Moreover, we found the required input energy storage, power throughput capacity, size, and weight of the overall source system to depend on the details of the candidate source system technology, physical configuration, and operating efficiencies required to achieve the desired target effects within the physical constraints imposed by the basing mode and engagement scenario parameters selected for the analyses.

Based on the above, we did a limited set of source system design and engagement performance trade-off studies for specific target and scenario

parameters selected. Operational tradeoffs involved analyses of the relationships among estimated source system size, weight, pulse shape/length, pulse repetition rate, pointing accuracy, and command/control timing required to achieve the desired radiated power and energy on target at various ranges for the most appropriate source technology options. We also included general risk assessment. Leading choices emerged from the studies for source system technologies and configurations best able to meet the requirements for achieving the desired effects with the least risk for specific selected combinations of target, source basing mode, and engagement scenario.

Publications

Other

Pate, R. C., P. D. Coleman, S. B. Dron, and M. T. Buttram. 1998. "Feasibility Study on the Design and Optimization of High-Power Electromagnetic Source Systems for Achieving Desired Effects on Specific Target Systems Under Selected Engagement Scenarios." Sandia Technical Report (classified). In preparation.

3532.190

Real-Time Design of Improved Powder Pressing Dies Using Finite-Element Method Modeling

K. G. Ewsuk, A. F. Fossum, J. G. Arguello, Jr.

We will apply and expand Sandia's extensive expertise in powder compaction science and technology to develop a user-friendly computer code that incorporates agile features to design complex geometry dies for powder compaction faster and more economically. This advanced technology will provide considerable advantages in designing and manufacturing advanced ceramic components, including (1) reducing manufacturing costs, cycle time, and waste, (2) enabling more cost-effective manufacturing of specialty components and small lot sizes, (3) reducing component development time, and (4) maximizing design and manufacturing flexibility (i.e., design and manufacturing agility). A successful project will significantly impact efforts to design and manufacture advanced ceramic components with improved performance and reliability for weapons systems, including cermets and lead zirconate titanate (PZT) voltage bars for neutron generators. The ultimate goal of this project is to develop a finite-element method (FEM) computer code that materials and design engineers can easily use on a commercial platform (i.e., ABAQUS) to systematically design and rapidly develop functional dies for pressing ceramic components from granulated powders.

We met all of our technical milestones: (1) determined realistic materials parameters/variability for FEM modeling to design powder compaction dies, (2) developed an agile FEM computer code with variable materials and geometric parameters to design complex geometry dies for pressing powder compacts, (3) established a dedicated workstation for die design/compaction simulations, and (4) successfully tested FEM modeling capability/code to design complex geometry dies. We also are looking into the possibility of patenting the concept we used to design the templates used in the computer code.

We set out to prove a concept that we could develop user-friendly computer code to simulate compaction using existing Sandia FEM code and compaction expertise and a new concept that involves a unique template architecture. We devised a unique concept to design a variable dimension and parameter template and demonstrated that this concept is a valid one to develop a user-friendly compaction code. We used this code to demonstrate 3-D compaction simulation capability whereby one can build/design a die on the computer in real time and define the compaction conditions simply by responding to straightforward questions from the computer screen. We used the new code to simulate the compaction of a complex geometry part (e.g., a bushing) fabricated by companies we collaborate with on a Cooperative Research and Development Agreement (CRADA). Of significant note is the simplicity with which the die design and compaction simulation can now be completed and at significantly reduced time. When we originally ran a similar simulation under the CRADA, it took about 2 weeks to set up the component geometry and mesh-up the part to complete the FEM compaction simulation on the computer, and it took another 8–12 hours to run the compaction simulations. With the new, user-friendly, template–based code, a non-expert is now able to set up and mesh the part geometry in about 5 minutes, and the compaction simulation can be run in 20 minutes. We reduced the total time from weeks to minutes to design a die and run a compaction simulation. With the template–based code developed, we demonstrated the inherent flexibility to systematically change the die design to simulate mechanical compaction of almost any axisymmetric cylindrical compact geometry imaginable (i.e., of currently manufactured ceramic components). The new template takes 1000 steps to run the compaction simulation, and we made a movie of the densification of a bushing geometry to demonstrate the new capability.

We anticipate that this computational technology can be used as a design tool to reduce or eliminate die and/or component prototyping, saving much time and expense in product development and commercialization. This is particularly important in advanced ceramics manufacturing, as ceramic components are typically more expensive to manufacture than either metals or polymers (i.e., this tool will allow ceramic component manufacturing to be more cost-competitive with other materials). The computer template also is a tool that will be valuable in designing and manufacturing small-lot-size specialty parts (e.g., cermets and v-bars for neutron generators for Defense Programs [DP]).

3532.210

Development of Fiber-Laser–Based LIF for Detection of SO_2

D. A. Kliner

Current understanding of many aspects of the Earth's climate system is limited by the available data. Measurements of critical species and processes are required to gain a detailed and quantitative understanding of past and present climates, to assess and narrow the uncertainties in climate models, and to develop the predictive capability required to discern natural and anthropogenic influences on the future climate. Providing such measurements requires development of new diagnostic methods for key atmospheric species and their incorporation into chemical sensors with high sensitivity, specificity, and time response. Sandia will develop these new chemical-sensing capabilities.

The species we will target initially are oxides of nitrogen and sulfur, specifically NO and SO_2 (sulfur dioxide). These molecules play a central role in the Earth's climate, and anthropogenic activities (primarily fossil-fuel combustion) are the dominant source of both species. Existing measurement methods for NO and SO_2 lack adequate sensitivity and/or time response to address many outstanding questions in studies of the Earth's climate.

We will explore the use of single-mode fiber lasers (developed for optical telecommunications) as compact, lightweight sources of tunable, narrow-bandwidth, deep-ultraviolet (UV) radiation. We will also perform spectroscopic studies to optimize laser-induced fluorescence (LIF) for detection of NO and SO_2 with high sensitivity and specificity.

We performed two types of experiments: (1) spectroscopic studies of SO_2 to optimize the LIF detection scheme, and (2) development of a compact fiber laser for generation of narrow-bandwidth, UV radiation.

We measured absorption, fluorescence-excitation, and dispersed fluorescence spectra of SO_2 at pressures of 7–700 Torr (the range relevant for detection throughout the atmosphere) with the bath gases N_2 and O_2. We tuned the excitation wavelength between 210 and 220 nm and detected fluorescence from 210 to 400 nm. We measured quenching rates for two absorption bands.

We determined the optimum excitation wavelength to be 216.9 nm (alpha2(0,5) band). The optimum detection wavelength is ~ 230 nm, and the detection bandwidth should be > 10 nm. Pressure broadening only slightly reduces the peak absorption cross-section of the 216.9 nm band, and the baseline is well resolved even at the highest pressures (on-line/off-line contrast ratio of 6/1 at 700 Torr). The sharp features present in the low-pressure fluorescence spectrum are broadened at elevated pressure, but the overall shape of the spectrum does not vary significantly with pressure, thereby simplifying the calibration of the LIF detection scheme. Radiative decay, predissociation, and collisional quenching make comparable contributions to the depopulation of electronically excited SO_2; the LIF sensitivity therefore varies with pressure, and the measured quenching rates are necessary for calibration of the detection scheme.

Future experiments will investigate quenching of electronically excited SO_2 by H_2O and the temperature-dependence of the quenching rates.

Development of a portable, LIF–based SO_2 sensor requires development of a compact source of tunable, narrow-bandwidth, UV radiation. We performed initial development of such a source in collaboration with the Naval Research Laboratory (NRL). Specifically, we built and tested a Q-switched (pulsed), Yb-doped fiber laser pumped by a high-power diode laser. The gain medium consisted of a single-mode optical fiber whose core was doped with 2.5 wt.% Yb3+ ions. We surrounded the core by a multimode cladding into which we launched ~ 200 mW of 974 nm pump radiation. The laser cavity included a Faraday mirror to compensate for the birefringence of the fiber, thereby ensuring linear output polarization (necessary for nonlinear frequency conversion). We accomplished wavelength tuning with an angle-tuned dichroic filter (1060–1090 nm). We used a standard Pockels cell as the Q-switch.

The laser system produced pulses of 5 ns duration and up to 2.0 kW of peak power at a repetition rate of 1–5 kHz. The power consumption (electrical) was < 1 W. The UV wavelengths required for LIF detection of SO_2 are accessible by frequency-quintupling of this source. Future experiments will entail implementing the nonlinear conversion scheme and further characterization and optimization of this new laser system.

Publications

Other

Kliner, D. A. V., J. P. Koplow, L. Goldberg, and R. L. Farrow. 1998. "Laser Development and Spectroscopic Studies for Development of a New SO_2 Sensor." Sandia Technical Report, in preparation.

3532.220

Penetration and Defeat of Hardened Underground Facilities Using a Microhole Drilling Robot

D. J. Holcomb, E. H. Ahrens

There is an increasing need to attack buried, hardened targets that are beyond the reach of conventional penetrators because of their depth or hardening, or both. As the physical limits of materials for penetration depending on kinetic energy are approached, it is time to tap the enormous technological base that exists in the drilling industry. Drilling 100 meters into rock is trivial using conventional technology. The nontrivial task is doing this with a package that can survive in a hostile environment. The essence of Sandia's work was to analyze the application of available technologies for cutting small (2–5 cm) holes in rock at very high rates. Many of the size, weight, and power requirements for conventional drilling arise from the need to apply high thrust and torque to the bit. The new technologies require neither. The combination of small hole size and low-thrust, low-torque cutting means that the apparatus can be made very small and light. Our goal was a system sized to fit a conventional penetrator body that would carry the drilling robot below the surface, making discovery and destruction of the system unlikely during the estimated one hour required to drill to the target.

We identified two enabling technologies, DTHH (down-the-hole hammer) drilling and the use of anaerobic OTTO fuel (OTTO is the inventor's first name), that make it possible to construct a drilling system that is small and light with penetration rates predicted to be as high as 5 meters/minute. Experts prepared and reviewed system design in drilling, penetrators, lethality, and OTTO fuel, and found it to be feasible, if difficult. Advances in the predicted rates of penetration reopened the possibility of a surface-landed system that would need only 15–20 minutes to drill into the facility.

Our goal was to determine if available or near-term-available technologies were sufficient to allow construction of a drilling apparatus that could be air-dropped and drilled into a deeply buried, hardened structure in a time of one hour or less. The system had to operate unattended and survive attempts to destroy it. We will accomplish survival by a combination of speed and system burial. We produced a system design that allowed the complete drilling apparatus to be contained in a large penetrator that would bury itself on impact and, in about one hour, drill through 100 meters of granite using a guided DTHH driven by OTTO torpedo fuel. OTTO fuel is high-energy, anaerobic fuel whose combustion products can be used directly to drive a DTHH, which is essentially a jack hammer driving a star drill. Penetration rates are in excess of 1 meter per minute with existing hammers, and analysis predicts up to 5 meters per minute, using the high energies that can be applied using the OTTO fuel. The two enabling technologies, DTHH drilling and OTTO fuel, are well-understood, mature technologies, but linking them will require development work.

We organized a design review of the proposed system involving experts in drilling, OTTO fuel, lethality agents, and penetrators. The review team found the concept to be feasible, with some areas of difficulty. Most of the difficult areas center on making the system survive 2000 G impact accelerations. We showed that the concept of a penetrator-contained drilling system is plausible with existing technology. In fact, the combination of direct use of the OTTO fuel for driving the hammer and DTHH drilling technology promises penetration rates high enough to reopen the possibility of a surface-landed system. Expected survival times would be much shorter, but penetration rates are projected to be so high that an armored system could survive long enough to accomplish its goal. The importance of the problem presented by deeply buried, hardened targets, combined with the probability that kinetic energy penetrators are near an end-point in their development, leads to the recommendation that the drilling approach be seriously pursued. Demonstration of the application of OTTO fuel as a power source for a DTHH drilling apparatus would be a productive first step, addressing the least-developed aspect of the required technologies.

Publications

Other

Holcomb, D. J., and E. Ahrens. 1998. "Evaluation of a Microhole Drilling Robot for Penetration and Defeat of Deeply Buried, Hardened Targets." Sandia Technical Report SAND98-2651 (October). Sandia National Laboratories, Albuquerque, NM.

3532.230

IFSAR Tree Phenomenology and Coherence Normalization

J. R. Fellerhoff

Recent developments in interferometric synthetic aperture radar (IFSAR) indicate a need to more completely understand the phenomenology relating to IFSAR digital terrain elevation data (DTED) measurements in vegetation. Several different research activities in the literature showed a failure to properly map tree heights with current IFSAR terrain mapping algorithms, even though theoretical predictions indicated that these experiments should correctly compute tree height in these digital maps. Sandia developed a detailed understanding of radar phenomenology and is seeking to apply this knowledge to the problem of IFSAR tree-height measurement.

This analysis comes at a critical time for the U.S.'s future involvement in IFSAR development. We initiated an advanced concept technology demonstration (ACTD), called rapid terrain visualization *(RTV), to demonstrate the feasibility of mapping large areas at extreme accuracy for battlefield planning and precision navigation and guidance. This system will require more accuracy in the measurement of tree height in terrain maps than can be demonstrated with current algorithms. A successful Sandia phenomenology study will greatly benefit the future of U.S. IFSAR airborne and spaceborne terrain mapping systems by providing more accurate digital terrain elevation maps.*

In addition to DTED maps, airborne and spaceborne IFSAR systems produce an extremely useful product called the coherence image. *The coherence image contains information about both the performance of the radar system and the characteristic of measured objects in the image. Target and scene recognition techniques could be improved if radar system effects could be separated from vegetation phenomenology. This project will address the vegetation phenomenology as the separation of systematic radar coherence effects from the effects of scene content.*

Success of this project will position Sandia as a national leader in IFSAR terrain mapping, a necessary product for future operational military training, as well as for the precision navigation and guidance of weapons, both conventional and nuclear.

We collected SAR data with the Twin Otter SAR system and initiated a detailed analysis effort to look at tree coherence and the wave problem. We made substantial progress toward analytical predictions and empirical observance of the phenomenon. There are over 30 potential error sources that could contribute to the phenomenon we are experiencing. Initial analysis of the physics governing the effects eliminated some, and analysis of the flight data allowed us to further focus our research activities in the future.

We initiated additional analysis governing the effects of tree phenomenology. The prevailing consensus is that decorrelation due to volumetric scattering may not be the dominant error source, as previously believed. Instead, it appears the decorrelation in the layover regions and shadow regions may be causing the phase unwrapper to improperly reconstruct the trees. We believe a previously proposed multibaseline technique that will eliminate the need for phase unwrapping is the correct solution to this problem.

Publications

Other

Burns, B. 1998. "Analysis of IFSAR Error Sources." Internal memorandum, Sandia Technical Report, in preparation. Sandia National Laboratories, Albuquerque, NM.

3532.240

Electric Launcher for Defense Applications

D. M. Rondeau, K. W. Reed, L. X. Schneider, B. E. Swanson, R. B. Asher, W. P. Schimmel, E. A. Weinbrecht, S. L. Shope, J. I. Crowther, Jr., B. M. Marder

We conducted a study assessing the application of Sandia-developed coil-gun technology for two airborne applications in support of Sandia's Emerging Threats Strategic Business Unit. An electric gun, of which a coil gun is one type, provides kinetic energy to a projectile from stored electrical or magnetic energy delivered in a few milliseconds. The primary elements are the power source, an energy storage device, a power peaking device, and the conversion elements from electric to kinetic energy. Potential advantages of this technology over conventional, chemically fired munitions include significantly higher velocities and kinetic energy levels, elimination of explosive propellants along with combustion gases and their issues, simplified loading and lower manning levels, increased stand-off range, increased penetrator lethality, and mission flexibility.

Two types of electric guns are of interest for large aircraft and fighter applications: a rail gun and a coil gun. In a rail gun, the conversion from electrical to kinetic energy is obtained from the magnetic fields generated by current flowing through sets of parallel rails, with the projectile armature being pushed by the interaction of the magnetic field with the current flowing through the armature. Current flow through the moving armature is established and maintained through contact with the rail, and this generates a plasma with substantial resistive loss and rail wear. In a coil gun, kinetic energy is imparted to the projectile through a series of sequentially switched magnetic coils. The coil gun has no electrical contact since it

couples magnetically, and the forces are such that the projectile tends to be self-centered within the barrel and is magnetically levitated on the centerline. The coil gun consists of a sequence of coils surrounding a flyway through which a conducting armature passes. A rapidly rising magnetic field associated with energizing the coils induces a current in the armature, producing a force. We achieved velocities in excess of 1 km/s with a 2-inch-diameter, 240-gram aluminum projectile in a 1.6-meter tube. Past experiments demonstrated coil strength, operating reliability and controllability, and benchmarking of simulations. We achieved coil strength and launch pressure of 1.1 kbar. We presume that an increase in coil strength to 2.0 kbar by 2005 is very feasible, and a 3–4 kbar pressure range by 2015 is possible.

We are evaluating two general applications for electric-gun technology: a replacement for a 105 mm Howitzer aboard a large aircraft gunship, and an integral frame-mounted weapon for the future-generation Joint Strike Fighter. For the large aircraft application, we are analyzing projectiles of 4 to 8 kg in mass, and muzzle velocities of 1.5 to 2.0 km/s. For the fighter aircraft, we are assessing projectile masses of 0.4 to 1.2 kg and muzzle velocities of 1.7 to 2.5 km/s. Several integral technology areas will require significant development and some research to realize the full potential of a coil gun in these applications: high-strength coil design, energy supply and storage, and fire-control system.

Preliminary assessments indicate that the system weight for the large aircraft application is on the order of 6,500 to 11,500 pounds by the year 2015 for a 4 kg, 1.7 km/s projectile and an 8 kg, 1.7 km/s projectile, respectively, utilizing a compulsator/capacitor power conditioning system. Fighter aircraft systems weights ranged between 1,900 pounds in 2015 for a 0.4 kg, 1.7 m/s projectile, and 6,000 pounds for a 1.0 kg, 2.5 km/s projectile.

We established a development program schedule and resource estimate to provide for significant design and development efforts in coil-gun operations, power supply storage, switching, smart and maneuvering projectiles, trainable gun with assisted target recognition, and aircraft integration testing and demonstration.

Publications

Other

Rondeau, D. M. 1998. “Application of Coilgun Technology for Military Aircraft.” Paper presented to the Directed Energy Technology Review, Dayton, OH, 29 September.

3533.180

Power-Grid Reliability and Restructuring Policy Changes

D. G. Robinson, A. B. Baker

The objective of this project is to provide additional insight into the effect of policy issues associated with restructuring of the power industry on the ability of the industry to provide adequate and secure power to the consumer. This project suggests that two interrelated areas of investigation be undertaken: (1) availability of off-site power to nuclear power plants, and (2) power-grid reliability. Research undertaken in this project was limited to characterizing the impact of restructuring on the availability of quality power to the consumer.

This research was the result of a cooperative effort between Sandia, Associated Power Analysts, Inc. (APAI), and Texas A&M University to characterize the impact of a changing regulatory environment on the reliability of customer electrical service. We desired to assess the impact in as realistic an environment as possible. Because of the availability of data, the initial study centered on the electric power grid in Texas. Specifically, we used data from the Electric Reliability Council of Texas (ERCOT) for the 1997 operational year in the research. Based on geography and location of generation and transmission lines, we considered ten basic areas and modeled each area as a single-point generation and load. Sandia developed a number of restructuring scenarios that APAI investigated using their N-Area Reliability Program (NARP). The present study is limited to an assessment of the adequacy aspects of reliability: sufficiency of installed generation and transmission capacity to satisfy the needs of all consumers in a steady-state sense. The results are, on one hand, conservative in that they address only the impact of peak loading. Alternatively, they are optimistic in that the transmission lines are assumed to be in continuous operation. The major results of this study indicate that, in a new regulatory era, the reliability of customer service will be significantly impacted, possibly in a negative fashion, unless the effects of the ensuing economic pressures are understood and appropriate actions are taken.

Publications

Refereed

Patton, A. D., C. Singh, and D. Robinson. 1998. “Impacts of Deregulation on the Reliability of a Multi-Area Power Pool.” *Proc. IEEE Power Sys. Computation Conf.*, accepted.

Other

Patton, A. D., C. Singh, and D. Robinson. 1998. “The Impact of Restructuring Policy Changes on Power-Grid Reliability.” Sandia Technical Report SAND98-2178 (October). Sandia National Laboratories, Albuquerque, NM.

3533.050

SAM Telemetry for Measurements While Drilling

S. Ballard, G. T. Barker, T. W. Caffey, A. J. Mansure, R. G. Keefe, L. C. Bartel

The need for a reliable, fast, wireless telemetry system in the drilling industry is great, but the technical challenge to develop such a system is huge. Sandia tested a downhole wireless telemetry system based on surface area modulation (SAM). SAM telemetry modulates an electrical current flowing along the drillstring. We monitor the current modulation at the surface with an ammeter. We encode downhole data and transmit them to the surface as a pattern of current oscillations.

In a field test, the SAM system successfully transmitted downhole information from depths of 1,400 feet below the fluid level to the surface at a rate of 110 baud. One of the configurations tested improved the data transmission rate at a given depth by more than an order of magnitude, and increased the maximum depth from which successful data telemetry could be achieved by more than a factor of two.

The need for a reliable, fast, wireless telemetry system in the drilling industry is great, but the technical challenge to develop such a system is huge. We field-tested the SAM system for measurement-while-drilling (MWD) well applications. During the test, we transmitted data successfully at 300 baud from depths of 550 feet below the fluid level using a coaxial configuration (configuration #1), and from depths of 1400 feet below the fluid level at a rate of 110 baud using an align electrode configuration (configuration #2). These performances were limited by the signal power generated by SAM, by the attenuation of the signal as it traveled back to the surface, and by the hardware used to encode and decode the data. For example, we recorded signals from 900 feet below the fluid level with configuration #1, but could not decode them. The risetime of these signals suggests that with proper modulation/demodulation, 110-baud data may have been transmitted from 900 feet below the fluid level with configuration #1.

Clearly the test did not achieve the dream of kilobaud data from 20,000 feet. Pretest predictions were that for configuration #1 data transmission would drop to below 110 baud before the bottom of the ~ 2,000-foot test well, and it did. We also predicted that configuration #2 would provide considerable benefit, and it did. In terms of actual measured performance, configuration #2 improved the data transmission rate at a given depth by an order of magnitude and increased the depth to which telemetry was successful by more than a factor of two.

Because the test well was only ~ 2,000 feet deep, extrapolation is required to predict what telemetry rates might be achievable at depths at which MWD becomes economic. We analyzed the data using three different approaches that arrived at essentially the same conclusions, lending credibility to their extrapolations. Extrapolation of the configuration #1 results suggests that data rates of 1 to 10 bits per second should be possible at 10,000-foot depth, the same rates achievable by conventional electromagnetic (EM) systems. It would appear that the difference between conventional EM systems and configuration #1 SAM is primarily a function of the signal power at the SAM package.

We found that configuration #2 provides, at a fixed depth, 100 times the bandwidth or, at a fixed bandwidth, 10 times the depth before signal drops below noise. Compared to configuration #1, configuration #2 provides the maximum signal power at the SAM package. Whereas extrapolations of configuration #1 to depth gave the same bit rates as conventional EM systems, we demonstrated configuration #2 to have significantly better performance.

Considerations beyond the scope of this test and analysis are changes in performance due to changes in geology, cultural noise, and input power. The test well penetrated shaly sand formations with 10-ohm-meter resistivity, which, while not a worst-case geology, was not favorable to data transmission. Although the test well was surrounded by producing wells, and some of the time the engines of the workover rig on the well were on, we measured no variations in cultural noise, and thus no conclusion should be made as to whether the tests were noise-favorable or -unfavorable. In theory, we can increase the signal by increasing the power supply output, provided the power supply does not contribute to the noise; however, such considerations are beyond the scope of this work.

The field test was not successful in demonstrating configuration #1 SAM telemetry as an improvement over current MWD EM telemetry, but it did demonstrate that configuration #2 has the potential to significantly improve the rates of data transmission.

Publications

Other

Mansure, A. J., R. G. Keefe, T. W. H. Caffey, L. C. Bartel, and S. Ballard. 1998. "The Surface Area Modulation Downhole Telemetry System for Measurement While Drilling." Sandia Technical Report SAND98-0778 (April). Sandia National Laboratories, Albuquerque, NM.

3533.160

Advanced Geosphere Transport Simulation

M. J. Martinez, P. L. Hopkins, P. C. Reeves

Numerical simulation is a key technology in system design, regulatory assessment, and decision analysis for radioactive-waste disposal and subsurface environmental remediation. Present limitations in computational technology drive model simplifications in the range of physical processes simulated, site

geometry, and geologic realism, with significant negative impacts: (1) simplifications become regulatory points of contention, (2) critical details about fast-path transport are lost, and (3) turnaround times for assessing uncertainty are too long to drive project decisions. A massively parallel (MP) geosphere transport model will overcome these limitations and place Sandia in an advanced position with respect to repository simulation capabilities. Sandia has a unique opportunity to leverage major Defense Program (DP) investments in computational simulation and to develop a fast, flexible geosphere transport simulation capability, running on MP computers and networked workstations. We are building this project on a recently completed MP research code, which will be a key component of the long-term strategic initiative to significantly enhance performance assessment capability. This code will also have the potential to enhance R&D in other technologies whose performance hinges on understanding and controlling geosphere transport.

(1) *Code upgrades*. (a) To efficiently manage this multideveloper software project, we placed the source code under the CVS (concurrent versions system) software control system. This enables simultaneous software development among the many developers in the MPSalsa family of codes and enables continuation of our collaborations in a much more cost-effective way. We implemented several key code capability upgrades that facilitate implementation of a liquid-phase advective/dispersive transport capability. The more important upgrades completed include enabled linking with updated NEMESIS parallel input/output (I/O) library and the updated AZTEC parallel solver libraries for improved performance; implemented user-driven specification of relative permeability and capillary pressure models, with automatic Jacobian calculation; and extended and improved the equation-of-state (EOS) models for phase appearance/disappearance. By leveraging on-going work, these upgrades also enable coupled physics modeling and mesh adaptation developments. (b) We implemented a control-volume–based stabilization method for convection-dominated flows and for dealing with phase transitions and verified it on several test problems, including 1-D heat-pipe and 2-D and 3-D Jornada Trench problems. The method is control-volume conservative, but allows general unstructured gridding. We developed and implemented a special quadrature rule. This feature is essential for stable numerical treatment of phase appearance and disappearance in the flow equations.

(2) *Geostatistical simulation capability*. The aim of this task is to facilitate flow and transport simulations over a fully heterogeneous field in which multiple formation and hydrologic properties have been generated by geostatistical simulation (GSLIB) software. The GSLIB software is the current industry standard and allows for the estimation and simulation of spatially correlated properties in two and three dimensions. Both maximum entropy (multigaussian) and indicator–based spatial fields can be created as input to the simulator. We developed a preprocessor both as a means of generating heterogeneous property fields and as an interface between the transport simulator and the GSLIB software. The current version of the preprocessor includes embedded logic for generating spatially uncorrelated material properties according to uniform, random, normal, and lognormal distributions. Properties generated with more sophistication by GSLIB software can be written to an ASCII (American Standard Code for Information Interchange) file and used as input to the preprocessor. These properties are typically generated on a well-defined, structured grid. We developed a nearest-neighbor method for mapping the heterogeneous properties from the geostatistical simulation grid onto the finite-element (FE) grid (structured or unstructured) used in the transport simulator.

(3) *Verifications*. For purposes of verification, we tested the code on a set of standard problems designed to exercise different aspects of the code. In addition, we applied the code to a series of sample problems modeled after the proposed Gas Migration Test being conducted by the Japanese Radioactive Waste Management Center at the Grimsel site in Switzerland. This test will assess the gas migration behavior of a 1/10th-scale repository containment placed in a crystalline rock that contains a steeply dipped fracture zone. These efforts demonstrated our abilities to model multiphase flow in complex 3-D geologic systems (200,000 grid points, 400,000 unknowns) running over a local-area network (LAN).

Publications

Refereed

Martinez, M. J., and P. L. Hopkins. 1998. "A Two-Phase Thermal Model for Subsurface Transport on Massively Parallel Computers." *Proc. 10th Internat. Conf. on Finite Elements in Fluids* **1** (Tucson, AZ, 5–8 January): 468–473.

Martinez, M. J., P. L. Hopkins, and J. N. Shadid. 1997. "Multiphase Nonisothermal Subsurface Transport on Parallel Computers." *Proc. 1997 ASME Internat. Mechanical Engin. Congress and Expo.* **224** (Dallas, TX, 16–21 November): 413–422.

Other

Martinez, M. J., P. L. Hopkins, and P. C. Reeves. 1998. "Progress Report on Advanced Geosphere Transport Simulation LDRD." Sandia internal memorandum to Distribution (10 July). Sandia National Laboratories, Albuquerque, NM.

Martinez, M. J., P. L. Hopkins, S. A. Altman, and P. B. Davies. 1997. "Numerical Simulation of Nonisothermal Flow on Massively Parallel Computer Architectures." Brochure/Poster for ASCI–Sandia Booth at Super Computing '97 Conference, San Jose, CA, 15–21 November.

3533.070

Design-for-Manufacturability Applied to Photovoltaic Modules

J. M. Gee, S. E. Garrett, W. P. Morgan

The purpose of this project is to apply modern manufacturing design procedures (e.g., design for manufacturability) and manufacturing processes from other mature industries (e.g., printed circuit boards and flexible circuits) to photovoltaic (PV) module manufacturing. The goal of the project is to reduce module assembly cost by a factor of two, which corresponds to a 25% decrease in the manufacturing cost of the PV module. The new concept (Monolithic Module Assembly) encapsulates and electrically connects all the cells in the module in a single step, which can be achieved only with significant changes in the PV cell and module design. Sandia will develop an assembly process that (1) uses back-contact cells, (2) uses a module backplane that has both the electrical circuit and encapsulation material in a single piece, and (3) uses a single-step process for assembly of these components into a module. This process reduces cost by reducing the number of steps, by eliminating the low-throughput (e.g., individual cell tabbing) steps, and by using completely planar processes that are easy to automate. Back-contact cells are crucial for this project because the coplanar geometry allows attachment of leads to both polarities in the same step. This work will use a Sandia-proprietary solar-cell concept (emitter wrap-through cell) that has both contacts on the back surface. A variety of materials and conductor application methods from the printed circuit board industry can be used for the module backplane. Similarly, the printed circuit board industry routinely bonds a large number of devices to a board in a single step using a variety of methods (e.g., solder and conductive epoxies). If successful, this work will lead to patentable advances in technology, will help position PV technology for substantial capacity additions at lower cost, and will be applicable to future PV technologies (thin-film and concentrator).

The goal of this final year of the project was to develop a prototype using more cost-effective materials. During the first year of the project, we developed a prototype that demonstrated the concept—electrical and mechanical assembly of a PV module in a single step. This first-year prototype used a fairly expensive material (conductive epoxy) that also did not perform very well in thermal cycling tests. Hence, we examined low-temperature solders. Solder is less expensive, has lower electrical resistance, and is likely to be more reliable than conductive epoxy. We examined relatively low-temperature, bismuth–based solders to be compatible with standard encapsulation materials (ethylene vinyl acetate) and process time-temperature-pressure cycles. We were concerned about the ability of the solder to wet the solar cell and interconnect during the lamination cycle. The problem is that the encapsulation material melts and flows during the lamination cycle and might prevent formation of the solder bond. We were successful in laminating modules with low-temperature solders. Cross-sectional analysis of the bonds suggested that the bonds were not very continuous, and initial thermal cycling testing also indicated problems with the bonds. We believe that we could improve the continuity of the solder bonds with some simple changes in the process (geometry of the solder bond and stabilization of the interconnect). We assembled PV modules using the new process with low-temperature solder bonds and achieved a solar-to-electric conversion efficiency of 13%. This is a substantial improvement over the 11% efficiency achieved in the first year of the project.

Publications

Refereed

Gee, J. M., D. D. Smith, S. E. Garrett, M. D. Bode, and J. C. Jimeno. 1998. "Back-Contact Crystalline-Silicon Solar Cells and Modules." *Proc. NCPV Program Review Mtg.* (Denver, CO, September).

3533.170

Low-Work-Function Thermionic Emission Materials

D. B. King, J. A. Ruffner, K. R. Zavadil

Thermionic converters or diodes are two electrode devices that convert heat energy to electrical power. The electrodes are spaced opposite each other. A heat source elevates the temperature of the emitter electrode. Electrons are then thermally evaporated into the interelectrode space between the emitter and collector electrode. The high working temperatures represent an operational limitation. A process to fabricate low-work-function electrode materials will allow the diode to operate at substantially lower temperatures. Promising materials for use as a cathode are scandia-stabilized, alkaline earth oxides. Scandia appears to provide two critical functions in a cathode, depending on how the cathode is fabricated. For mixed matrix-oxide cathodes, scandia appears to stabilize an emitter like barium (Ba), prolonging its surface residence time and reducing its loss rate from the near-surface region and from the bulk of the oxide. Sandia will develop methods of thin-film deposition amenable to incorporation into microelectronic fabrication schemes. The mixed matrix oxide is the more attractive alternative for microelectronic applications predominantly because of reported lower operating temperatures and an anticipated greater stability of Ba. The mixed oxide should allow a move away from the traditional, bulky

dispenser structure with a large capacity to a thin-film technology. In addition, we will investigate alternate evaporation and chemical vapor deposition (CVD) routes for cathode formation. We will deposit mixed Ba and scandium (Sc) oxide films by co-evaporating the metals followed by thermal oxidation. Metallic deposition affords an opportunity to gradate the Ba concentration in the film and preserve an excess concentration of zero-valent Ba at the film/substrate interface. This excess represents the additional capacity required with slow loss of Ba from the surface of the film.

The aim of this project is to develop a low-work-function thermionic emission material with appreciable electron emission at modest operating temperatures. The material must also be compatible with all microelectronic fabrication processes that will be used to create the new converters.

We successfully developed a method for fabricating scandate–based thermionic emitters in thin-film form. Our approach was to incorporate BaSrO (BSCO) into a Sc_2O_3 matrix using RF sputtering to produce thin films. Testing shows the resulting films to be electron emissive at temperatures as low as 900°K with current densities of 0.1 mA¾cm^{-2} at 1100°K and saturation voltages. We estimate an approximate maximum work function of 1.7 eV. Film compositional and structural analysis shows that a significant subsurface alkaline earth hydroxide phase can form and probably explains the limited utilization and stability of Ba and its surface complexes.

We deposited a variety of thin bilayer films onto a tantalum (Ta) electrode on silicon (Si). The films have four discrete layers sitting on top of the Si substrate: (1) 400 nm of thermally grown SiO_2, (2) 500 nm of sputter-deposited Ta, (3) < 400 nm of BSCO, and (4) 400 nm of Sc_2O_3. The BSCO layer forms platelet crystals oriented parallel to the surface, and Sc_2O_3 forms columnar crystals oriented perpendicular to the substrate. The films have a specular surface finish when first removed from vacuum, but rapidly develop surface texture with exposure to atmosphere. We found that thicker scandia capping layers, elevated temperature deposition (300°C), and introduction of O_2 into the RF plasma all slow the development of this surface texture. Mass-gain measurements made as a function of post-deposition atmospheric exposure are consistent with the uptake of H_2O to form a hydroxide phase. We believe that the columnar scandia crystal structure is largely responsible for the high permeability to H_2O and subsequent hydroxide formation.

We used surface spectroscopy to verify the existence of the hydroxide. X-ray photoelectron spectroscopy shows that Ba and strontium (Sr) are always present on the surface of these films. The relative hydroxide-to-oxide surface concentration scales with the amount of surface Ba and Sr. This finding argues that these species are transported through the scandia overlayer due to the activity of H_2O. We achieved the lowest degree of Ba and Sr conversion and transport with deposition at temperature, in oxygen, and with thicker capping layers. Cross-section scanning electron microscopy (SEM) analysis shows that the hydroxide presence is localized. Using energy dispersive x-ray fluorescence, we are able to collect compositional information from each of the discrete layers and the hydroxide layer. We find that the scandia capping layer is still intact below and to either side of the hydroxide. We also find that the relative 0°K level emission is significantly greater in the surface feature than either the underlying Sc_2O_3 or BSCO. This observation is evidence of localized hydroxide formation in the surface feature. We concluded that H_2O ingress occurs locally, first permeating and forming an underlayer hydroxide, then hydrating to an extent where transport of Ba_2+ and Sr_2+ through the scandia is possible. Hydroxide phase formation then continues locally at the surface. The hydroxide is an undesirable phase because electron emission would not be occurring exclusively from a Ba-Sc_2O_3 surface complex. We do find that the sample is electron emissive. Emission data show expected diode characteristics with a nearly zero current region corresponding to the work-function difference of the emitter and collector, a linear region of retarded mode operation, a decrease in current rise with diode voltage indicative of space charge, and, finally, a slow rise in current with voltage evidence of saturation. We estimate that the emitter work function is less than 1.7 eV. We find that the current output of these emitters is not stable with time, resulting in eventual decrease. This instability is a result of first depleting Ba from the hydroxide phase, explaining the high initial currents, followed by Ba diffusion from the BSCO underlayer, and electron emission from discrete local regions of the surface.

Publications

Refereed

King, D. B., J. R. Luke, and F. J. Wyant. 1998. "Results from the Microminiature Thermionic Converter Demonstration Testing Program." *AIP Conf. Proc. 13th Symp. on Space Nucl. Power and Propulsion*, accepted.

3534.030

LIGA Micromachining

J. M. Hruby, B. V. Hess, A. M. Morales, R. H. Nilson, S. K. Griffiths, M. X. Tan, D. R. Boehme, W. D. Bonivert

The LIGA (German for lithography, electroforming, molding) process uses synchrotron radiation to create patterns of fine-featured structures in polymethylmethacrylate (PMMA). These patterns, once developed, become a high-aspect-ratio mold that can be filled with other materials chosen for the intended application. Most commonly, metal is electrodeposited into the PMMA mold to produce metal or metal alloy micromachines. The micromachines produced through the LIGA process typically have aspect ratios greater than 10:1, can be made from a variety of metal or plastic materials, and are well suited to actuation as well as sensing functions. LIGA bridges a gap in miniaturization between silicon (Si) micromachining (a few microns) and precision machining (a few millimeters). At Sandia, LIGA micromachining complements our expertise in Si surface micromachining and compound semiconductor patterning.

In this project, we established capabilities to conduct all the LIGA process steps at Sandia except the synchrotron exposure and negotiated dedicated beam lines. The infrastructure developed includes the design and procurement of a flexible LIGA scanner for synchrotron exposures, LIGA mask making, chemical development of high-aspect-ratio patterns in resist, a better understanding of electroplating of high-aspect ratios, nonsynchrotron high-aspect-ratio mold making, and Web–based software for process predictions. Through this project Sandia has established a world-class LIGA capability that will be used by many customers.

During FY98 we accomplished the following:

(1) Completed the design of a LIGA scanner for synchrotron exposure. This scanner allows masks larger than 3 inches, multiple masks to be mounted at one time, mask rotation for 3-D exposures, and a user-friendly control architecture. We procured this scanner and began initial testing.

(2) Established and optimized the processing of Si substrate mask-making capability. This work was accomplished in collaboration with the University of California–Berkeley clean rooms. In parallel, we established clean-room capabilities onsite and procured an ultraviolet (UV) aligner. We also successfully explored alternative substrate mask-making capability.

(3) Procured and installed a new plating line that was specially designed for plating LIGA hardware. This plating line includes the capability to precisely control the current, to continuously monitor the plating conditions, and to have as many as eight chemistries available for plating LIGA parts. In addition, we studied and documented modeling to improve our understanding of the effects of natural convection on electroplating. This work led to both new understanding and suggested methodologies to improve electroplating uniformity. We initiated testing on the new, improved methodology.

(4) Implemented a LIGA software architecture that included Web-site design and installation, image library with remote upload and download capability, and remote Web-browser version of LEX (LIGA exposure) codes.

(5) Explored options for nonsynchrotron-exposure high-aspect-ratio structures. This work led to alternatives for structures that are 50 to 100 microns in depth.

Publications

Refereed

Griffiths, S. K., R. H. Nilson, R. W. Bradshaw, A. Ting, W. D. Bonivert, J. T. Hachman, and J. M. Hruby. 1998. "Transport Limitations in Electrodeposition for LIGA Microdevice Fabrication." *Proc. SPIE, Micromachining and Microfabrication Process Technol. IV* **3511** (Santa Clara, CA, 21–22 September): 364–375.

3534.040

Applied Microfluidics Science

E. B. Cummings, T. L. Prast, A. J. Salmi, S. K. Griffiths, R. H. Nilson, P. H. Paul

We developed a microparticle-image-velocimetry system and analysis software for measuring fluid velocity fields, electric fields, and viscosity fields in microchannels. We developed a means of rapidly and inexpensively microfabricating microfluidic systems using SU-8, a photopatternable clear epoxy. Our theoretical and numerical investigations into electrokinetically pumped microfluidics reveal that, in a

wide class of geometries, these flows are irrotational and subject to simple numerical and even analytical treatment. We also derived analytical expressions for hydrodynamic dispersion in capillaries with applications to optimizing the design of electrophoretic and capillary electrochromatographic columns. In collaboration with colleagues from the University of Florida and Washington State University, we studied boiling in microchannels numerically and experimentally.

(1) *Developed experimental techniques*. To supplement our caged-dye fluorescence imaging tool, we developed an epifluorescence multiple-camera video microscopy system for performing particle-image velocimetry (PIV) and ratiometric fluorescence imaging measurements in optically accessible microchannels. The PIV system uses dyed latex nanospheres (20–200 nm-diameter) that fluoresce strongly enough that individuals can be tracked. Behaving like macromolecules in solution, these particles permit measurement of electrophoretic, convective, and Brownian motion fields via PIV. Because many of the flows of interest are electrically driven, a component of the particle motion arises from electrophoresis. The contributions of convection and electrophoresis to the motion of the particles are independently inferred by simultaneously observing with two cameras the motion of particles with different electrophoretic mobilities and fluorescence wavelengths.

To analyze the particle-image data, we utilized µPIV, an in-house interactive and automated graphical user interface (GUI)–based image-processing code written in C++ for this program. This code utilizes fast Fourier transforms to perform image cross-correlation. An arbitrary number of sequential images can be incorporated into the same analysis, allowing averaging of the correlation functions for stationary flows. The innovative features of the code are automatic grid refinement, averaging of the correlation, and an ability to measure gradients and curvature in the velocity profile in the unresolved direction (normal to the imaging plane).

(2) *Developed fabrication methods*. We developed a capacity to design and microfabricate microfluidic test structures in house. Microelectronics at Sandia provides a photoplot of our computer-aided design (CAD) with ~ 30 µm resolution that we use as a mask for patterning SU-8, a photodefinable epoxy. We fabricated channels with SU-8 walls, floors, and ceilings by (a) spinning SU-8 (~ 1 µm) onto the surface of a wafer, photopatterning the desired channel floor, dissolving the undesired sections, and curing at ~ 130°C; (b) spinning the wall layer (typically 50 µm thick) of SU-8 onto this coated wafer or slide, photopatterning the channels, dissolving the channels, and curing at ~ 130°C; and (c) spinning SU-8 onto a microscope cover slip for the channel ceiling, baking out excess solvent, assembling the top and bottom pieces, placing in a vacuum bag, and baking at ~ 130°C, producing a sealed, all-epoxy channel. The SU-8 is chemically inert and nonfluorescent and features high-aspect-ratio walls (50:1). The development of this rapid and inexpensive fabrication technique is ongoing.

(3) *Developed theory of microfluidics*. We made strides in understanding the nature of electrokinetic (EK) flows when the electrical double layer is much smaller than boundary dimensions, as is typical for microfabricated devices. We showed theoretically and numerically that purely EK flow away from conducting surfaces and surface and fluid inhomogeneities is irrotational except in the electrical double layer. Thus bulk electrokinetically pumped flows are potential flows, a much-studied and tractable class of flows that are exact solutions to the Navier-Stokes equations for all Reynolds numbers. We also explored how inhomogeneities and conducting walls can produce vorticity and pressure fields.

We also derived analytical expressions for hydrodynamic dispersion in an open cylindrical channel. These solutions will assist designers with understanding the optimum scaling for electrophoresis columns and capillary electrochromatographic columns.

(4) Investigated boiling in microchannels. In our ongoing university collaboration, we began to explore phenomena related to boiling in microchannels. We experimentally explored the boiling of water, FC-72, and pentane in capillaries and microchannels using standard resistance heaters and a novel 100-element feedback-controlled microheater array provided by one colleague. Another colleague helped with physically modeling the liquid-vapor meniscus in boiling. Boiling and bubble formation are either useful or problematic for a wide range of microdevices.

3535.130

Computational Simulations of Self-Assembling Macro-Systems by Direct Fabrication of Microscopic Structured Materials

S. Istrail, J. Cesarano, III, V. Tikare

Sandia is modeling and testing the processes that direct self-assembly of macroscopic components in an effort to understand and establish control over spontaneous structure formation of small Janus bricks. (The simplest Janus particle has one side hydrophobic, the other hydrophilic.) Janus bricks can be programmed with varying affinities for each other on their faces and edges so that red surfaces (e.g., hydrophobic) stick to red but not to blue (e.g., hydrophilic). With unlimited colors, any macroshape could be self-assembled if the bricks had sufficient mobility and time to find their proper neighbors by low-temperature direct fabrication in a parallel self-assembling mode. Disparate materials could be accommodated in neighboring bricks, and near-net-shape structures could be formed out of fully dense bricks with minimal shrinking from sintering. It is an open question what shapes are possible with just two colors and only one or two brick shapes. Moreover, since it is not clear what process is required to sinter a Janus assembly, we are developing a phase-field sintering model to predict the end-state structures. We are using small, experimental systems to discover the phenomenology of simple Janus tiles, which have the attractive possibility of self-assembling very simple virus-like capsules from only six triangular tiles.

We explored isomorphism between Janus and Potts models. As a specific case of hydrophobic-hydrophilic interactions, we found the boundary of computational tractability for obtaining analytic, closed-form partitions functions for the Ising model, specifically for the Ising Spin-Glass problem. In the process, we made progress solving long-standing conjectures due to Onsager, Fisher, and Feynman related to the 3-D Ising problem, the 2-D versus planarity problem, and the second-neighbor interaction models. Using a phase-field formalism, we began to study the special problems that arise in sintering an assembly of ceramic Janus bricks.

As a simple realization of Janus objects, we worked experimentally with glass microballoons. We coated these 100-micron-diameter bubbles with a hydrophobic agent, then crushed them into approximately flat plates having one side hydrophobic, the other (interior side) hydrophilic. We examined the interactions between uncrushed microballoons with both treated and pristine surfaces in water by optical microscopy, then studied the behavior of shards in and on water. By far the strongest driving forces were found when we captured particles at a water-air interface: We found Janus plates to be oriented hydrophobic-side up regardless of initial deposition method. Somehow the plates spontaneously flipped over, even though their width greatly exceeds their thickness (exceeding 100:1). On a water surface, these Janus plates attracted very strongly, apparently via long-range capillary interactions. Untreated plates had little or no interaction. We have begun experiments to make LIGA-defined ceramic bricks.

Publications

Refereed

Hurd, A., and S. Istrail. 1997. "Prediction Algorithms for Nanobrick Self-Assembly." Presentation to the American Mathematics Society, Albuquerque, NM, 8 November.

3535.140

Self-Stabilizing Optical Solitons and High-Intensity Laser Plasma Channels for Diffraction-Free Propagation and Robust Power Compression

S. M. Cameron, D. E. Bliss

Optical channeling or refractive guiding processes involving the nonlinear interaction of intense femtosecond optical pulses with matter in the self-focusing regime have created exciting opportunities for next-generation laser plasma–based x-ray sources and atmospheric remote-sensing applications. This fundamentally new form of extended paraxial electromagnetic (EM) propagation in nonlinear dispersive media such as clear air or underdense plasma is attributed to the interplay between normal optical diffraction and intensity-dependent nonlinear focusing and refraction contributions in the dielectric response. Superposition of these mechanisms on the intrinsic index profile acts to define the propagating energy in a dynamic self-guiding longitudinal waveguide structure, which is stable for power transmission and robust compression. The laser-driven channels are hypothesized to support a degree of solitonic transport behavior, simultaneously stable in the space and time domains (group velocity dispersion balances self-phase modulation), and are believed to be self-compensating for diffraction and dispersion over many Rayleigh lengths in contrast to the defining characteristics of conventional diffractive imaging and beamforming. By combining concentrated power deposition with well-ordered spatial localization, this phenomenon will also create new possibilities for production and regulation of physical interactions, including electron beams, enhanced material

coupling, and modulated wakefields, over extended gain distances with unprecedented energy densities. Harmonious combination of short-pulse x-ray production with plasma channeling resulting from a relativistic charge-displacement nonlinearity mechanism in the terawatt regime has been shown to generate high-field conditions conducive to efficient multikilovolt x-ray amplification and peak spectral brightness. We recently utilized white-light conical emission generated by Kerr-induced atmospheric filamentation to collect remote backscatter spectrum from altitudes exceeding 10 kilometers. Channeled optical propagation with intense short-pulse lasers will impact several critical mission areas at Sandia, including x-ray backlighting of pinch implosions, nondestructive radiographic imaging of aging weapons components, high-power ultra–wide-bandwidth (UWB) single-cycle EM pulse generation, remote sensing, and laser micromachining.

In collaboration with researchers at the University of Illinois–Chicago, we used a self-focused femtosecond ultraviolet (UV) terawatt-class laser with a focused irradiance of 1018 W/cm^2 to produce L-shell x-ray emission from gold targets. We acquired spectra using an imaging crystal spectrometer of von Hamos type in mica (7th order) with an aluminized polycarbonate/kapton titanium filter set. The single-shot integrated x-ray yield near 10–14 keV exceeded our predicted value of 1 mJ/2p sr, and the observed spectrum, although occurring generally in the expected spectral region for the neon (Ne)-like gold (Au) transitions, exhibited a predominant asymmetrical broadband feature (~ 700 eV) superimposed on Bremsstrahlung continuum and line emission ($L_{a,b,g}$). Such a characteristic nonthermal emission signature arises from core-excited ionic state configurations (3d-2p, n > 3) and is direct evidence of a dynamical hollow atom excitation mechanism in which the energetic laser field collectively drives correlated multi-electron motion to produce anomalously strong coupling in the propagation channel. To our knowledge, this is the first reported measurement of gold L-shell emission from a laser-produced plasma and is the direct result of the unique interaction conditions that can be produced with high-intensity, short-pulse lasers. The achievable spectral radiances scaled to an existing hybrid Nd:glass laser deployed on the Z accelerator using our experimentally measured conversion efficiency (~ 1%) above 10 keV would facilitate an efficient, ultrabright, hard x-ray backlighting source capable of opacity penetration of pinch/capsule implosions with compressed area densities (rr ~ l–10). Corroborative measurements of the self-trapping channeling morphology with spatially resolved Thomson scattering and x-ray pinhole imagery indicated the presence of a longitudinally extended multifoci filament structure exceeding 50 Rayleigh lengths with < 5 mm radial extent characteristic of the relativistic self-focusing/charge-displacement mechanism. We also observed strong EM transients and coherent far-infrared (IR) emission at terahertz frequencies as the result of space-charge fields generated at the focus of the optical pulse due to the large pondermotive force. We recorded preliminary evidence of hot electron filaments or streamers generated by a wakefield or current pulse mechanism associated with the channeling process in xenon. As part of the experimental campaign, we also used the short picosecond x-ray bursts (recombination time < 5 ps) created by M-shell xenon (~ 1 keV) and L-shell barium fluoride (~ 4–5 keV) to directly measure the impulse response of x-ray detector (XRD) and photoconductive device (PCD) devices. The measured risetime for both devices, deconvolved for instrument response, was found to be approximately 100 ps, which may have important implications for diagnostic analysis of mix and Rayleigh-Taylor contributions in recent hydrodynamic evolution studies.

In parallel with experiments, modeling efforts have been ongoing toward spectroscopic analysis and developing predictive capability and stability criteria for the channeling mechanism. The theoretical analysis seeks to define stable eigenmodes in the nonlinear Schrödinger equation governing the guiding process and electrostatic force balance in the channel. By correlating the model results with our experimental data, such as x-ray spectra and spatially resolved images, we established first-order optimization parameters and stability maps for efficient x-ray conversion. The basic computational procedure developed in this work will find general usefulness in a variety of cases involving propagation in saturable nonlinear media different from plasma, including Kerr self-focusing in atmosphere. High-intensity, short-pulse experiments in this regime in conjunction with adaptive pulse shaping are being pursued under another project for remote-sensing and directed-energy applications.

Publications

Refereed

Borisov, A. B., J. W. Longworth, K. Boyer, and C. K. Rhodes. 1998. "Stable Relativistic/Charge-Displacement Channels in Ultrahigh-Power-Density Plasmas." *Proc. Nat. Academy of Sciences* **95** (June).

Cameron, S. M., D. E. Bliss, and C. K. Rhodes. 1998. "Self-Guided Laser Optical Channeling in Air with High-Intensity Ultrashort Pulses: Applications to Remote Sensing." Paper presented to the International Workshop on Ultrafast Intense Laser Pulse Propagation and Its Applications, Quebec City, Quebec, Canada, 19–20 June.

3535.160

Optical Communication System for Remote Monitoring and Adaptive Control of Distributed Ground Sensors Exhibiting Collective Intelligence

J. S. Wagner, K. M. Stantz, G. M. Loubriel, S. M. Cameron, M. W. Trahan

Comprehensive management of the battlespace has created new requirements in information management, communication, and interoperability as they affect surveillance and situational awareness. The objective of this project is to expand intelligent controls theory to produce a uniquely powerful implementation of distributed ground–based measurement incorporating both local collective behavior and interoperative global optimization for sensor fusion and mission oversight. By using a layered hierarchical control architecture to orchestrate adaptive reconfiguration of semiautonomous robotic agents, Sandia can improve overall robustness and functionality in dynamic tactical environments without information bottlenecking. In this concept, each sensor is equipped with a miniaturized optical reflectance modulator that is interactively monitored as a remote transponder using a covert laser communication protocol from a remote mothership or operative. We can leverage robot data-sharing at the ground level with global evaluation criteria, including terrain overlays and remote imaging data. Information sharing and distributed intelligence open up a new class of remote-sensing applications in which small, single-function autonomous observers at the local level can collectively optimize and measure large-scale, ground-level signals. As the need for coverage and the number of agents grow to improve spatial resolution, cooperative behavior orchestrated by a global situational awareness umbrella will be an essential ingredient to offset increasing bandwidth requirements within the net. A system of the type used in this project will be capable of sensitively detecting, tracking, and mapping spatial distributions of measurement signatures that are nonstationary or obscured by clutter and interfering obstacles by virtue of adaptive reconfiguration. This methodology could be used, for example, to field an adaptive ground-penetrating radar (GPR) for detection of underground structures in urban environments and to detect chemical species concentrations in migrating plumes.

Highlighted achievements concerning the theoretical components are the development of two physics–based collective behavior simulation codes, the development of a parallelized genetic algorithm (GA) for optimization of behavioral characteristics, and new results focused on local/global coordination of collective behavior and adaptive reconfiguration of swarms looking at plumes and underground structures. Two new physics–based collective models, a lattice gas (LG) and a particle-in-cell (PIC) (plasma–based) code, model collective behavior in a validated framework that enables theoretical comparisons with statistical mechanical behavioral theory, taking advantage of well-benchmarked physics models as an overall design tool. Each robot's potential fields modeled by the LG or PIC simulations provide fast trip-wire responses to an immediate target or event, point-sensor information/transformation for further processing (targets vector direction), application of pseudo-potential fields (linked to genetically trained [recurrent] neural network decisions) to adapt to local disturbances, and global imaging-like capabilities to study and respond to the environment. We developed and implemented a parallel GA on top of these collective behavior models to optimize spatial- and time-dependent nearest-neighbor potential interactions that realize adaptability in the swarm's performance (obstacle avoidance, GPR, remediation). We also studied behavioral performance versus other physical parameters, such as friction and drag during flight dynamics, to determine swarm behavioral changes for the ballistic missile (PIC) and fighter-planes in dog-fight scenarios.

Laser optical communication potentially offers significant advantages for remote coordination and data exfiltration from covert distributed ground-sensing networks. The spatial coherence of laser transmitters offers favorable gain scaling with low probability of intercept, and the relative temporal coherence of the optical carrier can support tremendous information bandwidth without baseband interference or frequency allocation problems. A major weakness limiting the operational utility of nonideal optical communication channels propagating in atmosphere, however, has been adverse effects of extinction (loss), scattering (dispersion), turbulence (degraded coherency), and fade, which degrade realizable transmission bandwidth and gain aperture for acceptable bit error rate. We investigated the use of a

previously developed active reflectance imaging technique based on an optical parametric amplifier (OPA) receiver to enhance detector sensitivity and error rate performance for unguided digital communication links affected by cloudlike conditions. Using a kilohertz repetition-rate femtosecond laser system operating at eyesafe wavelengths, we evaluated the role of signal-spontaneous OPA beat noise amplified spontaneous emission (s-ASE) on amplified signal, noise figure, and channel sampling capacity for various binary modulation formats in both direct and coherent detection modes to establish fundamental response limitations as a function of turbidity.

As an example of the new type of cooperative remote sensing and synchronization that can be addressed with a distributed collective operating synergistically at local and expert levels, we completed a field test in a stationary sandbox configuration that emulates an adaptive ground-penetrating impulse radar that is capable of detecting underground structures in cluttered or propagationally dispersive backgrounds. In these experiments, we used a fiber-coupled avalanche diode to trigger multiple ultra–wide-bandwidth (UWB) RF transceivers (Yagi) at various time/phase delays (simulating a distributed aperture of dipole pulsers optically triggered by photoconductive switches) to study electromagnetic (EM) superposition and target detection as a function of range (depth) and aspect (obliqueness). We used UWB waveforms because of potential advantages associated with signal interaction and extraction and improved imaging discrimination. By properly assembling the array in phase, amplitude, and spatial orientation, a directive illumination pattern with adjustable transfer function can be created to match the local measurement environment, including terrain obstacles and soil-layer attenuation. We compared experimental iterative solutions qualitatively with the results obtained from intelligent (genetic) optimization algorithms for design variables of the radiating structure, including element spacing, sensor density, and sidelobe characteristics in relation to detection criteria. We examined the general synthesis problem of a sparse array of active EM elements subject to a fitness function that optimizes a matched filter for the scattering topology of plane waves in the context of joint finite-difference, time-domain, frequency-domain analysis.

Publications

Other

Cameron, S. M., and R. D. Robinett, III. 1998. “Adaptively Reconfigurable Ground–Based Remote-Sensing System for Monitoring Migrating Chemical/Biological Plumes and Detection of Underground Structures.” DARPA proposal in response to BAA 98-18 (miniature, unattended ground sensors and related technologies) (25 February).

Cameron, S. M., R. B. Asher, G. M. Loubriel, R. D. Robinett, III, K. M. Stantz, M. W. Trahan, and J. S. Wagner. 1998. “Adaptive Remote-Sensing Techniques Implementing Swarms of Mobile Agents.” Paper presented to WSD ’98, 4th Joint Workshop on Standoff Detection for Chemical and Biological Defense, Williamsburg, VA, 30 October.

Stantz, K. M., C. G. Diniz, M. W. Trahan, and J. S. Wagner. 1998. “Character Recognition Using Genetically Trained Neural Networks.” Sandia Technical Report SAND98-2145 (October). Sandia National Laboratories, Albuquerque, NM.

Stantz, K. M., S. M. Cameron, G. M. Loubriel, M. W. Trahan, and J. S. Wagner. 1998. “Optical Communication System for Remote Monitoring and Adaptive Control of Distributed Ground Sensors Exhibiting Collective Intelligence.” Sandia Technical Report SAND98-2752 (November). Sandia National Laboratories, Albuquerque, NM.

Stantz, K. M., S. M. Cameron, M. W. Trahan, and J. S. Wagner. 1998. “Adaptive Remote-Sensing Techniques Implementing Swarms of Intelligent Mobile Agents Guided by Physics–Based Models.” Technical Advance SD-6225 (21 July).

Trahan, M. W., J. S. Wagner, K. M. Stantz, P. C. Gray, and R. D. Robinett, III. 1998. “Swarms of UAVs and Fighter Aircraft.” Paper presented to ICNPAA, The International Conference on Nonlinear Problems in Aviation and Aerospace, Daytona Beach, FL, 29 April.

Wagner, J. S., and M. W. Trahan. 1998. “A Method of Designing, Controlling, and Simulating the Collective Behavior of Autonomous, Heterogeneous Actors, Robots, UAVs and Mobile Vehicles.” Technical Advance SD-6230/S-91404 (5 August).

3534.020

Low-Cost Cadmium Zinc Telluride Radiation Detectors Based on Electron-Transport-Only Designs

J. C. Lund, N. R. Hilton, B. A. Brunett, E. Y. Lee

The goal of this project is to utilize a novel device design to build a compact, high-resolution, room-temperature–operated semiconductor gamma-ray sensor. Sandia constructed this improved sensor from a cadmium zinc telluride (CZT) crystal. It was able to both detect radiation and determine the particular isotopes responsible for the emitted radiation. CZT detectors produced today have excellent electron charge carrier collection, but suffer from poor hole collection. For conventional gamma-ray spectrometers, both the electrons and holes must be collected with high efficiency to preserve energy resolution. The requirement to collect the hole carriers, which have relatively low lifetimes, limits the efficiency and performance of existing experimental devices. By implementing novel device designs such that the devices rely only on the electron signal for energy information, we substantially increased the sensitivity of the sensors for detecting radiation. The availability of new CZT sensors with enhanced sensitivity would find immediate application in the safeguarding of stored nuclear materials, detecting nuclear smuggling and weapons facilities, enhancing arms-control and treaty-verification operations, detecting landmines and unexploded ordnance (UXO), and improving environmental monitoring and remediation activities.

We designed, built, and tested several electron-only devices of two general new designs. We also developed computational methods for designing devices. These computational methods are a vast improvement over the qualitative methods used to design our first device and allowed us to design optimized device structures. The computational methods include a full 3-D finite-element code and a simpler 2-D code for rapid execution and quick idea trials. We developed experimental methods to characterize the behavior of the devices and the crystalline semiconductor material from which the devices were built. These experimental methods included techniques to map the electrical and transport properties of the crystal used to construct the device. We also developed a method of reading out these new devices that provides both position resolution and pulse-height energy resolution. We also developed a novel method for rejecting unwanted signals arising in the detector, which was simple to implement yet extremely effective.

Publications

Refereed

Yoon, H., J. M. Van Scyoc, M. S. Goorsky, H. Hermon, M. Schieber, J. C. Lund, and R. B. James. 1997. "Investigation of the Effects of Polishing and Etching on the Quality of Cadmium Zinc Telluride Crystals and Detectors Using Spatial Mapping Techniques." *J. Electron. Mater.* **26** (December): 529–533.

3535.150

Novel Materials for Hydrogen Storage

B. P. Somerday, S. E. Guthrie, R. A. Causey

A professor at Chuo University demonstrated that exposure of nickel (Ni) to extremely high-pressure (5 GPa, diamond anvil) hydrogen (H) and high temperature (800°C) produces a material with up to 20% isolated vacancies. Such atomically porous materials have potential applications as H-storage devices. Sandia is investigating the feasibility of producing an atomically porous structure in a low-density material such as aluminum (Al). In addition, we will identify the salient factors that affect the stability of atomically porous materials by examining a well-characterized system, i.e., Ni. This work relies on numerical simulations to assess the stability of the atomically porous Al and Ni structures.

We conducted numerical simulations of Al and Ni lattices containing high concentrations of vacancies (0.05 to 0.20 vacancies/lattice site) using the Embedded Atom Method (EAM). The salient conclusions are as follows:

• High-vacancy concentrations cause the Al lattice to disorder at 300°K. Al is not a viable candidate for development as an atomically porous H-storage material.

• Vacancy concentration and H content are important variables in determining the lattice stability of Ni at 300°K.

– Ni retains the face-centered cubic structure for vacancy concentrations up to 0.15/lattice site, but lattices with 0.15 vacancies are more stable than lattices with 0.10 or 0.20 vacancies.

– Ni lattices with 0.15 vacancies are more stable with random vacancies compared to ordered vacancies. This finding is contrary to experimental results that suggest the stable structure in Ni is an ordered array of vacancies.

– Ni lattices with 0.15 vacancies exhibit rotations. This unexpected result may provide insight into the behavior of other systems that contain elevated vacancy concentrations, i.e., heavily cold-worked structures.

• Lattice structures of Ni and Al containing vacancies and H are less stable compared to structures with vacancies only at 300°K.

Publications

Other

Somerday, B. P., and M. I. Baskes. 1998. "Numerical Modeling of the Stability of Face-Centered Cubic Metals with High-Vacancy Concentrations." Presentation to Hiroshima University (Invited), Hiroshima, Japan, September. Sandia Technical Report SAND98-8624A.

3535.170

Inversion of Passive Electromagnetic Fields to Locate Weapons of Mass Destruction

G. A. Newman, D. M. Day

Weapons of mass destruction (WMD) pose grave threats to the security of the U.S. and the rest of the free world. Identifying and locating these facilities are therefore of critical importance. Because many facilities are buried at depths greater than several tens of meters, remote-sensing methods may be necessary for their detection. Here Sandia will focus on very low frequency (VLF) electromagnetic (EM) fields (< 10k Hz) to detect, locate, and characterize WMD facilities. The use of VLF fields is required since the Earth is a high-loss medium, and higher-frequency fields such as synthetic aperture radar (SAR) cannot effectively penetrate to the required depths. While passive seismic monitoring methods are currently under investigation for the WMD problem, the use of VLF fields is also now receiving attention.

Two types of VLF passive measurements are most promising for detecting WMD facilities. The first, addressed by this project, uses natural VLF emissions or magnetotelluric (MT) fields that arise from interaction of the solar wind with the Earth's ionosphere. The second employs emissions from the powerlines directly feeding the facility.

A major obstacle in employing passive VLF fields to image WMD facilities has been the inability to interpret the data. The observed VLF field depends on both the facility and the local geology. To accurately locate and characterize the facility, we must also characterize the geology. Unfortunately the facility response is coupled to the geology in a nonlinear fashion, and the geology, including the topography, of WMD sites is often complex and rugged. Another problem is that the (minimal) amount of data sufficient to reliably characterize and locate buried WMD facilities is unknown. Data sets with high spatial sampling are desirable, but are not practical to collect.

We carried out a resolution study to examine the applicability of using passive MT fields to locate and characterize facilities housing WMD. The key questions this study attempted to answer were (1) the ability to locate buried facilities in the presence of topography and local variations in near-surface geology, and (2) the minimum amount of data and quality necessary to characterize WMD facilities. Using nonlinear 3-D optimization techniques, we found that a single MT sounding, if properly located, can recover critical information on facility location, including its depth of burial. To provide enhanced resolution, however, requires much greater field sampling, which may not be practical. The findings also demonstrated that if sounding stations could be set up on the perimeter of a facility such that the sounding stations surround the facility, it is also possible to infer critical information on facility location and its depth of burial. Results from this investigation show that the use of passive MT fields to locate and characterize WMD facilities has significant potential.

Publications

Refereed

Newman, G. A., and D. L. Alumbaugh. 1998. "Three-Dimensional Magnetotelluric Inversion Using Nonlinear Conjugate Gradients." *Proc. Copper Mountain Conf. on Iterative Meth. II* (Copper Mountain, CO, 30 March–4 April): 1.

Other

Newman, G. A., and D. L. Alumbaugh. 1998. "Three-Dimensional Magnetotelluric Inversion Using Nonlinear Conjugate Gradients." *Geophys. J. Internat.*, submitted.

3535.180

Z-Pinch–Driven Isentropic Compression

S. A. Slutz, J. R. Asay, R. B. Spielman

The attainment of controlled fusion has to be one of the grand challenges of this century. The economic and environmental impact of commercial fusion would be enormous. In the near term, inertial fusion would be invaluable to the study of weapons physics and effects in the absence of nuclear testing. The achievement of inertial confinement fusion (ICF) requires the compression of hydrogen isotopes (deuterium-tritium [DT]) to high density and temperatures. High densities can be achieved most efficiently by isentropic compression, which requires relatively slow pressure pulses (~ 10^{-8} s). In contrast, high temperatures can be reached most efficiently with short, high-power pulses (~ 10^{-11} s). Z-pinches and lasers currently are being developed as alternative routes to inertial fusion. The purpose of this project is to determine if fusion could be reached more efficiently by using a z-pinch to compress the fuel, and a laser to heat and ignite this compressed fuel. This approach would use the strengths of these two technologies and could dramatically reduce the cost of a high-gain inertial fusion facility, which is important for stockpile stewardship. Furthermore, isentropic compression could provide valuable equation-of-state (EOS) information at high pressures and densities. This information is important for weapons physics, astrophysics, and planetary interiors, and may provide a means of generating new material states. We show that the laser energy needed to ignite a propagating burn is proportional to the reciprocal of the DT density squared and that trapping alpha particles with a magnetic field does not change this result. We performed numerical simulations that indicate a quasi-spherical z-pinch implosion using magnetic flux compression can efficiently compress DT to high densities. Furthermore, we performed experiments showing that high currents can be delivered to loads the small size of ICF targets.

The minimum hot-spot energy required for ignition is determined by the requirement that a significant fraction of the alpha particles be absorbed within the hot spot. Thus the radius of the hot spot, $R_h < R_a/r$, where the range of an alpha particle, $R_a \sim 0.4$ gm/cm^2. The hot-spot mass is $M_h=(4/3)\pi r r^3$. The temperature of the hot spot must be raised above the ideal ignition temperature. Assuming 3 kT/2 of energy/particle at 10 keV, the minimum hot-spot energy is $E_h=320/r^2$ MJ. This yields approximately 3 kJ at a density 1200 times the solid density of frozen DT. Numerical simulations indicate that hot electrons can be generated at about 40% efficiency by a high-intensity laser, $Il^2 = 10^{20}$ W cm^{-2} mm^2. Thus at this density approximately 7.5 kJ of laser energy would be required. This laser energy must be delivered in less time than the hot-spot disassembly time, $t_D \sim R_a/c_s r$, which is about 10 ps at r = 300 gm/cm^2.

The natural geometry of *z*-pinch implosions is cylindrical. The convergence ratio $h = r_0/r$ is limited by the Rayleigh-Taylor instability. Values of 10–20 are generally believed to be possible, even assuming h = 20, $E_h \sim 40$ kJ, which would require approximately 100 kJ of laser energy. This is a rather large laser. We considered the application of a strong magnetic field to inhibit the transport of the alpha particles and thus lower the hot-spot energy requirement. Numerical simulations show that although the gain within the hot spot is improved by the presence of the magnetic field, the propagation of the burn into the surrounding cold fuel is inhibited. We conclude that high densities are needed to keep the laser energy at an affordable level.

High densities with acceptable convergence ratios can be achieved only with quasi-spherical *z*-pinch implosions. Numerical simulations show that the current profile typical of a pulsed-power accelerator does not produce an isentropic compression because the current rises too quickly early in the pulse and not fast enough late in the pulse. This generates shock waves that increase the entropy of the fuel, and relatively low densities are obtained. Analytic modeling and numerical simulations show that an appropriate current profile can be generated by a *z*-pinch compressing a previously generated magnetic field. This is termed *flux compression* and works in a manner analogous to explosive generators. Ideal 1-D simulations of this approach yield compressed fuel densities of 300 gm/cm^2, with an accelerator drive current of only 20 MA, which can be delivered by the Z-accelerator. Of course, 2-D effects will degrade this performance, but the approach looks promising.

Current must be delivered to a very small load (1–2 mm) as compared to typical *z*-pinch loads, with an initial radius ~ 1 cm. To address the power-flow issue, we carried out experiments driving small cylindrical targets. Current was efficiently delivered to a 3 mm-radius tube. We diagnosed the pressure generated by the magnetic field near the tube using VISAR (velocity interferometer system for any reflector). For the first time, we observed high-pressure phase transition data in iron. These data indicate that valuable EOS information should be attainable with this technique. Further shots to measure isentropic compression are in the shot schedule.

Publications

Refereed

Slutz, S. A., R. Spielman, and J. Asay. 1999. "Z-Pinch–Driven Isentropic Compression for Inertial Fusion." *Proc. 8th Internat. Conf. on Megagauss Magnetic Field Generation and Related Topics* (Tallahassee, FL, 18–23 October).

3535.190

Covert, Distributed Biosensors for UXO/CW Based on Amplified Immunoassays Conducted in Porous Inorganic Media

C. J. Brinker, C. S. Ashley, A. K. Singh, J. S. Schoeniger, R. J. Simonson

Sandia's goal in this project is to demonstrate a revolutionary bio-inorganic sensor for UXO/CW (unexploded ordnance/chemical warfare) with the potential to combine sample preconcentration, molecular recognition, amplification, and optical transduction in a porous, inorganic media (SiO_2 aerogel or xerogel) with no requirement for external power. This approach exploits the unparalleled selectivity and sensitivity of antibody/antigen molecular recognition and amplified luminescent immunoassays (ALI) with the advantage of deployment by practical, dispersible means. We prepared samples in granular form for analysis by immunoassay of their local vapor or liquid environment. We incorporated commercially available antibodies along with corresponding antigen-enzyme complexes and dye precursors into a silica gel host using biocompatible aqueous processing. We examined enzyme activity and enzyme-catalyzed dye production over the range of relative humidities encountered in real-world environments. We identified commercial assays for the specific detection of small analytes that may be similar in size and solubility to common UXO agents and determined assay detection limits.

This project focused on three major areas: (1) development of a sol-gel host matrix compatible (i.e., with regard to structure and chemistry) with biomolecules of interest, (2) stability of host-enzyme-dye systems, and (3) identification, synthesis, and incorporation of TNT-specific enzyme systems and assay methods.

Specific accomplishments include the following:

(1) We established synthesis methods of an inorganic silica matrix for encapsulation of enzymes. These aqueous sol-gel processing methods completely eliminate the use of alcohol (deleterious to most biomolecules) as well as the formation of alcohol as a reaction by-product. We demonstrated enzyme-catalyzed dye production, which signals the formation of the enzyme-substrate complex, and response amplification of the dye signal. Enzyme-doped aerogels, prepared using the aqueous sol-gel process, showed bioactivity following processing. Retention of activity is critical in biosensor applications where the sensor is exposed to a range of temperature and humidity conditions.

(2) We dried silica gels (aerogels and xerogels) containing encapsulated enzymes and dye precursor molecules at humidities ranging from 1%–50%. The enzymes retained complete activity over a three-week period.

(3) To test the concept of vapor-phase sensing with these sol-gel sensors, we incorporated alcohol dehydrogenase into the silica matrix. This enzyme, which catalyzes reaction with alcohol, showed bioactivity when encapsulated within the inorganic sol-gel matrix and exposed to alcohol vapor. To extend this work to UXO applications, we identified commercial assays for the specific detection of small analytes that may be comparable in size and solubility to common UXO agents. EMIT assays are specifically designed for detection of analytes with molecular weights < 2000 daltons. EMIT assays have extensive applications in drug screening (e.g., digoxin, theophylline) and are robust to the presence of complex sample matrices such as blood, plasma, or urine. We used digoxin as a model analyte and modified the commercial assay to work in solution in a format directly applicable to our sensor format. The detection limit demonstrated in this test was 0.2 ng/ml, which correlates well with 0.1–0.5 ng/ml reported in the literature for systems using automated analyzers. We also identified a commercial source for specific antibodies against TNT and various TNT-enzyme conjugates. We synthesized a TNT-glucose PDH (phosphate dehydrogenase) conjugate (the enzyme of choice for most commercial EMIT assays) for potential use in a modified EMIT assay for TNT.

Publications

Refereed

Bhatia, R. B. (UNM), C. J. Brinker, C. S. Ashley, and T. M. Harris (U. Tulsa). 1998. "Synthesis of Sol-Gel Matrices for Encapsulation of Enzymes Using an Aqueous Route." *Organic/Inorganic Hybrid Materials, Proc. MRS* (San Francisco, CA, 13–17 April).

3535.210

Semiconductor Filament Lasers

F. J. Zutavern, S. M. Cameron, G. L. Benavides, A. G. Baca

Miniature, short-pulse lasers are being developed for use in at least three general applications that are very important to Sandia: (1) active optical sensors for Defense Programs (DP) and DoD weapons systems in limited-visibility environments (optical fuzing, LADAR [laser radar], 3-D imaging, and secure communications), (2) direct optical ignition (DOI) of fuels and explosives for military and commercial applications, and (3) micromachining micron-size features patterned over large areas of metals and alloys. At present, the highest-energy short-pulse semiconductor lasers deliver only 100 nJ in 100 ps and 130 mrad.

Sandia will make a new type of high-beam-quality semiconductor laser that can potentially produce over 1000 times more peak-power or short-pulse energy than the conventional semiconductor laser. We would create these new lasers from the current filaments that are formed in high-gain photoconductive semiconductor switches (PCSS). Low-field, avalanche-carrier generation is the mechanism by which lightning bolt-like channels of high-density, charge-neutral plasma are formed across the semi-insulating gap of the switch. We plan to make a completely revolutionary semiconductor laser from the electron-hole plasma inside these filaments.

We tested this new concept by building some devices that allowed us to produce a filament in a reflecting cavity and observe optical emission from the ends of the current filaments. We measured the optical and electrical properties of these devices and obtained very convincing evidence of lasing. We see low divergence (2.5 degrees), high energy (30–100 nJ), spectral (0.5 nm), and temporal (0.5 ns) narrowing, which are characteristic of lasing. However, the conclusive test is to resolve the laser mode structure. Because these lasers are larger than conventional semiconductor lasers, their modes are much closer together, and we were not able to resolve them with our present spectrometer.

We have started to test this new concept with some small devices that allowed us to produce a current filament in a reflecting cavity and observe optical emission from the ends of the filament. When we fabricated our first devices, we encountered stability problems with filament formation and contact degradation. We significantly improved stability by reducing the optical trigger image width from approximately 200 to 30 microns. We significantly improved contacts to high-gain PCSS with a deep diffusion process.

From the end of a 20–40 A current filament, we observed a round spot of light being emitted from the edge of the switch with relatively low divergence (2.5 degrees). The spot is 50–75 microns in diameter and approximately 50 times brighter than the emission that we observed from the surface of the switch. We measured 75 nJ emitted from one end of the filament in a subnanosecond pulse. This is more energy than has been obtained from the highest-energy, short-pulse conventional semiconductor lasers (CSL). (Wide-stripe, edge-emitting lasers can produce 10–50 nJ in subnanosecond pulses.) The semiconductor filament laser appears to be *Q* or gain switching because its pulsewidth is less than 500 ps, while the current pulse that forms the filament is 18 ns wide. We claim only strong evidence because the accepted criterion to demonstrate lasing is the resolution of cavity mode structure in the optical spectrum. Our spectrum shows an instrument-limited linewidth of 0.5 nm or 0.7 meV. The mode spacing for this 1 mm-long cavity is 0.1 nm, which is presently beyond the capability of our spectrometer. However, the spontaneous surface-emission spectrum is 50 nm wide due to the high temperature of the carriers in the filaments. The most likely explanation for this narrowing is lasing.

3537.010

Development of Membrane Devices Using AlN and SiC Films

W. K. Schubert

The objective of this project is to develop membrane devices for sensor applications. Researchers at Sandia showed that thin, freestanding membranes can be fabricated on silicon (Si) substrates. Using an appropriate transduction scheme, the membrane can be excited into a resonant mode. Since the membrane's resonant frequency is extremely sensitive to membrane tension and areal mass density, it can be configured as a sensor for pressure, strain, acceleration, or chemical species (using a sorptive film).

Researchers at Howard University (HU) developed deposition processes for crystalline aluminum nitride (AlN) and silicon carbide (SiC) films. When the AlN layer is oriented with c*-axis normal to the surface, it is piezoelectric and can be used, along with an interdigitated electrode pattern, to form a transducer on the resonant membrane structure. SiC is an extremely tough layer that can be used as a support for the AlN layer to form thin, freestanding membranes. SiC films can also serve as an etch-mask layer for the silicon micromachining required to fabricate the sensors. Alternatively, using a new magnetic excitation scheme that obviates the need for a piezoelectric layer, the nonpiezoelectric SiC layer could be used alone to form the membrane device. This excitation scheme relies on Lorentz forces generated by the current lines on the membrane in combination with an externally applied magnetic field.*

Researchers at HU, in collaboration with Sandia, developed a photolithographic mask set to implement the process of depositing SiC thin films ranging from 0.6 to 1.2 microns in thickness on 50 mm-diameter silicon (Si) wafers. Sandia wants to develop a process flow for fabricating flexural plate-wave (FPW) devices. This process involves bulk micromachining of the Si wafer using an anisotropic

etch solution (potassium hydroxide [KOH]) to release the precisely sized SiC membrane from the underlying Si. The area exposed to the KOH solution is defined with a photopatterned chrome/gold-masking layer on the backside of the wafer. We will define metal transducers used to impose a standing FPW on the front side of the released membranes. Process optimization of the membrane definition and release steps has begun.

In addition to the process development, we received two SiC-coated wafers for fabrication of FPW devices using existing photomasks. The Sandia process will define the metal transducers on the front side first, then use a photoresist mask and dry-etch process to release the membranes. We are currently testing minor adjustments to the membrane release process required to accommodate the SiC film. (Sandia's FPW devices normally use silicon nitride [SiN] films.)

The objective of this project was to test the suitability of SiC and AlN thin films for use in FPW devices. We have not yet met this objective, although we have made progress. Earlier work on these materials deposited the films in small research reactors on substrates that were too small for meaningful process development (about 1 cm). We succeeded in transferring the SiC process to larger-scale reactors and producing films with reasonable thickness uniformity on 50 mm-diameter wafers. We have begun the work required to test the suitability of the SiC films for FPW devices. Critical questions that must be answered to determine suitability include whether or not the films are compatible with the bulk micromachining methods used to release the membranes, and whether intrinsic stress levels in the films are compatible with membrane devices. If the films are under compressive stress, they will buckle when released, and the FPW device will not function. If stress levels are tensile but too high, the films fracture when the underlying Si is removed. The quality factor of FPW devices (resonant frequency/bandwidth) is highest when the membrane stress is below 100 megapascals.

These questions will be answered for the SiC films when the first membranes are released.

3537.020

Spectral Information Content in Ion-Mobility Spectra for Explosives, Interferants, and Other Negative-Ionizing Chemicals

J. E. Parmeter

Ion-mobility spectrometry (IMS) is one of the most powerful techniques currently available for the trace chemical detection of several important classes of compounds, including explosives and drugs. In IMS, analyte molecules are first ionized, then identified based on their time of flight (TOF) through an electric field. Attractive features of IMS include parts-per-trillion sensitivity, good selectivity, and near instantaneous response time. However, theoretical understanding of IMS lags behind practice, and there is currently no known way to abstract from an unknown IMS spectrum information about the type of molecule represented. However, some recent work at New Mexico State University (NMSU) indicates that it may be possible to abstract information on the chemical moieties present in an IMS spectrum by using artificial intelligence (AI) tools such as neural networks. In collaboration with NMSU, Sandia will focus on negative-ion IMS spectra (the mode of operation relevant to explosives detection), and investigate the ability of trained neural networks to classify spectra of chemicals that the networks have not been exposed to during training.

(1) To initiate the project, we constructed an experimental apparatus consisting of an IMS interfaced to a gas chromatograph (GC). The use of the GC allowed IMS spectra of test compounds to be obtained without concerns about interference from impurities, since the GC afforded a means of prefractioning the sample and delivering clean standards to the IMS. In the experiments carried out in this study, we ran the IMS at 160°C using carbon-tetrachloride reagent gas.

(2) We developed a reference library of negative polarity IMS spectra by obtaining spectra for 13 chosen compounds: o-nitrophenol, p-nitrophenol, 2,4-dinitrophenol, 2-nitrotoluene, 4-nitrotoluene, 2,4-dinitrotoluene, 2,6-dinitrotoluene, 3,4-dinitrotoluene, 1-chloro-2-nitrobenzene, 1-chloro-3-nitrobenzene, 1-chloro-4-nitrobenzene, pentachloronitrobenzene, and 2,4,6-trinitrotoluene. In most cases, we obtained 8–15 IMS spectra at different concentrations for each compound. The resulting library contains a total of 163 original IMS spectra for study using neural networks. The spectra followed reasonable interpretations of structure and stability for the ions created for each chemical.

(3) We used over 150 spectra from 13 chemicals (drawn from the GC/IMS library created here) to train a neural network, using a 400 MHz Pentium–based computer and NeuralWare II software.

(4) We subsequently challenged the neural net with additional spectra from the library, which had not previously been seen by the neural net, and attempted chemical identification. We found that the neural network was able to successfully identify these spectra as to compound. Thus, the system was able to use AI to identify IMS spectra of a given compound at one concentration, when the network had already been trained with a spectrum of the same compound at a different concentration.

(5) In another set of studies, we trained the network according to chemical class (nitrotoluenes, nitrophenols, and chloronitrobenzenes). The purpose of this training is to conduct experiments to see whether the neural network can classify compounds whose spectra it has never seen (at any concentration) according to chemical class. Preliminary results suggest that this is possible.

3537.040

Picosecond Particle Velocity Measurements

K. G. Holland

Sandia plans to develop an experimental capability to obtain subnanosecond particle velocity measurements in single-event shock-wave experiments. Such a capability will permit examination of fast transient phenomena at the continuum level in collaboration with the picosecond optical spectroscopy work being carried out at Washington State University (WSU).

Currently, we use both EMV (electromagnetic velocity) gauges (~ 10 ns risetime and restricted to nonmetallic solids) and laser interferometry (VISAR [velocity interferometer system for any reflector]) developed at Sandia to obtain particle velocity histories in shocked samples. The time resolution of electronic recording VISAR measurements is currently limited to 1–2 ns.

The development of a subnanosecond-velocity recording capability will enable strong interactions with comparable efforts currently under way in Sandia's shock physics programs.

The configuration used to acquire signals on the streak camera from the existing VISAR system consisted of the following components. We placed a beam splitter near each of the three photomultiplier tubes (PMTs) such that a portion of the light incident on the PMT photocathodes was diverted to a lens-coupled optical fiber (100/140-micron core/clad diameter, 0.29 numerical aperture [NA] gradient index fiber). The fibers from the two VISAR signal legs were equal length (230 cm), and the fiber carrying the beam intensity monitor (BIM) signal was 305 cm long, to compensate for the propagation time delay in the signal legs relative to the BIM sample location. We cemented the three fibers into a brass block in a linear array and polished the signal leg fibers on either side of the centered BIM. The assembly was mounted on the streak camera frame and the fibers imaged onto the streak camera photocathode with a Nikon 50 mm, f/1.4 lens at 1:1 magnification. This configuration allowed for simultaneous recording of VISAR data via the streak camera and the PMTs.

The charge-coupled device (CCD) ordered for use in this system did not arrive in time to be used for the feasibility demonstration; instead, we mated an existing CCD and image intensifier to the IMACON 790 streak camera for the test shot. The CCD array consisted of 24-micron square pixels on a 1024 x 1024 array. The image of each input fiber had a five-pixel full-width half-medium (FWHM) in the two orthogonal directions. At the setting selected for the first test shot, the overall streak rate on the CCD was 1.12 ns per pixel over an 800 ns recording window.

We used a simple impactor/target configuration in the feasibility demonstration shot. The lapped front surface of an aluminum (Al) projectile impacted a nominal 3 mm-thick Al disk, which was backed by a polymethylmethacrylate (PMMA) window. The PMMA window had a highly specular mirror surface at the PMMA/Al interface. The shot was fired in the ISP 2.5-inch light-gas gun. The expected velocity profile of the monitored surface consisted of the arrival of an elastic precursor followed by a plastic wave approximately 80 ns later, with a final particle velocity of 0.32 mm/msec within the recording interval. The streak/CCD records were fit by eye to a quadrature ellipse. We referred to the PMT records for guidance in the fit analysis, but did not use them to correct the velocity profile obtained from the streak data. The resulting velocity histories obtained via the two recording techniques showed excellent agreement in event timing and velocity magnitude. The largest deviations occurred after the final velocity was nearly reached, with maximum deviations of approximately 3%. The mean values for the final velocity plateau from the two measurements agreed to 1.3%.

We did not realize the highest possible time resolution in this first feasibility demonstration, but the test was nevertheless successful. Further work will consist of adapting the new CCD, improving the camera streak rate through the purchase of a faster plug-in streak unit, reducing the diameter of the coupling fibers, and optimizing the light-coupling scheme for light-collecting efficiency.

3537.050

Particle-Level Modeling of Flows of Concentrated Suspensions

A. J. Hurd

It is well established that the flow of concentrated suspensions of particles cannot be modeled in a satisfactory manner using currently available macroscopic constitutive equations because particles in the suspension may form structures that are flow-dependent. In addition, particle migration/segregation may occur under certain conditions. Modeling the interactions between large numbers of particles in a flowing suspension is essential to understand the above phenomena and to be able to construct accurate macroscopic constitutive equations. The boundary element method (BEM) is ideal for solving this class of problem. However, until recently, large dynamic particle-level simulations were not practical due to the $O(N_2)$ to $O(N_3)$ scaling of the necessary computational resources. The application of fat multipole methods (FMM) to the BEM results in O(N) scaling. In collaboration with researchers at the University of New Mexico, Sandia will use FMM combined with the scalability of BEM for parallel processing to enable large-scale, particle-level simulations to be performed.

We used the BEM to model the flow of highly loaded particle suspensions. This approach allows the simulation of particles of any shape in arbitrary flow geometries. Currently, the simulations are in two dimensions; however, a 3-D code is under construction.

The use of the BEM for this purpose has so far been limited to

relatively small numbers of particles due to the high computational cost of this technique, which scales as N_2, where N is the number of collocation points used in the boundary discretization. In this work, we used a multipole acceleration technique to reduce the computational cost from $O(N_2)$ to O(N log N). This allows the simulation of much larger systems.

The ability to simulate large numbers of particles is essential in understanding the macroscopic behavior of suspensions. Being able to simulate large systems eliminates the need for repeat cell simulations, where effects such as structure formation may be artificially induced.

The solution of boundary integral equations using the BEM involves the calculation of integrals, which become nearly singular when the collocation point is very close to the surface where the integration is taking place. This situation is inevitably encountered in the simulation of highly concentrated systems. A large part of the current work was the development of coordinate transformations that provide accurate integrations by reducing the singularity with appropriate jacobians. The efficacy of this technique is demonstrated by the quality of solutions produced by the simulations. The error in the calculation of the velocity for each particle is less than one percent with a 12-node particle discretization.

A practical application of immediate concern is the simulation of the extrusion of highly loaded suspensions of fine ceramic particles. This type of operation is used to produce complex-shaped ceramic components without the use of a mold. Because of the size of the particles, Brownian forces and colloidal forces act on each particle in the suspension in addition to the hydrodynamic interactions. We added the capacity to model such forces, as well as body forces such as gravity, to the BEM code.

We performed initial simulations using a wide-gap Couette geometry. Experimental data are available for this type of geometry, and the BEM code correctly predicted experimentally observed phenomena such as irreversible particle migration. We also correctly predicted sedimentation patterns. The shape of the sedimented particle bed predicted by the BEM code is very similar to the experimentally determined shape.

Currently, we are implementing geometries of more practical interest for the abovementioned application. In particular, the flow of a highly loaded suspension through a contraction is of immediate interest. In addition, the 3-D version of the BEM code is under development. While 2-D simulations have been shown to provide accurate qualitative predictions, quantitative predictions will require fully 3-D geometries.

Publications

Other

Mammoli, A. I. 1998. "Particle-Level Modeling of Flows of Concentrated Suspensions." Web site *www.unm.edu*, September.

3537.060

Efficient Processing of Materials Microstructures with Intelligent Feature Extraction for Quantitative Stereology

E. A. Holm

In collaboration with Lehigh University, Sandia will develop methodologies for the analysis of electron micrographs that will substantially enhance the acquisition of terascale microstructural information (e.g., distributions of grain size and shape) in a variety of systems. This project seeks to dramatically improve on the current situation by creating new deterministic and stochastic algorithms of sufficient generality that mitigate the contrast ambiguities peculiar to a number of microscopies. Such algorithms will necessarily complement many existing image-processing techniques and will be employed in conjunction with them to develop robust, systematic, automated tools. This research addresses the issue of image data reduction in the use of the Accelerated Strategic Computing Initiative's (ASCI's) microstructural evolution models.

The primary difficulty in analyzing and interpreting transmission electron micrographs (TEM) is that contrast variations in these images are often complex, owing to multiple contrast sources, which results in a large amount of spurious information. This project focuses on developing computational algorithms that minimize and eliminate erroneously identified microstructural features. Our strategy for attacking this problem includes both standard image-processing techniques and our own image filters, combined in optimal and novel ways. We utilize standard noise reduction, edge, and thresholding filters with newly developed automated thresholding, segment, tangle, and cluster filters. We developed the new filters with the geometry and topology of grain structures in mind. The microstructural investigation of some metallic systems presents additional challenges due to high proportions of low-angle twin boundaries, which should not be considered in a grain-size or topology analysis. We began work in developing new filters that use the geometric and topological characteristics of twins to eliminate twin boundaries during automated image analysis.

Publications

Refereed

Carpenter, D. T., J. M. Rickman, and K. Barmak. 1998. "A Methodology for Automated Quantitative Microstructural Analysis of Transmission Electron Micrographs." *J. Appl. Phys.*, accepted.

3537.030

Magnetic Field Profile Measurements in Wire-Array Z-Pinches by Faraday Rotation

R. B. Spielman

This research was directed toward the implementation of laser–based diagnostics for wire-array z-pinches. Sandia was able to carry out all the necessary preparations to set up the laser diagnostics to complement our x-ray backlighting measurements of the early phase of exploding-wire z-pinch plasma formation.

These new diagnostics will augment the capabilities of our present x-ray backlighting diagnostic to allow simultaneous laser illumination and x-ray backlighting of wire plasmas. Initially, schlieren imaging and interferometry with the laser will allow measurement of lower plasma densities than the x-ray backlighter. Eventually we hope to implement polarimetry (Faraday rotation) to determine the magnetic-field profile and therefore the current density profile flowing in the wire plasmas.

Diagnostic development. We determined the laser parameters needed for these laser–based techniques in combination. Although the nominal minimum laser pulsewidth is 4 ns, we were able to arrange with the manufacturer for an operating procedure that permits a 2 ns pulse in frequency-tripled light to be included within the warranted operating conditions because of our low intended pulse repetition rate (1 pps).

The Nd-YAG laser is set up to operate in either the fundamental, first, or second harmonic modes, and we can also use any of them in combination. After we established satisfactory laser operation in the first harmonic, we made measurements of laser-trigger throughput delay to determine possible approaches for the design of a system to trigger the laser with minimum possible time jitter with respect to the wire-array current pulse and the x-ray backlighter. This design was not straightforward because this laser, which was the only one available within our budget constraint having the required optical parameter for our applications, is supplied only in a configuration that is intended to be used in a free-run, repetitive-pulse mode of operation. However, we must synchronize a single laser pulse with the x-ray backlighter pulsed-power system. We chose a design for the trigger system that selects a pulse from the free-running repetitive firing of the laser flashlamp to trigger the wire-array current pulse and the x-ray backlighter driver when both are fully charged. The trigger for the laser Q-switch (Pockels cell) is then generated from a current monitor located after the main output switch of the x-ray backlighter driver, which minimizes jitter between the backlighter and the laser. We determined that the Pockels cell-trigger throughput delay is just short enough to allow this ideal low-jitter mode of operation. This system is presently under construction.

We were able to carry out all the necessary preparations to set up the laser diagnostics to complement our x-ray backlighting measurements of the early phase of exploding-wire, *z*-pinch plasma formation. We are now taking the initial steps to integrate the laser into the existing experimental system.

Publications

Other

Greenley, J. B. 1998. “Faraday Rotation Measurements on Z-Pinches Final Report.” Sandia Technical Report SAND98-2372 (November). Sandia National Laboratories, Albuquerque, NM.

3537.070

Nondestructive Evaluation of Wind Turbine Blades

T. W. Simmermacher

The failure of a wind turbine blade in the field is usually accompanied by damage to other wind turbine components and sometimes to other wind turbines. The event means loss of revenue, loss of equipment, usually negative public relations, and, at the very least, a hit on the credibility of the wind turbine manufacturer. It would be advantageous to avoid these outcomes altogether. There will be an increasing need, as a fleet of wind turbines ages, to be able to assess the health of the structures, particularly wind turbine blades.

Sandia is conducting an ongoing study in the nondestructive evaluation of wind turbine blades. Efforts concentrated on in-service evaluations that create minimal interference with operations in the field. Inherent in these studies is the need for algorithms that will quickly evaluate a set of data to determine the structural state of a blade.

Modal–based evaluation techniques and algorithms developed at North Carolina A&T State University provide a type of nondestructive evaluation that is particularly well suited for structurally simple systems such as wind turbines. These methods utilize data that are typically gathered in the course of a modal test. These data include frequency response functions (FRFs), mode shapes, damping, and natural frequencies. Changes in these data, as compared to a set of assumed undamaged set of data, can indicate the presence of damage and possibly the location of the damage. We can use this information to signal a problem with a particular blade that would indicate the need for maintenance.

These techniques offer the potential for application to weapon systems and other more complicated structures. Changes in modal parameters could indicate critical variations in tolerances of such parameters as bolt tension, metal fatigue of supporting brackets, and debonds in the aeroshell of a reentry vehicle, for example.

We used a scanning laser vibrometer and piezoceramic actuators to detect damage on a section of a wind turbine blade. The laser is a noncontact sensor that can measure vibration at a large number of points on a structure over a wide frequency range. We used piezoceramic patches to generate the vibration without mass loading the structure. We used three different methods for detecting damage, based on changes in transmittance functions, FRFs, and operational deflection shapes. We detected damage simulated by a steel plate clamped to the blade by the three techniques.

This experiment indicated the feasibility of using piezoceramic patches for excitation and a scanning laser vibrometer to measure vibration to detect damage. To increase the frequency range of the test and repeatability, we could place a second large piezoceramic patch on the opposite side of the blade and use a slower sweep input. A finer measurement grid would also increase the resolution of damage.

Publications

Other

Sundaresan, M. J., M. J. Schulz, J. Hill, E. A. Wheater, and F. Ferguson. 1998. "Damage Detection on a Wind Turbine Section." *Proc. 17th Internat. Modal Anal. Conf.* **1** (Orlando, FL, 8 February 1999).

3537.080

Very Small Arrays: Designing Self-Assembled Systems of Light-Antennae and Reaction Centers for Artificial Photosynthesis

J. A. Shelnutt

The goal of this project is to develop structure-function relationships to guide computer-aided design (CAD) of improved molecular elements for very small arrays. The photosynthetic apparatus is composed of a reaction center protein, containing six porphyrin–based pigments and other molecules surrounded by hundreds of similar porphyrins that act as a light antenna. The antenna collects light energy and feeds the reaction center by energy transfer. These pigment molecules are highly organized to bring about the efficient capture and conversion of light energy in the form of chemical fuels, principally ATP (adenosine triphosphate). Researchers at Arizona State University (ASU) are developing highly organized structures that mimic the photosynthetic apparatus. These amazing structures enable singlet electron transfer much like the pigments in the biological photosynthetic reaction center. Singlet transfer is important because more of the light energy absorbed by antennae pigments is made available for conversion to chemical energy than for triplet electron transfer. In collaboration with ASU researchers, we will perform molecular simulations on porphyrin-fullerene electron-transport complexes and validate the calculations with resonance Raman measurements.

We completed initial molecular simulations of porphyrin-fullerene and porphyrin-porphyrin dyads and used experimental studies using resonance Raman to validate the calculated structures of the dyads. For the fullerene systems, covalently bound fullerene-porphyrin dyads in which the nature of the porphyrin substituents was varied were energy-optimized to determine the stable conformations of the molecules. We performed similar molecular mechanics calculations for which the porphyrin substituents were varied for porphyrin-porphyrin covalently bound dyads. These included octaethyl-, etio-, and coproporphyrins. We found multiple conformers for some of these dyads. In some cases, the conformational energies are nearly equal, indicating the possibility that they will coexist at ambient temperatures. Initial resonance Raman studies of the dyads show spectral differences that validate the structural differences for different porphyrin substituents. Thus, we demonstrated the potential for using resonance Raman spectroscopy in combination with molecular simulations methods for designing small arrays.

Publications

Refereed

Ma, J. G., J. Zhang, R. Franco, S. L. Jia, I. Moura, J. G. Moura, P. M. H. Kroneck, and J. A. Shelnutt. 1998. "The Structural Origin of Nonplanar Heme Distortions in Tetraheme Ferricytochromes c3." *Biochemistry* **37** (1 September): 12431–12442.

Other

Ma, J. G., J. Zhang, R. Franco, S. L. Jia, and J. A. Shelnutt. 1998. "Structural Origin of the Nonplanar Hemes in Cytochromes c3." *Papers of the Amer. Chem. Soc.* **215** (Dallas, TX, 29 March): 308.

3537.110

Enzyme-Mediated Electrochemical Redox Polymer Biosensor for V- and G-Type Chemical Weapons

R. P. Janek, A. W. Flounders, K. Wally

This work seeks to further understand the direct intersection of biology and microelectronics. The benefits of such an understanding can be exploited to make robust sensors for biological and chemical weapons (BW/CW). Nature has successfully solved the problem of surviving in complex environments by miniaturizing task-specific enzymes and communicating with those enzymes via electronic pathways. One example of this scheme is the operation of the human brain. The field of bioelectronics is quite large and, although research efforts can require a substantial investment in resources, the work proposed here can be executed readily to yield high-quality information about the electrified interface. Sandia plans to embed organophosphate hydrolase (OPH) in a matrix of siloxane polymers containing naphthoquinone (NQ) and benzylviologen (BV) subunits. We will immobilize the polymers on carbon electrodes exposed to a solution of organophosphate. The NQ and BV form a redox couple that is capable of transporting charge from the polymer to the carbon electrode. This charge transport mechanism is mediated by the local pH of the polymer network. If an organophosphate agent is present, the OPH will hydrolyze this compound to form protons and therefore change the conductivity of the polymer.

The OPH enzyme used in this study is available from an internal Sandia source, as are methods for testing the electrical properties of the electrode materials. We will synthesize the redox polymer in collaboration with the University of California–Davis. We will probe the electrical properties of the interface with impedance spectroscopy and cyclic voltammetry as a function of organophosphate activity to evaluate the response of this sensor to analyte concentration.

Samples of NQ- and BV-containing siloxanes were synthesized and the compounds characterized using cyclic voltammetry and impedance spectroscopy. Although NQ/BV siloxanes were previously studied, this project is their first known use as bioelectronic sensor platforms.

We performed successful laboratory experiments using NQ-siloxane deposited on glassy carbon electrode surfaces with immobilized OPH enzyme. Data supported the hypothesis tested in this study. We tested this novel sensor with the organophosphate nerve agent paraoxon (commercial pesticide), and it responded to five micromolar concentration levels (about 1 ppm). This test result was garnered with little optimization of coating chemistry and should be considered as an upper detection limit of the sensor.

We immobilized the OPH enzyme that selectively cleaves paraoxon to form protons onto the carbon electrode surface with aminopropyltrimethoxysilane and glutaraldehyde prior to NQ-siloxane treatment. We prepared the pH-sensitive NQ-siloxane film in aqueous solution and deposited it in approximately 25 minutes. We monitored the film growth electrochemically and verified the presence of OPH enzyme and NQ redox polymer in an independent experiment. We measured the impedance of the carbon electrode at 200 Hz to yield the paraoxon-dependent signal.

3537.120

Novel Biosensor Fabrication Techniques

A. W. Flounders

Most chemical sensors consist of a recognition element that provides sensor specificity and a transduction platform that translates chemical presence into a measurable signal. The term biosensor *describes a specific class of chemical sensors that utilize a biological component (usually a protein such as an antibody or enzyme) as the chemical recognition element. Biological components are paired with optical, piezoelectric, and microelectronic transduction platforms.*

To date, all biosensor fabrication has been a two-step process. Automated wafer-scale microelectronic fabrication is followed by dicing, packaging, and manual chip-scale biochemical processing. Chip-scale biochemical processing is tedious, difficult to reproduce, and expensive; it completely negates all economy-of-scale advantages of the semiconductor manufacturing process.

Sandia is developing techniques that will enable wafer-scale processing of biochemical components. Recently, we demonstrated the ability to etch immobilized protein layers with an oxygen plasma system. We will investigate the compatibility of other semiconductor processing tools with biochemical components. We will investigate the use of a photoresist priming oven for deposition of organosilane monolayers in collaboration with University of California, Berkeley (UC–Berkeley). This process would enable wafer-scale preparation of surface layers ideally suited for biochemical attachment. This surface will then be reacted with protein solutions applied from a spray-head photoresist development station. The combination of vapor-phase monolayer formation followed by spray-dispense protein attachment and oxygen-plasma etching may enable a fully integratable wafer-scale protein process flow.

Silicon (Si) substrates with thermally grown Si dioxide (SiO_2) or thermally grown SiO_2 plus low-pressure chemical vapor-deposited Si nitride (SiN) films were prepared at the UC–Berkeley Microfabrication Laboratory. These films were then characterized via ellipsometry, static contact angle, and electrolyte insulator semiconductor (EIS) impedance spectroscopy. We selected aminopropyltriethoxysilane (APTS) and glycidoxypropyltriethoxysilane as best candidates for silane surface modification and protein immobilization based on their solubility and flammability properties.

We identified an equipment vendor with demonstration equipment suitable for the silane deposition testing, and vapor-phase silane treatment is under way.

Process compatibility also made impossible the use of the photoresist dispense station for application of protein solutions. Protein solutions typically have a high sodium content that is a significant contaminant for Si processing.

Process compatibility issues not previously considered precluded the use of already committed equipment. We prepared test substrates and identified an alternate path for testing vapor-phase silane; testing is under way. We have not addressed the additional component of spray dispense of proteins.

3537.140

Enhancing Multilevel Linear Equation Solvers Using Domain Decomposition Strategies

J. R. Red-Horse

Sandia's Accelerated Strategic Computing Initiative (ASCI)-funded structural dynamics finite-element (FE) software package, SALINAS, is an accurate scalable linear equation solver suitable for a massively parallel (MP) computing platform. One approach that has proven itself as a candidate is the so-called Finite Element Tearing and Interconnecting (FETI) solver conceived and developed by researchers at the University of Colorado (UC).

The FETI method is a domain decomposition–based iterative solver that has gained wide acceptance in the structural analysis community for solving large-scale FE problems of ASCI type. It is also an important component of the SALINAS project. In collaboration with UC's FETI group, we will improve the performance of the FETI solver for the highly heterogeneous problems that are often encountered at DOE.

• *Partitioning a structure along its materials boundaries.* The module domain decomposition module, DOMDEC, of UC's parallel FE structural mechanics code, TOP/DOMDEC, has been upgraded to understand the concept of substructures (each of them corresponding to a different material zone), and to incorporate a partitioning scheme for the global structure on a substructure-by-substructure basis. We are currently validating this module.

• *Constructing an edge–based coarse problem for improving the initial residual.* We developed a general theoretical framework for a FETI method with enriched search directions. This framework improved our insight into convergence issues and guided our construction of a new set of search directions for improving the initial residual obtained for heterogeneous problems. We programmed this new development into the existing FETI code, and will validate it and benchmark it on SALINAS problems.

3537.130

Design for 100-Year-Life Prototype

T. W. Simmermacher

The great majority of design specifications are based on meeting quantitative performance objectives (e.g., structural, electrical, thermal, radiation). Exhaustive studies and tests are typically performed to ensure the stated performance. Design optimization focuses on the ability of the product to meet its prescribed function for the lowest acquisition cost. A new design approach for increasing the long-term versatility of complex structures was developed recently at MIT. Titled "Design for 100-Year Life," this novel design methodology (D100) directly addresses life-cycle issues in an engineering design. Robust optimization of cost and performance over extreme service lives are key innovations in this approach. In collaboration with MIT, Sandia will (1) identify life-cycle design trade-off criteria and (2) demonstrate the principles in the design of a prototype structure. We will also review many of the surety (reliability, safety, and security) design approaches developed at Sandia, and compare and contrast them with the D100 methodology. This looks at extremely long life cycles. This is a radical approach in that it involves consideration of new types of materials, construction techniques, embedded sensors, and novel maintenance and dismantlement techniques.

Our success in nuclear weapon stockpile stewardship requires that we utilize new technology to evaluate system performance over extended life cycles.

The three scenarios developed in this research build on the developing capabilities of Sandia's Structural Health Monitoring program and the concepts within the Architectural Surety program, envisioning the capability within a structure to monitor and respond to the dynamic forces acting upon it. The scenarios explored the potential time to application to construction, ranging from the nearer term for the component performance database to the long term for the active control system. We based the scenarios on a system–based approach to structural monitoring and active control versus the component–based approach, where the latter approach defines a majority of the current research and development activities. The complementary technologies within Sandia could provide other essential elements of the system, and their existence displays the potential opportunities for creation of a larger system relating to other subsystems and controls within the home.

3537.150

In Situ and *Ex Situ* Investigations of Lateral Composition

S. R. Lee

Spontaneous lateral composition modulation during short-period superlattice (SPS) growth shows great potential as an alternative method to obtain quantum-size features in compound semiconductor alloys. Recent work elucidated some of the growth conditions required for the spontaneous modulation to occur, but the specific physical mechanisms producing lateral composition modulation formation are not fully understood.

In collaboration with researchers at the University of Michigan (UM), we began the process of examining the growth surface of SPS structures that are known to exhibit lateral composition modulation with in situ *scanning-tunneling microscopy (STM). Once successful, this technique will provide a first examination of the growing surface of the SPS.*

We undertook further ex situ *studies to examine the role of specific growth conditions on lateral composition modulation formation using X-Ray Diffraction Reciprocal Space Mapping (K-Mapping). These data resulted in improved understanding of lateral composition modulation formation and aided in the development of these materials and structures for use in novel, low-dimensional device applications.*

The scope of this project was to investigate some specific proposed formation mechanisms associated with lateral composition modulation in AlAs-InAs SPSs grown on (001) InP. We successfully characterized numerous samples *ex situ* using x-ray reciprocal space mapping to test the latest hypotheses concerning spontaneous lateral composition modulation formation. We made more limited progress during attempts to grow and image modulated structures *in situ* using STM due to technical difficulties with the STM instrumentation over the course of the project.

One major hypothesis examined in the present *ex situ* experiments is the idea that the lateral modulation period is controlled by the growth temperature in a manner consistent with a nucleation-and-growth/diffusion-length argument. X-ray diffraction reciprocal space maps of samples grown at temperatures ranging from T=500°C to T=555°C show that lateral modulation is present at all temperatures above T ~ 515°C. The periodicity of the modulation, however, remains approximately constant at a value of ~ 25 nm for all temperatures examined. Therefore, we demonstrated that the modulation wavelength is, in fact, not controlled by surface-diffusion length effects associated with the growth temperature as previously believed.

A second hypothesis examined in the *ex situ* experiments was the idea that lateral composition modulation forms only for those structures where the InAs-layer thickness in the superlattice exceeds some critical thickness. This hypothesis came about as a result of previous experiments that strongly suggested that a minimum of 1.65 ml of InAs is required for AlAs-InAs SPS structures to develop lateral composition modulation. X-ray reciprocal space maps of samples grown to explicitly test this hypothesis show that in spite of sufficiently thick InAs layers, lateral composition modulation does not occur for SPS samples where the average InAs composition deviates by more than ± 0.10 from the InP-lattice–matched composition of 0.52 (these composition bounds correspond to average lattice mismatches of approximately ± 0.7%). Thus, we demonstrated that simply exceeding an InAs critical layer thickness of 1.65 ml during SPS growth will not alone lead to compositional modulation. An overriding parameter that determines whether modulation occurs is the average alloy composition (or the associated average in-plane biaxial strain) of the SPS.

Publications

Refereed

Lee, S. R., J. M. Millunchick, R. D. Twesten, D. M. Follstaedt, J. L. Reno, S. P. Ahrehkiel, and A. G. Norman. 1998. "Reciprocal-Space Analysis of Compositional Modulation in Short-Period Superlattices Using Position-Sensitive X-Ray Detection." *J. Mater. Sci.: Mater. in Electron.*, submitted.

3537.160

Approximate Methods for Computing Eigensolutions Using Automated Multilevel Substructuring

J. R. Red-Horse

Recently, Sandia developed a method for frequency response analysis of structures, known as Automated Multi-Level Substructuring (AMLS). This method divides a large finite-element (FE) model automatically into thousands of substructures and transforms it so that response is represented in terms of the modal models for these substructures. Apparently, AMLS is suitable for obtaining very accurate approximations of global eigenpairs in a massively parallel (MP) environment with potentially large savings in computation time and memory requirements. In collaboration with researchers at the University of Texas–Austin, Sandia will develop an initial interface between SALINAS and AMLS software and explore the feasibility of incorporating AMLS directly into the SALINAS package. We will direct our efforts toward coupling SALINAS-generated global mass and stiffness matrices from the serial version of the code with the stand-alone AMLS code and subsequently calculating approximate global eigenvalue/eigenvector pairs using it.

(1) We modified existing AMLS software to enable the input of global structural matrices (those associated with the system stiffness and mass) from data files produced by Sandia's ASCI-funded structural dynamics FE code, SALINAS. Now it is possible to calculate approximate global eigenpairs, in stand-alone fashion, for the generalized eigenvalue problem associated with those matrices.

(2) We performed an in-depth investigation into how SALINAS handles connectivity between subdomains in a parallel computing environment. The result was the production of a document that describes how stiffness, mass, and connectivity data associated with individual subdomains can be written to files by SALINAS, in either serial or parallel mode, so that AMLS software can read these files, then process the FE model. This document will also provide information on the feasibility of incorporating AMLS as a solution sequence that can be called from within SALINAS itself.

3537.170

Living Tissue Engineering

S. N. Kempka

Living tissue engineering is the development of biological substitutes through the use of living cells and materials of synthetic or natural origin and the fostering of tissue regeneration and/or remodeling to repair, replace, or enhance function. This area is being driven by patient needs since there are insufficient native tissues to address existing needs. A new industry is emerging in this area. Techniques for tissue growth and preservation are presently categorized as art forms; that is, they are not determined using a scientific or engineering basis. This work will apply the formidable capabilities of numerical analysis on the development of two important tissue engineering processes: bioreactor design and cryopreservation.

It is not known how to most efficiently operate bioreactors, so Sandia will explore the use of numerical simulation to engineer the best operating parameters. Another area to be examined is cryopreservation, which has been successfully achieved for single cells, but attempts at cryopreservation of multicellular masses such as organs have not been successful.

The dominant physics that dominate the bioreactor operation and cryopreservation are convection and diffusion, for which numerical algorithms have been developed. In collaboration with researchers at the Georgia Institute of Technology, we will use these numerical algorithms in conjunction with experiments to optimize bioreactor operation and cryopreservation techniques for multicellular bodies.

Discussions with Georgia Tech staff and literature surveys in these areas allowed us to focus on the cryopreservation topic and eliminate the bioreactor topic. The cryopreservation area will focus on the inclusion of complex phase diagrams for the fluids involved, which describe highly complex behavior. This approach will benefit the cryopreservation project by providing a much more detailed predictive capability than is presently used in the industry.

Our efforts resulted in the decision to focus on cryopreservation. We based this decision on our findings that the phenomena associated with cryopreservation are more suitable to make significant progress in a relatively short time, which is important in developing an initial program. In particular, our numerical simulation capabilities in the cryopreservation area are more mature than in the bioreactor area. This allows us to focus on the implementation of highly advanced details of cryopreservation within a well-developed numerical technology.

We initiated an extensive literature review and developed a research plan. The literature review indicates that many of the data needed to describe cryopreservation are available, and that much of the complexity of cryopreservation phenomena has not yet been included in numerical models. This situation provides us with a unique opportunity to help remove the art associated with cryopreservation by using simulation to provide understanding of the complex phenomena associated with cryopreservation, and to use this understanding to design new procedures to preserve multicellular masses such as organs.

Our approach is to use a diffusion–based model in which convection is omitted and include complex phase phenomena.

THIS PAGE
INTENTIONALLY BLANK

A B C D E F G H I J K L M N O P Q R S T U V W X Y Z

A

Adams, D. P. 106, 192
Adolf, D. B. 91
Adriaans, M. J. 178
Ahrens, E. H. 209
Aidun, J. B. 90
Alam, M. K. 148
Alber, E. S. 90
Allen, J. J. 102
Allendorf, S. W. 92
Allerman, A. A. 57, 58, 60, 62, 64, 65, 74, 76, 198, 202
Alvin, K. F. 46, 94
Ames, A. L. 114, 116
Ammerlahn, H. R. 113
Anderson, C. 68
Anderson, D. J. 165
Anderson, R. A. 26
Anderson, R. J. 111, 118
Anex, D. S. 19, 136, 148
Arguello, J. G., Jr. 207
Armstrong, R. C. 52, 130
Asay, J. R. 224
Asbill, R. E. 64
Ashby, C. I. H. 60, 70, 105
Asher, R. B. 210
Ashley, C. S. 225
Aselage, T. L. 190
Attaway, S. W. 177
Atwood, C. L. 98
Aurand, J. F. 70, 206

B

Baca, A. G. 73, 75, 156, 226
Baer, M. R. 25, 90
Baeza, A. R. 179
Baker, A. B. 211
Baldwin, J. M. 107
Baldwin, M. D. 198
Ballard, S. 212
Bammann, D. J. 83, 86
Barker, G. T. 212
Barnaby, M. L. 38
Bartel, L. C. 138, 212
Bartelt, N. C. 22
Bartholomew, J. W. 67
Barton, D. L. 167
Battaile, C. C. 42
Baty, R. S. 44
Baucom, K. C. 59
Benavides, G. L. 102, 106, 192, 226
Bennett, P. C. 171
Benson, D. A. 66, 167
Berg, T. M. 194
Bespalko, S. J. 123
Bickel, D. L. 138
Biefeld, R. M. 20, 62
Bieg, L. F. 102
Blair, D. S. 154
Blake, R. J. 136
Bliss, D. E. 192, 218
Boehme, D. R. 216
Boettcher, G. E. 182
Bogdan, C. W. 165
Bonivert, W. D. 216
Borns, D. J. 150
Boslough, M. B. 200
Bouchard, A. M. 20
Bow, W. J. 142
Boyack, K. W. 53
Boyle, T. J. 10
Brady, P. V. 150
Brainard, J. P. 183
Braithwaite, J. W. 166
Brandt, J. M. 124
Brazee, J. L. 114
Breiland, W. G. 70
Brightwell, R. B. 50
Brinker, C. J. 10, 135, 152, 186, 225
Brockmann, J. E. 24, 165
Brooks, J. A. 29
Brown, K. H. 84
Brown, R. G. 114, 116, 117
Brunett, B. A. 222
Buchheit, T. E. 42, 104
Bujewski, G. E. 154
Burchett, S. N. 66
Burns, A. R. 15
Burns, S. P. 34, 44
Buss, R. J. 105
Butler, M. A. 191
Butler, P. C. 160, 168
Byrne, R. H. 68

C

Caffey, T. W. 212
Calton, T. L. 114, 118
Cameron, S. M. 192, 198, 199, 204, 218, 220, 226
Campbell, A. N. 106
Campbell, J. E. 162
Campbell, P. L. 126
Carichner, S. A. 172
Carlson, D. C. 179
Carlson, J. J. 103, 149, 180
Carr, M. J. 26, 148
Carr, R. D. 50
Casalnuovo, S. A. 14, 75, 77, 78
Causey, R. A. 222
Cesarano, J., III 25, 191, 218
Chambers, R. S. 91
Chambers, W. B. 172
Chang, H. 198
Chen, H. Y. 124, 130
Chen, K. S. 93
Chhabildas, L. C. 90
Choquette, K. D. 57, 58, 60, 74, 76
Chow, W. W. 10, 57, 65, 74
Christenson, T. R. 68, 78, 97
Christon, M. A. 44
Chrzan, D. C. 12
Chu, D. D. 142
Claassen, J. P. 138
Coats, R. S. 38
Cochran, R. J. 34
Cole, E. I., Jr. 167, 179
Coleman, P. D. 206
Collins, E. W. 106
Coltrin, M. E. 59, 93
Cordaro, J. T. 137
Craft, R. L. 162
Crawford, M. H. 10, 58, 73, 77, 171
Crowder, S. V. 106
Crowther, J. I., Jr. 210
Cummings, E. B. 216
Current, K. 61
Curro, J. G. 41, 100, 148, 184

D

Daniels, J. W. 136
Day, D. M. 36, 223
Dean, L. B. 126, 198
De Boer, M. P. 21, 102
Dec, J. E. 150
Denison, G. J. 156
De Sapio, V. 102, 107
Desiena, T. H. 179
Desjardin, P. E. 88
Devine, K. D. 34, 36
Diegert, C. F. 35
Diegert, K. V. 46
Dike, J. J. 82
Dimos, D. B. 16
Dison, H. L. 123
Dodd, P. E. 70
Dohner, J. L. 171
Dohrmann, C. R. 84, 100
Doran, L. M. 35
Douglas, M. R. 201

Doyle, B. L. 106
Draelos, T. J. 130
Draper, B. L. 62
Dreeben, T. D. 89
Drennen, T. E. 196
Dron, S. B. 206
Drummond, T. J. 59, 77
Dugger, M. T. 12, 15
Durant, J. L., Jr. 34
Dykhuizen, R. C. 24

E

Eaton, W. P. 159
Echekki, T. 89
Eichel, P. H. 142
Einfeld, W. 203
Elbring, G. J. 138
Emerson, J. A. 100
Engi, D. 196
Ensz, M. T. 25, 104
Espinoza, J. 128
Evans, G. H. 93
Ewsuk, K. G. 207

F

Falcone, P. K. 203
Fan, D. 52
Fang, H. E. 42
Farino, A. J. 66
Faulon, J. M. 43
Feddema, J. T. 97, 103, 194
Federico, P. J. 206
Feibelman, P. J. 22, 184
Fellerhoff, J. R. 138, 210
Filter, W. F. 160
Fisk, L. A. 52
Fleetwood, D. M. 62
Fleming, J. G. 66, 77
Fleming, R. P. 179
Flores, R. S. 70
Floro, J. A. 22, 71
Flounders, A. W. 142, 232
Foiles, S. M. 86
Follstaedt, D. M. 12, 58, 71, 77, 202
Ford, D. M. 33
Fossum, A. F. 207
Fredrich, J. T. 84
Friedman-Hill, E. J. 34
Friedmann, T. A. 12, 188
Friesen, J. A. 124, 125
Frink, L. J. D. 36
Fritz, I. J. 9
Frye-Mason, G. C. 75, 135, 172
Fuerschbach, P. W. 27
Funkhouser, D. R. 162
Fye, R. M. 41, 42, 52

G

Garbin, H. D. 138
Garcia, E. J. 61
Gardner, T. J. 10, 152
Garino, T. J. 68
Garrett, S. E. 214
Gee, J. M. 198, 202, 214
Geib, K. M. 74, 76
Gentile, A. C. 52
Gentry, S. M. 136
Gilliom, L. R. 194
Gilmore, D. L. 24
Gladwell, T. S. 111, 118
Glass, S. J. 42
Godfrey, A. W. 86
Goeke, R. S. 183
Goldsborough, S. S. 153
Goldsmith, S. Y. 119, 194, 204
Gonzales, R. A. 130
Gourley, P. L. 9
Griffith, M. L. 25, 98, 104
Griffiths, S. K. 216
Gritzo, L. A. 88, 92, 165
Grotbeck, C. L. 179
Guess, T. R. 91, 148
Guthrie, S. E. 222

H

Haaland, D. M. 148
Hadley, G. R. 57, 65
Hamilton, J. C. 17, 22, 43
Hamilton, V. A. 130
Hammons, B. E. 9, 74, 76
Han, J. 10, 73, 77
Harmony, D. W. 142
Haroldsen, B. L. 203
Harrington, J. J. 180
Harris, D. L. 164, 196
Hart, W. E. 48, 50, 108
Harwell, L. D. 104
Haynes, R. A. 38
Hebner, G. A. 105
Heffelfinger, G. S. 33
Heinstein, M. W. 84
Heller, E. J. 68, 75
Helms, C. J. 58
Henderson, C. L. 61
Hendrickson, B. A. 53
Henry, T. R. 123
Hess, B. V. 216
Heustess, J. E. 178
Hicken, G. K. 107
Hickerson, D. 114
Hickox, C. E., Jr. 84
Hiebert-Dodd, K. L. 196
Hietala, S. L. 75
Hietala, V. M. 58, 75
Hillaire, R. G. 107
Hilton, N. R. 222
Hinckley, M. K. 136
Ho, C. K. 81
Hobbs, D. J. 33
Holcomb, D. J. 209
Holland, K. G. 228
Hollowell, J. A. 137
Holm, E. A. 42, 86, 229
Hopkins, P. L. 212
Horn, K. M. 20, 59
Horstemeyer, M. F. 43
Hosking, F. M. 64
Hough, P. D. 129
Houston, J. E. 15, 17
Hruby, J. M. 216
Hu, T. C. 130
Hughes, D. A. 83, 86
Hughes, R. C. 10, 74, 142, 182
Hunter, K. O. 48
Hurd, A. J. 228
Hurtado, J. E. 47
Hutchinson, R. L. 119, 126
Hwang, R. Q. 17, 28
Hwang, Y. K. 123

I

Ingersoll, D. 198
Irwin, L. W. 159, 160
Istrail, S. 141, 218

J

Jackson, N. B. 196
Jacobs, J. A. 199
Jakowatz, C. V., Jr. 137
Jamison, G. M. 26
Janek, R. P. 142, 232
Janssen, C. L. 40
Jefferson, K. J. 179
Jennison, D. R. 20, 26, 28
Johnsen, H. A. 92
Johnson, A. J. 106
Johnson, D. K. 53
Johnson, M. M. 113, 129
Johnston, A. M. 130
Jones, D. A. 50, 108
Jones, E. D. 9, 10, 188
Jortner, J. N. 125
Jung, J. 100

K

Kasunic, K. J. 154
Keck, J. D. 99
Keefe, R. G. 212
Kegelmeyer, W. P. 131

Kellogg, G. L. 22
Kelly, M. J. 154
Kemme, S. A. 154
Kempka, S. N. 235
Kent, M. S. 18
Kern, J. P. 198
Kerstein, A. R. 34, 89
Key, S. W. 84
Kiefer, M. L. 38
King, C. 102
King, D. B. 214
King, R. K. 204
Kjeldgaard, E. A. 50
Klarer, P. R. 171
Klein, P. A. 90
Klem, J. F. 9, 59, 60, 71, 202
Kliner, D. A. 208
Knapp, J. A. 12, 21
Knorovsky, G. A. 42
Koch, M. W. 140
Koller, M. H. 53
Kottenstette, R. J. 75, 135
Kozlowski, D. M. 102
Kravitz, S. H. 58, 66, 78, 139, 142, 172
Krumel, L. J. 136
Kurtz, S. R. 9, 62, 72, 202

L

Ladd, M. D. 138
Lafarge, R. A. 49, 123
Laguna, G. A. 114
Lanes, K. R. 179
Larson, R. S. 93
Larson, W. L. 160
Lavigne, G. F. 192
Lee, E. Y. 222
Lee, S. R. 10, 71, 77, 202, 234
Lemen, E. K. 113
Leonard, C. M., Jr. 107
Leung, K. 45
Leung, V. J. 100
Lewis, C. L. 49, 171
Lewis, P. R. 135
Lin, S. Y. 9, 72
Lindgren, E. R. 36
Link, H. E. 194
Little, C. Q. 103, 114, 116, 149, 180
Lo, C. S. 91
Lockwood, S. J. 99
Loehman, R. E. 185
Lopez, E. P. 100
Loubriel, G. M. 156, 199, 220
Loy, D. A. 26, 148
Lu, W. 82
Ludowise, P. D. 92
Lund, J. C. 222
Lyo, S. K. 9, 72

M

MacCallum, D. O. 104
Mah, B. A. 128
Mansure, A. J. 212
Mar, A. 65
Marder, B. M. 210
Marlman, K. S. 106
Marozas, D. C. 164
Martin, J. E. 26
Martin, M. F. 106
Martinez, L. G., Jr. 128
Martinez, M. J. 212
Martino, A. 19, 154
Marx, K. D. 162
Matalucci, R. V. 177
Mayer, T. M. 14, 15, 21
Mazarakis, M. G. 199
McCarty, K. F. 12
McDonald, M. J. 112
McWhorter, P. J. 15
Medlin, D. L. 12
Meirans, L. 123
Melius, C. F. 34, 40
Meyers, C. E. 1
Michalske, T. A. 15, 171
Miles, P. C. 150
Miller, J. C. 193
Miller, J. E. 154, 196
Miller, P. A. 105
Miller, S. L. 15, 192
Miodownik, M. A. 86
Missert, N. A. 12, 189
Mitchell, E. A. 114
Mix, L. P., Jr. 38
Modine, N. A. 45
Moen, C. D. 51
Moffat, H. K. 59
Montague, S. 66
Montoya, T. V. 99
Moody, N. R. 17, 83
Moore, R. H. 99
Morales, A. M. 216
Morgan, W. P. 214
Mosher, D. A. 83
Moya, M. M. 140
Moyer, R. D. 178
Murray, J. R. 62
Myers, S. M., Jr. 73, 183

N

Napolitano, L. M. 194
Neilsen, M. K. 42
Neiser, R. A., Jr. 24
Nelson, C. L. 149, 180
Nelson, J. S. 20
Nenoff, T. M. 147
Nevers, J. A. 76
Newman, G. A. 223
Neyer, D. W. 136, 148
Ngujo, M. A. 126
Nicolette, V. F. 165
Nilsen, V. 89
Nilson, R. H. 216
Noble, D. R. 84
Nowlen, S. P. 165

O

Oberkampf, W. L. 46
O'Connor, R. M. 84
Olson, C. L. 199
Osbourn, G. C. 20, 135, 171, 194
Ottesen, D. K. 92

P

Paez, T. L. 88
Palmer, D. W. 124
Paradiso, N. J., Jr. 153
Parmeter, J. E. 227
Pasik, M. F. 38
Pate, R. C. 206
Patterson, P. E. 206
Paul, P. H. 201, 216
Peace, G. L. 156
Peña, E. A. 114
Peña, J. G. 126
Peng, L. W. 82
Peters, R. R. 114, 118
Peterson, D. W. 166
Peterson, K. A. 159
Phillips, C. A. 48, 50, 108
Phillips, L. R. 194
Pierson, L. G. 58, 126, 198
Plantenga, T. D. 40, 113
Plimpton, S. J. 17, 38, 40, 45, 50, 52
Plymale, D. L. 102, 106
Polosky, M. A. 97
Prast, T. L. 216
Provencio, P. N. 12, 26
Pryor, R. J. 47, 164, 194

R

Rader, D. J. 139
Rakestraw, D. J. 172
Ray, L. P. 123
Red-Horse, J. R. 88, 233, 235
Redmond, J. M. 21
Reed, K. W. 210
Reedy, E. D., Jr. 18, 91, 100
Reese, G. M. 36

Reeves, P. C. 212
Renlund, A. M. 193
Reno, J. L. 72, 75
Renzi, R. F. 139
Ricco, A. J. 14, 62, 67, 142
Rieger, D. J. 105
Riesen, R. E. 50
Riley, D. J. 38, 206
Rinehart, L. F. 206
Rintoul, M. D. 42
Rivord, G. E. 119
Roach, D. W. 44
Robertson, P. J. 58, 124, 126
Robino, C. V. 66
Robinson, A. C. 51
Robinson, D. G. 88, 160, 166, 168, 211
Rodacy, P. J. 191
Rodgers, M. S. 61, 102
Roe, D. C. 141, 203
Romero, V. J. 88, 94
Rondeau, D. M. 210
Ross, J. R. 92
Ruby, D. S. 105
Ruffner, J. A. 16, 28, 214
Rupley, F. M. 93
Rutherford, B. M. 46, 94
Ryba, G. N. 172

S

Sackos, J. T. 35
Salazar, J. S. 140
Salinger, A. G. 34, 36
Salmi, A. J. 216
Sands, D. N. 38
Sarfaty, R. A. 119
Sasaki, D. Y. 135
Sault, A. G. 10, 28, 152, 196
Saunders, R. S. 26, 148
Schimmel, W. P. 210
Schlienger, M. E. 98, 180
Schmidt, R. C. 34, 89
Schmitt, D. J. 25, 102, 111, 149
Schmitt, R. G. 203
Schneider, L. X. 210
Schoeneman, J. L. 198
Schoeniger, J. S. 136, 141, 142, 148, 225
Schriner, H. K. 61
Schubert, W. K. 16, 78, 226
Schultz, P. A. 45
Schunk, P. R. 51
Schwank, J. R. 62
Schwegel, J. 125
Scofield, T. W. 99
Scott, S. H. 148
Seager, C. H. 73
Sears, M. P. 20, 45, 50
Seidel, D. B. 38
Seidl, E. T. 34
Sellinger, A. 135
Sexton, F. W. 70
Shadid, J. N. 34, 51
Shaddix, C. R. 92, 165
Shaneyfelt, M. R. 62
Shea, L. E. 58
Sheaffer, D. A., Jr. 107
Shelnutt, J. A. 26, 147, 154, 187, 231
Shepodd, T. J. 19
Shinn, N. D. 17
Sholander, P. E. 128
Shope, S. L. 199, 210
Shul, R. J. 73, 77, 78
Siebers, D. L. 150
Siegel, M. D. 150
Silva, B. L. 105
Simmermacher, T. W. 230, 233
Simmons, J. A. 72
Simonson, K. M. 142
Simonson, R. J. 225
Singh, A. K. 225
Sipola, D. L. 99
Sleefe, G. E. 138
Slutz, S. A. 224
Small, D. E. 149, 180
Smith, A. V. 60
Smith, D. A. 136
Smith, J. H. 16, 64, 192
Smith, M. F. 24
Smith, N. F. 159
Smith, T. M. 34
Smithberger, G. L. 179
Smugeresky, J. E. 98
Sniegowski, J. J. 15, 21, 61, 66
Somerday, B. P. 222
Sorensen, N. R. 166
Spahn, O. B. 60, 64
Spielman, R. B. 201, 224, 230
Spires, S. V. 119, 194
Spletzer, B. L. 47, 171, 194
Spooner, J. T. 106
Stallard, B. R. 136
Stans, L. 130
Stantz, K. M. 220
Staple, B. D. 66
Staton, A. W. 67
Stechel, E. B. 45
Stevens, M. J. 15, 18
Stockman, H. W. 84
Stone, C. M. 84
Strickland, J. H. 88
Sturtevant, J. E. 38
Sullivan, C. T. 60, 198, 204
Sullivan, J. P. 60, 188, 189
Swanson, B. E. 210
Swartzentruber, B. S. 14, 22, 28
Sweatt, W. C. 136, 154
Sweet, J. N. 166
Swiler, L. P. 88

T

Tan, M. X. 97, 139, 216
Tanaka, T. J. 165
Tangyunyong, P. 159, 167
Tanner, D. M. 159
Tappan, A. S. 193
Tarbell, W. W. 204
Tarman, T. D. 126, 130
Thacher, P. D. 178
Thomas, D. H. 136
Thomas, E. V. 130
Thomas, G. A. 203
Thompson, A. P. 33
Thompson, B. M. 162
Thorne, L. R. 92
Tigges, C. P. 59
Tikare, V. 52, 104, 218
Tolendino, L. F. 128
Tong, C. H. 40, 51, 129
Toth, R. P. 205
Trahan, M. W. 220
Trinkle, J. C. 114, 118
Trott, W. M. 90
Trucano, T. G. 94
Tsang, R. P. 124
Tsao, J. Y. 71
Tuminaro, R. S. 36, 51
Turman, B. N. 199
Tuttle, B. A. 16, 99

U

Ulibarri, T. A. 148

V

Van Blarigan, P. 153
Vandernoot, V. A. 136
Vandewart, R. L. 162
Van Leeuwen, B. P. 128
Van Swol, F. B. 41
Vawter, G. A. 9, 60, 64, 65, 70
Vedula, V. R. 42
Venturini, E. L. 68
Voigt, J. A. 99
Volponi, J. V. 136
Voth, T. E. 44

W

Wagner, J. F. 199
Wagner, J. S. 48, 220

Walker, T. R. 107
Walkup, J. W. 179
Wally, K. 139, 142, 232
Walsh, D. S. 70, 202
Warren, M. E. 19, 58, 64, 76, 171
Warren, W. L. 62
Watterberg, P. A. 117
Webb, S. W. 81
Weber, T. M. 171
Wehlburg, J. C. 179, 199
Weinbrecht, E. A. 210
Wellman, G. W. 42
Wendt, J. R. 9, 64, 72
Wessendorf, K. O. 78
Wheeler, D. R. 26, 148
Wilcoxon, J. P. 26
Williams, A. B. 51
Williams, J. S. 179
Witkowski, W. R. 100
Witzke, E. L. 126
Wolfer, W. 171
Womble, D. E. 44
Wong, C. C. 171
Woodworth, J. R. 70
Wright. A. F. 10, 45, 73
Wright, S. A. 172
Wu, J. 153
Wu, K. L. 153
Wunsch, S. E. 89
Wyckoff, P. S. 130
Wylie, B. N. 53
Wyss, G. D. 162

X

Xavier, P. G. 116, 123, 171

Y

Yang, P. 105, 106
Yarberry, V. R. 102, 192
Yazzie, S. H. 160
Yee, A. A. 138
Yee, M. L. 138
Yelton, W. G. 67
Yocky, D. A. 140
Yoshimura, A. S. 113
Young, W. F. 119

Z

Zanini, D. V. 153
Zavadil, K. R. 214
Zhang, P. 150
Zutavern, F. J. 65, 226

THIS PAGE
INTENTIONALLY BLANK

Page Number	Title	Project Number
10	Catalytic Membrane Sensors	3502.030
9	Photonic Bandgap Structures as a Gateway to Nanophotonics	3502.040
10	Wide-Bandgap Compound Semiconductors to Enable Novel Semiconductor Devices	3502.050
12	Ultra-Hard Multilayer Coatings	3502.080
14	Scanning Probe–Based Processes for Nanometer-Scale Device Fabrication	3502.090
15	Molecular-Scale Lubricants for Micromachine Applications	3502.110
16	Surface-Micromachined Flexural Plate-Wave Device Integrated on Silicon	3502.120
17	Smart Interface Bonding Alloys (SIBA): Tailoring Thin-Film Mechanical Properties	3502.140
20	Recognizing Atoms in Atomically Engineered Nanostructures: An Interdisciplinary Approach	3502.170
18	Molecular-to-Continuum Fracture Analysis of Thermoset Polymer/Solid Interfaces	3502.190
19	Monolithic Structures for Nanoseparation	3502.210
21	Fundamental Aspects of Micromachine Reliability	3502.220
24	Enabling Science and Technology for Cold-Spray Direct Fabrication	3502.230
22	Atomic-Level Studies of Surfactant-Directed Materials Growth	3502.240
26	Intelligent Polymers for Nanodevice Performance Control	3502.250
25	Freeforming of Ceramics and Composites from Colloidal Slurries	3502.260
26	Quantum Dot Arrays	3502.270
27	Laser-Assisted Arc Welding for Aluminum Alloys	3502.280
28	Reactivity of Metal-Oxide Surfaces	3502.310
29	Exploiting LENS Technology Through Novel Materials	3502.320
34	Parallel Quantum Chemistry for Material Aging and Synthesis	3504.010
34	Modeling Complex Turbulent Chemically Reacting Flows on Massively Parallel Supercomputers	3504.020
35	Automated Geometric Model Builder Using Range Image Sensor Data	3504.050
36	A Massively Parallel Sparse Eigensolver for Structural Dynamics Finite Element	3504.060
36	Density-Functional Theory for Classical Fluids at Complex Interfaces	3504.070
33	Gradient-Driven Diffusion of Multi-Atom Molecules Through Macromolecules and Membranes	3504.090
38	Fast and Easy Parallel I/O for Efficient Scientific Computing	3504.120
38	Novel Load-Balancing for Scalable, Parallel Electromagnetic and Plasma Physics Simulation Software	3504.130
40	Parallel Computational Chemistry Using Constraints	3504.140
40	Massively Parallel *Ab Initio* Validation for ASCI Materials Aging	3504.160
42	Computational Methods for Coupling Microstructural and Micromechanical Materials Response Simulations	3504.170

Page Number	Title	Project Number
44	An Investigation of Wavelet Bases for Multiscale, Grid–Based Simulation	3504.180
41	Integrated Quantum/Classical Modeling of Hydrogenic Materials	3504.190
45	The Next Generation of Teraflop Density-Functional Electronic Structure Codes	3504.210
46	Methodology for Characterizing Modeling and Discretization Uncertainties in Computational Simulation	3504.220
48	Global Optimization for Engineering Science Problems	3504.230
49	Dynamic Simulation of Mechanical Systems with Intermittent Contacts	3504.240
43	From Atom-Picoseconds to Centimeter-Years in Simulation and Experiment	3504.250
47	Emergent Behavior of Large Swarms of Intelligent Agents	3504.260
50	Parallel Combinatorial Optimization for Scheduling Problems	3504.270
50	Programming Paradigms for Massively Parallel Computers	3504.280
51	Multilevel Techniques for Unstructured Grid Problems on Massively Parallel Computers	3504.290
52	Scalable Tools for Massively Parallel Distributed Computing	3504.310
52	Massively Parallel Methods for Simulating the Phase Field Model	3504.320
53	Visual Explanation and Insight	3504.330
58	Wafer Fusion for Integration of Semiconductor Materials and Devices	3506.110
58	Highly Parallel, Low-Power, Photonic Interconnects for Inter-Board Signal Distribution	3506.120
59	Virtual Reactor for the Semiconductor Manufacturing Plant of the Future	3506.140
60	Selective Oxidation Technology and Its Applications Toward Electronic and Optoelectronic Devices	3506.160
61	Agile Prototyping of Microelectro-mechanical Systems (MEMS)	3506.180
57	Advanced Concepts for High-Power VCSELs and VCSEL Arrays	3506.190
62	Midwave-Infrared (2–6 µm) Emitter–Based Chemical Sensor Systems	3506.210
62	A Novel Nondestructive Silicon-on-Insulator Nonvolatile Memory	3506.230
64	Integration of Optoelectronics and MEMS by Free-Space Microoptics	3506.240
65	Advanced Laser Structures for Short-Pulsed Power in Active Optical Sensor Systems	3506.250
66	Metal Micro-Heat-Pipe Substrates for High-Power-Density Electronics	3506.260
68	Integration of Microsensor Technology into a Miniature Robotic Vehicle	3506.270
66	Vacuum Encapsulation of MEMS Structures	3506.280
67	Massively Parallel Sensor Arrays for Volatile Organic Detection	3506.290
70	Agile Dry Etching of Compound Semiconductors for Science–Based Manufacturing Using *In Situ* Process Control	3506.310
68	Precision-Formed Micromagnets	3506.320
70	Time-Resolved Ion-Beam–Induced Charge-Collection (TRIBICC) Imaging	3506.330
74	Composite-Resonator Surface-Emitting Lasers	3506.340

Page Number	Title	Project Number
73	Role of Defects in III-Nitride–Based Electronics	3506.350
74	Ultra–Low-Power Sensors for Microtelemetry Systems	3506.360
72	Double Quantum-Well Long-Wavelength Optoelectronic Devices	3506.370
75	The Development of Integrated Chemical Microsensors in GaAs	3506.380
76	Monolithic Integration of VCSELs and Detectors for Microsystems	3506.410
77	AlGaN Materials Engineering for Integrated Multifunction Systems	3506.420
71	Compliant Substrates for Epitaxial Integration of Dissimilar Materials	3506.430
78	Post-Processed Integrated Microsystems	3506.440
83	Using Higher-Order Gradients to Modeling Localization Phenomena	3508.040
81	Enhanced Vapor-Phase Diffusion in Porous Media	3508.060
82	Stress Evaluation and Model Validation Using Laser Ultrasonics	3508.110
84	Altered Simulation Properties for Tetrahedral Finite Elements for Use in Engineering Simulation	3508.120
84	Development, Implementation, and Experimental Validation of the Lattice Boltzmann Method for Modeling Three-Dimensional Complex Flows	3508.130
86	Capturing Recrystallization of Metals with a Multiscale Material Model	3508.140
88	Nondeterministic Modeling in Engineering Science	3508.150
88	Lagrangian Modeling of Radiative Transport	3508.160
89	High-Resolution Modeling of Multiscale Transient Phenomena in Turbulent Boundary Layers	3508.170
90	Dispersive Measurements of Velocity in Heterogeneous Materials	3508.180
90	A Physically–Based Computational Method for Predicting Generalized Fracture	3508.190
92	Development of *In Situ* Diagnostics for Simultaneous Measurement of Transient Gas Species and Soot in Large Fires	3508.210
91	Micromechanical Failure Analyses for Finite-Element Polymer Modeling	3508.220
94	Methodology Optimal Selection of Test and Simulation Levels for Problems Involving Computational Simulation	3508.230
93	A Phenomenological Model for Multicomponent Transport with Electrochemical Reactions in Concentrated Solutions	3508.240
98	Laser-Spray Fabrication for Net-Shape Rapid Product Realization	3510.460
99	Solution Synthesis and Processing of PZT Materials for Neutron-Generator Applications	3510.510
97	Ultra-Precise Assembly of Micro-electromechanical Systems (MEMS)	3510.540
100	Finite-Element Meshing Approached as a Global Minimization Process	3510.570
102	Application of Parallel Mechanism Technology to Manufacturing	3510.580
100	Investigation of the Impact of Cleaning on Adhesive Bond and the Process Implications	3510.590
102	Standard Cells for Microelectro-mechanical Systems (MEMS)	3510.610

Page Number	Title	Project Number
104	Laser Wire Deposition for Fully Dense Shapes	**3510.620**
105	High-Throughput Dry Processes for Large-Area Devices	**3510.630**
106	Assuring High Reliability and Production Readiness in Low-Volume Manufacturing	**3510.640**
103	Scripting for Video Inspection	**3510.660**
106	Advanced Machining Processes for Microfabrication	**3510.670**
107	Fusion of Product and Process Data Using Real-Time Streaming Visualization	**3510.680**
108	Advanced Production Planning Models	**3510.690**
112	Automatic Generation of Multimedia Documentation for Assembly Operations	**3511.010**
113	Distributed Life-Cycle Models in Enterprise Simulations to Answer System Questions	**3511.020**
114	Immersive CAD	**3511.040**
114	Automatic Planning of Life-Cycle Assembly Processes	**3511.050**
116	Analysis of Very Large Assemblies	**3511.070**
111	Enabling Human Skills with Cooperative Automation	**3511.080**
116	Cloud To CAD	**3511.090**
118	Ergonomics in Life-Cycle Assembly Processes	**3511.110**
117	Feature Reduction of Geometric Solid Models for Analysis Tools	**3511.120**
119	System Surety Life-Cycle Engineering	**3511.130**
123	Content–Based Search of Geometric Databases	**3512.160**
124	Integrated Service Provisioning in an "IPv6 over ATM" Research Network	**3512.170**
125	Virtual Desktop Engineering with Integrated Multimedia Data	**3512.180**
123	Mission Surety for Large-Scale Real-Time Information Systems	**3512.190**
126	Scaled ATM End-to-End Encryption	**3512.220**
128	Network Surety Modeling for Wireless ATM Networks	**3512.230**
130	Low-Power, Reduced-Computation, Public-Key Protocols	**3512.240**
126	Ten-to-One-Hundred-Gigabit/Second Network Enabling R&D	**3512.250**
130	High-Performance Commodity Interconnects for Clustered Scientific and Engineering Computing	**3512.260**
131	AVATAR—Navigating and Mining in Massive Data	**3512.270**
129	Algorithm–Based Fault Tolerance on Heterogeneous Massively Parallel Computers	**3512.280**
136	Electrokinetic Immunoaffinity Chemical Sensors	**3516.050**
136	Information-Efficient Spectral Imaging System (ISIS)	**3516.060**
137	Imaging of Moving Targets Using Simultaneous Synthetic Aperture Radar (SAR) and Moving Target Indicator (MTI) Radar	**3516.070**
135	Sampling and Sensing Systems for High-Priority Analytes	**3516.080**
138	Automated Vegetation Height Measurement for Automatic Terrain Mapping	**3516.090**

Page Number	Title	Project Number
138	Sparse Geophysical Networks for Monitoring Deep Targets	3516.110
139	Miniature Bioaerosol Concentrator	3516.120
140	Recognizing Partially Obscured Targets by Combining Multiple Data Sources Using Evidential Reasoning	3516.130
141	Computational Engineering of Sensor Materials and Integration with a Novel Biological Weapon Detection System	3516.140
142	Biological Weapon Detector Using Bioaffinity Array Impedance Analysis with Chemical Amplification Through Redox Recycling	3516.150
142	ATR / Exploitation Utilizing Ultra–High-Resolution, Complex SAR Imaging	3516.160
147	Designed Molecular Recognition Materials for Chiral Sensors, Separations, and Catalytic Materials	3518.030
148	Rapid Screening of Complex Chemical Samples Via Capillary Array Analysis	3518.050
148	Designed Synthesis of Controlled Degradative Materials	3518.060
150	Mechanistic Models for Radionuclide Desorption from Soils	3518.070
150	Development of Innovative Combustion Processes for a Direct-Injection Diesel Engine	3518.080
152	Hydrogen Production for Fuel Cells by Selective Dehydrogenation of Alkanes in Catalytic Membrane Reactors	3518.090
153	Hybrid Vehicle Engine Development	3518.110
149	Adaptive 3-D Sensing	3518.120
154	Aqueous Organic Sensor	3518.130
154	Designed Ionophores for Liquid-Membrane Separation and Extraction of Metal Ions	3518.140
156	An Electromagnetic Imaging System for Environmental Site Reconnaissance	3518.150
160	Reliability Degradation Due to Stockpile Aging	3520.210
159	Integrated Approach to Develop Microelectromechanical (MEMS) Reliability Tools	3520.220
160	Precursors to Failure of Oxides and Metal Lines in CMOS Technology	3520.230
162	An Extensible Object-Oriented Framework for Risk and Reliability Analysis	3520.240
162	Simulation/Optimization Tools for System Variability Analysis	3520.270
164	A Massively Parallel Microsimulation Model of Infrastructure Interdependency	3520.280
166	Physical Models for Predicting the Effect of Atmospheric Corrosion on Microelectronic Reliability	3520.290
167	Backside Localization of Open and Shorted IC (Integrated Circuits) Interconnections	3520.310
165	Reliability Predictions for Advanced Electronics in Smoke Environments	3520.320
168	Security of Bulk Power Systems	3520.330
171	Science on the Microdomain	3522.010
172	Autonomous MicroChem Laboratory (µChemLab)	3522.020
171	Cooperative, Distributed Sensing and Action Using Microminiature, Intelligent Agents	3522.030

Page Number	Title	Project Number
177	Computational Methods for Predicting the Response of Critical As-Built Infrastructure to Dynamic Loads (Architectural Surety)	3530.030
178	Background Radiation Anisotropy Measurement Sensor (BRAMS)	3530.050
178	Exploitation of Satellite Communications Systems and Networks for Intelligence Applications	3530.090
179	Microcode Evaluation	3530.110
179	Real-Time Image Analysis Using Field-Programmable Gate Arrays	3530.120
180	Advanced 3-D Sensing and Visualization System for Unattended Monitoring	3530.130
180	System-of-Labs Direct Fabrication Technology	3531.020
182	Poco Switch Tubes	3531.140
182	Chemiresistors Based on Metal-Loaded Polymers for Solvent Spill Detection	3531.150
183	Advanced Neutron-Tube Design and Producibility	3531.160
183	Surface Hardening by Nanoparticle Precipitation and Atomic Clustering in Ni(Al,O)	3531.170
184	Dynamical Properties of Polymers: Computational Modeling	3531.180
188	Broadening Mechanism in 2-D Excitonic and Electron Gases	3531.190
184	Calculation and Interpretation of the Energies that Underlie Transition-Metal Surface Structure	3531.210
185	Interfacial Reactions in Ceramic Systems	3531.220
186	Direct Fabrication of Multifunctional Nanocomposites Via Supramolecular Self-Assembly	3531.230
187	Biophotonic Materials for Optical Encryption and Noncomputing	3531.240
188	Low-Stress Amorphous Diamond: A New Material for Sensors	3531.250
189	Nanoengineered Cu-Al Defects in Al: A Prototype System for Corrosion	3531.260
190	Novel Energy-Conversion Devices of Icosahedral Borides	3531.270
191	Ion-Mobility Spectroscopy of Biological Materials	3531.280
192	Visualization Tools for MEMS Designs in a Virtual 3-D World	3531.290
191	Direct Fabrication of Planar Solid-Oxide Fuel Cells	3531.310
192	Micromachining with Ultra-Short Pulsewidth Lasers	3531.320
193	Molecular Characterization of Energetic Material Initiation	3531.330
196	Chemical Feedstocks for the Future: Oxidative Dehydrogenation	3532.010
196	Global Approaches to Infrastructural Analysis (GAIA)	3532.030
194	Engineering Complex Distributed Systems	3532.070
198	Laser Communication Nanosatellites	3532.080
200	Collection and Data Synthesis of Atmospheric Explosion Ground Truth for Global Monitoring Systems	3532.090
201	Advanced Radiation Sources: Rayleigh-Taylor Mitigation Via Perturbation Reduction	3532.110

Page Number	Title	Project Number
201	Microfluidic Engineering	**3532.120**
199	Accelerator Technologies for Emerging Threats	**3532.130**
204	Technologies for System-Level Innovations in Ballistic Missile Defense	**3532.140**
202	InGaAsN: A Novel Material for High-Efficiency Solar Cells and Advanced Photonic Devices	**3532.150**
203	Technologies for Countering C/B Terrorism	**3532.160**
205	Aerosol Stand-Off Detection Test-Bed	**3532.170**
206	Design and Optimization of High-Power Electromagnetic Source Systems and Engagement Scenarios for Achieving Functional Upset or Damage in Specific Target Electronic Systems	**3532.180**
207	Real-Time Design of Improved Powder Pressing Dies Using Finite-Element Method Modeling	**3532.190**
208	Development of Fiber-Laser–Based LIF for Detection of SO_2	**3532.210**
209	Penetration and Defeat of Hardened Underground Facilities Using a Microhole Drilling Robot	**3532.220**
210	IFSAR Tree Phenomenology and Coherence Normalization	**3532.230**
210	Electric Launcher for Defense Applications	**3532.240**
212	SAM Telemetry for Measurements While Drilling	**3533.050**
214	Design-for-Manufacturability Applied to Photovoltaic Modules	**3533.070**
212	Advanced Geosphere Transport Simulation	**3533.160**
214	Low-Work-Function Thermionic Emission Materials	**3533.170**
211	Power-Grid Reliability and Restructuring Policy Changes	**3533.180**
222	Low-Cost Cadmium Zinc Telluride Radiation Detectors Based on Electron-Transport-Only Designs	**3534.020**
216	LIGA Micromachining	**3534.030**
216	Applied Microfluidics Science	**3534.040**
218	Computational Simulations of Self-Assembling Macro-Systems by Direct Fabrication of Microscopic Structured Materials	**3535.130**
218	Self-Stabilizing Optical Solitons and High-Intensity Laser Plasma Channels for Diffraction-Free Propagation and Robust Power Compression	**3535.140**
222	Novel Materials for Hydrogen Storage	**3535.150**
220	Optical Communication System for Remote Monitoring and Adaptive Control of Distributed Ground Sensors Exhibiting Collective Intelligence	**3535.160**
223	Inversion of Passive Electromagnetic Fields to Locate Weapons of Mass Destruction	**3535.170**
224	Z-Pinch–Driven Isentropic Compression	**3535.180**
225	Covert, Distributed Biosensors for UXO/CW Based on Amplified Immunoassays Conducted in Porous Inorganic Media	**3535.190**
226	Semiconductor Filament Lasers	**3535.210**
226	Development of Membrane Devices Using AlN and SiC Films	**3537.010**

Page Number	Title	Project Number
227	Spectral Information Content in Ion-Mobility Spectra for Explosives, Interferants, and Other Negative-Ionizing Chemicals	3537.020
230	Magnetic Field Profile Measurements in Wire-Array Z-Pinches by Faraday Rotation	3537.030
228	Picosecond Particle Velocity Measurements	3537.040
228	Particle-Level Modeling of Flows of Concentrated Suspensions	3537.050
229	Efficient Processing of Materials Microstructures with Intelligent Feature Extraction for Quantitative Stereology	3537.060
230	Nondestructive Evaluation of Wind Turbine Blades	3537.070
231	Very Small Arrays: Designing Self-Assembled Systems of Light-Antennae and Reaction Centers for Artificial Photosynthesis	3537.080
232	Enzyme-Mediated Electrochemical Redox Polymer Biosensor for V- and G-Type Chemical Weapons	3537.110
232	Novel Biosensor Fabrication Techniques	3537.120
233	Design for 100-Year-Life Prototype	3537.130
233	Enhancing Multilevel Linear Equation Solvers Using Domain Decomposition Strategies	3537.140
234	*In Situ* and *Ex Situ* Investigations of Lateral Composition	3537.150
235	Approximate Methods for Computing Eigensolutions Using Automated Multilevel Substructuring	3537.160
235	Living Tissue Engineering	3537.170

Awards/Recognition	Project Number	Project Title
Peter Mark Award of the American Vacuum Society: Brian Swartzentruber	3502.240	Atomic-Level Studies of Surfactant-Directed Materials Growth
Discover Magazine Technology Award: Computer Hardware and Electronics (protonic memory)	3506.230	A Novel Nondestructive Silicon-on-Insulator Nonvolatile Memory
1997 *Industry Week* Technology Award		
New Mexico Inventor of the Year Award	3506.280	Vacuum Encapsulation of MEMS Structures
1998 Award for Excellence: The Gunter Wittenberg Award for Best (Outstanding) Paper, on Assembly Automation, from the Literati Club	3511.050	Automatic Planning of Life-Cycle Assembly Processes
Paper selected for Best of the Best Paper session, Transportation Research Board of the National Research Council, 1998 Winter Meeting	3512.190	Mission Surety for Large-Scale Real-Time Information Systems
1998 VeriBest Superior Systems Award, for most unusual circuit board design	3512.220	Scaled ATM End-to-End Encryption
Distinguished Lecturer for the American Vacuum Society	3522.010	Science on the Microdomain
R&D 100 Award, *R&D Magazine*: COMRAD	3534.020	Low-Cost Cadmium Zinc Telluride Radiation Detectors Based on Electron-Transport-Only Designs
Discover Magazine Award: protonic memory	3536.250	Silicon–Based Nondestructive Read-out Memories
BES Materials Science Award: Microcavity Laser	3539.220	Biocavity Laser Microscopy/Spectroscopy of Cells

THIS PAGE
INTENTIONALLY BLANK

Legend

		Performance Statistics (Number of)											Project Qualitative Assessment		
Project Title	Project #	Refereed Publications	All Other Reports and Publications	Patent Disclosures	Patent Applications	Patents	Copyrights	Students	Post-docs	Permanent Staff Hired*	Awards	New Non-LDRD-Funded Projects†	% Milestones Completed	Goals Status**	Hypotheses Status***

* Permanent Staff Hired. Laboratories operate under manpower cap. Therre are no increases in permanent staff.

** Goals Status

1 - Goals Met
2 - Goals Substantially Met
3 - Goals Partially Modified
4 - Goals Substantially Modified
5 - Goals Not Met
11- Project Terminated

***Hypothesis Status

6 - Hypothesis Proved
7 - Hypothesis Remains Unchanged
8 - Hypothesis Modified
9 - Hypothesis Redefined
10 - Hypothesis Disproved
11 - Project Terminated

		Performance Statistics (Number of)											Project Qualitative Assessment		
Project Title	Project #	Refereed Publications	All Other Reports and Publications	Patent Disclosures	Patent Applications	Patents	Copyrights	Students	Post-docs	Permanent Staff Hired*	Awards	New Non-LDRD-Funded Projects†	% Milestones Completed	Goals Status**	Hypotheses Status***
Catalytic Membrane Sensors	3502.030	3		1	1								90%	2	7
Photonic Bandgap Structures as a Gateway to Nanophotonics	3502.040	2		2									100%	1	6
Wide-Bandgap Compound Semiconductors to Enable Novel Semiconductor Devices	3502.050	9											80%	2	6
Ultra-Hard Multilayer Coatings	3502.080	34		1	1			1					100%	2	8
Scanning Probe–Based Processes for Nanometer-Scale Device Fabrication	3502.090	2	1										50%	3	7
Molecular-Scale Lubricants for Micromachine Applications	3502.110	5							2				90%	2	6
Surface-Micromachined Flexural Plate-Wave Device Integrated on Silicon	3502.120	5						2	1	1			70%	2	7
Smart Interface Bonding Alloys (SIBA): Tailoring Thin-Film Mechanical Properties	3502.140	2							1				83%	1	7
Recognizing Atoms in Atomically Engineered Nanostructures: An Interdisciplinary Approach	3502.170	1											90%	2	6
Molecular-to-Continuum Fracture Analysis of Thermoset Polymer/Solid Interfaces	3502.190	1	4					2	1				70%	2	7
Monolithic Structures for Nanoseparation	3502.210			2				2					75%	3	8
Fundamental Aspects of Micromachine Reliability	3502.220	2			1					1			85%	2	7
Enabling Science and Technology for Cold-Spray Direct Fabrication	3502.230	2		1	1								100%	1	7
Atomic-Level Studies of Surfactant-Directed Materials Growth	3502.240	23	14								1		100%	2	7
Intelligent Polymers for Nanodevice Performance Control	3502.250	1											90%	2	7
Freeforming of Ceramics and Composites from Colloidal Slurries	3502.260	4	2	1	1			2	1				100%	1	7
Quantum Dot Arrays	3502.270	5						1	1				100%	1	6
Laser-Assisted Arc Welding for Aluminum Alloys	3502.280		1		1			2					100%	2	7
Reactivity of Metal Oxide Surfaces	3502.310	1											100%	1	7
Exploiting LENS Technology Through Novel Materials	3502.320	3											100%	1	7
Parallel Quantum Chemistry for Material Aging and Synthesis	3504.010												100%	1	6
Modeling Complex Turbulent Chemically Reacting Flows on Massively Parallel Supercomputers	3504.020	2							1			2	60%	3	7
Automated Geometric Model Builder Using Range-Image Sensor Data	3504.050												100%	1	7

		Performance Statistics (Number of)											Project Qualitative Assessment		
Project Title	Project #	Refereed Publications	All Other Reports and Publications	Patent Disclosures	Patent Applications	Patents	Copyrights	Students	Post-docs	Permanent Staff Hired*	Awards	New Non-LDRD-Funded Projects†	% Milestones Completed	Goals Status**	Hypotheses Status***
A Massively Parallel Sparse Eigensolver for Structural Dynamics Finite Element	3504.060	1								1			80%	2	6
Density Functional Theory for Classical Fluids at Complex Interfaces	3504.070	4	5										80%	2	6
Gradient-Driven Diffusion of Multi-Atom Molecules Through Macromolecules and Membranes	3504.090	5	7					1	3				80%	2	6
Fast and Easy Parallel I/O for Efficient Scientific Computing	3504.120	1											60%	3	7
Novel Load-Balancing for Scalable, Parallel Electromagnetic and Plasma Physics Simulation Software	3504.130						1						85%	2	7
Parallel Computational Chemistry Using Constraints	3504.140		3					5					100%	1	8
Massively Parallel *Ab Initio* Validation for ASCI Materials Aging	3504.160												100%	1	7
Computational Methods for Coupling Microstructural and Micromechanical Materials Response Simulations	3504.170	17						1	1	3			85%	1	7
An Investigation of Wavelet Bases for Multiscale, Grid–Based Simulation	3504.180	4	5		2				1				90%	2	6
Integrated Quantum/Classical Modeling of Hydrogenic Materials	3504.190	4						1	1				90%	2	7
The Next Generation of Teraflop Density Functional Electronic Structure Codes	3504.210	4						1	2				95%	2	7
Methodology for Characterizing Modeling and Discretization Uncertainties in Computational Simulation	3504.220	4	1										70%	3	7
Global Optimization for Engineering Science Problems	3504.230	8	14					1		1			90%	2	7
Dynamic Simulation of Mechanical Systems with Intermittent Contacts	3504.240	3						3					100%	1	7
From Atom-Picoseconds to Centimeter-Years in Simulation and Experiment	3504.250												90%	1	7
Emergent Behavior of Large Swarms of Intelligent Agents	3504.260	1											100%	1	7
Parallel Combinatorial Optimization for Scheduling Problems	3504.270		1										82%	2	7
Programming Paradigms for Massively Parallel Computers	3504.280												80%	3	7
Multilevel Techniques for Unstructured Grid Problems on Massively Parallel Computers	3504.290		3										90%	2	7
Scalable Tools for Massively Parallel Distributed Computing	3504.310	2	1					1					100%	1	7
Massively Parallel Methods for Simulating the Phase Field Model	3504.320								1				100%	1	6

		Performance Statistics (Number of)											Project Qualitative Assessment		
Project Title	Project #	Refereed Publications	All Other Reports and Publications	Patent Disclosures	Patent Applications	Patents	Copyrights	Students	Post-docs	Permanent Staff Hired*	Awards	New Non-LDRD-Funded Projects†	% Milestones Completed	Goals Status**	Hypotheses Status***
Visual Explanation and Insight	3504.330	1		2	2		1			1			100%	1	7
Wafer Fusion for Integration of Semiconductor Materials and Devices	3506.110	3						1					80%	2	7
Highly Parallel, Low-Power, Photonic Interconnects for Inter-Board Signal Distribution	3506.120		1										85%	2	6
Virtual Reactor for the Semiconductor Manufacturing Plant of the Future	3506.140	1											100%	1	7
Selective Oxidation Technology and Its Applications Toward Electronic and Optoelectronic Devices	3506.160	16	4										80%	2	6
Agile Prototyping of Microelectromechanical Systems (MEMS)	3506.180	2											95%	1	6
Advanced Concepts for High-Power VCSELs and VCSEL Arrays	3506.190	10	1			1							100%	1	6
Midwave-Infrared (2-6 µm) Emitter–Based Chemical Sensor Systems	3506.210	2									1	1	80%	2	7
A Novel Nondestructive Silicon-on-Insulator Nonvolatile Memory	3506.230	7	2	1							3		100%	3	7
Integration of Optoelectronics and MEMS by Free-Space Microoptics	3506.240		2	1				1	1			1	75%	2	7
Advanced Laser Structures for Short-Pulsed Power in Active Optical Sensor Systems	3506.250	2		2	1			1					85%	2	8
Metal Micro-Heat-Pipe Substrates for High-Power-Density Electronics	3506.260	2	2	1	1	1						1	100%	1	6
Integration of Microsensor Technology into a Miniature Robotic Vehicle	3506.270	1								1			100%	1	7
Vacuum Encapsulation of MEMS Structures	3506.280			2		2				1	1		100%	1	7
Massively Parallel Sensor Arrays for Volatile Organic Detection	3506.290							1				1	80%	2	6
Agile Dry Etching of Compound Semiconductors for Science–Based Manufacturing Using *In Situ* Process Control	3506.310												100%	1	7
Precision-Formed Micromagnets	3506.320		1		1			2					80%	2	7
Time-Resolved Ion-Beam–Induced Charge-Collection (TRIBICC) Imaging	3506.330	1	1										90%	2	7
Composite-Resonator Surface-Emitting Lasers	3506.340	2	1						1				80%	2	7
Role of Defects in III-Nitride–Based Electronics	3506.350	9											90%	1	7
Ultra–Low-Power Sensors for Microtelemetry Systems	3506.360	1		1				1	1			1	90%	2	7
Double Quantum-Well Long-Wavelength Optoelectronic Devices	3506.370	3	1	1	1			2	1				60%	3	8

		Performance Statistics (Number of)											Project Qualitative Assessment		
Project Title	Project #	Refereed Publications	All Other Reports and Publications	Patent Disclosures	Patent Applications	Patents	Copyrights	Students	Post-docs	Permanent Staff Hired*	Awards	New Non-LDRD-Funded Projects†	% Milestones Completed	Goals Status**	Hypotheses Status***
The Development of Integrated Chemical Microsensors in GaAs	3506.380		1	1									100%	1	7
Monolithic Integrated of VCSELs and Detectors for Microsystems	3506.410	6	1					1	1			4	100%	1	7
AlGaN Materials Engineering for Integrated Multifunction Systems	3506.420	4											90%	2	6
Compliant Substrates for Epitaxial Integration of Dissimilar Materials	3506.430												50%	3	7
Post-Processed Integrated Microsystems	3506.440	1											35%	2	7
Using Higher-Order Gradients to Modeling Localization Phenomena	3508.040		6						1				90%	2	6
Enhanced Vapor-Phase Diffusion in Porous Media	3508.060	7	3									1	100%	1	6
Stress Evaluation and Model Validation Using Laser Ultrasonics	3508.110	6				1		2					95%	2	6
Altered Simulation Properties for Tetrahedral Finite Elements for Use in Engineering Simulation	3508.120	4											100%	2	6
Development, Implementation, and Experimental Validation of the Lattice Boltzmann Method for Modeling Three-Dimensional Complex Flows	3508.130	6	12				1	3	2	1		3	100%	1	6
Capturing Recrystallization of Metals with a Multiscale Material Model	3508.140	6	16					1	2				80%	2	7
Nondeterministic Modeling in Engineering Science	3508.150		2										90%	2	7
Lagrangian Modeling of Radiative Transport	3508.160	3						1					90%	2	7
High-Resolution Modeling of Multiscale Transient Phenomena in Turbulent Boundary Layers	3508.170								3				100%	1	7
Dispersive Measurements of Velocity in Heterogeneous Materials	3508.180									1			100%	1	6
A Physically–Based Computational Method for Predicting Generalized Fracture	3508.190									1		1	100%	2	7
Development of *In Situ* Diagnostics for Simultaneous Measurement of Transient Gas Species and Soot in Large Fires	3508.210		1						1				80%	2	7
Micromechanical Failure Analyses for Finite-Element Polymer Modeling	3508.220												95%	1	7
Methodology Optimal Selection of Test and Simulation Levels for Problems Involving Computational Simulation	3508.230	2											90%	2	7
A Phenomenological Model for Multicomponent Transport with Electrochemical Reactions in Concentrated Solutions	3508.240												85%	2	7

		Performance Statistics (Number of)											Project Qualitative Assessment		
Project Title	Project #	Refereed Publications	All Other Reports and Publications	Patent Disclosures	Patent Applications	Patents	Copyrights	Students	Post-docs	Permanent Staff Hired*	Awards	New Non-LDRD-Funded Projects†	% Milestones Completed	Goals Status**	Hypotheses Status***
Laser-Spray Fabrication for Net-Shape Rapid Product Realization	3510.460	5	2	4		1		2	1	1		3	95%	1	6
Solution Synthesis and Processing of PZT Materials for Neutron-Generator Applications	3510.510	1	1	1	1							1	100%	1	6
Ultra-Precise Assembly of Microelectromechanical Systems (MEMS)	3510.540	4	2					1				1	100%	1	6
Finite-Element Meshing Approached as a Global Minimization Process	3510.570	1		1				1	1				75%	3	8
Application of Parallel Mechanism Technology to Manufacturing	3510.580			2	5			4			2	1	95%	1	7
Investigation of the Impact of Cleaning on Adhesive Bond and the Process Implications	3510.590	2	2					5			1	1	100%	1	7
Standard Cells for Microelectromechanical Systems (MEMS)	3510.610	3			1		1	2			1		100%	2	7
Laser Wire Deposition for Fully Dense Shapes	3510.620	1	2	1	1				1	1			100%	2	9
High-Throughput Dry Processes for Large-Area Devices	3510.630		2	2	2								80%	3	7
Assuring High Reliability and Production Readiness in Low-Volume Manufacturing	3510.640	1						1					90%	2	6
Scripting for Video Inspection	3510.660											1	90%	4	8
Advanced Machining Processes for Microfabrication	3510.670							1				1	95%	2	7
Fusion of Product and Process Data Using Real-Time Streaming Visualization	3510.680												90%	2	7
Advanced Production Planning Models	3510.690		1							1		1	100%	1	7
Automatic Generation of Multimedia Documentation for Assembly Operations	3511.010							1					100%	2	6
Distributed Life-Cycle Models in Enterprise Simulations to Answer System Questions	3511.020	1											100%	1	6
Immersive CAD	3511.040		1										70%	2	6
Automatic Planning of Life-Cycle Assembly Processes	3511.050	3	8		1		1				1		100%	2	7
Analysis of Very Large Assemblies	3511.070												100%	1	7
Enabling Human Skills with Cooperative Automation	3511.080												100%	1	7
Cloud To CAD	3511.090											1	100%	1	7
Ergonomics in Life-Cycle Assembly Processes	3511.110												80%	3	7
Feature Reduction of Geometric Solid Models for Analysis Tools	3511.120												100%	2	7
System Surety Life-Cycle Engineering	3511.130												100%	2	7
Content–Based Search of Geometric Databases	3512.160		1				1			1			80%	2	7

		Performance Statistics (Number of)											Project Qualitative Assessment		
Project Title	Project #	Refereed Publications	All Other Reports and Publications	Patent Disclosures	Patent Applications	Patents	Copyrights	Students	Post-docs	Permanent Staff Hired*	Awards	New Non-LDRD-Funded Projects†	% Milestones Completed	Goals Status**	Hypotheses Status***
Integrated Service Provisioning in an "IPv6 over ATM" Research Network	3512.170		2		2								100%	4	6
Virtual Desktop Engineering with Integrated Multimedia Data	3512.180											2	80%	2	9
Mission Surety for Large-Scale Real-Time Information Systems	3512.190	2			1			1			1		100%	1	6
Scaled ATM End-to-End Encryption	3512.220	1		3							1		90%	2	7
Network Surety Modeling for Wireless ATM Networks	3512.230	1	3										95%	1	7
Low-Power, Reduced-Computation, Public-Key Protocols	3512.240												90%	2	7
Ten-to-One-Hundred-Gigabit/Second Network Enabling R&D	3512.250			1				1					100%	2	7
High-Performance Commodity Interconnects for Clustered Scientific and Engineering Computing	3512.260		1										100%	2	7
AVATAR—Navigating and Mining in Massive Data	3512.270	2						2					90%	1	7
Algorithm–Based Fault Tolerance on Heterogeneous Massively Parallel Computers	3512.280												90%	2	7
Electrokinetic Immunoaffinity Chemical Sensors	3516.050	1						1	1	1			85%	2	7
Information Efficient Spectral Imaging System (ISIS)	3516.060		4	1	1			3				1	100%	1	6
Imaging of Moving Targets Using Simultaneous Synthetic Aperture Radar (SAR) and Moving Target Indicator (MTI) Radar	3516.070												100%	1	7
Sampling and Sensing Systems for High-Priority Analytes	3516.080	2							1			1	80%	2	6
Automated Vegetation Height Measurement for Automatic Terrain Mapping	3516.090		1									1	50%	3	7
Sparse Geophysical Networks for Monitoring Deep Targets	3516.110												100%	1	7
Miniature Bioaerosol Concentrator	3516.120			1									90%	2	7
Recognizing Partially Obscured Targets by Combining Multiple Data Sources Using Evidential Reasoning	3516.130		3										95%	1	7
Computational Engineering of Sensor Materials and Integration with a Novel Biological Weapon Detection System	3516.140	1					1	1					100%	2	7
Biological Weapon Detector Using Bioaffinity Array Impedance Analysis with Chemical Amplification Through Redox Recycling	3516.150								1				95%	2	7
ATR / Exploitation Utilizing Ultra–High-Resolution, Complex SAR Imaging	3516.160												98%	2	7

		Performance Statistics (Number of)											Project Qualitative Assessment		
Project Title	Project #	Refereed Publications	All Other Reports and Publications	Patent Disclosures	Patent Applications	Patents	Copyrights	Students	Post-docs	Permanent Staff Hired*	Awards	New Non-LDRD-Funded Projects†	% Milestones Completed	Goals Status**	Hypotheses Status***
Designed Molecular Recognition Materials for Chiral Sensors, Separations, and Catalytic Materials	3518.030	9			1			2	1			1	95%	1	6
Rapid Screening of Complex Chemical Samples Via Capillary Array Analysis	3518.050		5					1	1				80%	2	6
Designed Synthesis of Controlled Degradative Materials	3518.060												100%	1	8
Mechanistic Models for Radionuclide Desorption from Soils	3518.070	6										1	100%	1	7
Development of Innovative Combustion Processes for a Direct-Injection Diesel Engine	3518.080		3						1			3	100%	1	7
Hydrogen Production for Fuel Cells by Selective Dehydrogenation of Alkanes in Catalytic Membrane Reactors	3518.090	3						1	1				50%	3	8
Hybrid Vehicle Engine Development	3518.110	4	1	1	1			3				1	90%	2	7
Adaptive 3-D Sensing	3518.120									5			100%	1	7
Aqueous Organic Sensor	3518.130								1	2			100%	1	7
Designed Ionophores for Liquid-Membrane Separation and Extraction of Metal Ions	3518.140	1	1					2	1				90%	2	6
An Electromagnetic Imaging System for Environmental Site Reconnaissance	3518.150		1									1	100%	1	7
Reliability Degradation Due to Stockpile Aging	3520.210	2	1									1	100%	1	6
Integrated Approach to Develop Microelectromechanical (MEMS) Reliability Tools	3520.220	1	6				1						78%	2	7
Precursors to Failure of Oxides and Metal Lines in CMOS Technology	3520.230									2			30%	3	9
An Extensible Object-Oriented Framework for Risk & Reliability Analysis	3520.240	2						1					75%	3	6
Simulation/Optimization Tools for System Variability Analysis	3520.270												75%	2	7
A Massively Parallel Microsimulation Model of Infrastructure Interdependency	3520.280		1					5		1		3	90%	1	7
Physical Models for Predicting the Effect of Atmospheric Corrosion on Microelectronic Reliability	3520.290		1					2					90%	2	7
Backside Localization of Open and Shorted IC (Integrated Circuits) Interconnections	3520.310	2	1		1					4		1	100%	1	6
Reliability Predictions for Advanced Electronics in Smoke Environments	3520.320	1						1				1	80%	3	8
Security of Bulk Power Systems	3520.330												50%	3	7
Science on the Microdomain	3522.010			7	2					1	1		90%	2	6
Autonomous MicroChem Laboratory (µChemLab)	3522.020	26		5	3	1		6	6	3		5	90%	2	7

		Performance Statistics (Number of)											Project Qualitative Assessment		
Project Title	Project #	Refereed Publications	All Other Reports and Publications	Patent Disclosures	Patent Applications	Patents	Copyrights	Students	Post-docs	Permanent Staff Hired*	Awards	New Non-LDRD-Funded Projects†	% Milestones Completed	Goals Status**	Hypotheses Status***
Cooperative, Distributed Sensing and Action Using Microminiature, Intelligent Agents	3522.030											5	100%	1	7
Computational Methods for Predicting the Response of Critical As-Built Infrastructure to Dynamic Loads (Architectural Surety)	3530.030		2										80%	2	7
Background Radiation Anisotropy Measurement Sensor (BRAMS)	3530.050		1					2	1				70%	2	8
Exploitation of Satellite Communications Systems and Networks for Intelligence Applications	3530.090											2	100%	1	6
Microcode Evaluation	3530.110												100%	2	7
Real-Time Image Analysis Using Field Programmable Gate Arrays	3530.120		1						1	1		1	80%	2	8
Advanced 3-D Sensing and Visualization System for Unattended Monitoring	3530.130							2				2	100%	1	6
System-of-Labs Direct Fabrication Technology	3531.020	4	1									2	75%	2	8
Poco Switch Tubes	3531.140												50%	2	6
Chemiresistors Based on Metal-Loaded Polymers for Solvent Spill Detection	3531.150												100%	1	7
Advanced Neutron-Tube Design and Producibility	3531.160												70%	3	7
Surface Hardening by Nanoparticle Precipitation and Atomic Clustering in Ni(Al,O)	3531.170												100%	1	6
Dynamical Properties of Polymers; Computational Modeling	3531.180							1					100%	1	7
Broadening Mechanism in 2-D Excitonic and Electron Gases	3531.190												100%	1	7
Calculation and Interpretation of the Energies That Underlie Transition-Metal Surface Structure	3531.210	1	1						1				100%	3	7
Interfacial Reactions in Ceramic Systems	3531.220	1	1					1					90%	2	7
Direct Fabrication of Multifunctional Nanocomposites Via Supramolecular Self-Assembly	3531.230	1	1					1	1				90%	1	6
Biophotonic Materials for Optical Encryption and Noncomputing	3531.240	1	3		1			1					90%	2	6
Low-Stress Amorphous Diamond: A New Material for Sensors	3531.250		1					1					100%	1	6
Nanoengineered Cu-Al Defects in Al: A Prototype System for Corrosion	3531.260												70%	2	7
Novel Energy Conversion Devices of Icosahedral Borides	3531.270		1									1	100%	1	7
Ion-Mobility Spectroscopy of Biological Materials	3531.280	1						1					100%	1	7

		Performance Statistics (Number of)											Project Qualitative Assessment		
Project Title	Project #	Refereed Publications	All Other Reports and Publications	Patent Disclosures	Patent Applications	Patents	Copyrights	Students	Post-docs	Permanent Staff Hired*	Awards	New Non-LDRD-Funded Projects†	% Milestones Completed	Goals Status**	Hypotheses Status***
Visualization Tools for MEMS Designs in a Virtual 3-D World	3531.290			1			1						100%	1	6
Direct Fabrication of Planar Solid Oxide Fuel Cells	3531.310												100%	1	6
Micromachining with Ultra-Short Pulsewidth Lasers	3531.320		1										90%	2	6
Molecular Characterization of Energetic Material Initiation	3531.330	1								1			100%	1	7
Chemical Feedstocks for the Future: Oxidative Dehydrogenation	3532.010	2	2									2	100%	1	7
Global Approaches to Infrastructural Analysis (GAIA)	3532.030												100%	1	7
Engineering Complex Distributed Systems	3532.070	10	4	3						1			80%	2	7
Laser Communication Nanosatellites	3532.080	1	1	6								3	90%	2	7
Collection and Data Synthesis of Atmospheric Explosion Ground Truth for Global Monitoring Systems	3532.090		1										80%	2	7
Advanced Radiation Sources: Rayleigh-Taylor Mitigation Via Perturbation Reduction	3532.110							1				1	90%	2	7
Microfluidic Engineering	3532.120			6	3								100%	1	6
Accelerator Technologies for Emerging Threats	3532.130											1	100%	1	7
Technologies for System-Level Innovations in Ballistic Missile Defense	3532.140	1											100%	2	7
InGaAsN: A Novel Material for High-Efficiency Solar Cells and Advanced Photonic Devices	3532.150	2	1									2	100%	1	7
Technologies for Countering C/B Terrorism	3532.160											2	100%	1	6
Aerosol Stand-Off Detection Test-Bed	3532.170	1	2	1									100%	1	7
Design and Optimization of High-Power Electromagnetic Source Systems and Engagement Scenarios for Achieving Functional Upset or Damage in Specific Target Electronic Systems	3532.180		1										100%	1	7
Real-Time Design of Improved Powder Pressing Dies Using Finite-Element Method Modeling	3532.190				1		1						80%	2	6
Development of Fiber-Laser-Based LIF for Detection of SO_2	3532.210		1										75%	2	7
Penetration and Defeat of Hardened Underground Facilities Using a Microhole Drilling Robot	3532.220		1										100%	1	6
IFSAR Tree Phenomenology and Coherence Normalization	3532.230		1									1	50%	4	9
Electric Launcher for Defense Applications	3532.240		1									1	100%	1	6
SAM Telemetry for Measurements While Drilling	3533.050		1	3	1								100%	1	7

		Performance Statistics (Number of)											Project Qualitative Assessment		
Project Title	Project #	Refereed Publications	All Other Reports and Publications	Patent Disclosures	Patent Applications	Patents	Copyrights	Students	Post-docs	Permanent Staff Hired*	Awards	New Non-LDRD-Funded Projects†	% Milestones Completed	Goals Status**	Hypotheses Status***
Design-for-Manufacturability Applied to Photovoltaic Modules	3533.070	1		2	2								100%	1	6
Advanced Geosphere Transport Simulation	3533.160	2	2							1		1	90%	2	7
Low-Work-Function Thermionic Emission Materials	3533.170	1										2	75%	2	7
Power-Grid Reliability and Restructuring Policy Changes	3533.180	1	1										100%	1	6
Low-Cost Cadmium Zinc Telluride Radiation Detectors Based on Electron-Transport-Only Designs	3534.020	1		4	2		1	3	1			1	100%	1	6
LIGA Micromachining	3534.030	1						2			2		90%	1	6
Applied Microfluidics Science	3534.040						1	1					80%	2	7
Computational Simulations of Self-Assembling Macro-Systems by Direct Fabrication of Microscopic Structured Materials	3535.130	1						1	1			1	30%	1	9
Self-Stabilizing Optical Solitons and High-Intensity Laser Plasma Channels for Diffraction-Free Propagation and Robust Power Compression	3535.140	2						1		2			100%	2	6
Novel Materials for Hydrogen Storage	3535.150		1										50%	3	8
Optical Communication System for Remote Monitoring and Adaptive Control of Distributed Ground Sensors Exhibiting Collective Intelligence	3535.160		7	2				1	1	5		4	90%	1	6
Inversion of Passive Electromagnetic Fields to Locate Weapons of Mass Destruction	3535.170	1	1							2		1	90%	2	6
Z-Pinch-Driven Isentropic Compression	3535.180	1											75%	3	7
Covert, Distributed Biosensors for UXO/CW Based on Amplified Immunoassays Conducted in Porous Inorganic Media	3535.190	1						2	1				80%	2	7
Semiconductor Filament Lasers	3535.210				1							1	90%	1	6
Development of Membrane Devices Using AlN and SiC Films	3537.010							1					50%	3	7
Spectral Information Content in Ion-Mobility Spectra for Explosives, Interferants, and Other Negative-Ionizing Chemicals	3537.020							1					70%	3	7
Magnetic-Field Profile Measurements in Wire-Array Z-Pinches by Faraday Rotation	3537.030		1										100%	1	7
Picosecond Particle Velocity Measurements	3537.040									2			95%	1	6
Particle-Level Modeling of Flows of Concentrated Suspensions	3537.050		1					1					100%	1	6
Efficient Processing of Materials Microstructures with Intelligent Feature Extraction for Quantitative Stereology	3537.060	1						1					100%	1	7

		Performance Statistics (Number of)											Project Qualitative Assessment		
Project Title	Project #	Refereed Publications	All Other Reports and Publications	Patent Disclosures	Patent Applications	Patents	Copyrights	Students	Post-docs	Permanent Staff Hired*	Awards	New Non-LDRD-Funded Projects†	% Milestones Completed	Goals Status**	Hypotheses Status***
Nondestructive Evaluation of Wind Turbine Blades	3537.070		1					1	1				100%	1	7
Very Small Arrays: Designing Self-Assembled Systems of Light-Antennae and Reaction Centers for Artificial Photosynthesis	3537.080	1	1					1					100%	1	6
Enzyme-Mediated Electrochemical Redox Polymer Biosensor for V- and G-Type Chemical Weapons	3537.110			1									100%	1	6
Novel Biosensor Fabrication Techniques	3537.120												75%	3	7
Design for 100-Year-Life Prototype	3537.130							1					100%	1	7
Enhancing Multilevel Linear Equation Solvers Using Domain Decomposition Strategies	3537.140												100%	1	6
In Situ and *Ex Situ* Investigations of Lateral Composition	3537.150	1						1					75%	3	8
Approximate Methods for Computing Eigensolutions Using Automated Multilevel Substructuring	3537.160												100%	1	6
Living Tissue Engineering	3537.170												100%	1	8
		407	223	79	48	7	12	124	58	51	16	87			

† Identification of new non-LDRD-funded projects is now completed in the fiscal year following the annual report.

Pg #	Title	Case Number	Science of Complex Systems	Modeling & Simulation of Complex Systems	High-Performance Computing	Nuclear Weapons Predictive Capability (Classified)	Safety Assessments & Engineering	Use Control & Verification	Nonproliferation & Verification	Dynamic Testing in Severe Environments	High-Energy-Density Materials	Laser Technology	Pulsed Power and Accelerators	Microelectronics and Photonics	Nuclear Materials	Engineered Materials	Flexible Manufacturing	Environmentally Conscious Manufacturing	Intelligent Machines and Robotics	Waste Management	Other
10	Catalytic Membrane Sensors	3502.030															•				•
9	Photonic Bandgap Structures as a Gateway to Nanophotonics	3502.040			•			•	•			•		•		•					
10	Wide-Bandgap Compound Semiconductors to Enable Novel Semiconductor Devices	3502.050	•	•	•				•			•		•							
12	Ultra-Hard Multilayer Coatings	3502.080			•					•				•		•					
14	Scanning Probe–Based Processes for Nanometer-Scale Device Fabrication	3502.090												•							
15	Molecular-Scale Lubricants for Micromachine Applications	3502.110												•		•					
16	Surface-Micromachined Flexural Plate-Wave Device Integrated on Silicon	3502.120							•		•			•							
17	Smart Interface Bonding Alloys (SIBA): Tailoring Thin-Film Mechanical Properties	3502.140	•													•					
20	Recognizing Atoms in Atomically Engineered Nanostructures: An Interdisciplinary Approach	3502.170												•		•					
18	Molecular-to-Continuum Fracture Analysis of Thermoset Polymer/Solid Interfaces	3502.190	•	•	•	•								•		•					
19	Monolithic Structures for Nanoseparation	3502.210	•	•		•	•	•	•	•	•				•	•	•	•	•		
21	Fundamental Aspects of Micromachine Reliability	3502.220														•			•		
24	Enabling Science and Technology for Cold-Spray Direct Fabrication	3502.230		•								•		•		•	•	•			•
22	Atomic-Level Studies of Surfactant-Directed Materials Growth	3502.240												•		•					
26	Intelligent Polymers for Nanodevice Performance Control	3502.250						•								•					
25	Freeforming of Ceramics and Composites from Colloidal Slurries	3502.260	•	•												•	•				

Pg #	Title	Case Number	Science of Complex Systems	Modeling & Simulation of Complex Systems	High-Performance Computing	Nuclear Weapons Predictive Capability (Classified)	Safety Assessments & Engineering	Use Control & Verification	Nonproliferation & Verification	Dynamic Testing in Severe Environments	High-Energy-Density Materials	Laser Technology	Pulsed Power and Accelerators	Microelectronics and Photonics	Nuclear Materials	Engineered Materials	Flexible Manufacturing	Environmentally Conscious Manufacturing	Intelligent Machines and Robotics	Waste Management	Other
26	Quantum Dot Arrays	3502.270														•					
27	Laser-Assisted Arc Welding for Aluminum Alloys	3502.280										•				•	•				
28	Reactivity of Metal Oxide Surfaces	3502.310			•											•					
29	Exploiting LENS Technology Through Novel Materials	3502.320										•				•	•		•		
34	Parallel Quantum Chemistry for Material Aging and Synthesis	3504.010				•					•					•					
34	Modeling Complex Turbulent Chemically Reacting Flows on Massively Parallel Supercomputers	3504.020	•	•	•				•					•		•		•			
35	Automated Geometric Model Builder Using Range Image Sensor Data	3504.050		•	•				•			•							•		
36	A Massively Parallel Sparse Eigensolver for Structural Dynamics Finite Element	3504.060	•	•	•	•			•								•		•		
36	Density-Functional Theory for Classical Fluids at Complex Interfaces	3504.070	•	•												•					
33	Gradient-Driven Diffusion of Multi-Atom Molecules Through Macromolecules and Membranes	3504.090		•	•						•					•	•	•			
38	Fast and Easy Parallel I/O for Efficient Scientific Computing	3504.120		•	•																
38	Novel Load-Balancing for Scalable, Parallel Electromagnetic and Plasma Physics Simulation Software	3504.130		•	•	•						•	•	•							
40	Parallel Computational Chemistry Using Constraints	3504.140		•	•											•					
40	Massively Parallel *Ab Initio* Validation for ASCI Materials Aging	3504.160			•	•										•					
42	Computational Methods for Coupling Microstructural and Micromechanical Materials Response Simulations	3504.170	•	•										•		•	•				

Pg #	Title	Case Number	Science of Complex Systems	Modeling & Simulation of Complex Systems	High-Performance Computing	Nuclear Weapons Predictive Capability (Classified)	Safety Assessments & Engineering	Use Control & Verification	Nonproliferation & Verification	Dynamic Testing in Severe Environments	High-Energy-Density Materials	Laser Technology	Pulsed Power and Accelerators	Microelectronics and Photonics	Nuclear Materials	Engineered Materials	Flexible Manufacturing	Environmentally Conscious Manufacturing	Intelligent Machines and Robotics	Waste Management	Other
44	An Investigation of Wavelet Bases for Multiscale, Grid–Based Simulation	3504.180	•	•	•	•	•														
41	Integrated Quantum/Classical Modeling of Hydrogenic Materials	3504.190	•	•	•											•					
45	The Next Generation of Teraflop Density-Functional Electronic Structure Codes	3504.210		•	•																
46	Methodology for Characterizing Modeling and Discretization Uncertainties in Computational Simulation	3504.220	•	•	•			•	•								•		•		
48	Global Optimization for Engineering Science Problems	3504.230	•	•	•		•		•							•	•		•		
49	Dynamic Simulation of Mechanical Systems with Intermittent Contacts	3504.240	•	•			•										•		•		
43	From Atom-Picoseconds to Centimeter-Years in Simulation and Experiment	3504.250	•	•	•	•								•		•					
47	Emergent Behavior of Large Swarms of Intelligent Agents	3504.260	•	•					•										•		
50	Parallel Combinatorial Optimization for Scheduling Problems	3504.270			•												•				
50	Programming Paradigms for Massively Parallel Computers	3504.280	•	•	•																
51	Multilevel Techniques for Unstructured Grid Problems on Massively Parallel Computers	3504.290		•	•																
52	Scalable Tools for Massively Parallel Distributed Computing	3504.310			•																
52	Massively Parallel Methods for Simulating the Phase Field Model	3504.320		•	•																
53	Visual Explanation and Insight	3504.330	•	•					•												
58	Wafer Fusion for Integration of Semiconductor Materials and Devices	3506.110			•			•	•			•		•							

Pg #	Title	Case Number	Science of Complex Systems	Modeling & Simulation of Complex Systems	High-Performance Computing	Nuclear Weapons Predictive Capability (Classified)	Safety Assessments & Engineering	Use Control & Verification	Nonproliferation & Verification	Dynamic Testing in Severe Environments	High-Energy-Density Materials	Laser Technology	Pulsed Power and Accelerators	Microelectronics and Photonics	Nuclear Materials	Engineered Materials	Flexible Manufacturing	Environmentally Conscious Manufacturing	Intelligent Machines and Robotics	Waste Management	Other
58	Highly Parallel, Low-Power, Photonic Interconnects for Inter-Board Signal Distribution	3506.120			•			•				•		•							
59	Virtual Reactor for the Semiconductor Manufacturing Plant of the Future	3506.140												•		•	•				
60	Selective Oxidation Technology and Its Applications Toward Electronic and Optoelectronic Devices	3506.160			•			•	•			•		•							
61	Agile Prototyping of Microelectromechanical Systems (MEMS)	3506.180						•	•				•	•					•		
57	Advanced Concepts for High-Power VCSELs and VCSEL Arrays	3506.190			•			•	•			•		•							
62	Midwave-Infrared (2–6 µm) Emitter–Based Chemical Sensor Systems	3506.210			•			•	•			•		•							
62	A Novel Nondestructive Silicon-on-Insulator Nonvolatile Memory	3506.230			•									•							
64	Integration of Optoelectronics and MEMS by Free-Space Microoptics	3506.240			•			•	•			•		•							
65	Advanced Laser Structures for Short-Pulsed Power in Active Optical Sensor Systems	3506.250						•				•		•							
66	Metal Micro-Heat-Pipe Substrates for High-Power-Density Electronics	3506.260												•							
68	Integration of Microsensor Technology into a Miniature Robotic Vehicle	3506.270	•						•					•					•		
66	Vacuum Encapsulation of MEMS Structures	3506.280						•	•	•				•		•			•		
67	Massively Parallel Sensor Arrays for Volatile Organic Detection	3506.290							•					•							
70	Agile Dry Etching of Compound Semiconductors for Science–Based Manufacturing Using *In Situ* Process Control	3506.310												•			•				
68	Precision-Formed Micromagnets	3506.320	•					•						•		•					

Pg #	Title	Case Number	Science of Complex Systems	Modeling & Simulation of Complex Systems	High-Performance Computing	Nuclear Weapons Predictive Capability (Classified)	Safety Assessments & Engineering	Use Control & Verification	Nonproliferation & Verification	Dynamic Testing in Severe Environments	High-Energy-Density Materials	Laser Technology	Pulsed Power and Accelerators	Microelectronics and Photonics	Nuclear Materials	Engineered Materials	Flexible Manufacturing	Environmentally Conscious Manufacturing	Intelligent Machines and Robotics	Waste Management	Other
70	Time-Resolved Ion-Beam–Induced Charge-Collection (TRIBICC) Imaging	3506.330												•							
74	Composite-Resonator Surface-Emitting Lasers	3506.340										•		•							
73	Role of Defects in III-Nitride–Based Electronics	3506.350										•		•							
74	Ultra–Low-Power Sensors for Microtelemetry Systems	3506.360						•	•					•					•		
72	Double Quantum-Well Long-Wavelength Optoelectronic Devices	3506.370			•			•	•			•		•							
75	The Development of Integrated Chemical Microsensors in GaAs	3506.380							•					•					•		
76	Monolithic Integrated of VCSELs and Detectors for Microsystems	3506.410			•			•	•			•		•							
77	AlGaN Materials Engineering for Integrated Multifunction Systems	3506.420	•									•		•							
71	Compliant Substrates for Epitaxial Integration of Dissimilar Materials	3506.430										•		•			•				
78	Post-Processed Integrated Microsystems	3506.440							•					•			•		•		
83	Using Higher-Order Gradients to Modeling Localization Phenomena	3508.040	•	•	•	•	•			•					•	•	•				
81	Enhanced Vapor-Phase Diffusion in Porous Media	3508.060	•	•																	
82	Stress Evaluation and Model Validation Using Laser Ultrasonics	3508.110	•	•		•	•			•	•	•		•	•		•				
84	Altered Simulation Properties for Tetrahedral Finite Elements for Use in Engineering Simulation	3508.120		•	•	•	•	•	•								•				
84	Development, Implementation, and Experimental Validation of the Lattice Boltzmann Method for Modeling Three-Dimensional Complex Flows	3508.130	•	•	•		•		•							•					

Pg #	Title	Case Number	Science of Complex Systems	Modeling & Simulation of Complex Systems	High-Performance Computing	Nuclear Weapons Predictive Capability (Classified)	Safety Assessments & Engineering	Use Control & Verification	Nonproliferation & Verification	Dynamic Testing in Severe Environments	High-Energy-Density Materials	Laser Technology	Pulsed Power and Accelerators	Microelectronics and Photonics	Nuclear Materials	Engineered Materials	Flexible Manufacturing	Environmentally Conscious Manufacturing	Intelligent Machines and Robotics	Waste Management	Other
86	Capturing Recrystallization of Metals with a Multiscale Material Model	3508.140	•	•	•	•	•			•					•	•	•			•	
88	Nondeterministic Modeling in Engineering Science	3508.150	•	•	•			•	•								•		•		
88	Lagrangian Modeling of Radiative Transport	3508.160	•	•	•		•														
89	High-Resolution Modeling of Multiscale Transient Phenomena in Turbulent Boundary Layers	3508.170		•			•														
90	Dispersive Measurements of Velocity in Heterogeneous Materials	3508.180	•	•	•											•					
90	A Physically–Based Computational Method for Predicting Generalized Fracture	3508.190		•	•		•									•					
92	Development of *In Situ* Diagnostics for Simultaneous Measurement of Transient Gas Species and Soot in Large Fires	3508.210	•	•			•					•		•							
91	Micromechanical Failure Analyses for Finite-Element Polymer Modeling	3508.220		•		•	•	•						•		•	•				
94	Methodology Optimal Selection of Test and Simulation Levels for Problems Involving Computational Simulation	3508.230	•	•	•	•	•														
93	A Phenomenological Model for Multicomponent Transport with Electrochemical Reactions in Concentrated Solutions	3508.240	•	•			•							•		•	•				
98	Laser-Spray Fabrication for Net-Shape Rapid Product Realization	3510.460	•	•	•			•				•				•	•	•	•		
99	Solution Synthesis and Processing of PZT Materials for Neutron-Generator Applications	3510.510		•										•							
97	Ultra-Precise Assembly of Microelectromechanical Systems (MEMS)	3510.540												•			•		•		
100	Finite-Element Meshing Approached as a Global Minimization Process	3510.570	•	•	•	•	•									•	•				

Pg #	Title	Case Number	Science of Complex Systems	Modeling & Simulation of Complex Systems	High-Performance Computing	Nuclear Weapons Predictive Capability (Classified)	Safety Assessments & Engineering	Use Control & Verification	Nonproliferation & Verification	Dynamic Testing in Severe Environments	High-Energy-Density Materials	Laser Technology	Pulsed Power and Accelerators	Microelectronics and Photonics	Nuclear Materials	Engineered Materials	Flexible Manufacturing	Environmentally Conscious Manufacturing	Intelligent Machines and Robotics	Waste Management	Other
102	Application of Parallel Mechanism Technology to Manufacturing	3510.580	•	•												•	•	•	•		•
100	Investigation of the Impact of Cleaning on Adhesive Bond and the Process Implications	3510.590	•	•													•	•			
102	Standard Cells for Microelectromechanical Systems (MEMS)	3510.610						•						•							
104	Laser Wire Deposition for Fully Dense Shapes	3510.620		•												•	•	•			
105	High-Throughput Dry Processes for Large-Area Devices	3510.630		•										•				•			
106	Assuring High Reliability and Production Readiness in Low-Volume Manufacturing	3510.640		•			•										•				
103	Scripting for Video Inspection	3510.660		•													•		•		
106	Advanced Machining Processes for Microfabrication	3510.670										•				•	•				
107	Fusion of Product and Process Data Using Real-Time Streaming Visualization	3510.680		•													•		•		
108	Advanced Production Planning Models	3510.690		•	•				•								•				
112	Automatic Generation of Multimedia Documentation for Assembly Operations	3511.010		•													•		•		
113	Distributed Life-Cycle Models in Enterprise Simulations to Answer System Questions	3511.020	•	•	•	•															
114	Immersive CAD	3511.040	•	•	•														•		
114	Automatic Planning of Life-Cycle Assembly Processes	3511.050		•													•	•	•		
116	Analysis of Very Large Assemblies	3511.070	•	•													•	•	•		
111	Enabling Human Skills with Cooperative Automation	3511.080		•													•		•		

Pg #	Title	Case Number	Science of Complex Systems	Modeling & Simulation of Complex Systems	High-Performance Computing	Nuclear Weapons Predictive Capability (Classified)	Safety Assessments & Engineering	Use Control & Verification	Nonproliferation & Verification	Dynamic Testing in Severe Environments	High-Energy-Density Materials	Laser Technology	Pulsed Power and Accelerators	Microelectronics and Photonics	Nuclear Materials	Engineered Materials	Flexible Manufacturing	Environmentally Conscious Manufacturing	Intelligent Machines and Robotics	Waste Management	Other
116	Cloud To CAD	3511.090		•	•												•		•		
118	Ergonomics in Life-Cycle Assembly Processes	3511.110		•			•										•		•		
117	Feature Reduction of Geometric Solid Models for Analysis Tools	3511.120	•	•	•												•	•	•		
119	System Surety Life-Cycle Engineering	3511.130		•				•	•										•		
123	Content–Based Search of Geometric Databases	3512.160		•	•												•	•	•		
124	Integrated Service Provisioning in an “IPv6 over ATM” Research Network	3512.170			•																
125	Virtual Desktop Engineering with Integrated Multimedia Data	3512.180		•	•			•									•		•		
123	Mission Surety for Large-Scale Real-Time Information Systems	3512.190	•	•					•												
126	Scaled ATM End-to-End Encryption	3512.220						•	•												
128	Network Surety Modeling for Wireless ATM Networks	3512.230		•	•																•
130	Low-Power, Reduced-Computation, Public-Key Protocols	3512.240			•			•	•												
126	Ten-to-One-Hundred-Gigabit/Second Network Enabling R&D	3512.250	•	•	•									•							
130	High-Performance Commodity Interconnects for Clustered Scientific and Engineering Computing	3512.260			•																
131	AVATAR — Navigating and Mining in Massive Data	3512.270		•	•	•	•														•
129	Algorithm–Based Fault Tolerance on Heterogeneous Massively Parallel Computers	3512.280		•	•																
136	Electrokinetic Immunoaffinity Chemical Sensors	3516.050							•					•							

Pg #	Title	Case Number	Science of Complex Systems	Modeling & Simulation of Complex Systems	High-Performance Computing	Nuclear Weapons Predictive Capability (Classified)	Safety Assessments & Engineering	Use Control & Verification	Nonproliferation & Verification	Dynamic Testing in Severe Environments	High-Energy-Density Materials	Laser Technology	Pulsed Power and Accelerators	Microelectronics and Photonics	Nuclear Materials	Engineered Materials	Flexible Manufacturing	Environmentally Conscious Manufacturing	Intelligent Machines and Robotics	Waste Management	Other
136	Information-Efficient Spectral Imaging System (ISIS)	3516.060	•	•					•					•					•		
137	Imaging of Moving Targets Using Simultaneous Synthetic Aperture Radar (SAR) and Moving Target Indicator (MTI) Radar	3516.070		•					•												•
135	Sampling and Sensing Systems for High-Priority Analytes	3516.080							•					•		•		•			
138	Automated Vegetation Height Measurement for Automatic Terrain Mapping	3516.090		•					•												
138	Sparse Geophysical Networks for Monitoring Deep Targets	3516.110	•	•					•												
139	Miniature Bioaerosol Concentrator	3516.120							•									•			
140	Recognizing Partially Obscured Targets by Combining Multiple Data Sources Using Evidential Reasoning	3516.130							•										•		
141	Computational Engineering of Sensor Materials and Integration with a Novel Biological Weapon Detection System	3516.140		•	•											•					
142	Biological Weapon Detector Using Bioaffinity Array Impedance Analysis with Chemical Amplification Through Redox Recycling	3516.150							•					•							
142	ATR/Exploitation Utilizing Ultra–High-Resolution, Complex SAR Imaging	3516.160		•	•				•										•		
147	Designed Molecular Recognition Materials for Chiral Sensors, Separations, and Catalytic Materials	3518.030							•							•					•
148	Rapid Screening of Complex Chemical Samples Via Capillary Array Analysis	3518.050							•									•			
148	Designed Synthesis of Controlled Degradative Materials	3518.060						•								•					
150	Mechanistic Models for Radionuclide Desorption from Soils	3518.070	•	•																	

Pg #	Title	Case Number	Science of Complex Systems	Modeling & Simulation of Complex Systems	High-Performance Computing	Nuclear Weapons Predictive Capability (Classified)	Safety Assessments & Engineering	Use Control & Verification	Nonproliferation & Verification	Dynamic Testing in Severe Environments	High-Energy-Density Materials	Laser Technology	Pulsed Power and Accelerators	Microelectronics and Photonics	Nuclear Materials	Engineered Materials	Flexible Manufacturing	Environmentally Conscious Manufacturing	Intelligent Machines and Robotics	Waste Management	Other
150	Development of Innovative Combustion Processes for a Direct-Injection Diesel Engine	3518.080																			•
152	Hydrogen Production for Fuel Cells by Selective Dehydrogenation of Alkanes in Catalytic Membrane Reactors	3518.090														•					
153	Hybrid Vehicle Engine Development	3518.110																			•
149	Adaptive 3-D Sensing	3518.120					•	•	•			•			•		•		•		
154	Aqueous Organic Sensor	3518.130							•									•			•
154	Designed Ionophores for Liquid-Membrane Separation and Extraction of Metal Ions	3518.140		•					•							•		•			
156	An Electromagnetic Imaging System for Environmental Site Reconnaissance	3518.150							•			•	•	•							•
160	Reliability Degradation Due to Stockpile Aging	3520.210	•	•	•	•								•		•					
159	Integrated Approach to Develop Microelectromechanical (MEMS) Reliability Tools	3520.220												•					•		
160	Precursors to Failure of Oxides and Metal Lines in CMOS Technology	3520.230												•							
162	An Extensible Object-Oriented Framework for Risk and Reliability Analysis	3520.240		•			•														
162	Simulation/Optimization Tools for System Variability Analysis	3520.270		•	•	•		•													
164	A Massively Parallel Microsimulation Model of Infrastructure Interdependency	3520.280	•	•	•																
166	Physical Models for Predicting the Effect of Atmospheric Corrosion on Microelectronic Reliability	3520.290												•							
167	Backside Localization of Open and Shorted IC (Integrated Circuit) Interconnections	3520.310						•						•							

Pg #	Title	Case Number	Science of Complex Systems	Modeling & Simulation of Complex Systems	High-Performance Computing	Nuclear Weapons Predictive Capability (Classified)	Safety Assessments & Engineering	Use Control & Verification	Nonproliferation & Verification	Dynamic Testing in Severe Environments	High-Energy-Density Materials	Laser Technology	Pulsed Power and Accelerators	Microelectronics and Photonics	Nuclear Materials	Engineered Materials	Flexible Manufacturing	Environmentally Conscious Manufacturing	Intelligent Machines and Robotics	Waste Management	Other
165	Reliability Predictions for Advanced Electronics in Smoke Environments	3520.320					•			•											
168	Security of Bulk Power Systems	3520.330	•	•	•																
171	Science on the Microdomain	3522.010	•					•	•										•		
172	Autonomous MicroChem Laboratory (µChemLab)	3522.020	•	•		•		•	•		•			•		•	•				
171	Cooperative, Distributed Sensing and Action Using Microminiature, Intelligent Agents	3522.030	•	•					•										•		
177	Computational Methods for Predicting the Response of Critical As-Built Infrastructure to Dynamic Loads (Architectural Surety)	3530.030		•	•		•									•					
178	Background Radiation Anisotropy Measurement Sensor (BRAMS)	3530.050																			•
178	Exploitation of Satellite Communications Systems and Networks for Intelligence Applications	3530.090				•		•	•												
179	Microcode Evaluation	3530.110	•					•													
179	Real-Time Image Analysis Using Field-Programmable Gate Arrays	3530.120		•	•				•												
180	Advanced 3-D Sensing and Visualization System for Unattended Monitoring	3530.130					•	•	•			•			•						•
180	System-of-Labs Direct Fabrication Technology	3531.020										•				•	•				
182	Poco Switch Tubes	3531.140																			•
182	Chemiresistors Based on Metal-Loaded Polymers for Solvent Spill Detection	3531.150							•					•							
183	Advance Neutron-Tube Design and Producibility	3531.160														•	•				
183	Surface Hardening by Nanoparticle Precipitation and Atomic Clustering in Ni(Al,O)	3531.170														•	•	•	•		

Pg #	Title	Case Number	Science of Complex Systems	Modeling & Simulation of Complex Systems	High-Performance Computing	Nuclear Weapons Predictive Capability (Classified)	Safety Assessments & Engineering	Use Control & Verification	Nonproliferation & Verification	Dynamic Testing in Severe Environments	High-Energy-Density Materials	Laser Technology	Pulsed Power and Accelerators	Microelectronics and Photonics	Nuclear Materials	Engineered Materials	Flexible Manufacturing	Environmentally Conscious Manufacturing	Intelligent Machines and Robotics	Waste Management	Other
184	Dynamical Properties of Polymers: Computational Modeling	3531.180		•	•											•					
188	Broadening Mechanism in 2-D Excitonic and Electron Gases	3531.190	•	•										•							
184	Calculation and Interpretation of the Energies that Underlie Transition-Metal Surface Structure	3531.210			•											•					
185	Interfacial Reactions in Ceramic Systems	3531.220												•		•	•				
186	Direct Fabrication of Multifunctional Nanocomposites Via Supramolecular Self-Assembly	3531.230												•		•	•				
187	Biophotonic Materials for Optical Encryption and Noncomputing	3531.240	•	•	•				•					•		•					
188	Low-Stress Amorphous Diamond: A New Material for Sensors	3531.250							•					•							
189	Nanoengineered Cu-Al Defects in Al: A Prototype System for Corrosion	3531.260	•													•					
190	Novel Energy-Conversion Devices of Icosahedral Borides	3531.270																			•
191	Ion-Mobility Spectroscopy of Biological Materials	3531.280						•													•
192	Visualization Tools for MEMs Designs in a Virtual 3-D World	3531.290		•				•						•			•		•		
191	Direct Fabrication of Planar Solid-Oxide Fuel Cells	3531.310														•	•				
192	Micromachining with Ultra-Short Pulsewidth Lasers	3531.320										•	•				•		•		
193	Molecular Characterization of Energetic Material Initiation	3531.330		•						•		•									
196	Chemical Feedstocks for the Future: Oxidative Dehydrogenation	3532.010														•		•			
196	Global Approaches to Infrastructural Analysis (GAIA)	3532.030	•	•	•																

Pg #	Title	Case Number	Science of Complex Systems	Modeling & Simulation of Complex Systems	High-Performance Computing	Nuclear Weapons Predictive Capability (Classified)	Safety Assessments & Engineering	Use Control & Verification	Nonproliferation & Verification	Dynamic Testing in Severe Environments	High-Energy-Density Materials	Laser Technology	Pulsed Power and Accelerators	Microelectronics and Photonics	Nuclear Materials	Engineered Materials	Flexible Manufacturing	Environmentally Conscious Manufacturing	Intelligent Machines and Robotics	Waste Management	Other
194	Engineering Complex Distributed Systems	3532.070	•	•	•														•		
198	Laser Communication Nanosatellites	3532.080	•	•							•	•		•		•					
200	Collection and Data Synthesis of Atmospheric Explosion Ground Truth for Global Monitoring Systems	3532.090							•												
201	Advanced Radiation Sources: Rayleigh-Taylor Mitigation Via Perturbation Reduction	3532.110		•		•							•								
201	Microfluidic Engineering	3532.120												•					•		
199	Accelerator Technologies for Emerging Threats	3532.130											•								
204	Technologies for System-Level Innovations in Ballistic Missile Defense	3532.140	•						•	•	•	•	•	•		•					
202	InGaAsN: A Novel Material for High-Efficiency Solar Cells and Advanced Photonic Devices	3532.150												•		•					
203	Technologies for Countering C/B Terrorism	3532.160		•					•			•									
205	Aerosol Stand-Off Detection Test-Bed	3532.170																			•
206	Design and Optimization of High-Power Electromagnetic Source Systems and Engagement Scenarios for Achieving Functional Upset or Damage in Specific Target Electronic Systems	3532.180		•			•		•	•			•								
207	Real-Time Design of Improved Powder Pressing Dies Using Finite-Element Method Modeling	3532.190		•												•	•	•			
208	Development of Fiber-Laser–Based LIF for Detection of SO_2	3532.210	•									•		•				•			•
209	Penetration and Defeat of Hardened Underground Facilities Using a Microhole Drilling Robot	3532.220								•	•					•					
210	IFSAR Tree Phenomenology and Coherence Normalization	3532.230			•				•												

Pg #	Title	Case Number	Science of Complex Systems	Modeling & Simulation of Complex Systems	High-Performance Computing	Nuclear Weapons Predictive Capability (Classified)	Safety Assessments & Engineering	Use Control & Verification	Nonproliferation & Verification	Dynamic Testing in Severe Environments	High-Energy-Density Materials	Laser Technology	Pulsed Power and Accelerators	Microelectronics and Photonics	Nuclear Materials	Engineered Materials	Flexible Manufacturing	Environmentally Conscious Manufacturing	Intelligent Machines and Robotics	Waste Management	Other
210	Electric Launcher for Defense Applications	3532.240											•								
212	SAM Telemetry for Measurements While Drilling	3533.050								•											•
214	Design-for-Manufacturability Applied to Photovoltaic Modules	3533.070												•			•	•			
212	Advanced Geosphere Transport Simulation	3533.160		•	•																
214	Low-Work-Function Thermionic Emission Materials	3533.170												•		•					
211	Power-Grid Reliability and Restructuring Policy Changes	3533.180	•	•																	•
222	Low-Cost Cadmium Zinc Telluride Radiation Detectors Based on Electron-Transport-Only Designs	3534.020						•	•					•	•	•					
216	LIGA Micromachining	3534.030		•												•					
216	Applied Microfluidics Science	3534.040						•						•					•		
218	Computational Simulations of Self-Assembling Macro-Systems by Direct Fabrication of Microscopic Structured Materials	3535.130		•	•											•					
218	Self-Stabilizing Optical Solitons and High-Intensity Laser Plasma Channels for Diffraction-Free Propagation and Robust Power Compression	3535.140							•	•		•	•								
222	Novel Materials for Hydrogen Storage	3535.150	•	•							•					•					
220	Optical Communication System for Remote Monitoring and Adaptive Control of Distributed Ground Sensors Exhibiting Collective Intelligence	3535.160							•			•		•					•		
223	Inversion of Passive Electromagnetic Fields to Locate Weapons of Mass Destruction	3535.170	•	•	•				•			•					•		•		
224	Z-Pinch–Driven Isentropic Compression	3535.180								•	•		•			•					

Pg #	Title	Case Number	Science of Complex Systems	Modeling & Simulation of Complex Systems	High-Performance Computing	Nuclear Weapons Predictive Capability (Classified)	Safety Assessments & Engineering	Use Control & Verification	Nonproliferation & Verification	Dynamic Testing in Severe Environments	High-Energy-Density Materials	Laser Technology	Pulsed Power and Accelerators	Microelectronics and Photonics	Nuclear Materials	Engineered Materials	Flexible Manufacturing	Environmentally Conscious Manufacturing	Intelligent Machines and Robotics	Waste Management	Other
225	Covert, Distributed Biosensors for UXO/CW Based on Amplified Immunoassays Conducted in Porous Inorganic Media	3535.190							•							•					
226	Semiconductor Filament Lasers	3535.210								•	•	•	•	•		•	•				
226	Development of Membrane Devices Using AlN and SiC Films	3537.010												•		•			•		
227	Spectral Information Content in Ion-Mobility Spectra for Explosives, Interferants, and Other Negative-Ionizing Chemicals	3537.020						•	•										•		
230	Magnetic-Field Profile Measurements in Wire-Array Z-Pinches by Faraday Rotation	3537.030		•									•								
228	Picosecond Particle Velocity Measurements	3537.040																			
228	Particle-Level Modeling of Flows of Concentrated Suspensions	3537.050	•	•							•							•			
229	Efficient Processing of Materials Microstructures with Intelligent Feature Extraction for Quantitative Stereology	3537.060	•		•											•					
230	Nondestructive Evaluation of Wind Turbine Blades	3537.070		•						•											
231	Very Small Arrays: Designing Self-Assembled Systems of Light-Antennae and Reaction Centers for Artificial Photosynthesis	3537.080	•	•										•		•					
232	Enzyme-Mediated Electrochemical Redox Polymer Biosensor for V- and G-Type Chemical Weapons	3537.110							•					•		•					
232	Novel Biosensor Fabrication Techniques	3537.120							•					•							
233	Design for 100-Year-Life Prototype	3537.130		•			•			•				•		•					
233	Enhancing Multilevel Linear Equation Solvers Using Domain Decomposition Strategies	3537.140		•	•	•															

Pg #	Title	Case Number	Science of Complex Systems	Modeling & Simulation of Complex Systems	High-Performance Computing	Nuclear Weapons Predictive Capability (Classified)	Safety Assessments & Engineering	Use Control & Verification	Nonproliferation & Verification	Dynamic Testing in Severe Environments	High-Energy-Density Materials	Laser Technology	Pulsed Power and Accelerators	Microelectronics and Photonics	Nuclear Materials	Engineered Materials	Flexible Manufacturing	Environmentally Conscious Manufacturing	Intelligent Machines and Robotics	Waste Management	Other
234	*In Situ* and *Ex Situ* Investigations of Lateral Composition	3537.150										•		•							
235	Approximate Methods for Computing Eigensolutions Using Automated Multilevel Substructuring	3537.160		•	•										•						
235	Living Tissue Engineering	3537.170		•												•					

Pg #	Title	Case Number	Waste Management	Energy Efficiency	Renewable Energy	ES&H	Environmental Restoration	Fossil Energy	Radioactive-Waste Management	Economic Impact	Energy Research	Intelligence & National Security	Nuclear Energy	Science Education & Technical Information	Defense Programs	Department of Defense (DoD)	Other Federal Agencies*	Other (Industry, Consortia,…)**	Other Federal Agencies* (Industry, Consortia…)**
10	Catalytic Membrane Sensors	3502.030										•			•				
9	Photonic Bandgap Structures as a Gateway to Nanophotonics	3502.040								•		•			•	•			
10	Wide-Bandgap Compound Semiconductors to Enable Novel Semiconductor Devices	3502.050		•								•			•				
12	Ultra-Hard Multilayer Coatings	3502.080		•						•	•			•	•	•		•	
14	Scanning Probe–Based Processes for Nanometer-Scale Device Fabrication	3502.090								•	•				•				
15	Molecular-Scale Lubricants for Micromachine Applications	3502.110								•					•				
16	Surface-Micromachined Flexural Plate-Wave Device Integrated on Silicon	3502.120	•			•	•					•			•				
17	Smart Interface Bonding Alloys (SIBA): Tailoring Thin-Film Mechanical Properties	3502.140		•															
20	Recognizing Atoms in Atomically Engineered Nanostructures: An Interdisciplinary Approach	3502.170								•									
18	Molecular-to-Continuum Fracture Analysis of Thermoset Polymer/Solid Interfaces	3502.190													•	•		•	Industry
19	Monolithic Structures for Nanoseparation	3502.210	•	•	•	•	•	•	•	•	•	•	•	•	•	•	•	•	*EPA, NIH **auto, steel, glass, chemical, etc.
21	Fundamental Aspects of Micromachine Reliability	3502.220								•	•	•			•				
24	Enabling Science and Technology for Cold-Spray Direct Fabrication	3502.230		•		•		•		•				•	•	•	•	•	*Department of Commerce, NIST **U.S. auto industry and other U.S. industries
22	Atomic-Level Studies of Surfactant-Directed Materials Growth	3502.240									•				•				
26	Intelligent Polymers for Nanodevice Performance Control	3502.250										•			•				

Pg #	Title	Case Number	Waste Management	Energy Efficiency	Renewable Energy	ES&H	Environmental Restoration	Fossil Energy	Radioactive-Waste Management	Economic Impact	Energy Research	Intelligence & National Security	Nuclear Energy	Science Education & Technical Information	Defense Programs	Department of Defense (DoD)	Other Federal Agencies*	Other (Industry, Consortia,…)**	Other Federal Agencies* (Industry, Consortia…)**
25	Freeforming of Ceramics and Composites from Colloidal Slurries	3502.260	•	•											•				
26	Quantum Dot Arrays	3502.270						•			•								
27	Laser-Assisted Arc Welding for Aluminum Alloys	3502.280		•	•			•		•					•	•		•	**Industry
28	Reactivity of Metal-Oxide Surfaces	3502.310		•				•			•								
29	Exploiting LENS Technology Through Novel Materials	3502.320	•	•						•					•	•	•	•	*DOC **Industry
34	Parallel Quantum Chemistry for Material Aging and Synthesis	3504.010										•			•	•			
34	Modeling Complex Turbulent Chemically Reacting Flows on Massively Parallel Supercomputers	3504.020		•				•		•	•	•			•	•			
35	Automated Geometric Model Builder Using Range Image Sensor Data	3504.050								•	•	•			•	•			
36	A Massively Parallel Sparse Eigensolver for Structural Dynamics Finite Element	3504.060	•	•	•		•				•		•	•	•	•			
36	Density-Functional Theory for Classical Fluids at Complex Interfaces	3504.070					•				•					•			
33	Gradient-Driven Diffusion of Multi-Atom Molecules Through Macromolecules and Membranes	3504.090		•	•		•	•	•		•				•				
38	Fast and Easy Parallel I/O for Efficient Scientific Computing	3504.120									•	•			•	•			
38	Novel Load-Balancing for Scalable, Parallel Electromagnetic and Plasma Physics Simulation Software	3504.130								•	•	•			•	•		•	**Microelectronics
40	Parallel Computational Chemistry Using Constraints	3504.140										•			•	•			

Pg #	Title	Case Number	Waste Management	Energy Efficiency	Renewable Energy	ES&H	Environmental Restoration	Fossil Energy	Radioactive-Waste Management	Economic Impact	Energy Research	Intelligence & National Security	Nuclear Energy	Science Education & Technical Information	Defense Programs	Department of Defense (DoD)	Other Federal Agencies*	Other (Industry, Consortia,…)**	Other Federal Agencies* (Industry, Consortia…)**
40	Massively Parallel *Ab Initio* Validation for ASCI Materials Aging	3504.160													•	•			
42	Computational Methods for Coupling Microstructural and Micromechanical Materials Response Simulations	3504.170									•	•			•				
44	An Investigation of Wavelet Bases for Multiscale, Grid–Based Simulation	3504.180									•	•	•	•	•	•			
41	Integrated Quantum/Classical Modeling of Hydrogenic Materials	3504.190		•							•	•			•	•			
45	The Next Generation of Teraflop Density-Functional Electronic Structure Codes	3504.210									•	•			•				
46	Methodology for Characterizing Modeling and Discretization Uncertainties in Computational Simulation	3504.220	•	•	•		•				•		•	•	•	•			
48	Global Optimization for Engineering Science Problems	3504.230		•			•			•	•	•			•	•			
49	Dynamic Simulation of Mechanical Systems with Intermittent Contacts	3504.240								•		•			•				
43	From Atom-Picoseconds to Centimeter-Years in Simulation and Experiment	3504.250		•	•			•			•				•				
47	Emergent Behavior of Large Swarms of Intelligent Agents	3504.260	•				•					•			•				
50	Parallel Combinatorial Optimization for Scheduling Problems	3504.270													•				
50	Programming Paradigms for Massively Parallel Computers	3504.280									•				•	•			
51	Multilevel Techniques for Unstructured Grid Problems on Massively Parallel Computers	3504.290													•				
52	Scalable Tools for Massively Parallel Distributed Computing	3504.310									•				•				
52	Massively Parallel Methods for Simulating the Phase Field Model	3504.320								•	•				•	•			

Pg #	Title	Case Number	Waste Management	Energy Efficiency	Renewable Energy	ES&H	Environmental Restoration	Fossil Energy	Radioactive-Waste Management	Economic Impact	Energy Research	Intelligence & National Security	Nuclear Energy	Science Education & Technical Information	Defense Programs	Department of Defense (DoD)	Other Federal Agencies*	Other (Industry, Consortia,…)**	Other Federal Agencies* (Industry, Consortia…)**
53	Visual Explanation and Insight	3504.330								●		●		●	●	●			
58	Wafer Fusion for Integration of Semiconductor Materials and Devices	3506.110								●		●			●	●			
58	Highly Parallel, Low-Power, Photonic Interconnects for Inter-Board Signal Distribution	3506.120													●	●	●		*NSA, CIA
59	Virtual Reactor for the Semiconductor Manufacturing Plant of the Future	3506.140									●				●	●			
60	Selective Oxidation Technology and Its Applications Toward Electronic and Optoelectronic Devices	3506.160								●		●			●	●			
61	Agile Prototyping of Microelectromechanical Systems (MEMS)	3506.180								●					●	●		●	**Aerospace
57	Advanced Concepts for High-Power VCSELs and VCSEL Arrays	3506.190								●		●			●	●			
62	Midwave-Infrared (2–6 µm) Emitter–Based Chemical Sensor Systems	3506.210								●		●			●	●			
62	A Novel Nondestructive Silicon-on-Insulator Nonvolatile Memory	3506.230										●			●	●	●	●	*DOE **Industry
64	Integration of Optoelectronics and MEMS by Free-Space Microoptics	3506.240								●					●	●			
65	Advanced Laser Structures for Short-Pulsed Power in Active Optical Sensor Systems	3506.250								●		●			●	●	●		3-letter
66	Metal Micro-Heat-Pipe Substrates for High-Power-Density Electronics	3506.260										●			●	●		●	**Electronics manufacturers
68	Integration of Microsensor Technology into a Miniature Robotic Vehicle	3506.270													●	●			
66	Vacuum Encapsulation of MEMS Structures	3506.280					●					●			●	●		●	**Analog Devices, Inc., Rockwell International, Texas Instruments
67	Massively Parallel Sensor Arrays for Volatile Organic Detection	3506.290					●					●			●				

Pg #	Title	Case Number	Waste Management	Energy Efficiency	Renewable Energy	ES&H	Environmental Restoration	Fossil Energy	Radioactive-Waste Management	Economic Impact	Energy Research	Intelligence & National Security	Nuclear Energy	Science Education & Technical Information	Defense Programs	Department of Defense (DoD)	Other Federal Agencies*	Other (Industry, Consortia,…)**	Other Federal Agencies* (Industry, Consortia…)**
70	Agile Dry Etching of Compound Semiconductors for Science–Based Manufacturing Using *In Situ* Process Control	3506.310								•		•			•				
68	Precision-Formed Micromagnets	3506.320								•	•	•			•	•			
70	Time-Resolved Ion-Beam–Induced Charge-Collection (TRIBICC) Imaging	3506.330								•					•	•	•	•	*NSA, Air Force, NASA **IC industries
74	Composite-Resonator Surface-Emitting Lasers	3506.340										•			•	•			
73	Role of Defects in III-Nitride–Based Electronics	3506.350										•			•	•			
74	Ultra–Low-Power Sensors for Microtelemetry Systems	3506.360	•			•	•					•			•	•			
72	Double Quantum-Well Long-Wavelength Optoelectronic Devices	3506.370								•		•			•	•			
75	The Development of Integrated Chemical Microsensors in GaAs	3506.380										•			•		•		*EPA
76	Monolithic Integration of VCSELs and Detectors for Microsystems	3506.410								•		•			•	•			
77	AlGaN Materials Engineering for Integrated Multifunction Systems	3506.420		•							•	•			•				
71	Compliant Substrates for Epitaxial Integration of Dissimilar Materials	3506.430								•		•			•	•			
78	Post-Processed Integrated Microsystems	3506.440										•			•	•	•		3-letter
83	Using Higher-Order Gradients to Modeling Localization Phenomena	3508.040		•								•		•	•	•		•	**NCMS, USCAR
81	Enhanced Vapor-Phase Diffusion in Porous Media	3508.060	•	•			•		•		•								
82	Stress Evaluation and Model Validation Using Laser Ultrasonics	3508.110		•	•					•	•	•	•	•	•	•	•	•	*NRC, EPA **Auto, glass, steel, energy, & chemical industries

Pg #	Title	Case Number	Waste Management	Energy Efficiency	Renewable Energy	ES&H	Environmental Restoration	Fossil Energy	Radioactive-Waste Management	Economic Impact	Energy Research	Intelligence & National Security	Nuclear Energy	Science Education & Technical Information	Defense Programs	Department of Defense (DoD)	Other Federal Agencies*	Other (Industry, Consortia,…)**	Other Federal Agencies* (Industry, Consortia…)**
84	Altered Simulation Properties for Tetrahedral Finite Elements for Use in Engineering Simulation	3508.120	●	●	●			●	●			●			●	●		●	**Auto, aerospace industries
84	Development, Implementation, and Experimental Validation of the Lattice Boltzmann Method for Modeling Three-Dimensional Complex Flows	3508.130	●			●	●	●	●	●	●				●	●	●		*NASA
86	Capturing Recrystallization of Metals with a Multiscale Material Model	3508.140		●								●		●	●	●		●	**NCMS, USCAR, aluminum & steel suppliers
88	Nondeterministic Modeling in Engineering Science	3508.150	●	●	●		●				●		●	●	●	●			
88	Lagrangian Modeling of Radiative Transport	3508.160													●	●	●	●	*FAA, NASA **Insurance
89	High-Resolution Modeling of Multiscale Transient Phenomena in Turbulent Boundary Layers	3508.170	●	●				●			●	●			●				
90	Dispersive Measurements of Velocity in Heterogeneous Materials	3508.180			●						●				●	●	●		*NASA
90	A Physically–Based Computational Method for Predicting Generalized Fracture	3508.190		●				●			●	●	●	●	●	●			
92	Development of *In Situ* Diagnostics for Simultaneous Measurement of Transient Gas Species and Soot in Large Fires	3508.210		●	●						●				●	●	●		*DOC/NIST, EPA
91	Micromechanical Failure Analyses for Finite-Element Polymer Modeling	3508.220								●		●			●	●	●	●	*Department of Commerce **Aerospace, automotive, coatings
94	Methodology Optimal Selection of Test and Simulation Levels for Problems Involving Computational Simulation	3508.230	●				●		●			●			●				

Pg #	Title	Case Number	Waste Management	Energy Efficiency	Renewable Energy	ES&H	Environmental Restoration	Fossil Energy	Radioactive-Waste Management	Economic Impact	Energy Research	Intelligence & National Security	Nuclear Energy	Science Education & Technical Information	Defense Programs	Department of Defense (DoD)	Other Federal Agencies*	Other (Industry, Consortia…)**	Other Federal Agencies* (Industry, Consortia…)**
93	A Phenomenological Model for Multicomponent Transport with Electrochemical Reactions in Concentrated Solutions	3508.240	●				●								●	●	●	●	*DOE **Polymeric thin-film coating & semiconductor manufacturing industries
98	Laser-Spray Fabrication for Net-Shape Rapid Product Realization	3510.460	●	●		●				●					●			●	**LENS Consortium
99	Solution Synthesis and Processing of PZT Materials for Neutron-Generator Applications	3510.510													●				
97	Ultra-Precise Assembly of Microelectromechanical Systems (MEMS)	3510.540																●	**Industry
100	Finite-Element Meshing Approached as a Global Minimization Process	3510.570	●	●			●	●	●		●				●				
102	Application of Parallel Mechanism Technology to Manufacturing	3510.580								●				●	●	●	●	●	*NIST **Hexapod Users Group
100	Investigation of the Impact of Cleaning on Adhesive Bond and the Process Implications	3510.590	●			●				●					●	●		●	**NCMS, Sematech, industry
102	Standard Cells for Microelectromechanical Systems (MEMS)	3510.610								●					●	●		●	**Aerospace
104	Laser Wire Deposition for Fully Dense Shapes	3510.620								●				●	●	●			
105	High-Throughput Dry Processes for Large-Area Devices	3510.630			●						●				●			●	**Semiconductor industry
106	Assuring High Reliability and Production Readiness in Low-Volume Manufacturing	3510.640										●			●	●			
103	Scripting for Video Inspection	3510.660													●	●			
106	Advanced Machining Processes for Microfabrication	3510.670								●		●		●	●	●			
107	Fusion of Product and Process Data Using Real-Time Streaming Visualization	3510.680													●				
108	Advanced Production Planning Models	3510.690										●			●				

Pg #	Title	Case Number	Waste Management	Energy Efficiency	Renewable Energy	ES&H	Environmental Restoration	Fossil Energy	Radioactive-Waste Management	Economic Impact	Energy Research	Intelligence & National Security	Nuclear Energy	Science Education & Technical Information	Defense Programs	Department of Defense (DoD)	Other Federal Agencies*	Other (Industry, Consortia,…)**	Other Federal Agencies* (Industry, Consortia…)**
112	Automatic Generation of Multimedia Documentation for Assembly Operations	3511.010										●			●	●		●	**Consortia
113	Distributed Life-Cycle Models in Enterprise Simulations to Answer System Questions	3511.020										●			●	●			
114	Immersive CAD	3511.040									●				●	●			
114	Automatic Planning of Life-Cycle Assembly Processes	3511.050													●	●		●	**Consortia
116	Analysis of Very Large Assemblies	3511.070										●			●	●		●	**Consortia
111	Enabling Human Skills with Cooperative Automation	3511.080					●		●						●	●			
116	Cloud To CAD	3511.090					●	●							●	●			
118	Ergonomics in Life-Cycle Assembly Processes	3511.110							●	●					●			●	**Consortia
117	Feature Reduction of Geometric Solid Models for Analysis Tools	3511.120								●		●			●			●	**Consortia
119	System Surety Life-Cycle Engineering	3511.130								●		●		●	●	●	●	●	*DoT **FSTC
123	Content–Based Search of Geometric Databases	3512.160					●			●		●			●			●	**Industry
124	Integrated Service Provisioning in an “IPv6 over ATM” Research Network	3512.170								●					●			●	**Communications & Networking
125	Virtual Desktop Engineering with Integrated Multimedia Data	3512.180													●				
123	Mission Surety for Large-Scale Real-Time Information Systems	3512.190		●								●			●	●			
126	Scaled ATM End-to-End Encryption	3512.220										●			●				
128	Network Surety Modeling for Wireless ATM Networks	3512.230								●					●	●		●	**Telecom Standards

Pg #	Title	Case Number	Waste Management	Energy Efficiency	Renewable Energy	ES&H	Environmental Restoration	Fossil Energy	Radioactive-Waste Management	Economic Impact	Energy Research	Intelligence & National Security	Nuclear Energy	Science Education & Technical Information	Defense Programs	Department of Defense (DoD)	Other Federal Agencies*	Other (Industry, Consortia,…)**	Other Federal Agencies* (Industry, Consortia…)**
130	Low-Power, Reduced-Computation, Public-Key Protocols	3512.240										●	●		●	●		●	**IAGA, Cellular Telephony
126	Ten-to-One-Hundred-Gigabit/Second Network Enabling R&D	3512.250								●					●	●		●	**Telecommunications & computer networking companies
130	High-Performance Commodity Interconnects for Clustered Scientific and Engineering Computing	3512.260													●				
131	AVATAR — Navigating and Mining in Massive Data	3512.270									●	●	●		●				
129	Algorithm–Based Fault Tolerance on Heterogeneous Massively Parallel Computers	3512.280									●				●				
136	Electrokinetic Immunoaffinity Chemical Sensors	3516.050	●				●								●	●			
136	Information-Efficient Spectral Imaging System (ISIS)	3516.060	●		●		●	●				●			●	●			
137	Imaging of Moving Targets Using Simultaneous Synthetic Aperture Radar (SAR) and Moving Target Indicator (MTI) Radar	3516.070									●				●	●			
135	Sampling and Sensing Systems for High-Priority Analytes	3516.080	●			●	●		●	●		●			●	●	●		**CIA, FBI
138	Automated Vegetation Height Measurement for Automatic Terrain Mapping	3516.090													●	●	●		**NIMA, DOE-NN, Army Tec
138	Sparse Geophysical Networks for Monitoring Deep Targets	3516.110													●	●			
139	Miniature Bioaerosol Concentrator	3516.120							●						●	●			
140	Recognizing Partially Obscured Targets by Combining Multiple Data Sources Using Evidential Reasoning	3516.130													●	●			
141	Computational Engineering of Sensor Materials and Integration with a Novel Biological Weapon Detection System	3516.140													●	●			

Pg #	Title	Case Number	Waste Management	Energy Efficiency	Renewable Energy	ES&H	Environmental Restoration	Fossil Energy	Radioactive-Waste Management	Economic Impact	Energy Research	Intelligence & National Security	Nuclear Energy	Science Education & Technical Information	Defense Programs	Department of Defense (DoD)	Other Federal Agencies*	Other (Industry, Consortia,…)**	Other Federal Agencies* (Industry, Consortia…)**
142	Biological Weapon Detector Using Bioaffinity Array Impedance Analysis with Chemical Amplification Through Redox Recycling	3516.150	•				•					•			•	•			
142	ATR/Exploitation Utilizing Ultra–High-Resolution, Complex SAR Imaging	3516.160													•	•			
147	Designed Molecular Recognition Materials for Chiral Sensors, Separations, and Catalytic Materials	3518.030													•	•		•	**Chemical & pharmaceutical industries
148	Rapid Screening of Complex Chemical Samples Via Capillary Array Analysis	3518.050	•				•								•		•		*EPA
148	Designed Synthesis of Controlled Degradative Materials	3518.060													•	•			
150	Mechanistic Models for Radionuclide Desorption from Soils	3518.070	•				•		•	•					•				
150	Development of Innovative Combustion Processes for a Direct-Injection Diesel Engine	3518.080		•							•							•	**Diesel engine manufacturers
152	Hydrogen Production for Fuel Cells by Selective Dehydrogenation of Alkanes in Catalytic Membrane Reactors	3518.090		•				•			•				•	•			
153	Hybrid Vehicle Engine Development	3518.110		•	•			•			•								
149	Adaptive 3-D Sensing	3518.120	•				•		•			•			•	•			
154	Aqueous Organic Sensor	3518.130				•	•								•				
154	Designed Ionophores for Liquid-Membrane Separation and Extraction of Metal Ions	3518.140	•	•		•	•	•	•	•	•				•	•	•	•	*EPA **Industry
156	An Electromagnetic Imaging System for Environmental Site Reconnaissance	3518.150				•	•								•	•	•		*CIA
160	Reliability Degradation Due to Stockpile Aging	3520.210													•	•		•	**Industry

Pg #	Title	Case Number	Waste Management	Energy Efficiency	Renewable Energy	ES&H	Environmental Restoration	Fossil Energy	Radioactive-Waste Management	Economic Impact	Energy Research	Intelligence & National Security	Nuclear Energy	Science Education & Technical Information	Defense Programs	Department of Defense (DoD)	Other Federal Agencies*	Other (Industry, Consortia…)**	Other Federal Agencies* (Industry, Consortia…)**
159	Integrated Approach to Develop Microelectromechanical (MEMS) Reliability Tools	3520.220													●	●			
160	Precursors to Failure of Oxides and Metal Lines in CMOS Technology	3520.230													●	●			
162	An Extensible Object-Oriented Framework for Risk and Reliability Analysis	3520.240											●		●	●		●	**Industry
162	Simulation/Optimization Tools for System Variability Analysis	3520.270													●	●			
164	A Massively Parallel Microsimulation Model of Infrastructure Interdependency	3520.280								●					●	●	●		*FEMA, CIA
166	Physical Models for Predicting the Effect of Atmospheric Corrosion on Microelectronic Reliability	3520.290								●					●	●			
167	Backside Localization of Open and Shorted IC (Integrated Circuit) Interconnections	3520.310													●	●		●	**Microelectronics, Sematech
165	Reliability Predictions for Advanced Electronics in Smoke Environments	3520.320				●							●		●	●	●	●	*NRC, FAA **Telecommunications
168	Security of Bulk Power Systems	3520.330									●		●		●	●	●	●	*FBI, CIA **Public utilities
171	Science on the Microdomain	3522.010	●			●	●				●	●			●	●			
172	Autonomous MicroChem Laboratory (µChemLab)	3522.020	●	●	●	●	●	●		●	●				●	●	●	●	*NIJ, EPA, Veterans, DARPA, NIH **Industry, universities
171	Cooperative, Distributed Sensing and Action Using Microminiature, Intelligent Agents	3522.030	●				●					●			●				
177	Computational Methods for Predicting the Response of Critical As-Built Infrastructure to Dynamic Loads (Architectural Surety)	3530.030													●	●	●	●	*GSA, DOS, DOE TSWG **Building Construction Architect-Engineering
178	Background Radiation Anisotropy Measurement Sensor (BRAMS)	3530.050															●	●	*NASA **University Collaboration

Pg #	Title	Case Number	Waste Management	Energy Efficiency	Renewable Energy	ES&H	Environmental Restoration	Fossil Energy	Radioactive-Waste Management	Economic Impact	Energy Research	Intelligence & National Security	Nuclear Energy	Science Education & Technical Information	Defense Programs	Department of Defense (DoD)	Other Federal Agencies*	Other (Industry, Consortia,…)**	Other Federal Agencies* (Industry, Consortia…)**
178	Exploitation of Satellite Communications Systems and Networks for Intelligence Applications	3530.090					•								•	•	•		*Tagging & Tracking, DEA, Customs, FBI
179	Microcode Evaluation	3530.110										•			•	•			
179	Real-Time Image Analysis Using Field-Programmable Gate Arrays	3530.120													•				
180	Advanced 3-D Sensing and Visualization System for Unattended Monitoring	3530.130					•					•			•	•	•		*DOE, EM
180	System-of-Labs Direct Fabrication Technology	3531.020													•	•			
182	Poco Switch Tubes	3531.140													•	•			
182	Chemiresistors Based on Metal-Loaded Polymers for Solvent Spill Detection	3531.150	•			•	•								•	•			
183	Advance Neutron-Tube Design and Producibility	3531.160													•	•			
183	Surface Hardening by Nanoparticle Precipitation and Atomic Clustering in Ni(Al,O)	3531.170		•						•	•				•	•			
184	Dynamical Properties of Polymers: Computational Modeling	3531.180								•	•				•				
188	Broadening Mechanism in 2-D Excitonic and Electron Gases	3531.190												•					
184	Calculation and Interpretation of the Energies that Underlie Transition-Metal Surface Structure	3531.210									•				•				
185	Interfacial Reactions in Ceramic Systems	3531.220		•	•			•		•	•				•	•			
186	Direct Fabrication of Multifunctional Nanocomposites Via Supramolecular Self-Assembly	3531.230			•			•			•				•	•			

Pg #	Title	Case Number	Waste Management	Energy Efficiency	Renewable Energy	ES&H	Environmental Restoration	Fossil Energy	Radioactive-Waste Management	Economic Impact	Energy Research	Intelligence & National Security	Nuclear Energy	Science Education & Technical Information	Defense Programs	Department of Defense (DoD)	Other Federal Agencies*	Other (Industry, Consortia,…)**	Other Federal Agencies* (Industry, Consortia…)**
187	Biophotonic Materials for Optical Encryption and Noncomputing	3531.240													•	•			
188	Low-Stress Amorphous Diamond: A New Material for Sensors	3531.250													•	•			
189	Nanoengineered Cu-Al Defects in Al: A Prototype System for Corrosion	3531.260									•				•				
190	Novel Energy-Conversion Devices of Icosahedral Borides	3531.270		•							•				•	•			
191	Ion-Mobility Spectroscopy of Biological Materials	3531.280								•		•			•	•			
192	Visualization Tools for MEMs Designs in a Virtual 3-D World	3531.290								•					•	•			
191	Direct Fabrication of Planar Solid-Oxide Fuel Cells	3531.310		•							•				•	•			
192	Micromachining with Ultra-Short Pulsewidth Lasers	3531.320		•						•	•				•				
193	Molecular Characterization of Energetic Material Initiation	3531.330													•	•			
196	Chemical Feedstocks for the Future: Oxidative Dehydrogenation	3532.010		•				•		•	•								
196	Global Approaches to Infrastructural Analysis (GAIA)	3532.030	•	•	•			•		•		•	•	•					
194	Engineering Complex Distributed Systems	3532.070									•	•			•	•			
198	Laser Communication Nanosatellites	3532.080										•			•	•	•		*NASA
200	Collection and Data Synthesis of Atmospheric Explosion Ground Truth for Global Monitoring Systems	3532.090													•	•			
201	Advanced Radiation Sources: Rayleigh-Taylor Mitigation Via Perturbation Reduction	3532.110													•	•			

Pg #	Title	Case Number	Waste Management	Energy Efficiency	Renewable Energy	ES&H	Environmental Restoration	Fossil Energy	Radioactive-Waste Management	Economic Impact	Energy Research	Intelligence & National Security	Nuclear Energy	Science Education & Technical Information	Defense Programs	Department of Defense (DoD)	Other Federal Agencies*	Other (Industry, Consortia,…)**	Other Federal Agencies* (Industry, Consortia…)**
201	Microfluidic Engineering	3532.120					•					•			•	•			
199	Accelerator Technologies for Emerging Threats	3532.130													•	•			
204	Technologies for System-Level Innovations in Ballistic Missile Defense	3532.140										•			•	•			
202	InGaAsN: A Novel Material for High-Efficiency Solar Cells and Advanced Photonic Devices	3532.150								•	•	•				•	•		*NRO
203	Technologies for Countering C/B Terrorism	3532.160										•			•	•			
205	Aerosol Stand-Off Detection Test-Bed	3532.170										•			•	•	•		*FBI, FEMA
206	Design and Optimization of High-Power Electromagnetic Source Systems and Engagement Scenarios for Achieving Functional Upset or Damage in Specific Target Electronic Systems	3532.180										•			•	•			
207	Real-Time Design of Improved Powder Pressing Dies Using Finite-Element Method Modeling	3532.190													•	•		•	**Ceramic, metallurgical, & pharmaceutical industries
208	Development of Fiber-Laser–Based LIF for Detection of SO_2	3532.210						•			•				•		•		*NASA, EPA
209	Penetration and Defeat of Hardened Underground Facilities Using a Microhole Drilling Robot	3532.220										•			•	•			
210	IFSAR Tree Phenomenology and Coherence Normalization	3532.230					•	•				•			•	•			
210	Electric Launcher for Defense Applications	3532.240									•				•	•			
212	SAM Telemetry for Measurements While Drilling	3533.050		•				•			•								

Pg #	Title	Case Number	Waste Management	Energy Efficiency	Renewable Energy	ES&H	Environmental Restoration	Fossil Energy	Radioactive-Waste Management	Economic Impact	Energy Research	Intelligence & National Security	Nuclear Energy	Science Education & Technical Information	Defense Programs	Department of Defense (DoD)	Other Federal Agencies*	Other (Industry, Consortia,…)**	Other Federal Agencies* (Industry, Consortia…)**
214	Design-for-Manufacturability Applied to Photovoltaic Modules	3533.070			•					•	•								
212	Advanced Geosphere Transport Simulation	3533.160					•		•		•								
214	Low-Work-Function Thermionic Emission Materials	3533.170		•							•				•				
211	Power-Grid Reliability and Restructuring Policy Changes	3533.180		•						•	•		•		•	•	•		*Federal Energy Regulatory Commission (FERC) & North American Electric
222	Low-Cost Cadmium Zinc Telluride Radiation Detectors Based on Electron-Transport-Only Designs	3534.020	•			•	•		•	•	•		•		•	•	•	•	
216	LIGA Micromachining	3534.030								•	•	•			•				
216	Applied Microfluidics Science	3534.040	•								•				•				
218	Computational Simulations of Self-Assembling Macro-Systems by Direct Fabrication of Microscopic Structured Materials	3535.130									•				•				
218	Self-Stabilizing Optical Solitons and High-Intensity Laser Plasma Channels for Diffraction-Free Propagation and Robust Power Compression	3535.140													•	•			
222	Novel Materials for Hydrogen Storage	3535.150									•				•				
220	Optical Communication System for Remote Monitoring and Adaptive Control of Distributed Ground Sensors Exhibiting Collective Intelligence	3535.160													•	•			
223	Inversion of Passive Electromagnetic Fields to Locate Weapons of Mass Destruction	3535.170		•			•	•		•	•				•	•			
224	Z-Pinch–Driven Isentropic Compression	3535.180									•				•	•			

Pg #	Title	Case Number	Waste Management	Energy Efficiency	Renewable Energy	ES&H	Environmental Restoration	Fossil Energy	Radioactive-Waste Management	Economic Impact	Energy Research	Intelligence & National Security	Nuclear Energy	Science Education & Technical Information	Defense Programs	Department of Defense (DoD)	Other Federal Agencies*	Other (Industry, Consortia,…)**	Other Federal Agencies* (Industry, Consortia…)**
225	Covert, Distributed Biosensors for UXO/CW Based on Amplified Immunoassays Conducted in Porous Inorganic Media	3535.190										•				•	•		*NSA, CIA
226	Semiconductor Filament Lasers	3535.210									•		•		•	•			
226	Development of Membrane Devices Using AlN and SiC Films	3537.010												•	•				
227	Spectral Information Content in Ion-Mobility Spectra for Explosives, Interferants, and Other Negative-Ionizing Chemicals	3537.020										•			•	•		•	**Any security operation involving explosives detection
230	Magnetic-Field Profile Measurements in Wire-Array Z-Pinches by Faraday Rotation	3537.030									•		•		•	•			
228	Picosecond Particle Velocity Measurements	3537.040												•	•	•			
228	Particle-Level Modeling of Flows of Concentrated Suspensions	3537.050		•							•				•			•	**Coatings Consortium
229	Efficient Processing of Materials Microstructures with Intelligent Feature Extraction for Quantitative Stereology	3537.060												•					
230	Nondestructive Evaluation of Wind Turbine Blades	3537.070									•			•	•	•			
231	Very Small Arrays: Designing Self-Assembled Systems of Light-Antennae and Reaction Centers for Artificial Photosynthesis	3537.080		•							•	•			•				
232	Enzyme-Mediated Electrochemical Redox Polymer Biosensor for V- and G-Type Chemical Weapons	3537.110	•				•					•			•	•			
232	Novel Biosensor Fabrication Techniques	3537.120	•				•					•			•	•			
233	Design for 100-Year-Life Prototype	3537.130												•	•	•	•	•	*FEMA **Civil construction, insurance

Pg #	Title	Case Number	Waste Management	Energy Efficiency	Renewable Energy	ES&H	Environmental Restoration	Fossil Energy	Radioactive-Waste Management	Economic Impact	Energy Research	Intelligence & National Security	Nuclear Energy	Science Education & Technical Information	Defense Programs	Department of Defense (DoD)	Other Federal Agencies*	Other (Industry, Consortia,…)**	Other Federal Agencies* (Industry, Consortia…)**
233	Enhancing Multilevel Linear Equation Solvers Using Domain Decomposition Strategies	3537.140													•	•			
234	*In Situ* and *Ex Situ* Investigations of Lateral Composition	3537.150		•							•			•	•				
235	Approximate Methods for Computing Eigensolutions Using Automated Multilevel Substructuring	3537.160													•	•			
235	Living Tissue Engineering	3537.170								•									

THIS PAGE
INTENTIONALLY BLANK

Pg #	Title	Case Number	Aeronautics	Applied Molecular Biology	Ceramics	Composites	Computer Simulation & Modeling	Data Storage & Peripherals	Electronics & Photonics	Energy	Flexible Computer-Integrated Manufacturing	High-Definition Imaging & Displays	High-Performance Computing & Networking	High-Performance Metals & Alloys	Intelligent Processing Equipment	Materials Synthesis & Processing	Medical Technology	Micro- & Nanofabrication	Micro- & Optoelectronics	Photonic Materials	Pollution Min., Remediation, & Waste Mgmt.	Sensors & Signal Processing	Software	Surface Transportation Technologies	Systems Management Technologies	Defense-Related (mostly or purely)	Dual-Use (defense and non-defense-related)	Non-Defense-Related (mostly or purely)
10	Catalytic Membrane Sensors	3502.030													•			•			•			•				
9	Photonic Bandgap Structures as a Gateway to Nanophotonics	3502.040							•				•						•			•					•	
10	Wide-Bandgap Compound Semiconductors to Enable Novel Semiconductor Devices	3502.050					•	•	•	•		•				•			•	•		•					•	
12	Ultra-Hard Multilayer Coatings	3502.080						•	•	•		•				•		•	•			•					•	
14	Scanning Probe–Based Processes for Nanometer-Scale Device Fabrication	3502.090							•							•		•	•								•	
15	Molecular-Scale Lubricants for Micromachine Applications	3502.110														•		•	•			•					•	
16	Surface-Micromachined Flexural Plate-Wave Device Integrated on Silicon	3502.120			•				•							•		•	•		•	•					•	
17	Smart Interface Bonding Alloys (SIBA): Tailoring Thin-Film Mechanical Properties	3502.140				•	•											•				•						•
20	Recognizing Atoms in Atomically Engineered Nanostructures: An Interdisciplinary Approach	3502.170							•			•				•			•			•	•					•
18	Molecular-to-Continuum Fracture Analysis of Thermoset Polymer/Solid Interfaces	3502.190				•	•						•			•			•								•	
19	Monolithic Structures for Nanoseparation	3502.210		•						•						•	•				•	•		•			•	
21	Fundamental Aspects of Micromachine Reliability	3502.220																•									•	
24	Enabling Science and Technology for Cold-Spray Direct Fabrication	3502.230	•			•	•			•	•		•			•					•			•			•	

Pg #	Title	Case Number	Aeronautics	Applied Molecular Biology	Ceramics	Composites	Computer Simulation & Modeling	Data Storage & Peripherals	Electronics & Photonics	Energy	Flexible Computer-Integrated Manufacturing	High-Definition Imaging & Displays	High-Performance Computing & Networking	High-Performance Metals & Alloys	Intelligent Processing Equipment	Materials Synthesis & Processing	Medical Technology	Micro- & Nanofabrication	Micro- & Optoelectronics	Photonic Materials	Pollution Min., Remediation, & Waste Mgmt.	Sensors & Signal Processing	Software	Surface Transportation Technologies	Systems Management Technologies	Defense-Related (mostly or purely)	Dual-Use (defense and non-defense-related)	Non-Defense-Related (mostly or purely)
22	Atomic-Level Studies of Surfactant-Directed Materials Growth	3502.240							•									•									•	
26	Intelligent Polymers for Nanodevice Performance Control	3502.250														•											•	
25	Freeforming of Ceramics and Composites from Colloidal Slurries	3502.260			•	•				•						•											•	
26	Quantum Dot Arrays	3502.270								•						•		•		•								•
27	Laser-Assisted Arc Welding for Aluminum Alloys	3502.280	•							•	•			•	•	•											•	
28	Reactivity of Metal-Oxide Surfaces	3502.310					•			•						•												•
29	Exploiting LENS Technology Through Novel Materials	3502.320	•			•					•		•		•												•	
34	Parallel Quantum Chemistry for Material Aging and Synthesis	3504.010				•	•						•			•											•	
34	Modeling Complex Turbulent Chemically Reacting Flows on Massively Parallel Supercomputers	3504.020	•				•		•	•			•			•			•			•					•	
35	Automated Geometric Model Builder Using Range Image Sensor Data	3504.050					•						•				•										•	
36	A Massively Parallel Sparse Eigensolver for Structural Dynamics Finite Element	3504.060	•			•	•			•	•		•		•				•			•	•	•			•	
36	Density-Functional Theory for Classical Fluids at Complex Interfaces	3504.070			•		•									•		•				•						•

Pg #	Title	Case Number	Aeronautics	Applied Molecular Biology	Ceramics	Composites	Computer Simulation & Modeling	Data Storage & Peripherals	Electronics & Photonics	Energy	Flexible Computer-Integrated Manufacturing	High-Definition Imaging & Displays	High-Performance Computing & Networking	High-Performance Metals & Alloys	Intelligent Processing Equipment	Materials Synthesis & Processing	Medical Technology	Micro- & Nanofabrication	Micro- & Optoelectronics	Photonic Materials	Pollution Min., Remediation, & Waste Mgmt.	Sensors & Signal Processing	Software	Surface Transportation Technologies	Systems Management Technologies	Defense-Related (mostly or purely)	Dual-Use (defense and non-defense-related)	Non-Defense-Related (mostly or purely)
33	Gradient-Driven Diffusion of Multi-Atom Molecules Through Macromolecules and Membranes	3504.090		•		•	•		•	•			•	•		•	•	•			•	•	•	•			•	
38	Fast and Easy Parallel I/O for Efficient Scientific Computing	3504.120					•	•					•										•				•	
38	Novel Load-Balancing for Scalable, Parallel Electromagnetic and Plasma Physics Simulation Software	3504.130					•		•			•	•						•			•	•				•	
40	Parallel Computational Chemistry Using Constraints	3504.140											•			•											•	
40	Massively Parallel *Ab Initio* Validation for ASCI Materials Aging	3504.160				•	•						•			•										•		
42	Computational Methods for Coupling Microstructural and Micromechanical Materials Response Simulations	3504.170			•	•	•		•							•		•								•		
44	An Investigation of Wavelet Bases for Multiscale, Grid–Based Simulation	3504.180	•				•			•			•														•	
41	Integrated Quantum/Classical Modeling of Hydrogenic Materials	3504.190					•						•			•										•		
45	The Next Generation of Teraflop Density-Functional Electronic Structure Codes	3504.210					•						•										•				•	
46	Methodology for Characterizing Modeling and Discretization Uncertainties in Computational Simulation	3504.220	•			•	•			•	•		•		•	•			•			•	•				•	
48	Global Optimization for Engineering Science Problems	3504.230	•	•	•		•				•		•				•					•	•	•	•		•	

Pg #	Title	Case Number	Aeronautics	Applied Molecular Biology	Ceramics	Composites	Computer Simulation & Modeling	Data Storage & Peripherals	Electronics & Photonics	Energy	Flexible Computer-Integrated Manufacturing	High-Definition Imaging & Displays	High-Performance Computing & Networking	High-Performance Metals & Alloys	Intelligent Processing Equipment	Materials Synthesis & Processing	Medical Technology	Micro- & Nanofabrication	Micro- & Optoelectronics	Photonic Materials	Pollution Min., Remediation, & Waste Mgmt.	Sensors & Signal Processing	Software	Surface Transportation Technologies	Systems Management Technologies	Defense-Related (mostly or purely)	Dual-Use (defense and non-defense-related)	Non-Defense-Related (mostly or purely)
49	Dynamic Simulation of Mechanical Systems with Intermittent Contacts	3504.240	•				•				•				•								•				•	
43	From Atom-Picoseconds to Centimeter-Years in Simulation and Experiment	3504.250			•	•	•		•	•			•	•		•		•		•			•				•	
47	Emergent Behavior of Large Swarms of Intelligent Agents	3504.260					•						•		•						•						•	
50	Parallel Combinatorial Optimization for Scheduling Problems	3504.270									•		•										•				•	
50	Programming Paradigms for Massively Parallel Computers	3504.280	•				•	•					•										•				•	
51	Multilevel Techniques for Unstructured Grid Problems on Massively Parallel Computers	3504.290					•						•										•				•	
52	Scalable Tools for Massively Parallel Distributed Computing	3504.310											•										•				•	
52	Massively Parallel Methods for Simulating the Phase Field Model	3504.320			•		•						•														•	
53	Visual Explanation and Insight	3504.330		•			•																•		•		•	
58	Wafer Fusion for Integration of Semiconductor Materials and Devices	3506.110							•				•						•			•					•	
58	Highly Parallel, Low-Power, Photonic Interconnects for Inter-Board Signal Distribution	3506.120							•			•	•						•	•		•					•	
59	Virtual Reactor for the Semiconductor Manufacturing Plant of the Future	3506.140					•		•		•					•			•	•							•	

Pg #	Title	Case Number	Aeronautics	Applied Molecular Biology	Ceramics	Composites	Computer Simulation & Modeling	Data Storage & Peripherals	Electronics & Photonics	Energy	Flexible Computer-Integrated Manufacturing	High-Definition Imaging & Displays	High-Performance Computing & Networking	High-Performance Metals & Alloys	Intelligent Processing Equipment	Materials Synthesis & Processing	Medical Technology	Micro- & Nanofabrication	Micro- & Optoelectronics	Photonic Materials	Pollution Min., Remediation, & Waste Mgmt.	Sensors & Signal Processing	Software	Surface Transportation Technologies	Systems Management Technologies	Defense-Related (mostly or purely)	Dual-Use (defense and non-defense-related)	Non-Defense-Related (mostly or purely)
60	Selective Oxidation Technology and Its Applications Toward Electronic and Optoelectronic Devices	3506.160							•				•						•			•					•	
61	Agile Prototyping of Microelectromechanical Systems (MEMS)	3506.180	•						•			•						•	•			•					•	
57	Advanced Concepts for High-Power VCSELs and VCSEL Arrays	3506.190							•				•						•			•					•	
62	Midwave-Infrared (2–6 µm) Emitter–Based Chemical Sensor Systems	3506.210							•				•						•			•					•	
62	A Novel Nondestructive Silicon-on-Insulator Nonvolatile Memory	3506.230						•	•				•						•								•	
64	Integration of Optoelectronics and MEMS by Free-Space Microoptics	3506.240							•				•						•			•					•	
65	Advanced Laser Structures for Short-Pulsed Power in Active Optical Sensor Systems	3506.250							•							•		•	•	•		•					•	
66	Metal Micro-Heat-Pipe Substrates for High-Power-Density Electronics	3506.260	•						•				•					•	•			•					•	
68	Integration of Microsensor Technology into a Miniature Robotic Vehicle	3506.270																	•			•				•		
66	Vacuum Encapsulation of MEMS Structures	3506.280	•						•						•		•	•	•	•		•		•			•	
67	Massively Parallel Sensor Arrays for Volatile Organic Detection	3506.290							•										•			•	•				•	

Pg #	Title	Case Number	Aeronautics	Applied Molecular Biology	Ceramics	Composites	Computer Simulation & Modeling	Data Storage & Peripherals	Electronics & Photonics	Energy	Flexible Computer-Integrated Manufacturing	High-Definition Imaging & Displays	High-Performance Computing & Networking	High-Performance Metals & Alloys	Intelligent Processing Equipment	Materials Synthesis & Processing	Medical Technology	Micro- & Nanofabrication	Micro- & Optoelectronics	Photonic Materials	Pollution Min., Remediation, & Waste Mgmt.	Sensors & Signal Processing	Software	Surface Transportation Technologies	Systems Management Technologies	Defense-Related (mostly or purely)	Dual-Use (defense and non-defense-related)	Non-Defense-Related (mostly or purely)
70	Agile Dry Etching of Compound Semiconductors for Science–Based Manufacturing Using *In Situ* Process Control	3506.310							•							•		•	•	•							•	
68	Precision-Formed Micromagnets	3506.320			•				•							•		•				•					•	
70	Time-Resolved Ion-Beam–Induced Charge-Collection (TRIBICC) Imaging	3506.330																	•								•	
74	Composite-Resonator Surface-Emitting Lasers	3506.340							•							•			•	•		•					•	
73	Role of Defects in III-Nitride–Based Electronics	3506.350							•										•	•							•	
74	Ultra–Low-Power Sensors for Microtelemetry Systems	3506.360							•								•	•			•	•					•	
72	Double Quantum-Well Long-Wavelength Optoelectronic Devices	3506.370							•				•						•			•					•	
75	The Development of Integrated Chemical Microsensors in GaAs	3506.380							•									•	•			•					•	
76	Monolithic Integrated of VCSELs and Detectors for Microsystems	3506.410							•				•						•			•					•	
77	AlGaN Materials Engineering for Integrated Multifunction Systems	3506.420						•	•	•	•	•				•		•	•	•		•					•	
71	Compliant Substrates for Epitaxial Integration of Dissimilar Materials	3506.430							•							•		•	•	•							•	
78	Post-Processed Integrated Microsystems	3506.440							•									•	•			•				•		
83	Using Higher-Order Gradients to Modeling Localization Phenomena	3508.040					•							•		•											•	

Pg #	Title	Case Number	Aeronautics	Applied Molecular Biology	Ceramics	Composites	Computer Simulation & Modeling	Data Storage & Peripherals	Electronics & Photonics	Energy	Flexible Computer-Integrated Manufacturing	High-Definition Imaging & Displays	High-Performance Computing & Networking	High-Performance Metals & Alloys	Intelligent Processing Equipment	Materials Synthesis & Processing	Medical Technology	Micro- & Nanofabrication	Micro- & Optoelectronics	Photonic Materials	Pollution Min., Remediation, & Waste Mgmt.	Sensors & Signal Processing	Software	Surface Transportation Technologies	Systems Management Technologies	Defense-Related (mostly or purely)	Dual-Use (defense and non-defense-related)	Non-Defense-Related (mostly or purely)
81	Enhanced Vapor-Phase Diffusion in Porous Media	3508.060			•		•			•											•							•
82	Stress Evaluation and Model Validation Using Laser Ultrasonics	3508.110	•		•	•	•			•				•		•		•				•		•			•	
84	Altered Simulation Properties for Tetrahedral Finite Elements for Use in Engineering Simulation	3508.120	•				•				•			•					•								•	
84	Development, Implementation, and Experimental Validation of the Lattice Boltzmann Method for Modeling Three-Dimensional Complex Flows	3508.130			•		•			•			•	•		•											•	
86	Capturing Recrystallization of Metals with a Multiscale Material Model	3508.140					•							•		•		•									•	
88	Nondeterministic Modeling in Engineering Science	3508.150	•			•	•			•	•		•		•				•			•	•				•	
88	Lagrangian Modeling of Radiative Transport	3508.160																							•	•		
89	High-Resolution Modeling of Multiscale Transient Phenomena in Turbulent Boundary Layers	3508.170					•			•																	•	
90	Dispersive Measurements of Velocity in Heterogeneous Materials	3508.180			•	•	•			•						•		•									•	
90	A Physically–Based Computational Method for Predicting Generalized Fracture	3508.190			•	•	•			•			•	•				•									•	
92	Development of *In Situ* Diagnostics for Simultaneous Measurement of Transient Gas Species and Soot in Large Fires	3508.210					•			•											•	•					•	

Pg #	Title	Case Number	Aeronautics	Applied Molecular Biology	Ceramics	Composites	Computer Simulation & Modeling	Data Storage & Peripherals	Electronics & Photonics	Energy	Flexible Computer-Integrated Manufacturing	High-Definition Imaging & Displays	High-Performance Computing & Networking	High-Performance Metals & Alloys	Intelligent Processing Equipment	Materials Synthesis & Processing	Medical Technology	Micro- & Nanofabrication	Micro- & Optoelectronics	Photonic Materials	Pollution Min., Remediation, & Waste Mgmt.	Sensors & Signal Processing	Software	Surface Transportation Technologies	Systems Management Technologies	Defense-Related (mostly or purely)	Dual-Use (defense and non-defense-related)	Non-Defense-Related (mostly or purely)
91	Micromechanical Failure Analyses for Finite-Element Polymer Modeling	3508.220	•			•	•		•		•					•			•								•	
94	Methodology Optimal Selection of Test and Simulation Levels for Problems Involving Computational Simulation	3508.230					•						•										•				•	
93	A Phenomenological Model for Multicomponent Transport with Electrochemical Reactions in Concentrated Solutions	3508.240					•				•					•					•						•	
98	Laser-Spray Fabrication for Net-Shape Rapid Product Realization	3510.460	•		•	•				•	•			•	•	•					•		•				•	
99	Solution Synthesis and Processing of PZT Materials for Neutron-Generator Applications	3510.510			•				•							•		•								•		
97	Ultra-Precise Assembly of Microelectromechanical Systems (MEMS)	3510.540							•		•							•	•								•	•
100	Finite-Element Meshing Approached as a Global Minimization Process	3510.570	•		•	•	•				•																•	
102	Application of Parallel Mechanism Technology to Manufacturing	3510.580	•								•				•												•	
100	Investigation of the Impact of Cleaning on Adhesive Bond and the Process Implications	3510.590	•			•			•	•	•					•		•			•						•	
102	Standard Cells for Microelectromechanical Systems (MEMS)	3510.610	•						•			•						•	•			•					•	
104	Laser Wire Deposition for Fully Dense Shapes	3510.620	•								•			•	•	•							•				•	

Pg #	Title	Case Number	Aeronautics	Applied Molecular Biology	Ceramics	Composites	Computer Simulation & Modeling	Data Storage & Peripherals	Electronics & Photonics	Energy	Flexible Computer-Integrated Manufacturing	High-Definition Imaging & Displays	High-Performance Computing & Networking	High-Performance Metals & Alloys	Intelligent Processing Equipment	Materials Synthesis & Processing	Medical Technology	Micro- & Nanofabrication	Micro- & Optoelectronics	Photonic Materials	Pollution Min., Remediation, & Waste Mgmt.	Sensors & Signal Processing	Software	Surface Transportation Technologies	Systems Management Technologies	Defense-Related (mostly or purely)	Dual-Use (defense and non-defense-related)	Non-Defense-Related (mostly or purely)
105	High-Throughput Dry Processes for Large-Area Devices	3510.630							•	•									•								•	
106	Assuring High Reliability and Production Readiness in Low-Volume Manufacturing	3510.640	•								•				•			•	•			•					•	
103	Scripting for Video Inspection	3510.660			•		•		•		•				•							•	•				•	
106	Advanced Machining Processes for Microfabrication	3510.670	•		•						•			•	•	•		•				•					•	
107	Fusion of Product and Process Data Using Real-Time Streaming Visualization	3510.680					•				•				•							•	•				•	
108	Advanced Production Planning Models	3510.690					•				•		•								•		•	•	•	•		
112	Automatic Generation of Multimedia Documentation for Assembly Operations	3511.010	•				•				•										•		•				•	
113	Distributed Life-Cycle Models in Enterprise Simulations to Answer System Questions	3511.020					•						•														•	
114	Immersive CAD	3511.040	•				•				•		•														•	
114	Automatic Planning of Life-Cycle Assembly Processes	3511.050	•				•		•						•								•				•	
116	Analysis of Very Large Assemblies	3511.070	•				•		•						•								•				•	
111	Enabling Human Skills with Cooperative Automation	3511.080					•								•						•	•					•	
116	Cloud To CAD	3511.090	•				•					•	•										•				•	
118	Ergonomics in Life-Cycle Assembly Processes	3511.110	•				•				•				•						•		•				•	

Pg #	Title	Case Number	Aeronautics	Applied Molecular Biology	Ceramics	Composites	Computer Simulation & Modeling	Data Storage & Peripherals	Electronics & Photonics	Energy	Flexible Computer-Integrated Manufacturing	High-Definition Imaging & Displays	High-Performance Computing & Networking	High-Performance Metals & Alloys	Intelligent Processing Equipment	Materials Synthesis & Processing	Medical Technology	Micro- & Nanofabrication	Micro- & Optoelectronics	Photonic Materials	Pollution Min., Remediation, & Waste Mgmt.	Sensors & Signal Processing	Software	Surface Transportation Technologies	Systems Management Technologies	Defense-Related (mostly or purely)	Dual-Use (defense and non-defense-related)	Non-Defense-Related (mostly or purely)
117	Feature Reduction of Geometric Solid Models for Analysis Tools	3511.120	•				•				•		•		•						•	•	•				•	
119	System Surety Life-Cycle Engineering	3511.130					•								•								•				•	
123	Content–Based Search of Geometric Databases	3512.160					•	•			•		•		•								•				•	
124	Integrated Service Provisioning in an “IPv6 over ATM” Research Network	3512.170									•	•	•														•	
125	Virtual Desktop Engineering with Integrated Multimedia Data	3512.180					•				•		•														•	
123	Mission Surety for Large-Scale Real-Time Information Systems	3512.190	•	•			•						•				•					•	•				•	
126	Scaled ATM End-to-End Encryption	3512.220							•				•														•	
128	Network Surety Modeling for Wireless ATM Networks	3512.230					•						•														•	
130	Low-Power, Reduced-Computation, Public-Key Protocols	3512.240						•					•		•							•	•		•		•	
126	Ten-to-One-Hundred-Gigabit/Second Network Enabling R&D	3512.250					•		•				•														•	
130	High-Performance Commodity Interconnects for Clustered Scientific and Engineering Computing	3512.260					•						•														•	
131	AVATAR — Navigating and Mining in Massive Data	3512.270	•				•			•					•		•										•	
129	Algorithm–Based Fault Tolerance on Heterogeneous Massively Parallel Computers	3512.280					•	•			•		•		•							•	•			•		

Pg #	Title	Case Number	Aeronautics	Applied Molecular Biology	Ceramics	Composites	Computer Simulation & Modeling	Data Storage & Peripherals	Electronics & Photonics	Energy	Flexible Computer-Integrated Manufacturing	High-Definition Imaging & Displays	High-Performance Computing & Networking	High-Performance Metals & Alloys	Intelligent Processing Equipment	Materials Synthesis & Processing	Medical Technology	Micro- & Nanofabrication	Micro- & Optoelectronics	Photonic Materials	Pollution Min., Remediation, & Waste Mgmt.	Sensors & Signal Processing	Software	Surface Transportation Technologies	Systems Management Technologies	Defense-Related (mostly or purely)	Dual-Use (defense and non-defense-related)	Non-Defense-Related (mostly or purely)
136	Electrokinetic Immunoaffinity Chemical Sensors	3516.050		•					•								•	•	•			•					•	
136	Information-Efficient Spectral Imaging System (ISIS)	3516.060					•		•						•							•					•	
137	Imaging of Moving Targets Using Simultaneous Synthetic Aperture Radar (SAR) and Moving Target Indicator (MTI) Radar	3516.070																				•				•		
135	Sampling and Sensing Systems for High-Priority Analytes	3516.080			•				•							•		•	•		•	•					•	
138	Automated Vegetation Height Measurement for Automatic Terrain Mapping	3516.090																				•					•	
138	Sparse Geophysical Networks for Monitoring Deep Targets	3516.110					•															•	•			•		
139	Miniature Bioaerosol Concentrator	3516.120																•				•				•		
140	Recognizing Partially Obscured Targets by Combining Multiple Data Sources Using Evidential Reasoning	3516.130													•		•					•					•	
141	Computational Engineering of Sensor Materials and Integration with a Novel Biological Weapon Detection System	3516.140		•			•						•			•						•					•	
142	Biological Weapon Detector Using Bioaffinity Array Impedance Analysis with Chemical Amplification Through Redox Recycling	3516.150		•					•								•		•			•					•	
142	ATR/Exploitation Utilizing Ultra–High-Resolution, Complex SAR Imaging	3516.160									•				•							•				•		

Pg #	Title	Case Number	Aeronautics	Applied Molecular Biology	Ceramics	Composites	Computer Simulation & Modeling	Data Storage & Peripherals	Electronics & Photonics	Energy	Flexible Computer-Integrated Manufacturing	High-Definition Imaging & Displays	High-Performance Computing & Networking	High-Performance Metals & Alloys	Intelligent Processing Equipment	Materials Synthesis & Processing	Medical Technology	Micro- & Nanofabrication	Micro- & Optoelectronics	Photonic Materials	Pollution Min., Remediation, & Waste Mgmt.	Sensors & Signal Processing	Software	Surface Transportation Technologies	Systems Management Technologies	Defense-Related (mostly or purely)	Dual-Use (defense and non-defense-related)	Non-Defense-Related (mostly or purely)
147	Designed Molecular Recognition Materials for Chiral Sensors, Separations, and Catalytic Materials	3518.030					•	•								•	•	•				•					•	
148	Rapid Screening of Complex Chemical Samples Via Capillary Array Analysis	3518.050																			•						•	
148	Designed Synthesis of Controlled Degradative Materials	3518.060				•										•											•	
150	Mechanistic Models for Radionuclide Desorption from Soils	3518.070																			•						•	
150	Development of Innovative Combustion Processes for a Direct-Injection Diesel Engine	3518.080								•														•				•
152	Hydrogen Production for Fuel Cells by Selective Dehydrogenation of Alkanes in Catalytic Membrane Reactors	3518.090			•					•						•		•									•	
153	Hybrid Vehicle Engine Development	3518.110								•														•				•
149	Adaptive 3-D Sensing	3518.120										•					•				•	•					•	
154	Aqueous Organic Sensor	3518.130																				•					•	
154	Designed Ionophores for Liquid-Membrane Separation and Extraction of Metal Ions	3518.140		•			•			•				•		•	•	•			•	•					•	
156	An Electromagnetic Imaging System for Environmental Site Reconnaissance	3518.150							•										•		•	•					•	
160	Reliability Degradation Due to Stockpile Aging	3520.210	•		•	•	•		•					•					•								•	

Pg #	Title	Case Number	Aeronautics	Applied Molecular Biology	Ceramics	Composites	Computer Simulation & Modeling	Data Storage & Peripherals	Electronics & Photonics	Energy	Flexible Computer-Integrated Manufacturing	High-Definition Imaging & Displays	High-Performance Computing & Networking	High-Performance Metals & Alloys	Intelligent Processing Equipment	Materials Synthesis & Processing	Medical Technology	Micro- & Nanofabrication	Micro- & Optoelectronics	Photonic Materials	Pollution Min., Remediation, & Waste Mgmt.	Sensors & Signal Processing	Software	Surface Transportation Technologies	Systems Management Technologies	Defense-Related (mostly or purely)	Dual-Use (defense and non-defense-related)	Non-Defense-Related (mostly or purely)
159	Integrated Approach to Develop Microelectromechanical (MEMS) Reliability Tools	3520.220																	•			•					•	
160	Precursors to Failure of Oxides and Metal Lines in CMOS Technology	3520.230																	•								•	
162	An Extensible Object-Oriented Framework for Risk and Reliability Analysis	3520.240					•			•			•		•		•								•		•	
162	Simulation/Optimization Tools for System Variability Analysis	3520.270	•				•		•		•		•														•	
164	A Massively Parallel Microsimulation Model of Infrastructure Interdependency	3520.280					•						•										•		•		•	
166	Physical Models for Predicting the Effect of Atmospheric Corrosion on Microelectronic Reliability	3520.290					•		•									•	•			•				•		
167	Backside Localization of Open and Shorted IC (Integrated Circuit) Interconnections	3520.310																	•								•	
165	Reliability Predictions for Advanced Electronics in Smoke Environments	3520.320	•							•			•														•	
168	Security of Bulk Power Systems	3520.330					•			•			•														•	
171	Science on the Microdomain	3522.010															•	•	•		•	•					•	
172	Autonomous MicroChem Laboratory (µChemLab)	3522.020		•			•	•	•	•	•				•	•	•	•	•	•	•	•		•	•		•	
171	Cooperative, Distributed Sensing and Action Using Microminiature, Intelligent Agents	3522.030					•								•						•						•	

Pg #	Title	Case Number	Aeronautics	Applied Molecular Biology	Ceramics	Composites	Computer Simulation & Modeling	Data Storage & Peripherals	Electronics & Photonics	Energy	Flexible Computer-Integrated Manufacturing	High-Definition Imaging & Displays	High-Performance Computing & Networking	High-Performance Metals & Alloys	Intelligent Processing Equipment	Materials Synthesis & Processing	Medical Technology	Micro- & Nanofabrication	Micro- & Optoelectronics	Photonic Materials	Pollution Min., Remediation, & Waste Mgmt.	Sensors & Signal Processing	Software	Surface Transportation Technologies	Systems Management Technologies	Defense-Related (mostly or purely)	Dual-Use (defense and non-defense-related)	Non-Defense-Related (mostly or purely)
177	Computational Methods for Predicting the Response of Critical As-Built Infrastructure to Dynamic Loads (Architectural Surety)	3530.030				•	•					•											•				•	
178	Background Radiation Anisotropy Measurement Sensor (BRAMS)	3530.050																				•						•
178	Exploitation of Satellite Communications Systems and Networks for Intelligence Applications	3530.090																				•		•	•		•	
179	Microcode Evaluation	3530.110																								•		
179	Real-Time Image Analysis Using Field-Programmable Gate Arrays	3530.120					•								•							•				•		
180	Advanced 3-D Sensing and Visualization System for Unattended Monitoring	3530.130													•						•	•					•	
180	System-of-Labs Direct Fabrication Technology	3531.020												•		•											•	
182	Poco Switch Tubes	3531.140																									•	
182	Chemiresistors Based on Metal-Loaded Polymers for Solvent Spill Detection	3531.150							•								•	•	•		•	•					•	
183	Advance Neutron-Tube Design and Producibility	3531.160			•																					•		
183	Surface Hardening by Nanoparticle Precipitation and Atomic Clustering in Ni(Al,O)	3531.170												•		•		•									•	
184	Dynamical Properties of Polymers: Computational Modeling	3531.180					•						•			•											•	
188	Broadening Mechanism in 2-D Excitonic and Electron Gases	3531.190							•										•									•

Pg #	Title	Case Number	Aeronautics	Applied Molecular Biology	Ceramics	Composites	Computer Simulation & Modeling	Data Storage & Peripherals	Electronics & Photonics	Energy	Flexible Computer-Integrated Manufacturing	High-Definition Imaging & Displays	High-Performance Computing & Networking	High-Performance Metals & Alloys	Intelligent Processing Equipment	Materials Synthesis & Processing	Medical Technology	Micro- & Nanofabrication	Micro- & Optoelectronics	Photonic Materials	Pollution Min., Remediation, & Waste Mgmt.	Sensors & Signal Processing	Software	Surface Transportation Technologies	Systems Management Technologies	Defense-Related (mostly or purely)	Dual-Use (defense and non-defense-related)	Non-Defense-Related (mostly or purely)
184	Calculation and Interpretation of the Energies that Underlie Transition-Metal Surface Structure	3531.210					•		•	•				•		•		•									•	
185	Interfacial Reactions in Ceramic Systems	3531.220			•	•				•						•			•								•	
186	Direct Fabrication of Multifunctional Nanocomposites Via Supramolecular Self-Assembly	3531.230			•	•			•	•		•				•		•	•	•		•					•	
187	Biophotonic Materials for Optical Encryption and Noncomputing	3531.240					•	•	•							•			•	•		•					•	
188	Low-Stress Amorphous Diamond: A New Material for Sensors	3531.250							•									•	•			•					•	
189	Nanoengineered Cu-Al Defects in Al: A Prototype System for Corrosion	3531.260			•													•									•	
190	Novel Energy-Conversion Devices of Icosahedral Borides	3531.270							•	•																	•	
191	Ion-Mobility Spectroscopy of Biological Materials	3531.280																				•				•		
192	Visualization Tools for MEMs Designs in a Virtual 3-D World	3531.290					•		•		•							•	•								•	
191	Direct Fabrication of Planar Solid-Oxide Fuel Cells	3531.310			•	•				•						•		•									•	
192	Micromachining with Ultra-Short Pulsewidth Lasers	3531.320	•						•	•							•	•				•					•	
193	Molecular Characterization of Energetic Material Initiation	3531.330								•						•										•		
196	Chemical Feedstocks for the Future: Oxidative Dehydrogenation	3532.010																										•

Pg #	Title	Case Number	Aeronautics	Applied Molecular Biology	Ceramics	Composites	Computer Simulation & Modeling	Data Storage & Peripherals	Electronics & Photonics	Energy	Flexible Computer-Integrated Manufacturing	High-Definition Imaging & Displays	High-Performance Computing & Networking	High-Performance Metals & Alloys	Intelligent Processing Equipment	Materials Synthesis & Processing	Medical Technology	Micro- & Nanofabrication	Micro- & Optoelectronics	Photonic Materials	Pollution Min., Remediation, & Waste Mgmt.	Sensors & Signal Processing	Software	Surface Transportation Technologies	Systems Management Technologies	Defense-Related (mostly or purely)	Dual-Use (defense and non-defense-related)	Non-Defense-Related (mostly or purely)
196	Global Approaches to Infrastructural Analysis (GAIA)	3532.030					•			•			•									•	•		•			•
194	Engineering Complex Distributed Systems	3532.070					•	•					•									•	•		•		•	
198	Laser Communication Nanosatellites	3532.080							•	•			•	•				•	•	•							•	
200	Collection and Data Synthesis of Atmospheric Explosion Ground Truth for Global Monitoring Systems	3532.090					•																				•	
201	Advanced Radiation Sources: Rayleigh-Taylor Mitigation Via Perturbation Reduction	3532.110					•																			•		
201	Microfluidic Engineering	3532.120																•	•			•					•	
199	Accelerator Technologies for Emerging Threats	3532.130				•										•										•		
204	Technologies for System-Level Innovations in Ballistic Missile Defense	3532.140	•					•	•				•			•			•	•		•				•		
202	InGaAsN: A Novel Material for High-Efficiency Solar Cells and Advanced Photonic Devices	3532.150							•										•	•							•	
203	Technologies for Countering C/B Terrorism	3532.160	•	•	•		•						•						•			•				•		
205	Aerosol Stand-Off Detection Test-Bed	3532.170																						•			•	
206	Design and Optimization of High-Power Electromagnetic Source Systems and Engagement Scenarios for Achieving Functional Upset or Damage in Specific Target Electronic Systems	3532.180							•																	•		

Pg #	Title	Case Number	Aeronautics	Applied Molecular Biology	Ceramics	Composites	Computer Simulation & Modeling	Data Storage & Peripherals	Electronics & Photonics	Energy	Flexible Computer-Integrated Manufacturing	High-Definition Imaging & Displays	High-Performance Computing & Networking	High-Performance Metals & Alloys	Intelligent Processing Equipment	Materials Synthesis & Processing	Medical Technology	Micro- & Nanofabrication	Micro- & Optoelectronics	Photonic Materials	Pollution Min., Remediation, & Waste Mgmt.	Sensors & Signal Processing	Software	Surface Transportation Technologies	Systems Management Technologies	Defense-Related (mostly or purely)	Dual-Use (defense and non-defense-related)	Non-Defense-Related (mostly or purely)
207	Real-Time Design of Improved Powder Pressing Dies Using Finite-Element Method Modeling	3532.190	•		•	•	•				•			•		•							•				•	
208	Development of Fiber-Laser–Based LIF for Detection of SO_2	3532.210							•												•	•					•	
209	Penetration and Defeat of Hardened Underground Facilities Using a Microhole Drilling Robot	3532.220																				•				•		
210	IFSAR Tree Phenomenology and Coherence Normalization	3532.230					•	•				•										•	•				•	
210	Electric Launcher for Defense Applications	3532.240	•																					•		•		
212	SAM Telemetry for Measurements While Drilling	3533.050								•																		•
214	Design-for-Manufacturability Applied to Photovoltaic Modules	3533.070							•	•																		•
212	Advanced Geosphere Transport Simulation	3533.160					•			•			•								•							•
214	Low-Work-Function Thermionic Emission Materials	3533.170								•						•											•	
211	Power-Grid Reliability and Restructuring Policy Changes	3533.180					•			•																	•	
222	Low-Cost Cadmium Zinc Telluride Radiation Detectors Based on Electron-Transport-Only Designs	3534.020							•	•		•		•		•	•	•	•	•	•	•					•	
216	LIGA Micromachining	3534.030												•		•		•				•					•	
216	Applied Microfluidics Science	3534.040		•			•		•									•	•			•					•	

Pg #	Title	Case Number	Aeronautics	Applied Molecular Biology	Ceramics	Composites	Computer Simulation & Modeling	Data Storage & Peripherals	Electronics & Photonics	Energy	Flexible Computer-Integrated Manufacturing	High-Definition Imaging & Displays	High-Performance Computing & Networking	High-Performance Metals & Alloys	Intelligent Processing Equipment	Materials Synthesis & Processing	Medical Technology	Micro- & Nanofabrication	Micro- & Optoelectronics	Photonic Materials	Pollution Min., Remediation, & Waste Mgmt.	Sensors & Signal Processing	Software	Surface Transportation Technologies	Systems Management Technologies	Defense-Related (mostly or purely)	Dual-Use (defense and non-defense-related)	Non-Defense-Related (mostly or purely)
218	Computational Simulations of Self-Assembling Macro-Systems by Direct Fabrication of Microscopic Structured Materials	3535.130					•						•										•				•	
218	Self-Stabilizing Optical Solitons and High-Intensity Laser Plasma Channels for Diffraction-Free Propagation and Robust Power Compression	3535.140								•						•	•										•	
222	Novel Materials for Hydrogen Storage	3535.150								•				•		•											•	
220	Optical Communication System for Remote Monitoring and Adaptive Control of Distributed Ground Sensors Exhibiting Collective Intelligence	3535.160							•											•		•					•	
223	Inversion of Passive Electromagnetic Fields to Locate Weapons of Mass Destruction	3535.170					•		•	•			•										•				•	
224	Z-Pinch–Driven Isentropic Compression	3535.180								•				•		•											•	
225	Covert, Distributed Biosensors for UXO/CW Based on Amplified Immunoassays Conducted in Porous Inorganic Media	3535.190			•	•										•		•				•					•	
226	Semiconductor Filament Lasers	3535.210	•		•	•			•	•	•	•		•			•	•	•	•		•					•	
226	Development of Membrane Devices Using AlN and SiC Films	3537.010							•													•					•	
227	Spectral Information Content in Ion-Mobility Spectra for Explosives, Interferants, and Other Negative-Ionizing Chemicals	3537.020													•							•	•				•	

Pg #	Title	Case Number	Aeronautics	Applied Molecular Biology	Ceramics	Composites	Computer Simulation & Modeling	Data Storage & Peripherals	Electronics & Photonics	Energy	Flexible Computer-Integrated Manufacturing	High-Definition Imaging & Displays	High-Performance Computing & Networking	High-Performance Metals & Alloys	Intelligent Processing Equipment	Materials Synthesis & Processing	Medical Technology	Micro- & Nanofabrication	Micro- & Optoelectronics	Photonic Materials	Pollution Min., Remediation, & Waste Mgmt.	Sensors & Signal Processing	Software	Surface Transportation Technologies	Systems Management Technologies	Defense-Related (mostly or purely)	Dual-Use (defense and non-defense-related)	Non-Defense-Related (mostly or purely)
230	Magnetic-Field Profile Measurements in Wire-Array Z-Pinches by Faraday Rotation	3537.030								•																	•	
228	Picosecond Particle Velocity Measurements	3537.040				•	•																				•	
228	Particle-Level Modeling of Flows of Concentrated Suspensions	3537.050			•	•	•								•	•	•	•									•	
229	Efficient Processing of Materials Microstructures with Intelligent Feature Extraction for Quantitative Stereology	3537.060	•																									•
230	Nondestructive Evaluation of Wind Turbine Blades	3537.070	•			•	•			•																	•	
231	Very Small Arrays: Designing Self-Assembled Systems of Light-Antennae and Reaction Centers for Artificial Photosynthesis	3537.080		•			•		•							•			•	•							•	
232	Enzyme-Mediated Electrochemical Redox Polymer Biosensor for V- and G-Type Chemical Weapons	3537.110							•							•		•				•					•	
232	Novel Biosensor Fabrication Techniques	3537.120		•					•								•	•	•			•					•	
233	Design for 100-Year-Life Prototype	3537.130					•															•		•	•			
233	Enhancing Multilevel Linear Equation Solvers Using Domain Decomposition Strategies	3537.140	•				•				•												•				•	
234	*In Situ* and *Ex Situ* Investigations of Lateral Composition	3537.150						•	•	•						•		•	•	•							•	

Pg #	Title	Case Number	Aeronautics	Applied Molecular Biology	Ceramics	Composites	Computer Simulation & Modeling	Data Storage & Peripherals	Electronics & Photonics	Energy	Flexible Computer-Integrated Manufacturing	High-Definition Imaging & Displays	High-Performance Computing & Networking	High-Performance Metals & Alloys	Intelligent Processing Equipment	Materials Synthesis & Processing	Medical Technology	Micro- & Nanofabrication	Micro- & Optoelectronics	Photonic Materials	Pollution Min., Remediation, & Waste Mgmt.	Sensors & Signal Processing	Software	Surface Transportation Technologies	Systems Management Technologies	Defense-Related (mostly or purely)	Dual-Use (defense and non-defense-related)	Non-Defense-Related (mostly or purely)
235	Approximate Methods for Computing Eigensolutions Using Automated Multilevel Substructuring	3537.160	•				•				•												•				•	
235	Living Tissue Engineering	3537.170				•	•																					•

THIS PAGE
INTENTIONALLY BLANK

A B C D E F G H I J K L M N O P Q R S T U V W X Y Z

A

Accelerated Strategic Computing Initiative (ASCI)
    Turbulent flows, 34-35
    Materials aging, 40-41
Acceleration
    Multipole, 229
    Sensor, 226
Accelerators
    Pulse-powered, 199
    Z-pinch, 38
Acetylene, 92
ACIS
    see Applications of Collective Intelligence Systems
Acoustic
    see Surface Acoustic Wave
Acoustoelasticity, 82
ActiveX, 107
Adams, D. P.
    Advanced machining, 106
    Laser micromachining, 192
Adaptive visualization (AVATAR), 131
    see also: Data mining
Adenosine triphosphate, 231
Adolf, D. B. 91
Adriaans, M. J. 178
Adsorbate kinetics, 28
Aerodynamic lens
    Bioaerosol, 139
    Cold-spray, 24
Aerogel, 225
Aeroshell, 231
Agent
    Distributed systems, 194-195
    Infrastructure, 164-165
    Intelligent, 47
Ahrens, E. H. 209
Aidun, J. B. 90
Alam, M. K. 148
Alber, E. S. 90
ALEGRA (code)
    Parallel I/O, 38
    Rayleigh-Tayor, 201
    Unstructured, grid, 51
Alkanes
    Hydrogen production, 152
    Oxidative dehydrogenation, 196-197
Allen, J. J. 102
Allendorf, S. W. 92
Allerman, A. A.
    Chemical sensor, 62
    Composite resonator, 74
    High-power Vertical-Cavity Surface-Emitting Laser, 57
    Microsystems, 76
    Nanosatellite, 198
    Optical sensor, 65
    Optoelectronics, 64
    Selective oxidation, 60
    Solar and photonic, 202
    Wafer fusion, 58
Alternator, 153
Altimeter,
    see High Altitude Doppler Radar Altimeter
Alvin, K. F.
    Characterizing uncertainty, 46
    Test and simulation levels, 94
Ames, A. L.
    Cloud to Computer Aided Design, 116
    Immersive Computer Aided Design, 114
AMLS,
    see Automated Multilevel Substructuring
Ammerlahn, H. R. 113
Anderson, C. 68
Anderson, D. J. 165
Anderson, R. A. 26
Anderson, R. J.
    Automation, 111
    Ergonomics, 118
Anex, D. S.
    Capillary analysis, 148
    Chemical sensor, 136
    Nanoseparation, 19
Animation
    Documentation, 112-113
    Virtual engineering, 125
Anisotropy
    Background Radiation Anisotropy Measurement Sensor, 178
    Magnet, 69
Anneal
    Nonvolatile memory, 63
    Solar cells, 202
Antenna, 206
Anthrax sensor, 142
Antibody
    Bioaffinity array, 142
    Electrokinetic sensors, 136
    Fabrication, 232
    Immunoassay, 225
Antitoxin development, 203
Applications of Collectively Intelligent Systems, 117
ARCHIMEDES (code), 130
Architectural Surety
    100-year-life, 233
    PRONTO3D, 177
Arc welding, 27
Arguello, J. G., Jr. 207
Armature, 210-211
Armor penetration, 209
Armstrong, R. C.
    Commodity interconnects, 130
    Distributed computing, 52

Asay, J. R. 224
Asbill, R. E. 64
ASCI
see Accelerated Strategic Computing Initiative
Aselage, T. L. 190
Ashby, C. I. H.
Dry etching, 70
Large-area etching, 105
Selective oxidation, 60
Asher, R. B. 210
Ashley, C. S. 225
Assay
Bead, 141
Immuno, 225
Asteroid, 5
Asynchronous Transfer Mode
High-performance interconnects, 130
Mobile switches, 128
Scalable, 126
Wireless, 128
Atom
Adatom, 184
Defect chemistry, 28
Diffusion, 33
Materials growth, 22
Nanostructures, 20
Picoseconds, 43
Parallel computation, 40
Porous structures, 222
Recrystallization, 86
Surface hardening, 183
Atom-Tracker (AT-STM)
see Scanning-Tunneling Microscopy
ATM
see Asynchronous Transfer Mode
ATP
see Adenosine TriPhosphate
ATR
see Automatic Target Recognition
Attaway, S. W. 177
Attenuation (monitored natural), 150
Atwood, C. L. 98
Aurand, J. F.
Electromagnetic attack, 206
Imaging, 70
Authenticate, 130
AutoCAD
Geometric databases, 123
Microelectromechanical Systems, 192
Automated
Cooperative assistants, 111
Documentation, 112
Intelligent controls, 111
Life-cycle assembly, 114
Model builder, 35
Terrain mapping, 138
Automated Multilevel Substructuring, 235
Automatic Target Recognition
Obscured targets, 142
Synthetic Aperture Radar, 140
Ultra-high-resolution, 142
AVATAR
see Adaptive Visualization
AZTEC (code), 50-51

B

Baca, A. G.
Chemical microsensors, 75
Electronic defect, 73
Environmental reconnaissance, 156
Semiconductor laser, 226
Bacteria
Sensor, 136
Spectroscopy, 191
Bacteriorhodopsin, 187
Baer, M. R.
Colloidal slurry, 25
Heterogeneous materials, 90
Baeza, A. R. 179
Baker, A. B. 211
Baldwin, J. M. 107
Baldwin, M. D. 198
Ballard, S. 212
Ballistic missile, 204
Bammann, D. J.
Localization modeling, 83
Recrystallization modeling, 86
Bandgap
Nanophotonics, 9
Solar cells, 202-203
Wide, 10-11
Barker, G. T. 212
Barnaby, M. L. 38
Bartel, L. C.
Geophysical networks, 138
Surface Area Modulation telemetry, 212
Bartelt, N. C. 22
Bartholomew, J. W. 67
Barton, D. L. 167
Battaile, C. C. 42
Battery, 93
Baty, R. S. 44
Baucom, K. C. 59
Benavides, G. L.
Filament laser, 226
Laser micromachining, 192
Manufacturing, 102
Microfabrication, 106
Bennett, P. C. 171
Benson, D. A.
Integrated circuit interconnections, 167
Micro-heat-pipe, 66
Berg, T. M. 194
Bespalko, S. J. 123
Bickel, D. L. 138
Bicrystal
Compliant substrates, 71
Metal recrystallization, 86
Biefeld, R. M.
Chemical sensor, 62

Engineered nanostructure, 20
Bieg, L. F. 102
Bioaerosol, 139
Bioaffinity, 142
Biocavity, 251
Biodetection, 203
Biological Warfare Agent, 139
Biophotonic, 187
Bioreactor, 235
Biosensor
Bioaffinity, 142
Electrochemical redox, 232
Fabrication, 232
Immunoaffinity, 136
Immunoassays, 225
Blair, D. S. 154
Blake, R. J. 136
Bliss, D. E.
Laser micromachining, 192
Power compression, 218
Boehme, D. R. 216
Boettcher, G. E. 182
Bogdan, C. W. 165
Bombardment, 190
Bonivert, W. D. 216
Borns, D. J. 150
Boslough, M. B. 200
Bouchard, A. M. 20
Bow, W. J. 142
Boyack, K. W. 53
Boyle, T. J. 10
Brady, P. V. 150
Brainard, J. P. 183
Braithwaithe, J. W. 166
Brandt, J. M. 124
Brazee, J. L. 114
Breiland, W. G. 70
Brightwell, R. B. 50
Brinker, C. J.
Catalytic sensor, 10
Fuel cells, 152
Immunoassay biosensor, 225
Nanocomposite, 186
Sensing systems, 135
Brockmann, J. E.
Cold-spray fabrication, 24
Smoke environment, 165
Brooks, J. A. 29
Brown, K. H. 84
Brown, R. G.
Geometric solid model, 117
Life-cycle assembly, 114
Very large assemblies, 116
Brunett, B. A. 222
Buchheit, T. E.
Laser wire deposition, 104
Micro simulations, 42
Bujewski, G. E. 154
Burchett, S. N. 66
Burns, A. R. 14
Burns, S. P.
Grid-based simulation, 44
Modeling turbulent flows, 34
Buss, R. J. 105
Butler, M. A. 191
Butler, P. C.
Power system security, 168
Stockpile aging, 160
BWA
see Biological Warfare Agent
Byrne, R. H. 68

C

CAD
see Computer Aided Design
CAEC
see Capillary Affinity Electrochromatography
Caffey, T. W. 212
Calibrate, 41
Calton, T. L.
Ergonomics, 118
Life-cycle assembly, 114
Camera (video), 103
Cameron, S. M.
Ballistic missiles, 204
Emerging threats, 199
Filament lasers, 226
Laser micromachining, 192
Nanosatellite, 198
Optical communication, 220
Power compression, 218
Campbell, A. N. 106
Campbell, J. E. 162
Capillary Affinity Electrochromotography, 136
Capillary (electrochromotography), 216-217
Carichner, S. A. 172
Carlson, D. C. 179
Carlson, J. J.
3-D sensing, 149
Unattended monitoring, 180
Video inspection, 103
Carr, M. J.
Degradative materials, 148
Intelligent polymers, 26
Carr, R. D. 50
Casalnuovo, S. A.
Chemical microsensor, 75
Device fabrication, 14
Integrated microsystems, 78
Materials engineering, 77
Cascade (lasers), 62
Catalytic
Chiral sensors, 147
Membrane reactor, 152
Membrane sensor, 10
Oxidative dehydrogenation, 196-197
Cathode, 214-215
Causey, R. A. 222

Cavity
see Vertical-Cavity Surface-Emitting Laser
CBR
see Cosmic Background Radiation
Centimeter-Years, 43
Ceramic
Free-form fabrication, 25
Interfacial reaction, 185
Multilayer coating, 12
Powder pressing, 207
Switch tube, 182
Cesarano, J., III
Colloidal slurries, 25
Fuel cells, 191
Self-assembling macrosystems, 218
Chambers, R. S. 91
Chambers, W. B. 172
Chang, H. 198
Charge-Collection, 70-71
Chemiresistor
Low-power sensor, 74-75
Metal-loaded polymer, 182
Chen, H. Y.
Asynchronous Transfer Mode network, 124
Commodity interconnects, 130
Chen, K. S. 93
Chhabildas, L. C. 90
Chiral, 147
Choquette, K. D.
Composite resonator, 74
Microsystems, 76
Optoelectronics, 60
Vertical-Cavity Surface-Emitting Laser array, 57
Wafer fusion, 58
Chow, W. W.
Composite resonator, 74
Novel semiconductor devices, 10
Optical sensor, 65
Vertical-Cavity Surface-Emitting Laser array, 57
Christenson, T. R.
Microelectromechanical Systems assembly, 97
Micromagnet, 68
Microsystems, 78
Christon, M. A. 44
Chromatography, 136
Chrzan, D. C. 12
Chu, D. D. 142
Circuit, 167
Claassen, J. P. 138
Clean-up (soil), 150
Climate, 208
Cluster
Atomic, 183
Computing, 130
CMOS
see Complementary Metallic Oxide Semiconductors
Coats, R. S. 38
COBE
see Cosmic Background Radiation
Cochran, R. J. 34
Coherence, 210
Coil gun, 210-211
Cold-Spray Processing, 24
Cole, E. I., Jr.
Integrated Circuit interconnects, 167
Microcode evaluation, 179
Coleman, P. D. 206
Collective, 194-195
Collector, 139
Collins, E. W. 106
Coltrin, M. E.
Multicomponent transport, 93
Virtual reactor, 59
Column (capillary), 148
Combustion, 153
Complementary Metallic Oxide Semiconductors, 160-161
Comprehensive Test Ban Treaty, 200
Complex
Distributed systems, 194-195
Flows, 84-85
Imaging, 142-143
Sample screening, 148
Compliant (substrates), 71
Composite
Colloidal slurry, 25
Interfacial reaction, 185
Vertical-Cavity Surface-Emitting Laser, 74
Compression
Engine, 153
Isentropic, 224
Power, 218-219
Computer-Aided Design
Fabrication, 98
Immersive, 114
Scanned data, 116
Concentrator (bioaerosol), 139
Constraint (modeling), 40
Contaminant
Adhesive bond, 100-101
Environmental reconnaissance, 156
Soil, 150
Conversion (energy), 190
Cooperative monitoring, 172
Cordaro, J. T. 137
Corrosion, 166
see also: Degradation
Cosmic Background Radiation, 178
Coupled-resonator, 74
Covert systems, 178-179
CPlant (code)
Commodity interconnects, 130
Fault tolerance, 129
Scalable tools, 52
Crack
Fabrication, 180-181
Finite element, 83
Simulation, 42
see also: Fracture

Craft, R. L. 162
Crawford, M. H.
Electronic defect, 73
Materials engineering, 77
Microdomain, 171
Novel semiconductor devices, 10
Wafer fusion, 58
Crosstalk, 57-58
Crowder, S. V. 106
Crowther, J. I., Jr. 210
Cryptography, 179
Crystal
Cadmium, 222
Growth, 22
Photonic, 9
see also: Bicrystal
CSP
see Cold-Spray Processing
CTBT
see Comprehensive Test Ban Treaty
CTH (code)
Architectural surety, 177
Integrated service provisioning, 124
Cummings, E. B. 216
Current, K. 61
Curro, J. G.
Cleaning, 100
Degradative materials, 148
Hydrogenic materials, 41
Polymer modeling, 184

D

Daniels, J. W. 136
Database (geometric), 123
Data mining, 53
see also: Adaptive Visualization
Day, D. M.
Sparse eigensolver, 36
Weapons of mass destruction, 223
Dean, L. B.
High-speed networks, 126
Nanosatellites, 198
De Boer, M. P.
Microelectromechanical Systems, 102
Micromachine reliability, 21
Dec, J. E. 150
Decay, 190
Decontamination, 199
Deep-target, 138
Defects
Chemistry, 28
Cu-Al, 189
III-Nitride electronics, 73
Degradation
Controlled, 148-149
Stockpile, 160
see also: Corrosion
Dehydrogenation, 152
Denison, G. J. 156
Deposition
Cold-spray, 24
Laser, 98-99
Laser wire, 104
Laser-Engineered Net Shaping, 180-181
Thermionic materials, 214-215
Ultra-hard, 12-13
De Sapio, V.
Manufacturing, 102
Streaming visualization, 107
Desiena, T. H. 179
Desjardin, P. E. 88
Desorption, 150
Detection
Aqueous sensor, 154
Bioaerosol, 139
Biological weapons, 141
Buried waste, 156
High-priority analytes, 135
Immunoaffinity, 136
Massively parallel, 67
Optoelectronic, 72
Photo, 76
Redox, 142
Solvent, 182
Soot, 92
Targets, 140
Volatile organic, 154
Devine, K. D.
Density function theory, 36
Modeling turbulent flows, 34
Diamond
Coating, 12-13
Sensor, 188-189
Diegert, C. F. 35
Diegert, K. V. 46
Diesel, 150-151
Diffusion
Calculation, 184
Gradient-driven, 33
Materials growth, 22-23
Model, 93
Photonic, 202-203
Vapor-phase, 81
Digital (video), 124
Dike, J. J. 82
Dimos, D. B. 16
Diode
Pulsed power, 65
Sensor, 62
Dison, H. L. 123
Dispersion
Nanoparticle precipitation, 183
Velocity, 90
Disruption (infrastructure), 164
Dodd, P. E. 70
Dohner, J. L. 171
Dohrmann, C. R.
Finite-element meshing, 100
Tetrahedral finite elements, 84

Doped, 188
Doran, L. M. 35
Douglas, M. R. 201
Downhole, 212
    see also: Hole
Download (microcode), 179
Doyle, B. L. 106
Draelos, T. J. 130
Draper, B. L. 62
Dreeben, T. D. 89
Drennen, T. E. 196
Drill
    Laser, 192-193
    Robot, 209
    Surface Area Modulation, 212
Dron, S. B. 206
Drummond, T. J.
    Materials engineering, 77
    Virtual reactor, 59
Dugger, M. T.
    Molecular-scale lubricants, 15
    Multilayer coatings, 12
Durant, J. L., Jr. 24
Dyads, 221
Dykhuizen, R. C. 24

E

Eaton, W. P. 159
Echekki, T. 89
Eichel, P. H. 142
Eigensolution
    Massively parallel, 38
    Multilevel substructuring, 235
Einfeld, W. 203
EKP
    see Electrokinetic Pump
Elasticity, 91
Elbring, G. J. 138
Electrical
    Digital, 58
    Engine, 153
    Failure, 160-161
    Field, 14-15
    Fuel cell, 152-153
    Launcher, 210-211
    Photovoltaic module, 214
    Power generation, 190
    Power-grid, 211
    Property, 26-27
    Security, 168
    Simulation, 162-163
    Solar, 202-203
    see also: Piezoelectric
Electrochemical
    Reaction, 93-94
    Redox, 232-233
    Spectroscopy, 154
Electrode
    Detector, 142
    Polymer biosensor, 232
    Thermionic, 214-215
Electroform
    see LIGA
Electrokinetic
    Immunoaffinity sensors, 136
    Pump, 201
Electromigration, 160-161
Electrophoresis, 216-217
Electroplate, 216
Electrospray, 191
Elliptic, 44-45
Emergent behavior, 47
Emerging threat, 199
Emerson, J. A. 100
Emissions
    Diesel, 150-151
    Hybrid drive train, 153
    Laser, 218-219
    Thermionic, 214-215
Emulsion, 150-151
Encapsulant
    Enzyme, 225
    Microelectromechanical Systems, 66
    Polymer modeling, 90
    Surface cleaning, 100-101
    Weapons systems, 166
Encryption
    see Cryptography
Encryptor, 126
Energetic materials, 193
Energy
    Binding, 188
    Conversion, 190
    Hot-spot, 224
    Infrastructure, 164-165
    Kinetic, 210-211
    Micromagnet, 68-69
    Photosynthesis, 231
    Potential, 40
    Power system, 168
    Release, 200
    Short-pulse laser, 226
    Transition metal, 184
    Vehicle, 153
Engi, D. 196
Enhanced Vapor Diffusion, 81
Ensz, M. T.
    Colloidal slurries, 25
    Laser wire deposition, 104
Environment
    Electromagnetic imaging, 156
    Soil, 150
    Virtual, 125
Enzyme
    Biosensor, 225
    Redox, 232-233
Epitaxy
    Compliant substrate, 71
    Materials growth, 22-23
    Molecular beam, 58

Epoxy
Conductive, 214
Interfacial fracture, 18-19
Ergonomic, 118-119
Espinoza, J. 128
Etch
Dry, agile, 70
Dry, large-area, 105
Microoptic, 64
Microsystems, 78
Neutron-tube, 183
Ethernet, 130
Evans, G. H. 93
Evaporation
Electron, 214-215
Self-assembly, 186
EVD,
see Enhanced Vapor Diffusion
Ewsuk, K. G. 207
Excimer, 106-107
Excitation (fluorescence), 208
Exciton
Gas, 188
Wide bandgap, 10-11
Exfiltrate, 178
Explosive
Attack, 177
Material, 193
Microchem lab, 172-173
Monitoring, 200
Spectral information, 227
Extraction, 154-155

F

FAA
see Federal Aviation Administration
Failure
Architectural, 177
Complementary Metallic Oxide Semiconductors, 160-161
Computer, 129
Fracture prediction, 90-91
Integrated circuits, 167
Microelectromechanical Systems reliability, 159
Modeling, 83
Polymer modeling, 91
System variability analysis, 162-163
Falcone, P. K. 203
Fan, D. 52
Fang, H. E. 42
Faraday Rotation, 230
Farino, A. J. 66
Fatigue, 42-43
Faulon, J. M. 43
Fault, 129
Feddema, J. T.
Distributed systems, 194
Microelectromechanical Systems assembly, 97
Video inspection, 103
Federal Aviation Administration, 191
Federico, P. J. 206
Feeder, 98
see also: Wire
Feedstocks, 196-197
Feibelman P. J.
Materials growth, 22
Surface structure energies, 184
Fellerhoff, J. R.
Interferometric Synthetic Aperture Radar, 210
Terrain mapping, 138
FE
see Finite Element
FIB
see Focused Ion Beam
Fiber
Laser, 208
Particle velocity, 228
Field Programmable Gate Array, 179
Fighter (aircraft), 210-211
Filaments, 226
Filter
Digital, 70
Image, 229
Filter, W. F. 160
Finite Element
Automated substructuring, 235
Laser ultrasonics, 82-83
Meshing, 100
Modeling localization phenomena, 83
Modeling turbulent flows, 34-35
Multilevel linear equation solvers, 233
Polymer modeling, 91
Powder pressing, 207
Sparse eigensolver, 36
Tetrahedral, 84
Unstructured grid problems, 51
see also: Mesh
Fire
Smoke environments, 165
Soot, 92
Fireball, 200
Fisk, L. A. 52
Fleetwood, D. M. 62
Fleming, J. G.
Materials engineering, 77
Vacuum encapsulation, 66
Fleming, R. P. 179
Flexural Plate-Wave
Sensor membrane devices, 226-227
Surface micromachining, 16-17
Flip-chip, 64
Flores, R. S. 70
Floro, J. A.
Compliant substrates, 71
Materials growth, 22
Flounders, A. W.
Biological weapon detector, 142
Polymer biosensor, 232
Flows
Bioaerosol concentrator, 139
Concentrated suspensions, 228-229

Laser-spray fabrication, 98-99
Lattice Boltzman, 84-85
Microfluidic engineering, 201
Microfluidics, 216-217
Modeling turbulent, 34-35
Radiative transport, 88-89
Transient phenomena, 89
Transport simulation, 212-213
Virtual reactor, 59
Fluorescence, 216-217
Focus
Cold-spray fabrication, 24
Power compression, 218-219
Synthetic Aperture Radar, 137
Focused Ion Beam
Integrated circuit interconnections, 167
Microfabrication, 106-107
Foiles, S. M. 86
Follstaedt, D. M.
Compliant substrates, 71
Materials engineering, 77
Multilayer coatings, 12
Solar cells, 202
Wafer fusion, 58
Ford, D. M. 33
Fossum, A. F. 207
FPGA
see Field Programmable Gate Array
FPW
see Flexural Plate-Wave
Fracture
Predicting, 90-91
Thermoset interface, 18-19
see also: Crack
Framework, 162
Fredrich, J. T. 84
Freeforming, 25
Frequency (electromagnetic), 156
Friction
Lubricants, 15
Reliability, 21
Friedman-Hill, E. J. 34
Friedmann, T. A.
Diamond, 188
Multilayer coatings, 12
Friesen, J. A.
Integrated Asynchronous Transfer Mode service, 124
Virtual desktop, 125
Frink, L. J. D. 36
Fritz, I. J. 9
Frye-Mason, G. C.
Chemical microsensors, 75
Microchem lab, 172
Sensing systems, 135
Fuel-cells
Hydrogen production, 152
Solid-oxide, 191
Fuel-injection, 150-151
FUEGO (code), 37
Fuerschbach, P. W. 27
Funkhouser, D. R. 162
Fye, R. M.
Computational materials, 42
Hydrogenic materials, 41
Phase field model, 52

G

GAIA
see Global Approaches to Infrastructure Analysis
Gamma-ray, 222
Garbin, H. D. 138
Garcia, E. J. 61
Gardner, T. J.
Catalytic sensor, 10
Fuel cells, 152
Garino, T. J. 68
Garrett, S. E. 214
Gas
Cold-spray, 24
Electron, 188
Laser-spray, 98-99
Soot, 92
Vapor-phase diffusion, 81
Velocity, 90-91
Gate
Arrays, 179
Optoelectronic, 72
Gaussian, 188
Gear, 97
Gee, J. M.
Nanosatellite, 198
Photovoltaic modules, 214
Solar cells, 202
Geib, K. M.
Composite resonator, 74
Microsystems, 76
Gentile, A. C. 52
Gentry, S. M. 136
Geology, 223
Geometric databases, 123
Geophysical, 138-139
Geosphere, 212-213
Gilliom, L. R. 194
Gilmore, D. L. 24
Gladwell, T. S.
Cooperative automation, 111
Ergonomics, 118
Glass, S. J. 42
Global Approaches to Infrastructure Analysis, 196
GLRS
see Grating Light Reflection Spectroscopy
Godfrey, A. W. 86
Goeke, R. S. 183
Goldsborough, S. S. 153
Goldsmith, S. Y.
Ballistic missiles, 204
Distributed systems, 194
System surety, 119

GOMA (code)
Electrochemical reactions, 93
Unstructured grid, 51
Gonzales, R. A. 130
Gourley, P. L. 9
Grain (metal), 86
Graphite, 41
Grating Light Reflection Spectroscopy, 154
Grid
Electromagnetic simulation, 38-39
Multiscale simulation, 44
Radiative transport, 88-89
Unstructured, 51
see also: Power
Griffith, M. L.
Colloidal slurries, 25
Laser-spray fabrication, 98
Laser wire deposition, 104
Griffiths, S. K. 216
Gritzo, L. A.
Radiative transport, 88
Smoke environments, 165
Soot, 92
Grotbeck, C. L. 179
Ground-level, 138
Ground
Environmental reconnaissance, 156
Explosion monitoring, 200
Sensors, 220
GSLIB (software)
see Geosphere
Guess, T. R.
Degradative materials, 148
Polymer modeling, 91
Guns, 210-211
Guthrie, S. E. 222

H

Haaland, D. M. 148
Hadley, G. R.
Optical sensor, 65
Vertical-Cavity Surface-Emitting Laser arrays, 57
Half-life (boride), 190
Hamilton, J. C.
Materials growth, 22
Smart Interface Bonding Alloys, 17
Simulation, 43
Hamilton, V. A. 130
Hammons, B. E.
Composite resonator, 74
Microsystems, 76
Nanophotonics, 9
Han, J.
Electronic defects, 73
Materials engineering, 77
Novel semiconductor devices, 10
Hard-coded tools, 52
Hardness
Diamond, 188
Drilling, 209
Nanocomposites, 186
Surface, 183
Harmony, D. W. 142
Haroldsen, B. L. 203
Harrington, J. J. 180
Harris, D. L.
Global Approaches to Infrastructure Analysis, 196
Infrastructure interdependency, 164
Hart, W. E.
Engineering optimization, 48
Production planning, 108
Scheduling optimization, 50
Harwell, L. D. 104
Haynes, R. A. 38
Heat-pipe, 66
Heat transfer, 89
Heavy-ion, 70-71
Hebner, G. A. 105
Heffelfinger, G. S. 33
Heinstein, M. W. 84
Heller, E. J.
Chemical microsensor, 75
Robotic vehicle, 68
Helms, C. J. 58
Henderson, C. L. 61
Hendrickson, B. A. 53
Henry, T. R. 123
Hess, B. V. 216
Heterogeneous materials, 90
Heustess, J. E. 178
Hicken, G. K. 107
Hickerson, D. 114
Hickox, C. E., Jr. 84
Hiebert-Dodd, K. L. 196
Hierarchical (wavelets), 44
Hietala, S. L. 75
Hietala, V. M.
Chemical microsensors, 75
Photonic interconnects, 58
HIDRA
see High-Altitude Doppler Radar Altimeter
High-Altitude Doppler Radar Altimeter, 138
High-aspect, 216
High-explosive, 193
High-level tools, 52
High-Power Microwave, 206
Hillaire, R. G. 107
Hilton, N. R. 222
Hinckley, M. K. 136
HMX
see High-explosive
Ho, C. K. 81
Hobbs, D. J. 33
Holcomb, D. J. 209
Hole
Laser micromachining, 192-193
Robot drilling, 209
see also: Downhole

Holland, K. G. 228
Hollowell, J. A. 137
Holm, E. A.
    Computational materials, 42
    Materials microstructures, 229
    Recrystallization of metals, 86
Hopkins, P. L. 212
Horn, K. M.
    Nanostructures, 20
    Virtual reactor, 59
Horstemeyer, M. F. 43
Hosking, F. M. 64
Hot-press, 68-69
Hot-spot, 224
Hough, P. D. 129
Houston, J. E.
    Molecular-scale lubricants, 15
    Smart Interface Bonding Alloys, 17
HPM
    see High-Power Microwave
Hruby, J. M. 216
HSI
    see Hyperspectral Imaging
Hu, T. C. 130
Hughes, D. A.
    Modeling localization phenomena, 83
    Recrystallization of metals, 86
Hughes, R. C.
    Biological weapon detector, 156
    Catalytic sensors, 10
    Chemiresistors, 182
    Microtelemetry, 74
Human (adaptive sensing), 149
Hunter, K. O. 48
Hurd, A. J. 228
Hurtado, J. E. 47
Hutchinson, R. L.
    High-speed networks, 126
    System surety, 119
Hwang, R. Q.
    Metal-oxide surfaces, 28
    Smart Interface Bonding Alloys, 17
Hwang, Y. K. 123
Hybrid (engine), 153
Hydrogen production, 152
Hydrogenic, 41
Hydrophilic, 218
Hydrophobic
    Nanocomposites, 186
    Self-assembling macrosystems, 218
Hyperbolic, 44
Hyperspectral, 179
Hyperspectral Imaging, 136-137

I

Icosahedral, 190
IC
    see Integrated Circuit
IDES
    see Infrastructure for Distributed Enterprise Simulations
Imager
    Electromagnetic, 156
    Electron micrograph, 229
    Geometric model builder, 35
    Microfluidics, 216-217
    Video, 103
    see also: Scanning-Tunneling Microscopy, Synthetic Aperture Radar, Information-Efficient Spectral Imaging System, Optically Recording Velocity Interferometer System
Immersive (Computer Aided Design), 114
Immunoaffinity, 136
Immunoassay, 225
Impact-loading, 90
Implants, 183
Implosion, 224
Impurities, 12
Inclusion, 91
Index (databases), 123
Information-Efficient Spectral Imaging
System, 136
Infrasound, 200
Infrastructure
    Architectural surety, 177
    Global Approaches to Infrastructure Analysis, 196
    Power, 168
    Simulation, 162
Infrastructure for Distributed
Enterprise Simulations
    Fault tolerance, 129
    System questions, 113
Ingersoll, D. 198
Initiation (explosive), 193
Injection (engine), 150-151
Inspection (video), 103
Instability (radiation), 201
Insulator
    Nonvolatile memory, 62
    Optoelectronics, 60
Integrated Circuit
    Complementary Metallic Oxide Semiconductors, 160-161
    Interconnections, 167
Internal combustion, 153
Ion-beam, 70-71
Ion-exchange
    Catalytic sensor, 10
    Fuel cells, 152
Ion-mobility
    Biological materials, 191
    Explosives, 227
Ionophore, 154-155
Irwin, L. W.
    Complementary Metallic Oxide Semiconductors, 160
    Microelectromechanical Systems reliability, 159
Isentropic, 224

ISIS
see Information-Efficient Spectral Imaging System
Islands (materials growth), 22
Isothermal, 160-161
Isotope
Boride, 190
Detectors, 222
Z-pinch, 224
Istrail, S.
Biological weapon detection, 141
Self-assembling macrosystems, 218

J

Jackson, N. B. 196
Jacobian, 36-37
Jacobs, J. A. 199
Jakowatz, C. V., Jr. 137
Jamison, G. M. 26
Janek, R. P.
Biological weapon detector, 142
Polymer biosensor, 232
Janssen, C. L. 40
Janus, 218
Jefferson, K. J. 179
Jennison, D. R.
Quantum dot arrays, 26
Metal-oxide surfaces, 28
Nanostructures, 20
Johnsen, H. A. 92
Johnson, A. J. 106
Johnson. D. K. 53
Johnson, M. M.
Enterprise simulation, 113
Fault tolerance, 129
Johnston, A.M. 130
Jones, D. A.
Production planning, 108
Scheduling optimization, 50
Jones, E. D.
Broadening mechanism, 188
Nanophotonics, 9
Novel semiconductor devices, 10
Jortner, J. N. 125
Jung, J. 100

K

Kasunic, K. J. 154
Keck, J. D. 99
Keefe, R. G. 212
Kegelmeyer, W. P. 131
Kellogg, G. L. 22
Kelly, M. J. 154
Kemme, S. A. 154
Kempka, S. N. 235
Kent, M. S. 18
Kern, J. P. 198
Kerstein, A. R.
Modeling turbulent flows, 34
Transient phenomena, 89
Key, S. W. 84
Kiefer, M. L. 38
Kinematic, 118-119
King, C. 102
King, D. B. 214
King, R. K. 204
Kjeldgaard, E. A. 50
Klarer, P. R. 171
Klein, P. A. 90
Klem, J. F.
Compliant substrates, 71
Nanophotonics, 9
Optoelectronics, 60
Solar cells, 202
Virtual reactor, 59
Kliner, D. A. 208
Knapp, J. A.
Micromachine reliability, 21
Multilayer coatings, 12
Knorovsky, G. A. 42
Knowledge mining, 53
Koch, M. W. 140
Koller, M. H. 53
Kottenstette, R. J.
Chemical microsensors, 75
Sensing systems, 135
Kozlowski, D. M. 102
Kravitz, S. H.
Bioaerosol concentrator, 139
Biological weapon detector, 142
Microchem lab, 172
Micro-heat-pipe, 66
Microsystems, 78
Wafer fusion, 58
Krumel, L. J. 136

L

LADAR
see Laser Radar
Ladd, M. D. 138
Lafarge, R. A.
Geometric databases, 123
Intermittent contacts, 49
Lagrangian, 88-89
Laguna, G. A. 114
LAMA
see Laser Mapper
Laminated (nanocomposites), 186
LAMMPS
see Large-Scale Atomic/Molecular Massively Parallel Simulator
Landmine detection, 172-173
Lanes, K. R. 179
Large-Scale Atomic/Molecular Massively Parallel Simulator, 40
Larson, R. S. 93
Larson, W. L. 160
Laser
Biodetection, 203
Communications, 220-221

Diode, 62
Flared, 65
Mapper, 180
Microfabrication, 106-107
Micromachining, 192-193
Nanosatellites, 198-199
Nonflared, 65
Optoelectronics, 72
Plasma channels, 218
Ultrasonics, 82-83
Welding, 27
WireFeed, 104
Z-pinch, 224
Z-pinch diagnostics, 230-231
see also: Vertical-Cavity Surface-Emitting Lasers
Laser Mapper, 180
Laser Radar, 226
Lattice Boltzmann, 84-85
Launcher, 210-211
Lavigne, G. F. 192
Leaky, 57
Lee, E. Y. 222
Lee, S. R.
Compliant substrates, 71
Lateral composition, 234
Materials engineering, 77
Novel semiconductor devices, 10
Solar cells, 202
Lemen, E. K. 113
Leonard, C. M., Jr. 107
Leung, K. 45
Leung, V. J. 100
Lewis, C. L.
Intelligent agents, 171
Intermittent contacts, 49
Lewis, P. R. 135
LIGA (lithography, electroforming, molding)
Microelectromechanical Systems, 97
Microfabrication, 106-107
Micromachining, 216
Light-absorbing, 187
Light-antennae, 231
Lin, S. Y.
Nanophotonics, 9
Optoelectronics, 72
Lindgren, E. R. 36
Link, H. E. 194
Liquid-membrane, 154-155
Lithography, 69
Little, C. Q.
3-D sensing, 149
Cloud to Computer Aided Design, 116
Immersive Computer Aided Design, 114
Unattended monitoring, 180
Video inspection, 103
Lo, C. S. 91
Load-balancing, 38-39
Lockwood, S. J. 99
Loehman, R. E. 185
Lopez, E. P. 100
Loubriel, G. M.
Collective intelligence, 220
Emerging threats, 199
Environmental reconnaissance, 156
Loy, D. A.
Degradative materials, 148
Intelligent polymers, 26
Lu, W. 82
Lubricant (micromachine), 15
Ludowise, P. D. 92
Lund, J. C. 222
Lyo, S. K.
Nanophotonics, 9
Optoelectronics, 72

M

MacCallum, D. O. 104
Macromolecule, 33
Macrosystems, 218
Magnet
see Micromagnet
Mah, B. A. 128
Mansure, A. J. 212
Manufacture
Automated, 138
Cleaning, 130-131
Interferometric Synthetic Aperture Radar, 210
Laser Mapper, 180
Low-volume, 106
Parallel mechanism, 102
Photovoltaic modules, 214
Powder pressing, 207
Semiconductors, 70
Mar, A. 65
Marder, B. M. 210
Marlman, K. S. 106
Marozas, D. C. 164
Martin, J. E. 26
Martin, M. F. 106
Martinez, L. G., Jr. 128
Martinez, M. J. 212
Martino, A.
Ionophores, 154
Nanoseparation, 19
Marx, K. D. 162
Mask
Membrane devices, 226-227
Micromachining, 216
Neutron-tube, 183
Massively Parallel Processing, 126-127
Matalucci, R. V. 167
Mayer, T. M.
Micromachine reliability, 21
Molecular-scale lubricants, 15
Nanometer-scale fabrication, 14
Mazarakis, M. G. 209
MBE
see Molecular Beam Epitaxy
McCarty, K. F. 12
McDonald, M. J. 112

McWhorter, P. J. 15
Medlin, D. L. 12
Meirans, L. 123
Melius, C. F.
    Material aging, 34
    Parallel computational chemistry, 40
Mesh
    Computational materials, 42
    Global minimization, 100
    Modeling localization phenomena, 83
    Multiscale simulation, 44
    Tetrahedral finite elements, 84
    Unstructured grid problems, 51
    see also: Finite Element
Metal-loaded, 182
Metalorganic Chemical Vapor Deposition
    Chemical sensors, 62
    Electronic defects, 73
    Materials engineering, 77
    Virtual reactor, 59
Metal-oxide, 28
Meteorite, 200
Meyers, C. E. 1
Micelles, 186
Michalske, T. A.
    Microdomain, 171
    Molecular-scale lubricants, 15
Microchannels, 216-217
Microchem, 172
Microdomain, 171
Microencapsulate, 205
Microfluidic
    Applied, 216-217
    Engineering, 201
Micro-heat-pipe, 66
Microhole, 209
Micromachine
    Molecular-scale lubricants, 15
    Reliability, 21
Micromachining
    Flexural plate-wave, 16-17
    Laser, 192-193
    LIGA, 216
    Microelectromechanical Systems, 61
    Microfabrication, 106-107
    Reliability tools, 159
Micromagnet, 68
Micromechanics
    Failure analysis, 91
    Materials simulations, 42
Microminiature, 171
Microoptics, 64
Microporous, 152
Microsensor
    Integrated chemical, 75
    Robotic vehicle, 68
    Solvent detection, 182
Microsimulation, 164
Microsystem
    Post-processed, 78
    Vertical-Cavity Surface-Emitting Laser, 76
Microtelemetry, 74
Microtools, 106-107
Miles, P. C. 150
Mill, 106-107
Miller, J. C. 193
Miller, J. E.
    Ionophores, 154
    Oxidative dehydrogenation, 196
Miller, P. A. 105
Miller, S. L.
    Molecular-scale lubricants, 15
    Visualization tools, 192
Miniature
    Bioaerosol concentrator, 139
    Robotic vehicle, 68
Mining
    see Data mining
Miodownik, M. A. 86
Missert, N. A.
    Corrosion, 189
    Multilayer coatings, 12
Missile, 204
Mitchell, E. A. 114
Mix, L. P., Jr. 38
MNA
    see Monitored Natural Attenuation
MOCVD
    see Metalorganic Chemical Vapor Deposition
Modine, N. A. 45
Moen, C. D. 51
Moffat, H. K. 59
Mold, 68-69
Molecular Beam Epitaxy, 59
Monitor
    Atmospheric explosion, 200
    Deep targets, 138
    Remote, 220
    Unattended, 180
Monitored Natural Attenuation, 150
Monolayer, 15
Monolithic
    Microsystems, 76
    Nanoseparation, 19
Monomer, 186
Montague, S. 66
Montoya, T. V. 99
Moody, N. R.
    Modeling localization phenomena, 83
    Smart Interface Bonding Alloys, 17
Moore, R. H. 99
Morales, A. M. 216
Morgan, W. P. 214
Mosher, D. A .83
Motion
    Ergonomics, 118-119
    Human, 102
    Targets, 137
Motor, 68-69
Movie, 112-113
Moving Target Indicator, 137

Moya, M. M. 140
Moyer, R. D. 178
MPP
see Massively Parallel Processing
MPSalsa (code)
Turbulent flows, 20-21
Unstructured grid, 37
MTI
see Moving Target Indicator
Multilayer (coatings), 12
Multiplex, 92
Murray, J. R. 62
Myers, S. M., Jr.
Electronic defects, 73
Surface hardening, 183

N

Nanocluster, 26-27
Nanocomposite, 186
Nanodevice, 26
Nanoengineered, 189
Nanofabrication, 14
Nanoparticle, 183
Nanophotonics, 9
Nanosatellite, 198-199
Nanoseparation, 19
Nanostructure
Fabrication, 14
Recognizing atoms, 20
Nanotubes, 41
Napolitano, L. M. 193
Navigating, *see* Data mining
Neilsen, M. K. 42
Neiser, R. A., Jr. 24
Nelson, C. L.
3-D sensing, 149
Unattended monitoring, 180
Nelson, J. S. 20
Nenoff, T. M. 149
Net-shape, 98-99
Network
Commodity interconnects, 130
Surety, 128
Neural network, 227
Neutron-tube, 183
Nevers, J. A. 76
Newman, G. A. 223
Neyer, D. W.
Capillary array analysis, 148
Chemical sensors, 136
Ngujo, M. A. 126
Nicolette, V. F. 165
Nilsen, V. 89
Nilson, R. H. 216
Noble, D. R. 84
Nonproliferation, 172
Nowlen, S. P. 165
Nucleation, 86

O

Oberkampf, W. L. 46
O'Connor, R. M. 84
Olson, C. L. 199
Optical
Channeling, 218-219
Smoke, 165
see also: Photonic
Optically Recording Velocity
Interferometer System, 90
Optoelectronics
Free-space microoptics, 64
Quantum-well, 72
Ordination, 53
Organophosphate, 232
Orthogonal
Motion, 102
Wavelets, 44
ORVIS
see Optically Recording Velocity
Interferometer System
Osbourn, G. C.
Distributed systems, 194
Microdomain, 171
Nanostructures, 20
Sensing systems, 135
Oscillator, 75
Ottesen, D. K. 92
Oxidative, 196-197
Oxides
Complementary Metallic Oxide Semiconductors, 160-161
Nonvolatile memory, 62-63
Thermionic material, 214-215

P

Paez, T. L. 88
Palmer, D. W. 124
Paradiso, N. J., Jr. 153
Parmeter, J. E. 227
Partnership for a New
Generation Vehicle, 150
Pasik, M. F. 38
Pate, R. C. 206
Patterson, P. E. 206
Paul, P. H.
Microfluidic engineering, 201
Microfluidic science, 216
Peace, G. L. 156
PEM,
see Plastic-Encapsulated
Microelectronics
Peña, E. A. 114
Peña, J. G. 126
Penetrate
Drilling robot, 209
Environmental reconnaissance, 156
Peng, L. W. 82

Peters, R. R.
Automatic assembly planning, 114
Ergonomics, 118
Peterson, D. W. 166
Peterson, K. A. 159
PFM
see Phase Field Model
Phase Field Model, 52-53
Philips, C. A.
Optimization engineering, 48
Production planning, 108
Scheduling optimization, 50
Phillips, L. R. 194
Photodetector, 76
Photonic
Biophotonic, 187
Interconnects, 58-59
Nanophotonics, 9
Solar cells, 202
see also: Optical
Photosynthesis, 231
Photovoltaic, 214
Pierson, L. G.
Asynchronous Transfer Mode encryption, 126
Nanosatellites, 198
Photonic interconnects, 58
Piezoceramic, 230-231
Piezoelectrics
Chemical microsensors, 75
Flexural plate-wave, 16-17
see also: Electrical
Pigment, 231
Plantenga, T. D.
Computational chemistry, 40
Enterprise simulations, 113
Plasma
Dry etching, 70
Large-scale, dry processes, 105
Power compression, 218-219
Rayleigh-Taylor mitigation, 201
Simulation software, 38
Wire-array Z-pinch, 230
Plastic-Encapsulated Microelectronics, 166
Plate-wave, 16
PLD
see Pulsed-Laser Deposition
Plimpton, S. J.
Computational chemistry, 40
Electromagnetic simulation, 38
Electronic structure codes, 45
Phase field model, 52
Programming paradigms, 50
Smart Interface Bonding Alloys, 17
Plymale, D. L.
Manufacturing, 102
Microfabrication, 106
PNGV
see Partnership for a New Generation Vehicle
Poco, 182
Polosky, M. A. 97
Polymeric, 148-149
Portable (sensor), 136
Portal detector, 191
Post-processed, 78
Power
Reliability, 211
Security, 168
Prast, T. L. 216
Probe, 14
Projectiles, 210-211
PRONTO3D (code), 177
Propagation, 218-219
Protein
Chemical sensors, 136
Novel biosensor, 232-233
Proton, 62-63
Provencio, P. N.
Multilayer coatings, 12
Quantum dot arrays, 26
Pryor, R. J.
Distributed systems, 194
Infrastructure interdependency, 164
Intelligent agents, 47
Pulsed
Accelerator, 199
Filament laser, 226
Ground-penetrating radar, 156
Micromachining, 192
Optical sensor, 65
Power compression, 218
Z-pinch, 230
Pulsed-Laser Deposition, 12
Pumped
Bioaerosol concentrator, 139
Microfluidic engineering, 201

Q

Quantum
Dot arrays, 26
Hydrogenic materials, 41
Materials aging, 34
Optoelectronics, 72
Solar cells, 202-203
see also: Vertical-Cavity Surface-Emitting Laser
QUICKSILVER (code), 39

R

Radar, 137
see also: Synthetic Aperture Radar
Rader, D. J. 139
Radiation-hardened, 62-63
Radiation
Advanced sources, 201
Background Radiation Anisotropy Measurement Sensor, 178
Detectors, 222
Emerging threats, 199
Icosahedral borides, 190
Microsystems, 76

Radioisotopes
see Isotope
Radionuclide, 150
Rail (gun), 214-215
Rakestraw, D. J. 172
Range-image, 35
Rayleigh-Taylor, 201
Ray, L. P. 123
RCPD,
see Resonant-Cavity Photodetectors
Reconnaissance, 156
Recycling, 142
Red-Horse, J. R.
Automated substructuring, 235
Linear equation solvers, 233
Nondeterministic modeling, 88
Redmond, J. M. 21
Reed, K. W. 21
Reedy, E. D., Jr.
Cleaning, 100
Fracture analysis, 18
Polymer modeling, 91
Reese, G. M. 36
Reeves, P. C. 212
Remote
Collective intelligence, 220-221
Intelligence, 178-179
Sensing, 218-219
Unattended monitoring, 180
Renlund, A. M. 193
Reno, J. L.
Chemical microsensors, 75
Optoelectronics, 72
Renzi, R. F. 139
Reproducing Kernel Particle Method, 44
Resistor, 67
Resonant-Cavity Photodetectors, 76
Resonator
Chemical microsensors, 76
Composite, 74
Ricco, A. J.
Biological weapon detector, 142
Chemical sensors, 62
Nanometer-scale fabrication, 14
Organic detection, 67
Rieger, D. J. 105
Riesen, R. E. 50
Riley, D. J.
Electromagnetic simulation, 38
High-power microwave, 206
Rinehart, L. F. 206
Ring
Laser, 65
Polymer, 41
Rintoul, M. D. 42
Risk, 162
see also: Surety
Rivord, G. E. 119
RKPM,
see Reproducing Kernel Particle Method
Roach, D. W. 44
Robertson, P. J.
Asynchronous Transfer Mode encryption, 126
Asynchronous Transfer Mode integrated service, 124
Photonic interconnects, 58
Robino, C. V. 66
Robinson, A. C. 51
Robinson, D. G.
Atmospheric corrosion, 168
Nondeterministic modeling, 88
Power reliability, 211
Power security, 168
Stockpile aging, 160
Robot
3-D sensing, 149
Collective intelligence, 220-221
Cooperative automation, 111
Distributed systems, 194-195
Drilling, 209
Intelligent agents, 171
Microelectromechanical Systems assembly, 97
Miniature vehicle, 68
Rodacy, P. J. 191
Rodgers, M. S,
Microelectromechanical Systems prototyping, 61
Standard cell, 102
Roe, D. C.
Biological weapons detection, 141
Chem/bio terrorism, 203
Romero, V. J.
Nondeterministic modeling, 88
Simulation optimization, 94
Rondeau, D. M. 210
Ross, J. R. 92
Rotation
Virtual reactor, 59
Z-pinch, 230
Ruby, D. S. 105
Ruffner, J. A.
Flexural plate-wave, 16
Metal-oxide surfaces, 28
Thermionic materials, 214
Rupley, F. M. 93
Rutherford, B. M.
Modeling uncertainties, 48
Simulation optimization, 94
Ryba, G. N. 172

S

Sackos, J. T. 35
Salazar, J. S. 140
Salinger, A. G.
Density-function theory, 36
Modeling turbulent flows, 34
Salmi, A. J. 216
SAM
see Surface Area Modulation
Sands, D. N. 38
SAR
see Synthetic Aperture Radar

Sarfaty, R. A. 119
Sasaki, D. Y. 135
Satellite
    Global monitoring, 200
    Intelligence, 178
    Nanosatellite, 198
Sault, A. G.
    Catalytic sensors, 10
    Fuel cells, 152
    Metal-oxide surfaces, 28
    Oxidative dehydrogenation, 196
Saunders, R. S.
    Degradative materials, 148
    Intelligent polymers, 26
SAW,
    see Surface Acoustic Wave
Scanning-Tunneling Microscopy
    Lateral composition, 234
    Metal-oxide surfaces, 28
    Materials growth, 24
    Nanometer-scale fabrication, 14
    Nanostructures, 20
Schimmel, W. P. 210
Schlienger, M. E.
    Direct fabrication, 180
    Laser-spray fabrication, 98
Schmidt, R. C.
    Modeling turbulent flows, 34
    Transient phenomena, 89
Schmitt, D. J.
    3-D sensing, 149
    Colloidal slurries, 25
    Cooperative automation, 111
    Parallel manufacturing, 102
Schmitt, R. G. 203
Schneider, L. X. 210
Schoeneman, J. L. 198
Schoeniger, J. S.
    Bioaffinity array, 142
    Biological weapon detection, 141
    Capillary array analysis, 148
    Chemical sensors, 136
    Covert biosensors, 225
Schriner, H. K. 61
Schubert, W. K.
    Flexural plate-wave, 16
    Membrane devices, 226
    Microsystems, 78
Schultz, P. A. 45
Schunk, P. R. 51
Schwank, J. R. 62
Schwegel, J. 125
Scofield, T. W. 99
Scott, S. H. 148
Seager, C. H. 73
Sears, M. P.
    Electronic structure codes, 45
    Nanostructures, 20
    Programming paradigms, 50
Seidel, D. B. 38
Seidl, E. T. 34
Self-assembled
    Nanocomposites, 186
    Photosynthesis, 231
    Simulation, 218
Self-focusing (laser), 218-219
Self-healing (boride), 190
Self-stabilizing, 218-219
Sellinger, A. 135
Semiconductor
    Dry etching, 70
    Filament lasers, 226
    Icosahedral borides, 190
    Novel devices, 10
    Optoelectronics, 72
    Solar cells, 202-203
    Virtual reactor, 59
    Wafer fusion, 58
Sensor
    Adaptive 3-D sensing, 149
    Background Radiation Anisotropy Measurement Sensor, 178
    Catalytic membrane, 10
    Chemical (integrated), 75
    Chemiresistors, 182
    Chiral, 147
    Collective intelligence, 220
    Cooperative automation, 111
    Cadmium Zinc Telluride, 222
    Diamond, 188-189
    Intelligent agents, 171
    Information-Efficient Spectral Imaging System, 136-137
    Laser-spray, 98-99
    Microelectromechanical Systems , 66
    Microtelemetry, 74-75
    Midwave-infrared, 62
    Model builder, 35
    Optical, 65
    Robotic, 68
    Stand-off, 205
    Unattended monitoring, 180
    Volatile organic, 67
    see also: Biosensor, Detection,
SEU
    see Single-Event Upset
Sexton, F. W. 70
Shaddix, C. R.
    Smoke environments, 165
    Soot, 92
Shadid, J. N.
    Modeling turbulent flows, 34
    Unstructured grid problems, 51
Shaneyfelt, M. R. 62
Shared-Memory Processing, 50-51
Shea, L. E. 58
Sheaffer, D. A., Jr. 107
Shelnutt, J. A.
    Artificial photosynthesis, 231
    Biophotonics, 187
    Chiral sensors, 147
    Intelligent polymers, 26

Ionophores, 154
Shepodd, T. J. 19
Shield, 190
Shinn, N. D. 17
Shock-waves, 228
Sholander, P. E. 128
Shope, S. L.
Electric launcher, 210
Emerging threats, 199
Short-Period Superlattice, 234
Shul, R. J.
Electronic defects, 73
Integrated microsystems, 78
Materials engineering, 77
Siebers, D. L. 150
Siegal, M. D. 150
Sieving, 41
Signal
Asynchronous Transfer Mode, 124
Chemiresistors, 182
Collective intelligence, 220-221
Complementary Metallic Oxide Semiconductors, 160-161
Distribution, 58-59
Geophysical networks, 138-139
Particle velocity, 228
Surface Area Modulation telemetry, 212
Silva, B. L 105
Simmermacher, T. W.
100-year-life, 233
Wind turbines, 230
Simmons, J. A. 72
Simonson, K. M. 142
Simonson, R. J. 225
Singh, A. K. 225
Single-Event Upset, 70-71
Sinter
Micromagnets, 68
Self-assembling macrosystems, 218
Sipola, D. L. 99
Sleefe, G. E. 138
Slurry
Colloidal, 25
Fuel cells, 191
Slutz, S. A. 224
Small, D. E.
3-D sensing, 149
Unattended monitoring, 180
Smith, A. V. 60
Smith, D. A. 136
Smith J. H.
Flexural plate-wave, 16
Microelectromechanical Systems, 192
Microoptics, 64
Smithberger, G. L. 179
Smoke (environments), 165
SMP
see Shared-Memory Processing
Smugeresky, J. E. 98
Sniegowski, J. J.
Microelectromechanical Systems prototyping, 61
Micromachine reliability, 21
Molecular-scale lubricants, 15
Vacuum encapsulation, 66
SOFC
see Solid-Oxide Fuel Cell
Soil
Environmental reconnaissance, 156
Radionuclide desorption, 150
Solar-cell
Dry processes, 105
Nanosatellites, 198-199
Novel material, 202-203
Photovoltaic modules, 214
Solder
Microoptics, 64
Photovoltaic modules, 214
Solid-model
Analysis tools, 117
Immersive Computer Aided Design, 114
Solid-Oxide Fuel Cell, 191
Soliton, 218
Somerday, B. P. 222
SONET
see Synchronous Optical Network
Sorensen, N. R. 166
Spahn, O. B.
Microoptics, 64
Optoelectronics, 60
Spectroelectrochemical
see Electrochemical
Spectroscopy
Analysis tools, 117
Organic sensor, 154
Ion mobility, 191
Spielman, R. B.
Faraday rotation, 230
Isentropic compression, 224
Rayleigh-Taylor mitigation, 201
Spill (detection), 182
Spires, S. V.
Distributed systems, 194
System surety, 119
Spletzer, B. L.
Distributed systems, 194
Emergent behavior, 47
Intelligent agents, 171
Spooner, J. T. 106
Spray
Cold-spray, 24
Laser, 98
Laser-Engineered Net Shaping, 180-181
Sprytron, 182
SPS
see Short-Period Superlattice
Stallard, B. R. 136
Stans, L. 130
Stantz, K. M. 220
Staple, B. D. 66
Staton, A. W. 67
Stechel, E. B. 45
Stereology, 229

Stevens, M. J.
Fracture analysis, 18
Molecular-scale lubricants, 15
Stewardship
see Stockpile
STM
see Scanning-Tunneling Microscopy
Stockman, H. W. 84
Stockpile
Aging simulation, 43
Enterprise simulations, 113
Production planning, 108
Reliability, 160
Stone, C. M. 84
Streaming, 107
Strickland, J. H. 88
Sturtevant, J. E. 38
Sullivan, C. T.
Ballistic missiles, 204
Nanosatellite, 198
Optoelectronics, 60
Sullivan, J. P.
Corrosion, 189
Diamond, 188
Optoelectronics, 60
Supercomputer, 34
Superlattice, 234
Surety
Asynchronous Transfer Mode, 128
Information systems, 123
Life-cycle, 119
see also: Architecture, Risk
Surface Acoustic Wave
Flexural plate-wave, 16
Integrated microsensors, 75
Microdomain, 171
Sensor arrays, 67
Surface Area Modulation, 212
Supramolecular, 186
Surfactant
Fuel cells, 152
Materials growth, 22
Swanson, B. E. 210
Swartzentruber, B. S.
Materials growth, 22
Metal-oxide surfaces, 28
Nanometric fabrication, 14
Sweatt, W. C.
Information-Efficient Spectral Imaging System, 136
Organic sensors, 154
Sweet, J. N. 166
Swiler, L. P. 88
Synchronous Optical Network
Asynchronous Transfer Mode encryption, 126
High-speed network, 126-127
Synchrotron, 216
Synthetic Aperture Radar
Automatic Target Recognition, 142-143
Interferometric Synthetic Aperture Radar, 210
Moving targets, 137
Obscured targets, 140

T

Tag (microtelemetry), 74
Tan, M. X.
Bioaerosol concentrator, 139
LIGA, 216
Microelectromechanical Systems, 97
Tanaka, T. J. 165
Tangyunyong, P.
Integrated Circuit interconnections, 167
Microelectromechanical Systems, 159
Tanner, D. M. 159
Tappan, A. S. 193
Tarbell, W. W. 204
Target
Automatic Recognition, 142-143
High-power microwave, 206-207
Imagining, 90
Recognizing, 140
Synthetic Aperture Radar, 137
see also: Deep-Target
Tarman, T. D.
Asynchronous Transfer Mode encryption, 126
Commodity interconnects, 130
TDL
see Tunable Diode Laser
Telecommunication, 164-165
Teraflop, 45
Terrorism
Chemical/biological, 203
Emerging threats, 199
Thacher, P. D. 178
Thermal-battery, 93
Thermionic, 214-215
Thermometric, 178
Thermoset, 18
Thomas, D. H. 136
Thomas, E. V. 130
Thomas, G. A. 203
Thompson, A. P. 33
Thompson, B. M. 162
Thorne, L. R. 92
Tigges, C. P. 59
Tikare, V.
Laser wire deposition, 104
Phase field model, 52
Self-assembling macrosystems, 218
Time-Resolved Ion-Beam–Induced
Charge Collection, 70-71
Tips (Scanning-Tunneling Microscopy), 20-21
Tissue (engineering), 235
Tolendino, L. F. 128
Tong, C. H.
Fault tolerance, 129
Materials aging, 40
Unstructured grid problems, 51
Topography (atomic), 20
Topological, 114
Toth, R. P. 205
Toxin, 136
Trajectory, 200

Trahan, M. W. 220
Transducer
    Flexural plate-wave, 16
    Membrane devices, 226-227
Translator, 112
Transmitter
    Environmental reconnaissance, 156
    Surface Area Modulation telemetry, 212
TRIBICC
    see Time-Resolved Ion-Beam–Induced Charge Collection
Trinkle, J. C.
    Ergonomics, 118
    Life-cycle assembly, 114
Trott, W. M. 90
Trucano, T. G. 94
Tsang, R. P. 124
Tsao, J. Y. 71
Tuminaro, R. S.
    Sparse eigensolver, 36
    Unstructured grid problems, 51
Tunable Diode Laser, 92
Turbine, 230-231
Turbulence (modeling), 89
Turman, B. N. 199
Tuttle, B. A.
    Flexural plate-wave, 16
    Neutron generators, 99

U

Ulibarri, T. A. 148
Ultrasonic, 82-83
Unstructured-grid, 38-39
UTOPIA (code), 126-127

V

Vacuum (encapsulation), 66
Van Blarigan, P. 153
Vandernoot, V. A. 136
Vandewart, R. L. 162
Van Leeuwen, B. P. 128
Van Swol, F. B. 41
Vapor
    Biosensor, 232-233
    Diffusion, 81
    Spill detection, 182
Vawter, G. A.
    Dry etching, 70
    Microoptics, 64
    Optical sensor, 65
    Optoelectronics, 60
VCSEL
    see Vertical-Cavity Surface-Emitting Laser
Vedula, V. R. 42
Vegetation, 138
Velocity Interferometer System for Any Reflector
    Heterogeneous materials, 90
    Picosecond measurements, 228
Venturini, E. L. 68
Vertical-Cavity Surface-Emitting Laser
    High-power, 57
    Wafer fusion, 58
    Selective oxidation, 60-61
    Composite-resonator, 74
    Microsystems, 76
    see also: Laser, Quantum
Very Low Frequency, 223
Vibrations (wind turbine blade), 230-231
Video
    Asynchronous Transfer Mode, 124-125
    Explosion monitoring, 200
    Inspection, 103
Virtual
    Desktop, 125
    Microelectromechanical Systems, 192
    Reactor, 59
Virus (biological), 191
VISAR
    see Velocity Interferometer System for Any Reflector
Visualization, 192
VLF
    see Very Low Frequency
VOC
    see Volatile Organic Compounds
Voigt, J. A. 99
Volatile Organic Compounds
    Detection, 67
    Robotic vehicles, 68
Volponi, J. V. 136
VOLMAX (code), 24-25
Vortex, 88-89
Voth, T. E. 44
VxInsight, 53

W

Wafer, 58
Wagner, J. F. 199
Wagner, J. S.
    Collective intelligence, 220
    Engineering optimization, 48
Walker, T. R. 107
Walkup, J. W. 179
Wally, K.
    Bioaerosol concentrator, 139
    Biological weapons detector, 142
    Polymer biosensor, 232
Walsh, D. S.
    Solar cells, 202
    Time-Resolved Ion-Beam–Induced Charge Collection, 70
Warren, M. E.
    Microoptics, 64
    Microsystems, 76
    Microdomain, 171
    Nanoseparation, 19
    Photonic interconnects, 58
Warren, W. L. 62

Watterberg, P. A. 117
Wave
    Chemical sensors, 62
    Flexural plate-wave, 16-17
    Laser ultrasonics, 82-83
    Microchem lab, 172-173
    Optical sensor, 65
    Optoelectronics, 72
    Wavelet, 44-45
    see also: Surface Acoustic Wave
Webb, S. W. 81
Weber, T. M. 171
Wehlburg, J. C.
    Emerging threats, 199
    Image analysis, 179
Weinbrecht, E. A. 210
Weld
    Laser arc welding, 27
    Laser wire deposition, 104
Wellman, G. W. 42
Wendt, J. R.
    Microoptics, 64
    Nanophotonics, 9
    Optoelectronics, 72
Wessendorf, K. O. 78
Wheeler, D. R.
    Degradative materials, 148
    Intelligent polymers, 26
Wide-bandgap, 10
Wilcoxon, J. P. 26
Williams, A. B. 51
Williams, J. S. 179
Wire
    Array, 230
    Laser deposition, 104
    see also: Feeder
Witkowski, W. R. 100
Witzke, E. L. 126
Wolfer, W. 171
Womble, D. E. 44
Wong, C. C. 171
Woodworth, J. R. 70
World Wide Web
    Multimedia documentation, 112-113
    Streaming visualization, 107
Wright, A. F.
    Electronic defects, 73
    Novel semiconductor devices, 10
    Structure codes, 45
Wright, S. A. 172
Wu, J. 153
Wu, K. L. 153
Wunsch, S. E. 89
Wyckoff, P. S. 130
Wylie, B. N. 53
Wyss, G. D. 162

X

Xavier, P. G.
    Cloud to Computer Aided Design, 116
    Geometric databases, 123
    Intelligent agents, 171

Y

Yang, P.
    Dry processes, 105
    Microfabrication, 106
Yarberry, V. R.
    Microelectromechanical Systems, 102
    Visualization tools, 192
Yazzie, S. H. 160
Yee, A. A. 138
Yee, M. L. 138
Yelton, W. G. 67
Yocky, D. A. 140
Yoshimura, A. S. 113
Young, W. F. 119

Z

Zanini, D. V. 153
Zavadil, K. R. 214
Zhang, P. 150
Z-pinches
    Faraday rotation, 230
    Isentropic compression, 224
    Rayleigh-Taylor mitigation, 201
Zutavern, F. J.
    Filament laser, 226
    Optical sensor, 65

END OF
DOCUMENT